



SEATTLE PUBLIC LIBRARY

R629.435 C813i

010117

Corliss, William R.

031

The interplanetary pionee

337037



0000100437508



TECHNOLOGY

STACK

SEATTLE PUBLIC LIBRARY

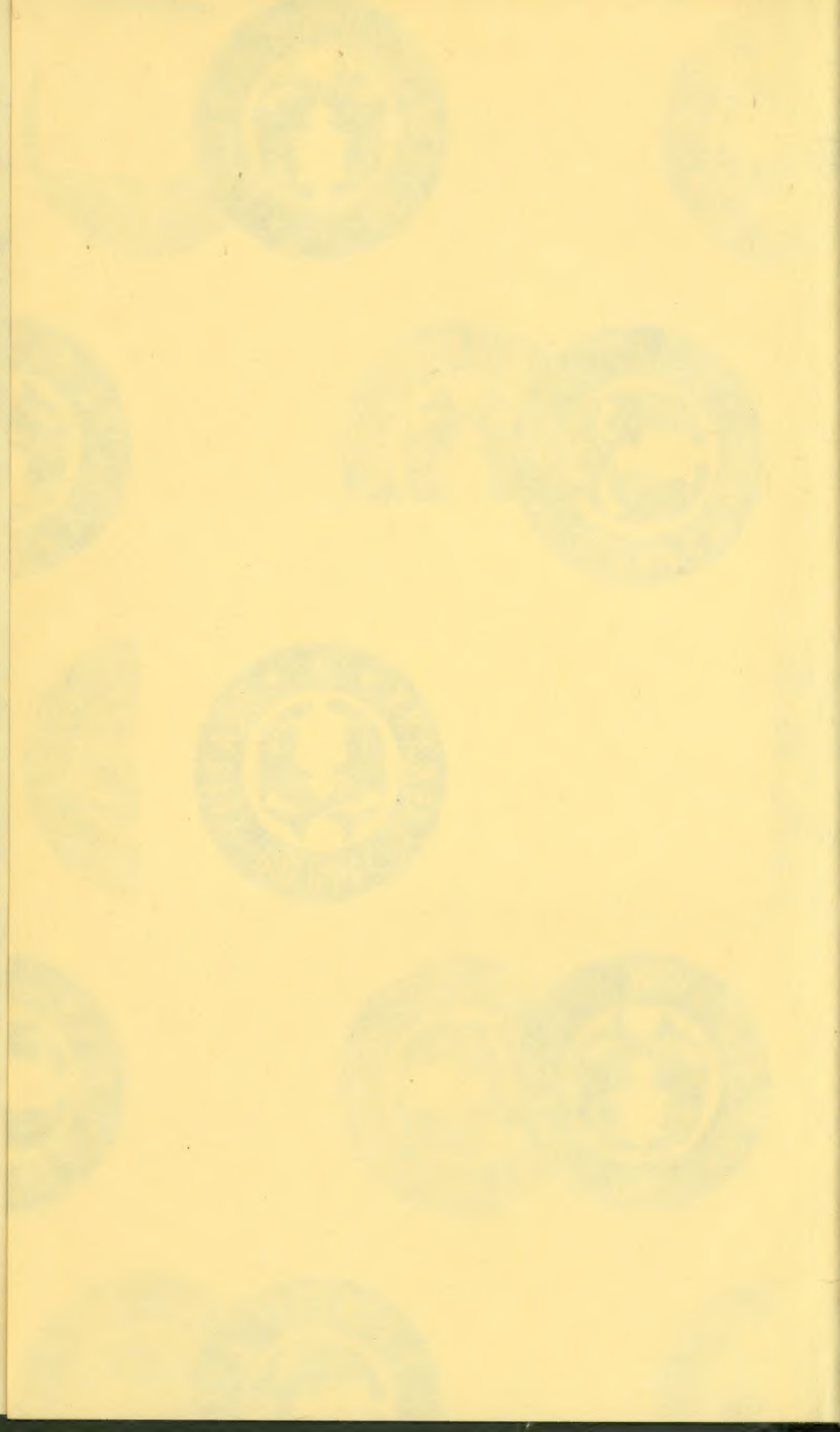
REFERENCE BOOK

NOT TO BE TAKEN FROM THIS ROOM

R629.435  
C813i

2768227  
v.1-3





Seattle Public Library

JAN 23 1973  
NASA SP-278

# THE INTERPLANETARY PIONEERS

## VOLUME I: SUMMARY

by

William R. Corliss



Scientific and Technical Information Office  
NATIONAL AERONAUTICS AND SPACE ADMINISTRATION  
Washington, D.C.

1972

R 629.435  
C 8/3e  
v.1-3



---

For sale by the Superintendent of Documents  
U.S. Government Printing Office, Washington, D.C. 20402  
Price \$1.25 (paper cover) Stock Number 3300-0447  
Library of Congress Catalog Card Number 74-176234

## Foreword

SOME EXPLORATORY ENTERPRISES start with fanfare and end with a quiet burial; some start with hardly a notice, yet end up significantly advancing mankind's knowledge. The Interplanetary Pioneers more closely fit the latter description. When the National Aeronautics and Space Administration started the program a decade ago it received little public attention. Yet the four spacecraft, designated Pioneers 6, 7, 8, and 9, have faithfully lived up to their name as defined by Webster, "to discover or explore in advance of others." These pioneering space-craft were the first to systematically orbit the Sun at widely separated points in space, collecting information on conditions far from the Earth's disturbing influence. From them we have learned much about space, the solar wind, and the fluctuating bursts of cosmic radiation of both solar and galactic origin.

These Pioneers have proven to be superbly reliable scientific explorers, sending back information far in excess of their design lifetimes over a period that covers much of the solar cycle.

This publication attempts to assemble a full accounting of this remarkable program. Written by William R. Corliss, under contract with NASA, it is organized as Volume I: Summary (NASA SP-278); Volume II: System Design and Development (NASA SP-279); and Volume III: Operations and Scientific Results (NASA SP-280). In a sense it is necessarily incomplete, for until the last of these remote and faithful sentinels falls silent, the final word is not at hand.

HANS MARK  
*Director*  
*Ames Research Center*  
*National Aeronautics and*  
*Space Administration*

TECHNOLOGY

2768227

to which they will submit, and upon which they will be compelled to act, in accordance with their own best judgment. They will be compelled to act, because they will be compelled to submit. They will be compelled to submit, because they will be compelled to act.

It is not to be denied, however, that the people of Boston, and of Massachusetts, are not, in this matter, to be regarded as a mere mass of individuals, but as a body corporate, having, like all other bodies corporate, a right to self-government, and a right to be represented in the Legislature.

The Legislature, however, is not to be regarded as a mere mass of individuals, but as a body corporate, having, like all other bodies corporate, a right to self-government, and a right to be represented in the Legislature.

But the Legislature, like all other bodies corporate, has a right to self-government, and a right to be represented in the Legislature.

But the Legislature, like all other bodies corporate, has a right to self-government, and a right to be represented in the Legislature.

But the Legislature, like all other bodies corporate, has a right to self-government, and a right to be represented in the Legislature.

But the Legislature, like all other bodies corporate, has a right to self-government, and a right to be represented in the Legislature.

But the Legislature, like all other bodies corporate, has a right to self-government, and a right to be represented in the Legislature.

But the Legislature, like all other bodies corporate, has a right to self-government, and a right to be represented in the Legislature.

But the Legislature, like all other bodies corporate, has a right to self-government, and a right to be represented in the Legislature.

# Contents

|  | Page       |
|--|------------|
| <b>Chapter 1. ORIGIN AND HISTORY OF THE INTERPLANETARY<br/>PIONEER PROGRAM</b> | <b>1</b>   |
| The Scientific Challenge of Interplanetary Space                               | 1          |
| The Ames Solar Probe Studies   | 2          |
| Selecting a Contractor   | 4          |
| The Pioneer Organization   | 5          |
| The Pioneer Schedule   | 11         |
| The Pioneer Cost Picture   | 14         |
| Pioneer Chronology   | 22         |
| <b>Chapter 2. PIONEER SYSTEM DESIGN AND DEVELOPMENT</b>                        | <b>25</b>  |
| Defining the Pioneer System  | 25         |
| Pioneer Launch Trajectory and Solar Orbit Design                               | 29         |
| Spacecraft Design Approach and Evolution                                       | 34         |
| The Spacecraft Subsystems  | 37         |
| Scientific Instruments   | 62         |
| The Delta Launch Vehicle   | 76         |
| Tracking and Communicating with the Pioneer Spacecraft                         | 78         |
| Pioneer Data Processing Equipment  | 84         |
| <b>Chapter 3. PIONEER FLIGHT OPERATIONS</b>                                    | <b>89</b>  |
| Prelaunch Activities   | 89         |
| Launch to DSS Acquisition  | 93         |
| From DSS Acquisition to the Beginning of the Cruise Phase                      | 98         |
| Spacecraft Performance during the Cruise Phase                                 | 99         |
| <b>Chapter 4. PIONEER SCIENTIFIC RESULTS</b>                                   | <b>103</b> |
| The Goddard Magnetic Field Experiment  | 103        |
| The MIT Plasma Probe   | 105        |
| The Ames Plasma Probe  | 107        |
| The Chicago Cosmic-Ray Experiment  | 109        |
| The GRCSW Cosmic-Ray Experiment  | 111        |
| The Minnesota Cosmic-Ray Experiment  | 115        |
| The Stanford Radio Propagation Experiment                                      | 116        |
| TRW Systems Electric Field Experiment  | 120        |

|   | Page       |
|---|------------|
| The Goddard Cosmic Dust Measurements                        | 121        |
| The Pioneer Celestial Mechanics Experiment                  | 123        |
| Solar Weather Monitoring                                    | 125        |
| <b>BIBLIOGRAPHY</b>   | <b>127</b> |
| Appendix. MEMORANDUM: ORGANIZATION OF AMES SOLAR PROBE TEAM | 129        |

## Origin and History of the Interplanetary Pioneer Program

### THE SCIENTIFIC CHALLENGE OF INTERPLANETARY SPACE

WHEN WE LOOK UP AT THE STARS, we think we see the real universe, but the stars constitute only about 1 percent of the matter in the universe. The other 99 percent exists as dust and gas and occupies the space between the stars. The real drama of cosmic evolution may be unfolding in the cold space between the stars rather than in hot stellar interiors. But until recently, science has confined its study mainly to the astronomical bodies that shine by their own emissions or by reflected light. The bulk of the universe has been by necessity virtually ignored.

The only direct, *in situ* measurements we can make of this dominant fraction of the universe are from space probes and satellites that reach well beyond the distorting influences of the Earth's atmosphere and magnetic field. Even then, the probes measure interplanetary space rather than interstellar space. The region between the planets is swept by the solar wind and bursts of solar cosmic rays which usually overwhelm galactic phenomena. Still, this can be advantageous to science, because spacecraft in interplanetary space can monitor the interface between a typical star—the Sun—and interstellar space, recording the outward flow of solar electromagnetic energy, solar cosmic rays, and solar plasma. Similarly the inflow of galactic cosmic rays can be measured. Like all interface regions, interplanetary space is full of turmoil and is a rich region for scientific research.

The scientific mission of Pioneers 6 through 9<sup>1</sup> has been the synoptic measurement of the interplanetary milieu as it is affected by the Sun. The Pioneers have measured and transmitted back to Earth data on solar plasma, solar and galactic cosmic radiation, magnetic and electric fields, and the specks of cosmic dust that pervade interplanetary space. All of these phenomena, even the flux of galactic cosmic rays, are strongly affected by events occurring

<sup>1</sup> Also called Pioneers A through D prior to launch. Pioneer E, which would have been Pioneer 10, was a launch failure. Pioneers 1 through 5 were early lunar probes.

on the Sun. Spotted strategically around the Sun in the plane of the ecliptic, they have monitored the ever-changing fluxes and fields that wax and wane with solar activity. In purpose, the Pioneers have been akin to weather satellites, except that they are artificial planets of the Sun and not satellites of the Earth. In fact, data from the Pioneers have been used extensively in preparing "space weather" forecasts.

The main pulse of solar activity is the 11-year cycle of sunspots, a periodic phenomenon felt the length and breadth of the solar system. In 1961, when the National Aeronautics and Space Administration (NASA) formulated the Pioneer Program, scientists around the world were organizing a concentrated study of solar events expected during the 1964–1965 solar minimum. It seemed highly desirable to have some unmanned instrumented spacecraft out in deep space to support the growing number of International Quiet Sun Year (IQty) projects. Data radioed back from these proposed spacecraft would supplement those received from NASA's OGOs, OSOs, and Explorer satellites in orbit around the Earth and a worldwide array of scientific sensors on the ground. A unique feature of such spacecraft in heliocentric orbits lay in the fact that they would range far ahead and behind the Earth as it swung around the Sun, giving scientists a more comprehensive picture of interplanetary space at various azimuths along the plane of the ecliptic. As the following chapters will show, the unexpectedly long lives of the Pioneers extended deep-space scientific coverage through the 1969–1970 solar maximum. Furthermore, lunar and solar occultations and unusual spacecraft alignments have occurred which increased the scientific payoff of the Pioneer Program far beyond original expectations. As Chapter 4 demonstrates, the Pioneers added immeasurably to our knowledge of the region between 0.8 and 1.2 Astronomical Units (AU)<sup>2</sup> as well as to our knowledge of the Sun itself.

### THE AMES SOLAR PROBE STUDIES

The Pioneer Program began as an informal study of solar probes at the Ames Research Center in May 1960. At this time, NASA had been in existence only a year and a half, and the previous National Advisory Committee for Aeronautics (NACA) laboratories, such as Ames, were still working at defining their roles in space. The solar-probe study was an attempt to demonstrate Ames' potential as a spacecraft project manager and to also interest top management at

<sup>2</sup> The Astronomical Unit is equal to the mean distance from the Earth to the Sun; i.e. about 92.95 million miles or 149.6 million kilometers.

Ames in this role which departed from Ames' traditional function as an aeronautical research center.

The informal study team was headed by Charles F. Hall, who enlisted a dozen other Ames engineers in the effort.<sup>3</sup> The results of the study were published as an internal Ames report on July 22, 1960, bearing the title: "A Preliminary Study of a Solar Probe."

The spacecraft conceived during the study was conical in shape and was designed to point continuously at the Sun as it approached to about 0.3 AU. The Ames solar probe was quite different from the Pioneer spacecraft that it was to engender. However, the scientific rationale quoted in the report differed little from that adopted for the Pioneers: "The desirability of a solar probe was indicated by the thought that an increase in knowledge of solar phenomena through measurements made near the Sun would aid in an understanding of terrestrial phenomena in such areas as communication, weather prediction and control, and atomic and nuclear physics." The spacecraft was envisioned as small, simple, and long-lived, just as its progeny were to be in fact.

Although considerable opposition developed at Ames to getting into spacecraft project work, Smith J. DeFrance, the Center Director, among others, supported the solar-probe project. On September 14, 1960, DeFrance organized a formal Ames Solar Probe Team. (The text of the memorandum setting up the team is reproduced in the Appendix.) Headed by Hall, the team retained many of the members of the informal group and was charged with recommending a "practical system."

The Solar Probe Team now bent its efforts to fleshing out the skeleton concept described in the July 22, 1960, report. The objective was to show the practical feasibility of the Ames concept and demonstrate to NASA Headquarters Ames' capability for heading up a hardware project. The basic spacecraft concept changed somewhat during these studies. The major problem involved keeping the spacecraft and its instruments cool as it neared the Sun. Fuller descriptions of the spacecraft, its trajectory, and the proposed instruments can be found in references 1 and 2.

During late 1961 and early 1962, Hall and others tried to stimulate interest in the concept at NASA Headquarters. At one presentation, Jesse Mitchell, from NASA's Office of Space Science, became intrigued with the Ames spacecraft. Mitchell subsequently arranged a meeting between Hall and Edgar M. Cortright, who was the

<sup>3</sup> Specifically: Bader, M., Beam, B. H., Dimeff, J., Dugan, D. W., Eggers, A. J., Jr., Hansen, C. F., Hornby, H., Jones, R. T., Matthews, H. F., Mersman, W. A., Robinson, G. G., and Tingling B. E.

Deputy Director of the Office of Space Science at that time.<sup>4</sup> Cortright pointed out that Ames had no spacecraft experience, but he also remarked that he would like to see Ames get into the "hardware business." He posed the question: Would Ames be interested in building an Interplanetary Pioneer as a step on the way to the solar probe? Hall returned to Ames and received a go-ahead from Ames management. Ames management also recommended that an industrial contractor be brought in to do a feasibility study.

### SELECTING A CONTRACTOR

The industrial contractor chosen was Space Technology Laboratories (STL)<sup>5</sup> at Redondo Beach, California. STL, acquainted with the Ames work, submitted an unsolicited proposal that was subsequently funded. In April 1962 STL completed the 2½-month, \$250 000, feasibility study (ref. 3) under NASA Contract NAS2-884.

The STL Pioneer feasibility study was particularly significant because, during the 2½ months in early 1962, almost all of the important system-design decisions were made by STL engineers working in conjunction with NASA-Ames personnel. The key concept of a spin-stabilized spacecraft, with its spin axis perpendicular to the plane of the ecliptic, and a flat, fanlike, high-gain antenna pattern was originated by Herbert Lassen, of STL. As discussed in Vol. II, Chapter 1, this concept helped meet all the severe design constraints placed upon Pioneer by weight, cost, and schedule.

The next big step was obtaining formal project approval from Headquarters. The Ames group, backed by DeFrance, made the key presentation to NASA Associate Administrator Robert C. Seamans, Jr., on June 6, 1962. After Congress approved the NASA budget, Seamans signed the Project Approval Document (PAD) on November 9, 1962.

Pressing their advantage, STL followed up the feasibility study with an unsolicited proposal to design and fabricate four spacecraft, quoting a price of \$10 million on a cost-plus-fixed-fee basis (ref. 4). Ames wished to go ahead with a sole-source procurement, but this was disapproved and competitive selection was stipulated.

Using the STL feasibility study as a foundation, Ames wrote the specifications for the Pioneer spacecraft and on January 29, 1963, issued a Request for Proposal (RFP-6669) to industry. Eight companies responded on March 4, 1963. Because of the price dis-

<sup>4</sup> Interview with Charles F. Hall, January 26, 1971.

<sup>5</sup> STL's name was later changed to TRW Systems. TRW refers to Thompson-Ramo-Wooldridge, the parent company.

parity between the two technically superior proposals (from Hughes and STL), NASA requested that these two companies resubmit bids on a fixed-price-incentive (FPI) basis.<sup>6</sup> The second submissions were received on May 24, 1963. STL was selected over Hughes in the final competition (ref. 5). The terms of a letter contract were agreed upon in July, and the letter contract was awarded on August 5, 1963. The contract authorized expenditures up to \$1.5 million. Work began immediately at STL. The definitive contract (NAS2-1700) was negotiated later and was approved by NASA Headquarters on July 30, 1964. It is interesting to note here that the incentive provisions of the contract (as opposed to the cost-plus-fixed-fee contract then common in aerospace work) forced NASA to define everything it wanted with high precision. Contract negotiations were lengthy, and approximately 80 changes were made to the basic statement of work originally stated in RFP A-6669. With a contractor hard at work, Pioneer moved ahead rapidly toward the first launch, planned for 1965.

### THE PIONEER ORGANIZATION

The Pioneer hardware, described in the next chapter, consisted of four major systems:

- (1) The spacecraft itself
- (2) The scientific instruments
- (3) The launch vehicle
- (4) The ground-based tracking and data acquisition stations

NASA assigned teams of engineers and scientists to each of these four technical elements. Many contractor personnel, especially at TRW Systems and the Deep Space Network (DSN) stations, were closely involved in the program.

The purpose of this section is the general recounting of how Pioneer was organized and who some of the key personnel were.

The overall NASA Pioneer organization is shown in figure 1-1, beginning with the NASA Administrator and showing the principal chains of command. This diagram shows overall management responsibility but does not highlight the groups where the bulk of the work was done. The actual work entailed:

- (1) Spacecraft design, testing, and launching
- (2) The design and testing of the scientific instruments and the presentation of final scientific results

<sup>6</sup> While the contract was being firmed up, STL was given a small side study to investigate the effects of uprating the Delta launch vehicle and going to a larger spacecraft.

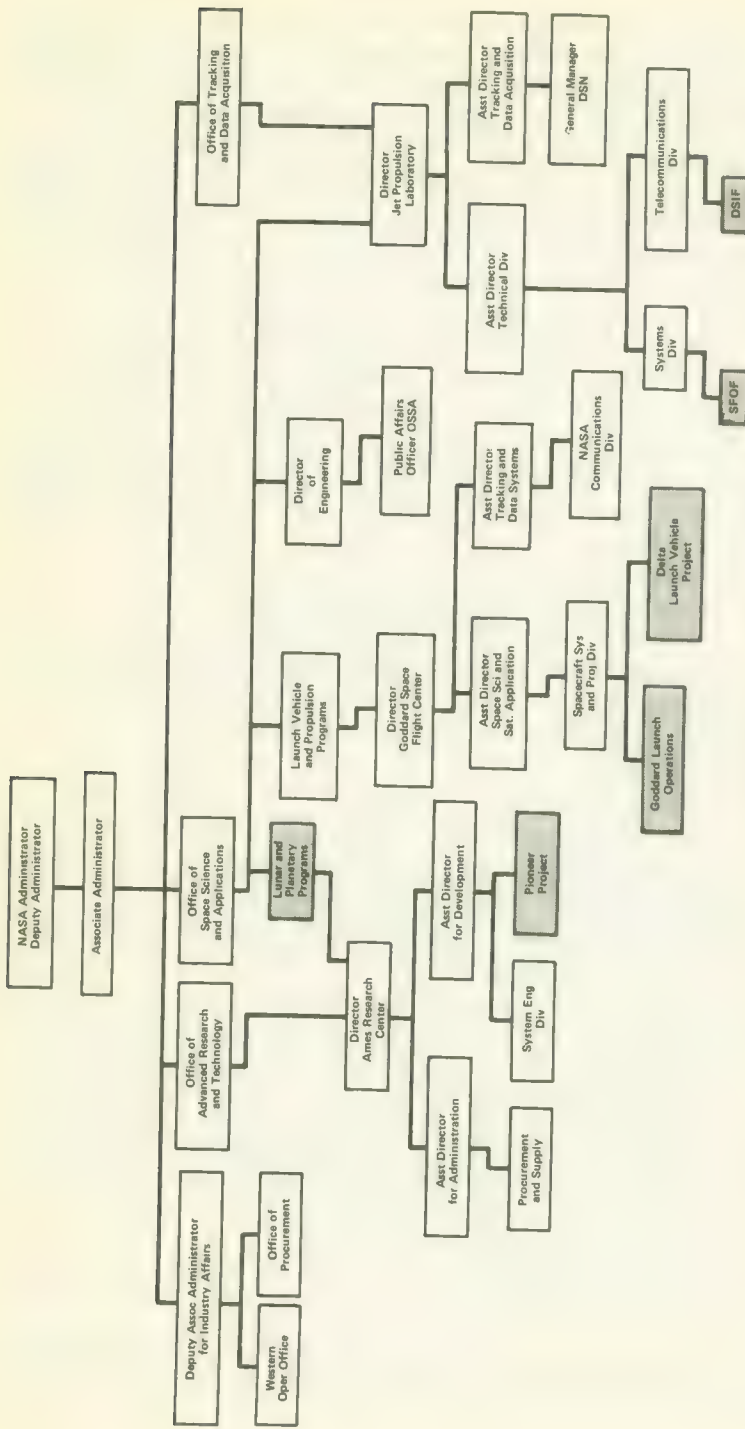


FIGURE I-1.—Principal elements of the NASA organization early in the Pioneer Program. The shaded boxes indicate where most personnel assigned to Pioneer were located.

(3) The routine, but highly important, day-by-day control of the spacecraft and its tracking and data acquisition

(4) The huge volume of management chores that accompanies a program of this size

The shaded boxes on the diagram indicate the focal points of activity, but only those within NASA. Important contractors—TRW Systems and the experimenters, in particular—are not shown. What figure 1-1 does show well is the dual nature of the NASA organization. The Ames Research Center, for example, reported administratively through the Headquarters Office of Advanced Research and Technology, but project direction came from the Headquarters Office of Space Sciences and Applications. The Pioneer Program was one of the few NASA spacecraft programs assigned to a NASA research-oriented center. Obviously, the unusual arrangement worked very well in the case of Pioneer.

Basically Ames built, tested, and controlled the spacecraft and the scientific instruments provided by the experimenters; Goddard procured a Delta rocket and launched the spacecraft; the Jet Propulsion Laboratory (JPL), which operated the DSN, tracked the spacecraft and passed the acquired data on to Ames. Headquarters provided overall direction. This situation is spelled out more thoroughly in table 1-1 and figure 1-2. Figure 1-2 shows how the Ames Pioneer Project Manager, C. F. Hall, organized his group to tie together the different elements of NASA into a smoothly functioning team. The

TABLE 1-1.—*Responsibilities in the Pioneer Program*

| Task   | Organization  | Individuals  |
|--|---|--|
| Overall program direction  | Lunar and Planetary Program Office, Office of Space Science and Applications, NASA Headquarters | Kochendorfer, F.D.<br>(1962-1963)<br>Reiff, G.A. (1963-1970)<br>Kochendorfer, F.D.<br>(1970 to date) |
| Project management   | Ames Research Center  | Hall, C.F.   |
| Spacecraft system  | Ames Research Center<br>TRW Systems   | Holtzclaw, R.W.<br>Mickelwait, A.G.<br>(1962-1967)<br>O'Brien, B.J.<br>(1967 to date)                |
| Scientific instrument system   | Ames Research Center  | Wolfe, J.H.  |
| Assuring that overall scientific objectives are met                                      | Ames Research Center  |  |
| Management of scientific instrument systems  | Ames Research Center  | Cross, H.V.<br>Lepetich, J.E.<br>(1962 to date)  |
| Providing scientific instruments, data reduction and analysis, and scientific reporting: |   |  |

TABLE 1-1.—*Responsibilities in the Pioneer Program—Concluded*

| Task  | Organization   | Individuals  |
|---|--|--|
| Magnetometer (Pioneers 6, 7, 8)   | Goddard Space Flight Center                                    | Ness, N.F.   |
| Magnetometer (Pioneers 9, E)  | Ames Research Center   | Sonett, C.P.   |
| Plasma probes (Pioneers 6, 7, 8, 9, E)  | Ames Research Center   | Wolfe, J.H.  |
| Plasma probes (Pioneers 6, 7)   | Massachusetts Institute of Technology<br>University of Chicago | Bridge, H.<br>Simpson, J.A.  |
| Cosmic-ray telescope (Pioneers 6, 7)  | Graduate Research Center of the Southwest                      | McCracken, K.G.  |
| Cosmic-ray experiment (Pioneers 6, 7, 8, 9, E)                                    | University of Minnesota  | Webber, W.R.   |
| Cosmic-ray experiment (Pioneers 8, 9, E)  | Stanford University  | Eshleman, V.R.   |
| Radio propagation experiment (Pioneers 6, 7, 8, 9, E)                             | TRW Systems  | Scarf, F.L.  |
| Electric-field detector (Pioneers 8, 9, E)  | Goddard Space Flight Center                                    | Berg, O.   |
| Cosmic dust detector (Pioneers 8, 9, E)   | Jet Propulsion Laboratory                                      | Anderson, J.D.   |
| Celestial mechanics (Pioneers 6, 7, 8, 9, E)                                      |  |  |
| Engineering instrument system   | Ames Research Center   | Lumb, D.R.   |
| Provision of a convolutional coder and analysis of results (Pioneers 9, E)        |  |  |
| Launch vehicle system   | Goddard Space Flight Center                                    | Schindler, W.R.  |
| Procurement of Delta launch vehicle   | McDonnell-Douglas Aircraft Company                             |  |
| Design and fabrication of the Delta launch vehicle                                |  |  |
| Launch activities   | Goddard Space Flight Center                                    | Gray, R.H.   |
| Direction of launch operations  | USAF Eastern Test Range  |  |
| Tracking and data acquisition during powered flight                               | Ames Research Center   | Hofstetter, R.U.   |
| Spacecraft-launch vehicle interface and coordination of launch vehicle operations |  |  |
| Flight operations   | Ames Research Center   | Jagiello, L.T.<br>(1962-1966)  |
| Mission planning and control  |  | Nunamaker, R.R.<br>(1966 to date)  |
| Tracking, data acquisition, and command transmission                              | Jet Propulsion Laboratory                                      | Thatcher, J.W.<br>(1962-1966)  |
| Data processing and analysis  | Ames Research Center   | Siegmeth, A.J.<br>(1966 to date)<br>Erickson, M.D.<br>(1966-1969)<br>Natwick, A.S.<br>(1969 to date) |

## ORIGIN AND HISTORY

2

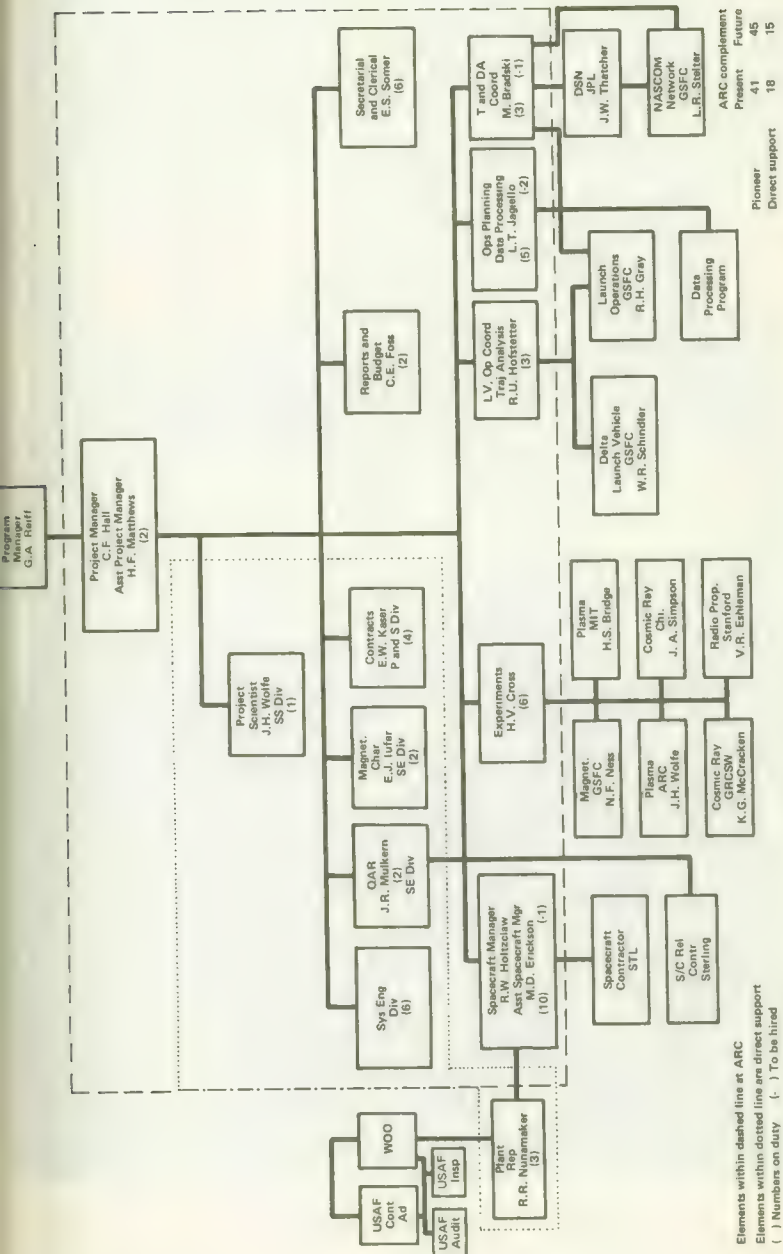


FIGURE 1-2.—The Pioneer team in 1964. This organization was remarkably stable. The few changes that were made are summarized in table 1-1.

Pioneer Project group at Ames was originally split into five groups, with almost a one-to-one correspondence with the four Pioneer systems—spacecraft, experiments, launch vehicle, tracking and data acquisition. Later, the correspondence was made exact when the five project groups were consolidated into four groups responsible for the spacecraft, the experiments, the flight operations (mainly tracking and data acquisition), and the launch vehicle and launch operations with groups from Goddard and JPL supporting the project. Figures 1-3 through 1-8 show some of the individuals who contributed to the Pioneer Program. In practice, Ames personnel from the Pioneer Project worked directly with those people in the support groups assigned to Pioneer, even though they reported through JPL, Goddard, or contractor managements. This synthesis of project-oriented and functionally oriented personnel has been quite common and very effective in the aerospace industry.

During any project extending over a decade, one would expect considerable turnover of key people within government and the contractor organizations. Pioneer is an exception to this rule in



FIGURE 1-3.—NASA Headquarters inspection of the mockup of the Pioneer instrument platform. Left to right: R. F. Garbarini, J. E. Naugle, C. F. Hall (Ames), A. B. Mickelwait (TRW Systems), O. W. Nicks, H. E. Newell, and H. A. Lassen (TRW Systems).



FIGURE 1-4.—Part of the Ames Pioneer Project team. Left to right: top row, G. J. Nothwang, C. F. Hall; middle row, A. J. Wilhelm, R. U. Hofstetter, R. L. Edens; bottom row, D. W. Lozier, J. E. Lepetich, R. W. Holtzclaw.

that personnel changes have been minor. People and organization structures have stayed remarkably stable. The important changes that have occurred are summarized in table 1-1. One of the most important factors in the success of the Pioneer Program has undoubtedly been the permanence, high capability, and dedication of the Ames Pioneer Project personnel.

### THE PIONEER SCHEDULE

The Pioneer Program consisted of five flight spacecraft, the five Delta rockets for launching them, the experiments, and all the

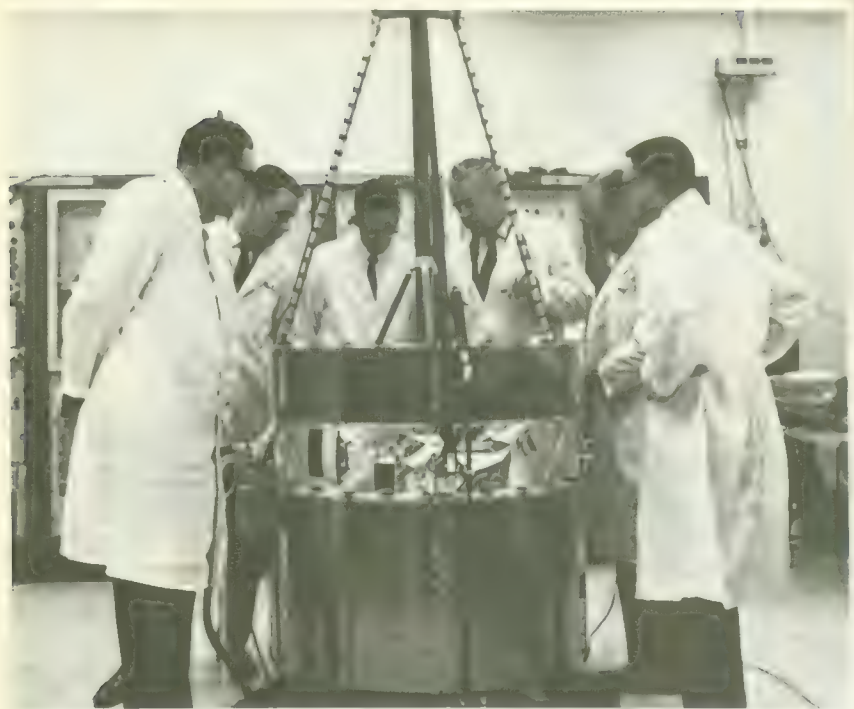


FIGURE 1-5.—Inspection of the Pioneer prototype at TRW Systems in 1965. Far left, A. B. Mickelwait; second from left, G. A. Reiff (NASA Headquarters); fourth from left, C. F. Hall (Ames). (Courtesy of TRW Systems.)



FIGURE 1-6.—Part of Pioneer management team at Cape Kennedy in 1967. Left to right: B. J. O'Brien (TRW Systems), J. Mitchell (NASA Headquarters), M. Aucremanne (NASA Headquarters), C. F. Hall (Ames).



FIGURE 1-7.—R. Gray, second from left, headed Goddard Operations at the Cape during the Pioneer Program. W. R. Schindler, third from left, managed Goddard's Delta program. At far left, J. Schwartz (WTR); at far right, H. Van Goey.



FIGURE 1-8.—JPL DSN personnel assigned to Pioneer. Left to right, A. J. Siegmeth, J. W. Thatcher, and N. A. Renzetti. (Courtesy of JPL.)

necessary ground equipment for tracking and the acquisition and processing of the data. Table 1-1 reveals many, but not all, of the government and contractor organizations that had to work together to produce scientific measurements from deep-space instrument platforms. In such a complex program, one can expect schedule slippages here and there. In the case of Pioneer, the schedule changes due to spacecraft engineering and fabrication were all relatively minor. The first two spacecraft were launched close to the original schedule, during the period of low solar activity as the scientists had intended.

Two kinds of schedules are presented here. First, figure 1-9 reproduces the Pioneer master schedule from the original Project Development Plan which was issued in March 1965. This particular schedule is of historical interest and, in addition, shows the many diverse program elements that had to be completed for a timely launch.

The second set of schedules is presented in figures 1-10 through 1-14—one for each of the five flight spacecraft. Each schedule slippage is explained in the right-hand margin; these explanations are indicative of the many different factors affecting the Pioneer Program.

Pioneers 6 and 7 were launched fairly close to the original target dates. The slippages in the launch schedules of the remaining three spacecraft were much greater. Many of the delays were attributable to troubles with the experiments. In the case of Pioneer 9, launch was delayed to provide a larger time interval between Pioneers 7 and 8 and to permit certain trajectories later. The launch date of the ill-fated Pioneer E was slipped for the same reasons.

### THE PIONEER COST PICTURE

One of the original constraints placed upon the Pioneer Program when it was being formulated in 1962 was that the total cost be around \$30 million.<sup>7</sup> During the years, the Pioneer Program was expanded for a number of reasons, as enumerated below and in figure 1-15. The net result has been that the entire Program has cost about \$70 million. Here are the major reasons for the cost increases:

- (1) Addition of data processing
- (2) Addition of a fifth spacecraft
- (3) Unexpected long lives of the spacecraft, requiring additional funds for tracking and data acquisition

<sup>7</sup>Other constraints were the use of the Delta launch vehicle, and the use of the Deep Space Network.

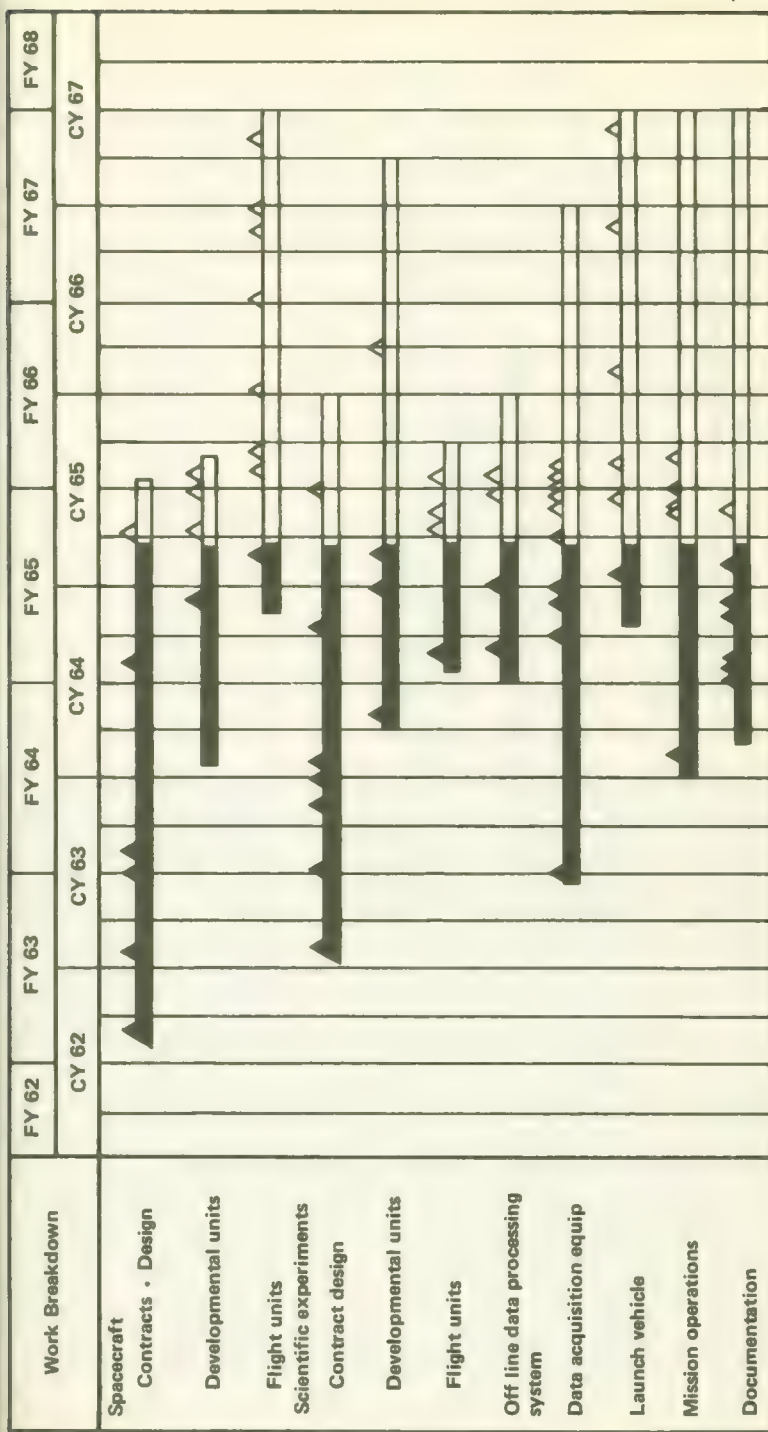


FIGURE I-9.—Project Pioneer master schedule as of March 15, 1965.

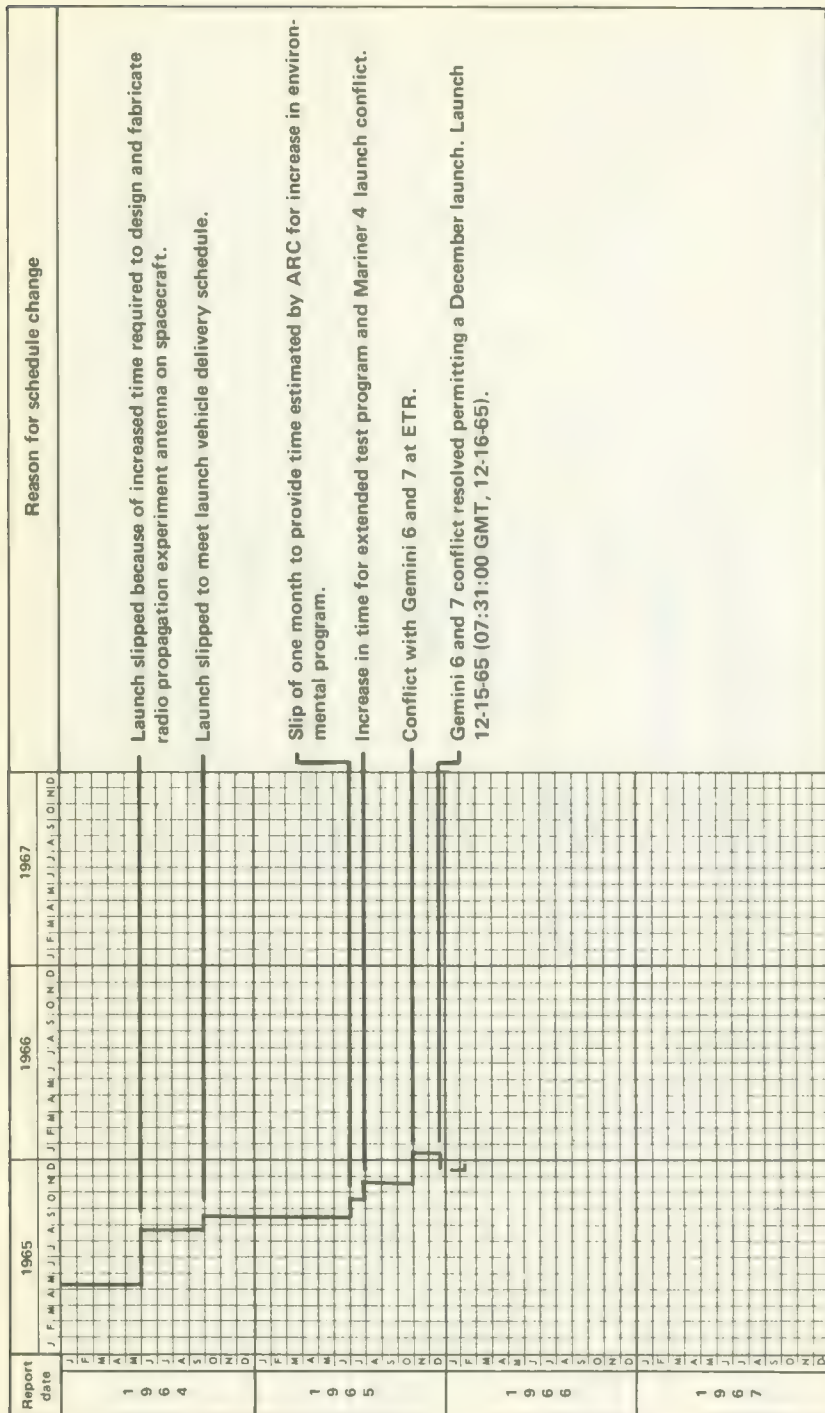


FIGURE 1-18.—Pioneer A schedule. Explanation for slippages are given at the right.

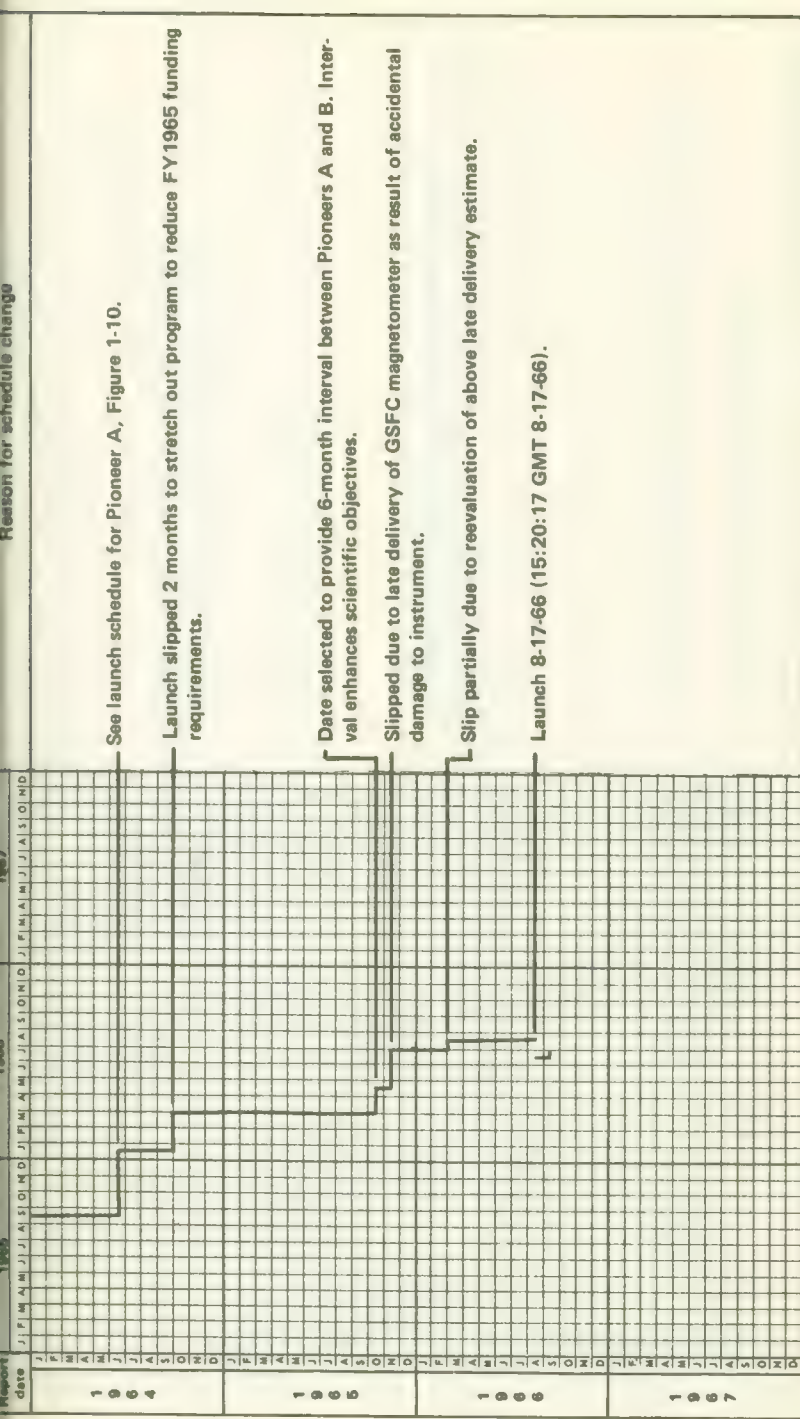


FIGURE 1-11.—Pioneer B schedule.

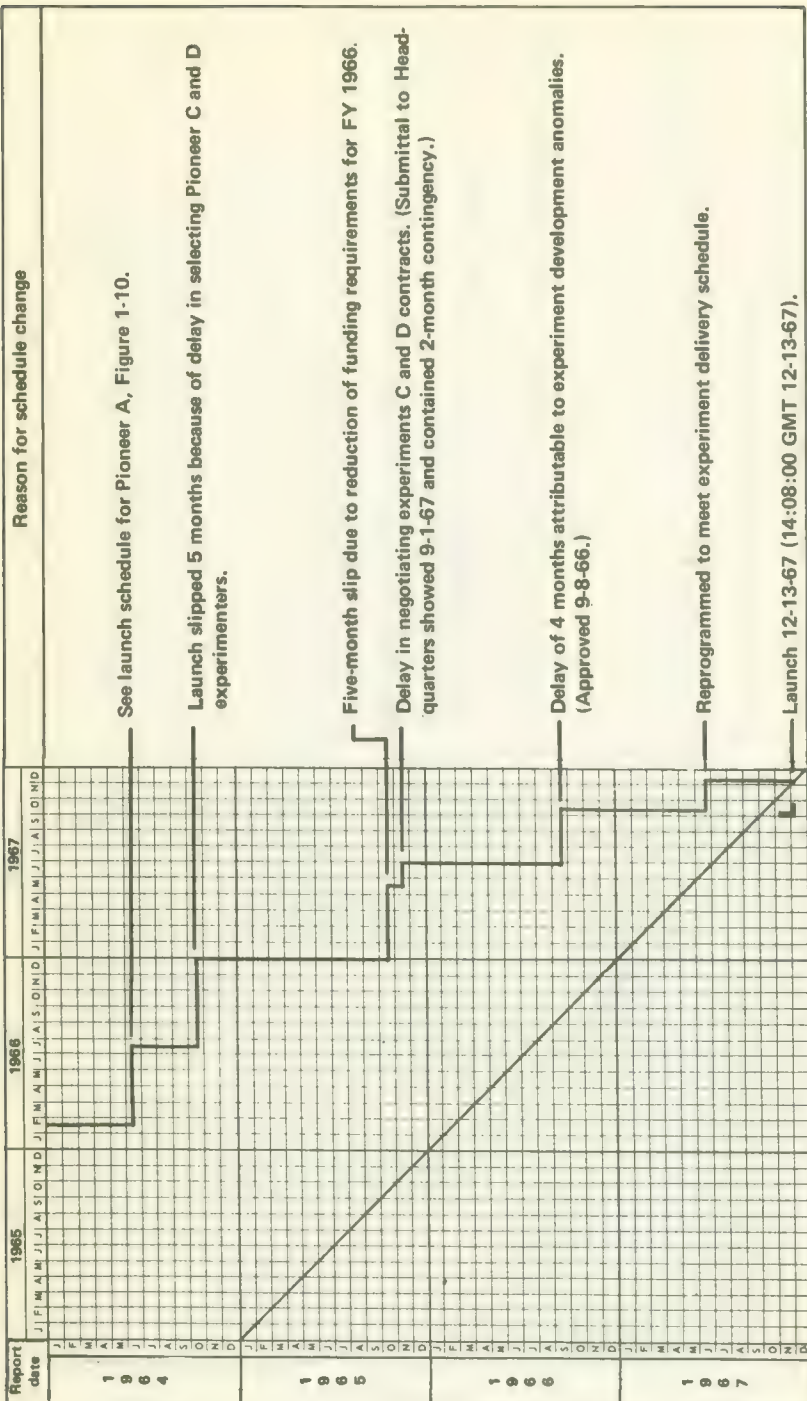


FIGURE I-12.—Pioneer C schedule.

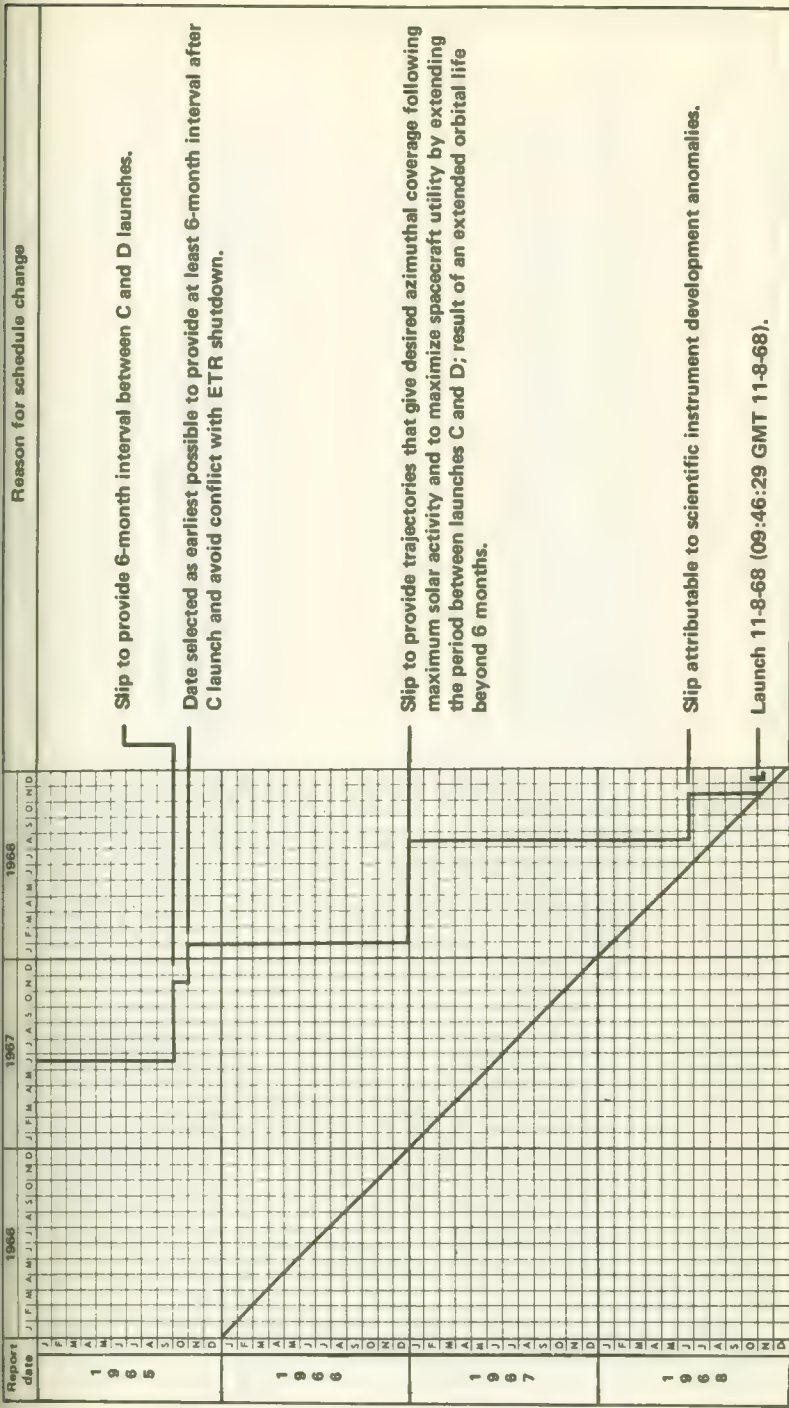


FIGURE 1-13.—Pioneer D schedule.

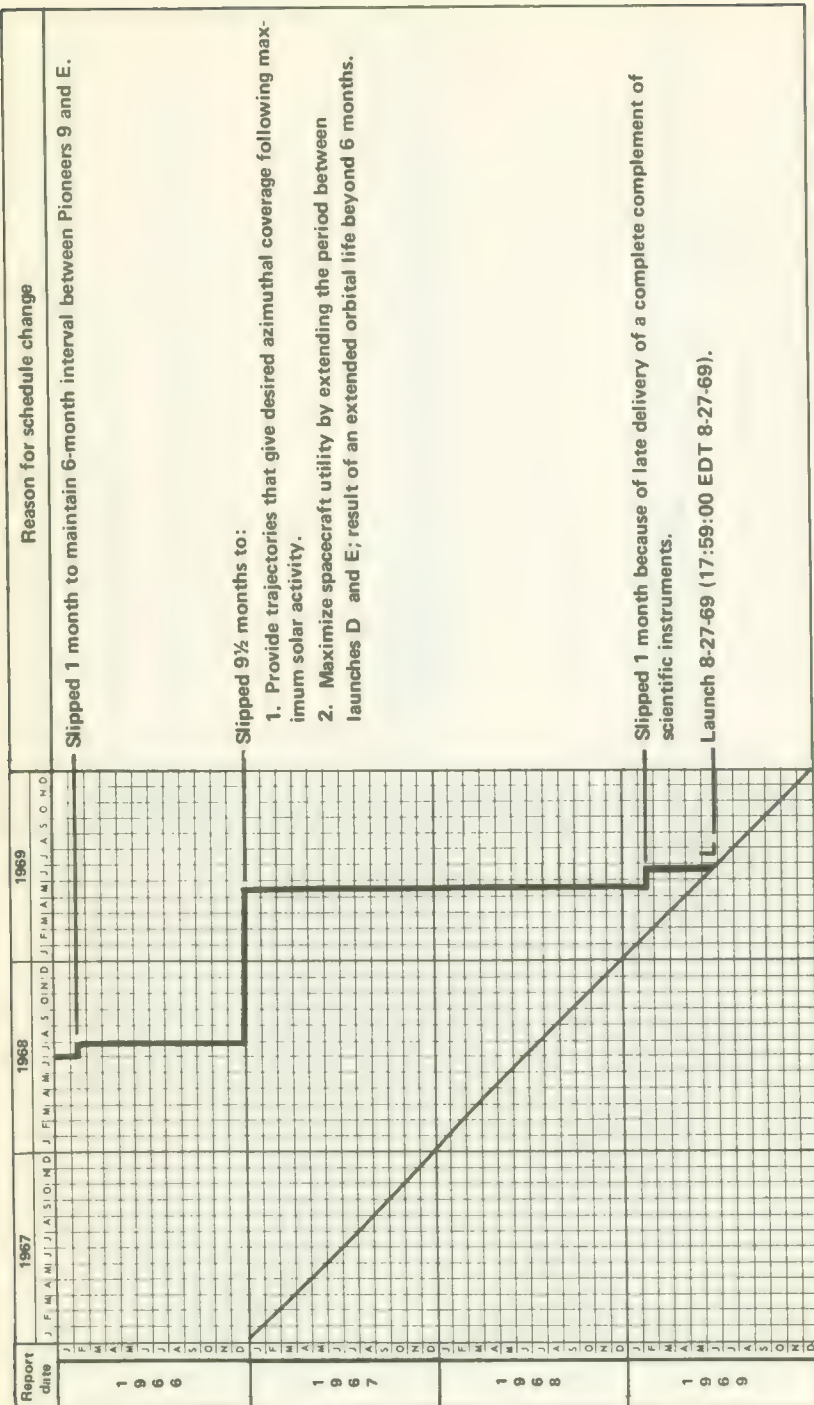


FIGURE 1-14.—Pioneer E schedule.

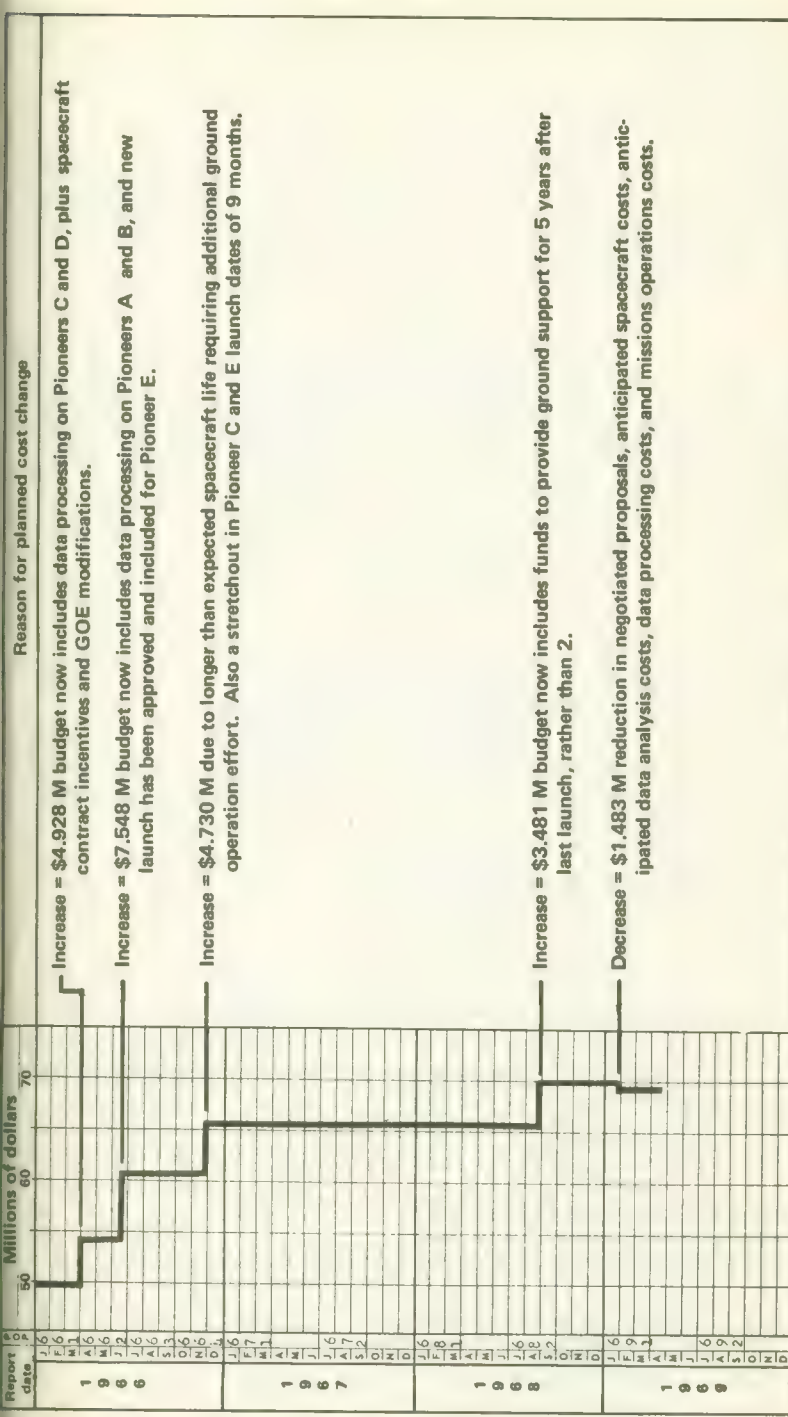


FIGURE 1-15.—Pioneer Program cost trends as of spring, 1969. Reasons for increases and decreases are indicated at the right.

(4) Delays due to late deliveries of experiments

(5) Differences between Pioneers 6 and 7 (the Block-I spacecraft) and Pioneers 8, 9, and E (the Block-II spacecraft) because different experiments were selected for each block

When the long useful lives of the four successfully launched Pioneers are considered (more than 5 years for Pioneer 6), this Program is incontestably one of the least expensive of all NASA spacecraft programs in terms of scientific results per dollar spent.

### PIONEER CHRONOLOGY

Table 1-2 is a chronology which summarizes the major historical events related in earlier pages and also adds a few points not brought out in the text. Much more detailed chronologies covering operations at Cape Kennedy and postlaunch events are presented in Volume III.

TABLE 1-2.—*Chronology of Major Historical Events in the Pioneer Program*

| Date           | Event   |
|----------------|---|
| July 22, 1960  | Release of Ames report, "A Preliminary Study of a Solar Probe"  |
| Sept. 14, 1960 | Formation of Ames Solar Probe Team  |
| Apr. 1962      | STL study of an interplanetary Pioneer completed  |
| June 6, 1962   | Presentation of Ames and STL work on interplanetary Pioneer to R.C. Seamans, Jr., and other NASA Headquarters personnel   |
| Nov. 9, 1962   | Pioneer PAD signed  |
| Jan. 10, 1963  | Pioneer procurement plan approved   |
| Jan. 29, 1963  | RFP for spacecraft sent to industry   |
| Feb. 1, 1963   | RFP for experiments sent to potential experimenters for Pioneers A and B  |
| Mar. 4, 1963   | Eight proposals received at Ames  |
| Mar. 30, 1963  | Spacecraft Selection Board evaluations complete   |
| Apr. 8, 1963   | Experiment proposals received by NASA Headquarters  |
| Apr. 11, 1963  | Procurement briefing to NASA Administrator. Decision to readvertise the Pioneer spacecraft to STL and Hughes on FPI basis |
| May 14, 1963   | New RFP to STL and Hughes   |
| May 24, 1963   | Second set of proposals received at Ames  |
| Jun. 7, 1963   | Second procurement briefing for NASA Administrator. Decision to negotiate with STL  |
| Aug. 5, 1963   | Letter contract signed with STL   |
| Apr. 1964      | Final spacecraft design review  |
| July 30, 1964  | Definitive contract with STL approved by NASA Headquarters  |
| Dec. 5, 1965   | Pioneer-A flight model arrives at Cape Kennedy  |
| Dec. 15, 1965  | Pioneer-6 launch successful   |
| Feb. 22, 1966  | Contract with TRW Systems amended to delete fifth spacecraft in series for budgetary reasons                              |
| Mar. 2, 1966   | Pioneer-6 inferior conjunction or syzygy  |

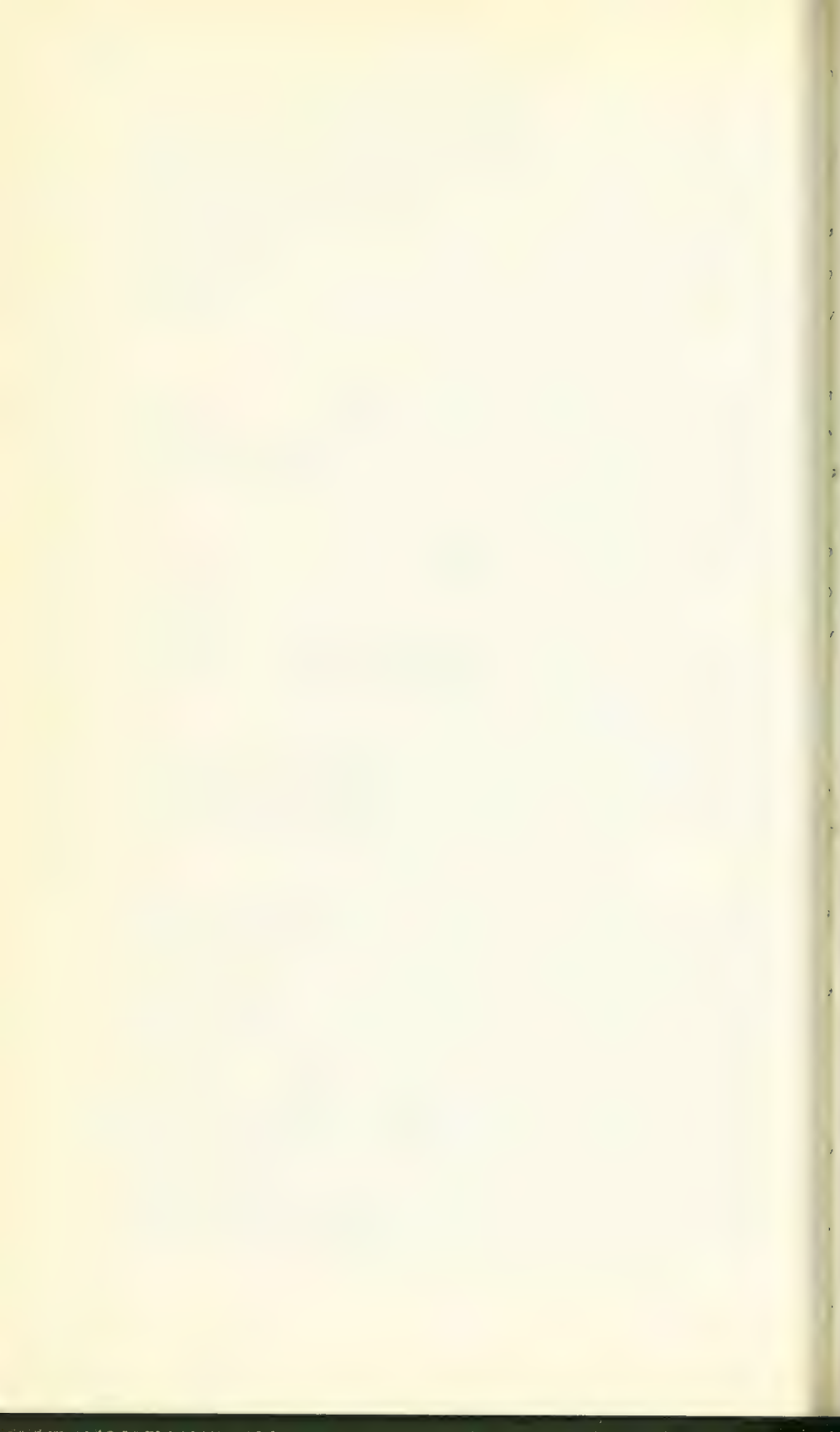
TABLE 1-2.—*Chronology of Major Historical Events in the Pioneer Program—Concluded*

| Date           | Event  |
|----------------|--|
| Apr. 28, 1966  | Contract with TRW Systems amended to fabricate fifth spacecraft out of spares                            |
| Aug. 17, 1966  | Pioneer-7 launch successful  |
| Aug. 31, 1966  | Traveling Wave Tube (TWT) 2 switched in to replace TWT 1 on Pioneer 7*                                   |
| Sept. 30, 1966 | Pioneer-7 inferior conjunction or syzygy   |
| Jan. 19, 1967  | Pioneer-7 lunar occultation  |
| Dec. 13, 1967  | Pioneer-8 launch successful  |
| Jan. 17, 1968  | Pioneer-8 inferior conjunction or syzygy   |
| Jan. 27, 1968  | Pioneer-8 emerges from geomagnetic tail  |
| Oct. 6, 1968   | First use of Deep Space Network-Manned Space Flight Network (DSN-MSFN) hybrid configuration on Pioneer-8 |
| Nov. 8, 1968   | Pioneer-9 launch successful  |
| Nov. 23, 1968  | Pioneer-6 superior conjunction (behind Sun)  |
| Jan. 30, 1969  | Pioneer-9 inferior conjunction or syzygy   |
| Feb. 16, 1969  | Sun pulse lost from Pioneer-7  |
| Aug. 27, 1969  | Pioneer-E launch unsuccessful due to failure of Delta rocket guidance system                             |
| Nov. 28, 1969  | First simultaneous tracking of two spacecraft (Pioneers 6 and 7)   |
| Jan. 20, 1970  | Electromagnetic interference tests of Pioneers 8 and 9 to check effects on cosmic dust experiment        |
| July 26, 1970  | Pioneer-6 magnetometer lost  |
| Oct. 30, 1970  | Simultaneous tracking of Pioneers 6 and 8  |
| Dec. 18, 1970  | Pioneer-9 superior conjunction (behind Sun)  |

\* The TWT is used in the transmitter power amplifier. This was the only serious trouble experienced with this vital component during all Pioneer flights.

## REFERENCES

1. DUGAN, D.W.: A Preliminary Study of a Solar-Probe Mission. NASA TN D-783, April 1961.
2. HALL, C.F.; NOTHWANG, G.J.; and HORNBY, H.: A Feasibility Study of Solar Probes. IAS Paper 62-21, 1962.
3. ANON: Space Technology Laboratories, Final report on the Interplanetary Probe Study. August 15, 1962.
4. ANON: Space Technology Laboratories, A Proposal for an Interplanetary Probe during the International Quiet Sun Year. STL Proposal No. 1536.00. August 1962.
5. ANON: Space Technology Laboratories, Proposal under RFP-A-6669 to Produce the Pioneer Spacecraft for Study of Particles and Fields in Interplanetary Space during the International Quiet Sun Year. STL Proposal No. 1943.00. March 4, 1963.
6. HALL, C.F.; and MICKELWAIT, A.B.: Development and Management of the Interplanetary Pioneer Spacecraft. NASA TM X-60264, 1967. (Also in Proc., 18th International Astron. Congress, vol. 2, M. Lunc, ed., Pergamon Press, Oxford, 1968, pp. 173-187.)



## CHAPTER 2

# Pioneer System Design and Development

### DEFINING THE PIONEER SYSTEM

THE PIONEER SYSTEM was predicated upon the use of the Delta launch vehicle and the Deep Space Network for tracking and data acquisition. The decision to use the Delta meant a spacecraft of modest weight—something just over 100 lb plus 20 to 40 lb of scientific instruments. Financial resources for the entire program were set at between \$50 and \$100 million. The scientific objectives also helped shape the design of the spacecraft. The more important of these follow:

- (1) The ability to point instruments at all azimuths along the plane of the ecliptic
- (2) Continuous data sampling from the instruments
- (3) High data transmission rates back to Earth
- (4) Many commandable modes of operation, enabling experimenters to modify their apparatus from Earth
- (5) A favorable instrument environment, particularly very low residual magnetic fields
- (6) A long life—at least 6 months, possibly longer
- (7) The inclusion of a wide variety of scientific instruments

Within the resources at hand, all of the scientific desiderata could not be realized, but some inspired design innovations increased the scientific payoff well beyond that expected from so small a spacecraft, as we shall see.

The overall Pioneer system consisted of the four systems portrayed in figure 2-1. The scientific instruments are considered a separate system rather than a spacecraft subsystem.

All four systems will be described in more detail later in this chapter. For the moment, let us consider the functions to be performed by the spacecraft. These functions are listed in table 2-1 where they are also assigned to one of the seven spacecraft subsystems. These subsystems are shown schematically in figure 2-2. By understanding how all of the subsystems fit together, one can appreciate better the many engineering tradeoffs that were considered in formulating the concept of the Pioneer spacecraft—a new and unusual

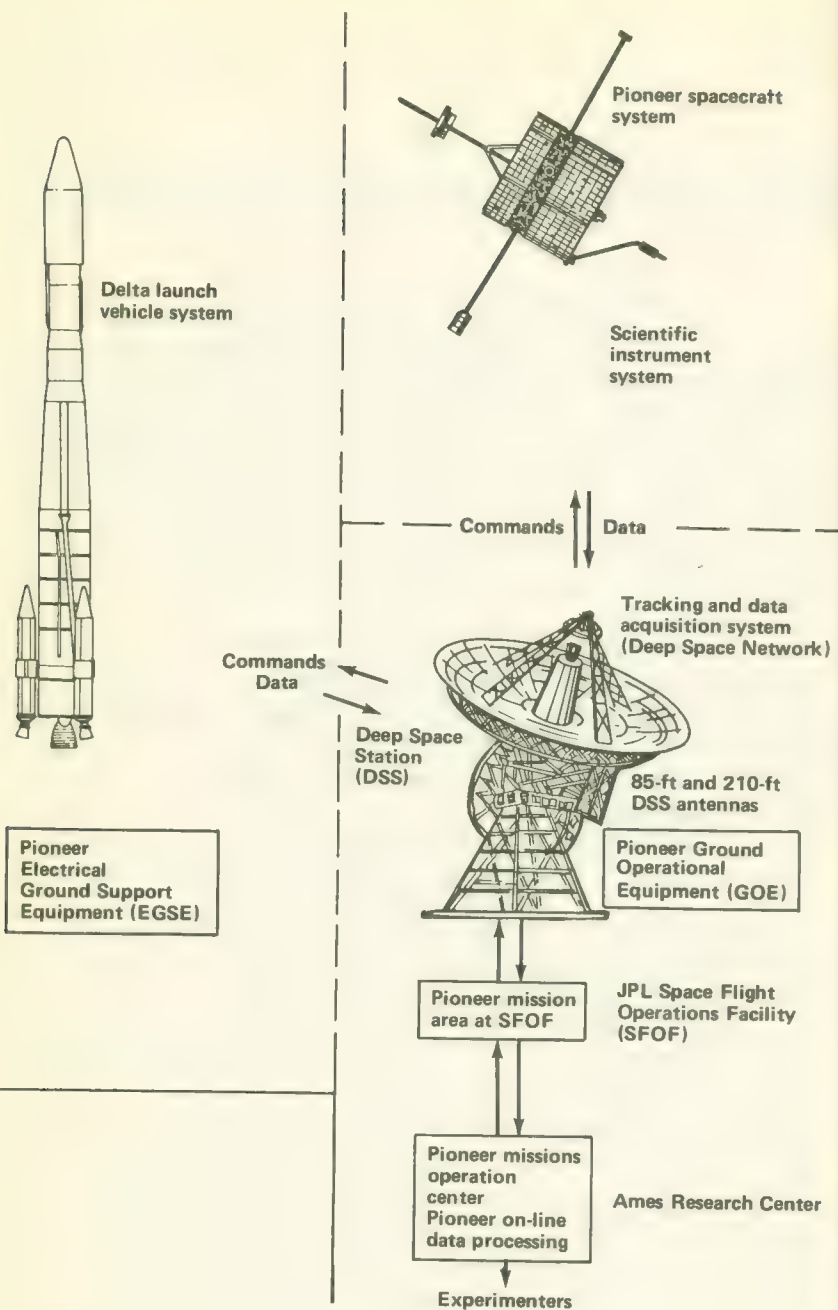


FIGURE 2-1.—The four Pioneer systems.

TABLE 2-1.—*Definition of Pioneer Spacecraft Subsystems*

| Subsystem       | Functions performed  |
|-----------------|--|
| Communication   | Relays scientific and spacecraft status data from the spacecraft to Earth. Receives commands from Earth. Makes possible the two-way Doppler shift measurements required for orbit determination. |
| Data-handling   | Accepts data from scientific and housekeeping instruments and arranges them in proper format for transmission back to Earth. Provides for limited data storage.                                  |
| Electric-power  | Provides electrical power to all spacecraft subsystems and the scientific instrument system.   |
| Orientation     | Orients the spacecraft spin axis as required; damps out wobble. Attitude sensors and gas jets are included within this subsystem.  |
| Thermal-control | Maintains temperatures within specified ranges within the spacecraft.  |
| Command         | Decodes commands received via the communication subsystem; distributes commands to the spacecraft subsystems specified in the command addresses.   |
| Structure       | Supports and maintains spacecraft configuration under design loads. Provides booms for instrument isolation.   |

concept that strongly affected the spacecraft's interfaces with the Deep Space Network and the scientific instruments.

Restricted weight and the simplicity necessary for high reliability dictated a spin-stabilized spacecraft. However, random spin stabilization entailed three problems:

(1) A high-gain transmitter antenna was needed on the spacecraft if it was going to telemeter data to the Earth across the wide expanse of the solar system. Yet a high-gain, highly directional antenna could not be aimed at the Earth from a spinning spacecraft without unacceptably complicated control equipment.

(2) The scientists preferred to have their instruments scan the plane of the ecliptic, not any of the infinity of other planes possible with a randomly oriented spinning spacecraft.

(3) If the spin vector of the spacecraft were random, solar cells would have to be mounted on all sides of the spacecraft, increasing the weight.

These thoughts led to the concept of an *orientable*, spin-stabilized spacecraft with a spin axis that could be torqued by a simple gas jet until it was aligned perpendicular to the plane of the ecliptic. The laws of motion predicted that such torquing would cause wobbling, but this could be largely eliminated by a simple wobble damper. If the spacecraft is spin stabilized with its equator in the

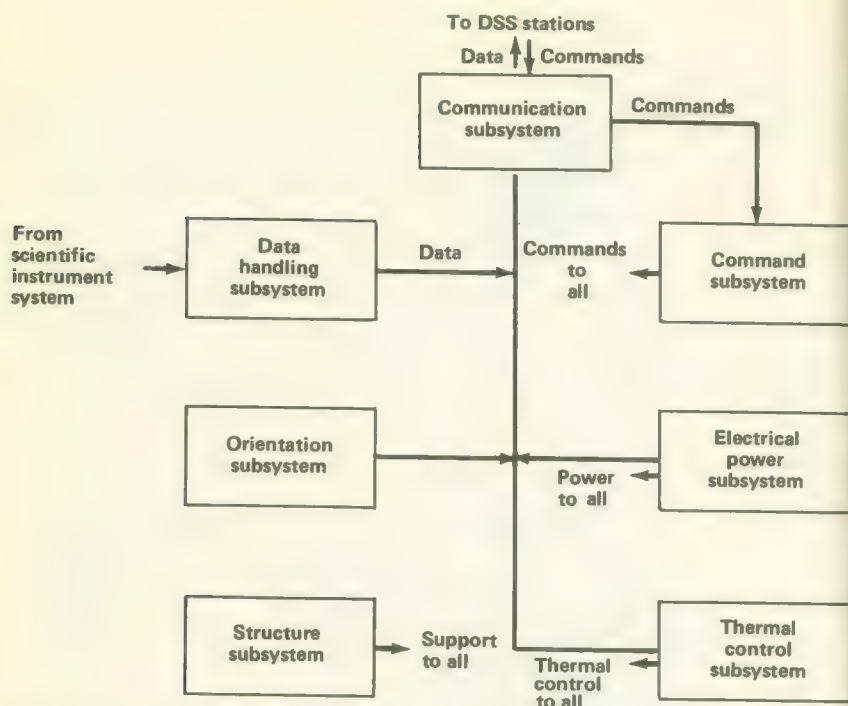


FIGURE 2-2.—Generalized block diagram showing Pioneer spacecraft subsystems. Magnetic, thermal, and other forces crossing subsystem interfaces are not shown.

plane of the ecliptic at all times, two of the three problems mentioned above could be solved easily. The scientific instruments could be mounted on an instrument platform perpendicular to the spin vector, and they could then scan the plane of the ecliptic as the spacecraft rotated. By making the spacecraft a right circular cylinder, solar cells need be mounted only on the curved sides because the Sun is in the plane of the ecliptic.

Only the antenna problem would remain. The capstone of the Pioneer concept is the use of a mastlike antenna (a modified Franklin array) mounted along the spin axis (fig. 2-3). This kind of antenna concentrates the radiated energy into a flat disk which, because of the unique spacecraft orientation, would lie in the plane of the ecliptic and thus be received by DSN antennas on Earth.

In fact, given the original weight constraints (imposed by the Delta and the mission), the Pioneer Project would not have been feasible without this novel concept; i.e., an orientable, spin-stabilized, cylindrical spacecraft with a disk-shaped antenna beam.



FIGURE 2-3.—View of the Pioneer spacecraft showing the three radial booms deployed, the telemetry antenna mast (top), and the Stanford radio propagation experiment antenna (bottom).

#### PIONEER LAUNCH TRAJECTORY AND SOLAR ORBIT DESIGN

The original plan for the Pioneer Program involved sending small spacecraft into orbits about the Sun where they could monitor solar events in interplanetary space without the perturbations of the Earth's magnetosphere and atmosphere. Trajectory analysis soon

showed that the scientific productivity of the flights could be enhanced greatly by shaping the launch trajectories and heliocentric orbits to:

- (1) Improve solar system coverage in the radial direction
- (2) "Create" astronomical phenomena, such as solar occultations,
- (3) Study Earth-induced space phenomena, such as the geomagnetic tail

The Pioneer flights were designed with these objectives in mind. Pioneers 6 and 9 followed an inward trajectory, perihelion near 0.8 AU, in order to extend solar system coverage by Pioneer instruments into the sector ahead of the Earth as it plies its orbit about the Sun. Solar occultation of the spacecraft as seen by the tracking antennas on Earth was also planned for these two flights.

Pioneers 7 and 8 followed an outward trajectory, aphelion near 1.1 AU, in order to extend solar system coverage in the Earth's "wake." A lagging spacecraft actually detects solar events before terrestrial instruments because the outwardly spiraling solar magnetic lines of force sweep around the solar system faster than the planets due to the Sun's 28-day rotation.

Since the trajectory of an outward-bound Pioneer can be designed to swing through the Earth's magnetic tail, plans for geomagnetospheric tail analysis were included for Pioneers 7 and 8.

On both inward- and outward-bound missions, scientists have a "sporting chance" to see an occultation of the Earth by the Moon through the "eyes" of the Pioneer instruments. Intrinsic launch vehicle inaccuracies precluded any guarantee, however. The first attempt at lunar occultation analysis was made with Pioneer 7.

Pioneer E was to follow an inward-outward combination trajectory, with final near-Earth (1.0 AU) heliocentric orbit. The objective was to have the spacecraft linger in the vicinity of the Earth, allowing the use of high-bit-rate telemetry over a period of several hundred days. The design of Pioneer E also included plans for geomagnetospheric tail analysis similar to Pioneer 7.

The trajectory designer had to program the Delta vehicle in such a way as to attain the proper heliocentric orbit and accomplish other scientific objectives, such as lunar occultation, as the spacecraft left the Earth's vicinity.

The Delta launch vehicles carrying Pioneer payloads were all launched southeastward from Cape Kennedy along the Eastern Test Range. During the flight, the Deltas passed over Ascension Island in the South Atlantic and NASA tracking stations in the vicinity of Johannesburg, Republic of South Africa (fig. 2-4). Approximately 500 sec after liftoff, the second-stage engines cut off (fig. 2-5). The Delta second and third stages, the Pioneer spacecraft, and any Test

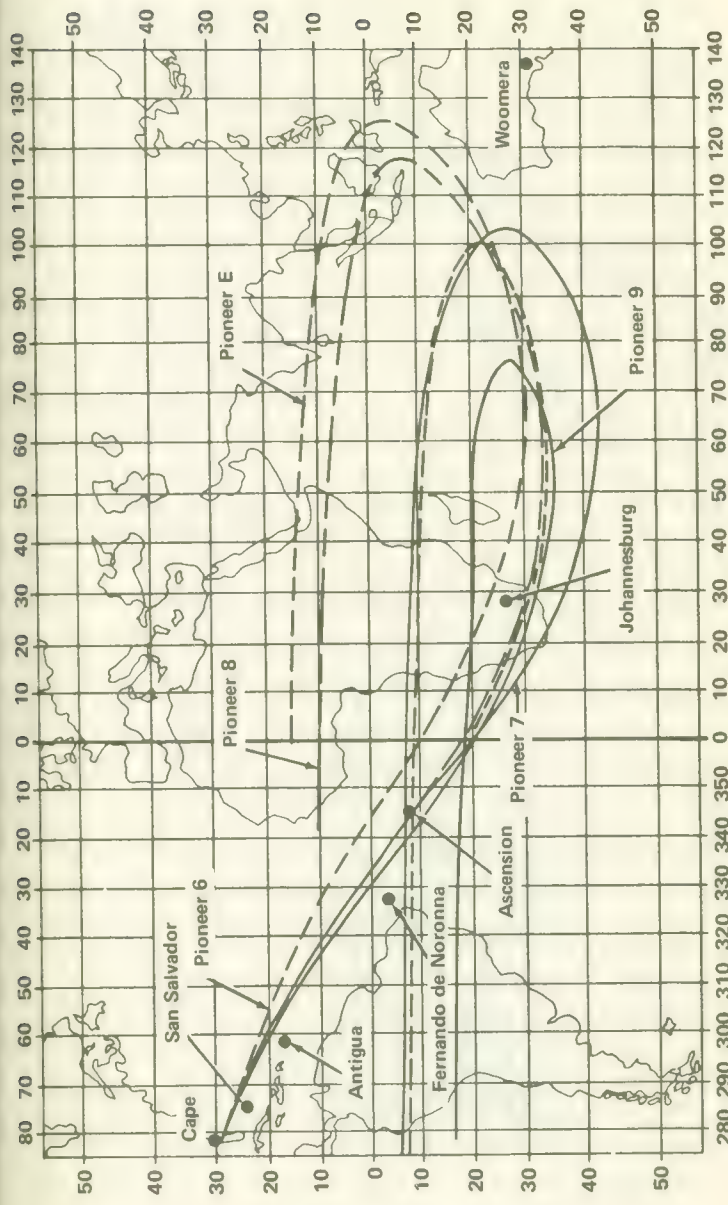


**FIGURE 2-4.**—Ground tracks of the four successful Pioneers plus the projected track of Pioneer E.

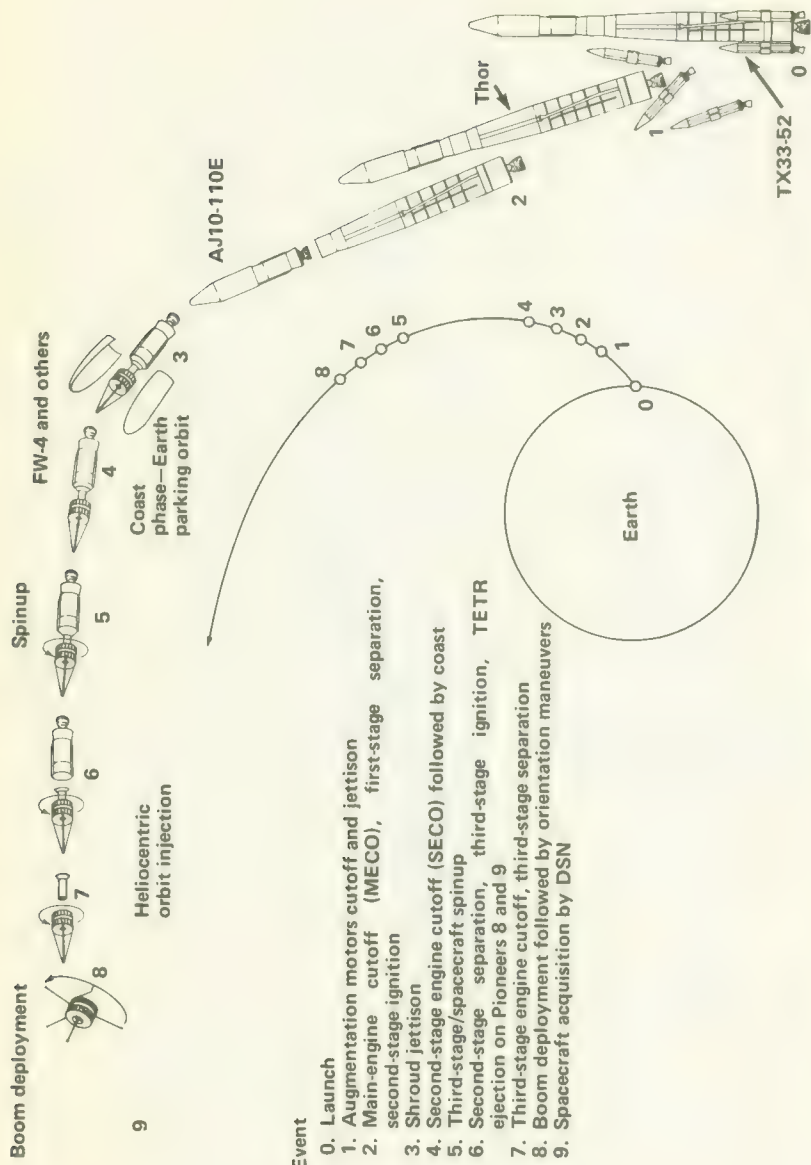


FIGURE 2-5.—The Pioneer launch sequence.

and Training Satellite (TTS) piggyback spacecraft are then in Earth orbit over Johannesburg.<sup>8</sup> This coast phase is essential if the spacecraft is to be launched properly into an orbital plane nearly parallel to that of the ecliptic. At a point before the spacecraft and attached Delta upper stages reach the plane of the ecliptic, the small rockets on the spin table on the Delta second stage fire, imparting a spin to the spacecraft and Delta third stage. Next, the Delta third stage fires at that precalculated point in the coast trajectory where the velocity added by the third stage will carry the spacecraft into an escape hyperbola and thence into orbit around the Sun. Only after third-stage ignition is the second-priority TTS injected into Earth orbit. The inward Pioneers (6 and 9) were injected with velocity vectors approximately opposite to the Earth's velocity. Thus slowed, they "fell" in toward the Sun and initially fell behind or lagged the Earth. The inward Pioneers essentially converted gravitational energy into orbital velocity and, after about 75 days, caught up with the Earth and led it by ever-increasing distances in its journey around the Sun. The outward Pioneers (7 and 8) were injected with velocities parallel to that of the Earth; they initially led the Earth but after 30 to 40 days they fell behind and, like the outer planets, lagged the Earth.

To achieve solar orbits that were very nearly in the plane of the ecliptic, Pioneer launches were ideally made during launch windows a few minutes wide that occur only once a day. The Pioneer Project Office at Ames Research Center required that launch windows be greater than 8 min, however, so that short holds would not scrub a mission for a whole day.

Several kinds of charts are employed to show how the Pioneers move in various coordinate systems once they are in heliocentric orbit. Only two of these plots are of general interest:

(1) the Sun-centered, vernal-equinox ecliptic reference (fig. 2-6), which shows how inward Pioneers draw farther and farther ahead of the Earth as both swing around the Sun; and

(2) the "snapshots" of the four successfully launched Pioneers (fig. 2-7) taken at four different times looking down on the plane of the ecliptic from the north ecliptic pole. The latter illustration has a physical meaning for those attempting to forecast solar weather. The Sun's spiral magnetic field, which rotates with the Sun, rotates much faster than the Pioneers and the Earth do in their heliocentric orbits. Therefore, the streams of plasma that propagate along the Sun's magnetic lines of force are always sweeping past the Pioneers and the Earth, spraying them with plasma like a rotary water

<sup>8</sup>The TTSs were used to give tracking stations practice prior to Apollo flights.

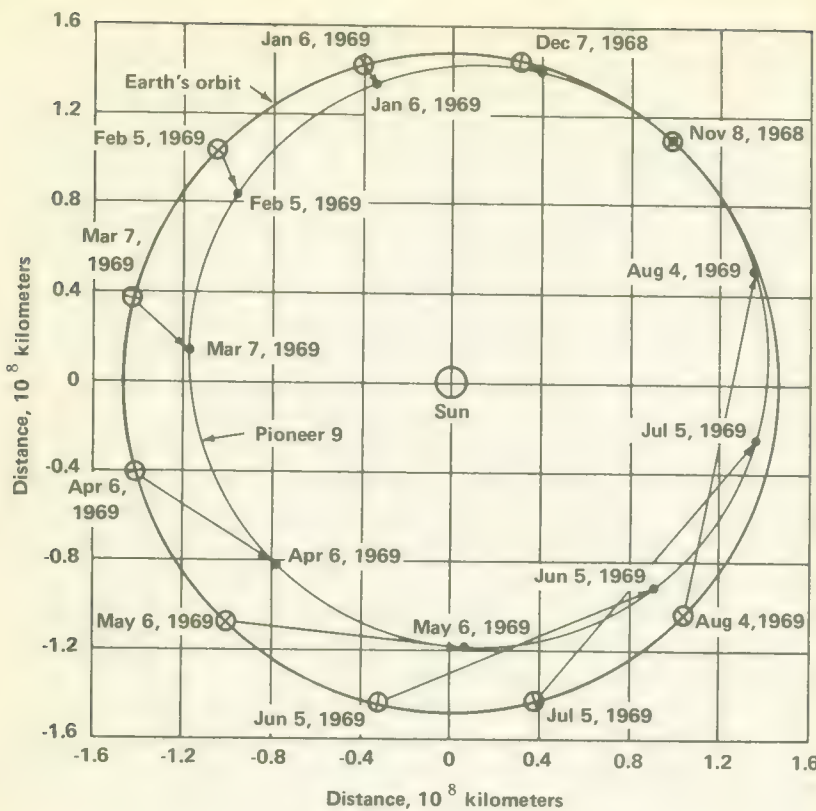


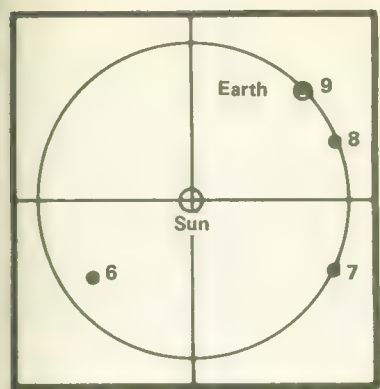
FIGURE 2-6.—Actual heliocentric orbit for Pioneer 9 using vernal equinox reference.

sprinkler. The Pioneers lagging the Earth are thus in good positions to forecast solar-related events for Earth.

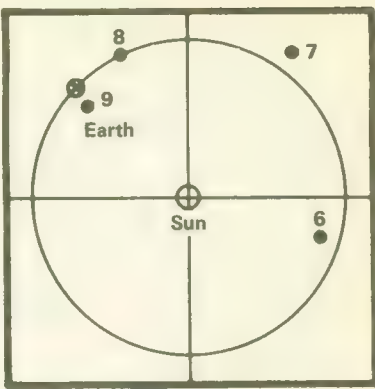
Finally, table 2-2 summarizes Pioneer trajectory and orbital data as of March 1969.

#### SPACECRAFT DESIGN APPROACH AND EVOLUTION

In addition to the constraints imposed by the selection of the Delta launch vehicle and the DSN, it was also stipulated that the spacecraft be state-of-the-art; i.e., no untried equipment was to be employed because it might affect the success and long-term reliability of the spacecraft. Two important exceptions were allowed. The TWTs, though unproven in deep-space use in 1962, had no acceptable alternatives. The convolutional coders used on Pioneers 9 and E were also new, but they were installed on an experimental basis



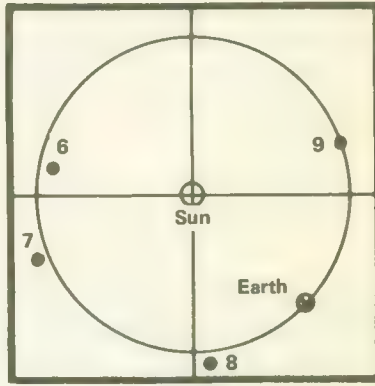
Nov 8, 1968



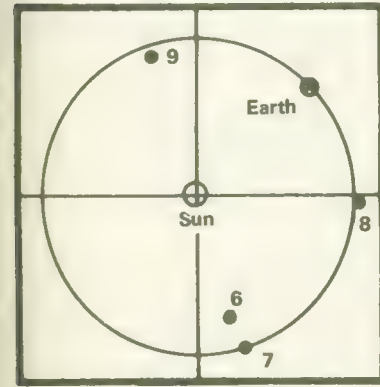
Feb 6, 1969



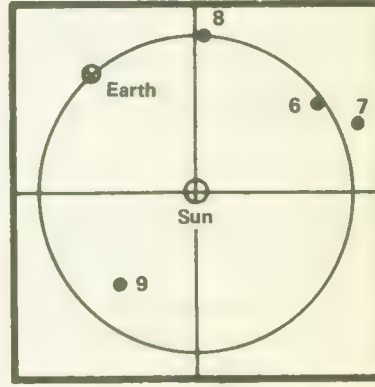
May 7, 1969



Aug 5, 1969



Nov 3, 1969



Feb 1, 1970

FIGURE 2-7.—Relative positions of the four successful Pioneers with respect to the Earth at various times.

TABLE 2-2.—*Pioneer Orbital Parameters*

| Parameters                             | 6           | 7           | 8           | 9           |
|--|-------------|-------------|-------------|-------------|
| <b>Orbital Injection Conditions</b>    |             |             |             |             |
| Date of injection                      | 12-16-65    | 8-17-66     | 12-13-67    | 11-8-68     |
| Time of injection<br>(GMT)             | 0756:41.1   | 1545:38.6   | 1439:32.5   | 1007:22.4   |
| Injection latitude                     | 7.8° S      | 14.48° S    | 22.83° S    | 3.36° S     |
| Injection longitude                    | 4.6° W      | 6.8° W      | 9.385° E    | 23.26° W    |
| Injection altitude (km)                | 564.1       | 378.476     | 486.02      | 467.054     |
| Injection velocity<br>(km/sec)         | 10.8488     | 10.939      | 10.7837     | 11.035674   |
| Flight path angle (deg)                | 1.7         | 2.1         | -0.364      | 2.413724    |
| Azimuth angle (deg)                    | 119.3       | 106.98      | 129.374     | 101.04027   |
| <b>Elements of Heliocentric Orbits</b> |             |             |             |             |
| Semimajor axis (km)                    | 134 481 910 | 159 713 300 | 155 372 610 | 130 500 710 |
| Eccentricity                           | 0.0942      | 0.05397     | 0.0476      | 0.1354      |
| Inclination to ecliptic<br>plane       | 0.1693      | 0.09767     | 0.0578      | 0.0865      |
| Aphelion (AU)                          | 0.936       | 1.1250      | 1.0880      | 0.9905      |
| Perihelion (AU)                        | 0.8143      | 1.0100      | 0.9892      | 0.7542      |
| Period (days)                          | 311.327     | 402.91      | 386.60      | 297.594     |

and could be bypassed if necessary. Although the TWTs did perform well, they caused much concern early in the program.

Given the mission objectives and the constraints enforced by the mission and the state-of-the-art, a design philosophy evolved to guide the hardware designers. The most important element of the Pioneer design philosophy was the desire for long spacecraft life and magnetic cleanliness. To meet the reliability goals, the following guidelines were set down:

- (1) Provide failure modes of operation wherever possible
- (2) Use only proven components (in practice, many components came from military space programs) except for the TWTs
- (3) Qualify parts rigorously
- (4) "Burn-in" components before use on spacecraft

Magnetic cleanliness was achieved by enforcing magnetic guidelines that permitted the use of only certain parts and specified certain construction practices. As a result the Pioneers have been the cleanest spacecraft—magnetically speaking—that the United States has built. The Pioneers have also been the longest lived spacecraft ever built. Both facts are a tribute to the design philosophy employed during the Pioneer Program and, of course, the capabilities of the engineers who designed and built the craft.

The major elements of the spacecraft design were sketched out in the STL feasibility contract. After the formal Pioneer contract was awarded, a more detailed design was made. A few minor features were changed in this process, as indicated in table 2-3.

The experiment complement was changed between the Block-I Pioneers (6 and 7) and the Block-II Pioneers (8, 9, and E). This change engendered a few more changes, noted in table 2-3. Overall spacecraft weight increased by more than 10 lb from Pioneer 6 to Pioneer E. This was permissible because the Delta was also improved as the Program progressed.

## THE SPACECRAFT SUBSYSTEMS

The seven Pioneer spacecraft subsystems are defined by their various functions (table 1-1). It is now appropriate to replace the very generalized subsystem block diagram in figure 2-2 by one that employs Pioneer terminology and indicates some of the major components in the subsystems (fig. 2-8).

### The Communication Subsystem

The basic problems in long-distance communication are distance and natural radio noise from the Sun and the rest of the galaxy. The following factors have given the relatively small Pioneer spacecraft the ability to telemeter data to and receive commands from the Earth over distances of nearly 200 million miles despite natural radio noise:

- (1) A relatively high transmitter power level (8 W) for such a small spacecraft
- (2) The focusing of radio energy into a flat disk-shaped beam by the Franklin-array antenna
- (3) The use of very low bit rates (8 bps) at great distances, reducing the bandwidth required as well as power
- (4) The very sensitive "ears" of the DSN—the 85-ft and 210-ft paraboloidal antennas (During the Pioneer Program, the DSN improved its signal detection capability by about 10 dB, mainly through the addition of the 210-ft antenna shown in figure 2-9.)

The major components of the communication subsystem are one high-gain and two low-gain antennas, two receivers, a transmitter-driver, two TWT power amplifiers, and five coaxial switches that can be activated by command from Earth to switch in redundant components should failures occur (fig. 2-8). Telemetry, commands, and tracking information are all handled by the communication

TABLE 2-3.—*Evolution of the Pioneer Spacecraft*

| Pioneer spacecraft | Point in time    | Weight   | Changes   |
|--------------------|------------------|--|---|
| 6                  | ComPLETED design | Spacecraft<br>Experiments<br><hr/> 102.7 lb<br>34.3<br><hr/> 137.0 lb    | (from first version A-6669)<br>Ames micrometeoroid experiment deleted<br>Stanford radio propagation experiment antenna added<br>Solar sail added to antenna mast<br>Three booms now located on spacecraft viewing band<br>Solar cells removed from viewing band<br>Thermal insulation added to protect spacecraft from X-258 exhaust plume<br>Magnetometer moved from antenna mast to radial boom |
| 7                  | ComPLETED design | Spacecraft<br>Experiments<br><hr/> 103.26 lb<br>35.09<br><hr/> 138.35 lb | (from Pioneer 6)<br>Magnetometer range reduced to $\pm 32\gamma$<br>Energy windows and angular resolution of cosmic-ray experiment changed  |
| 8                  | ComPLETED design | Spacecraft<br>Experiments<br><hr/> 106.1 lb<br>38.0<br><hr/> 144.1 lb    | (from Pioneer 7)<br>Block-II experiments substituted<br>Telemetry format altered<br>Larger battery added for experiments  |
| 9                  | ComPLETED design | Spacecraft<br>Experiments<br><hr/> 107.13 lb<br>41.27<br><hr/> 148.40 lb | (from Pioneer 8)<br>Ames magnetometer substituted for Goddard magnetometer<br>Convolutional coder experiment added<br>Texas Instruments solar cells substituted for RCA cells<br>Thick glass covers placed on Sun sensors   |
| E                  | ComPLETED design | Spacecraft<br>Experiments<br><hr/> 106.54 lb<br>41.06<br><hr/> 147.60 lb | (from Pioneer 9)<br>Ultraviolet filters substituted for thick glass covers on Sun sensors   |

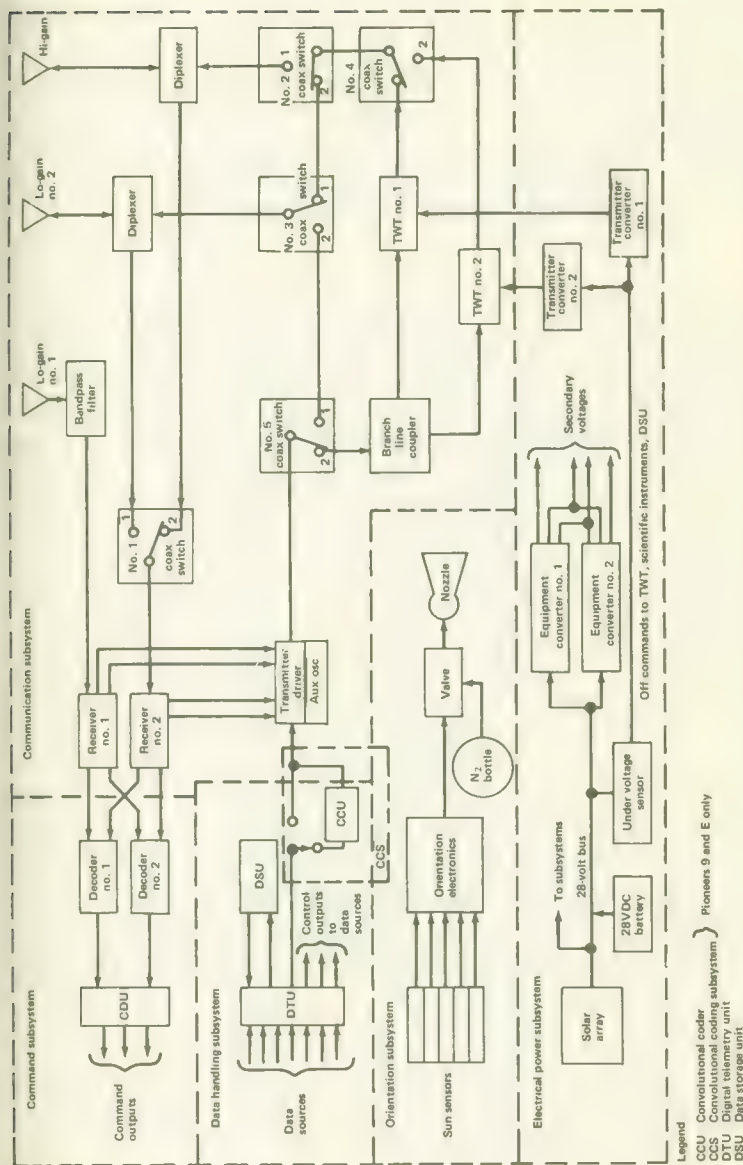


FIGURE 2-8.—Simplified block diagram showing the Pioneer spacecraft subsystems.

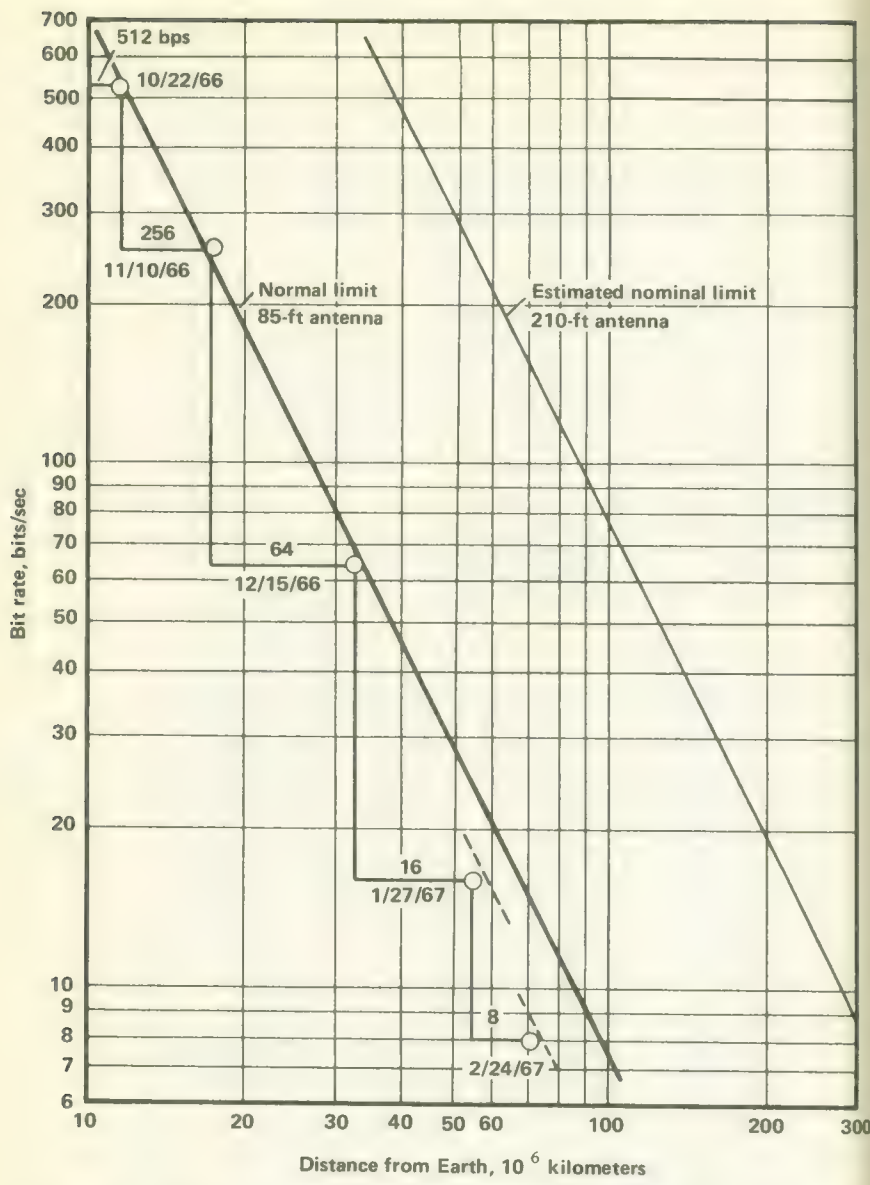


FIGURE 2-9.—Distance limitations for Pioneer 7, showing dates when telemetry bit rate was changed. Note the improved performance with the 210-ft antenna.

subsystem. The communication subsystem utilizes the phase-lock loop concept developed at JPL for deep-space and planetary probes.

To understand phase-lock loop operation, picture a Pioneer spacecraft 100 million miles or so ahead of the Earth in its orbit about

the Sun. Assume first that the terrestrial DSN antennas are busy with some other spacecraft. In this situation, both spacecraft receivers are waiting, as it were, for further instructions from Earth. The transmitter, however, still transmits any scientific and housekeeping information it receives from the data-handling subsystem even though no terrestrial antenna intercepts it. Thus, even if both spacecraft receivers should fail, DSN antennas can still acquire the spacecraft and record whatever data it transmits. During these periods when the spacecraft is "on its own," the spacecraft transmitter frequency is controlled by an internal crystal-controlled oscillator. This mode is called the *noncoherent* mode of operation. One-way Doppler tracking of limited accuracy can be accomplished by merely listening to the spacecraft.

Next, suppose that a DSN antenna is swung around to point in the direction where orbital computations predict the spacecraft will be. DSN receivers pick up the weak telemetry signal and lock onto it. Lock is attained by means of a feedback loop involving a narrow bandpass filter and a voltage-controlled oscillator. A down-link lock exists when the voltage-controlled oscillator generates a signal at precisely the carrier frequency received from the spacecraft but with a 90° phase change. The feedback circuit in essence operates as a servomechanism to force the oscillator to match the spacecraft carrier frequency. Once a down-link lock has been established, the ground transmitter sends its own carrier in the direction of the spacecraft. Since the two spacecraft receivers are tuned to operate at different frequencies, the ground transmitter can select either one by using the proper carrier frequency. The presence of a signal in the spacecraft receiver automatically disconnects the spacecraft crystal-controlled oscillator and switches in a voltage-controlled oscillator that generates a frequency precisely 12/221 times that received from the DSN. This frequency is then multiplied by 20 in the transmitter driver. A phase-coherent transmitter signal with a frequency 240/221 times the frequency received from Earth is amplified in the operational TWT and dispatched to Earth via the high-gain antenna. The waiting DSN antenna locks onto this signal, which may be slightly different from that originally acquired because the spacecraft's crystal-controlled oscillator may have drifted slightly. Only when the spacecraft and Deep Space Instrumentation Facility receivers are *both* locked on the signals received from Earth and spacecraft, respectively, can coherent, much more accurate, two-way tracking measurements be made. This coherent mode can be disabled on command, so that the transmitted frequency is always governed by the crystal-controlled oscillator.

The two tasks of the small, lightweight spacecraft receiver were:

(1) to detect, demodulate, and amplify the commands received from the DSN station working the spacecraft; and (2) to provide the transmitter-driver with a phase-coherent signal  $12/221$  times the frequency of the received DSN carrier. When an external signal is received from a DSN station, a threshold detector in the receiver disables the on-board, crystal-controlled, noncoherent oscillator when in the coherent mode. The coherent receiver then generates the phase-coherent signal which ultimately drives the TWT when in the coherent mode. The Pioneer receiver components were of the discrete-circuit type rather than the newer integrated circuits, that were not proven sufficiently for the Pioneer designers in 1962.

The transmitter driver consists of a transistorized amplifier-modulator and a varactor multiplier. The driver provides either the non-coherent signal from its crystal-controlled oscillator or a phase-coherent signal that is  $240/221$  times the DSN carrier frequency. The amplified signal of approximately 50 mW is fed to the power amplifier stage, which is built around the TWT.

Three antennas serve the communication subsystem. Two are low-gain, multislots types with broad beam widths. One of these is permanently connected to one of the receivers to guarantee that the spacecraft will always be able to receive commands regardless of the operability of the coax switches. The low-gain antennas are essential during spacecraft acquisition before the initial orientation maneuvers when the high-gain antenna is being torqued into a position perpendicular to the plane of the ecliptic. The high-gain antenna is a collinear broadside array (a modified Franklin array) consisting of nine driven and nine parasitic elements.

### The Data Handling Subsystem

The end product of most spacecraft—the Pioneers included—is information. Data flows not only between Earth and spacecraft but also among the various spacecraft subsystems. In the guises of telemetry, commands, and control signals, information is ubiquitous onboard a spacecraft. The data handling subsystem acts as a central clearinghouse where data are received, formatted, processed, stored, and sent back to Earth or to other Pioneer subsystems.

More formally, the functions of the data handling subsystem are:

- (1) The sampling and encoding of analog and digital measurements taken by the scientific instruments (In special cases, the encoding is done by the scientific instrument.)
- (2) The sampling and encoding of spacecraft engineering or "housekeeping" measurements

(3) The storage, upon command, of data when DSN stations are not available to acquire spacecraft data

(4) The storage, upon command, of special data formats when the spacecraft is communicating with the DSN

(5) The changing, upon command, of data bit rate and/or format as the spacecraft recedes and approaches Earth. (Bit rates available are 8, 16, 64, 256, and 512 bps.)

(6) The provision of sundry clock and control signals throughout the spacecraft (Clock signals, in effect, force spacecraft experiments and subsystems to work together in synchronism.)

Two elements make up the data handling subsystems: the digital telemetry unit (DTU) (really the data processor) and the data storage unit (DSU) (fig. 2-10). On Pioneers 9 and E, a third unit was added on an experimental basis, a convolutional coder unit (CCU), which could be switched in-line from a standby status or vice versa.

When the Pioneer Program was being formulated in 1962, there existed a trend toward pulse code modulation (PCM) for space telemetry. The Mariner space probes, NASA's observatory series of satellites, and both the Gemini and Apollo programs had adopted PCM. PCM has many advantages, such as unlimited accuracy (in principle), the existence of self-checking and error-correcting codes, and instant compatibility with computers. Because the Pioneers were going to interface with the DSN, with its already strong bias toward digital techniques, it was logical to follow the PCM trend.

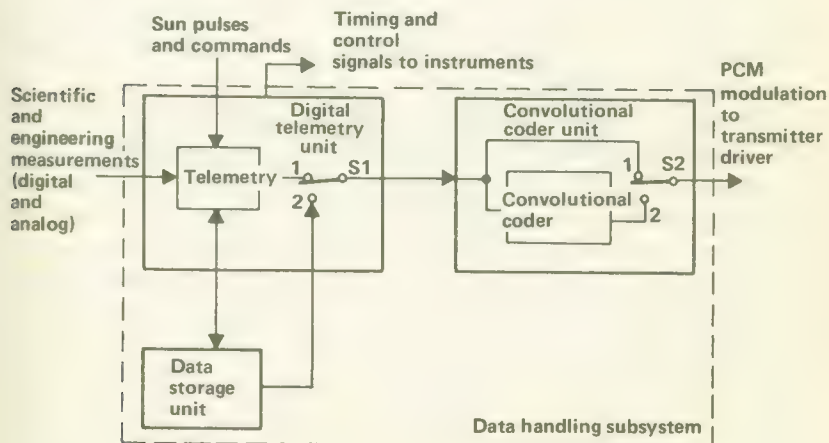


FIGURE 2-10.—Block diagram of the data handling subsystem.

The bits that constitute each PCM telemetry word can be communicated by any one of several two-valued properties of a modulated radio signal. Following JPL practice, Pioneer PCM bits are impressed upon the transmitter carrier by phase-modulating the 2048-Hz square wave subcarrier. More technically, the subcarrier is biphase modulated by a time-multiplexed train of bits, using a non-return-to-zero-mark (NRZ-M) format, and this subcarrier is used to phase-modulate the carrier.<sup>9</sup>

The basic unit of information in a telemetry message from a Pioneer spacecraft is a seven-bit word. The first six bits represent the instrument reading or datum, with the most significant bit appearing first. The last, or seventh, bit is a parity bit based upon the first, third, and fifth bits in the preceding word. If the sum of these bits is even, the parity bit will be odd; i.e., one.

The parity bit represents a self-checking feature of the code. Words containing errors introduced during transmission and the many processing steps along the way can be identified and flagged in most instances by recomputing and checking the parity bit for the word that finally arrives at its terrestrial destination. The parity bit, as used in Pioneer telemetry, was worth roughly 2 dB, in the sense that transmitted messages could be edited and made more accurate.

Just as bits are organized into words, the words themselves are ordered into "frames" consisting of 32 words each. The frames keep repeating one after the other, but the arrangement of words can be modified by command. This separation of words by interspersing them in the time dimension is called time-division multiplexing. In effect, each scientific and engineering instrument gets read periodically and the data are strung together in the 32-word frames. The flexibility of the formats represents one of the strong points of the Pioneer system design.

There are four basic Pioneer telemetry formats. The formats themselves are too long and overly complex to describe in detail here. They can be found in Volume II, Chapter 4. Formats A and B are primarily for scientific data. Format C consists mainly of engineering data and is employed during orientation maneuvers and when the spacecraft is in trouble. Format D consists of data from the Stanford radio propagation experiment only and is switched on during lunar occultations and other special events.

During the launch and reorientation maneuver, the spacecraft normally transmitted Format C. While the spacecraft was still near

<sup>9</sup>On Pioneers 9 and E, the non-return-to-zero-level (NRZ-L) format was introduced.

enough to the Earth to support a high bit rate, Format A was usually employed. As the spacecraft receded from Earth, forcing the use of lower bit rates, Format B was adopted. If the trajectory of a Pioneer should be favorable for lunar occultation, a command from Earth will switch to Format D. Out in the relatively calm reaches of deep space, the spacecraft transmits Format B most of the time.

Although variable bit rate and telemetry format confer considerable flexibility, provision is needed for storing and thus delaying data transmission back to Earth. Suppose, for example, that an important solar event occurs and one or more of the Pioneers are too far away to telemeter plasma-probe data rapidly enough to catch the details of the fast-breaking action. With onboard data storage, data could be recorded at a high rate during the event and then retransmitted later at a bit rate compatible with the spacecraft's transmitter power and distance from the Earth.

Based on the above illustration, three of the four Pioneer telemetry modes are easy to justify: (1) real-time operation, (2) telemetry store, and (3) memory read-out. The fourth mode, the duty-cycle store mode, simply stores data in the memory periodically, in short bursts a frame at a time, when the spacecraft is not being worked by a DSN station. Any of the four modes can be started with a specific command from Earth.

The digital telemetry unit is not only the central clearinghouse for all spacecraft-generated data, it is also the spacecraft coxswain that keeps all spacecraft components operating in step. To do this and impose order upon the variegated data requires a rather complex array of logic circuits, counters, and A/D converters (fig. 2-11).

The coxswain function is performed by a crystal-controlled-oscillator clock producing a 16 384-Hz output signal. This signal is then divided by 32, 64, 256, 1024, and 2048 to establish the five standard bit rates. Armed with timing signals, the multiplexers and sub-multiplexers sample the various analog and digital outputs of the scientific and engineering instruments. All instruments are usually on all the time, and the only stimulus needed to make them provide a reading is an electronic "gate." (An exception is the Stanford radio propagation experiment which is usually turned off at great ranges.) The multiplexers simply open and close gates leading to the instruments in the order specified by the last command from Earth. Electronic switches or gates are the mainstays of computers and other logic circuits. It is the spacecraft clock, of course, that ultimately drives all subsystem circuits.

The solid-state memory of the DSU is not large by terrestrial standards—only 15 232 bits—but this is sufficient for Pioneer's pur-

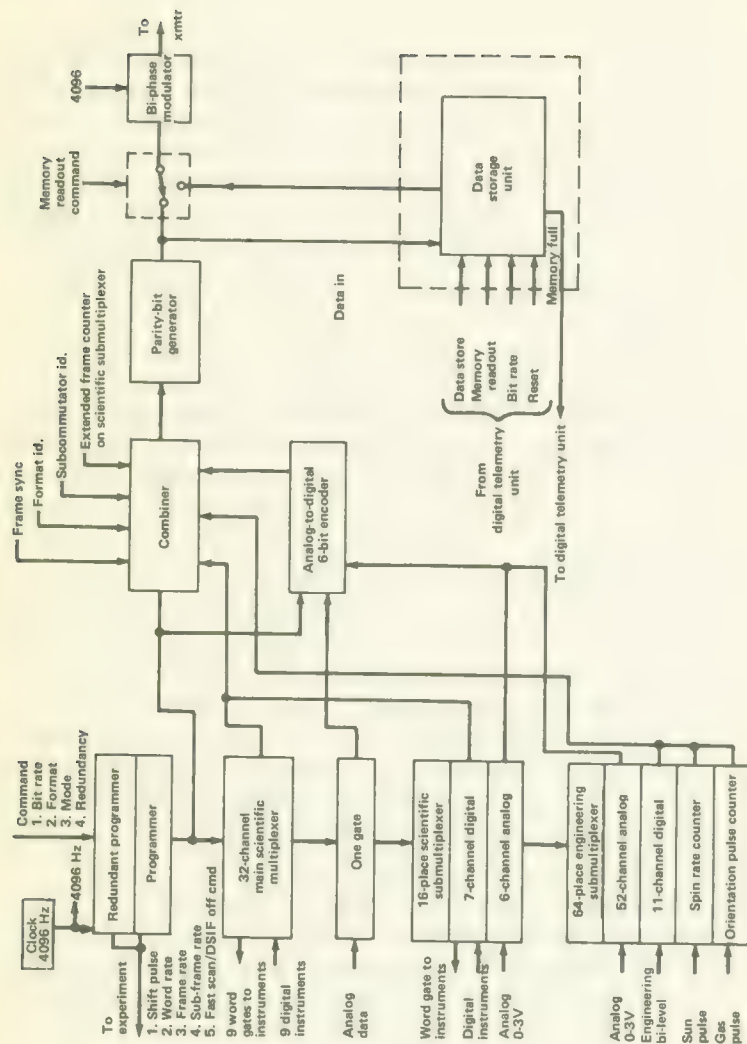


FIGURE 2-11.—Simplified block diagram of the digital telemetry unit (DTU).

poses in view of the very low data rates possible for transmission back to Earth. It takes more than half an hour to read out a 15 232 bit memory at 8 bps.

### The Command Subsystem

None of the flexibility and reliability gained through alternate modes of operation and redundancy can be realized without switches commandable from the Earth. To substitute a new TWT for one that falters or to change the bit rate, the mission controller dispatches a command to the spacecraft directing a specific switch to open or close. All told, the Pioneers employ between 57 and 67 commands (each spacecraft was slightly different) to activate the same numbers of spacecraft switches. About two-thirds of the commands pertain to spacecraft functions and the rest to experiments.

Let us say that the mission controller at Ames Research Center wishes to change Pioneer 6's bit rate from 16 bps to 8 bps because the spacecraft is too far from Earth for the higher bit rate to be received without an excessive error rate. He constructs a 23-bit command word that is sent through JPL along NASA's global communication system (NASCOM) lines to the DSN station working Pioneer 6. The command is modulated onto the up-link carrier in what is called frequency-shift keying (FSK). If a digital one is to be sent, a 240-Hz tone is phase-modulated (PM) on the DSN carrier. A 150-Hz tone represents a digital zero. The bit stream representing the command is thus a series of 23 beeps (in two pitches) on the DSN carrier.

The Pioneer command is much longer than the standard telemetry word—23 versus 7 bits. If merely the command number were sent, seven bits would be sufficient. Pioneer 9, which used the most commands (67), just barely needed seven bits. As figure 2-12 indicates, the basic Pioneer command number was actually seven bits long. Preceding the seven-bit segment, however, was a seven-bit complement of the command, in which the ones in the command number were replaced by zeros and vice versa. It is common space-craft practice to promote high command accuracy by sending considerable redundant information. The consequences of a garbled command are too serious to settle for simple parity checks. While the 23-bit command is in the decoder register, it is compared bit by bit with its complement. Complete correspondence is required before the command is released for execution. Incomplete or distorted commands are not executed.

Command tones are modulated on the DSN carrier at the rate of only 1 bps. Including the time required for processing the com-

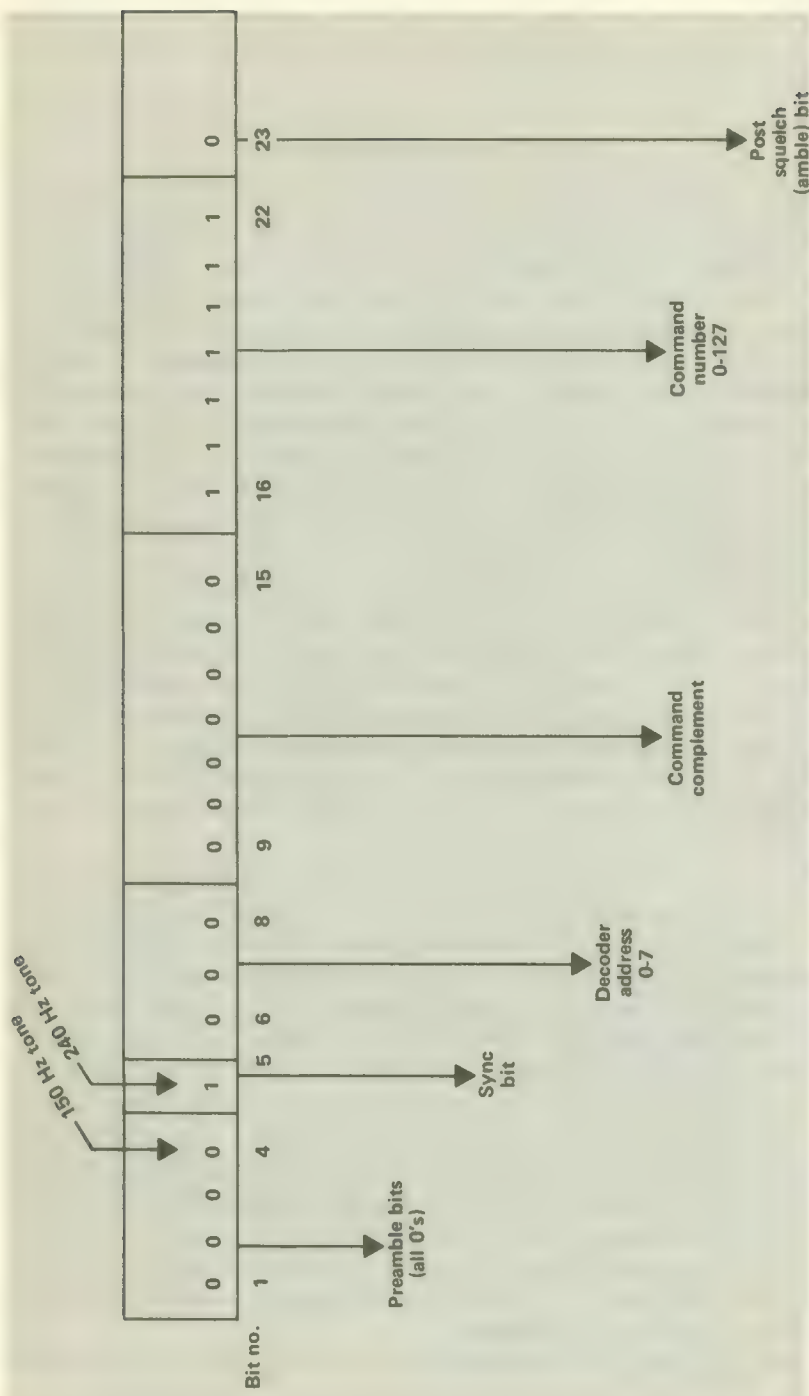


FIGURE 2-12.—Structure of the Pioneer command word.

mand in the decoder and executing it, it takes 27 sec to receive and execute a command aboard the spacecraft. Also, the Pioneers are often several light minutes away from Earth and are therefore out of touch to some degree, regardless of the low command rate.

The assigned task of the command decoder is the delivery of a verified bit train to the command distribution unit (CDU). Four different kinds of signals flow out of the CDU, each tailored for triggering a specific action—the end result of the command transmitted from Earth:

(1) Most command pulses are short ( $10 \mu\text{sec}$ ), low current (about 10 mA), at 10 V. These signals are sufficient to drive most Pioneer electronic circuits.

(2) Some devices, such as the coaxial switches, require somewhat longer pulses; the CDU provides a 160-msec, 28-V pulse for such devices.

(3) Where solid-state switches are inadequate because of the high currents involved, as in the case of the battery, the CDU activates relays.

(4) A "state" output, i.e., one of two voltage levels, is available for instrumentation. On the Pioneers, state commands were simply "voltage on" or "voltage off" commands.

### The Electric Power Subsystem

Once they leave the Earth far behind, the Pioneer spacecraft are in full sunlight. It is not surprising to find spacecraft so situated converting solar energy into electricity to operate its scientific instruments and also to drive the spacecraft subsystems that enable the vehicle to survive in outer space and maintain a communication link with the Earth.

The power picture becomes more complicated once the Pioneer mission is studied in detail. First, a basic program ground rule states that the spacecraft must be flexible enough to operate between 0.8 and 1.2 AU without modification. And second, for purposes of acquisition, the spacecraft must be operable while it is in the Earth's shadow prior to escaping the Earth and breaking into full sunlight. The Pioneer shadow problem is a one-time affair, not repeating every few hours like that of an Earth satellite. Yet it can be solved in the same way—with a battery serving as a reservoir of energy. In a satellite the battery is discharged and charged through several cycles each day; but with Pioneer, the battery becomes largely excess baggage once the Earth's shadow is traversed. "Largely" is appropriate here because even in full sunlight the spacecraft depends upon the battery for an assist in meeting sudden, brief surges in

power during normal operation, due in particular to pneumatic valve pulses and, on Pioneers 6 and 7, to the MIT experiment (fig. 2-13). The solar-cell array keeps the battery charged at a low level for this purpose if it is still in the subsystem. (Pioneer practice was to command the battery off after a year or so of operation.)

The total electric power subsystem consists of:

- (1) The solar array, the only source of new energy after launch
- (2) The battery, which acts as a temporary source of power during the shadow period and as a reservoir to supply peak demands in space
- (3) Converters that change bus power into the voltages and current levels required by the TWTs and other spacecraft equipment
- (4) Current and voltage sensors and protective devices
- (5) Power switching and distribution equipment

Pioneer power requirements changed slightly from mission to mission. The largest change took place between the 8 and 9 missions, when the convolutional coder was added and the Goddard magnetometer was replaced by one from Ames. These changes are summarized in table 2-4.

The Pioneer solar cell is a high-efficiency, solderless, n-on-p type, with 1 to 3 ohm-cm base resistivity. Each cell is 1 by 2 cm and is covered by a 0.15-mm glass slide for radiation protection. Early in the program, the average cell efficiency target was 12 percent; this was never achieved and the cells finally launched on the spacecraft average about 10.5 percent.

Individual cells were fabricated into two types of modules. In the first type, 12 cells were interconnected so that 3 were in series and 4 in parallel; in the second, there were 6 in series and 4 in parallel. A close look at figure 2-14 seems to show the cells "shingled together along the long edges according to conventional practice. Actually each cell was soldered to metal connectors that made the modules both self-supporting and flexible. It was this flexibility that allowed the modules to be affixed (with silicone rubber adhesive) to a curved substrate conforming to the cylindrical spacecraft surface.

Each of the 48 solar-cell strings was made from interconnected modules and a blocking diode. The diodes, in effect, permit power to flow out of, but not into, the strings. The strings cover a total area of 22.8 sq ft—essentially all of the spacecraft's cylindrical surface except for the 7.5-in. viewing band—also the locus of the heaviest boom shadowing. Solar cells along the edge of the belly-band are provided with shunt diodes arranged so that, even if they are shadowed, other cells in the string can still provide useful power to the spacecraft.

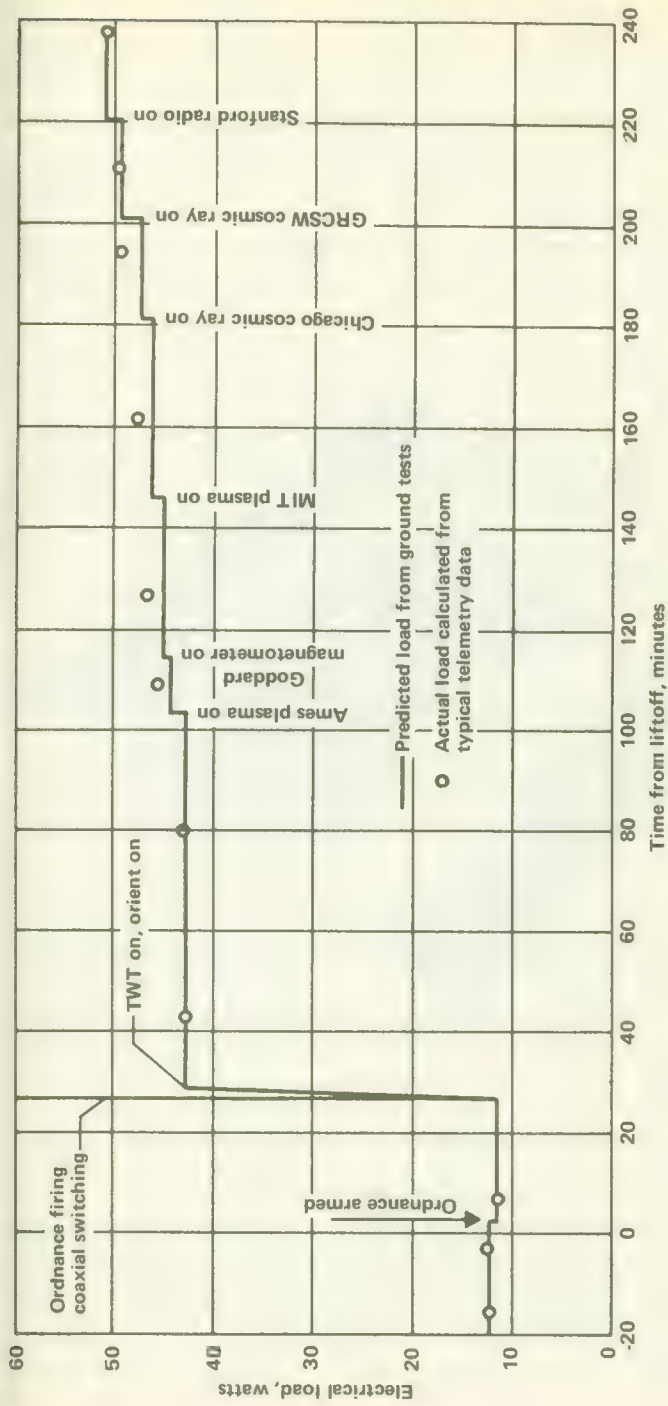


FIGURE 2-13.—Pioneer 6 power profile during the first 4 hr of flight. Superimposed upon the average power level are peaks up to 10 W high from the MIT experiment and 7 to 8 W from the pneumatic valve solenoid in the orientation subsystem.

TABLE 2-4.—*Pioneer Power Budgets*

| Pioneer spacecraft             | 6    | 7    | 8    | 9     | E     |
|--------------------------------|------|------|------|-------|-------|
| Average electrical loads,<br>W |      |      |      |       |       |
| Spacecraft system *            | 43.4 | 43.6 | 43.1 | 43.66 | 41.86 |
| Experiments                    | 9.2  | 8.2  | 12.3 | 17.57 | 17.80 |
| Total                          | 52.6 | 51.8 | 55.4 | 61.23 | 59.66 |

\* Includes 30 W for the TWTs.

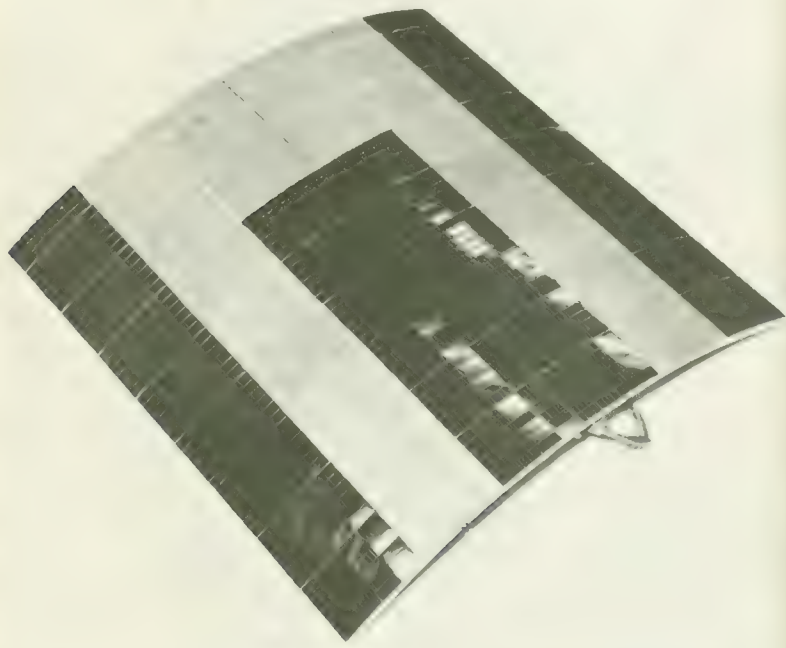


FIGURE 2-14.—One of the Pioneer solar panels, showing both 12- and 24-cell modules mounted on a curved substrate. (Courtesy of TRW Systems.)

A Pioneer is completely dependent upon its battery from the time ground power is severed on the launch pad until the fairing is jettisoned, as well as while the spacecraft is in the shadow cast by the Earth. During this latter period, the battery must supply about 12 W. After orientation, at the discretion of the mission controller back on Earth, the battery is left connected across the bus bar dominated by the solar-cell array. The mission controller can

disconnect the battery by command if it begins to compromise the mission for some reason. Normally, the battery is left on for 6 to 12 months to accommodate any temporary power shortages or overloads. So far as is known, no power shortages have occurred.

The battery chosen for Pioneer was of the sealed, silver-zinc type, which lends itself well to operation in the floating mode. The sealed case was made from fiberglass, a nonmagnetic material. As already mentioned, it can be wired for inward and outward missions. Built with 18 cells, taps were provided at 16, 17, and 18 cells, for the sake of mission flexibility.

### The Orientation Subsystem

The success of the Pioneer mission depended completely upon twisting the spacecraft's spin axis around after injection until its high gain antenna mast pointed within  $2^\circ$  of the south ecliptic pole. The same orientation equipment could also be used to adjust spacecraft orientation if the axis drifted out of the  $90^\circ \pm 2^\circ$  attitude range with respect to the plane of the ecliptic.

The most important components needed in such an orientation maneuver are:

- (1) A device to torque the angular momentum vector of the spacecraft
- (2) Sensors to distinguish the direction of precession
- (3) Sensors to signal the status of the orientation maneuver
- (4) A nutation or wobble damper to dissipate nutation energy induced during the orientation

A small solar sail was added at the tip of the high-gain antenna mast to offset any residual torque due to solar pressure.

Let us sketch out the orientation concept completely. After the spacecraft is injected into the plane of the ecliptic, two pairs of Sun sensors determine the attitude of the spacecraft with respect to a line joining Sun and spacecraft. The Type-I orientation maneuver commences automatically. The Sun sensors will cause the nitrogen gas jet to fire and torque the spacecraft spin axis through the smallest angle until it is perpendicular (within  $\pm 0.5^\circ$ ) to the space-craft-Sun line. At this point, thermal control is possible and the solar array generates full power. With the spin axis perpendicular to the Sun-spacecraft line, the Type-II orientation moves the spin axis in a plane perpendicular to the Sun-spacecraft line. The Type-II orientation is commanded from the ground and is controlled by monitoring the strength of the signal from the high-gain antenna. At maximum, the Pioneer spin axis is also perpendicular to the

spacecraft-Earth line. Here, the desired accuracy is  $\pm 1^\circ$ . If the spacecraft is perpendicular to both the spacecraft-Sun and spacecraft-Earth lines, it is also perpendicular to the plane of the ecliptic. Orientation is now complete. Spin-axis orientation is maintained through spin stabilization at roughly 60 rpm.

The sensitive elements of the Sun sensors were quad-redundant, photosensitive silicon-controlled rectifier (PSCR) chips, manufactured by Solid State Products, Inc. The chips were developed especially for Pioneer. They delivered a signal to the orientation-control circuitry whenever the Sun was in view. The view of each Sun sensor was restricted by aluminum shades. On Pioneers 6 and 7 the light-sensitive chips were protected against space radiation damage by 20-mil quartz covers. However, several months after launch, it was discovered that the Sun sensor thresholds had changed. Laboratory testing implied that radiation damage was the primary cause; therefore, the quartz covers on Pioneer 8 were made 100 mils thick. The trouble persisted. The real cause was discovered by chance at TRW Systems when the sensors were tested under ultraviolet light to see if it degraded the adhesives used in sensor construction. It was discovered that the sensors were ultraviolet-sensitive. In space, the ultraviolet light from the Sun had caused the change in the sensor thresholds. Simple ultraviolet filters were then added to 60-mil quartz covers on Pioneers 9 and E.

The five Pioneer Sun sensors are mounted on the spacecraft with the fields of view specified in figure 2-15. Sensors A and C, located on the spacecraft bellyband, looking up and down, respectively, help position the spacecraft during the Type-I orientation. As long as the spin axis does not point within  $10^\circ$  of the Sun, except for a small overlap of the field of view, sensors A and C will see the Sun once each revolution as the spacecraft spins. The Type-I orientation proceeds as sensor A or C, whichever one is illuminated, stimulates a succession of gas pulses from the jet on the end of the orientation boom. Each pulse lasts for  $45^\circ$  of spacecraft rotation and torques the spin axis about  $0.15^\circ$  in the direction of the smallest angular displacement toward maneuver completion. The pulses cease when the other sensor finally sees the Sun. When both sensors see the Sun at the same time, the spin axis will be perpendicular to the spacecraft-Sun line within about  $\pm 0.5^\circ$ .

The Type-II orientation employs sensors B and D, also located on the spacecraft bellyband, but with  $20^\circ$  fields of view centered on the spacecraft meridian plane. These sensors do not exercise complete control over the gas pulses that torque the spin axis during Type-II orientations; they only time the pulses. Sensor B, for ex-

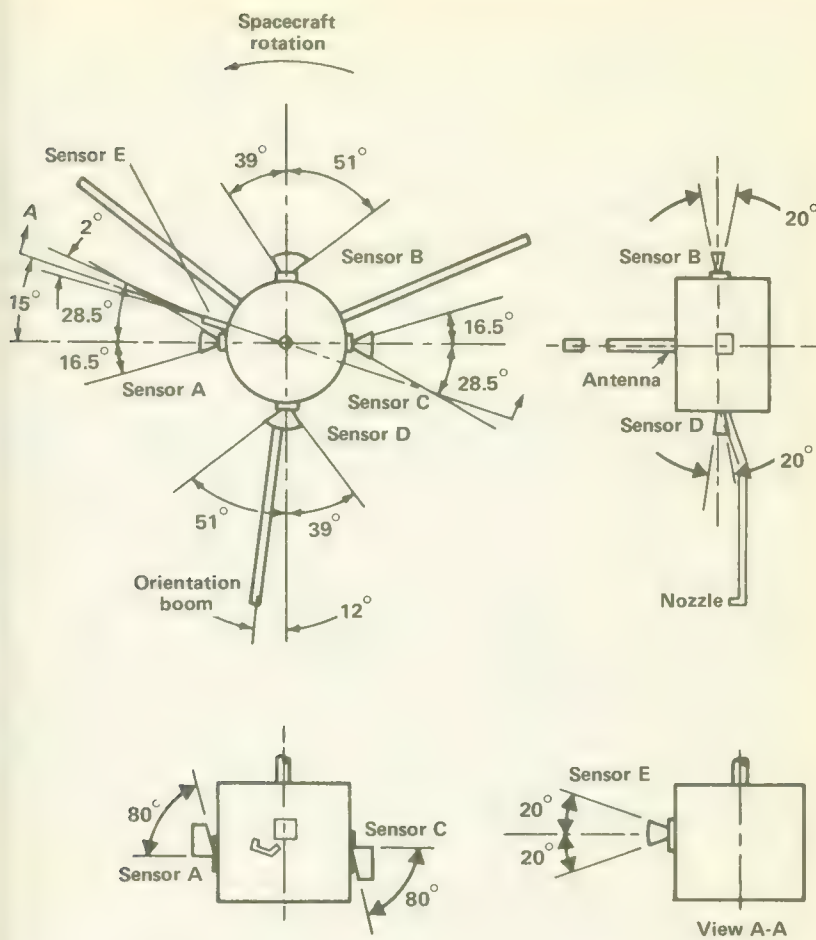


FIGURE 2-15.—Sun-sensor locations and fields of view.

ample, triggers the gas pulse at just the right time for clockwise rotation of the spin axis around the spacecraft-Sun line. (Note that the spacecraft is already perpendicular to the spacecraft-Sun line by virtue of the Type-I orientation. It retains this attitude during Type-II orientation.) Sensor D times the gas pulses for counterclockwise torquing of the spin axis. Thus, sensors B and D control the direction and pulse duration but not the extent of the rotation about the spacecraft-Sun line. The number of pulses for Type-II orientation is controlled by individual commands from the ground. As the angle change progresses, measurements are made of the strength of the carrier signal from the spacecraft's high-gain antenna. When maximum signal strength is obtained, the spin axis

is perpendicular to the spacecraft-Earth line, and orientation is perpendicular to the ecliptic plane established.

Sensor E establishes the reference position of the spacecraft with respect to the Sun and sends signals to the scientific experiments. Also mounted on the viewing band of the spacecraft, sensor E possesses only a  $2^\circ$  field of view that provides short, sharp pulses as it sees the Sun roughly once each second. Because the field of view is only  $40^\circ$  in the other direction (fig. 2-15), Sun pulses appear only when the spin axis is within  $20^\circ$  of being perpendicular to the spacecraft-Sun line. The appearance of Sun pulses also indicates that the Type-I orientation is proceeding successfully and near its end.

The pneumatic assembly is a titanium-alloy pressure vessel containing about 0.9 lb of nitrogen at 3250 psi, a pressure regulator, a solenoid valve, a pressure switch, and a nozzle. The nitrogen had to be very dry to preclude valve icing at low temperatures. An electrical signal opens the solenoid valve for a moment, releasing a burst of gas at about 50 psi which provides the desired impulse. The solenoid valve and nozzle are located at the end of a 62-in. boom to increase the angular impulse and isolate the valve solenoid's iron core from the magnetometer.

On the Pioneer spacecraft, the energy of nutation (wobble) was dissipated by beryllium-copper balls rolling inside and impacting at the ends of a pair of tubes located at the end of the 62-in. boom. Rolling friction and inelastic collisions at the ends of the tubes extracted the energy of nutation, converting it to heat.

### The Thermal Control Subsystem

The task of the thermal control subsystem is to keep the spacecraft cool enough (less than  $90^\circ$  F) on the inward missions and warm enough (more than  $30^\circ$  F) on those swinging away from the Sun to 1.2 AU. The solar heat flux varies between 690 and 307 Btu/hr-sq ft between 0.8 and 1.2 AU; and Pioneer ground rules stipulated that these conditions must be handled without spacecraft design changes for inward and outward missions. The internal heat loads were also variable as electrical equipment was switched on and off. These load changes were small, however, roughly a swing of 12 W or about 20 percent, compared to the greater than 2:1 fluctuation in solar flux.

NASA and STL engineers also had to examine several transient events or situations that occurred before the spacecraft broke into full sunlight following launch:

- (1) The launch-pad environment (The spacecraft determined air-conditioning requirements here.)
- (2) Aerodynamic heating of the shroud during launch and the consequent transfer of heat to the spacecraft
- (3) Aerodynamic heating of the spacecraft at very high altitudes after shroud ejection (Analysis showed that no problem existed here.)
- (4) Radiant heating of the bottom of the spacecraft by the third-stage rocket plume
- (5) Cooling during eclipse of the Sun by the Earth during ascent

Passive thermal control, employing no moving parts, would have been the simplest and most reliable approach in the Pioneer program. However, the more than 2:1 variation in solar flux and changing internal heat loads ruled out passive control.

The whole Pioneer mission depended upon the concept of a spin-stabilized spacecraft with a spin axis normal to the plane of the ecliptic. The curved sides of the cylinder receive essentially all solar radiation, while the ends point toward cold space. This situation is ideal for a thermally insulated spacecraft with active thermal control. Insulation around the sides of the structure allows only a small portion of the solar heat load to reach the inside of the spacecraft. Insulation on the top leaves the bottom as the only possible exit for heat (fig. 2-16). This heat leakage, which varies depending on the distance from the Sun, can be radiated out the spacecraft bottom along with the variable internally generated heat load. The variability is handled by changing the effective radiating area of the bottom of the spacecraft. Mechanization of the concept consisted of a set of louvers that varies the effective radiating area, increasing it as the internal temperature rises and reducing it when the inside of the spacecraft became too cool. The setting of the louvers is controlled by bimetallic actuators sensitive to internal temperature.

### The Structure Subsystem

The Pioneer structure (figs. 2-17 to 2-19) consists of the following major sections:

- (1) The interstage ring and cylinder
- (2) The equipment platform and struts
- (3) High-gain antenna mast supports
- (4) Solar-array substrate and supports
- (5) Boom dampers and wobble dampers
- (6) The booms and associated deployment and locking equipment
- (7) The Stanford experiment antenna

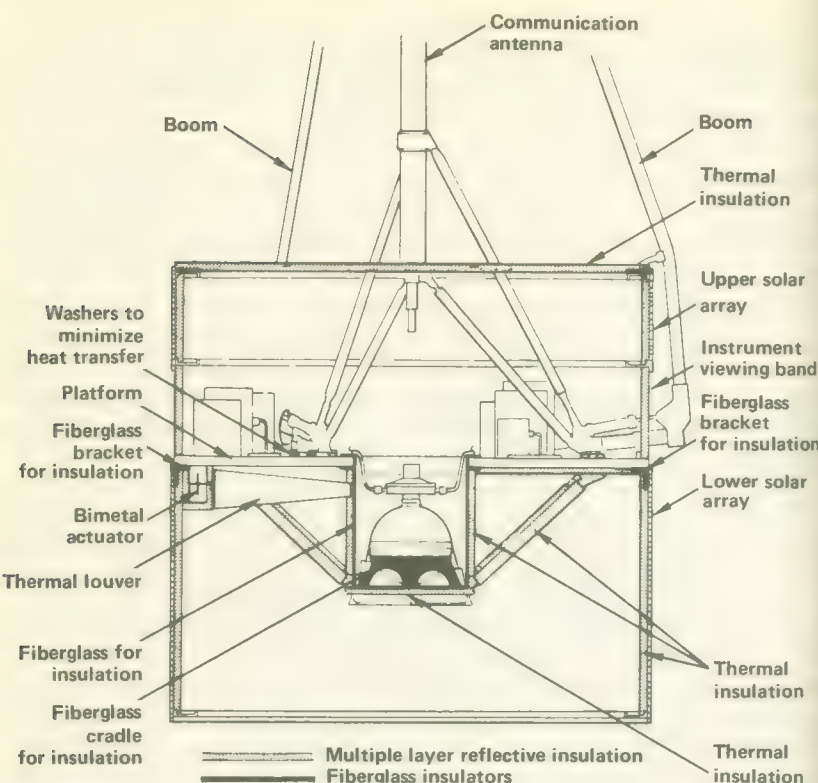


FIGURE 2-16.—Diagram of the components affecting thermal control.

Spin-stabilized spacecraft need not be cylindrical in shape; only symmetry about the spin axis is required. Spheres, for example, also lend themselves to spin stabilization. With Pioneer, however, there was good reason to choose a cylinder. The spacecraft was to be oriented with its spin axis perpendicular to the plane of the ecliptic. Thus, body-mounted solar cells would always be perpendicular to sunlight once each revolution (roughly once per second). Axis perpendicularity was a condition for maximum power generation and obviously a factor enhancing the whole Pioneer concept.

Externally, the Pioneers were cylinders 37.3 in. in diameter and 35.14 in. long, with three booms  $120^\circ$  apart extending 82.44 in. from the spin axis (fig. 2-17). The Stanford experiment antenna projects downward when deployed, being in appearance and complexity a fourth boom. The high-gain antenna mast projects roughly 53 in. above the top edge of the cylinder. Pioneer presents appendages in all directions, in contrast to the relatively clean configuration first suggested.

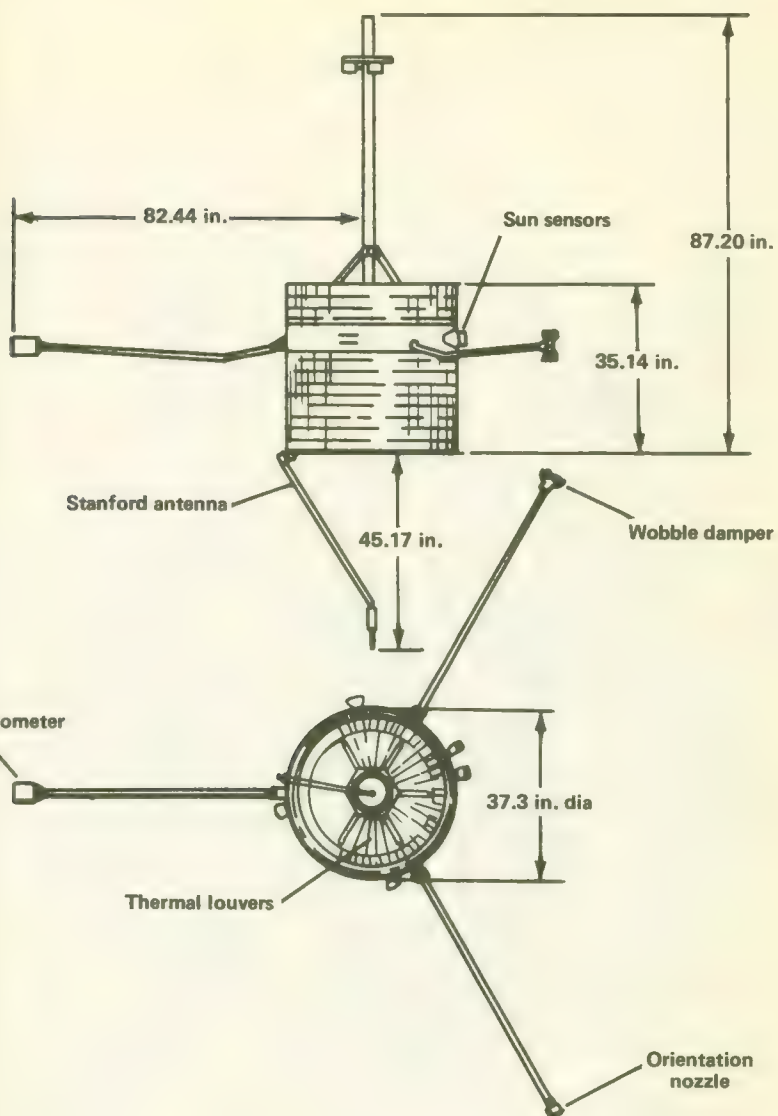


FIGURE 2-17.—External dimensions of spacecraft in-flight configuration.

Internally the major requirements were support for scientific instrumentation and spacecraft subsystems and, once again, spin-axis symmetry. Symmetry must be taken here to mean the judicious placement of mass around the spin axis to preclude the spacecraft's wobbling like a poorly loaded washing machine. Of course, the farther that components were located from the spin axis, the

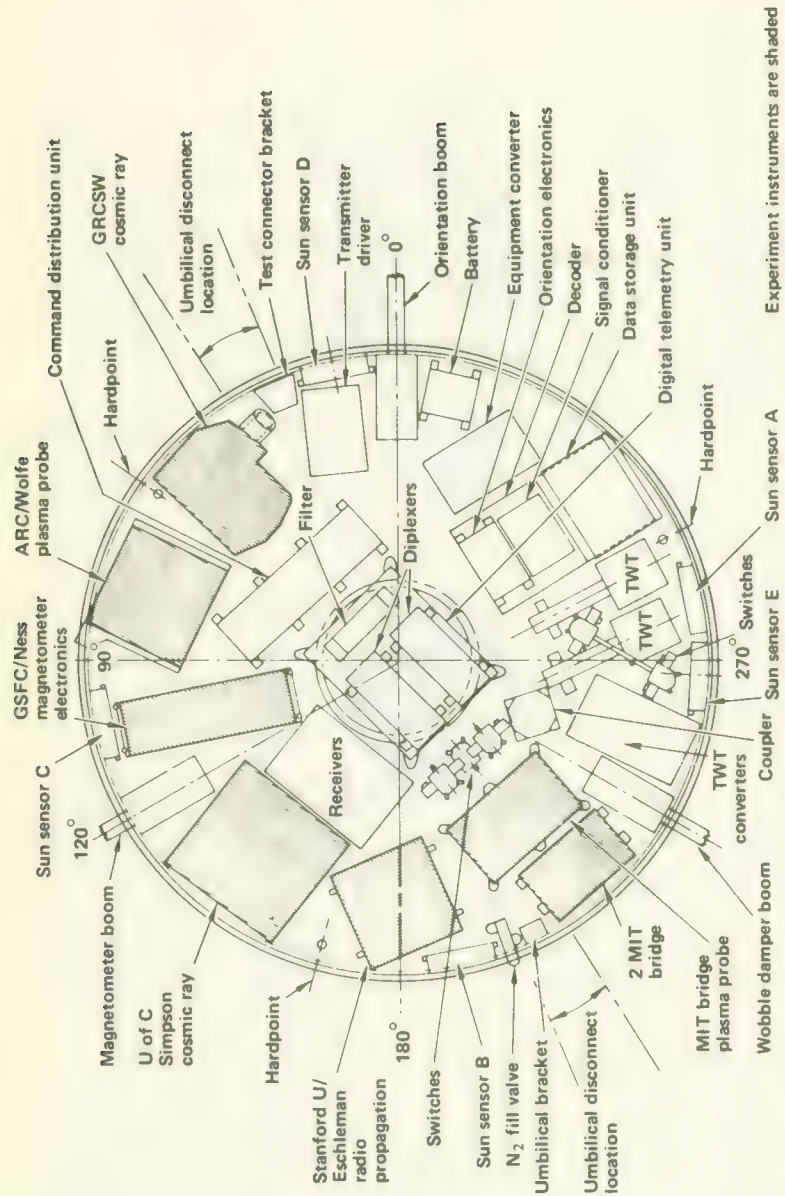


FIGURE 2-18.—Equipment platform layout for Pioneers 6 and 7. Layouts for the Block-II Pioneers were very similar.

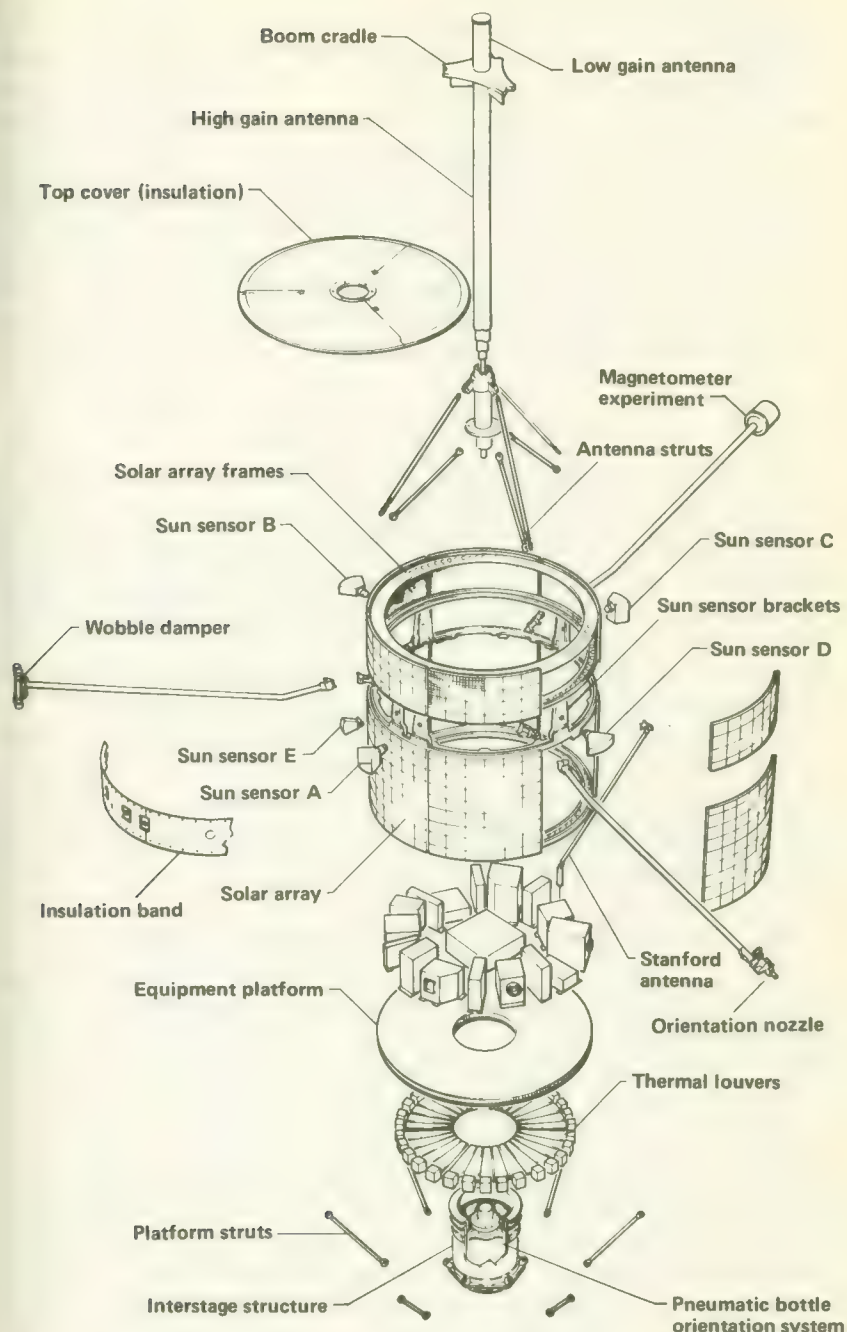


FIGURE 2-19.—Exploded view of the Pioneer spacecraft.

greater the spin stability; that is, the better the spinning spacecraft could resist destabilizing influences. The internal configuration (fig. 2-18) followed general spacecraft practice by making the major structural element a strong equipment platform. This platform supports all internal components, three radial booms, and the high-gain antenna mast. The equipment platform is the internal skeleton. The cylindrical shell, which is rigidly attached to the equipment platform, was constructed of aluminum honeycomb with fiberglass face sheets and is the structural skin that forms the base of the solar array. Sun sensors and the Stanford antenna are attached to the equipment platform. The major structural elements are equipment platform, appendages, and cylindrical shell.

## SCIENTIFIC INSTRUMENTS

The initial scientific objective of the Pioneer Program was the *in situ* measurement of interplanetary phenomena during the minimum in the solar cycle. The later launches in the program and the unexpected longevities of the first Pioneers extended coverage through the following solar maximum well into the 1970's. The facets of the space environment of interest were the solar plasma, solar and galactic cosmic rays, magnetic fields, electric fields, cosmic dust, and radio propagation properties—all with reference to solar activity.

The experiments for the Pioneers were selected carefully by NASA on the basis of scientific merit, pertinence to the Pioneer mission, and other factors detailed in Volume II, Chapter 5. The instruments selected, the experimenters and their affiliations, and the assigned flights are summarized in table 2-5.

### The Goddard Magnetometer (Pioneers 6, 7, and 8)

The interplanetary magnetic field is created by the Sun and modulated by the streams of plasma that stream out into interplanetary space. Magnetic field measurements, particularly those recording transients following solar activity, are critical to our understanding of the space surrounding the Sun.

The spin-stabilized Pioneers permitted the use of a unique magnetometer design whereby all three components of the magnetic field could be measured with a single-axis sensor. If the sensor axis is mounted at an angle of  $54^{\circ}45'$  to the spin axis and if the sensor is sampled at three equally spaced intervals during the rotation of the spacecraft, the experimenter receives three independent measurements of three orthogonal components of the magnetic field. These completely define the instantaneous magnetic field.

TABLE 2-5.—*Experiments Selected for Pioneer Flights*

| Instrument                        | Principal<br>experimenter                                  | Pioneer spacecraft |   |   |   |   |
|-----------------------------------|--|--------------------|---|---|---|---|
|                                   |  | 6                  | 7 | 8 | 9 | E |
| Single-axis fluxgate magnetometer | N. F. Ness, Goddard Space Flight Center                    | X                  | X | X |   |   |
| Triaxial fluxgate magnetometer    | C. P. Sonett, Ames Research Center                         |                    |   |   | X | X |
| Faraday-cup plasma probe          | H. Bridge, Massachusetts Institute of Technology           | X                  | X |   |   |   |
| Plasma analyzer                   | J. Wolfe, Ames Research Center                             | X                  | X | X | X | X |
| Cosmic-ray telescope              | J. Simpson, University of Chicago                          | X                  | X |   |   |   |
| Cosmic-ray anisotropy detector    | K. G. McCracken, Graduate Research Center of the Southwest | X                  | X | X | X | X |
| Cosmic-ray gradient detector      | W. R. Webber, University of Minnesota                      |                    |   | X | X | X |
| Radio propagation experiment      | V. R. Eshleman, Stanford University                        | X                  | X | X | X | X |
| Electric-field detector           | F. L. Scarf, TRW Systems                                   |                    |   | X | X | X |
| Cosmic dust detector              | O. Berg, Goddard Space Flight Center                       |                    |   | X | X | X |
| Celestial mechanics               | J. D. Anderson, Jet Propulsion Laboratory                  | X                  | X | X | X | X |

The sensor of the single-axis fluxgate magnetometer employed in the Goddard experiment is a saturable inductance driven by a gating magnetic field applied by a winding. The flux induced in the saturable core is modified by the presence of the external magnetic field in such a way that the contribution of the external field can be easily separated and quantified.

The fluxgate sensor is mounted on one of Pioneer's three booms at a distance of 2.1 m from the spin axis in a cannister employing passive thermal control. An unusual feature of this experiment is an explosive-actuated indexing device, which permits the experimenter back on Earth to flip the sensor over by 180° so that magnetic fields created by the spacecraft can be taken into account. The Goddard sensor is rotated by a spring-driven escapement mechanism. Because of their very high reliabilities, 11 pairs of small explosive charges were used to activate the escapement mechanism. Thus, 11-sensor flip-overs are possible by remote control.

Magnetic interference is a critical problem for the experimenter flying a magnetometer in interplanetary space. The fields are usually

less than  $10\gamma$  and may be overwhelmed by the fields generated by the spacecraft.<sup>10</sup> For this reason, the Pioneers were made as magnetically clean as possible, and the magnetometer sensor was located on a spacecraft boom 2.1 m from the spacecraft spin axis. Detailed mapping indicated that the magnetic interference from the spacecraft was less than  $0.125\gamma$ ,  $0.35\gamma$ , and  $0.2\gamma$  on Pioneers 6, 7, and 8, respectively. The Pioneers were among the cleanest spacecraft ever built from a magnetic standpoint. Therefore, the data telemetered to Earth have been of great utility in mapping the magnetic structure of solar disturbances and (from data gathered during the first few hours of flight) the Earth's magnetic tail.

### The Ames Magnetometer (Pioneers 9 and E)

The Ames magnetometer instrumentation consists of a fluxgate-sensor package located at the end of one of the 62-in. spacecraft booms and an electronics package mounted on the spacecraft equipment platform. Like the Goddard magnetometer, the Ames instrument is based on the fluxgate saturable inductance sensor. The instrument, however, employs three sensors mounted along mutually orthogonal axes rather than a single sensor as in the Goddard instrument. One fluxgate is parallel to the spacecraft spin axis and a second oriented radially. The Ames experimenters hoped that their three-axis magnetometer would provide a better measure of the interplanetary magnetic field during disturbances involving large, rapid magnetic fluctuations.

The three sensors comprise two packages: one single-axis fluxgate is located in a package mounted so that the sensor axis is parallel to the spacecraft boom axis; the second package contains two orthogonally mounted fluxgates with both axes perpendicular to the boom axis. The Ames instrument includes a flipping mechanism, but it is powered by two resistance-heated bimetallic motors rather than the pyrotechnic devices used by the Goddard magnetometer. The motors on the Ames instrument flip the dual sensor assembly  $90^\circ$  upon command from Earth. One motor flips the sensors clockwise; the other counterclockwise. The Ames magnetometer sensors can be flipped again and again and are not limited to the number of pyrotechnic charges launched with the spacecraft (11 flips for the Goddard instrument). However, an additional burden is placed upon the spacecraft power supply by the resistance heaters in the motors.

<sup>10</sup>  $1\gamma = 10^{-4}$  gauss.

### MIT Faraday-Cup Plasma Probe (Pioneers 6 and 7)

By 1965, plasma probes flown on several Earth satellites and planetary probes had confirmed that the interplanetary plasma originates in the Sun's corona and flows outward toward the planets at some 300 km/sec, remaining ionized out to several AU. Further, this plasma is electrically conductive and interacts in complex ways with solar and planetary magnetic fields. The scientific objectives of the MIT plasma probes were to measure the following characteristics of the interplanetary plasma:

- (1) Positive ion flux as a function of energy and direction
- (2) Electron flux as a function of energy and direction
- (3) The temporal and spatial variations of these physical quantities
- (4) Correlation of plasma measurements with magnetic field measurements

MIT scientists had flown Faraday-cup plasma probes on the Interplanetary Monitoring Platform (IMP) and Orbiting Geophysical Observatory (OGO) series of Earth satellites prior to the Pioneer 6 and 7 flights. The Pioneer instruments were basically similar to these flight-proven plasma probes. The Pioneer sensors (fig. 2-20), the Faraday cups, are 6 in. in diameter with the open side normal to the spacecraft spin axis so that it sweeps out the plane of the ecliptic as the spacecraft spins. At the bottom of the cup, two halves of a split collector intercept those electrons and positive ions from the external plasma that are able to pass through a modulator grid. This grid electrically sorts out the particles in the plasma according to species and energy. The collector is split parallel to the spacecraft equatorial plane to provide directional information about the plasma fluxes in the meridian plane.

The energy spectra of the plasma ions and electrons are measured by applying square waves at different voltage amplitudes to the modulator grid directly in front of the split collector. For example, an 1800-Hz square wave varying between  $V_1$  and  $V_2$  will admit only those particles in the plasma with energies between  $V_1$  and  $V_2$  eV. Further, the square wave will modulate the stream of particles impinging on the collectors so that the currents collected and resultant signals delivered to the electronics section of the experiment will vary at 1800 Hz, a signal that can be amplified and filtered conveniently. The amplitude of the square wave is varied between 100 and 10 000 V in 14 contiguous intervals to scan the positive ion spectrum and between 100 and 2000 V in four intervals for the electron spectrum.

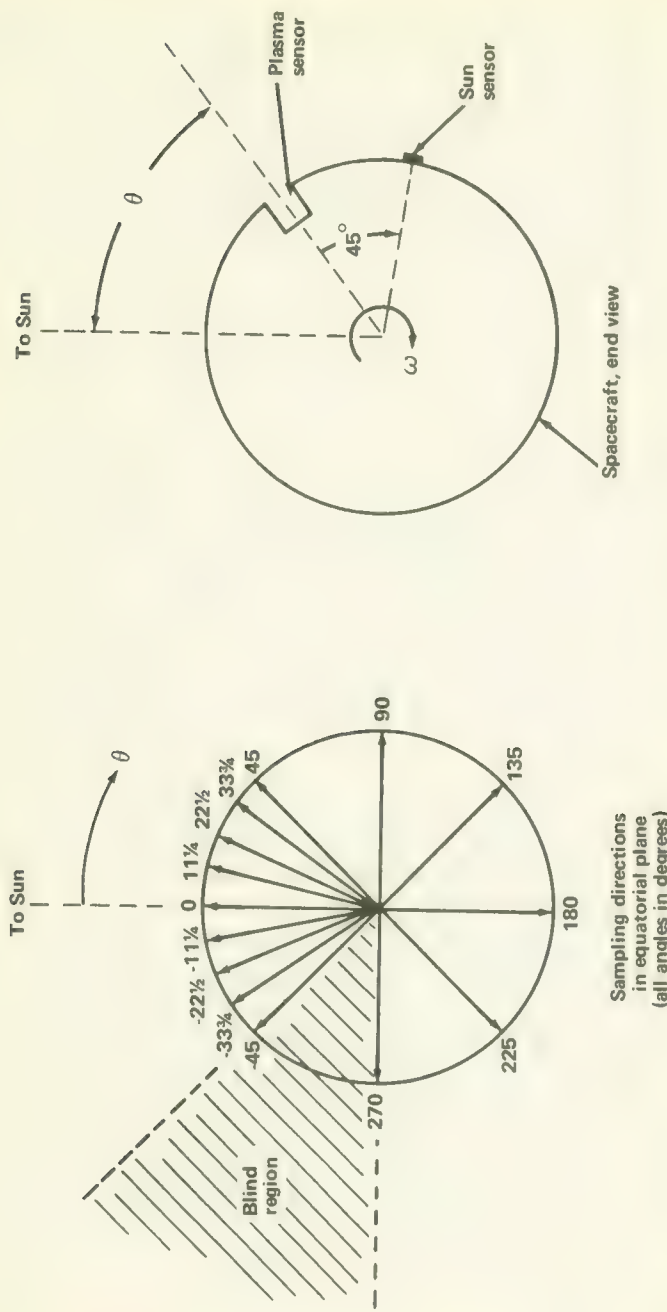


FIGURE 2-20.—Sampling intervals of the MIT plasma probe.

### Ames Plasma Probe (Pioneers 6, 7, 8, 9, and E)

When the angular distributions of the ions and electrons comprising the interplanetary plasma are not well known, the response of the Faraday-cup probe is often hard to interpret. The curved-surface electrostatic plasma analyzers provide more detail, but they are correspondingly more complex. Plasma analyzers work on a different principle. They separate the plasma components into different energy-per-unit-charge ( $E/q$ ) groups and also into much smaller solid angles. In other words, their  $E/q$  and solid-angle discriminations are better.

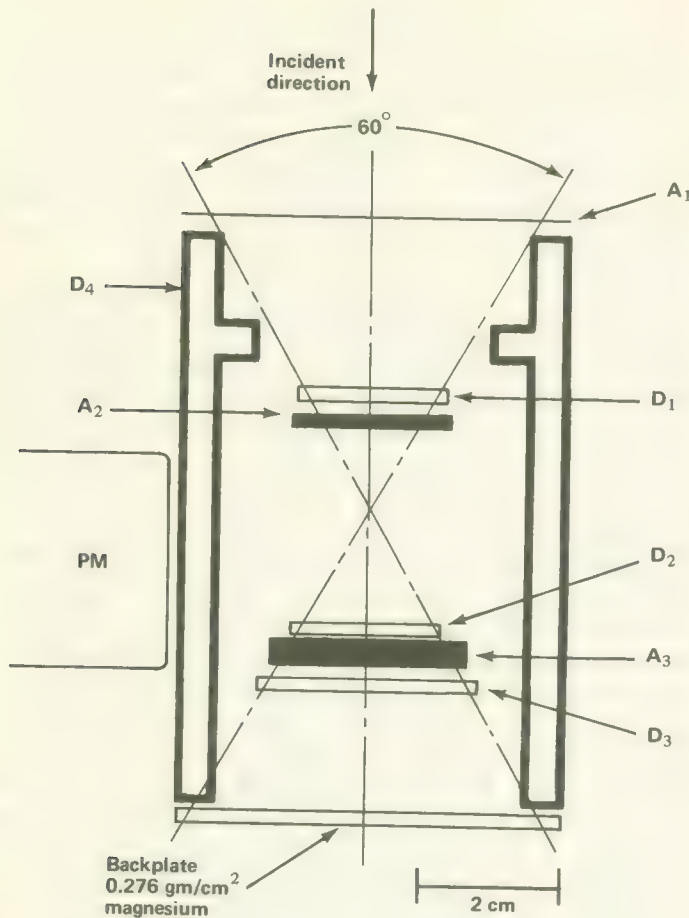
The curved-surface plasma analyzers work by applying stepped voltages to a pair of curved plates. Positively charged particles in the plasma are deflected toward one plate, negatively charged particles toward the other. Depending upon the voltage difference across the plates, only those particles within a narrow range of energy-to-charge ratio and within a narrow solid angle will reach the particle collector at the end of the curved plates. In effect, the curved plates form a filter through which passes only a certain range of energy-to-charge ratios. By making the plates portions of spherical surfaces and segmenting the collectors, the plasma flux arriving from different directions may be analyzed. Energy-to-charge spectrum scanning is possible by stepping the applied voltages.

Although the basic principles of operation were the same, the plasma analyzers flown on the Block-I Pioneer spacecraft were significantly different from those on Block-II spacecraft. The Block-I instruments used quadrисpherical plates, eight current collectors, 16 positive ion groups between 200 and 100 000 eV, and eight electron groups between 0 and 500 eV. Block-II instruments differed from Block-I instruments by using truncated hemispherical plates, three current collectors, 30 positive ion groups between 150 and 15 000 eV, and 14 electron groups between 12 and 1000 eV.

### The Chicago Cosmic-Ray Experiment (Pioneers 6 and 7)

The scientific objective of the Chicago cosmic-ray experiment was the measurement of the heliocentric, radial gradient of the proton and alpha particle fluxes in various energy ranges. Such information is useful in helping decide between various models of the interplanetary magnetic field that modulates solar cosmic rays.

The basic instrument is a four-element, solid-state, cosmic-ray telescope (fig. 2-21). Three telescope elements (D1, D2, and D3) are lithium-drifted silicon semiconductor wafers. These detectors are surrounded by a plastic scintillator (D4), which defines the 60°

**Legend**

|       |  |       |  |
|-------|--|-------|--|
| $A_1$ | Aluminized Mylar window $0.5 \text{ mg/cm}^2$          | $D_2$ | Lithium drift silicon detector $0.230 \text{ gm/cm}^2$ |
| $D_1$ | Lithium drift silicon detector $0.122 \text{ gm/cm}^2$ | $A_3$ | Platinum absorber $8.46 \text{ gm/cm}^2$               |
| $A_2$ | Aluminum absorber $0.103 \text{ gm/cm}^2$              | $D_3$ | Lithium drift silicon detector $0.22 \text{ gm/cm}^2$  |
|       |  | $D_4$ | Plastic scintillator                                   |
|       |  | PM    | Photomultiplier tube                                   |

FIGURE 2-21.—Arrangement of detectors and absorbers in the Chicago cosmic-ray telescope.

acceptance cone for incident charged particles. A photomultiplier tube monitors the plastic scintillator. The silicon wafers and the photomultiplier tube are all sensitive to sunlight, making a light-tight enclosure a necessity. Particle absorbers between the telescope elements define the response of the elements to various particles at various energies.

Consider particles entering the instrument through the solid angle defined by the plastic scintillator. The particles pass through D1, producing pulses with heights proportional to the amount of energy lost in transit through the silicon wafer. The detectors D2 and D3 have the same general characteristics. From this type of information, along with knowledge of the energy-loss characteristics of the absorbers placed between D1, D2, and D3, and with pulse-height analysis, the experimenters can deduce considerable information about the cosmic-ray environment seen by the instrument as it scans the plane of the ecliptic.

The energy discriminating capabilities of the experiment (when pulse-height analysis is employed) are summarized below:

- (1) For protons—6 to 8 MeV and 80 to 190 MeV
- (2) For alpha particles—8 to 80 MeV per nucleon and 80 MeV per nucleon to relativistic energies
- (3) For electrons—1 to 20 MeV in the mode  $D1\bar{D}2\bar{D}3\bar{D}4$ <sup>11</sup> and in excess of 160 keV when D1 counts are considered alone

Electrons can be distinguished in the pulse-height analysis of D1 signals because they cause mainly low-amplitude pulses. Counting rates alone without pulse-height analysis can also provide significant energy-and-particle discrimination in themselves. Two examples follow: (1) for protons plus alphas,  $D1\bar{D}2\bar{D}4$  logic provides counts in the 0.8 to 8 MeV per nucleon range; (2) for protons and alphas,  $DID2\bar{D}3\bar{D}4$  logic yields counts between 8 and 80 MeV per nucleon.

### The GRCSW Cosmic-Ray Experiments (Pioneers 6, 7, 8, 9, and E)<sup>12</sup>

The Earth-based study of cosmic-ray anisotropy has always been hampered by the presence of the Earth's magnetic field and atmosphere. Scientific satellites do not get far enough away from the Earth to avoid its magnetic field completely. The crucial test of one theory that describes the motion of cosmic rays within the

<sup>11</sup> A bar over a detector designation signifies anticoincidence. For example  $D1\bar{D}2$  "logic" means that detector D1 detects a particle at a given instant in time but D2 does not.

<sup>12</sup> GRCSW was later renamed Southwest Center for Advanced Studies (SCAS) and is now known as The University of Texas at Dallas.

solar system depends upon the careful measurement of cosmic-ray anisotropy at energies below 1000 MeV. For such measurements, the instruments must be carried well away from the Earth. The Pioneer probes were ideal for this purpose.

The Graduate Research Center of the Southwest (GRCSW) instruments were part of all five Pioneer payloads, but those on Pioneers 8, 9, and E (Block II) represented second-generation equipment. The later equipment was more sophisticated because additional low-energy measurements were made in, above, and below the plane of the ecliptic.

In both generations of equipment, the principal cosmic-ray detector consisted of a flat cylindrical CsI(Tl) scintillator crystal (detector C) contained within a cuplike cylindrical container of scintillating polytoluene (detector D), which functioned as a guard detector. On all five Pioneers the CsI(Tl) and plastic scintillators were connected in anticoincidence so that the detector was directional with an acceptance cone of about 107°. Particles with energies greater than 90 MeV/nucleon were also eliminated because even if they entered the instrument's aperture, they passed right through the CsI(Tl) scintillator and activated the guard scintillator. Separate photomultiplier tubes watched the two scintillators (fig. 2-22).

The same basic scintillator arrangement was employed for the Block-II flights, but it was supplemented with a three-way coincidence telescope consisting of four 100- $\mu$ , totally depleted silicon, surface-barrier detectors.

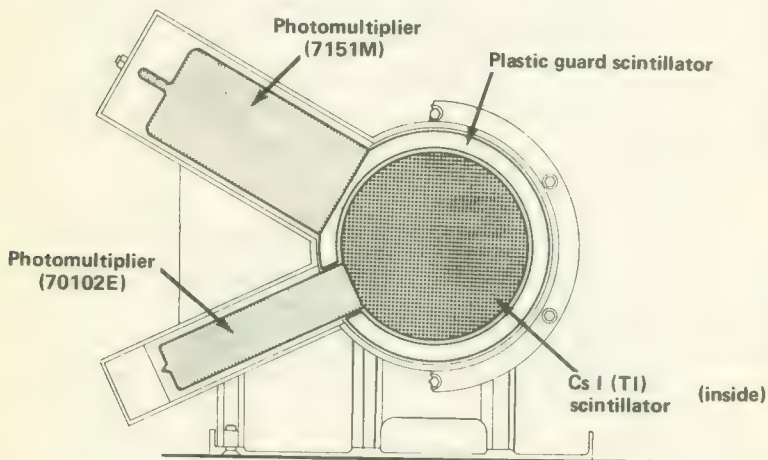


FIGURE 2-22.—Axial view of the GRCSW cosmic-ray telescope, Block-I Pioneers. The detector dimensions and positions were changed for the Block-II flights (see text).

The goal of the experiments was the study of cosmic-ray anisotropies as small as  $10^{-3}$  of the mean cosmic-ray flux. Consequently, the count-accumulation times for the four quadrant registers had to be identical to at least one part in  $10^4$  to provide meaningful experimental results. A unique and critical part of the experiment, therefore, was the precision, crystal-controlled aspect clock that controlled the gating pulses.

#### **Minnesota Cosmic-Ray Detector (Pioneers 8, 9, and E)**

The Minnesota cosmic-ray experiment had a purpose entirely different from that of the GRCSW instrument. The experiment objectives listed below are indicative of the lack of high precision cosmic-ray experiments flown on spacecraft prior to the spring of 1964.

- (1) Measure the quiet-time energy spectrum of protons, alphas, and heavier nuclei up to a charge of 14 over a wide energy range with better energy and background discrimination than previously obtained.
- (2) Measure the variations in these spectra, including the features of Forbush decreases as well as the 11-year variation during the solar cycle.
- (3) Measure the radial and azimuthal cosmic-ray gradients existing in interplanetary space during quiet and disturbed periods on the Sun.
- (4) Measure comprehensively the charge, isotopic composition, and energy spectrum of solar cosmic rays.

The Minnesota instrument incorporates seven separate detectors (fig. 2-23), which are, in effect, electronically arranged into five different telescopes by Earth commands. Detector G is a two-piece guard counter made of Pilot B plastic; it is viewed by a photomultiplier tube. Detector D, at the bottom of the telescope, is a 1-cm-thick piece of synthetic sapphire and functions as a Cerenkov counter. Another photomultiplier tube views this detector. The remaining five detectors—B1A, B1B, B2, B3, and C—are all of the semiconductor type. The coincidence-anticoincidence conditions that electronically create five different telescopic arrangements are listed in table 2-6, along with the ranges and particles which they can detect.

#### **The Stanford Radio Propagation Experiment (Pioneers 6, 7, 8, 9, and E)**

The Stanford experiment measured the integrated electron density along the radio transmission path between the Earth and space-

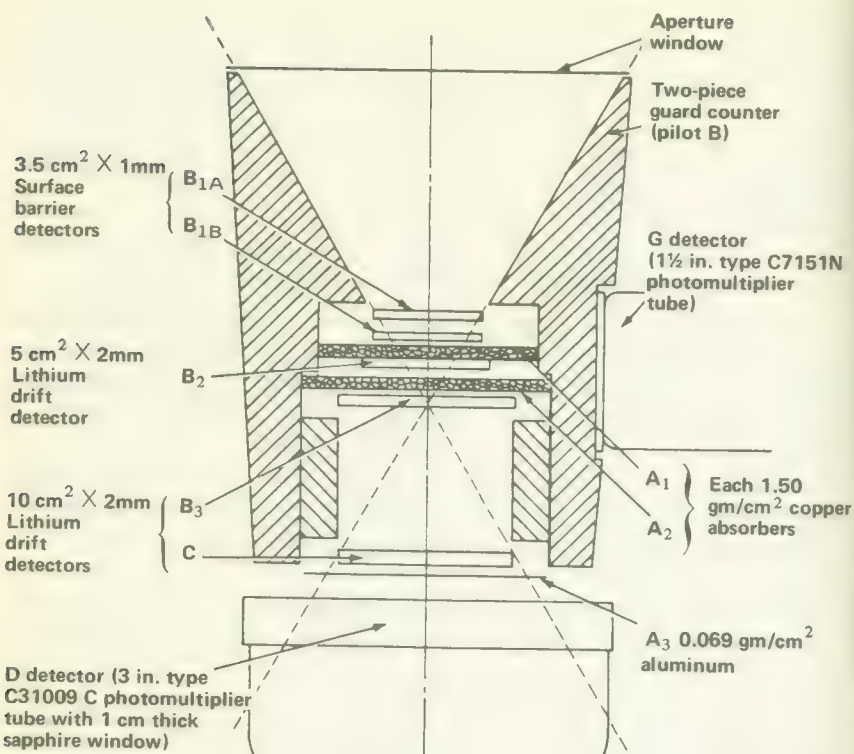


FIGURE 2-23.—Arrangement of detectors and absorbers in the Minnesota cosmic-ray telescope.

craft. For successful operation the experiment required that a special dual-channel, phase-locked-loop receiver in the spacecraft lock onto signals transmitted from the 150-ft parabolic antenna located on the Stanford campus. When the experiment is in progress, two modulated coherent carriers of approximately 49.8 and 423.3 MHz are sent to the spacecraft from the 150-ft Stanford antenna. The special Stanford receiver on the spacecraft measures the relative phase change between the modulation envelopes. Since the higher frequency is relatively unaffected by the presence of ionization, the comparison provides the information needed to compute the integrated electron number density, or the total number of electrons per square meter between Earth and spacecraft. The rate of phase change of one signal with respect to the other is also measured to very high precision to determine the time variation of the integrated electron number density. The experiment also measures the strength of the signals sent from Earth.

TABLE 2-6.—Minnesota Cosmic-Ray Telescope Arrangements

| Telescope | Coincidence-anticoincidence requirements                           |                              | Charge and energy ranges of the particles detected  |
|-----------|--|------------------------------|---|
| T1, T2    | B1A • B1B • B2 • B3 • C  | $Z \geq 1$<br>$e \pm$        | $E \gtrsim 64$ MeV per nucleon<br>$E \gtrsim 8.4$ MeV   |
| T3        | B1A • B1B • B2 • $\overline{C} \cdot \overline{G}$                 | $e \pm$<br>$,H^1$<br>$,He^4$ | 4.2 MeV $\leq E \leq$ 8.4 MeV<br>39.6 MeV $\leq E \leq$ 64.3 MeV<br>39.4 MeV per nucleon $\leq E \leq$ 64.1 MeV per nucleon |
| T4        | $B \cdot \overline{B2} \cdot \overline{G}$<br>( $B1 = B1A + B1B$ ) | $e \pm$<br>$,H^1$<br>$,He^4$ | 0.34 MeV $\leq E \leq$ 4.3 MeV<br>3.5 MeV $\leq E \leq$ 39.7 MeV<br>6.6 MeV per nucleon $\leq E \leq$ 39.7 MeV per nucleon  |
| T5        | B1A • B1B  | $Z \geq 1$<br>$e \pm$        | $E \gtrsim 14$ MeV per nucleon<br>$E \gtrsim 0.6$ MeV   |

Both the 49.8- and 423.3-MHz transmissions to the spacecraft originate at the Stanford computer-controlled "Big Dish." The 49.8-MHz signal is fed to a crossed, folded dipole and reflector located just below the focal point of the 150-ft dish. This signal is generated in a 300-kW linear amplifier transmitter. The high frequency signal, 423.3 MHz, is radiated directly from the horn of the dish.

Both carriers from the Earth are received by the Stanford antenna on the spacecraft and sent to the Stanford dual-channel receiver, which consists of two separate coherent phase-locked receivers. The main reasons for the phase-lock design are (1) to increase the sensitivity of the receiver and (2) to detect the difference in radio frequency cycles between the 49.8 MHz and the 2/17 harmonic of the 423.3-MHz carrier.

Because the Stanford experiment must have transmitter operators at Stanford in the loop during its operation, real-time teletype data are relayed directly from JPL's Space Flight Operations Facility (SFOF) to Stanford. Teletyped parameters include the modulation phase-difference measurements and the radio frequency difference counts. The Stanford operator uses this information to adjust the transmitter frequencies, powers, and modulation phase offset for best operation. At the experiment design range of 300 000 000 km, it takes about 33 min before the effects of transmitted changes are seen in the teletype messages from JPL.

### The TRW Systems Electric Field Detector (Pioneers 8, 9, and E)

The Stanford and TRW Systems experiments are closely related. In fact, the TRW Systems experiment makes direct use of the Stanford antenna. Whereas the purpose of the radio propagation experiment was essentially macroscopic in nature—measuring integrated electron density over long distances—the TRW Systems experiment is microscopic in design. Its purpose is the detection of charge differences over small distances in interplanetary space through the electric fields they create along the Stanford antenna. Plasma waves and other cooperative actions in the 100- to 100 000-Hz VLF range of charged particles in collisionless interplanetary space can be detected with the instrument.

The decision to add the electric field detector was made well after the Block-II payload was selected. Six spare words from the Pioneer telemetry format were made available. The weight of 0.9 lb and power drain of 0.5 W made it possible to squeeze this experiment onto the spacecraft without major changes, particularly since it could use the Stanford antenna. In a sense, it is an addendum to the Stanford experiment, and it is often treated as such in the literature.

The electric field experiment makes use of the short (6.4 in.) 423.3-MHz segment of the Stanford antenna as a capacitively coupled sensor with which local plasma waves can be detected. The sensor is relatively insensitive but adequate for the purposes of the experiment. A number of Earth satellites have carried similar VLF radio receivers for the same purpose.

The portion of the wave spectrum to be studied had to be selected carefully in advance on the basis of our limited knowledge of plasma waves in space. The high-frequency channel selected was at 22 kHz for Pioneer 8 and 30 kHz for Pioneers 9 and E. The low-frequency channels were at 400 Hz and 100 to 100 000 Hz (for the broadband survey) on all Block-II spacecraft.

### The Goddard Cosmic-Dust Experiment (Pioneers 8, 9, and E)

The cosmic-dust experiment objectives were:

- (1) To measure the cosmic-dust density in the solar system well away from the Earth
- (2) To determine the distribution of cosmic-dust concentrations (if any) in the Earth's orbit
- (3) To determine the radiant flux density and speeds of particles in meteor streams
- (4) To perform an in-flight determination of the reliability of the microphone as a cosmic-dust detector

The instrument consists of two film-grid sensor arrays spaced 5 cm apart followed by an acoustical impact plate (microphone) upon which the last film is mounted. Three types of cosmic-dust particles were considered in the design of the experiment:

- (1) High-energy, hypervelocity particles ( $> 1.0 \text{ erg}$ )
- (2) Low-energy, hypervelocity particles ( $< 1.0 \text{ erg}$ )
- (3) Relatively large, high-velocity particles ( $> 10^{-10} \text{ g}$ )

As a high-energy, hypervelocity particle pierces the front film sensor (fig. 2-24), some of its kinetic energy generates ionized plasma at the front, or "A" film. The electrons in the plasma are collected on the positively biased grid (+24 V) creating positive pulses as shown. The positive ions in the plasma are collected on the negatively biased film (-3.5 V), producing a positive pulse that is pulse-height-analyzed to measure the particle's kinetic energy. The same thing occurs at the rear sensor or "B" film, generating a second set of plasma pulses. Impact on the plate produces an acoustical pulse. A peak-pulse-height analysis is performed on the acoustical sensor output as a measure of the particle's remaining momentum.

A low-energy, hypervelocity particle will yield all of its kinetic energy at the "A" film. A pulse-height analysis measures the particle's kinetic energy. A high-energy hypervelocity particle may be erroneously registered as a low-energy hypervelocity particle if, because of its angle of entry, it fails to hit the "B" film. If a relatively large, high-velocity particle enters, it may pass through the front and rear film arrays without generating detectable plasma because of its comparatively low velocity; but it may still impart a measur-

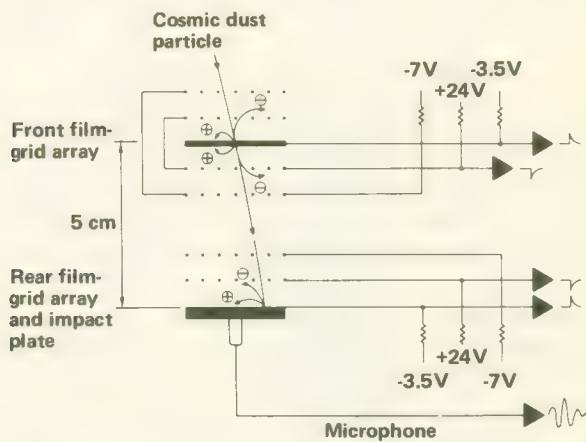


FIGURE 2-24.—Schematic of the Goddard micrometeoroid sensor.

able impulse to the acoustical sensor. An electronic "clock" registers the times of flight of particles. The time lapses between positive pulses from the "A" and "B" films are used to derive particle speeds.

The time-of-flight sensor is one of 256 similar sensors that comprise the portion of the Pioneer instrument measuring particle speed and direction. Four vertical film strips are crossed by four horizontal grid strips that create 16 front and 16 rear film sensor arrays (each 2.5 by 2.5 cm) or 256 total combinations. Each grid strip and film strip connects to a separate output amplifier. The output signals from these amplifiers are used to determine the segment in which an impact occurred. Thus, by knowing the front film-grid segments penetrated and the rear film-grid segment affected by the impact, one can determine the direction of the incoming particle with respect to the sensor axis and the spacecraft attitude. The solar-aspect sensor determines the Sunline at the time of an impact.

### **The JPL Celestial Mechanics Experiment (Pioneers 6, 7, 8, 9, and E)**

The celestial mechanics experiment required no special equipment on the spacecraft or at the tracking stations. The tracking data provided by the Deep Space Stations (DSS) were sufficiently accurate to support the following primary objectives:

- (1) To obtain better measurements of the masses of the Earth and Moon and of the Astronomical Unit (AU)
- (2) To improve the ephemeris of the Earth
- (3) To investigate the possibility of testing the General Theory of Relativity using Pioneer tracking data

The methods employed in obtaining the tracking data are discussed in Chapter 4, where the results from all experiments are presented.

## **THE DELTA LAUNCH VEHICLE**

The Delta launch vehicle, sometimes called the Thor-Delta, has been one of NASA's most successful launch vehicles. The use of the Delta was basic in planning the Pioneer Program, primarily because it was low cost and also because it had already proven to be a reliable spacecraft launcher when the Pioneer Program was being formulated in 1962.

The Delta is basically a three-stage rocket. The liquid-fueled first and second stages are topped by a small solid-propellant third stage (fig. 2-25). The first-stage core is the Thor military rocket, burning a hydrocarbon fuel similar to kerosene (RP-1, RJ-1, etc.) with liquid oxygen. This stage is manufactured by the McDonnell Douglas Astronautics Company. The liquid first-stage engines are made by

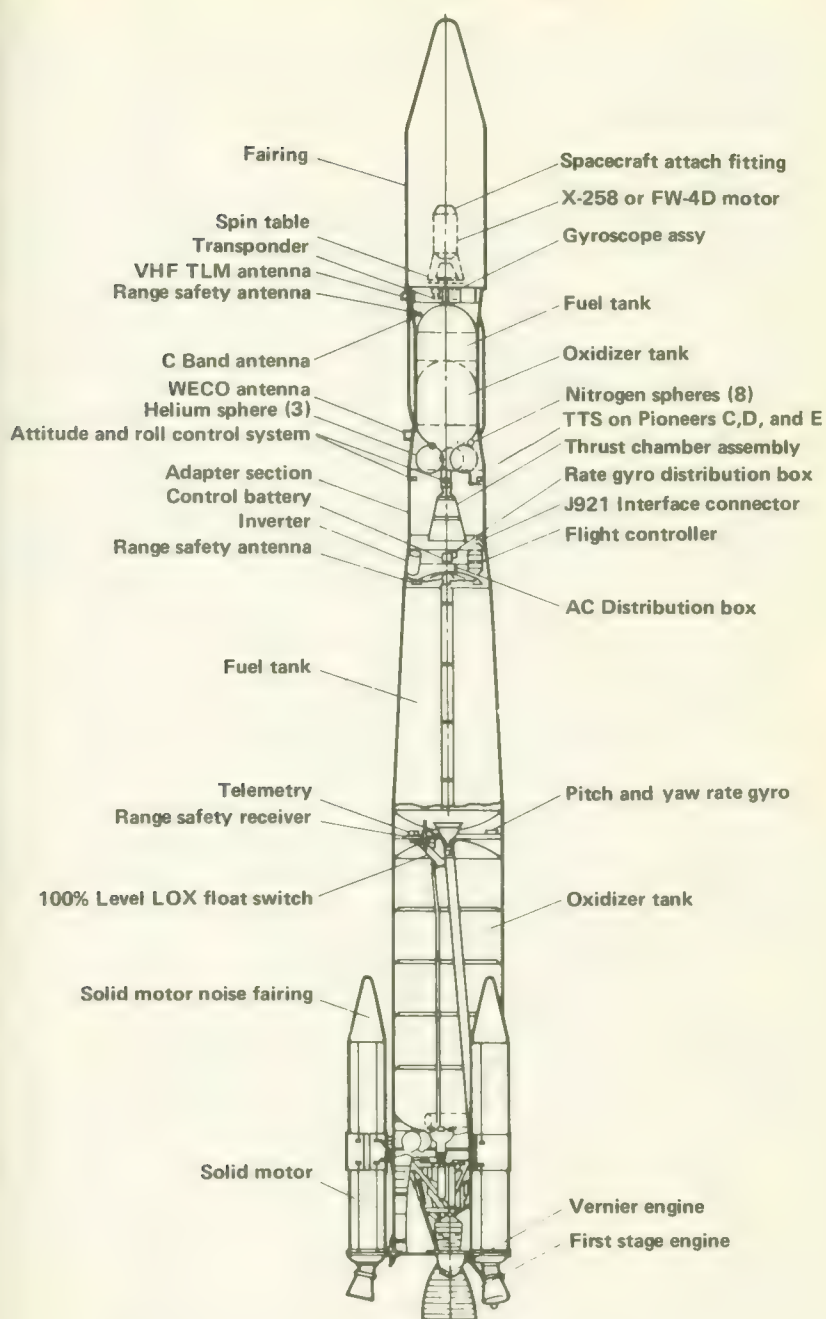


FIGURE 2-25.—The thrust-augmented improved Delta (TAID).

the Rocketdyne Division of North American Rockwell. The solid-thrust-augmentation rockets strapped on the first stages of later models are Castor rockets, usually produced by the Thiokol Chemical Corporation. The much smaller second stage uses unsymmetrical dimethyl hydrazine (UDMH) as fuel, oxidized by inhibited red fuming nitric acid (IRFNA). The second stage is also a product of McDonnell Douglas Corporation. It employs an Aerojet-General engine. The third-stage solid rockets have been manufactured by various concerns during the evolution of the Delta: Allegheny Ballistics Laboratory, United Technology Center, and Thiokol Chemical Corporation. The Delta is one of NASA's smaller launch vehicles (first-stage thrust, about 175 000 lb; plus about 160 000 lb from solid strap-ons on later models).

No launch vehicle that has seen as much use as the Delta remains unchanged. Almost every launch vehicle is different at least in some minor detail, because the interface with each payload is different. More significant changes arise when rocket motors are uprated, propellant tank sizes are changed, and solid-fuel rockets are strapped on for first-stage augmentation. The Delta has gone through over a dozen of these upratings and improvements. The characteristics of the Pioneer Deltas are summarized in table 2-7.

### TRACKING AND COMMUNICATING WITH THE PIONEER SPACECRAFT

When the Pioneer Program began in 1962 there was no question about network choice. The DSN was the only one of NASA's three networks that could track and communicate with a deep-space probe. Like the Delta launch vehicle, the DSN became a pillar of the Pioneer Program. It helped shape spacecraft design as well as the launch trajectories and heliocentric orbits.

Three basic concepts are necessary to the successful tracking of and acquisition of data from Pioneer space probes that are tens or hundreds of millions of miles out in space:

- (1) The concept of a high-gain, highly directional, paraboloidal antenna with a large diameter shown in figure 2-26. (High gain permits reception of very weak spacecraft signals; high directionality provides the accurate angular bearings needed for tracking.)
- (2) A measure of two-way Doppler shift (in the coherent mode) of radio signals between Earth and spacecraft and back again (Spacecraft radial velocity comes from these measurements.)
- (3) The JPL phase-lock-loop, conceived by JPL's Eberhardt Rechlin during the 1950's, and adopted by the DSN and later by the

TABLE 2-7.—Physical Characteristics of the Pioneer Deltas<sup>a</sup>

| Characteristic       |                           | Pioneer 6                  | Pioneer 7 | Pioneer 8 | Pioneer 9 | Pioneer E       |
|----------------------|---------------------------|----------------------------|-----------|-----------|-----------|-----------------|
| Delta popular name   |                           | TAID                       | TAID      | TAID      | TAID      | Long-tank Delta |
| Delta model number   |                           | E<br>35                    | E<br>40   | E<br>55   | E<br>60   | L<br>73         |
| Delta launch number  |                           | DSV-2C                     | DSV-2C    | DSV-2C    | DSV-2C    | DSV-2L-1B       |
| First stage          | Model                     | Height (ft) (with adapter) | 60.4      | 60.4      | 60.4      | 70.3            |
|                      | Height (ft)               | 8                          | 8         | 8         | 8         | 8               |
|                      | Diameter (ft)             | 2.6                        | 2.6       | 2.6       | 2.6       | 2.6             |
|                      | Weight (lb)               | 27 600                     | 27 600    | 27 600    | 29 600    | 29 600          |
|                      | Sealevel thrust (lb)      | 175 600                    | 175 600   | 175 600   | 175 600   | 172 000         |
| Second stage         | Model                     | Castor I                   | Castor I  | Castor I  | Castor II | Castor II       |
|                      | Height (ft) (with nozzle) | 24.3                       | 24.3      | 24.3      | 24.3      | 24.3            |
|                      | Diameter (ft)             | 2.6                        | 2.6       | 2.6       | 2.6       | 2.6             |
|                      | Weight (lb)               | 161 700                    | 161 700   | 161 700   | 156 450   | 156 450         |
|                      | Sealevel thrust (lb)      | 13                         | 13        | 13        | 13        | 13              |
| Third stage          | Model                     | X-258                      | FW-4D     | FW-4D     | FW-4D     | FW-4D           |
|                      | Height (ft)               | 5                          | 5         | 5         | 5         | 5               |
|                      | Diameter (ft)             | 1.7                        | 1.7       | 1.7       | 1.7       | 1.7             |
|                      | Weight (lb)               | 735                        | 663       | 663       | 663       | 663             |
|                      | Vacuum thrust (lb)        | 6 200                      | 5 600     | 5 600     | 5 600     | 5 600           |
| Total launch vehicle | Height (ft) (with shroud) | 92                         | 92        | 92        | 92        | 106             |
|                      | Weight (lb)               | 150 000                    | 150 000   | 150 000   | 150 000   | 200 000         |
|                      | Date                      | 12-16-65                   | 8-17-66   | 12-13-67  | 11-8-68   | 8-27-69         |
| Spacecraft           | Weight (lb)               | 140                        | 140       | 145       | 148       | 148             |

<sup>a</sup> Thrust and weight figures are approximate.



FIGURE 2-26.—The first 85-ft paraboloidal antenna installed at Goldstone (Pioneer site).

Manned Space Flight Network (MSFN) for its unified S-Band tracking during the Apollo Program (The phase-lock-loop concept is fundamental to the detection of signals by the DSN.)

In general terms, the DSN carries out the tracking, data acquisition, and command functions listed above using three distinct facilities:

(1) The Deep Space Instrumentation Facility (DSIF), which consists of the DSN tracking and data acquisition stations shown in table 2-8.

(2) The Space Flight Operations Facility (SFOF), located at

TABLE 2-8.—*The DSN Stations*

| Station number | Location                                 | Dish size | Primary during Pioneer flights |   |   |   |   | E |
|----------------|--|-----------|--------------------------------|---|---|---|---|---|
|                |  |           | 6                              | 7 | 8 | 9 |   |   |
| 11             | Goldstone, Calif. (Pioneer) <sup>a</sup> | 85 ft     |                                |   | X | X |   |   |
| 12             | Goldstone, Calif. (Echo)                 | 85 ft     | X                              | X | X | X |   |   |
| 13             | Goldstone, Calif. (Venus) <sup>b</sup>   | 85 ft     |                                |   |   |   |   |   |
| 14             | Goldstone, Calif. (Mars) <sup>c</sup>    | 210 ft    | X                              | X | X | X |   |   |
| 41             | Woomera, Australia                       | 85 ft     |                                |   |   | X |   |   |
| 42             | Canberra, Australia <sup>d</sup>         | 85 ft     | X                              | X |   |   | X |   |
| 51             | Johannesburg, South Africa               | 85 ft     | X                              | X |   | X | X |   |
| 61             | Madrid, Spain (Robledo) <sup>a</sup>     | 85 ft     |                                |   |   | X | X |   |
| 62             | Madrid, Spain (Cebreros)                 | 85 ft     |                                |   |   | X | X |   |
| 71             | Cape Kennedy, Florida                    | 4 ft      | X                              | X | X | X | X | X |

<sup>a</sup> MSFN Apollo Wing located here; used during some Pioneer flights.

<sup>b</sup> Used primarily for research and development.

<sup>c</sup> Used on extended Pioneer missions.

<sup>d</sup> Also called Tidbinbilla.

JPL, in Pasadena, California, which monitors all spacecraft data, issues commands, and performs all necessary mission calculations

(3) The Ground Communication Facility (GCF), which ties all DSIF stations to the SFOF with high-speed, real-time communications (The bulk of DSN communication traffic is carried via NASCOM, which contributes circuits to the GCF.)

Despite the size and capabilities of the DSN, NASA had to pool the following facilities to fully cover the Pioneer flights:

- (1) The DSN, which included the DSIF, GCF, and SFOF
- (2) The MSFN, which provided 85-ft dish support on occasion
- (3) NASCOM, which contributed many circuits to the DSN's GCF

(4) The Air Force Eastern Test Range (AFETR), which supplied much of the ground environment from the launch pad downrange 5000 miles to Ascension Island; i.e., the Near-Earth Phase Network

The Pioneer flights were divided logically into two main phases: near-Earth and deep-space. The successful injection of the spacecraft into a heliocentric orbit was the event that separated the two phases (fig. 2-27). At this point, somewhere over the Indian Ocean, the spacecraft would be handed over completely to the DSN and cooperating MSFN stations. Each phase of tracking required a different configuration of tracking, data acquisition, command, and ground communication equipment.

The equipment committed to the Pioneer Program during the near-Earth phase varied slightly from flight to flight, as detailed in table 2-9. The stations along the AFETR had the primary responsibility for tracking (or metric data) during the launch and Earth-

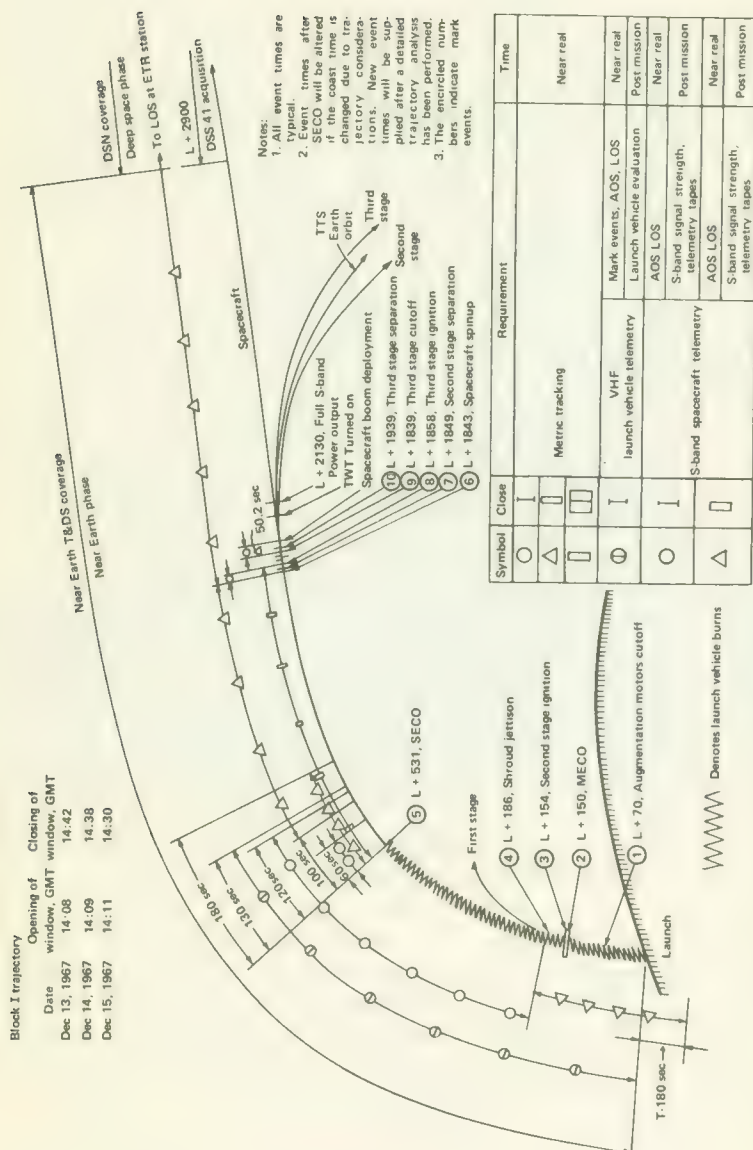


FIGURE 2-27.—Near-Earth tracking and telemetry requirements for the Pioneer 8 flight.

TABLE 2-9.—*Configuration of Tracking and Data Acquisition Stations during Near-Earth Phases*

| Station number | Location                                       | Tracking radars                           | Telemetry   | Used during Pioneer flights |   |   |   |   |
|----------------|--|---|-------------|-----------------------------|---|---|---|---|
|                |  |   |             | 6                           | 7 | 8 | 9 |   |
| AFETR 1        | Cape Kennedy                                   | FPQ-6<br>FPS-16, TPQ-18<br>FPS-16, TPQ-18 | VHF, S-band | X                           | X | X | X | X |
| 3              | Grand Bahama                                   | TPQ-18                                    | VHF         | X                           | X | X | X | X |
| 7              | Grand Turk                                     | TPQ-18                                    | VHF         | X                           | X | X | X | X |
| 91             | Antigua  | FPQ-6                                     | VHF, S-band | X                           | X | X | X | X |
| 12             | Ascension                                      | FPQ-18, FPS-16                            | VHF, S-band | X                           | X | X | X | X |
| 13             | Pretoria                                       | MPS-25                                    | VHF, S-band | X                           | X | X | X | X |
|                | <i>Twin Falls</i> (ship)                       | FPS-16                                    |             | X                           | X | X | X | X |
|                | <i>Coastal Crusader</i> (ship)                 |   |             | X                           | X | X | X | X |
| MSFN 1         | Bermuda  | FPS-16, FPQ-6                             | VHF         | X                           | X | X | X | X |
| 2              | Ascension                                      |   |             | X                           | X | X | X | X |
| 3              | Tananarive, Malagasy                           | Capri                                     | VHF         | X                           | X | X | X | X |
| 4              | Carnarvon, Australia                           | FPQ-6                                     | VHF         | X                           | X | X | X | X |
| 5              | Goddard Space Flight Center,<br>Greenbelt, Md. |   |             | X                           | X | X | X | X |
| 6              | Guam   |   |             | X                           | X | X | X | X |
| 7              | Hawaii   |   |             | X                           | X | X | X | X |
| DSN 71         | Cape Kennedy                                   |   |             | X                           | X | X | X | X |
| 72             | Ascension                                      |   |             | X                           | X | X | X | X |
| 51             | Johannesburg                                   |   |             | X                           | X | X | X | X |
|                | SFOF, Pasadena                                 |   |             | X                           | X | X | X | X |
|                | Building AO, Cape Kennedy                      |   |             | X                           | X | X | X | X |

orbit portions of the flights. The Cape itself is well-equipped with radars, radio interferometers, and a great variety of optical tracking equipment. AFETR and MSFN downrange stations and Range Instrumentation Ships (RIS) also possess full complements of tracking radars and telemetry receiving equipment. Data are fed back to the Cape via submarine cables and radio links.

The DSN station at the Cape (DSS 71) provided prelaunch support to assure spacecraft compatibility with DSN configurations supporting Pioneer flights. JPL also maintains a field station at Cape Kennedy that provides an operational tracking interface between the SFOF, in Pasadena, and the Kennedy Space Center and Goddard Space Flight Center groups. Considering the manifold operations at the Cape, their complex interactions, and the immense detail required for effective coordination, such interface groups are essential. The JPL Field Station also contained an Operations Center with displays to help JPL personnel monitor the status of range instrumentation during Pioneer launches. Critical tracking and telemetry data were also routed to the SFOF through the field station.

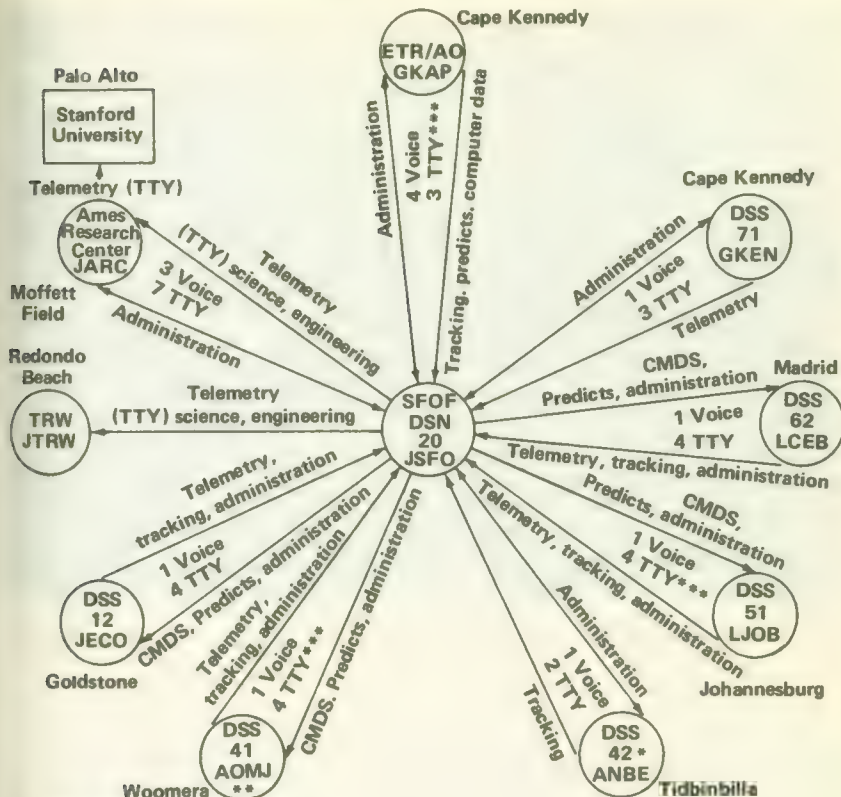
All launches at Cape Kennedy are under the direct control of the Air Force until the spacecraft leaves Eastern Test Range (ETR) jurisdiction somewhere beyond Ascension. Because it is responsible for range safety, the Air Force monitors launch vehicle status data and tracking information. Commands to terminate the mission through the destruction of the launch vehicle are also an Air Force prerogative—one that was exercised during the launch of Pioneer E on August 27, 1969.

After leaving Earth orbit, the Pioneer spacecraft quickly ascended beyond the 500 to 1000 mile ranges of the AFETR and MSFN tracking radars. From here on they were tracked, communicated with, and commanded by the primary DSN stations listed in table 2-8. MSFN and other DSN stations worked the Pioneer spacecraft on an as-needed basis (fig. 2-28).

Each of the primary DSN stations was outfitted with mission-dependent equipment that accommodated general-purpose DSIF machinery to specific Pioneer requirements. The DSN gear was called Ground Operational Equipment (GOE). No special equipment was installed at the SFOF, although a general-purpose mission-support area was reconfigured for the Pioneer missions. Additional mission-dependent equipment was installed at Ames.

### PIONEER DATA PROCESSING EQUIPMENT

Pioneer spacecraft radioed back to Earth two kinds of data: scientific data for the experimenters and engineering data for mis-



- \* DSS 42 backup for DSS 41
- \*\* DSS 41 prime acquisition station
- \*\*\* These TTY circuits (using CP) are to have hardwire backup.

FIGURE 2-28.—GCF channels established for Pioneer 8.

sion controllers to use in assessing the "health" of the spacecraft. The telemetry data follow two separate paths between the DSN stations (which receive it directly from the spacecraft) to the experimenters and Pioneer project personnel. As they arrive from deep space, Pioneer telemetry data are recorded directly on magnetic tape at the DSN stations and airmailed to JPL for verification and then to Ames Research Center. This is the first route, and all data follow it. At Ames, they are processed on the Pioneer Off-Line Data-Processing System (POLDPS) for subsequent transmission to the experimenters on digital magnetic tapes in formats compatible with their computer facilities. Some of the telemetry data also follow a second route. These are dispatched immediately from the DSN to Ames Research Center via teletype through JPL's SFOF. These



FIGURE 2-29.—Pioneer Off-line Data Processing System (POLDPS) at Ames Research Center.

are called "quick look" data; they are used for checking the scientific instruments and for retransmission (after some processing) to the Environmental Science Services Administration (ESSA) to help forecast solar activity. Data from the Stanford radio propagation experiment are handled differently. Proper operation of this experiment requires the near-real-time feedback to Stanford of information on the Stanford receiver status. This information is relayed by teletype from Ames Research Center to Stanford a few miles away. In addition, engineering data flow via teletype from the DSN to the SFOF and from there to both Ames and TRW Systems for analysis. At Ames, these engineering data are used to assess the health of the spacecraft and guide operational decisions.

Originally JPL had been assigned the task of processing Pioneer scientific data, but in 1964 JPL computers were heavily loaded, and it was decided to construct the processing line at Ames Research Center. Magnetic tape represented the only practical way to transmit the bulk of data from Pioneer spacecraft—teletype facilities could not handle the volume. At each DSN station, two Ampex FR-1400 tape recorders operating in parallel prepare analog tapes of the transmissions received from the Pioneers. Tape loading times for each machine are staggered to avoid the loss of data. One set of

tapes containing all recorded data is selected and shipped first to JPL where it is examined (verified) to ensure the quality of reproduction. The tapes are then sent to POLDPS at Ames Research Center.

During 1969, Pioneer tape shipments averaged four hundred 9200-ft tapes per month, each containing 4 hr of data with half-hour overlaps. POLDPS processed and sorted out these data, preparing an average of four hundred 2400-ft tapes per month for the experimenters. The preparation of over 15 experimenter tapes per working day indicated that POLDPS was extremely active during 1969, when four Pioneers were transmitting data back to Earth (fig. 2-29).

POLDPS processes these tapes in a two-level system. The first level, called the Tape Processing Station (TPS), produces a multifile digital tape that serves as the input to the second level of processing, which consists of the Pioneer Off-Line Direct Coupled System (POLDCS). POLDCS generates separate experimenter tapes that are IBM-compatible and in the formats and densities desired by the individual Pioneer experimenters.



# Pioneer Flight Operations

## PRELAUNCH ACTIVITIES

THE SUCCESSFUL COMPLETION of the spacecraft's Preship Review at the TRW Systems plant in Redondo Beach, California, signals the beginning of prelaunch activities. The spacecraft is carefully packed and shipped to Cape Kennedy by air. Its arrival at the Cape initiates a 6 to 10 week series of additional tests and checkout procedures designed to assure both the readiness of the spacecraft and its compatibility with the Delta launch vehicle, the DSN, and the ETR. If all goes well and the pieces fit together, the spacecraft is launched.

More people and facilities participate during the Pioneer prelaunch and launch activities than at any other time. Although the Cape Kennedy and ETR downrange stations are the focal points during this phase of operations, the Deep Space Network, JPL's Space Flight Operations Facility, and Ames Research Center's Pioneer Mission Operations Center are all involved. As the moment of launch approaches, more and more of the NASA and Air Force general-purpose facilities "come on the line" for the launch. During the minutes after liftoff, radars, optical instrumentation, and telemetry antennas at the Cape and downrange are all waiting for the Delta and its Pioneer payload. Likewise, critical antennas at some of the DSN's Deep Space Stations break off from tracking Mariner and Pioneers already out in space and swing toward the points where the new Pioneer is expected to come over the horizon.

The functions of the major facilities concerned with a Pioneer launch are:

(1) Cape Kennedy provides facilities for spacecraft tests, checkout, and integration and facilities for mating of spacecraft with launch vehicle and for launch vehicle assembly and launch. The Pioneer Electrical Ground Support Equipment (EGSE) provides an interface between the spacecraft and the launch pad environment.

(2) Eastern Test Range (ETR) provides tracking and data acquisition services from launch through DSN acquisition at Johannesburg.

(3) The Deep Space Network (DSN) provides tracking, data acquisition, and transmission of command signals to the spacecraft. The

Pioneer Ground Operational Equipment (GOE) at selected DSN stations provides an interface between the spacecraft and the generalized DSN equipment.

The prelaunch phase of activities consists of so many hundreds of separate items and events that the checkout and countdown lists are often printed by computers. Three groups of processes and events stand out as particularly important:

- (1) Training in operational procedures
- (2) Integrated systems tests (ISTS)
- (3) Operational readiness tests

Training in operational procedures was most important during the preparations for the launch of Pioneer A in 1965, when the Pioneer Program was new to ETR and DSN personnel. The Delta was already familiar, and the ETR and of course DSN had handled more complex spacecraft. The different aspects of the Pioneer launches were:

- (1) The unusual orientation maneuvers following launch
- (2) The narrow launch window associated with injecting the spacecraft into an orbit roughly parallel to the plane of the ecliptic
- (3) The ejection of the TTS satellites from the Block-II Pioneers
- (4) The occultations and flights through the Earth's magnetic tail.

The orientation maneuvers, especially, required careful training at the Goldstone DSS site and, in the case of Pioneers 6 and 9, at Johannesburg and Goldstone, respectively, where partial Type-II orientation maneuvers were carried out.

### Pioneer-A Prelaunch Narrative

Both the prototype and flight models were sent to the Cape. The prototype arrived October 1, 1965, for use in practicing prelaunch operations.

The Pioneer-A flight model arrived on December 5. During preliminary alignment checkout a Total Indicator Runout (TIR) of 0.25 in. was noted, indicating a physical mismatch. The attach fitting was modified to bring the alignment within tolerance. Tests and checkouts proceeded normally through F - 1 day, with only minor, easily corrected problems.

December 15, F - 0 Day, was relatively calm with visibility of only 0.125 to 2 miles. Countdown commenced 30 min early at 1630. Everything went smoothly until T - 90 min when the second-stage umbilical plug was inadvertently pulled, causing loss of power to the Delta second stage and the spacecraft itself. No one could be sure

exactly what would happen if the plug were reinserted. Conceivably, some unforeseen signal could cause serious damage by firing some of the ordnance. The spacecraft and the Delta were therefore revalidated. The built-in 60-min hold and ultimately the launch window had to be extended while further checks were made. The terminal count resumed at 0145, December 16, at T -35 min.

At T -2 min an abnormality in the radio guidance equipment caused another hold. The situation seemed to correct itself, and the count was recycled to T -8 min. Liftoff occurred at 0231:20 EST, December 16, 1965 (fig. 3-1).



FIGURE 3-1.—The launch of Pioneer A on Delta 35.

### Pioneer-B Prelaunch Narrative

The prelaunch operations for Pioneer B were comparatively uneventful. The flight spacecraft arrived at Building AM on July 17, 1966. On August 9, it was discovered that a connection opened when the Chicago cosmic-ray experiment warmed up, signalling a nonexistent low radiation level at all times. The experiment flew in this condition.

F - 0 day, August 17, had superb weather, with 5-knot winds and a visibility of 10 miles. The countdown proceeded normally to T - 3 min, when a hold was called due to the loss of communications downrange on the ETR. Communications were restored after 2 min and liftoff occurred at 1020:17 EST.

### Pioneer-C Prelaunch Narrative

Pioneer C was the first of the Block-II spacecraft. In addition, this flight was the first to carry a Test and Training Satellite mounted in the Delta second stage. The Pioneer-C flight model was received at Building AM on Nov. 11, 1967. The IST of November 15 identified a faulty decoder, which was replaced. On November 22, the Ames plasma probe was removed to correct a wiring error.

F - 2 day, December 11, was plagued by bad weather, twice forcing personnel to clear the pad. At 1520, electrical power was lost for 25 min, causing some concern because the spacecraft air conditioning was also lost. On F - 1 day, the fairing had to be removed to repair the wiring to the third-stage velocity meter. Terminal count began at 0543, December 13, and Pioneer C was launched successfully at 0908:00 on December 13, 1967.

### Pioneer-D Prelaunch Narrative

This spacecraft was the first to incorporate the convolutional coder experiment and the Ames magnetometer. Pioneer D arrived at Building AM on October 6, 1968. The beginning of the countdown was delayed for two days while tests and adjustments were made to the second-stage programmer. The countdown then proceeded smoothly to 0900 EST, when anomalies appeared in the experimental data and experiment performance. Holds were called to investigate these problems, which were found to be due to radio and electrical interference from the launch vehicle. No troubles were encountered during F - 1 day countdown activities. At 1850 EST, November 7, 1968, F - 0 day checks began. Spacecraft power was turned on at 1920. Spacecraft systems checks ran ahead of schedule and a 20-

min hold was called at 2015 to give the spacecraft receiver additional time to warm up. The terminal count began at 0050, November 8. Following a hold of 9.5 min due to high sheer winds aloft, the Delta lifted off at 0446:29.

### Pioneer-E Prelaunch Narrative

On July 18, 1969, the Pioneer-E spacecraft was received at Cape Kennedy. There were no unusual prelaunch events. A study of the launch vehicle test summary indicates a normal sequence of pre-launch events. Although a number of minor problems arose, nothing unusual occurred. Nothing in the prelaunch tests and checkout presaged the failure of the launch vehicle after lift-off.

Spacecraft and radio frequency checks, Task VII, began at 0835 EDT on F -0 day, August 27, 1969. Except for a thunderstorm that temporarily delayed work, weather was excellent with a visibility of 8 miles and light winds. The terminal countdown was uneventful. Lift-off was at 1759:00 EDT, August 27, 1969.

### LAUNCH TO DSS ACQUISITION

The phase of operations stretching from launch to DSS acquisition lasts less than 1 hr, but it is the only time when all four Pioneer systems are in operation together. Even then, the spacecraft systems and scientific instruments are essentially passive during powered flight and coast. Only housekeeping data are telemetered and all scientific instruments are off. The spacecraft comes to life when the TWTs are switched on, the booms deploy, and the Type-I orientation maneuver begins automatically. By this time, the spacecraft has been spun up and has separated from the Delta third stage. The ground-based Pioneer system, the DSN, is involved through the Near-Earth-Phase Network, which also incorporates some facilities from the Air Force Eastern Test Range and the Manned Space Flight Network. Figure 3-2 illustrates the chronology and terminology involved in the near-Earth phase of the mission.

It is best to view Pioneer operations from several vantage points so that the operations of all four systems can be appreciated. First, the sequence of events is portrayed schematically in figure 3-3. The nominal time frames for all of the launches are added to the picture in table 3-1. Of course, the timing of the critical events varies from mission to mission because the burn and coast times changed with each launch and the Delta rocket was upgraded during the Program. The nominal time frame, with its critical events, provides a yardstick against which to measure the success of the launch.

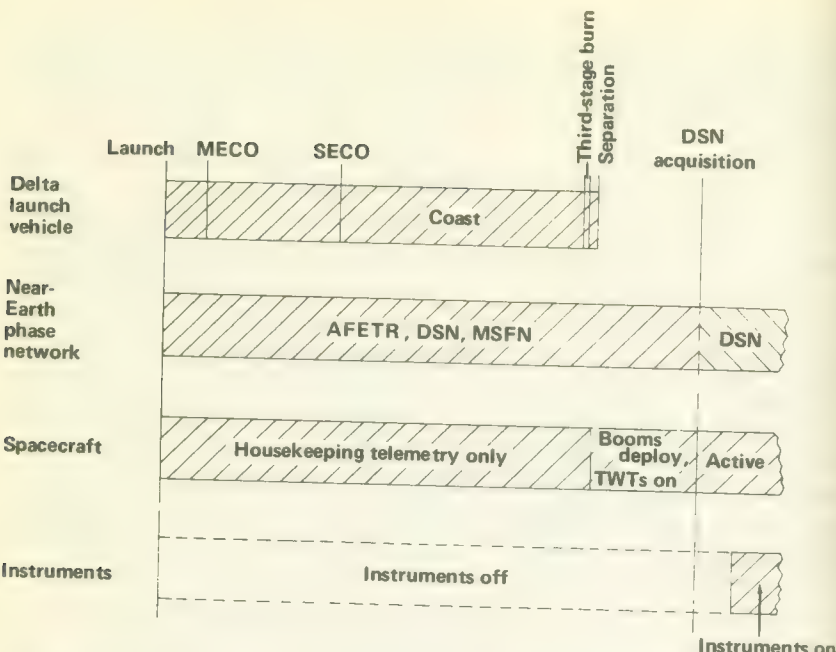


FIGURE 3-2.—Status of the four Pioneer systems from launch through DSS acquisition.

### Performance of the Delta Launch Vehicle

The Delta launch vehicle performed superbly during the first four Pioneer launches. The fifth mission, Pioneer E, had to be aborted by the Range Safety Officer when the vehicle began to stray off course.

### Tracking and Data Acquisition

As a spacecraft and its launch vehicle rise from the launch pad at Cape Kennedy, they are viewed downrange by a variety of radio and optical tracking devices. Until the spacecraft is handed over to the Johannesburg Deep Space Station, the pooled radars, optical trackers, guidance equipment, and telemetry receivers of the Air Force Eastern Test Range and some stations of NASA's Deep Space Network and Manned Space Flight Network are crucial to mission success.

The facilities assigned to each of the Pioneer missions from launch through DSS acquisition are listed in table 3-2. The AFETR was the primary agency responsible for providing metric (tracking) data during this phase. The MSFN stations in table 3-2 provided redundant radar support. Metric requirements were met by tracking

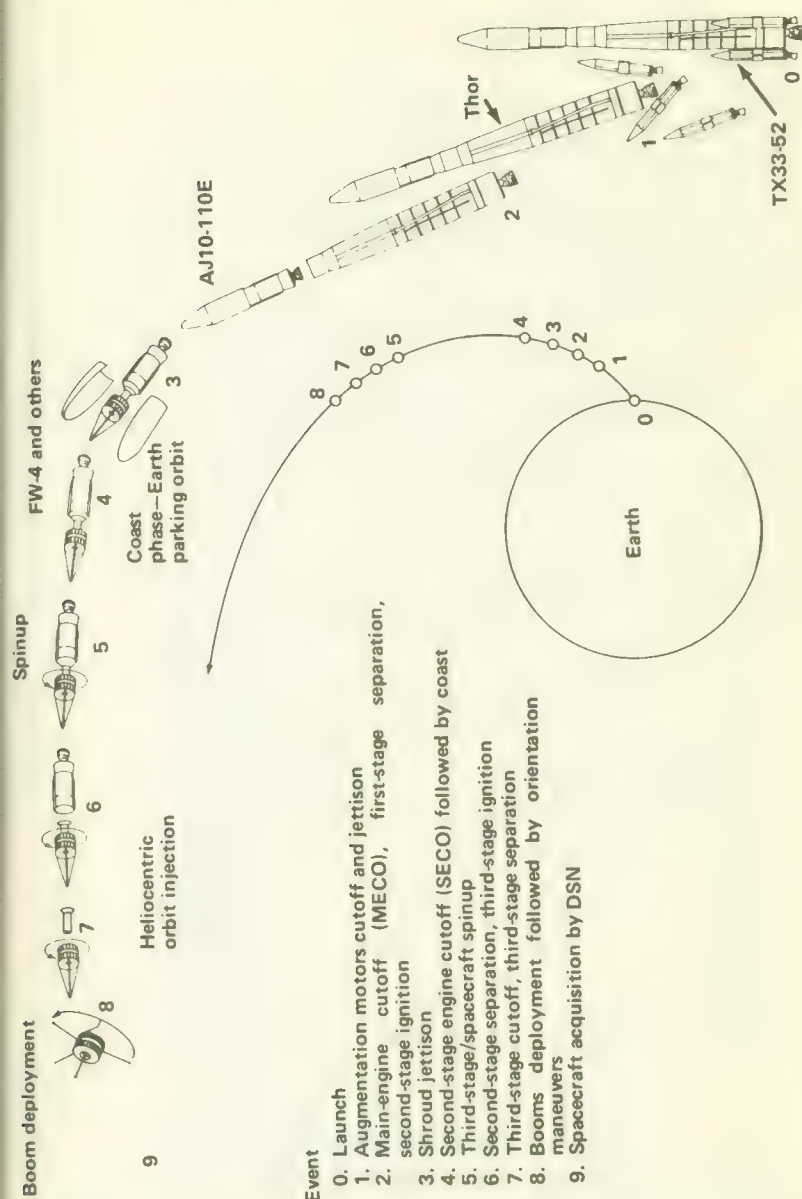


FIGURE 3-3.—A typical Pioneer launch sequence.

TABLE 3-1.—Summary of Critical Nominal and Actual Launch Events

|                                    | Pioneer 6     |               | Pioneer 7 |               | Pioneer 8 |         | Pioneer 9 |         | Pioneer E*    |          |
|------------------------------------|---------------|---------------|-----------|---------------|-----------|---------|-----------|---------|---------------|----------|
|                                    | Nominal       | Actual        | Nominal   | Actual        | Nominal   | Actual  | Nominal   | Actual  | Nominal       | Actual   |
| Liftoff (sec)                      | 0             | 0             | 0         | 0             | 0         | 0       | 0         | 0       | 0             | 0        |
| Solid motor burnout                | 43.00         | 42.23         | 42.65     | 41.60         | 41.90     | 42.25   | 38.19     | 39.4    |               |          |
| Solid motors jettisoned            | 70.00         | 69.97         | 70.00     | 70.79         | 70.00     | 70.3    | 70.00     | b69.94  | 70.00         | 69.8     |
| Main-engine cutoff                 | 149.21        | 148.01        | 149.52    | 148.10        | 149.75    | 149.45  | 150.53    | 151.35  | 220.0         | 215.4    |
| Second-stage ignition              | 153.21        | 152.03        | 153.52    | 152.13        | 153.75    | 153.50  | 154.53    | 155.42  | 224           | 224      |
| Fairing jettisoned                 | —             | —             | 178.84    | 175.52        | 174.74    | 185.75  | 186.16    | 169.53  | 171.01        | 229      |
| Second-stage engine cutoff command | 551.13        | 531.44        | 529.32    | 527.89        | 530.93    | 536.73  | 534.35    | 539.01  |               |          |
| Third-stage spinup                 | 1486.21       | 1485.03       | 1475.52   | 1474.12       | 1842.75   | 1842.42 | 1201.53   | 1202.40 |               |          |
| Second-stage jettisoned            | 1488.21       | 1487.03       | 1477.52   | 1476.12       | 1844.75   | 1844.43 | 1203.53   | 1204.37 |               |          |
| Third-stage ignition               | 1501.21       | 1496.94       | 1490.52   | 1488.98       | 1857.75   | 1857.98 | 1216.53   | 1218.54 |               |          |
| Third-stage burnout                | 1528.71       | 1520.74       | 1521.34   | 1519.80       | 1888.55   | 1888.78 | 1247.33   | 1249.34 |               |          |
| TTS separation                     | —             | —             | —         | —             | 1904.75   | 1904.25 | 1263.53   | 1264.4  |               |          |
| Actual launch date                 | Dec. 16, 1965 | Aug. 17, 1966 | —         | Dec. 13, 1967 | —         | —       | —         | —       | Aug. 27, 1969 | —        |
| Actual launch time                 | 0231:20 EST   | 1020:17 EST   | —         | 0908:00 EST   | —         | —       | —         | —       | 0946:29 GMT   | 1759 EDT |

<sup>a</sup> First stage hydraulic pressure lost at 214 sec. Destruction by Range Safety Officer at 483.9 sec.  
<sup>b</sup> For one motor; the other two augmentation motors were jettisoned at 69.992 sec.

the C-band beacon aboard the Delta and the S-band telemetry signal from the spacecraft. From liftoff to 5000 ft altitude, AFETR optical equipment provided additional metric data.

### Spacecraft Performance

The spacecraft were nearly dormant during powered-flight stages. About 5 min before launch, each spacecraft was put on internal power. The spacecraft low-gain antenna 2 was connected to the transmitter-driver rather than to one of the TWTs, to conserve battery power. Consequently, only about 40 mW of signal power were broadcast until the TWT was switched on. Housekeeping telemetry during launch was set at 64 bps—a relatively low rate—to increase the likelihood of obtaining good diagnostic data at the low power level should the TWT fail to turn on.

As soon as the spacecraft separated from the Delta third stage, the booms and Stanford antenna automatically deployed and locked

TABLE 3-2.—*Tracking and Data Acquisition Support Stations through DSS Acquisition*

| Range/<br>network | Station                                 | Used during Pioneer flights |   |   |   |                |
|-------------------|---|-----------------------------|---|---|---|----------------|
|                   |   | 6                           | 7 | 8 | 9 | E              |
| AFETR             | 1 Cape Kennedy and Patrick AFB          | X                           | X | X | X | X              |
|                   | 3 Grand Bahama I                        | X                           | X | X | X | X              |
|                   | 7 Grand Turk I                          | X                           | X | X | X | X              |
|                   | 91 Antigua I                            | X                           | X | X | X | X              |
|                   | 12 Ascension I                          | X                           | X | X | X | X              |
|                   | 13 Pretoria, S.A.                       | X                           | X | X | X | X              |
|                   | <i>Twin Falls</i> (ship)                | X                           | X | X | X |                |
|                   | <i>Coastal Crusader</i> (ship)          | X                           | X | X | X |                |
|                   | <i>Sword Knot</i> (ship)                |                             | X |   |   |                |
| MSFN              | Merritt I.                              |                             |   |   |   | X              |
|                   | Bermuda                                 | X                           | X | X | X | X              |
|                   | Grand Bahama                            |                             |   |   |   | X              |
|                   | Antigua                                 |                             |   |   |   | X              |
|                   | Ascension I                             | X                           | X | X | X | X              |
|                   | Tananarive, Malagasy Rep.               | X                           | X | X | X | X              |
| DSN               | <i>Vanguard</i> (ship)                  |                             |   |   |   | X              |
|                   | DSS-71, Cape Kennedy                    | X                           | X | X | X |                |
|                   | DSS-72, Ascension I.                    | X                           | X | X |   |                |
|                   | DSS-51, Johannesburg, S.A.              | X*                          | X | X | X | X <sup>b</sup> |
|                   | DSS-41, Woomera, Australia <sup>c</sup> |                             |   | X |   |                |

\* Commanded partial Type-II orientation. This maneuver was commanded from Goldstone on Pioneer 9.

<sup>b</sup> Scheduled, but not actually used due to abort.

<sup>c</sup> The primary DSN acquisition station for Pioneer 8.

into position. Power was applied to the TWT and the orientation subsystem, again automatically. The Type-I orientation maneuver then began and proceeded in the manner described in Chapter 2. When the low-gain antenna was switched from the transmitter driver to the TWT, the telemetry signal from the spacecraft faded for about a minute while the TWT warmed up. By the time Johannesburg rose, the spacecraft was transmitting at about 7 W. It was fully operational and had completed one Type-I orientation maneuver. Upon acquisition the first commands generally sent were:

- (1) Switch to 512 bps
- (2) Repeat the Type-I orientation maneuver.

### FROM DSS ACQUISITION TO THE BEGINNING OF THE CRUISE PHASE

The period of several hours stretching between the initial acquisition of the spacecraft by one of the DSN stations and the beginning of the cruise phase encompasses several events crucial to the success of the mission:

- (1) Two types of orientation maneuvers
- (2) Experiment turn-ons
- (3) The first thorough assessment of spacecraft health in flight
- (4) The first passes over all participating DSN stations

Prior to DSS acquisition, the spacecraft automatically went through the Type-I orientation maneuver. This event was started by switches triggered when the deploying appendages locked into position. By the time the spacecraft was acquired by DSN, spacecraft power was on and the transmitter was sending telemetry. In addition, the spin axis was almost perpendicular to the sunline by virtue of the automatic Type-I orientation maneuver.

The first command dispatched after a two-way lock had been established was usually that which changed the telemetry bit rate from Format C, 64 bps, to Format C, 512 bps. Next, a command initiating the Type-I orientation maneuver was sent to refine the alignment made automatically prior to acquisition and, more important, to preclude the possibility that the automatic orientation sequence may have terminated prematurely. The third in the series of preparatory commands was "Undervoltage Protection On," but this was sent only if analysis by the Spacecraft Analysis and Command (SPAC) Group (located at the SFOF during launch) was confident that the spacecraft power level was normal and that the spacecraft was operating properly. Following the spacecraft's execution of Undervoltage Protection On, the Pioneer was ready for experiment turn-on and the all important Type-II orientation maneuvers.

The purpose of the Type-II maneuver was the rotation of the spacecraft spin axis about the Sunline until the spin axis was perpendicular to the plane of the ecliptic. As explained more fully in Chapter 2, this maneuver was normally controlled from Goldstone where Operations Orientation Director (OOD) maximized the telemetry signal received from the Pioneer's high-gain telemetry antenna. Generally, hundreds of Type-II orientation commands were relayed to the spacecraft, each giving rise to a pulse of gas from the orientation subsystem. There was some jockeying back and forth across the peak in the signal-strength reception curve. On occasion, the normal Type-II orientation process was interrupted for another Type-I maneuver to remove any spin-axis misalignment inadvertently introduced by cross coupling during Type-II maneuvers.

Preliminary trajectory analysis in the cases of Pioneers 6 and 9 indicated that partial Type-II orientation would be desirable early in the flight to preclude an unfavorable spacecraft orientation later in the flight. This special maneuver was necessary because the low-gain omnidirectional antenna used for communication early in the flight had a very low gain within about  $10^{\circ}$  aft of the spin axis. During the partial Type-II orientation maneuver the gas pulses torqued the spin axis sufficiently so that Goldstone antennas would not be looking up this cone at the spacecraft during the final Type-II orientation maneuver. The final Type-II orientation maneuvers were always directed from Goldstone. Special equipment for this task, as well as the OOD and his team, were located there.

## SPACECRAFT PERFORMANCE DURING THE CRUISE PHASE

The Pioneer spacecraft were designed for a minimum life of 6 months each. Each greatly exceeded this goal. In fact, each spacecraft functioned well for several years, their longevity confirming the design decisions made by Ames and TRW Systems in the early 1960's. This section is concerned with spacecraft performance in orbit around the Sun.

### Pioneer-6 Performance

The nominal Pioneer-6 mission extended from December 16, 1965, to June 18, 1966—a total of 180 days. However, because spacecraft performance at the end of 180 days continued to be good and the 210-ft dish at DSS-14 became available for long-distance tracking, the mission was extended.

Although each Pioneer surpassed the goals set for it, each spacecraft had its share of minor problems. On Pioneer 6, for example, a

gas leak in the orientation control subsystem caused some concern. And the degradation of the Sun sensors plagued every Pioneer until Pioneer 9's ultraviolet filters finally solved the problem.

### Pioneer-7 Performance

As the spacecraft began the long cruise phase, all spacecraft subsystems appeared to be operating normally. On August 25, 1966, however, TWT 1 began to display anomalous performance in the noncoherent mode of operation, although operation was normal in the coherent mode. The helix current jumped to 10.2 mA as compared to the normal 6.1 mA, and the temperature rose to 180° F from the normal 101° F. On August 31, 1966, Ames personnel decided to switch in TWT 2. This TWT behaved normally in every respect. Except for this difficulty, which was overcome by design redundancy, spacecraft performance during the basic 180-day mission was excellent.

### Pioneer-8 Performance

The Earth-escape hyperbola for Pioneer 8 was less energetic than planned. Instead of occurring at roughly 500 Earth radii, syzygy took place at 463 Earth radii. The heliocentric orbit is less eccentric and more inclined than the planned orbit, but the differences are not significant. The spacecraft has performed normally except for the deviations noted below.

Early in the mission, trouble was experienced with the Ames plasma probe and it was subsequently turned off. However, the difficulty was ultimately traced to a corona discharge resulting from outgassing. Later, the Ames experiment was switched back on and it operated without further trouble.

During an orientation maneuver in March 1968, Sun sensor D was found to be inoperative. On another orientation attempt in June 1968, Sun sensors A, B, and C were also found to be out of commission. The heavier Sun-sensor covers installed on Pioneer 8 had obviously not solved the degradation problem.

### Pioneer-9 Performance

Pioneer 9, an inbound flight, was subjected to increasing solar radiation, higher solar-array temperatures, and, consequently, falling bus voltages. To prevent the discharge of the battery, it was switched off on January 14, 1969.

To check the effects of the newly installed ultraviolet filters on

the Sun sensors, a special test was conducted on February 5, 1969, the 89th day of flight. Telemetry indicated that Type-I and Type-II commands were executed properly. The ultraviolet filters had apparently solved the Sun-sensor degradation problem.

The spacecraft reached perihelion at 0.754 AU on April 8, 1969. The spacecraft was designed to penetrate to only 0.8 AU, but it reached 0.754 AU without overheating, although the cosmic-ray experiment reached its upper temperature limit.

All spacecraft systems operated normally throughout the 180-day mission. During the extended mission, in May 1969, the communication range reached 130 million km (78 million miles) using only the 85-ft DSN antennas. This extension of the communication range can be attributed to three factors:

- (1) Use of linear polarizers at some DSN stations
- (2) Improvement of noise temperatures at the DSN stations
- (3) Use of the Convolutional Coder Unit on Pioneer 9 (See below.)

The CCU, described in Chapter 2, was added to Pioneers D and E as an engineering experiment. It can be switched in or out of the telemetry stream. CCU performance has been good, contributing about 3 dB to the communication power budget. In effect, the CCU increased the maximum communication range for Pioneer 9 at each bit rate by 40 percent.

Between the launch date on November 6, 1968, and December 10, 1968, the spacecraft operated in the uncoded mode at 512 bps, except for CCU functional checks. Since December 10, the CCU has been in almost constant use except when the spacecraft was being worked by a DSN without Pioneer Ground Operational Equipment (GOE).

About January 7, 1969, Pioneer 9 was far enough away from the CCU to provide a "coding gain" for DSN stations configured for receiving circularly polarized waves.<sup>13</sup> Up to March 6, 1969, GOE-equipped DSN stations tracked Pioneer 9 for about 1000 hr with the CCU in operation; 680 hr were in the coding gain region. As a result of the CCU's coding gain,  $4.43 \times 10^8$  additional bits were received during this period. The 3 dB gain at 512 bps was verified by direct comparison with uncoded data at 256 bps. The CCU experiment has been so successful on Pioneer 9 that convolutional coding is being applied to other spacecraft.

<sup>13</sup> The Pioneers transmit linearly polarized signals. A 3 dB loss is incurred when a DSN receiving circularly polarized signals is used.



## Pioneer Scientific Results

THE SCIENTIFIC LEGACY of the Pioneer Program will not be complete for many years. Scientific papers based upon the data telemetered back from deep space are still being published in abundance. Meanwhile, all four successfully launched spacecraft at this writing continue to operate successfully. The Pioneer scientific record, though incomplete, is impressive—some 150 contributions to the literature as of early 1971. Some of these papers and their implications are summarized in the following pages.

### THE GODDARD MAGNETIC FIELD EXPERIMENT

By December 1965, when Pioneer 6 was launched, satellites had confirmed the theoretical prediction of a basically spiral solar magnetic field imbedded or "frozen" in the streaming solar plasma. The Sun's rotation about its axis imposed the "water sprinkler" pattern on the outwardly rushing plasma (fig. 4-1).

Pioneer-6 data confirmed that the interplanetary magnetic field often changes direction abruptly without changing magnitude. This phenomenon was interpreted at that time in terms of intertwined filamentary or tube-like structures in interplanetary space which, on a large scale, display the classical spiral structure but which, on a small scale, create a twisted microstructure.

Generally early Pioneer magnetometer data tended to confirm the Earth shock structure, the magnetopause, and the spiral sector structure of the interplanetary field inferred from previous spacecraft flights.

Outward-bound Pioneers carried Goddard magnetometers through the region where the geomagnetic tail was expected to exist. This region was crossed by Pioneer 7 between September 23 and October 3, 1966, at distances ranging from 900 to 1050 Earth radii. A coherent, well-ordered geomagnetic tail with an imbedded neutral sheet was not observed by Pioneer 7. However, the rapid field reversals recorded are characteristic of the neutral sheet region observed closer to Earth. The conclusion at Goddard was that the geometry of the tail changes to a complex set of intermingled filamentary

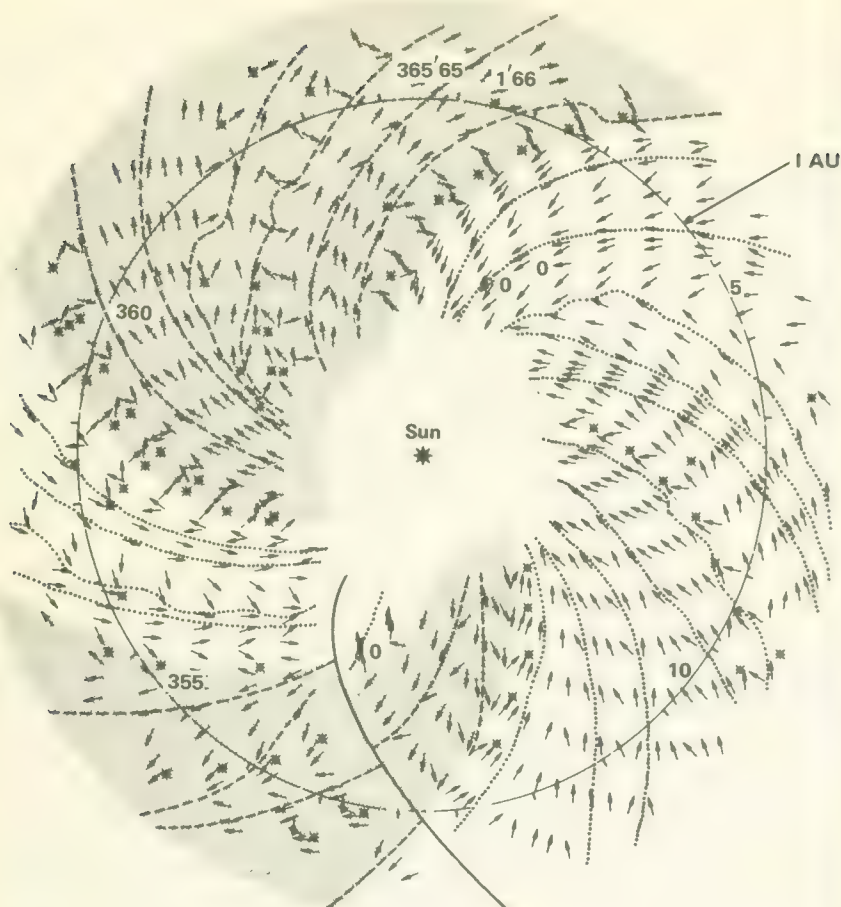


FIGURE 4-1.—Sector structure of the interplanetary magnetic field from Pioneer 6 data telemetered between Dec. 18, 1965, and Jan. 14, 1966. Each arrow represents an equivalent flux of  $5\gamma$  for 6 hr. Shaded regions are those where the field is directed away from the Sun; field was antisolar elsewhere. From: Schatten, Ness, and Wilcox: *Solar Physics*, vol. 5, p. 250, fig. 8, 1968.

flux tubes at several hundred Earth radii. Later analysis led to a "discontinuous" model.

The new model recognizes the fact that field discontinuities on the mesoscale and microscale—in both magnitude and direction—are more prevalent than previously suspected, and that their character does not always imply the existence of filaments.

Pioneer magnetometer results have also helped provide insight into what happens in interplanetary space when a major solar event, such as a large flare, occurs. The following observations based on

Pioneer-8 telemetry represent about what one would expect from the general model of a solar disturbance propagating through space.

(1) A rather steady field of  $4$  to  $6\gamma$  was observed during the early hours of February 25.

(2) The field increased rapidly to near  $10\gamma$  between 2000 and 2022, then it rose slowly to about  $14\gamma$ .

(3) Long-period variations were observed between 0200 and 0500, February 26.

(4) A very quiet field of about  $6\gamma$  occurred between 2000 and 0500, February 27.

(5) The next group of telemetered data at 2149, February 27, again revealed a high field (over  $10\gamma$ ). Large variations were noticed.

(6) In the last time interval telemetered, between 0200, February 28, and 0500, February 29, the field had dropped to normal values.

### THE MIT PLASMA PROBE

The preliminary MIT data indicated first, that sharp changes in the plasma density preceded the dramatic changes in the magnetic field recorded by the Goddard magnetometer, and second, that the peaks in number density were followed by periods of increased bulk velocity.

The MIT group later published additional correlations between their plasma-probe and magnetometer data. The simultaneous changes in plasma and magnetic parameters were consistent with what one would expect from tangential discontinuities. High-velocity shears were observed across these discontinuities; the largest was about 80 km/sec. The discontinuities observed by the MIT plasma probe were undoubtedly due to the same filament boundaries or discontinuities discussed in the papers published by the Goddard group.

The MIT plasma-probe and Goddard magnetometer data also showed that these discontinuities have preferred directions in space, with a tendency for the solar wind to be fast from the west and slow from the east. This east-west asymmetry in solar-wind velocity is a natural result of the rotation of the Sun—the water sprinkler effect again.

Pioneer 6 carried the MIT plasma probe through the magneto-sheath in the dusk meridian on December 16, 1965. While the data confirmed some portions of the various theories developed to describe the magnetosheath, the proton distribution measured was bi-Maxwellian rather than the classical single-peaked curve. Roughly 10 percent of the total number density was estimated to reside in the high-energy tail (fig. 4-2). Apparently the high-energy tail was

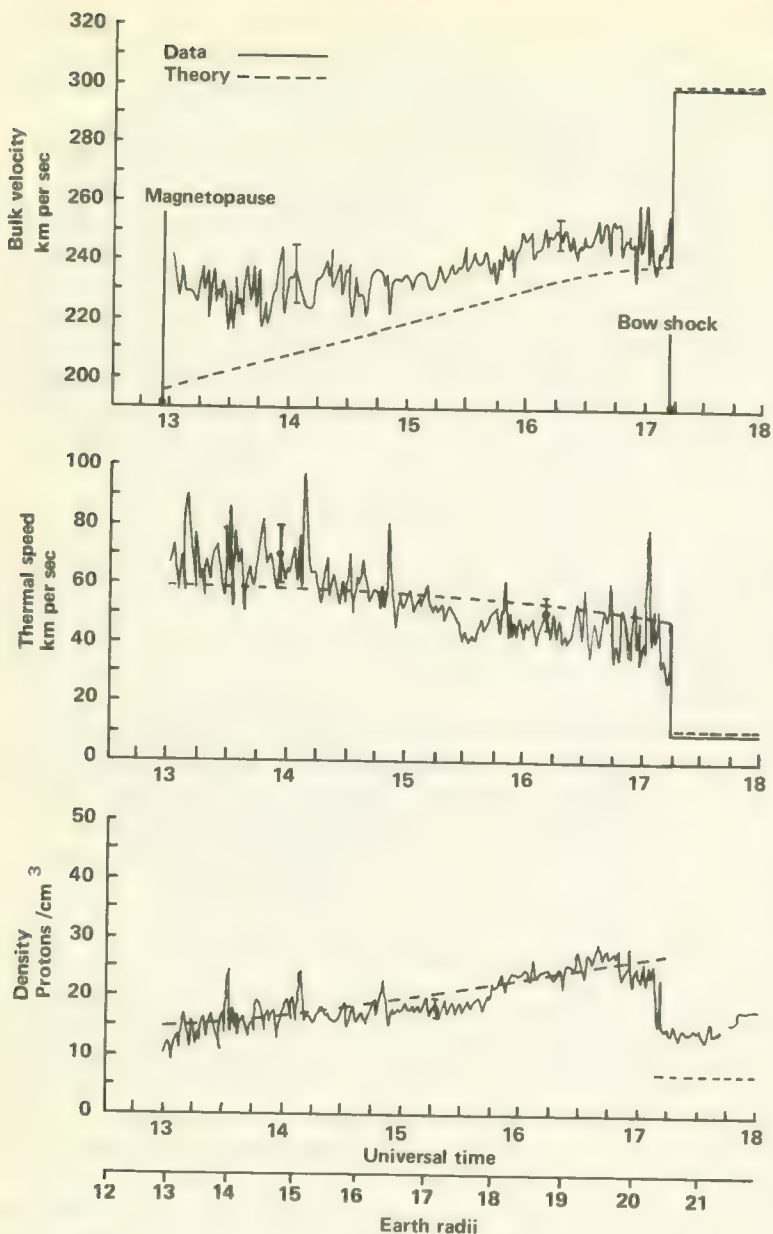


FIGURE 4-2.—Pioneer 6 magnetosheath proton observations showing velocity, thermal speed, and number density. From: Howe: J. Geophys. Res., vol. 75, p. 2434, fig. 4, May 1, 1970.

composed of solar plasma particles penetrating through the magnetosheath and eventually swerving to travel in the direction of the bulk flow within the magnetosheath.

The electron flux was more complex, with three distinct regions being observed. The first region, from 9 to 11.5 Earth radii, was characterized by angularly isotropic fluxes in all four electron channels. The electron energy spectrum indicated that the electrons formed a plasma sheet in this region. The second region, 1.5 Earth radii thick, was bounded at the outer edge by the magnetopause. The electron distribution in this region could be explained by two models. Using a thermodynamic model, the distribution matched that of a Maxwellian having a pressure of about 300 ev/cu cm, with the temperature parallel to the local magnetic field about twice that perpendicular to the field. In the third region, the magnetosheath, itself, the following parameters were typical: thermal electron energy—40 eV; electron speed—2700 km/sec; electron temperature—100 000° K.

### THE AMES PLASMA PROBE

The Block-I and Block-II plasma probes built by Ames Research Center record the energy spectra of electrons and positive ions in the solar plasma as functions of azimuth and elevation angles. For a more complete understanding of the interplanetary medium, it is essential to relate plasma probe results to the magnetometer data and, of course, the somewhat different perspectives apparent to the MIT Faraday-cup plasma probe and the TRW Systems electric field detector.

Figure 4-3 shows one type of data acquired by the Ames plasma probe: energy spectra and angular spectra. The energy spectrum indicates a proton peak at 1350 V, corresponding to a proton velocity of approximately 510 km/sec. The second peak in the curve was due to alpha particles. However, analysis of subsequent data revealed the possible presence of singly ionized helium in the solar wind—the first time this had been detected.

The early data also revealed an average solar wind electron temperature of about 100 000° K during quiet times when the solar wind was blowing at about 290 km/sec, with a maximum ion temperature of 50 000° K.

As Pioneer 6 passed through the Earth's magnetopause, the Ames plasma probe measured the temperature of solar electrons in the bow shock at 500 000° K. Here, ion temperatures were about the same as electron temperatures, but, in contrast, the ions did not cool off downstream from the Earth.

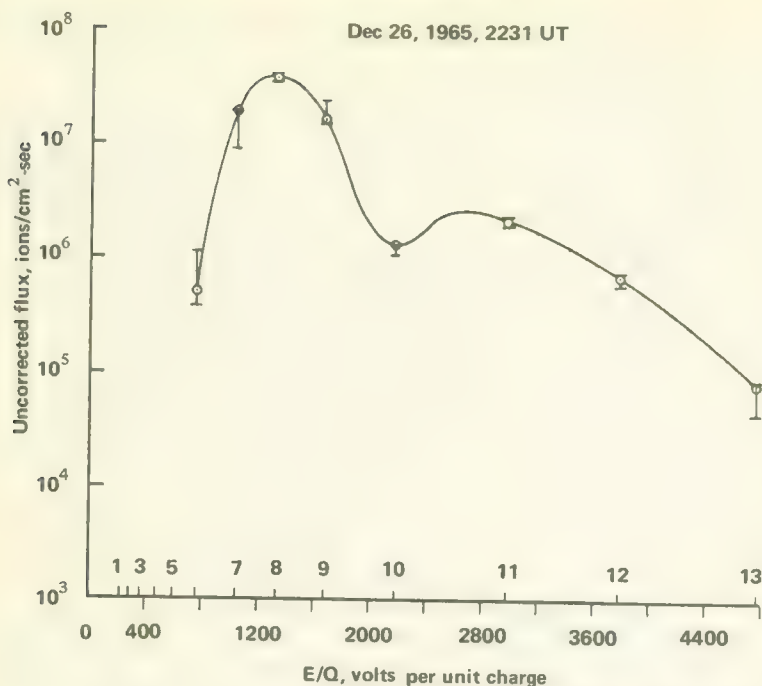


FIGURE 4-3.—Pioneer 6 Ames plasma probe  $E/Q$  spectrum, Dec. 26, 1965, 2231 UT, showing the hydrogen peak at approximately 1350 V, with the helium peak estimated at 2700 V. From Wolfe, et al.: J. Geophys. Res., vol. 71, p. 3330, fig. 2, July 1, 1966.

Pioneers 7 and 8 were outward missions and swept through the Earth's tail early in their flights. Instruments on both spacecraft detected evidence of the Earth's tail or "wake" with their magnetometers and plasma probes. The Ames plasma probes detected the wakes at about 1000 and 500 Earth radii for Pioneers 7 and 8, respectively.

The Ames investigators felt, on the basis of their data, that the following interpretations were possible:

- (1) The observations could represent a turbulent downstream wake if the Earth's magnetosphere closed between 80 and 500 Earth radii.
- (2) If the solar wind diffuses into the magnetic tail, the plasma probe measurements could be due to the tail "flapping" past the spacecraft.
- (3) The tail might have a filamentary structure at these distances (500 and 1000 Earth radii) and the disturbed data could arise at filament boundaries.

(4) Possibly, the tail might have disintegrated into "bundles" at these distances.

(5) If magnetic merging occurred, subsequent acceleration of pinched-off gas may have caused the disturbed conditions that were measured.

Prior to Pioneer 6, few spacecraft were capable of making detailed measurements of the solar wind. Consequently, the collisionless interplanetary plasma was treated as a single magnetofluid. However, the Ames plasma probes have revealed that the solar proton distribution is definitely anisotropic, with the temperature parallel to the local magnetic field being larger than that perpendicular to the local magnetic field.

### THE CHICAGO COSMIC-RAY EXPERIMENT

The Chicago cosmic-ray telescope on the Block-I Pioneers provided the opportunity for scientists to investigate the direction of arrival of cosmic-ray particles near the plane of the ecliptic. The experiment also had a short enough time resolution so that rapid fluctuations in cosmic-ray intensity could be recorded. The first test case came shortly after the launch of Pioneer 6, when solar-flare protons were detected on December 30, 1965.

The solar flare that erupted about 2 weeks after the launch of Pioneer 6 was given an importance rating of 2. The effects were noted for almost a week, as indicated in figure 4-4. Interplanetary conditions during most of this period were remarkable free of solar-flare blast effects capable of modulating the galactic cosmic-ray flux. Solar protons in the energy range 13 to 70 MeV first arrived at the spacecraft at about 0300 UT, December 30, 1965, with lower energy particles arriving later. The anisotropy of these protons was striking. The average direction of particle flow about halfway between the Sunline and the angle would be expected if the particles traveled along the water-sprinkler spiral lines. However, the detailed data reveal a more complex situation:

(1) The direction of the peak amplitude was highly variable, changing direction by as much as  $90^\circ$  within 10 min.

(2) Relative to the intensities in other directions, the peak intensive varies rapidly.

(3) Occasionally, the angular distribution was strongly peaked within a  $45^\circ$  sector.

(4) Rarely, two intensity peaks  $180^\circ$  apart were noted.

The strong collimation of solar protons with energies greater than 13 MeV suggests that there are few irregularities in the propagation path from the Sun that could scatter the protons. However, the

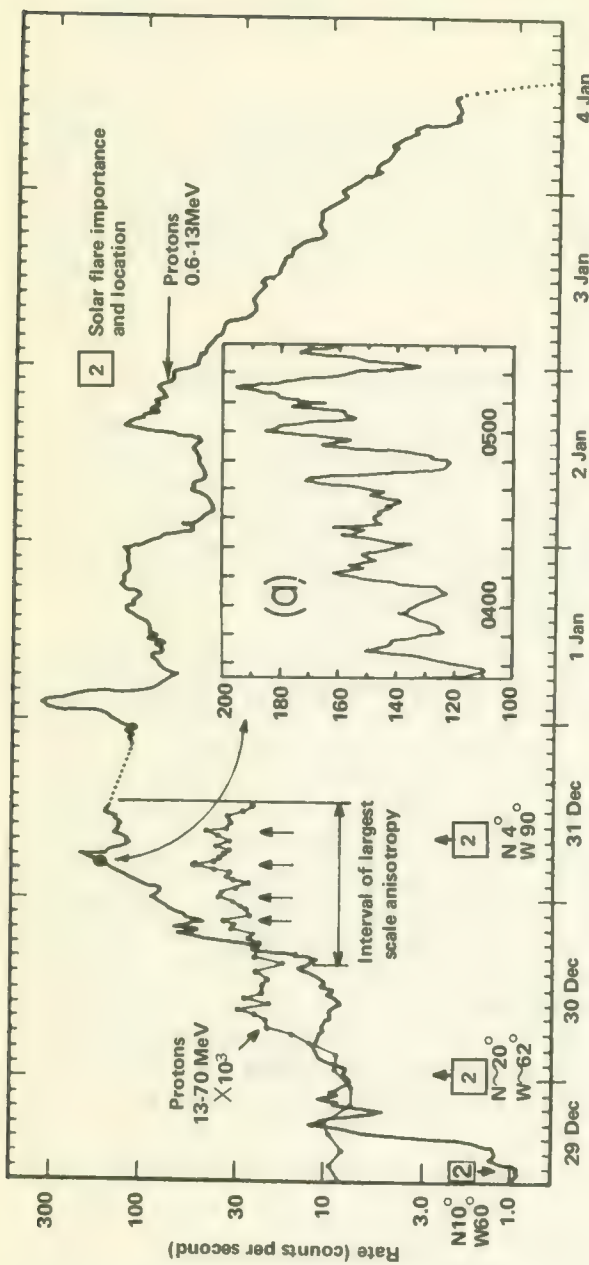


FIGURE 4-4.—The intensity-time distribution of protons of 0.6- to 13-MeV energy and protons of 13- to 70-MeV energy. Anisotropies were observed for a period of approximately 2 days after the flare of Dec. 30, 1965. The arrows refer to quasi-periodic bursts of period  $\sim 4$  hr. Insert (a) is an expansion of the region shown within the circle. Data points are  $\sim 56$  sec apart. Note the quasi-periodic oscillations of  $\sim 15$  min. From: Fan et al.: J. Geophys. Res., vol. 71, p. 3291, fig. 3, July 1, 1966.

rapid changes in direction of the peak flux vector supports the conclusion from Goddard magnetometer and GRCSW cosmic-ray antisotropy data that there are many short-term, rather localized changes in the Earth's magnetic field.

Corotation effects were noted early in flight by the Chicago instrument, supporting the joint observations of several other Pioneer-6 instruments and similar instruments on spacecraft elsewhere in the solar system.

Proton flux increases over the period from December 1965 through September 1966 have been unambiguously associated with specific solar flares. Enhanced solar proton fluxes in the energy range of 0.6 to 13 MeV have been recorded from specific active regions from ranges as great as  $180^\circ$  in longitude. The enhanced fluxes were characterized by definite onsets when their associated active centers reached points from  $60^\circ$  to  $70^\circ$  east of the central solar meridian. Cutoffs occurred at from  $100^\circ$  to  $130^\circ$  west. Coupled with the detection of associated modulations of the galactic cosmic-ray flux, these observations again point to the existence of corotating magnetic regions associated with the active centers on the Sun. Observations seem to show that solar-flare protons propagate along the spiral interplanetary field from the Sun's western hemisphere. Present evidence supports the view that the solar protons arise from processes continually occurring in the solar active centers.

Further inferences from the Chicago data are:

(1) Most of the particles observed during the solar minimum are of galactic origins.

(2) Relativistic electrons were detected only in the neutral sheet of the geomagnetic tail, pointing to the possible acceleration of these electrons by the split magnetic field.

### THE GRCSW COSMIC-RAY EXPERIMENT

The primary mission of the GRCSW experiment was the measurement of anisotropy in the distribution of cosmic rays within the solar system, but still far enough away from the Earth to avoid its perturbing magnetic field. The construction of a theoretical model describing how cosmic rays are propagated through the solar system depends upon the accurate measurement of cosmic rays with energies less than 1000 MeV. Because the weaker cosmic rays, especially those originating on the Sun, are affected by the solar magnetic field and the plasma in which it is imbedded, the GRCSW data must be examined in conjunction with the results of the Pioneer plasma and magnetometer experiments.

The extent of the anisotropy of low-energy solar protons during

early flight was striking. Since scattering normally reduces anisotropy, these results imply that little scattering transpired since the cosmic rays were injected into the interplanetary field near the Sun. In contrast, the anisotropy of relativistic cosmic rays is known to be obliterated quickly.

From Pioneer anisotropy data collected during 1965 and 1966 for periods when solar flare effects were not seen and considering only cosmic rays in the vicinity of 10 MeV/nucleon, the conclusions were:

- (1) The 10 MeV/nucleon cosmic rays possessed a density gradient directed toward the Sun; i.e., density increases sunward, as expected.
- (2) These low-energy cosmic rays are predominantly of solar origin even during the sunspot minimum.
- (3) The density gradient frequently reverses in the range  $10 < E < 1000$  MeV.
- (4) Cosmic radiation between 10 and  $10^5$  MeV corotates with the Sun.

Studies of the large-scale, steady-state structure of interplanetary space have also been made by comparing Pioneer data with those from other spacecraft. It was concluded that there exist numerous, long-lived regions of modulated cosmic-ray flux following the general spiral configuration of the interplanetary magnetic field as it corotates with the Sun.

The GRCSW and Goddard groups introduced the filament concept. The main thrust of this concept was that the observed anisotropies of low-energy cosmic rays could be divided into two groups:

(1) Equilibrium anisotropies are most evident toward the end of a solar-flare event. The maximum cosmic-ray flux is always directed away from the Sun (fig. 4-5), and the anisotropy amplitude is low (5 to 15 percent). Perhaps of most significance is the fact that the anisotropies are not dependent upon the detailed nature of the interplanetary magnetic field.

(2) Nonequilibrium anisotropies change direction in time and have amplitudes between 20 and 50 percent. These anisotropies are aligned—parallel or antiparallel—to the magnetic field.

These observations were interpreted as possible evidence of complex loops in the magnetic field.

The GRCSW group also related Pioneer cosmic-ray data to cosmic-ray flare effects and energetic-storm-particle events. The data used came from Pioneers 6 and 7 and covered 29 solar flares occurring between December 16, 1965, and October 31, 1966. Some of the more important conclusions expressed in the first paper on this subject were:

- (1) Solar cosmic rays are normally extremely anisotropic with

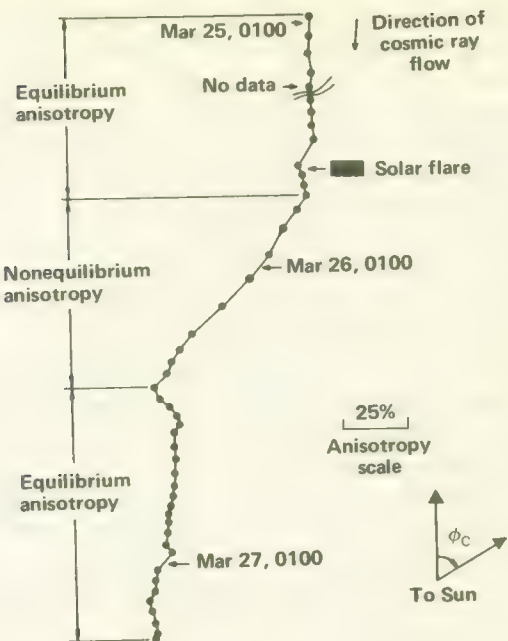


FIGURE 4-5.—The difference between the equilibrium and nonequilibrium classes of cosmic-ray anisotropy. The amplitudes and azimuths of the mean anisotropy for each hour are plotted as a vector addition diagram. Note definition of  $\phi_c$ . From: McCracken, Rao, and Ness: J. Geophys. Res., vol. 73, p. 4160, July 1, 1968.

the direction of maximum flux aligned parallel to the magnetic field vector during the first part of the solar event.

(2) During the late portion of the flare, the cosmic rays are in diffusive equilibrium.

(3) Under some circumstances, the propagation of cosmic rays from the Sun to Earth is completely dominated by a "bulk motion" propagation mode. Here, the cosmic rays do not reach the spacecraft until the magnetic regime into which they were injected engulfs the Earth.

(4) In two cases, the anisotropy and cosmic-ray times of flight infer diffusion of the cosmic rays to a point on the western portion of the solar disk before injection into the magnetic field.

(5) Simultaneous observation by both Pioneers when separated by  $54^\circ$  of azimuth indicate density gradients of about two orders of magnitude per  $60^\circ$  sector during the initial stages of a solar flare.

(6) A study of cosmic-ray scattering within the solar system indicates a mean free path of about 1.0 AU for large-angle scattering.

A second paper dealt with the energetic-storm-particle event,

which was defined as the very marked enhancement of cosmic rays in the 1 to 10 MeV range near the onset of a strong terrestrial magnetic storm. Data relating to seven such events were extracted from Pioneer-6 and Pioneer-7 telemetry. The data indicated a near 1-to-1 correspondence between the energetic-storm-particle events and the beginning of a Forbush decrease. It was shown further that the bulk of the energetic-storm particles are apparently not trapped in the magnetic regime associated with the Forbush decrease. The Pioneer cosmic-ray data tend to support the Parker "blast wave" model, in which the charged particles are accelerated by the magnetic field within the shock front.

The GRCSW group also compared the characteristics of corotating the flare-induced Forbush decreases as derived from cosmic-ray data obtained from Pioneers 6 and 7. The results of this investigation are summarized in table 4-1.

Several solar-flare events have been examined in detail in the light of GRCSW cosmic-ray data and readings taken at several ground stations. By way of illustration, the results of the studies of the January 28, 1967, and March 30, 1969, events are summarized below. The salient features of the first event were:

- (1) The probable location of the responsible solar flare was about  $60^\circ$  beyond the west limb of the Sun.
- (2) Low-energy particles ( $<100$  MeV) recorded by the Pioneers and the high-energy particles ( $>500$  MeV) detected at Earth arrived after diffusion across the interplanetary magnetic field. Both groups of particles displayed remarkable isotropy.
- (3) The flux that would be observed by a detector ideally located in azimuth would be greater than  $2000$  particles  $\text{cm}^{-2}\text{-sec}^{-1}\text{-sr}^{-1}$  above 7.5 MeV.

TABLE 4-1.—*Comparison of the Properties of Corotating and Flare-Initiated Forbush Decreases*

| Corotating Forbush decrease   | Flare-initiated Forbush decrease  |
|---|---|
| Not accompanied by solar-generated cosmic rays                          | Accompanied by solar cosmic rays and an energetic-storm-particle event                  |
| Onset time difference due to corotation                                 | Probably simultaneous onset up to $\sim 100^\circ$ off the axis of the Forbush decrease |
| No amplitude dependence over $\sim 60^\circ$ of solar azimuth           | Amplitude varies by a factor of $\sim 4.0$ over $\sim 60^\circ$ of solar azimuth        |
| The energy dependence of both classes of events is essentially the same |   |

(4) Pioneer observations indicated low-energy injection commencing several hours before the high-energy main event.

### THE MINNESOTA COSMIC-RAY EXPERIMENT

The Minnesota cosmic-ray telescopes replaced the Chicago instruments on the Block-II Pioneer flights. The energy range of the Minnesota instrument was considerably higher (100 MeV/nucleon to over 22 BeV/nucleon) and, as intended, the research results are primarily concerned with galactic cosmic rays rather than the lower-energy particles originating on the Sun.

Although the carbon, nitrogen, oxygen, and "M" (for medium) nuclei are the most abundant nuclei in cosmic rays except for hydrogen and helium, their relative abundances have been in question until recently. New measurements of cosmic-ray nitrogen from balloons and Pioneer 8 have provided better estimates. The energy spectrum of nitrogen was found to be identical with those of the other M nuclei over the range from 100 MeV to over 22 BeV/nucleon. The ratio of nitrogen nuclei to all M nuclei was found to be about 0.125, constant to within 10 percent over the above energy range (fig. 4-6). Assuming that some of the nitrogen in the cosmic-ray flux originates in fragmentation reactions with interstellar matter and knowing the proper cross sections, one can compute a "source" N/M ratio less than about 0.03. However, the solar atmospheric value for the N/M ratio is about 0.10—a disturbingly higher value. The implication is that galactic and solar cosmic rays may originate in fundamentally different processes.

The Pioneer-8 instrument also identified and measured fluorine nuclei in the galactic cosmic rays. The fluorine abundance was 1 to 2 percent than that of oxygen for energies above 500 MeV/nucleon. These data on fluorine are consistent with the hypothesis that the fluorine is created by the fragmentation of heavier nuclei as they traverse roughly 4 g/sq cm of hydrogen in their flights through the galaxy.

Although Pioneer 8's orbit takes it only from 1.0 to 1.12 AU, the Minnesota instrument is sensitive enough to estimate cosmic-ray radial gradients within the solar system. First, the instrument measured differential energy spectra of protons and helium nuclei between 40 MeV/nucleon and 2 BeV/nucleon; the analysis in this range was two-dimensional, greatly reducing the background. Second, each event was assigned to one of four quadrants, permitting a study of the anisotropies associated with the gradients. The results of these measurements are presented in table 4-2. In general the cosmic-ray seems close to zero, however, it may be slightly positive in some

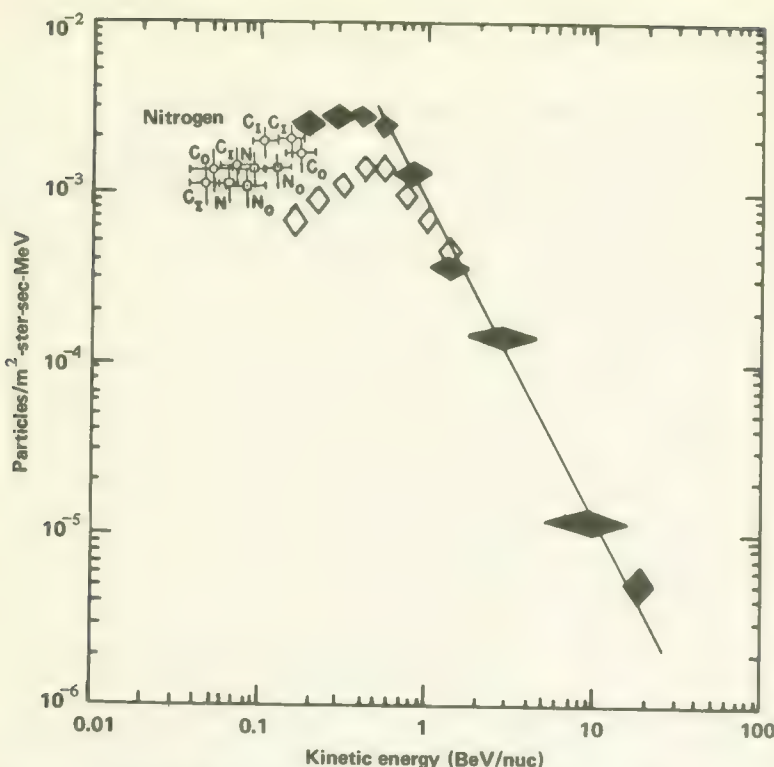


FIGURE 4-6.—Differential spectra of nitrogen nuclei measured by Pioneer 8 in 1968 (open diamonds) and from balloons in 1966 (solid diamonds). The low-energy points are from several satellites. From Lezniak et al.: *Astrophys. and Space Sci.*, vol 5, p. 106, fig. 1, 1969.

energy ranges. The data indicate that there are no significant anisotropies above about 240 MeV.

### THE STANFORD RADIO PROPAGATION EXPERIMENT

The Stanford radio propagation experiment operates in a closed loop which employs the 150-ft paraboloidal antenna and associated transmitting equipment at Stanford University, the spacecraft receiver and transmitter, and the facilities of NASA's Deep Space Network. Basically, the experiment measures the integrated electron content between the spacecraft and the Earth. Corrections for the Earth's ionosphere are made with the help of radio propagation measurements using Earth satellites, such as the Beacon Explorers.

Based upon Pioneer-6 data taken between February 2 and April

TABLE 4-2.—*Gradient and Anisotropy Proton Measurements on Pioneer 8*

| Energy           | Radial proton gradient, % | Radial proton anisotropy, % | Azimuthal proton anisotropy, % |
|------------------|---------------------------|-----------------------------|--------------------------------|
| >2 BeV           | -1.5±6                    | -0.31±0.28                  | -0.13±0.27                     |
| 1.25 BeV-2 BeV   | 0±7                       | +0.26±0.45                  | -0.38±0.44                     |
| 660 MeV-1.25 BeV | +23±8                     | +0.57±0.35                  | -0.55±0.44                     |
| 334 MeV-660 MeV  | +28±9                     | +0.36±0.38                  | -0.80±0.35                     |
| 240 MeV-334 MeV  | -7±11                     | +0.7±1.0                    | -0.60±1.0                      |
| 63 MeV-107 MeV   | +20±15                    |                             |                                |
| >60 MeV          | 0±5                       |                             |                                |
| 12 MeV-25 MeV    | 0±25                      |                             |                                |

9, 1966, the average electron number density was  $8.25 \text{ cm}^{-3}$ , with an rms value of  $4.43 \text{ cm}^{-3}$ . As Pioneer 6 moved farther out into space, it soon became apparent that the first values reported were unusually high due to high solar activity. The spread in measured values of the total interplanetary electron content is shown for Pioneer 6 in figure 4-7. The electron number density can be computed from the slopes of the lines drawn through these scattered points. The data in the figure yield an electron number density of  $5.74 \pm 4.1 \text{ cm}^{-3}$ . A similar procedure for Pioneer-7 data leads to the value of  $8.02 \pm 3.8 \text{ cm}^{-3}$ .

The measurements plotted in figure 4-7 owe their variation primarily to changes in solar activity and, consequently, the quantity of electrons injected into interplanetary space. Some of these injections—called plasma pulses or clouds—are fairly well-defined and have been mapped by the Stanford radio propagation experiment.

The Stanford group made a detailed study of the plasma cloud ejected by the July 7, 1966, solar flare. Although the radio propagation experiment was being operated beyond its nominal maximum range, the description of the plasma cloud derived from the measurements is compatible with data from the MIT plasma probe, which also measured the passage of a plasma shock at the same time. The shape and extent of the passing plasma cloud was calculated from the integrated electron content measured from Pioneer 6. Three cloud shapes—each deduced from a different data channel—seemed to fit the data (fig. 4-8).

When the Moon occulted the Pioneer-7 spacecraft on January 20, 1967, radio signals sent from the 150-ft Stanford antenna were diffracted by the edge of the lunar disk and also refracted by the lunar ionosphere. If there is no lunar ionosphere at all, only the classical Fresnel diffraction pattern will be measured. If an ionosphere

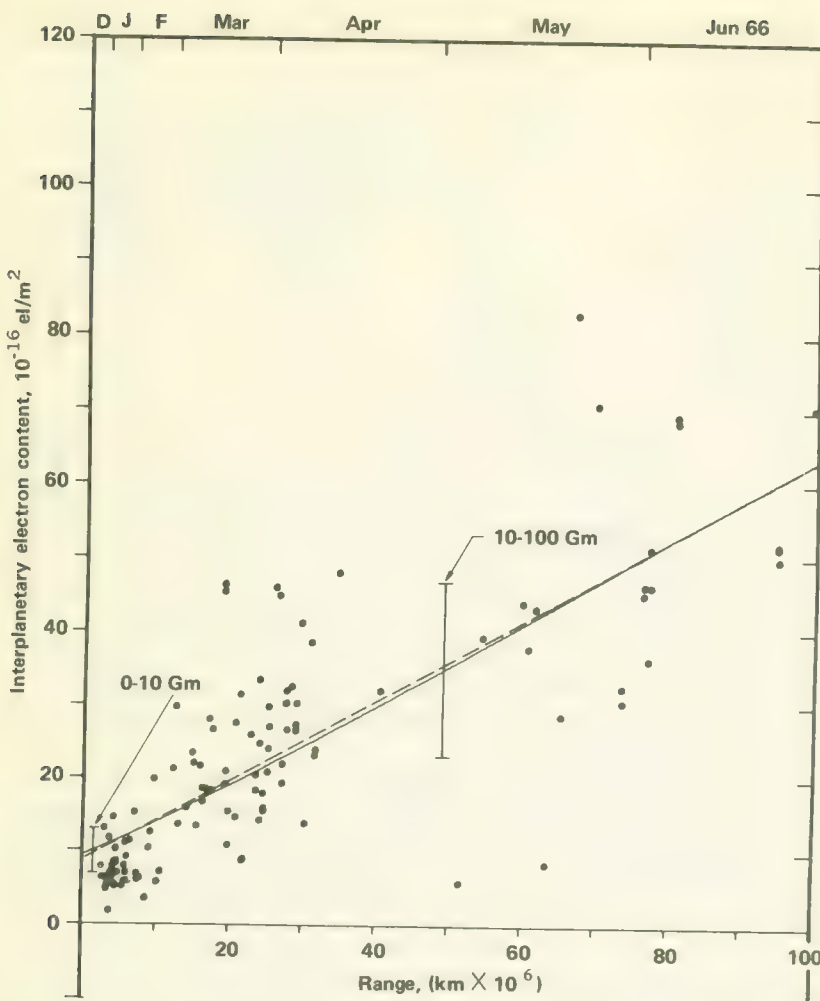


FIGURE 4-7.—Integrated electron content measured from Pioneer 6 to Earth as a function of spacecraft range. From: Koehler: SEL-67-051, p. 56, fig. 5-4, 1967.

is present, however, its refractive effects will displace the diffraction pattern in time. In this case, the difference in the angles of refraction for the 49.8- and 423.3-MHz signals was used to compute electron density.

The ray path from the Stanford antenna to Pioneer 7 was partially in the shadow of the Moon during immersion but was fully illuminated during emersion. The angles of refraction were  $-2.3$  microradians and  $-5.7$  microradians for immersion and emersion, respectively. The minus sign indicates that the electron density

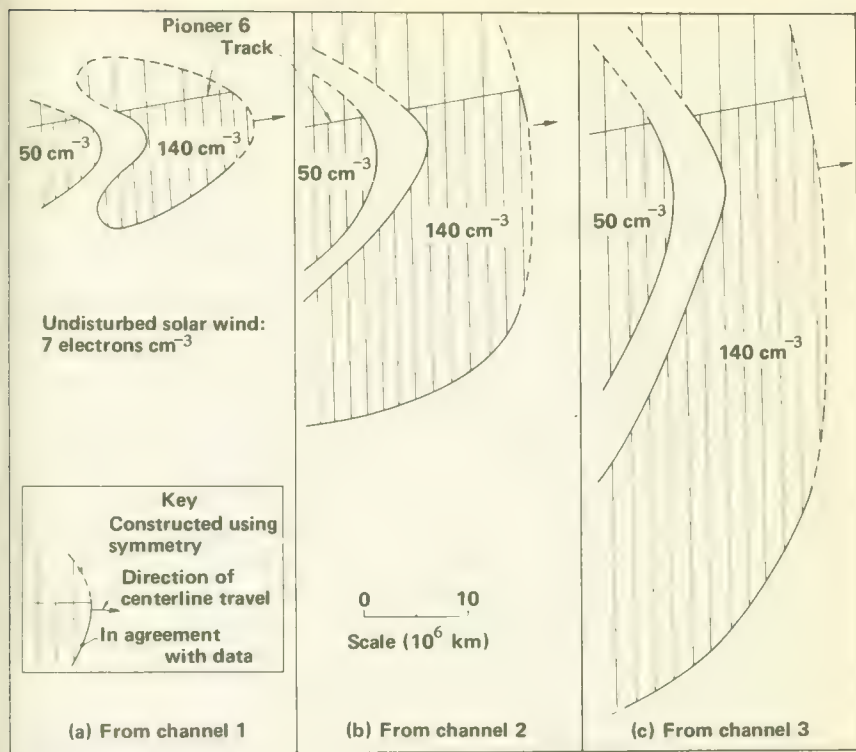


FIGURE 4-8.—Possible plasma cloud shapes. These shapes are consistent with measurements, but were restricted by simplifying assumptions and incorporate structural features based on prevailing theories about such cloud behavior. The configuration shown in (b) is considered the most likely. A gradient in density was actually measured along the Pioneer track and a lateral gradient also probably existed; consequently, the cloud must have been broader than the outlines shown. From: Landt and Croft: SU-SEL-70-001, 1970.

increases with height near the surface of the Moon, and that a tenuous ionosphere may be created—at least on the sunlit side—by the interaction of the solar wind with the lunar surface.

Useful scientific information can also be obtained concerning transient space phenomena by observing changes in the Faraday rotation of the signal from the spacecraft S-band transmitter. Levy and his associates at the California Institute of Technology and the University of Southern California have used the DSN 210-ft antenna at Goldstone to measure transient Faraday rotations during solar occultation of Pioneer 6. As the spacecraft line of sight approached the Sun, the S-band telemetry signal passed through increasingly dense regions of the solar corona. At three points between

6 and 11 solar radii, Faraday-rotation transients were recorded. The duration of each event was about 2 hours. The transients were poorly correlated with solar flares, but it was noted that bursts of radio noise in the dekameter range occurred prior to the observation of the Faraday rotation phenomena.

### TRW SYSTEMS ELECTRIC FIELD EXPERIMENT

Near the Earth's orbit the solar wind is very dilute, and the plasma is truly collisionless. Individual electrons and positive ions are influenced only by dc electromagnetic fields or by fields due to the organized motion of plasma particles in the form of ac plasma waves. The Pioneer Electric Field Experiment was designed to detect these microscopic plasma phenomena. The overall size of the Pioneer spacecraft and its appendages is small compared to the Debye length in interplanetary space and also the minimum wavelength for any undamped plasma oscillation. Thus, the spacecraft actually represents a "microscopic" measuring platform immersed in plasma phenomena of much greater fundamental size. The 423-MHz antenna of the radio propagation experiment is a relatively insensitive, but adequate, capacitively coupled sensor that detects plasma waves sweeping past the Pioneers in interplanetary space.

While magnetometers have helped scientists understand microscopic electromagnetic phenomena in space, the Pioneer Electric Field Experiment is electrostatic in nature—it was the first low-frequency (under 100 Hz) electric field experiment to be flown in space. The Pioneer instruments detect density fluctuations within the plasma rather than the motions of current systems indicated by magnetometers.

The following conclusions were made on the basis of early Pioneer-8 data:

- (1) Even when the Sun is quiet, low-frequency electric waves ( $\geq 100\text{Hz}$ ) can be detected in the solar wind.
- (2) Wave amplitudes at the lowest frequencies vary markedly with changing conditions in interplanetary space. These electric field changes are correlated with local changes in the plasma environment, as registered on the Ames plasma probe.
- (3) As Pioneer 8 moved away from the Earth, the effects of corotation and solar-wind travel times were evident when comparing disturbances recorded both on Earth and on the spacecraft.
- (4) Large-amplitude, high-frequency waves, detected when the spacecraft was far from Earth, are apparently the result of bursts of interplanetary electron oscillations.

Data from Pioneers 8 and 9 and OGO 5 were used to demonstrate

the several types of shock structures found in the high Mach-number solar plasma colliding with the Earth's magnetosphere. The most common structure reported was a large-amplitude magneto-hydrodynamic pulse having a characteristic length equal to the initial gradient and a trailing wavetrain.

The plasma-probe and electric-field data, recorded as Pioneer 8 crossed the Earth's geomagnetic tail during January 1968, indicated disturbances near the tail boundaries between 500 and 800 Earth radii downstream. The major conclusion of this paper was that tail breakup and field-line-reconnection phenomena begin within 500 Earth radii.

The initial results from the Pioneer-8 electric field experiment showed clearly their close correlations with terrestrially detected magnetic activity. Because the other Pioneer instruments also record space events—although from a different perspective—on-board correlations should also be obvious in many instances. Scarf has presented a three-way correlation during a Forbush decrease. Figure 4-9 indicates how the Pioneer-8 magnetometer, electric-field experiment, and the Minnesota cosmic-ray experiments all recorded the same event. Similar correlations have been made with data from other spacecraft.

### THE GODDARD COSMIC DUST MEASUREMENTS

During the early days of the Space Age, cosmic dust was thought to be a serious hazard to men and machines operating outside the Earth's protective atmosphere. More accurate measurements of cosmic dust particles have since shown these fears to have been unwarranted. Sensitive external surfaces on long-lived Earth satellites may suffer some degradation, but neither manned nor unmanned spacecraft have been compromised. Nevertheless, cosmic dust particles do exist and their presence in space demands a scientific explanation.

Are cosmic dust particles products of cometary disintegration or the debris from collisions within the asteroid belt? Most of our insight into this question at present comes from ground-based photographic and radar measurements of meteor trails. These data suggest that almost all cosmic dust trajectories are heliocentric with the orbital characteristics of comets rather than asteroids. Further, the particles seem "fluffy" and of low density. The Pioneer cosmic dust experiment, which flew on Pioneers 8 and 9, was designed to help answer this question of particle origin with *in situ* data from deep space.

During the first 390 days of continuous exposure of the Pioneer-8 sensors, numerous events (several per day) were recorded by the front sensor array *alone*, the rear sensor array *alone*, or the micro-

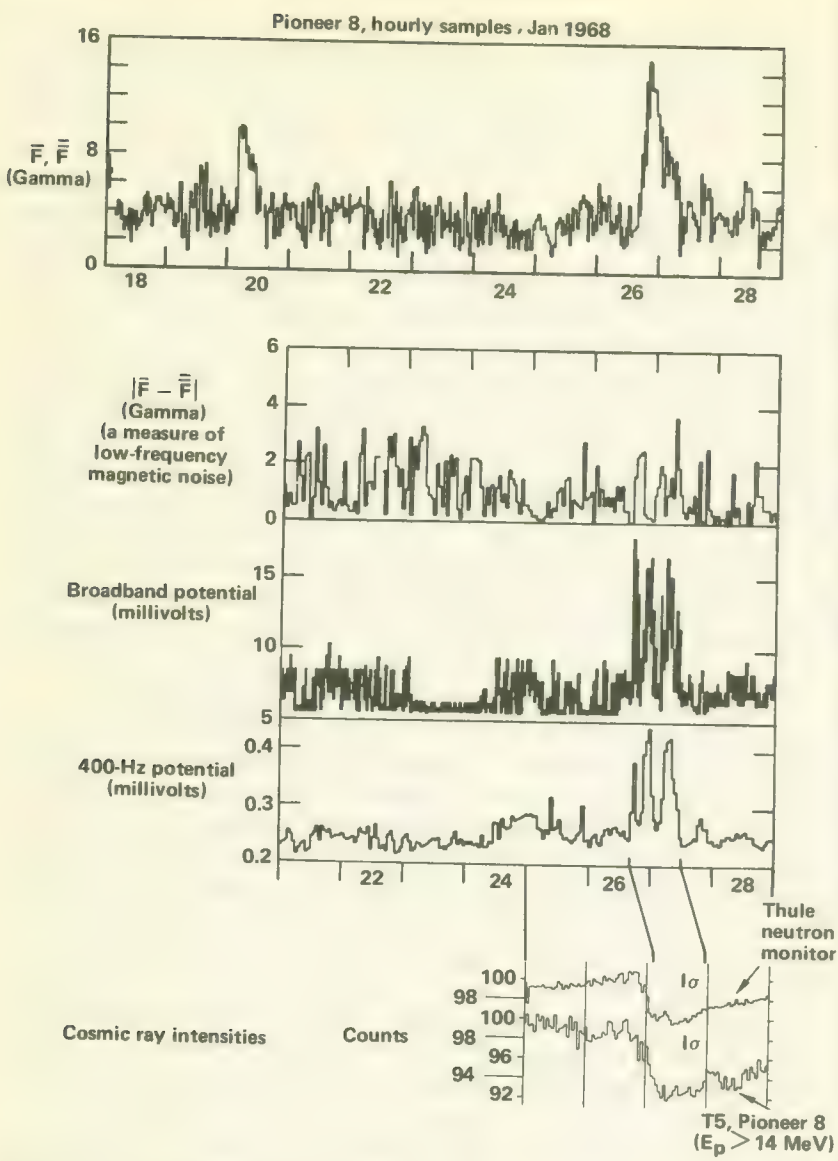


FIGURE 4-9.—Pioneer 8 magnetometer data (top) and electric-field data (middle) reveal interplanetary shock. Cosmic-ray readings (bottom) show attendant Forbush decrease.

phone sensor alone. Six time-of-flight events involving both front and rear sensor arrays were also registered. These are considered highly important to the question of cosmic dust origin because orbital information can be derived from the measurements.

The six time-of-flight events in a space of 390 days represent a rate  $3.8 \times 10^4$  lower than the rate recorded by a time of flight experiment on OGO 1. It is surmised that the high OGO-1 rate was due to coincident noise pulses in that experiment. Noise was a serious problem with early scientific satellite cosmic dust experiments. In general, early Pioneer-8 results confirm expectations from zodiacal light measurements.

From a knowledge of the spacecraft trajectory and orientation at the instant of each event and the telemetered data indicating times of flight and the specific sensors activated in the front and back arrays it was possible to derive the particle orbits (fig. 4-10). These data indicate a cometary origin for the six particles, reinforcing the conclusions derived from ground-based observations.

The most interesting of the six events reported occurred on April 13, 1968. Apparently, one front sensor segment and two rear sensors responded, inferring that the particle partially disintegrated upon first impact, showering the rear array with a conical spray of debris. No such fragmentation was observed during laboratory tests with particles fired from an electrostatic accelerator. In view of the possible friable nature of cosmic dust material, this type of event was not unexpected.

The April 13, 1968, event was notable in two other aspects: (1) its impact energy exceeded 80 ergs, more than any other particle recorded; and (2) it was the only particle that activated the acoustical sensor. Thus, independent measurements of the particle's mass were possible from the energy and momentum equations. These were  $2.3 \times 10^{-11}$  and  $1.6 \times 10^{-11}$  g—relatively good agreement for this kind of experiment. From this information, an orbit for the particle was computed.

### THE PIONEER CELESTIAL MECHANICS EXPERIMENT

All spacecraft launched out of the Earth's gravitational "well" provide opportunities for improving solar system constants and ephemerides. Although the Pioneer spacecraft did not pass close to any other solar system planets, their trajectories were affected by the Moon. Further, the launch of four similar spacecraft, of known mass, all equipped with tracking aids, into heliocentric orbits, made possible more accurate determinations of the Astronomical Unit (AU) as well as the Earth's ephemeris. The three formal objectives of the experiment were:

- (1) To obtain primary determinations of the masses of the Moon and Earth and of the AU
- (2) To improve the ephemeris of the Earth

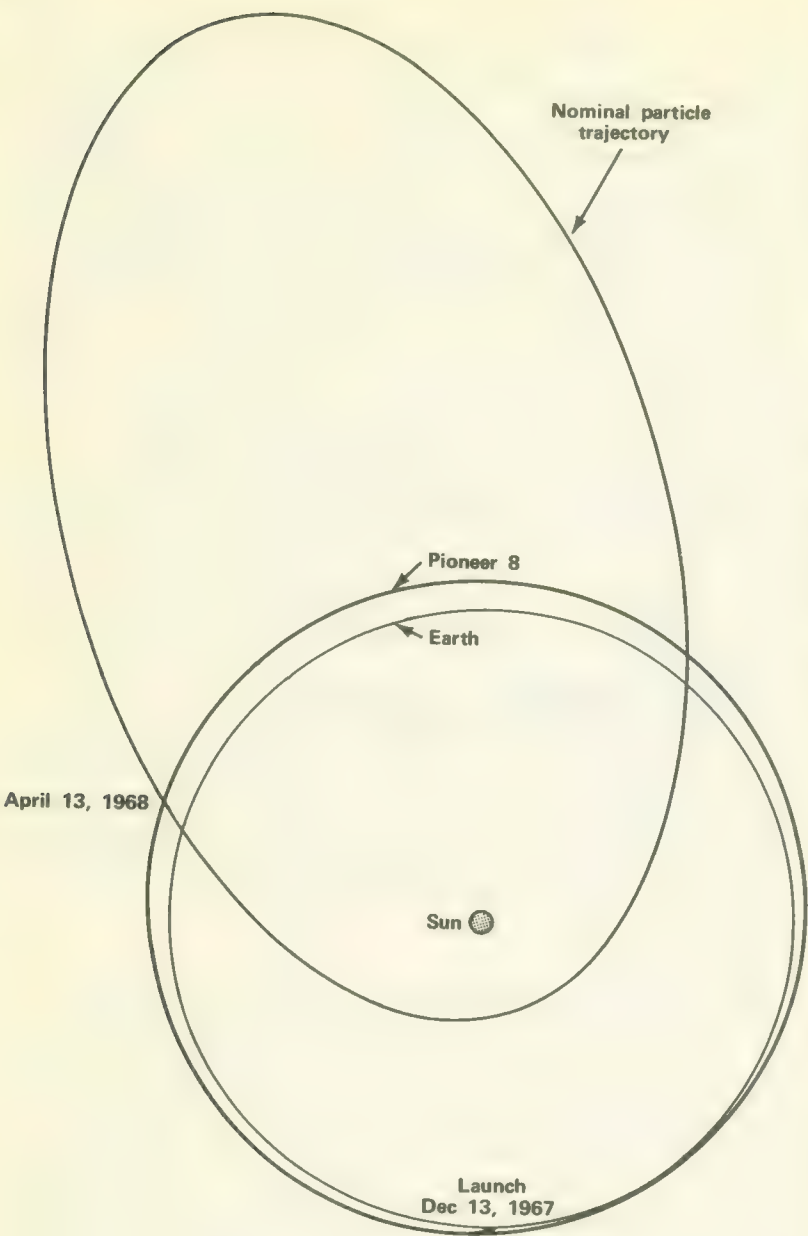


FIGURE 4-10.—Postulated orbit for the particle recorded on April 13, 1968. This was a time-of-flight event. From: Berg, 1969.

(3) To investigate the possibility of a General Relativity test, using Pioneer orbits and data

The following preliminary Earth-Moon data have been reported from this experiment:

$$\text{Geocentric gravitational constant} = GE = 398\,601.5 \pm 04 \text{ km}^3/\text{sec}^2$$

$$\text{Lunar gravitational constant} = GM = 4902.75 \pm 0.12 \text{ km}^3/\text{sec}^2$$

$$\text{Earth-Moon mass ratio} = \mu^{-1} = 81.3016 \pm 0.0020$$

### SOLAR WEATHER MONITORING

Because of these terrestrial effects of solar activity, several groups are interested in "solar weather"; i.e., the status of the interplanetary magnetic field, plasma fluxes, and cosmic radiation levels. The interest transcends pure science. NASA, for example, is concerned with solar events that might compromise manned space missions, particularly those that leave the shelter of the Earth's magnetosphere. The Environmental Science Services Administration (ESSA) desires advance information on magnetic storms and the injection of new, charged particles into the Earth's belt of trapped radiation. These are the events that sometimes upset terrestrial communications and have some not-so-well-understood effects on the planet's weather. The Department of Defense (DOD) has similar interests for military reasons.

Pioneer Solar Weather reports began in January 1967. Usually they are sent once a day to ESSA's Space Disturbance Forecast Center at Boulder, Colorado; to DOD's NORAD; and to other agencies. However, when manned flights are imminent, reports are sent hourly to NASA's Apollo Mission Control Center at Houston, Texas. The reports include:

- (1) The corotation delay, i.e., the expected time in days between the measurement of a disturbance at the spacecraft and its arrival at Earth
- (2) Solar wind velocity, density, and temperature
- (3) Cosmic-ray intensities in several energy bands
- (4) The general condition of the interplanetary magnetic field.



## Bibliography

- ANDERSON, J.D.; AND HILT, D.E.: Improvement of Astronomical Constants and Ephemerides from Pioneer Radio Tracking Data. Am. Astronaut. Soc. Paper, pp. 68-130, 1968.
- ANON.: TRW Systems, Pioneer Spacecraft Project Final Project Report. Rep. no. 8830-28, 1969.
- BARON, W.R.: The Solar Array for the Pioneer Deep Space Probe. Electronics and Power, vol. 14, March 1968, p. 261.
- BARTLEY, W.C.; McCracken, K.G.; AND RAO, U.R.: Pioneer VI Detector to Measure Degree of Anisotropy of Cosmic Radiation in Energy Range 7.5-90 MeV/Nucleon. Rev. Sci. Instr., vol. 38, Feb. 1967, p. 266.
- BERG, O.E.: The Pioneer 8 Cosmic Dust Experiment. NASA TN D-5267, 1969. (Also Rev. Sci. Inst., vol. 40, Oct. 1969.)
- BERG, O.E.; KRISHNA SWAMY, K.S.; AND SECRETAN, L.: Cosmic Dust Radiants and Velocities from Pioneer 8. Goddard Space Flight Center, X-616-69-145 and X-616-69-238, 1969.
- BURLAGA, L.F.: Microscale Structures in the Interplanetary Medium. Solar Phys., vol. 4, May 1968, p. 67.
- CANTARANO, S.C., ET AL.: Magnetic Field Experiment, Pioneers 6, 7, and 8. NASA TM-X-68395, 1968.
- FAN, C.Y. ET AL.: Differential Energy Spectra and Intensity Variation of 1-20 MeV/Nucleon Protons and Helium Nuclei in Interplanetary Space (1964-1966). Can. J. Phys., vol. 46, May 15, 1968, p. S498.
- HALL, C.F.; AND MICKELWAIT, A.B.: Development and Management of the Interplanetary Pioneer Spacecraft. NASA TM-X-60564, 1967. (Also in Proc., 18th International Astron. Congress, vol. 2, M. Lunc, ed., Pergamon Press, Oxford, 1968.)
- INTRILIGATOR, D.S. ET AL.: Preliminary Comparison of Solar Wind Plasma Observations in the Geomagnetic Wake at 1000 and 500 Earth Radii. Planetary and Space Sci., vol. 17, March 1969, p. 321.
- LAZARUS, A.J.; SISCOE, G.L.; AND NESS, N.F.: Plasma and Magnetic Field Observations during the Magnetosphere Passage of Pioneer 7. J. Geophys. Res., vol. 73, April 1968, p. 2399.
- LEZNIAK, J.A. ET AL.: Observations on the Abundance of Nitrogen in the Primary Cosmic Radiation. Astrophys. and Space Sci., vol. 5, Sept. 1969, p. 103.
- LUMB, D.R.: Test and Preliminary Flight Results on the Sequential Decoding of Convolutional Encoded Data from Pioneer IX. IEEE ICC Conference Publications, vol. 5, IEEE, New York, 1969, pp. 39-1 to 39-8.
- LUMB, D.R.; AND HOFFMAN, L.B.: An Efficient Coding System for Deep Space Probes with Specific Application to Pioneer Missions. NASA TN-D-4105, 1967.
- MARIANI, F.; AND NESS, N.F.: Observations of the Geomagnetic Tail at 500 Earth Radii by Pioneer 8. J. Geophys. Res., vol. 74, Nov. 1, 1969, p. 5633.

- MCCRACKEN, K.G.; RAO, U.R.; AND NESS, N.F.: Interrelationship of Cosmic-Ray Anisotropies and the Interplanetary Magnetic Field. *J. Geophys. Res.*, vol. 73, July 1, 1968, p. 4159.
- NESS, N.F.: Interplanetary Sector Structure, 1962-1966. *Solar Phys.*, vol. 2, Nov. 1967, p. 351.
- NESS, N.F.: Direct Measurements of Interplanetary Magnetic Field and Plasma. *Ann. of the IQSY*, vol. 4, 1969, p. 88.
- NUNAMAKER, R.R.; HALL, C.F.; AND FROSOLONE, A.: Solar Weather Monitoring—Pioneer Project. *Am. Inst. Astronaut. Aeron. Paper* 68-36, 1968.
- RAO, U.R.; MCCRACKEN, K.G.; AND BUKATA, R.P.: Cosmic-Ray Propagation Processes, 2. *J. Geophys. Res.*, vol. 72, Sept. 1, 1967, p. 4325.
- RAO, U.R.; MCCRACKEN, K.G.; AND BUKATA, R.P.: The Energetic Storm Particle Event. *J. Geophys. Res.*, vol. 72, Sept. 1, 1967, p. 4325.
- REIFF, G.A.: Radio Propagation Experiments with Interplanetary Spacecraft. *J. Spacecraft and Rockets*, vol. 6, May 1969, p. 551.
- REIFF, G.A.: The Pioneer Spacecraft Program. *AAS Paper*, 1969.
- SCARF, F.L. ET AL.: Initial Results of the Pioneer 8 VLF Electric Field Experiment. *J. Geophys. Res.*, vol. 73, Nov. 1, 1968, p. 6665.
- SCARF, F.L. ET AL.: Pioneer 8 Electric Field Measurements in the Distant Geomagnetic Tail. *J. Geophys. Res.*, vol. 75, June 1, 1970, p. 3167.
- SHERGALIS, L.D.: A Magnetically Clean Pioneer. *Electronics*, vol. 38, Sept. 20, 1965, p. 131.
- SISCOE, G.L.; GOLDSTEIN, B.; AND LAZARUS, A.J.: An East-West Asymmetry in the Solar Wind Velocity. *J. Geophys. Res.*, vol. 74, April 1, 1969, p. 1759.
- STAMBLER, I.: The New Pioneer Satellites. *Space/Aeron.*, vol. 40, Nov. 1963, p. 58.
- WOLFE, J.H. ET AL.: The Compositional, Anisotropic, and Non-radial Flow Characteristics of the Solar Wind. *J. Geophys. Res.*, vol. 71, July 1, 1966, p. 3329.

## APPENDIX

### MEMORANDUM: ORGANIZATION OF AMES SOLAR PROBE TEAM

NASA-Ames  
September 14, 1960

MEMORANDUM for Research Division Chiefs and Branch Chiefs

Subject: Organization of Ames Solar Probe Team

1. In the past few months a feasibility study of a solar probe has been made by members of the Ames staff. The purpose of such a vehicle would be to obtain valuable information on the spatial environment in the near vicinity of the sun which would permit a better understanding of the influence of the sun on weather and communication on earth and on the radiation hazard to manned flight in space. The results of this study have been compiled and a report entitled "A Preliminary Study of a Solar Probe" has been prepared and disseminated to interested personnel at Ames. The results of the study show that such a vehicle is feasible and have indicated a number of areas where research will be required in order to make the development of the solar probe practical.

2. In order to capitalize on the ideas and data that have resulted from this study the Ames Solar Probe Team is organized. It will be the responsibility of the team to consider the design problems of the vehicle, to recommend a practical system when it is judged feasible, and to recommend research programs that are desirable or necessary in this connection. Study of the vehicle system will be carried out by team members and their subordinates; recommendations of the team that require action by the Center should be brought to the attention of the Assistant Director's Office. This office will in turn organize a meeting of Branch Chiefs, Division Chiefs, and Team members for the required interchange and discussion so that decisions, approvals and assignment of responsibility can be accomplished expeditiously and with full backing of the Center Administration.

3. The following staff members are appointed to the Ames Solar Probe Team:

|                |                                 |
|----------------|---------------------------------|
| C. F. Hall     | Chairman                        |
| John Dimeff    | Instrumentation                 |
| C. F. Hansen   | Experiments                     |
| W. A. Mersman  | Trajectories                    |
| R. T. Jones    | Theory                          |
| H. F. Matthews | Guidance, Stability and Control |
| H. Hornby      | Boosters                        |
| W. J. Kerwin   | Communication, Auxiliary Power  |
| C. A. Hermach  | Thermal Protection              |

Smith J. DeFrance  
*Director*

NASA SP-279

TECHNOLOGY  
FEDERAL

# THE INTERPLANETARY PIONEERS

VOLUME II: SYSTEM DESIGN  
AND DEVELOPMENT



NATIONAL AERONAUTICS AND SPACE ADMINISTRATION

Challenger Collection

MAR 20 1973

NASA SP-279

# THE INTERPLANETARY PIONEERS

## VOLUME II: SYSTEM DESIGN AND DEVELOPMENT

by

William R. Corliss



Scientific and Technical Information Office

NATIONAL AERONAUTICS AND SPACE ADMINISTRATION

Washington, D.C.

1972

---

For sale by the Superintendent of Documents,  
U.S. Government Printing Office, Washington, D.C. 20402  
Price \$2.50 Stock Number 3300-0452  
*Library of Congress Catalog Card Number 74-176234*

## Foreword

SOME EXPLORATORY ENTERPRISES start with fanfare and end with a quiet burial; some start with hardly a notice, yet end up significantly advancing mankind's knowledge. The Interplanetary Pioneers more closely fit the latter description. When the National Aeronautics and Space Administration started the program a decade ago it received little public attention. Yet the four spacecraft, designated Pioneers 6, 7, 8, and 9, have faithfully lived up to their name as defined by Webster, "to discover or explore in advance of others." These pioneering spacecraft were the first to systematically orbit the Sun at widely separated points in space, collecting information on conditions far from the Earth's disturbing influence. From them we have learned much about space, the solar wind, and the fluctuating bursts of cosmic radiation of both solar and galactic origin.

These Pioneers have proven to be superbly reliable scientific explorers, sending back information far in excess of their design lifetimes over a period that covers much of the solar cycle.

This publication attempts to assemble a full accounting of this remarkable program. Written by William R. Corliss, under contract with NASA, it is organized as Volume I: Summary (NASA SP-278); Volume II: System Design and Development (NASA SP-279); and Volume III: Operations and Scientific Results (NASA SP-280). In a sense it is necessarily incomplete, for until the last of these remote and faithful sentinels falls silent, the final word is not at hand.

HANS MARK  
*Director*  
*Ames Research Center*  
*National Aeronautics and*  
*Space Administration*



# Contents

|   | Page      |
|---|-----------|
| <b>Chapter 1. DEFINING THE PIONEER SYSTEM.....</b>                      | <b>1</b>  |
| Motivation for Pioneer.....   | 1         |
| Desiderata and Constraints: Some Early Thoughts.....                    | 2         |
| A Hierarchy of Systems.....   | 5         |
| A Model of the Spacecraft System.....                                   | 7         |
| The Proper Order of Things.....   | 8         |
| A Look at the STL Feasibility Study.....                                | 10        |
| Some Constraints on the Feasibility Study.....                          | 11        |
| A New Flight Concept.....   | 12        |
| Escaping the Earth's Gravitational Field.....                           | 14        |
| Communications Reliability.....   | 14        |
| Getting Rid of Waste Heat.....  | 15        |
| Onboard Data Storage.....   | 15        |
| An Early Weight Breakdown.....  | 15        |
| Experiments Suggested by STL.....                                       | 16        |
| Impact of the Feasibility Study.....                                    | 17        |
| Reference.....  | 17        |
| <b>Chapter 2. PIONEER LAUNCH TRAJECTORY AND SOLAR ORBIT DESIGN.....</b> | <b>19</b> |
| Specific Mission Objectives: A Scientist's View.....                    | 19        |
| Other Factors Involved in Pioneer Trajectory and Orbit Design.....      | 20        |
| Pioneer 9 Trajectory Analysis.....                                      | 27        |
| Pioneer Orbit Parameters.....   | 34        |
| Spacecraft Orientation.....   | 35        |
| Reference.....  | 38        |
| <b>Chapter 3. SPACECRAFT DESIGN APPROACH AND EVOLUTION.....</b>         | <b>39</b> |
| Spacecraft Design Approach.....   | 39        |
| Evolution of the Spacecraft Design.....                                 | 49        |
| References.....   | 53        |
| <b>Chapter 4. THE SPACECRAFT SUBSYSTEMS.....</b>                        | <b>55</b> |
| The Communication Subsystem.....  | 55        |
| The Data Handling Subsystem.....  | 68        |
| The Command Subsystem.....  | 91        |
| The Electric Power Subsystem.....                                       | 100       |

|  | Page       |
|--|------------|
| The Orientation Subsystem.....   | 111        |
| The Thermal Control Subsystem.....   | 121        |
| The Structure Subsystem.....   | 128        |
| Overall Weight Breakdown.....  | 134        |
| References.....  | 136        |
|  |            |
| <b>Chapter 5. SCIENTIFIC INSTRUMENTS.....</b>                                  | <b>137</b> |
| Scientific Objectives.....   | 137        |
| Applications of Pioneer Data.....  | 139        |
| Instrument Interfaces and Specifications.....                                  | 139        |
| Instrument Selection.....  | 140        |
| The Goddard Magnetometer (Pioneers 6, 7, and 8).....                           | 142        |
| The Ames Magnetometer (Pioneers 9 and E).....                                  | 145        |
| MIT Faraday-Cup Plasma Probe (Pioneers 6 and 7).....                           | 148        |
| Ames Plasma Probe (Pioneers 6, 7, 8, 9, and E).....                            | 152        |
| The Chicago Cosmic Ray Experiment (Pioneers 6 and 7).....                      | 160        |
| The GRCSW Cosmic Ray Experiments (Pioneers 6, 7, 8, 9, and E).....             | 165        |
| Minnesota Cosmic Ray Detector (Pioneers 8, 9, and E).....                      | 170        |
| The Stanford Radio Propagation Experiment (Pioneers 6, 7, 8, 9,<br>and E)..... | 171        |
| The TRW Systems Electric Field Detector (Pioneers 8, 9, and E).....            | 176        |
| The Goddard Cosmic Dust Experiment (Pioneers 8, 9, and E).....                 | 181        |
| The JPL Celestial Mechanics Experiment (Pioneers 6, 7, 8, 9, and E).....       | 188        |
| References.....  | 188        |
|  |            |
| <b>Chapter 6. THE PIONEER TEST AND GROUND SUPPORT PROGRAM.....</b>             | <b>191</b> |
| Test Specifications.....   | 192        |
| Spacecraft Models.....   | 192        |
| Test Facilities.....   | 196        |
| Spacecraft Integration and Test Procedures.....                                | 202        |
| Electrical Ground Support Equipment.....                                       | 205        |
| Typical Test Results.....  | 207        |
| References.....  | 210        |
|  |            |
| <b>Chapter 7. THE DELTA LAUNCH VEHICLE.....</b>                                | <b>211</b> |
| Why the Delta?.....  | 211        |
| The Evolution of the Delta.....  | 211        |
| The Delta Spacecraft Interface.....  | 216        |
| Other Interfaces.....  | 224        |
| Trajectory Design.....   | 224        |
| Primary Launch Objectives.....   | 229        |
| The Launch Sequence.....   | 231        |

|  | <i>Page</i> |
|--|-------------|
| A Typical Weight Breakdown.....  | 235         |
| References.....  | 236         |
| <br>   |             |
| <b>Chapter 8. TRACKING AND COMMUNICATING WITH PIONEER<br/>SPACERCRAFT.....</b> | <b>237</b>  |
| Tracking the First Pioneers.....   | 237         |
| Some Generalities About Tracking and Data Acquisition.....                     | 239         |
| General Deep Space Network Capabilities.....                                   | 241         |
| Specific Pioneer Network Configurations.....                                   | 263         |
| Telemetry Capabilities.....  | 267         |
| Command Capabilities.....  | 267         |
| References.....  | 273         |
| <br>   |             |
| <b>Chapter 9. PIONEER DATA-PROCESSING EQUIPMENT.....</b>                       | <b>277</b>  |
| Pioneer Off-Line Data-Processing System.....                                   | 277         |
| Tape Processing Station.....   | 278         |
| Pioneer Off-Line Direct-Coupled System.....                                    | 280         |
| Data Processing at TRW Systems.....  | 283         |
| Reference.....   | 283         |
| <br>   |             |
| <b>BIBLIOGRAPHY.....</b>   | <b>285</b>  |
| <br>   |             |
| <b>PIONEER SPECIFICATIONS.....</b>   | <b>289</b>  |
| <br>   |             |
| <b>Appendix. RELIABILITY AND QUALITY ASSURANCE.....</b>                        | <b>293</b>  |



## CHAPTER 1

# Defining the Pioneer System

### MOTIVATION FOR PIONEER

THE SCIENTIFIC MISSION of Pioneers 6 through 9 was the synoptic measurement of the interplanetary milieu as it is affected by the Sun. The Pioneers measured and transmitted back to Earth data on solar plasma, cosmic radiation, magnetic and electric fields, and the specks of cosmic dust that drift through interplanetary space. All of these physical phenomena are dominated by the Sun. The Pioneer spacecraft described here were akin to weather satellites, except that they were artificial planets of the Sun rather than satellites of the Earth. Spotted strategically around the Sun in the plane of the ecliptic, they monitored the ever-changing fluxes and fields that wax and wane with solar activity.

Solar activity follows an eleven-year cycle of sunspot numbers—a periodic phenomenon felt throughout the solar system. In 1962, when NASA began to formulate its “follow-on” Pioneer Program, which would extend the earlier International Geophysical Year (IGY) Pioneers (Pioneers 1–5), scientists around the world were organizing an investigation of solar problems to take place during the solar minimum expected during the 1964–1965 period. They hoped to further the scientific advances recorded during the IGY (18 months in the span 1956–1958), a period that also saw the first satellites and the formation of NASA. The new effort was labeled the International Quiet Sun Year (IQS<sup>Y</sup>). The five Pioneers planned in 1962 would be in direct support of the IQSY, supplementing NASA’s Orbiting Geophysical Observatory (OGO) series, Orbiting Solar Observatory (OSO) series, and Explorer series in orbit around the Earth, and a worldwide array of scientific sensors on the ground and on sounding rockets. The Pioneers’ unique value to the IQSY lay in the fact that they would range far ahead and behind the Earth as it swung around the Sun. Further, they would make *in situ* measurements of deep-space phenomena, unperturbed by the Earth’s magnetic and gravitational fields.<sup>1</sup>

As the IQSY or Interplanetary Pioneer Program developed, it became apparent that the long lifetimes of the spacecraft and the schedule changes would extend deep-space solar monitoring through the 1969–1970 solar

<sup>1</sup> See Volume I for the detailed scientific objectives of the Pioneer Program, and Volume III for a summary of scientific results.

maximum—a scientific bonus. This extension of coverage also aided the Apollo lunar exploration effort. Scientists, as they take the Sun's pulse with their manifold instruments, are beginning to predict solar activity in much the same way that the Weather Bureau predicts tornado and hurricane activity from its array of terrestrial meteorological sensors. A violent storm on the Sun could endanger astronauts on the Moon with an intense burst of solar cosmic rays. The prediction of a severe solar disturbance a few hours ahead of time would give astronauts time to take shelter in the relative safety of their spacecraft.

Weather prediction of any kind is more reliable if data can be obtained from widely separated sites. The "inward" Pioneers (6 and 9) and "outward" Pioneers (7 and 8) ied and lagged the Earth by tens of millions of miles, respectively, providing a much broader data base than terrestrial sensors. Selected scientific parameters from the Pioneer spacecraft were teletyped from tracking and data acquisition sites to Ames Research Center, forty miles south of San Francisco, where they were processed and analyzed prior to transmission to the Space Disturbance Center of Environmental Science Services Administration (ESSA), at Boulder, Colorado. After combining Pioneer data with that from other sensors, in space and on the ground, ESSA issued daily Space Disturbance Forecasts. These forecasts not only alerted astronauts, but also signaled scientists around the world that interesting events were about to happen on the Sun. Solar weather monitoring was not one of the original objectives of the Pioneer Program, but the obvious value of Pioneer deep-space data led to its use in preparing the Space Disturbance Forecasts.

## DESIDERATA AND CONSTRAINTS: SOME EARLY THOUGHTS

The Pioneer mission as defined above was far too general to enable engineers to sit down and draw up a system design. A wide variety of spacecraft, weighing pounds or tons, costing millions or billions, could monitor interplanetary weather. In 1962, the practical considerations of money and available launch vehicles dictated that the spacecraft weigh only about 100 lb. The investment of resources had to be commensurate with the potential scientific payoff and not detract from NASA's major mission, the manned lunar landing. In this light, the Pioneers were closely related to the small Explorer-class satellites that NASA launches on geophysical missions.

As the scientific desiderata were defined more closely, the main engineering features of the Pioneers began to come into focus. As instrument carriers, scientists wanted the Pioneers to have:

- (1) The ability to point instruments in all directions, particularly all azimuths in the plane of the ecliptic
- (2) Capability for continuous data sampling of the experiments

- (3) High data transmission rates back to Earth
- (4) Many commandable modes of operation to permit them to modify their instruments from Earth
- (5) A stable environment for the instruments without temperature extremes, electromagnetic interference, or other perturbing forces
- (6) A very low residual magnetic field that would not obscure the slight interplanetary magnetic fields
- (7) A long reliable life, preferably a year or more
- (8) A maximum spacecraft penetration toward and away from the Sun
- (9) A wide variety of scientific instruments to measure the many interrelated features of interplanetary space

Vannevar Bush once described science as "an endless frontier." In this context, it would be desirable to carry a hundred instruments, approach the Sun to within a tenth of an Astronomical Unit (AU), and take excursions from the plane of the ecliptic. Such objectives were obviously beyond the scope and assigned resources of the I奎SY Pioneers, though certainly not beyond man's increasing capabilities in space. Despite the limitations, the final spacecraft were excellent instrument platforms that more than fulfilled all scientific objectives.

With the Pioneer Program thus characterized as a modest effort, available launch vehicles and proven technology had to be applied. The engineers on the Pioneer Program did not attempt to make technological breakthroughs. In addition, the horizons of the Pioneers had to be limited by available tracking and data acquisition facilities. The basic factor creating these constraints was, of course, cost. Scientific return had to be maximized within a framework of resources in the \$50 to \$100 million category.

Every engineer recognizes the trade-off problem just posed; that is, maximizing performance within fixed technological and financial constraints. The detailed trade-offs and design philosophy employed during the evolution of the Pioneer spacecraft will be described in later chapters. Here, only the identification of the major elements of the overall Pioneer system is important. The resources of NASA in 1962 allowed the Pioneer Project the following system elements (fig. 1-1):

(1) The Delta launch vehicle, a low cost, highly reliable rocket, capable of propelling about 150 pounds into orbit around the Sun, available, and well proven in many satellite launches.

(2) The Deep Space Network (DSN), comprising the Deep Space Instrumentation Facility (DSIF) of tracking and data acquisition antennas and the Space Flight Operations Facility (SFOF) at the Jet Propulsion Laboratory (JPL) in Pasadena, California. The DSN was built for NASA's planetary and lunar programs. It was the only NASA tracking and data acquisition network, capable of handling a small space probe tens of millions of miles from the Earth, and a reality that helped shape the Pioneer Program.

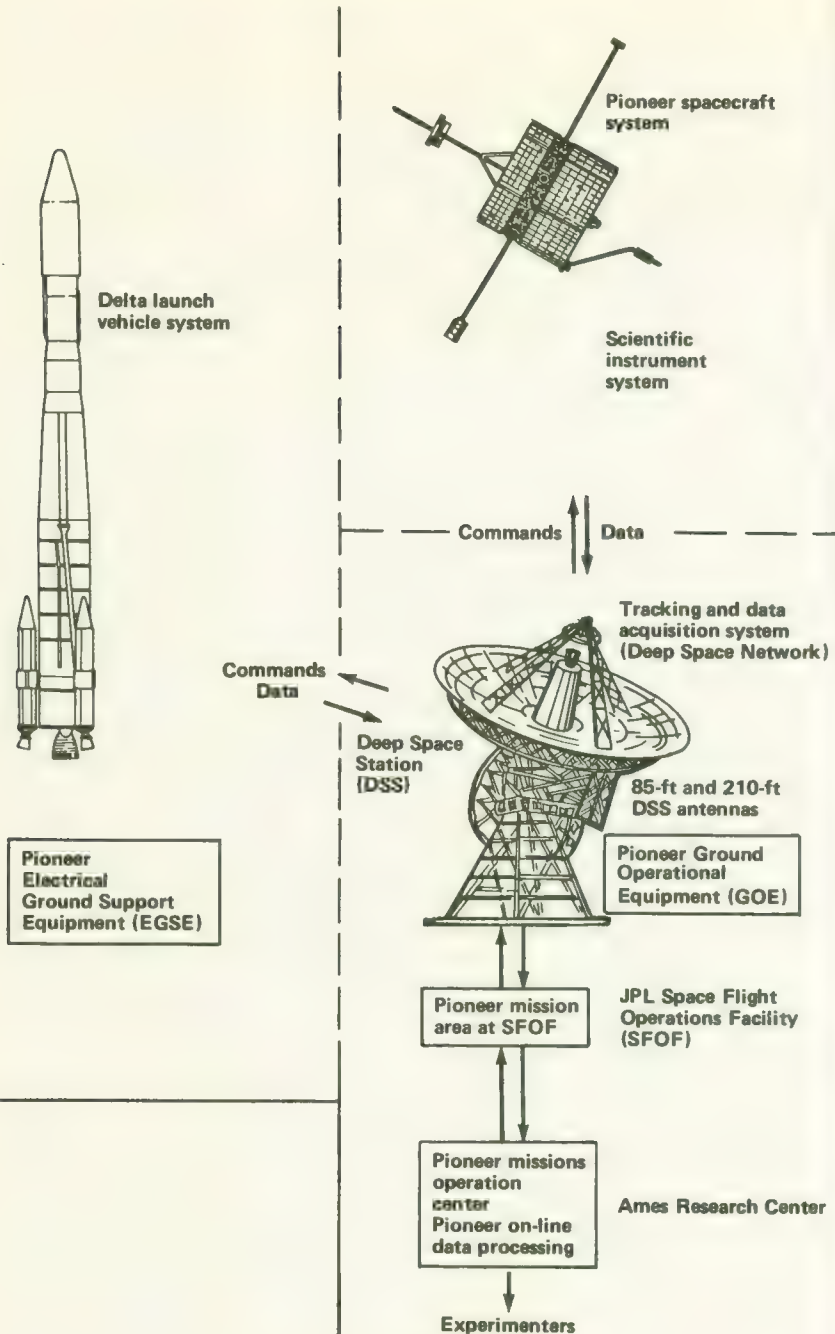


FIGURE 1-1.—The four Pioneer systems.

(3) The spacecraft system, a stable instrument carrier weighing something around 100 pounds, capable of communicating with experimenters through the DSN, and providing room for about 20 to 40 lb of scientific instruments.

(4) The scientific instrument system, made up of magnetometers, particle detectors, and whatever other instruments the scientific community deemed feasible and worthwhile within the payload limitations set by the launch vehicle, orbit, and spacecraft weight requirements.

Obviously, this is only the crudest sketch of the Pioneer System—about as far as one could go at that time, given NASA's resources and the broad scientific objectives. This was the starting point. To go further, someone needed to express things in numbers or “engineer” the system.

The purpose of this volume is to describe how this engineering was performed, what the critical design decisions were, and what the final system looked like. Pioneer operations and scientific results are related in Volume III.

### A HIERARCHY OF SYSTEMS

Before a description of the Pioneer feasibility study and subsequent design, fabrication, and test activities, a model of the spacecraft program is desirable. This model should not only define the various equipments and how they mesh physically, but also how the spacecraft project moves through the time dimension from feasibility study to launch pad.

The Pioneer spacecraft with about 20 lb of scientific instruments may be likened to the apex of a large pyramid. The small point of the pyramid depends completely upon the large supporting foundation. In this analogy, the base of the pyramid is represented by the launch vehicle, the ground support equipment, the test facilities, and the multifarious activities involved in the design, construction, and operation of the spacecraft. The spacecraft receives the fanfare, but thousands of people on the ground and hundreds of millions of dollars worth of facilities are also essential to success.

In the formal language of engineering, the complete system begins at the spacecraft sensor and ends with the publication of the scientific results in the literature. The major elements in the overall Pioneer System are the spacecraft itself, its cargo of scientific instruments, the launch vehicle, and the tracking and data acquisition network, as diagrammed in figure 1-1. Because these elements are frequently called systems in their own right, it is more proper to refer to them overall as the Pioneer supersystem. Nevertheless, to adhere to Pioneer Program terminology, the Pioneer System will be understood to consist of four lesser systems. Each of the four Pioneer systems can be further subdivided into subsystems, such as the spacecraft communication subsystem. These distinctions may seem overly complicated, but it is important to sketch out a general framework for the de-

scriptive material that follows. And, of course, from the standpoint of program management, the supersystem work must be parceled out to engineering groups in conveniently sized systems, subsystems, and even smaller pieces.

Engineers like to subdivide large supersystems into smaller pieces because this dissection helps them to see and to understand the inner workings of each part. The problem is putting the pieces back together again. The designer of the spacecraft's communication subsystem cannot ignore the antenna of the terrestrial data acquisition equipment, even though it may be designed by a company in another part of the country. Boundary regions between subsystems and systems are termed interfaces. The proper matching of interfaces is vital to the successful operation of the complete supersystem.

The management device used to ensure matching interfaces in many NASA programs is called the interface specification, a carefully written description of how various subsystems must fit together. The interface between a Pioneer spacecraft far out in space and the DSIF back on Earth involved such matters as radio frequencies, the type of telemetry employed, and the many other aspects of radio communication. The Pioneer supersystem was, in fact, a huge, remotely controlled, information-gathering machine. It is not surprising to find that communication and information interfaces existed between almost all systems and subsystems. A mechanical

TABLE 1-1.—*Types of Interfaces in Spacecraft Systems*

| Type                 | Design considerations  |
|----------------------|--|
| Mechanical.....      | Physical dimensions of mating parts must match. Shock and vibration may cause damage during launch.  |
| Spatial.....         | Competition for solid angle (view cones) by scientific instruments, solar cells, and navigation sensors.   |
| Thermal.....         | Heat flow across interfaces may degrade equipment; viz., aerodynamic heating during launch.  |
| Electrical.....      | Voltages, currents, and ac frequencies must match. The summation of the power profiles of equipment as functions of time must not exceed power subsystem capacity.   |
| Magnetic.....        | Magnetic materials and current loops must not interfere with magnetic instrumentation.   |
| Electromagnetic..... | Crosstalk between neighboring circuits is a common spacecraft problem.   |
| Radiative.....       | Particulate radiation from nuclear power supplies or the environment may interfere with instrumentation or, in extreme cases, damage materials and components. (Not a consideration on the IQLY Pioneers.) |
| Information.....     | Data flow across interfaces must be matched in terms of word format, the rate of data transmission, etc.   |

interface obviously must be matched when the launch vehicle and spacecraft come together at the launch pad. Within the spacecraft itself, the interfaces are more subtle, as illustrated in table 1-1. Magnetic cleanliness, for example, was a major goal on the Pioneer spacecraft. This requirement led to the establishment of magnetic interface specifications stipulating the maximum magnetic fields tolerable from each spacecraft subsystem. In the large sense, the spacecraft systems also had to be matched to the environment; that is, environmental forces, such as solar plasma, could not degrade spacecraft performance. The interface specifications strongly influenced the design of each component on the spacecraft and on the ground.

### A MODEL OF THE SPACECRAFT SYSTEM

The definition of the spacecraft subsystems is essential to the understanding of the chapters that follow. Subsystem definition varies somewhat from design group to design group. Generally, one attempts to lift out a well-defined piece of equipment with well-defined functions, and label it a subsystem. The electric power subsystem is a typical subsystem. After the electric power subsystem, the communication subsystem, and the other "removable" subsystems listed in table 1-2 are extracted, only the structure subsystem is left. The structure subsystem is the shell and/or framework that holds the other subsystems in place. Its design is just as critical to success as any other subsystem.

TABLE 1-2.—*Definition of Pioneer Spacecraft Subsystems*

| Subsystem       | Functions performed   |
|-----------------|---|
| Communication   | Relays scientific and spacecraft status data from the spacecraft to Earth; receives commands from Earth.  |
| Data-handling   | Accepts data from scientific and housekeeping instruments and arranges them in proper format for transmission back to Earth; provides for limited data storage.     |
| Electric-power  | Provides electrical power to all spacecraft subsystems and the scientific instrument system.  |
| Orientation     | Orients the spacecraft spin axis as required; damps out wobble. Attitude sensors and gas jets are included within this subsystem under Pioneer Program terminology. |
| Thermal-control | Maintains temperatures within specified ranges within the spacecraft.   |
| Command         | Decodes and distributes commands received via the communication subsystem to the spacecraft subsystems specified in the command addresses.                          |
| Structure       | Supports and maintains spacecraft configuration under design loads; provides booms for instrument isolation.  |

The Pioneer spacecraft subsystems delineated in figure 1-2 and table 1-2 are fairly consistent with nomenclature in other spacecraft projects. The major differences are as follows:

- (1) The Pioneer scientific instruments were considered to constitute a full-scale system by themselves and not a spacecraft subsystem as on many Earth satellites.
- (2) An onboard data-handling subsystem was separated from the communications subsystem.
- (3) The attitude-control subsystem was termed the "orientation subsystem" on Pioneer spacecraft.
- (4) Onboard propulsion and centralized onboard computer subsystems were not needed on Pioneer spacecraft.
- (5) Housekeeping sensors were included within each subsystem rather than considered collectively as a separate subsystem.

Interfaces had to be matched between each of the seven subsystems portrayed in figure 1-2 and table 1-2. Almost all of the Pioneer spacecraft subsystems required electrical power, and most also exchanged data and commands with the data handling and command subsystems. All subsystems had to fit together mechanically. (This is not so elementary a problem as it seems. Each spacecraft contains tens of thousands of parts, and cases have occurred where parts did not mesh properly the first time.) In view of spacecraft complexity, interface specifications were both voluminous and indispensable.

### THE PROPER ORDER OF THINGS

Equipment specifications stipulate what the equipment should be like; interface specifications insure that the various pieces of equipment will fit and work together satisfactorily. The omitted dimension is time. The flow of project events is specified by a milestone series familiar to every engineer and project manager.

As related in Volume I, the Pioneer Project began informally as a concept in Ames Research Center, NASA Headquarters, and industry during 1962. After considering the broad scientific objectives and its available resources, NASA management selected the major features of the Pioneer Project in 1962, as described in the preceding sections. However, many features of the spacecraft and mission-dependent equipment remained undefined. The next logical step was a feasibility study. The Pioneer feasibility study was made at Space Technology Laboratories, Inc. (STL)<sup>2</sup> and it went much further than the confirmation of feasibility; many design decisions were made and the spacecraft and other systems took on more detailed focus.

---

<sup>2</sup> Later renamed TRW Systems (July 1, 1965).

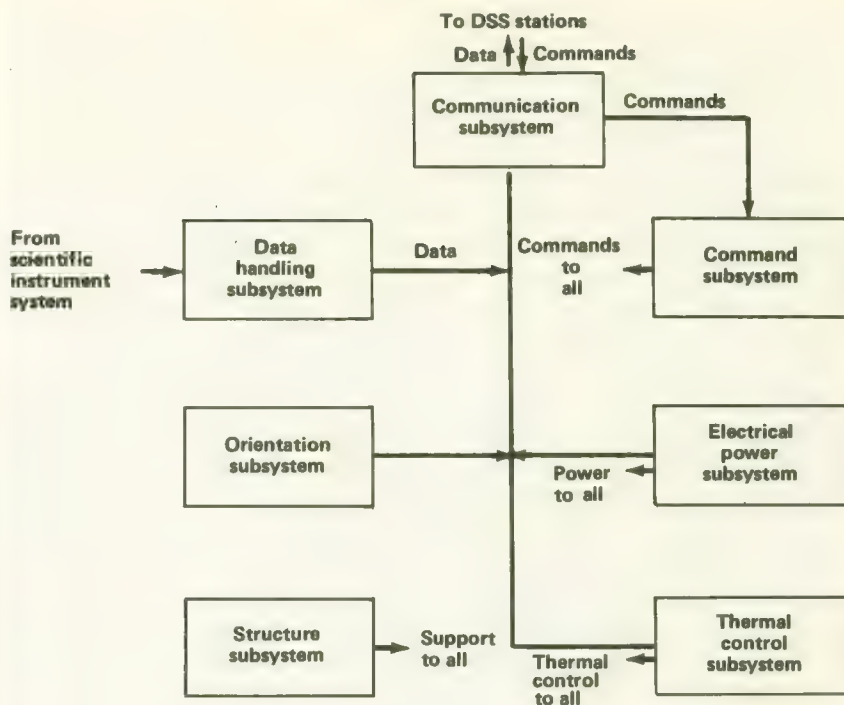


FIGURE 1-2.—Generalized block diagram showing Pioneer spacecraft subsystems. Magnetic, thermal, and other forces crossing subsystem interfaces are not shown.

With the feasibility study as a basis, Ames Research Center was able to draw up specifications to serve as the basis for hardware contracts. Two mainstreams of activity began with project approval on November 9, 1962; one stream each for the spacecraft and the scientific instruments. The evolution of the two other major systems, the Delta launch vehicle and the DSN, were not dictated by the Pioneer Program. The spacecraft and scientific instruments progressed through the phases of:

- (1) Contractor competition and selection
- (2) Detailed design and development
- (3) Hardware procurement and fabrication
- (4) Testing
- (5) Integration and checkout

The spacecraft, its instruments, the Delta, and DSN utilization ultimately converged at Cape Kennedy at the time of launch, when the four systems were integrated and checked out as a single supersystem. The Pioneer mission-dependent equipment, including the spacecraft and its scientific instruments, was completely new; while the mission-independent equipment (the DSN and Delta) required what are termed "project-

unique" modifications and auxiliaries. The general flow pattern of the Pioneer Project is illustrated for the first spacecraft, Pioneer 6, in figure 1-3. A major task of NASA Project management was the coordination of these four more-or-less parallel streams of effort. Specifications, schedules, and review meetings were the primary management tools employed in assuring that the four-way confluence was a successful one. The four straight Pioneer successes testify to the excellence of both engineering and management, in and out of the government, between Project approval in 1962 and the final launch in the series in 1969.

### A LOOK AT THE STL FEASIBILITY STUDY

Before NASA could embark upon a full-scale hardware program, it required a more precise definition of the Pioneer System. The general objectives and the rough delineation of major system components described in the preceding sections had to be confirmed by a hard-headed preliminary engineering design and then sketched out in more detail. The 1962 Pioneer feasibility study performed these tasks.

Feasibility studies are common in aerospace projects. The essentials of a system have to be known before realistic cost and schedule estimates can be made. If the Pioneer Program actually proved feasible within the

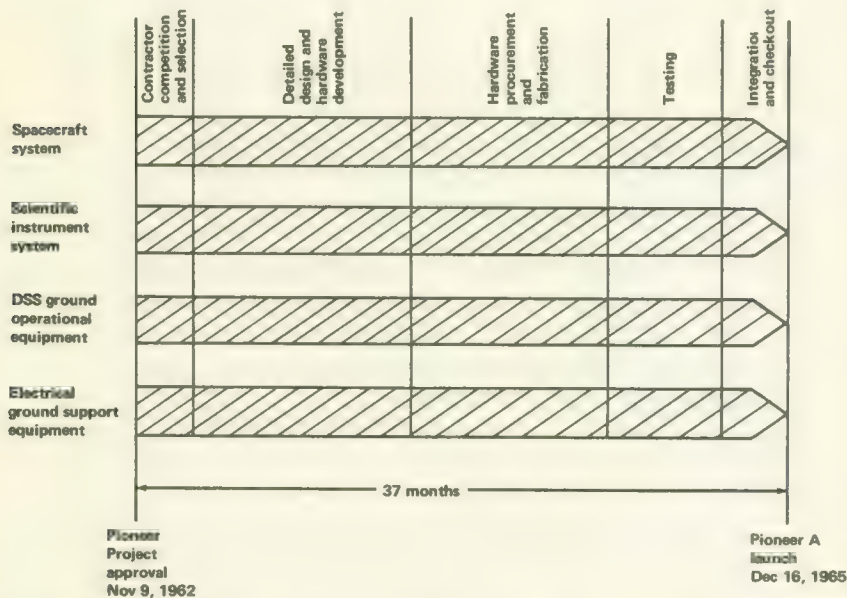


FIGURE 1-3.—Activity flow for the four Pioneer systems (shown for Pioneer A). Subsystems within each system followed similar paths. The phases were not synchronized precisely.

limitations of its resources, NASA intended to use the feasibility study as a basis for a Request for Proposal (RFP) which, in turn, would lead to contracts for the construction and testing of the spacecraft, the instruments, and the other project-unique equipment. This was, in fact, exactly what happened during 1962 and 1963.

In April 1962, STL completed a 2½-month study of an Interplanetary Probe under contract NAS2-884. That study was the basis for the I奎SY Pioneer Program and the spacecraft now called Pioneers 6 through 9. Armed with the STL study, Ames Research Center issued RFP A-6669 on January 29, 1963. STL won the final competition for the design, development, and construction of the spacecraft and certain ground-support equipment. NASA signed a letter contract with STL on August 4, 1963, and the Pioneer Program began to move out of the paper-study phase. The definitive contract with STL was not signed until May 1964. During the nine-month letter contract phase, STL and Ames engineers refined the spacecraft design considerably, making what might be called a "second iteration" on the design presented in the feasibility study.

The Pioneer feasibility study is especially important because, during the 2½ months in early 1962, almost all of the important system-design decisions were made by STL engineers working in conjunction with Ames personnel. A brief review of the most significant of these system-wide decisions is in order, for they refined considerably the definition of all systems and subsystems, and also revealed how well the general scientific objectives could be met within the scope of NASA's resources.

### SOME CONSTRAINTS ON THE FEASIBILITY STUDY

At the beginning of the feasibility study, NASA and STL personnel had at hand the general objectives and constraints mentioned earlier, the most important of which stipulated the use of the Delta (Thor-Delta) launch vehicle, the DSN, and, as far as possible, proven hardware. Applying numbers to its mission objectives, NASA specified that the Pioneer spacecraft should have a minimum probability of success of 0.8 for a 6-month life, with no absolute upper limit, and that it should be able to operate between 0.8 and 1.2 AU without spacecraft modifications.

The feasibility study proceeded on the basis of a contractual go-ahead on October 1, 1962, and a first flight in July 1964. Three other launches would follow at 6-month intervals and sufficient spare parts would be built for a fifth spacecraft. Furthermore, NASA imposed a fiscal constraint: the rate of cost buildup during the first 6 months of the program was not to be more than 15 percent of the total program cost.

The tight schedule, the desire to minimize costs, and the high space-craft-reliability target defined a modest total program with a very simple spacecraft built from off-the-shelf components.

## A NEW FLIGHT CONCEPT

The only significant experience U.S. astronautical engineers had with interplanetary spacecraft prior to early 1962 was with Pioneer 5 (launched June 26, 1960) and Mariner 2 (launched in August 1962). The Mariner was a sophisticated spacecraft, with solar panels that could be oriented toward the Sun and a high-gain, directional communication antenna that would point toward DSN antennas back on Earth. Weighing 447 pounds, Mariner 2 was too complex and too expensive under the Pioneer ground rules. Pioneer 5, on the other hand, was merely spin-stabilized in outer space and could not face its solar paddles to the Sun while rotating. It possessed an omnidirectional antenna that radiated radio energy wastefully in all directions. Still, Pioneer 5 had operated successfully for 2½ months (a good record in 1960) and had sent back signals from 22 million miles. At 75 lb, Pioneer 5 was a simple spacecraft and much closer than Mariner 2 to NASA's concept of the IQuSY Pioneers. STL had built Pioneer 5; this was one reason why STL was awarded the feasibility study and, ultimately, the IQuSY Pioneer spacecraft contract.

Weight and simplicity dictated a spin-stabilized spacecraft (almost all early U.S. spacecraft were spin-stabilized for this same reason). Spacecraft stabilization with gas jets and/or gyros was weight-consuming and risky from the reliability standpoint. Spin-stabilization also has the advantage of rotating the scientific instruments frequently through all azimuths. However, uncontrolled spin-stabilization entailed three problems:

(1) An ordinary dish-type directional antenna would be aimed at the Earth only once each rotation, a fact that would militate against achieving high data flow rates (high bit rates) over tens of millions of miles.

(2) The scientists preferred to have their instruments scan in the plane of the ecliptic, not any of the infinite number of other planes possible with a randomly oriented spacecraft.

(3) If the spin vector of the spacecraft was to be random, solar cells would have to be mounted on all sides of the spacecraft.

These thoughts led to the concept of an orientable, spin-stabilized spacecraft, with a spin axis that could be swung around with a simple gas jet until it was perpendicular to the plane of the ecliptic. The laws of motion predicted that torquing the spin vector would cause spacecraft precession or wobbling, but this could be largely eliminated by installing a simple "wobble damper." If the spacecraft were a cylinder (the preferred shape for many scientific spacecraft), with instruments and solar cells mounted around its curved surface, the last two of the three problems would be solved. The scientific instruments would scan in the plane of the ecliptic and solar cells would not be needed on the flat ends of the cylinder, freeing them for other components.

Only the antenna problem would remain. A paraboloidal spacecraft

antenna sweeping the plane of the ecliptic would be wasteful of spacecraft power, as would an omnidirectional antenna. A rather inspired solution to this conundrum was a mast-like antenna (a modified Franklin array) mounted along the spin axis. This kind of antenna would radiate a flat fan of radio energy in the plane of the ecliptic. The Earth and its DSN paraboloidal antennas would always be in this fan if the spacecraft spin axis were properly oriented. Of course, some radio energy would be wasted in other spacecraft azimuths; but the antenna fan was so narrow ( $\pm 5^\circ$  to the 3 dB points) that it was much less wasteful (10 dB), better than an omnidirectional antenna, and still far simpler than a pointable-dish antenna, such as that on Mariner 2. The combination of the unusual antenna plus spin stabilization perpendicular to the plane of the ecliptic were the key design decisions that conferred high reliability and the capability of very long distance communication on the IQuS Pioneers.

It is interesting to note how completely these elementary considerations define the spacecraft configuration (fig. 1-4). It had to have cylindrical symmetry (for spin stability); and it had to have a conspicuous antenna



FIGURE 1-4.—View of the Pioneer spacecraft showing the three radial booms deployed, the telemetry antenna mast (top), and the Stanford radio propagation experiment antenna (bottom).

mast at one end. Actually, these early design decisions were felt throughout the entire spacecraft design period and at every subsystem level. The effects were important at the systems level, too. The instrument system was aided by the spinning spacecraft platform; the high-gain antenna made the DSN's task easier; and the axis of spin symmetry simplified the dynamic interface with the Delta launch vehicle.

### ESCAPING THE EARTH'S GRAVITATIONAL FIELD

The STL feasibility study considered a launch from Cape Kennedy into the plane of the ecliptic. Cape Kennedy approaches to within about  $5^\circ$  of the plane of the ecliptic once each day. Propulsive requirements for Earth escape into the plane of the ecliptic are minimum at this time; however, the rocket must be fired in a given direction precisely at this moment. Payload can be traded for rocket propellant to gain the desired flexibility in launch time and direction. Rough calculations showed that a 9-lb payload penalty would permit a launch any time of day, in any direction from the Cape. (See ch. 2 for trajectory details.) Another launch trajectory trade-off concerned the altitude of main engine cutoff (MECO). Low-altitude MECOs (around 180 000 ft) produced important aerodynamic heating that required insulation on the Delta stages. The weight of this insulation reduced the payload. High-altitude MECOs demand less insulation, but payloads are again reduced because of higher propulsive requirements. These tradeoffs were investigated in detail in the feasibility study. The general conclusion was that there was ample margin in the Delta capabilities for launching a payload of about 126 lb.

Also examined was the possibility of exchanging the X-248 Delta third stage for the somewhat better X-258. Essentially NASA was offered a choice between a little more payload and less reliability with the newer stage. (This matter will be brought up again in ch. 7 because NASA ultimately did switch from the X-248 to the X-258 for Pioneer 6.)

### COMMUNICATIONS RELIABILITY

In the feasibility study, STL calculated a 0.83 probability of a 6-month life for the spacecraft, once in orbit. To attain this level of reliability, STL engineers employed redundancy, particularly for such critical communication components as the traveling wave tube, receiver, decoder, and elements of the digital telemetry unit. Conservative selection of parts was also a factor. For example, the traveling wave tube was selected over the more efficient but relatively new amplitron because reliability data were lacking for the latter. There was also doubt that a sufficiently reliable amplitron could be delivered in time for the first flight. Further, the amplitron's stray

magnetic field might have compromised magnetometer experiments in the payload.

### GETTING RID OF WASTE HEAT

NASA wished to send the IQUSY Pioneers on solar orbits both inside and outside that of the Earth. The accommodation of different thermal environments, without redesigning the spacecraft, dictated an active thermal control subsystem; that is, one with temperature-controlled vanes or louvers rather than static schemes employing fixed patterns of different surface absorptivity and emissivity. The relatively large variations in internal heat generation due to the variable transmitter power also added impetus to the choice of an active thermal control subsystem. The logical spot to install the vanes was on the bottom of the spacecraft which was unencumbered by solar cells or antenna. From here the spacecraft could radiate the waste heat directly to the cold sky seen perpendicular to the plane of the ecliptic.

### ONBOARD DATA STORAGE

Although the feasibility study did not absolutely recommend onboard data storage, the subject was considered carefully and left an option for NASA—an option that NASA did take.

Most Earth satellites carry tape recorders which are read out whenever the satellite passes over a data-acquisition site. A tape recorder allows instruments to record continuously when the satellite is out of sight of a station. The DSN has several 85-ft and 210-ft paraboloidal antennas suitable for Pioneer data acquisition at various sites around the world (see ch. 8 for list), but often they are busy on high priority programs, such as manned and unmanned lunar spacecraft. As a result, a data handling subsystem with limited data storage appeared in the final spacecraft design.

### AN EARLY WEIGHT BREAKDOWN

Of course, the feasibility study went into much more detail than the preceding paragraphs indicate. The chapters covering the various subsystems will trace the design from the feasibility study through final fabrication. The intent here has been to introduce the reader to more general considerations and the major design decisions that were made during the feasibility study.

The IQUSY Pioneer spacecraft emerging from the feasibility study had the same basic geometry as the final flight versions, except that booms were installed to isolate instruments in the flight models (fig. 1-4). The feasibility study's weight breakdown is presented in table 1-3.

TABLE 1-3.—*Spacecraft Weight Breakdown; STL Feasibility Study*

| Subsystem or component                         | Weight   |
|--|----------|
| Structure.....                                 | 17.4     |
| Communications.....                            | 27.6     |
| Electrical system.....                         | 15.8     |
| Reorientation system.....                      | 8.4      |
| Temperature control.....                       | 3.2      |
| Solar cell array.....                          | 17.7     |
| Balance weights.....                           | 1.5      |
|  | 91.6 lb  |
| 5 percent contingency.....                     | 4.6      |
|  | 96.2 lb  |
| Experiments, power conversion and cabling..... | 20.0     |
|  | 116.2 lb |
| Delta interstage structure.....                | 9.5      |
|  | 125.7 lb |
| Total.....                                     |          |

### EXPERIMENTS SUGGESTED BY STL

The IQSY Pioneers were considered precursor instrument carriers for the purposes of the feasibility study. The thought at NASA at that time was that more sophisticated space vehicles carrying better, more precise instruments would follow once the Pioneers blazed a path and radioed back a rough picture of the interplanetary domain. Because the interplanetary environment was only known imperfectly, the experiments were designed with a high dynamic range rather than high precision. As mentioned previously, instruments strongly affect spacecraft design, particularly in the matters of scanning, communication, and power requirements. Furthermore, the command subsystem and experiments should possess sufficient flexibility to allow experimenters to step up the sampling rates for instruments recording solar plasma, solar radiation, and magnetic fields during periods of high solar activity. In other words, the Pioneers were not to be regarded as passive instrument platforms set adrift on the interplanetary sea, but rather flexible arrays of instruments responsive to experimenters on Earth.

With flexibility in mind, STL suggested three alternative data handling systems offering various combinations of real-time transmission, fast scanning of selected instruments, and data storage prior to transmission. Data storage allowed the instruments to record data faster than the communication subsystem could transmit it to Earth—a valuable feature during

a solar flare, for example. As mentioned earlier, data storage capability also permitted data recording during periods when the spacecraft was not being tracked. The feasibility study, however, was based on a spacecraft without data storage for the sake of simplicity and reliability, although STL engineers clearly favored the addition of a data storage unit.

STL did examine specific types of experiments, although for the actual spacecraft NASA solicited experiments from the scientific community. The five types of instruments suggested by STL were:

- (1) Magnetometers, both fluxgates and search coils
- (2) Plasma probes
- (3) Lyman-alpha detectors
- (4) Micrometeoroid detectors
- (5) Cosmic-ray detectors

Detailed instrument design was not part of the feasibility study. The study of instrument types was aimed solely at defining interface problems. The Pioneer spacecraft that actually flew carried all of the instrument types suggested by STL with the exception of the Lyman-alpha detectors. As a result of the deliberations of its Space Science Steering Committee, NASA also added radio-propagation and electric-field experiments to the Pioneers (see ch. 5).

### **IMPACT OF THE FEASIBILITY STUDY**

The feasibility study was a solid foundation for the drawing up of specifications, the issuance of an RFP, and the eventual selection of a hardware contractor. The feasibility study did not provide all of the answers; some spacecraft features were changed later during the detailed design phase. Still, the basic concept was sketched out and strengthened by the application of STL's hardware experience with many other spacecraft in the same size class. The following chapters covering detailed system design will use the results of the feasibility study (ref. 1) as a point of departure in describing the technical evolution of the Pioneer interplanetary probe.

### **REFERENCE**

1. ANON.: Final Report on the Interplanetary Probe Study. Space Technology Laboratories Rept., Redondo Beach, Aug. 15, 1962.



## Pioneer Launch Trajectory and Solar Orbit Design

THE ORIGINAL PLAN for the Pioneer Program involved merely sending a small spacecraft into orbit about the Sun where it could monitor the environment in interplanetary space without the perturbations of the Earth's magnetosphere and atmosphere. Trajectory analysis soon showed that the scientific productivity of the missions could be increased greatly by shaping the trajectories and orbits to: (1) enhance solar system coverage, (2) create astronomical phenomena, such as solar occultations, and (3) study Earth-induced space phenomena, such as its magnetic tail. Trajectory and orbit planning thus became more complex as scientific objectives grew more ambitious.

Each Pioneer mission was different. Rather than burden the reader with the details of each, generalizations and summaries covering all Pioneer flights will be presented, supplemented by a detailed discussion of trajectory and orbit design for Pioneer 9.

### SPECIFIC MISSION OBJECTIVES: A SCIENTIST'S VIEW

To set the stage for the general treatment of trajectory trade-offs and other factors that influenced Pioneer celestial mechanics, consider the following special requirements levied on the five missions. The special requirements for Pioneer 6 were:

- (1) Inward trajectory, perihelion near 0.8 AU, in order to extend solar system coverage by Pioneer instruments into the sector ahead of the Earth as it plies its orbit about the Sun
- (2) Solar occultation of the spacecraft as seen by the tracking antennas on Earth

The special requirements for Pioneer 7 were:

- (1) Outward trajectory, aphelion near 1.1 AU, to extend solar system coverage in the Earth's "wake"—note that a lagging spacecraft actually detects solar events before terrestrial instruments because the outwardly spiraling solar magnetic lines of force sweep around the solar system faster than the planets due to the Sun's 28-day rotation.

- (2) Geomagnetospheric tail analysis—an outward-bound Pioneer can be designed to swing through the Earth's magnetic tail.

(3) Lunar occultation analysis—on both inward- and outward-bound missions, scientists had a “sporting chance” to see an occultation of the Earth by the Moon through the sensors of the Pioneer instruments. Intrinsic launch vehicle inaccuracies precluded any guarantees. The first attempt was made with Pioneer 7.

Pioneer 8 special requirements were the same as for Pioneer 7; Pioneer 9 special requirements were the same as for Pioneer 6.

The special requirements for Pioneer E were:

(1) Inward-outward combination trajectory, with final near-Earth (1.0 AU) heliocentric orbit—the objective was to have the spacecraft linger in the vicinity of the Earth, allowing the use of high-bit-rate telemetry over a period of several hundred days.

(2) Geomagnetospheric tail analysis was to be similar to that of Pioneer 7.

### OTHER FACTORS INVOLVED IN PIONEER TRAJECTORY AND ORBIT DESIGN

Before detailed trajectory studies could commence for any Pioneer mission, the science-oriented objectives had to be translated into quantitative goals which in turn were subject to quantitative constraints imposed by hardware and the laws of nature. Several new trajectory and orbit design factors are apparent in the following list of goals and constraints established for the Pioneer 9 mission, which is used here as an example:

- (1) 0.76 AU nominal perihelion
- (2) 0.00° inclination with respect to the ecliptic plane
- (3) To maximize the time the spacecraft remains close to superior conjunction (solar occultation)
- (4) Lunar occultation
- (5) To provide station-look angles of less than 150° and greater than 30° at Deep Space Station 51 (DSS-51 at Johannesburg); DSS-41 (Woomera); and DSS-12 (Goldstone) from launch plus 90 minutes to launch plus 48 hours (This goal was established to facilitate tracking and data acquisition during the spacecraft orientation maneuvers.)
- (6) To minimize the sensitivity of transit time to superior conjunction to deviations in launch vehicle performance

The following constraints or essential conditions were also established:

- (1) Three-sigma probability (99.73 percent) of Earth escape based on  $n$ -body escape velocity
- (2) Three-sigma probability of a Sun-look angle greater than 10° at spacecraft injection (This condition provides a high probability that the Sun will be seen by the spacecraft Sun sensors, which have a built-in 10° deadband where the Sun is invisible. Proper orientation of the spacecraft is impossible unless the Sun is in view of these sensors. See ch. 4.)

(3) Three-sigma probability of orbit inclination to the ecliptic plane less than 0.20°

(4) Total input heat rate to spacecraft less than 0.095 Btu/ft<sup>2</sup>-sec due to rocket plume radiation, Earth albedo, etc.

(5) Maximum internal fairing temperature less than 275° F

(6) Spacecraft total angular momentum vector to point at the southern celestial hemisphere after the first orientation maneuver (Type-I maneuver)

(7) Three-sigma probability that Earth shadow period (time in umbra) is less than 15 minutes (The spacecraft battery is of limited capacity and must not be exhausted before sunlight activates the solar cells) (fig. 2-1).

(8) Three-sigma probability that the spacecraft will not impact the Moon

(9) Spacecraft spinup acceleration to be less than 25 radians/sec<sup>2</sup> to avoid undue stresses on the spacecraft

(10) Launch window to be greater than eight minutes

(11) Sixty seconds of tracking from Antigua to be available after second-stage engine cutoff (SECO)

(12) The orbit attained by the second stage prior to the injection of the Pioneer spacecraft into an escape hyperbola to be suitable for the piggyback Test and Training Satellite (TETR-2 on Pioneer 9)

Quite obviously there was a need for the trajectory designer to balance many parameters as he attempted to program the Delta launch vehicle for a Pioneer mission.

### Early Phases of Trajectory

A general picture of the trajectory is useful amid these seemingly unrelated parameters. The Delta launch vehicles carrying Pioneer payloads were all launched southeastward from Cape Kennedy along the Eastern Test Range (ETR). During the flight, the Deltas passed over Ascension Island in the South Atlantic and tracking stations in the vicinity of Johannesburg, Republic of South Africa (fig. 2-2). Approximately 500 seconds after lift-off, the second-stage engines cut off (figs. 2-3 and 2-4). The Delta second and third stages, the Pioneer spacecraft, and any TETR piggyback spacecraft are then in Earth orbit over Johannesburg. This coast phase is essential if the spacecraft is to be launched properly into an orbital plane nearly parallel to that of the ecliptic. At a point before the spacecraft and attached Delta upper stages reach the plane of the ecliptic, the small rockets on the spin table on the Delta second-stage fire, imparting a spin to the spacecraft and Delta third stage. Next, the Delta third stage fires at that precalculated point in the coast trajectory where the velocity added by the third stage will carry the spacecraft into an escape hyperbola and thence into orbit around the Sun. Only after third-stage ignition is the second-priority TETR injected into Earth orbit from its berth near the top of the second stage. The inward Pioneers (6 and 9) were injected with

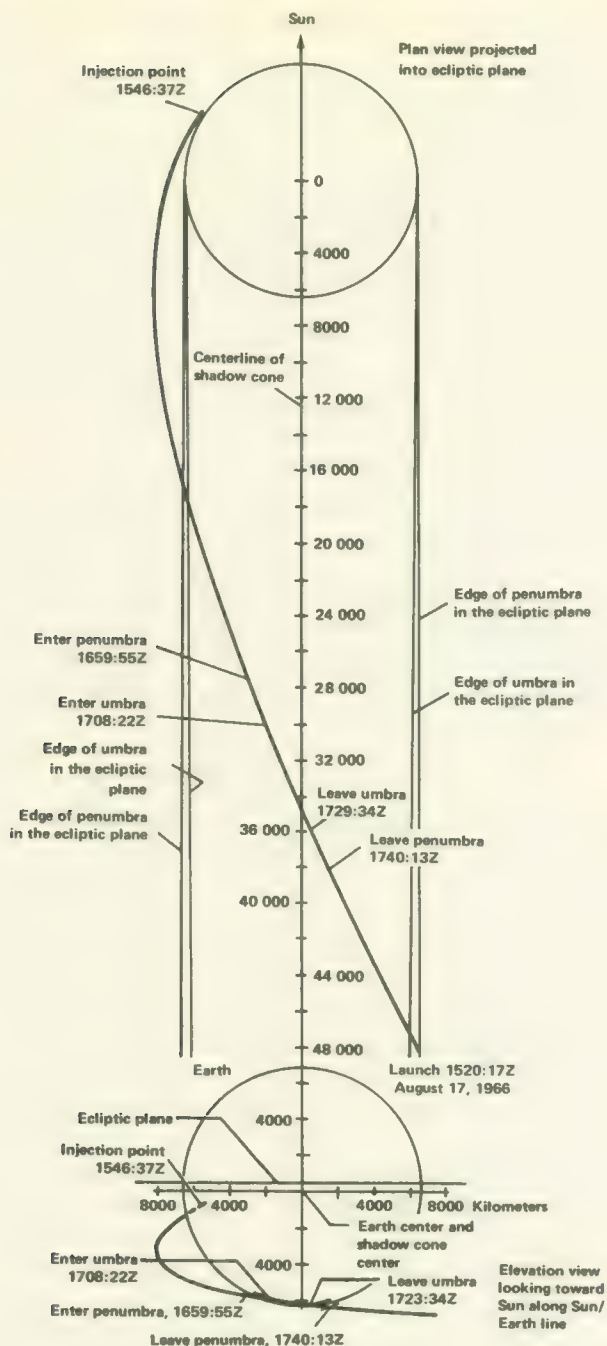


FIGURE 2-1.—The trajectory of Pioneer 7 as it passed through the Earth's shadow.

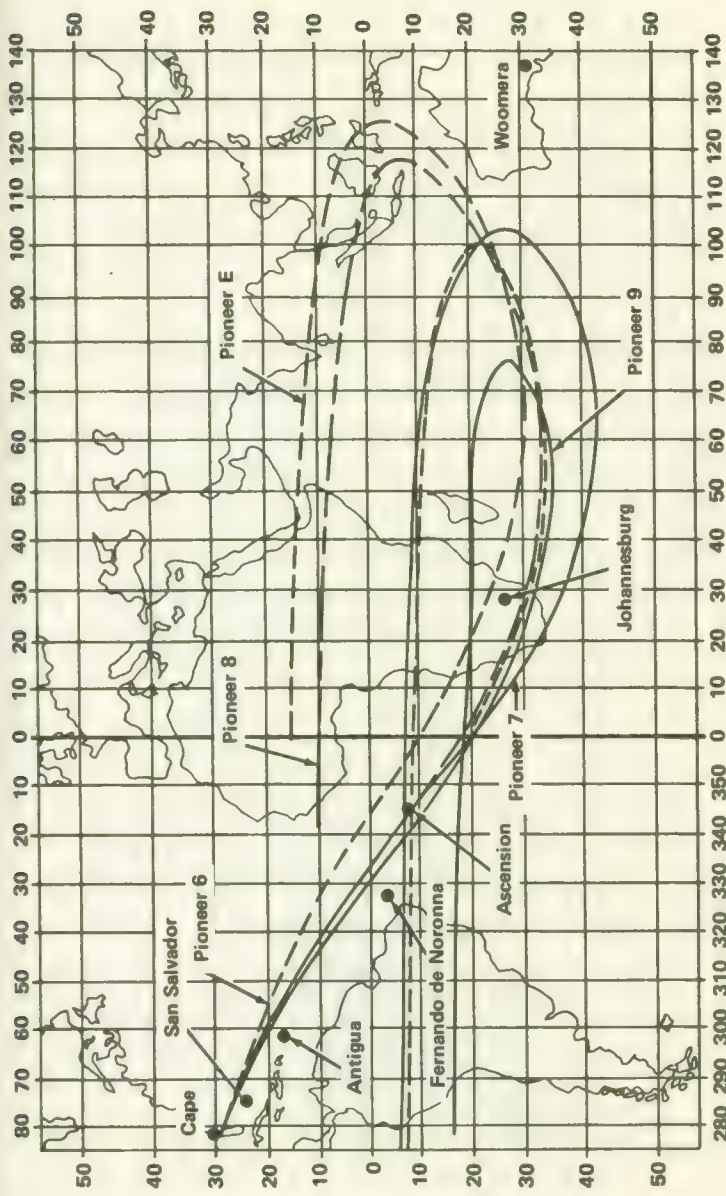


FIGURE 2-2.—Ground tracks for the four successful Pioneers plus the projected track of Pioneer E.

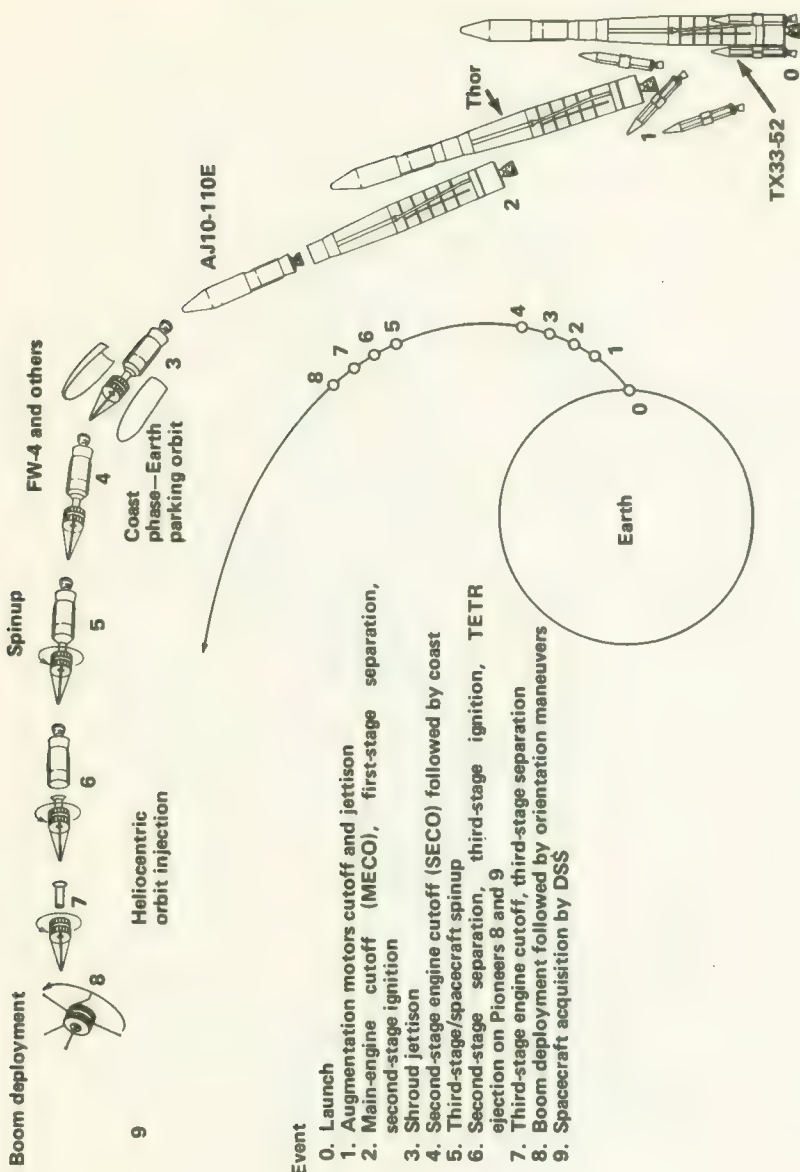


FIGURE 2-3.—The Pioneer launch sequence.

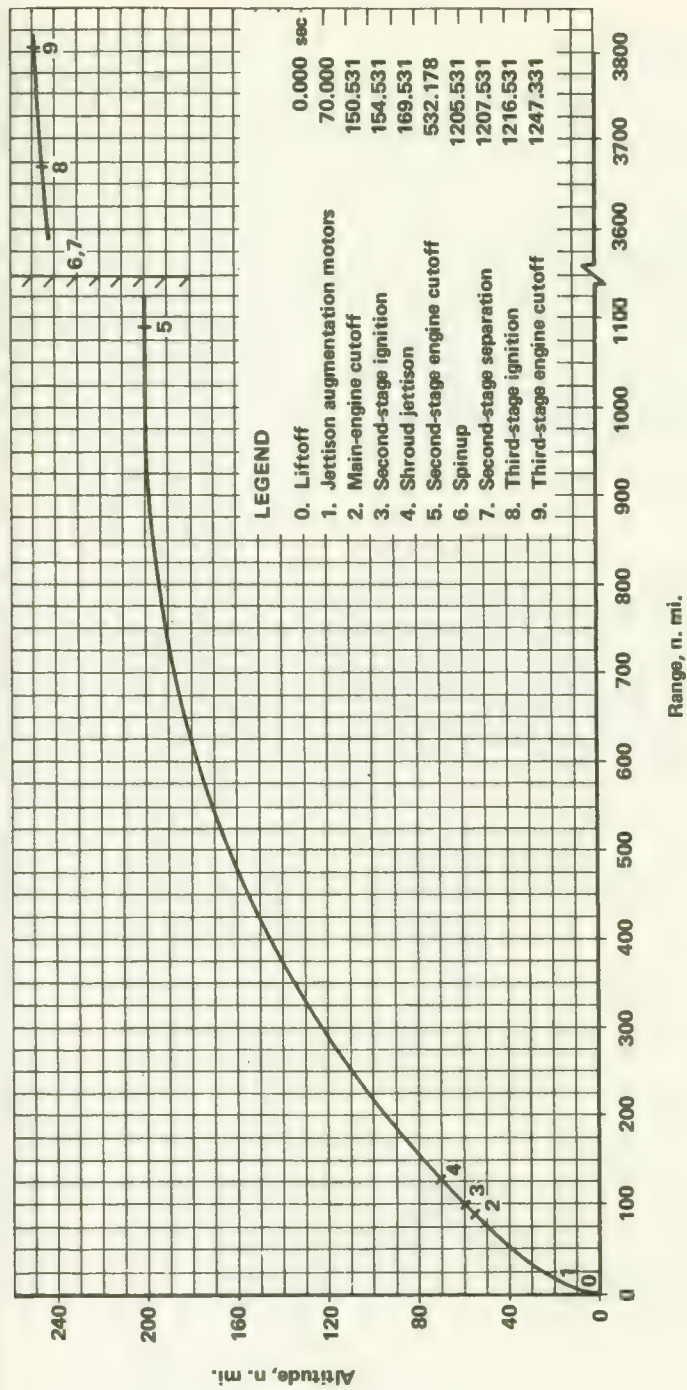


FIGURE 2-4.—The planned ascent profile for Pioneer 9.

velocity vectors approximately opposite to the Earth's velocity. Thus slowed, they "fall" in toward the Sun and initially fall behind or lag the Earth (fig. 2-5). The inward Pioneers essentially convert gravitational energy into orbital velocity and, after about 75 days, catch up with the Earth and lead it by ever-increasing distances in its journey around the Sun. The outward Pioneers (7 and 8) were injected with velocities parallel to that of the Earth. They initially lead the Earth but after 30 to 40 days they fall behind and, like the outer planets, lag the Earth.

The ground tracks of the Pioneers (or any other interplanetary probes) indicate a retrograde motion with respect to an observer on the Earth. This effect is due to the rotation of the Earth under the spacecraft as it moves off into deep space. The ground track is, of course, of vital importance in scheduling NASA's tracking and data acquisition stations around the world (ch. 8).

### Launch Windows

As the Earth turns on its axis, it carries Cape Kennedy to a position within approximately  $5^{\circ}$  of the plane of the ecliptic once a day. This is the optimum period for Pioneer launches. At this moment, only about 5 min of coast time are required to reach the plane of the ecliptic. Twelve hours later, a 30-min coast period is necessary; this would cost extra payload pounds. Pioneer launches, therefore, were best made during launch windows a few minutes wide that occur only once a day. The Pioneer Project Office

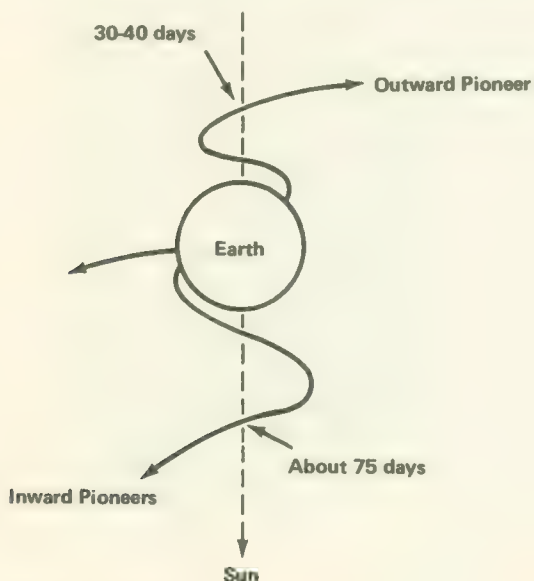


FIGURE 2-5.—Initial portions of inward and outward Pioneer trajectories (not to scale).

at Ames Research Center required that launch windows be greater than 8 min wide so that short holds would not scrub a mission for a whole day.

From the standpoint of scheduling the many intermeshing launch activities at Cape Kennedy, Pioneer launches had to be arranged months ahead of time. Precise times had to be specified so that tracking crews, range safety personnel, and all other Cape activities could be properly synchronized. Neither was a specific time window on a single specific day sufficient, because the launch might be postponed due to weather or some minor malfunction. In the Pioneer Program, "blocks" of launch windows, with windows about a day apart within each block, were established. If minor problems did crop up, it was hoped that they would be corrected in time for launch within a given block of days. If, however, serious difficulties arose affecting the launch—weather or a conflict with a higher priority program, for example—the first block of windows could be set aside and replaced by the second block. Two blocks of windows set aside for Pioneer 9 are described in table 2-1.

### PIONEER 9 TRAJECTORY ANALYSIS

The ascent trajectory for the Delta launching Pioneer 9 was designed by McDonnell-Douglas Astronautics Co., the launch vehicle contractor, subject to the objectives and constraints specified by the Pioneer Project Office of Ames Research Center (ref. 1). This was the usual procedure for all Pioneer launches. The objectives and constraints listed in the preceding section are essentially those applied to Pioneer 9.<sup>3</sup> The two blocks of desired launch days were also specified by Ames in accordance with mission requirements. All data presented in this section were computed for the nominal launch time of November 6, 1968, 9:47 GMT unless otherwise specified. They are applicable even though the launch was delayed until November 8.

A characteristic of all Pioneer missions is the common ascent trajectory for all days within a given launch block. Timing of the launch was, of course, dictated by the approach of the plane of the ecliptic to Cape Kennedy. The ascent profile for the Pioneer 9 launch is presented in figure 2-4.<sup>4</sup> Further details about the launch vehicle and its operational constraints may be found in chapter 7. For this specific launch the planned liftoff weight was 151 761 lb with a liftoff thrust of 255 367 lb. In the launch plan, the main first-stage engine burned for 150.5 sec and the three solid augmentation rockets burned for approximately 40 sec each. During the first-stage burn, pitch and yaw control was accomplished by the automatic

<sup>3</sup> According to NASA terminology, this spacecraft was called Pioneer D until it was successfully injected into Earth orbit.

<sup>4</sup> Launch trajectories were computed from a three-dimensional *n*-body computer program developed by JPL and designated DBH07.

TABLE 2-1.—*Pioneer-D Launch Windows*

| Block-IIA missions     |                    |                     |
|------------------------|--------------------|---------------------|
| Date                   | Window opens (GMT) | Window closes (GMT) |
| November 6, 1968-----  | 0945               | 0959                |
| November 7, 1968-----  | 0941               | 0955                |
| November 8, 1968*----- | 0937               | 0951                |
| November 13, 1968----- | 0917               | 0932                |
| November 20, 1968----- | 0849               | 0904                |
| November 22, 1968----- | 0841               | 0856                |

| Block-III missions     |                    |                     |
|------------------------|--------------------|---------------------|
| Date                   | Window opens (GMT) | Window closes (GMT) |
| November 27, 1968----- | 0843               | 0857                |
| December 4, 1968-----  | 0816               | 0829                |
| December 11, 1968----- | 0748               | 0802                |
| December 18, 1968----- | 0721               | 0734                |
| December 22, 1968----- | 0703               | 0717                |

\* Actual launch date; time 0946:29 GMT.

gimballing of the main engine in response to signals from an inertial reference package. Roll control was maintained by gimballed vernier engines and the inertial reference package. A radio guidance system in the second stage also supplied steering correction signals to the first stage.

The second-stage engine was ignited at an altitude of about 60 n. mi. This motor burned for a nominal 377.6 sec with a thrust of 7803 lb. Again, the main engine was gimballed. Roll was controlled by four cold-gas jets. Control signals originated in a second-stage programmer, an inertial reference package, and the radio guidance system.

The coast period following second-stage cutoff was computed to be 684.4 sec for Pioneer 9. As the spacecraft and the attached second and third stages approached the point of injection, gas jets turned the spacecraft axis so that it had an elevation angle of  $-2.0^\circ$  and a yaw angle of  $5.2^\circ$  about the local vertical to the right of the trajectory plane looking downrange. Next, the spin-table rockets atop the second stage were fired to spin up the spacecraft and attached third stage for purposes of dynamic stability. Just 9 sec before reaching the point of injection, the second stage was jettisoned. The combination third-stage-plus-spacecraft weighed 878.2 lb at this point.

The solid third-stage engine fired for 30.8 sec with a thrust of approximately 5605.5 lb, imparting 3282 m/sec velocity to the spacecraft before

cutoff. The resultant velocity vector was approximately parallel to the plane of the ecliptic. Attitude stability during third-stage burn was maintained by the spinning action. The third stage was jettisoned and the spacecraft headed on an escape hyperbola for heliocentric orbit. The ground trace for Pioneer 9 is shown in figure 2-2.

If all had gone well during the launch, the spacecraft would have embarked on the planned near-Earth trajectory illustrated in figure 2-6. As it turned out, a launch vehicle problem delayed the launch for about 48 hours. If the date in figure 2-6 is changed to Nov. 8, the figure applies equally well for the actual trajectory. The view in figure 2-6 is that seen from the north ecliptic pole with the Earth-Sun line fixed in space. As mentioned earlier, the inward-bound Pioneer 9 spacecraft initially lagged the Earth which was moving to the left.

One can see from figure 2-7 how lunar occultation by the Earth—as seen from spacecraft instruments—is possible. This astronomical event, however, is very sensitive to small dispersions in launch vehicle performance. A slight deviation from the nominal orbital plane, for example, will preclude occultation.

The actual trajectory of Pioneer 9 is shown in figure 2-8, on the same scale as figure 2-7. The critical difference is not the shape of the trajectory, which is almost identical, but the day of launch. During the two days' delay, the Moon had moved as shown. Further, a 9-min hold prior to launch resulted in excursions of 206 000 and 202 000 km below and above the plane of the ecliptic, respectively.

Figure 2-8 also has the Earth's magnetosphere (hardly spherical) superimposed upon it. The trajectory cuts through the "side" of the plasma sheath, but inward launches do not take the spacecraft far out into the magnetic tail like the outward launches do.

The event termed syzygy is noted on figure 2-9. This is simply that point in time when the Earth is between the Sun and the spacecraft and in a common plane perpendicular to the ecliptic. Unlike solar occultation, which occurs when the Sun is between the Earth and the spacecraft, syzygy holds little interest for the scientists.

Three other types of charts are commonly used in describing Pioneer heliocentric orbits. The first, figure 2-10, is based on a Sun-centered vernal equinox ecliptic reference. It shows clearly how Pioneer 9 draws farther and farther ahead of the Earth as both swing around the Sun. Perihelion for Pioneer 9 occurs roughly at the same spot in space where it was launched, but when it first returns to this location in 298 days, the Earth with its 365-day period will be far behind the spacecraft.

The second type of presentation shows Pioneer orbits plotted with respect to a fixed Earth-Sun line, figure 2-11. This figure is much like figures 2-6, 2-7, and 2-8 except that here the Sun is at the center of the polar coordinate paper. The distance between the Earth and Pioneer 9

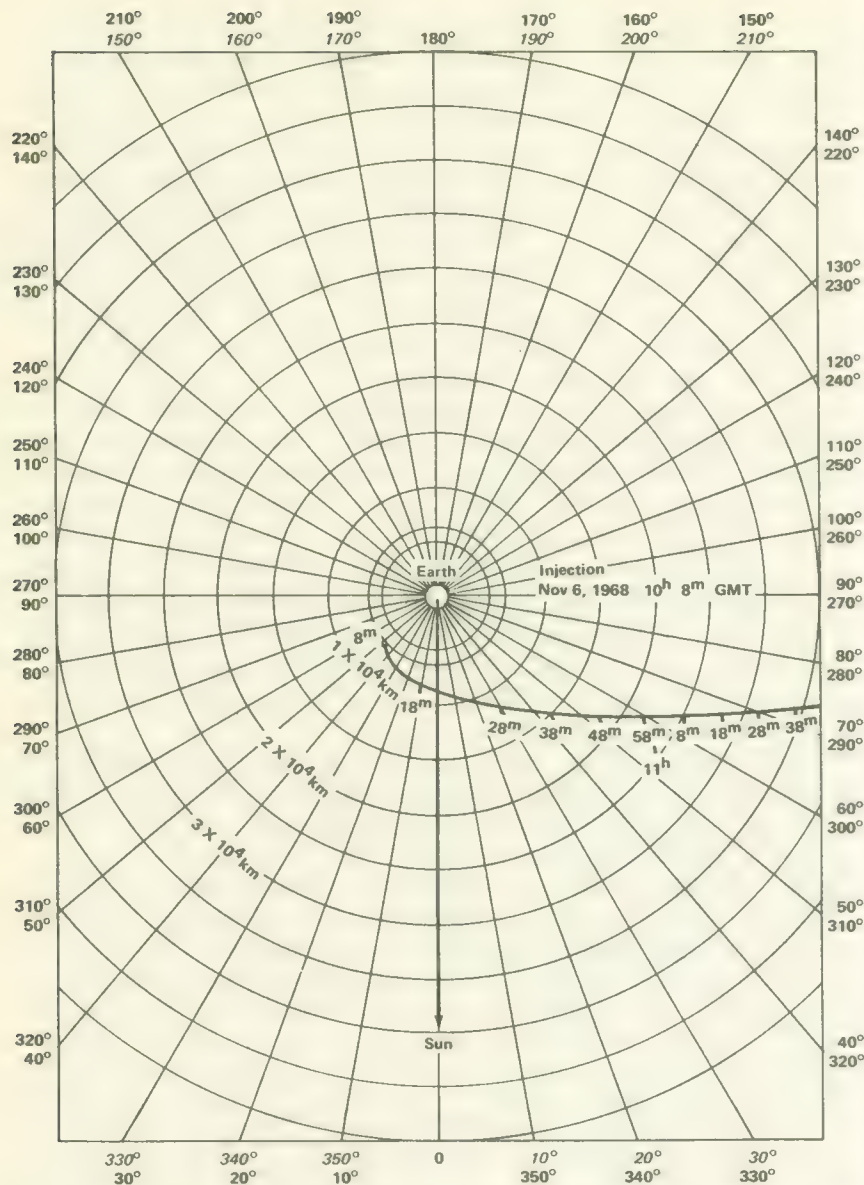


FIGURE 2-6.—The near-Earth trajectory of Pioneer 9 (as projected for a Nov. 6 launch).

grows ever greater, with the exception of the little loops of apparent retrograde motion at the aphelion points. Early in 1973, Pioneer 9 will lap the Earth for the first time. In the case of outward Pioneers, the Earth laps them, although not so quickly. The plots for outward-bound Pioneers show

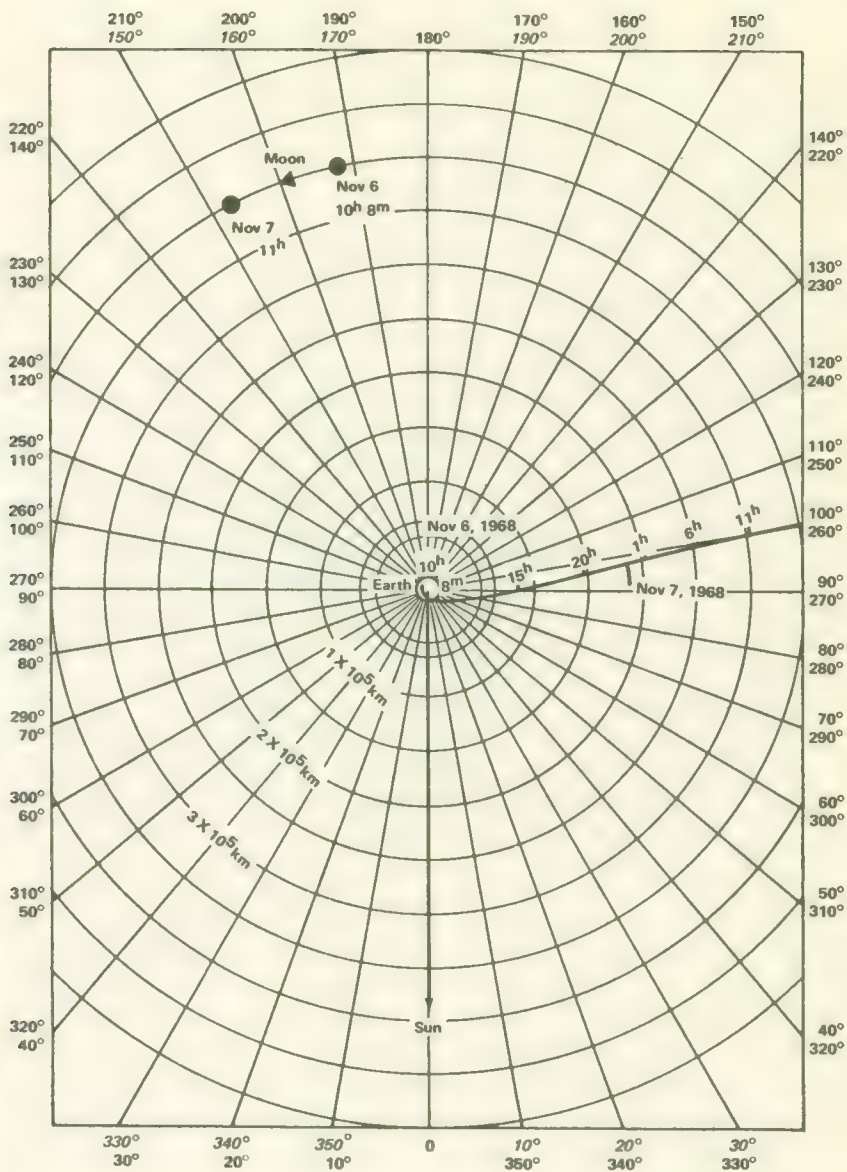


FIGURE 2-7.—Cislunar trajectory for Pioneer 9 (as projected for a Nov. 6 launch).

cusps at perihelion rather than the aphelion loops on figure 2-11. The scientifically important event shown on figure 2-11 occurred when the Sun occulted the Pioneer 9 spacecraft in late 1970. For a month or two on either

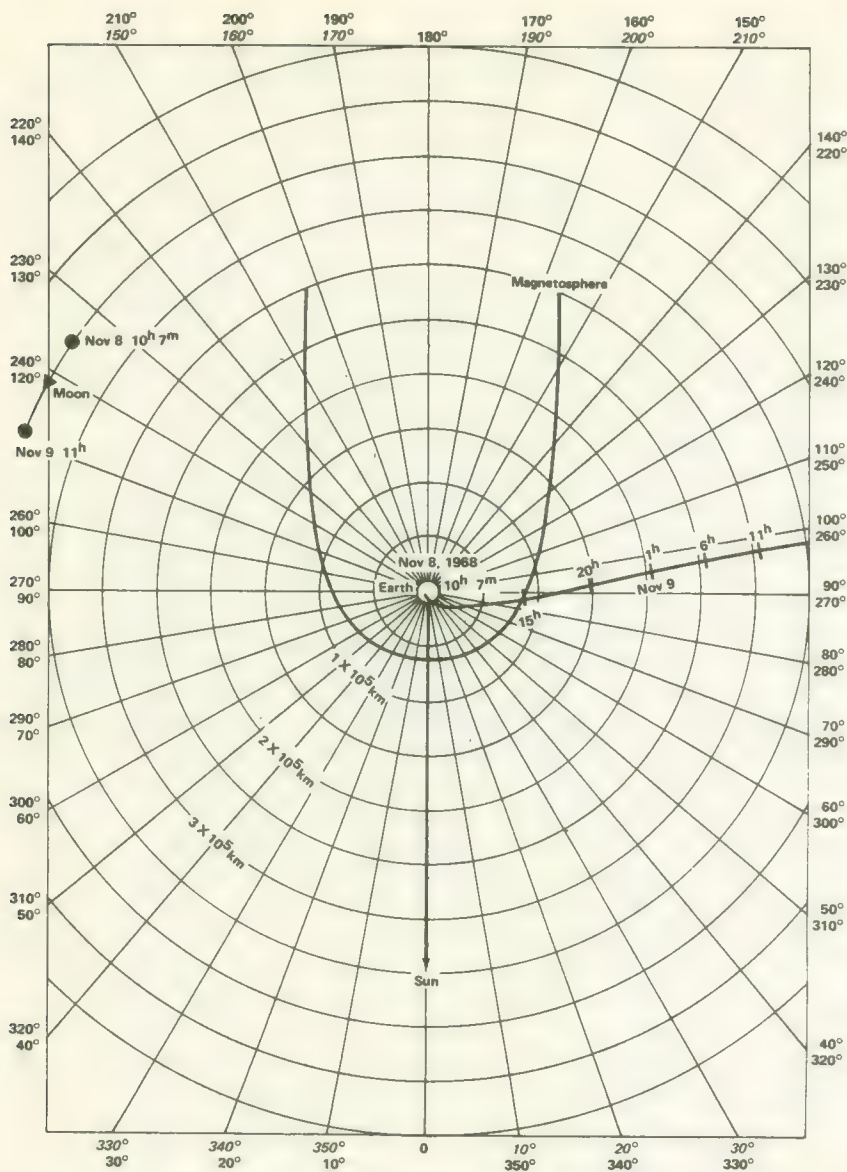


FIGURE 2-8.—Actual cislunar trajectory for delayed Pioneer 9 launch.

side of this date, the DSN 210-ft antenna at Goldstone recorded the effects of the solar corona and atmosphere on the spacecraft radio signals.

The last type of plot considered here shows the relative positions of all four successful Pioneers with respect to one another and the Earth at

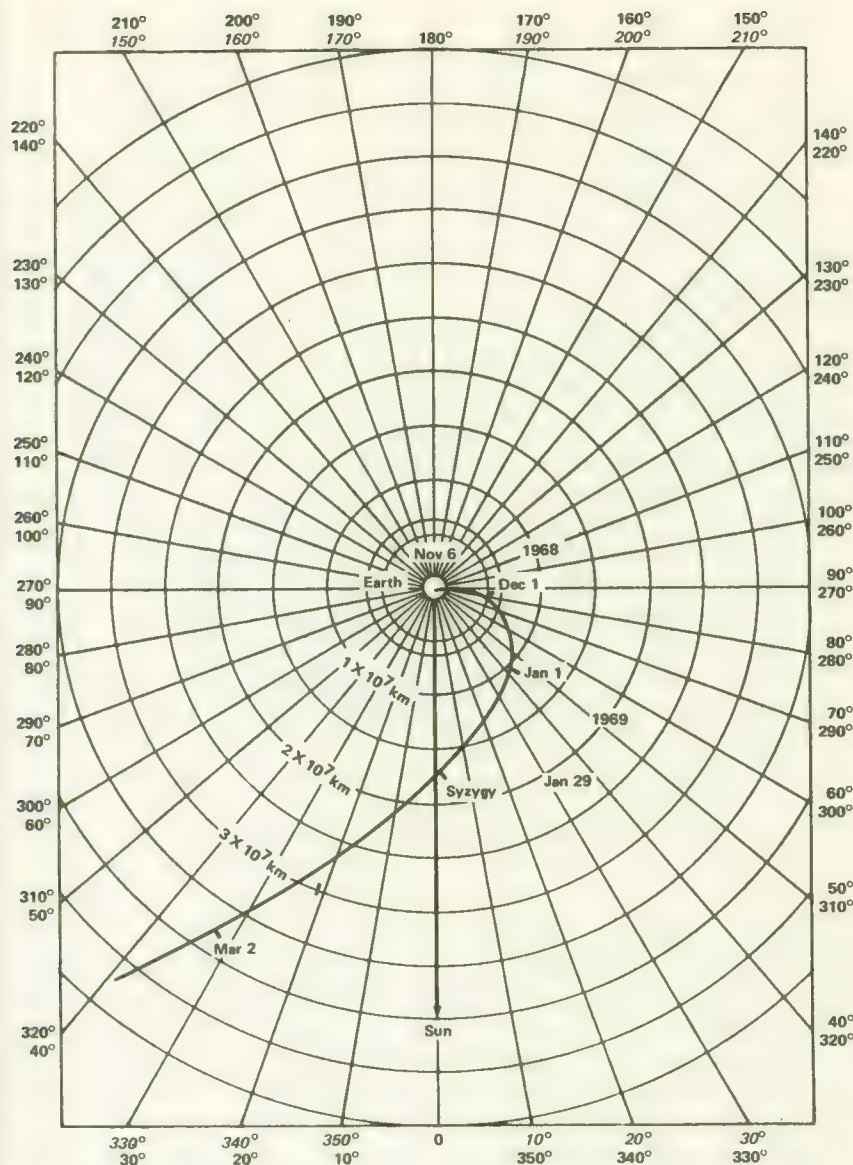


FIGURE 2-9.—Pioneer 9 trajectory through syzygy (as projected for a Nov. 6 launch).

various times. In a sense, figure 2-12 consists of a series of snapshots looking down on the plane of the ecliptic from the north ecliptic pole. The space-craft and Earth are moving counterclockwise about the Sun, with the inward objects moving faster than the outward objects, as both real and

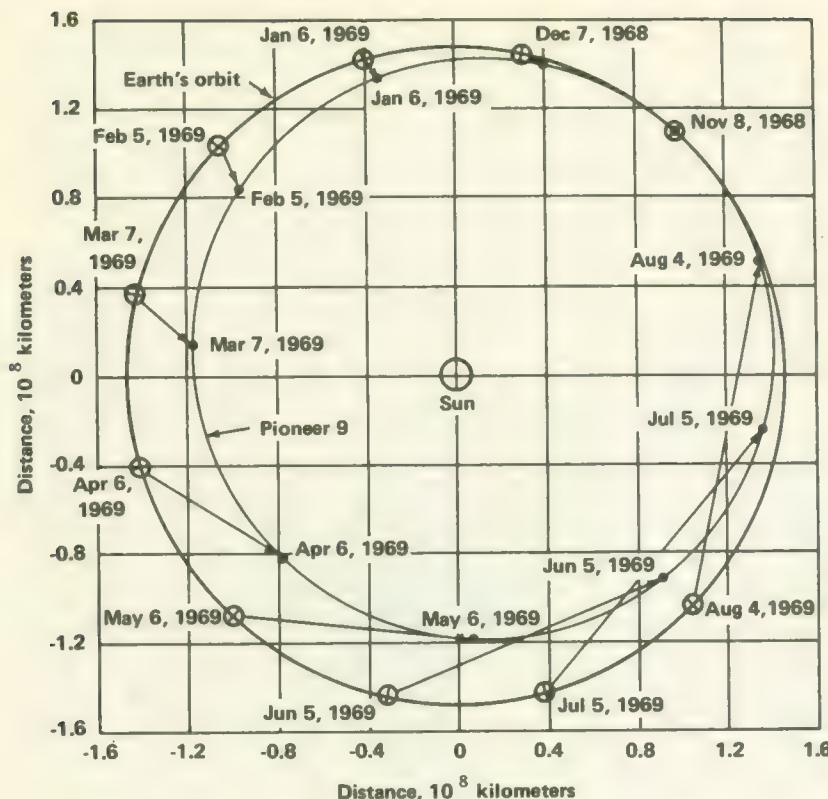


FIGURE 2-10.—Actual heliocentric orbit for Pioneer 9 using vernal equinox reference.

artificial planets should. This view has physical meaning for those attempting to forecast solar weather. The Sun rotates on its axis in the same direction as the Earth and the Pioneers circulate around it. With a 28-day period of rotation, however, the Sun's spiral magnetic field, which rotates with the Sun, turns much faster than the objects in heliocentric orbit. Therefore, the streams of plasma that follow the Sun's magnetic lines of force are always catching up with both the Earth and the probes and spraying them with plasma like a rotary water sprinkler. The lagging Pioneers are thus in a position to forecast solar-related events for the Earth.

### PIONEER ORBITAL PARAMETERS

The charts presented above are helpful in visualizing the Pioneer trajectories and orbits. For those interested in more precise information, table 2-2 summarizes Pioneer orbital data as of March 1969.

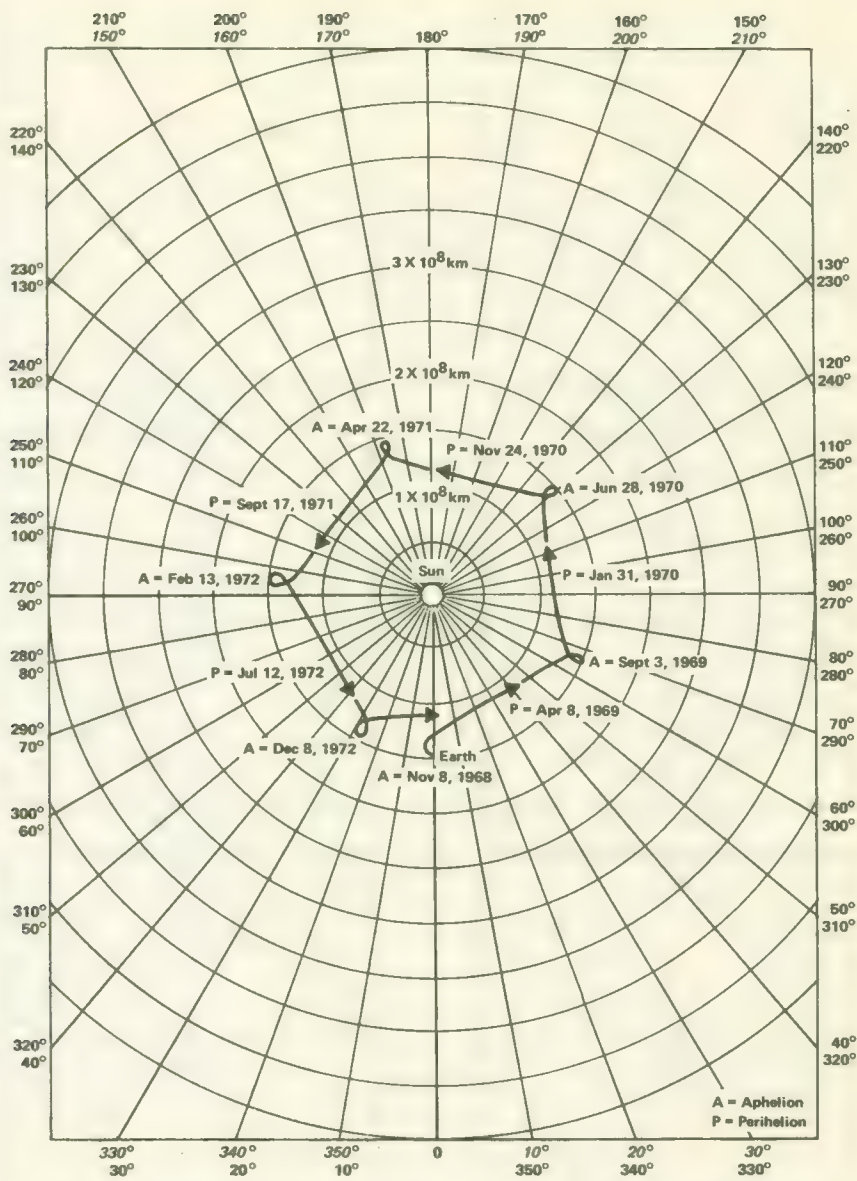
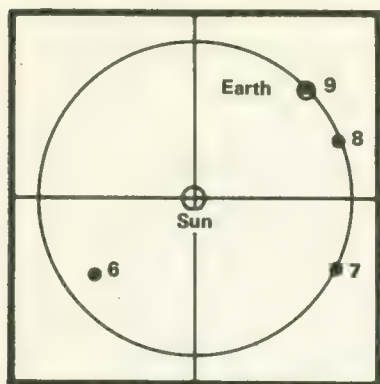


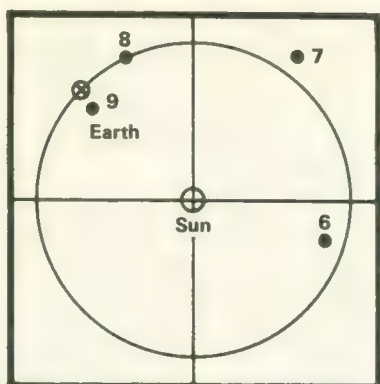
FIGURE 2-11.—Actual heliocentric orbit of Pioneer 9 in Earth-Sun-line reference frame.

### SPACECRAFT ORIENTATION

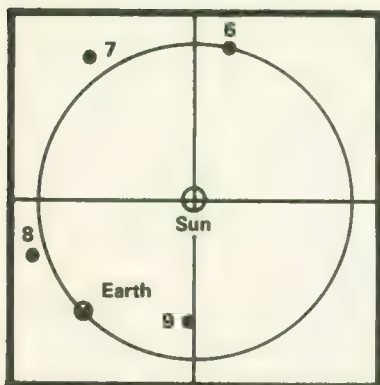
For the Pioneer spacecraft concept to be successful, the spacecraft spin axis had to be oriented so that it was perpendicular to the plane of the ecliptic. Only then would the spacecraft antenna patterns intercept the



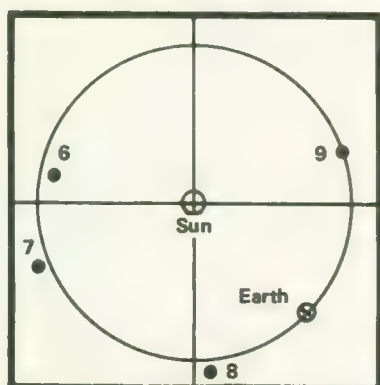
Nov 8, 1968



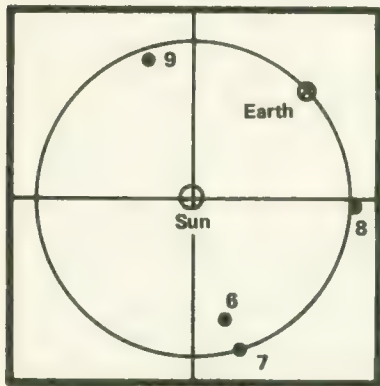
Feb 6, 1969



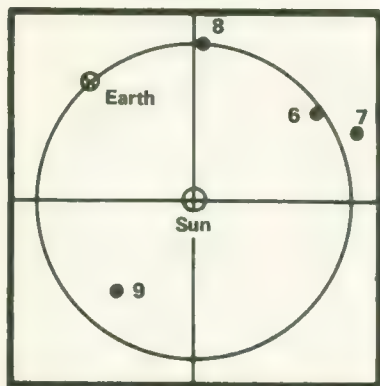
May 7, 1969



Aug 5, 1969



Nov 3, 1969



Feb 1, 1970

FIGURE 2-12—Relative positions of the four successful Pioneers with respect to the Earth at various times.

TABLE 2-2.—*Pioneer Orbital Parameters*<sup>a</sup>

| Parameter                                   | Orbital injection conditions |             |             |             |
|---|------------------------------|-------------|-------------|-------------|
|   | 6                            | 7           | 8           | 9           |
| Date of injection-----                      | 12-16-65                     | 8-17-66     | 12-13-67    | 11-8-68     |
| Time of injection (GMT)-----                | 0756:41.1                    | 1545:38.6   | 1439:32.5   | 1007:22.4   |
| Injection latitude-----                     | 7.8° S                       | 14.48° S    | 22.83° S    | 3.36° S     |
| Injection longitude-----                    | 4.6° W                       | 6.8° W      | 9.385° E    | 23.26° W    |
| Injection altitude (km)-----                | 564.1                        | 378.476     | 486.02      | 467.054     |
| Injection velocity<br>(km/sec)-----         | 10.8488                      | 10.939      | 10.7837     | 11.035674   |
| Flight path angle (deg)-----                | 1.7                          | 2.1         | -0.364      | 2.413724    |
| Azimuth angle (deg)-----                    | 119.3                        | 106.98      | 129.374     | 101.04027   |
| Elements of parking orbit                   |                              |             |             |             |
| Semimajor axis (km)-----                    | 7149.44                      | 7015        | 6775.1      | 7049.3      |
| Eccentricity-----                           | 0.071                        | 0.0549      | 0.0139      | 0.0424      |
| Inclination (deg)-----                      | 30.2                         | 33.0        | 32.906      | 32.88       |
| Height of perigee (km)-----                 | 270.6                        | 330.9       | 307.6       | 372.2       |
| Height of apogee (km)-----                  | 1288.1                       | 1342.5      | 495.1       | 970.0       |
| Anomalistic period<br>(min)-----            | 100.5                        | 97.4        | 92.4        | 98.17       |
| Elements of heliocentric orbit              |                              |             |             |             |
| Semimajor axis (km)-----                    | 134 481 910                  | 159 713 300 | 155 372 610 | 130 500 710 |
| Eccentricity-----                           | 0.0942                       | 0.05397     | 0.0476      | 0.1354      |
| Inclination to ecliptic<br>plane (deg)----- | 0.1693                       | 0.09767     | 0.0578      | 0.0865      |
| Aphelion (AU)-----                          | 0.936                        | 1.1250      | 1.0880      | 0.9905      |
| Perihelion (AU)-----                        | 0.8143                       | 1.0100      | 0.9892      | 0.7542      |
| Period (days)-----                          | 311.327                      | 402.91      | 386.60      | 297.594     |

<sup>a</sup> Support Instrumentation Requirements Document, Project Pioneer, NASA Headquarters, March 1969.

Earth and only then would the solar-cell arrays generate full power. After injection by the Delta third stage, the typical Pioneer spacecraft was spin-stabilized but its axis was not perpendicular to the ecliptic plane. The spacecraft onboard orientation subsystem automatically began the first or Type-I orientation maneuver. During this maneuver cold-gas jets torqued the spin axis around until it was perpendicular to the Sun-spacecraft line. The second, or Type-II, orientation maneuver was carried out through

ground commands from a DSN station, usually Goldstone. Under ground control, the gas jets were fired until the spacecraft transmitter signal received on Earth was maximized. The spacecraft spin axis was then approximately perpendicular to the plane of the ecliptic. A detailed description of these maneuvers and the spacecraft orientation subsystem may be found in chapter 4.

#### REFERENCE

1. ANON.: Pioneer D(IX) Trajectory and Orientation Analysis. TRW Systems Rept. 3432.8-5, 1968.

# Spacecraft Design Approach and Evolution

## SPACECRAFT DESIGN APPROACH

**S**PACECRAFT DESIGN is rarely a series of orderly, obviously logical steps. Instead, spacecraft design is usually iterative; that is, cyclic, with each successive iteration based on the experience of the previous one. The Pioneer spacecraft was no exception. It passed through a conceptual design phase, a feasibility study phase, an iteration on the feasibility study, a final design phase, and, before Pioneer 6 was finally mated to a Delta at Cape Kennedy, it had evolved not into a new species, but rather into a hardier, longer-lived subspecies. Furthermore, spacecraft evolution did not stop with the first launch; each of the five spacecraft and their instrument complements were slightly different, with the largest change occurring between Blocks I and II.

The Pioneer spacecraft evolved because of continuous pressure for improved reliability, telemetry capability, instrument payload, and other measures of performance. The direction of the spacecraft's evolutionary path was determined by the major spacecraft design objectives shown in table 3-1. The width of the path was established by the design constraints, some of which are noted in table 3-2. The achievement of the design objectives within the confines of the design constraints required a design philosophy, based on experience with other spacecraft of the same general type. Table 3-3 presents some of the major elements of Pioneer design philosophy. Quite obviously, design philosophy is really an astute combination of common sense and hard-earned experience.

It is not a foregone conclusion that spacecraft design objectives and constraints are compatible, even with the application of the best design philosophy. This fact is usually discovered during the feasibility study. Fortunately, the Pioneer spacecraft was feasible, and the long lifetimes achieved in space (several times the lifetime objective listed in table 3-1) demonstrate the success of the design philosophy.

### Spacecraft Weight

Spacecraft weight is usually an extremely critical parameter during the design history of any spacecraft. Along with reliability and magnetic cleanliness, weight was one of the three spacecraft-wide parameters that

TABLE 3-1.—*Major Spacecraft Design Objectives*

| Objective   | Remarks  |
|---|--|
| A success probability of 0.75 for a lifetime of six months----- | Lifetime figure was originally set by expected communication range of DSN 85-ft antennas (about 50 000 000 miles). (From Specification A-6669)   |
| A magnetically clean spacecraft-----                            | At 80 in. from the spin axis, on the magnetometer boom, the field perpendicular to the boom axis should not exceed: <ol style="list-style-type: none"> <li>0.5γ peak at 0–25 Hz</li> <li>16γ due to remanence after magnetization in a 25-G field parallel to the spacecraft axes</li> <li>1.0γ due to remanence after demagnetization in an ac field having an initial magnitude of 50 Oe (A-6669)</li> </ol> |
| Minimum cost-----   | The original cost goal for the spacecraft alone was to be about \$20 000 000.  |
| Minimum weight-----   | The upper limit of 111.24 lb was a constraint listed in Specification A-6669. (See table 3-2.)   |
| Wide flexibility in scientific instrument accommodation-----    | This would increase experimental options as more was learned about interplanetary space.   |
| Maximum bit rate-----   | The product of lifetime and bit rate is really the "pay-off function" for an interplanetary probe. Specific NASA objectives: <ul style="list-style-type: none"> <li>5 200 000 miles; 512 bits/sec</li> <li>7 300 000 miles; 256 bits/sec</li> <li>14 700 000 miles; 64 bits/sec</li> <li>29 400 000 miles; 16 bits/sec</li> <li>41 500 000 miles; 8 bits/sec</li> </ul>  |

had to be controlled with great care. These three important factors will now be covered to set the stage for the discussion of specific hardware in chapter 4.

The initial weight estimate is almost always optimistic, with the weight rising alarmingly—10 to 20 percent over the desired value—during the first few months of design. Then a concerted weight-reduction program usually pares off a few pounds until spacecraft weight is once again compatible with the launch vehicle capability and the mission requirements (fig. 3-1). In the case of the Pioneers, weight was very critical for the first flight. Indeed, with the early Delta launch vehicles and the DSN of 1964, the total Pioneer concept was really only marginally feasible; that is, with a 20 percent increase in spacecraft weight or, equivalently, a traveling wave tube (TWT) efficiency of 30 percent instead of 50 percent, the design would not have succeeded. The Delta and DSN, however, were not static systems.

TABLE 3-2.—*Major Spacecraft Design Constraints*

| Constraint  | Remarks  |
|---|--|
| Delta launch vehicle-----   | The spacecraft/launch vehicle interface is discussed in chapter 7.   |
| Deep Space Network (DSN)---   | The spacecraft/DSN interface is discussed in chapter 8.  |
| State-of-the-art-----   | Exceptions: TWTs, convolutional coder, and long-distance telemetry represented advances in the state-of-the-art.   |
| Maximum spacecraft weight:<br>111.24 lb-----  | This is exclusive of instruments, but includes payload penalties from launch-vehicle shroud and third-stage motor case thermal insulation (A-6669). See chapter 7. |
| Space environment between<br>0.8 and 1.2 AU-----  | Actually, little was known about this environment in 1963 and 1964. Environmental data were extrapolated from near-Earth measurements.                             |
| Ratio of spin-axis moment of<br>inertia to moments of inertia<br>about other axis be greater<br>than one----- | This would insure dynamic stability of spin-stabilized spacecraft.   |

The Delta was improved with each launch. Although Pioneer spacecraft weight did generally increase slightly from flight to flight (especially between Blocks I and II) as new experiments and improved equipment were added, the final two flights were launched with up to 30 lb of ballast and a piggyback TETR satellite on the Delta.

### Spacecraft Reliability

The Pioneer spacecraft have operated several years beyond their nominal 6-month lifetimes. This extra capability or overdesign has proven of great value to science, extending Pioneer coverage of interplanetary space past the 1969–1970 solar maximum. The original objective of 6-month life was set as the time it would take the spacecraft to forge beyond the 50 000 000-mile limitations of the extant 85-ft DSN antennas. The DSN improved, as explained earlier, and, fortunately, the spacecraft met the challenge, enabling scientific data to be received from spacecraft on the far side of the Sun, a distance of about 200 000 000 miles.

Several proven methods for increasing reliability are listed in table 3-3. Reliability is a somewhat more elusive parameter than weight. Weight may be measured precisely, and budgeted, as program dollars are. Re-

TABLE 3-3.—*Major Elements of Spacecraft Design Philosophy*

| Element of philosophy  | Remarks   |
|--|---|
| Failure modes of operation will be provided.   | The single failure of any control system, except the pneumatic assemblies of the orientation subsystem, would not result in the catastrophic failure of the mission (A-6669). This is the classical use of redundancy to attain higher reliability. (See further discussion in text.)   |
| Subsystems will be of modular form and interchangeable.                                      | This expedited testing, replacement, and repair (A-6669).   |
| Proven components will be used.  | Many entries on the Pioneer "approved parts" list came from the Air Force Minuteman ICBM program. (See "State-of-the-art," table 3-2.)  |
| Parts will be rigorously qualified; components will be "burned-in" before use on spacecraft. | The rather high percentage of early or incipient failures were eliminated in this way.  |
| "Magnetic guidelines" will be rigorous.  | Some guidelines established are: (1) use of Pioneer approved parts list, which eliminated the most offensive materials and components; (2) all magnetic leads to be less than 0.25 in. long; (3) all chokes, inductances, and transformers to be carefully designed and screened; (4) alloy 180 to be used for welded wire work and interconnections; (5) extreme caution to be employed with electrodeless nickel plating; (6) leads carrying 10 mA or more to be twisted with the return lead; (7) solar array to be backwired; and (8) ground loops to be avoided. |

liability, being a statistical parameter, cannot be measured for any single, specific part with any single, specific measuring instrument. Instead, the spacecraft engineer must rely upon collective experience with parts in applications similar to the intended one. In short, reliability assessment is as much an art as an engineering discipline. The attainment of high reliability in a spacecraft such as Pioneer requires the application of procedures and methods that have proven successful in the past. The two most successful general methods involve the use of carefully selected parts and the judicious application of redundancy. Added to the formal technique was the dedication of the program people to the goal of high reliability.

Mathematical assessments of Pioneer reliability were made by STL

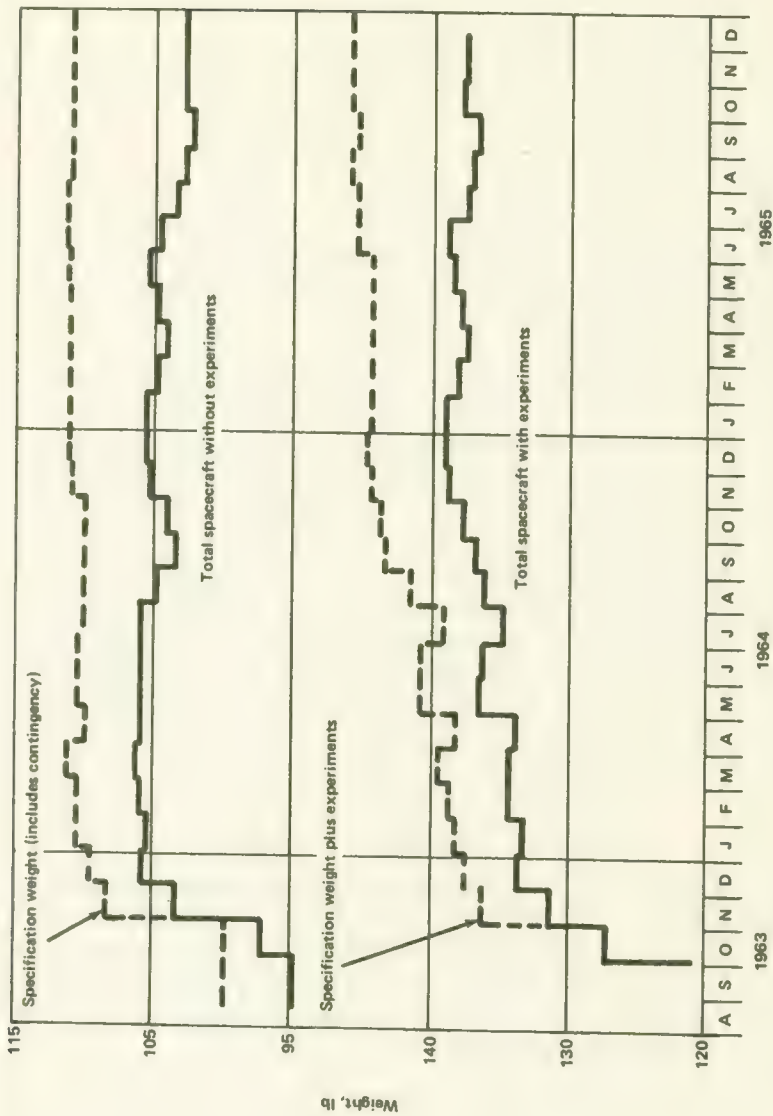


FIGURE 3-1.—Total spacecraft weight (Block I) without contingency as a function of calendar time.

during its feasibility study (ref. 1), and by Walter V. Sterling Co. during the performance of the following hardware design and development contract. Perhaps even more important to Pioneer's long life were the rigorous Quality Assurance and Failure Reporting programs established at STL and the equally severe test program that followed.

The high reliability of Pioneer is attributable to a three-level approach plus those elements of design philosophy listed in table 3-3. The three level approach was:

- (1) Mathematical analysis to identify weak points and the value of redundancy (described briefly below)
- (2) Selection and qualification of parts and subassemblies using very high standards (See Appendix for details on the STL Reliability and Quality Assurance Programs and Test Failure Reporting approach.<sup>5</sup>)
- (3) Testing in environments simulating those to be encountered by the spacecraft (covered in ch. 6)

During its 1962 feasibility study, STL estimated that using parts meeting military specifications but without the use of redundancy (except in the solar-cell array), overall system reliability would be an untenable 0.31. The use of the high-reliability parts developed during the Minuteman Intercontinental Ballistic Missile (ICBM) Program would boost system reliability to 0.59. Finally, the application of failure-mode protection (i.e., redundancy) would raise system reliability to an acceptable 0.86. The specific reliability model employed early in the program is portrayed in figure 3-2, while the effects of adding failure-mode protection are listed in table 3-4. It should be emphasized that figure 3-2 and table 3-4 are from the STL Pioneer proposal (ref. 3) and represent an early point in spacecraft design and not the spacecraft launched between 1965 and 1969, although most design features did not change significantly.

### Magnetic Cleanliness Campaign

In the Pioneer Program a third spacecraft-wide factor was added to those of weight and reliability control: magnetic cleanliness. Since all spacecraft subsystems might use magnetic materials and might also generate interfering electromagnetic fields, the cleaning of a magnetically "dirty" spacecraft demanded the cooperation of all spacecraft engineers. Magnetic cleanliness, like high reliability, owes more to design experience than any single device or technique.

Magnetic cleanliness becomes essential on scientific deep-space probes that venture out into the weak interplanetary fields which generally measure less than  $10\gamma$ . An ordinary capacitor, for example, may generate

<sup>5</sup> NASA Pioneer Specification A-6669.01 required the spacecraft contractor to establish these programs in accordance with NASA-wide product assurance guidelines. See A-6669 for details (ref. 2).

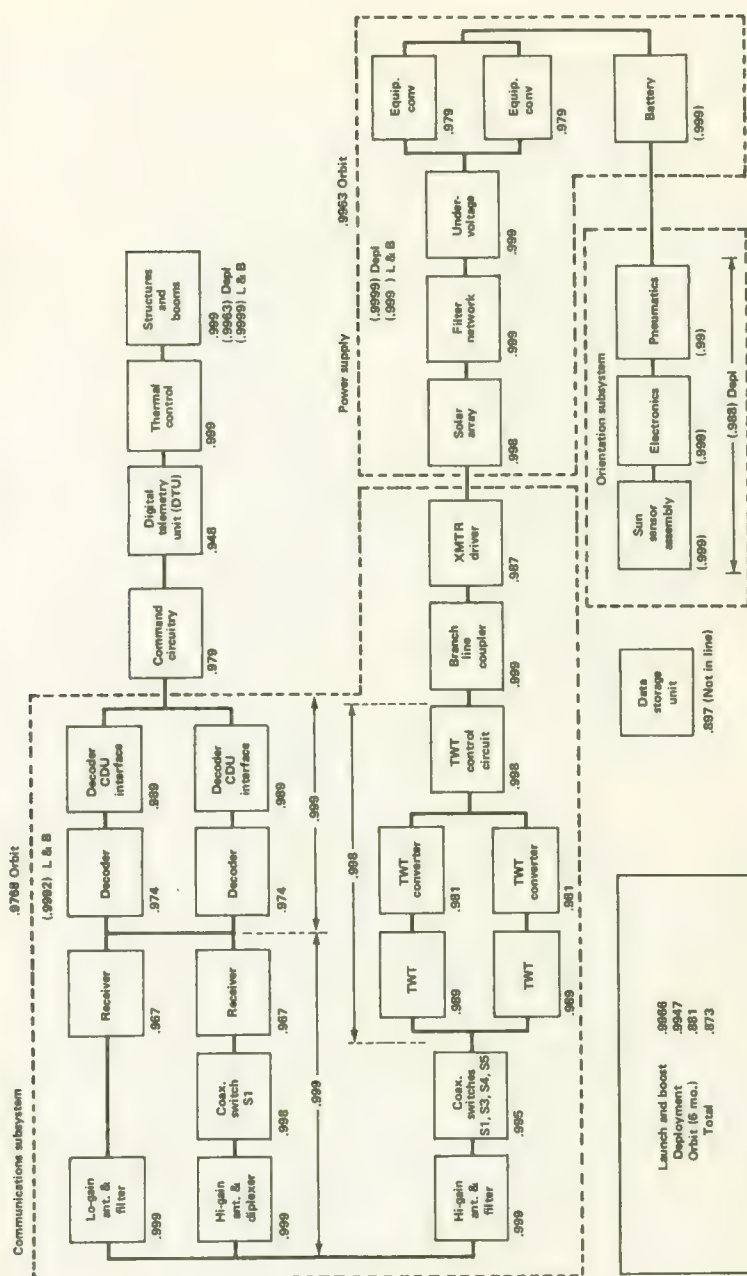


FIGURE 3-2.—Reproduction of the reliability diagram submitted in the STL Pioneer proposal.  
Redundancy of key components was essential to high reliability.

TABLE 3-4.—*Potential Elements of Failure Mode Protection<sup>a</sup>*

| Subsystem  | Redundancy  | Result  | R*   |
|--|---|---|------|
| Decoder  | Parallel redundant and cross-strapped to each receiver  | Command link is retained if internal failure occurs to one decoder.   | 12.4 |
| General-purpose converter                                      | General-purpose converter paralleled  | Internal failure of one converter allows operation of the nonredundant critical functions.  | 4.3  |
| Digital telemetry unit programmer and analog-digital converter | Programmer and analog-to-digital converter series parallel redundant; ground command able to select either path   | Internal failure of one programmer or converter in a series path does not catastrophically affect mission success.  | 8.9  |
| Receiver and antenna   | Receiver able to be switched from wideband to narrowband only; <sup>b</sup> receiver and general-purpose converter series-parallel redundant; receivers cross-strapped to the high- and low-gain antennas | Removes possibility of inadvertently switching from the high-gain mode during the extended mission (after 6 months). Internal failure of one receiver or associated converter does not catastrophically affect mission success. Ability to switch antennas gives greater reception flexibility. | 25.6 |
| Orientation subsystem  | Quad-redundancy provided at the part level for valves, valve drivers, sensors, sensor drive and filters, and flip-flops; dual-parallel redundancy provided at the part level for all other assemblies     | Two, or in some cases, three of the elements can fail without catastrophic results. Failure of Type-I orientation maneuver to begin at separation can be corrected by ground command.   | 3.1  |
| Command distribution unit                                      | Enable driver with parallel redundant coils and parallel series cross-strapped contacts   | One open enable driver coil or one or two open or shorted contacts and failure of two of the 16 silicon controlled rectifiers can occur without catastrophic results.   | 7.8  |
| TWT converter and TWT  | The TWT converter and TWT series-parallel sequence redundant,   | Internal failure of one transmitter converter or TWT in a series  | 35.3 |

TABLE 3-4.—*Potential Elements of Failure Mode Protection* (Concluded)

| Subsystem  | Redundancy   | Result   | R*   |
|--|--|--|------|
|  | ground command able to select either path; 8- and 5-W power modes and high- and low-gain antennas that can be selected by ground command <sup>b</sup> also available | path does not catastrophically affect mission success. The capability for switching antennas and/or power modes gives added flexibility. For example, if the available solar-array power is reduced by meteoroid damage, excessive radiation, etc., the 5-W power mode can be used as a backup. <sup>b</sup> |      |
| Power supply, solar array, battery, and undervoltage control | Oversize solar array incorporating multiple redundancy by means of extensive cross-strapping   | The array allows for output degradation and random failures; multiple cell cross-strapping allows for the anticipated failure mode.  | 2.7° |

\* See reliability diagram, fig. 3-1. The spacecraft components and subsystems are described in detail in ch. 4. This table from the STL feasibility study is intended to show the design approaches to high reliability; not all were used.

<sup>b</sup> This stratagem was not employed on the actual spacecraft.

<sup>c</sup> Solar array redundancy not included.

R\* = Reliability improvement, percent (total R = 0.59 to 0.86).

a field of  $1\gamma$  at a distance of 3 in. after the application and removal of a 25-G field. Inductances and relay coils with magnetic cores are even more offensive to the magnetometers on board. Unless some concerted action is taken, the cumulative fields of 10 000-plus parts on a Pioneer-class spacecraft can completely overwhelm the interplanetary field of a few gammas.

Early interplanetary craft, such as the first Mariner, were not very clean magnetically and absolute measurements of the interplanetary field were more difficult. The first intensive efforts to build clean spacecraft came with the Goddard Space Flight Center series of Interplanetary Monitoring Platforms (IMPs); the first three IMPs were Explorers 18, 21, and 28. The IMP techniques were borrowed and extended for the Ames Pioneers—the first spacecraft to be designed magnetically clean from the start (ref. 4).

Comparing the pro-reliability and pro-magnetic cleanliness philosophies

in table 3-3, one notes many similarities: approved parts lists, stipulations about components usage, and, of course, the same sorts of rigorous qualification and test programs. (See ch. 6 for magnetic test program.)

The TWTs in the communication subsystem were the "dirtiest" space-craft components, due to their platinum-cobalt magnet assemblies. Since the TWTs could not operate without the magnetic fields, the only solution lay in magnetic compensation; that is, placing other permanent magnets so that their fields combined to cancel those from the TWT magnets in the vicinity of the magnetometer.

In some cases, it was possible to arrange with manufacturers for a special run of nonmagnetic components for Pioneer. Tantalum capacitors, for example, were procured in this manner by STL and the experimenters.

The combination of all these philosophies—compensation, parts screening, use of twisted leads, avoidance of ground loops, and careful attention to details exemplified in table 3-3—made the Pioneers the cleanest space-

TABLE 3-5.—*Evolution of the Pioneer Spacecraft*

| Point in time:<br>STL feasibility<br>study complete | Point in time:<br>Ames Specification<br>A-6669 issued   | Point in time:<br>Pioneer 6<br>complete                                       |
|---|---|---|
| Spacecraft<br>Experiments      96.2 lb<br>20.0      | Spacecraft      111.24 lb<br>A-6669 issued              | Spacecraft      102.7 lb<br>Experiments      34.3                             |
| 116.2 lb  |   | 137.0 lb  |
| <hr/>   |   |   |
| Changes from early<br>STL conceptual study          | Changes from STL<br>feasibility study                   | Changes from first<br>version A-6669  |
| <hr/>   |   |   |
| Antenna supports removed                            | TWT substituted for<br>amplitron                        | Ames micrometeoroid<br>experiment deleted                                     |
| Battery added-----                                  | Flat solar-cell modules<br>changed to curved<br>modules | Stanford radio propagation<br>experiment added                                |
|   | Proposed experiment<br>complement changed<br>by NASA    | Solar sail added to antenna<br>mast   |
|   | Four booms added to top<br>of spacecraft (fig. 3-4)     | Three booms located on<br>spacecraft viewing band<br>(fig. 3-5)               |
|   |   | Solar cells removed from<br>viewing band                                      |
|   |   | Thermal insulation added<br>to protect spacecraft from<br>X-258 exhaust plume |
|   |   | Magnetometer moved from<br>antenna mast to radial<br>boom                     |

TABLE 3-5.—*Evolution of the Pioneer Spacecraft (Concluded)*

| Point in time:<br>Pioneer 7<br>complete   | Point in time:<br>Pioneer 8<br>complete  | Point in time:<br>Pioneer 9<br>complete   | Point in time:<br>Pioneer E<br>complete  |
|---|--|---|--|
| Space-<br>craft<br>Experi-<br>ments   | Space-<br>craft<br>Experi-<br>ments  | Space-<br>craft<br>Experi-<br>ments   | Space-<br>craft<br>Experi-<br>ments  |
| 103.26 lb<br>35.09  | 106.1 lb<br>38.0   | 107.13 lb<br>41.27  | 106.54 lb<br>41.06   |
| 138.35 lb   | 144.1 lb   | 148.40 lb   | 147.60 lb  |
| Changes from<br>Pioneer 6   | Changes from<br>Pioneer 7  | Changes from<br>Pioneer 8   | Changes from<br>Pioneer 9  |
| Magnetometer range<br>reduced to $\pm 32\gamma$<br>Energy windows and<br>angular resolution<br>of cosmic-ray<br>experiment<br>changed | Block-II experi-<br>ments substituted<br>Telemetry format<br>altered<br>Larger battery<br>added<br>for experiments | Ames magnetom-<br>eter substituted<br>for Goddard<br>magnetometer<br>Convolutional coder<br>experiment<br>added<br>Texas Instru-<br>ments solar cells<br>substituted for<br>RCA cells<br>Thick glass covers<br>placed on Sun<br>sensors | Ultraviolet filters<br>substituted for<br>thick glass covers<br>on Sun sensors |

craft built to date. The field due to the spacecraft in the vicinity of the magnetometer was roughly  $0.5\gamma$ , or an order-of-magnitude below the interplanetary field being measured.

## EVOLUTION OF THE SPACECRAFT DESIGN

The Pioneer spacecraft design changed in several minor ways during the seven years between conception and the launch of Pioneer E in 1969. The basic system design—a spin-stabilized spacecraft oriented with its spin axis perpendicular to the plane of the ecliptic, holding the Earth perpetually in its disk-shaped antenna pattern—was absolutely essential to the scientific success of a small, low cost interplanetary probe. Basic system design could not be changed, but spacecraft details could. It is appropriate here to survey the more important of these evolutionary (not revolutionary) changes before a large-scale perspective is lost in the next chapter's welter of details.

At the risk of some oversimplification, table 3-5 divides Pioneer spacecraft evolution into periods and lists the important changes that took place within each time frame. The original STL concept was born of its family of Able spacecraft. The most important changes were made during the feasibility study and NASA's issuance of the basic Pioneer Specifications (fig. 3-3). Understandably, this was the period of greatest flux, as NASA and STL focused on a design that would best meet the engineering, scienti-

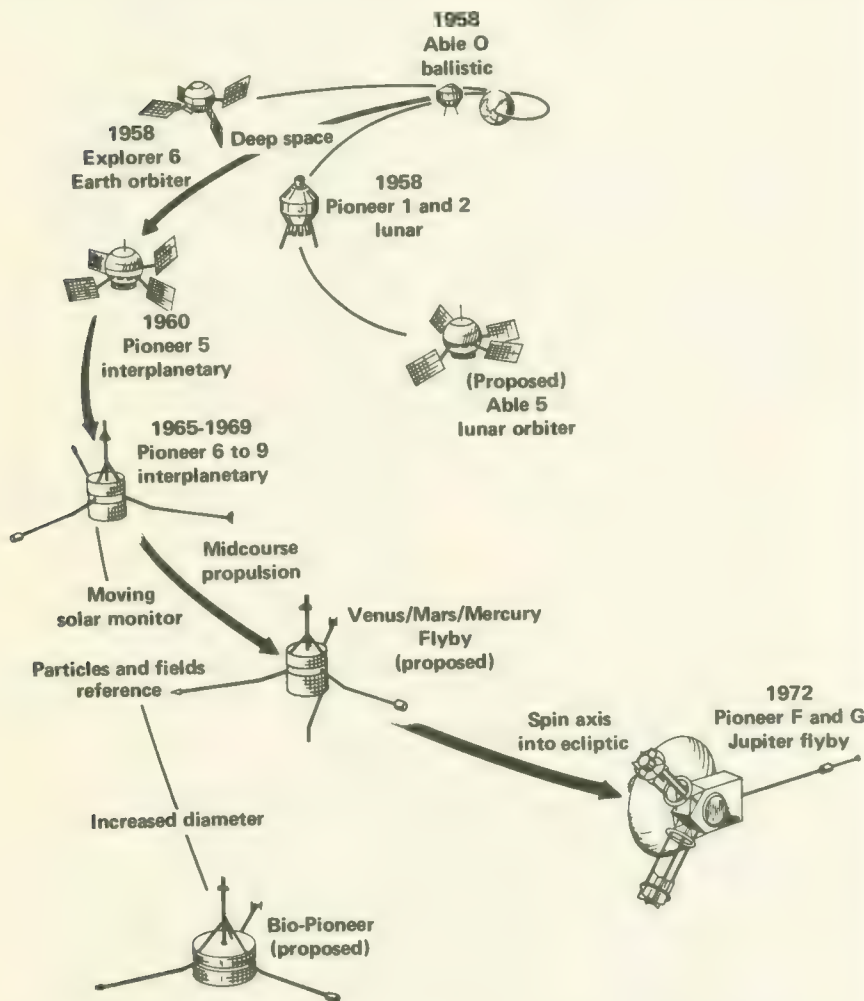


FIGURE 3-3.—Sketch showing the evolution of the STL Pioneer "family." Mainline evolution shows the changes from the spherical to cylindrical to box geometry and the changes from solar-cell paddles to body-mounted cells to radioisotope thermoelectric generators (RTGs). Note that the sketch of Pioneers F and G represents an early version.

tific, and political requirements. The flight of Pioneer 6 in late 1965 did not end spacecraft evolution, though it dampened the magnitude of the changes. There was little change within Block I (Pioneers 6 and 7). In fact, Pioneer 7 was originally intended to be a backup spacecraft for Pioneer 6, but this philosophy was changed in favor of two separate pairs of spacecraft making up Blocks I and II, with enough qualified spares for

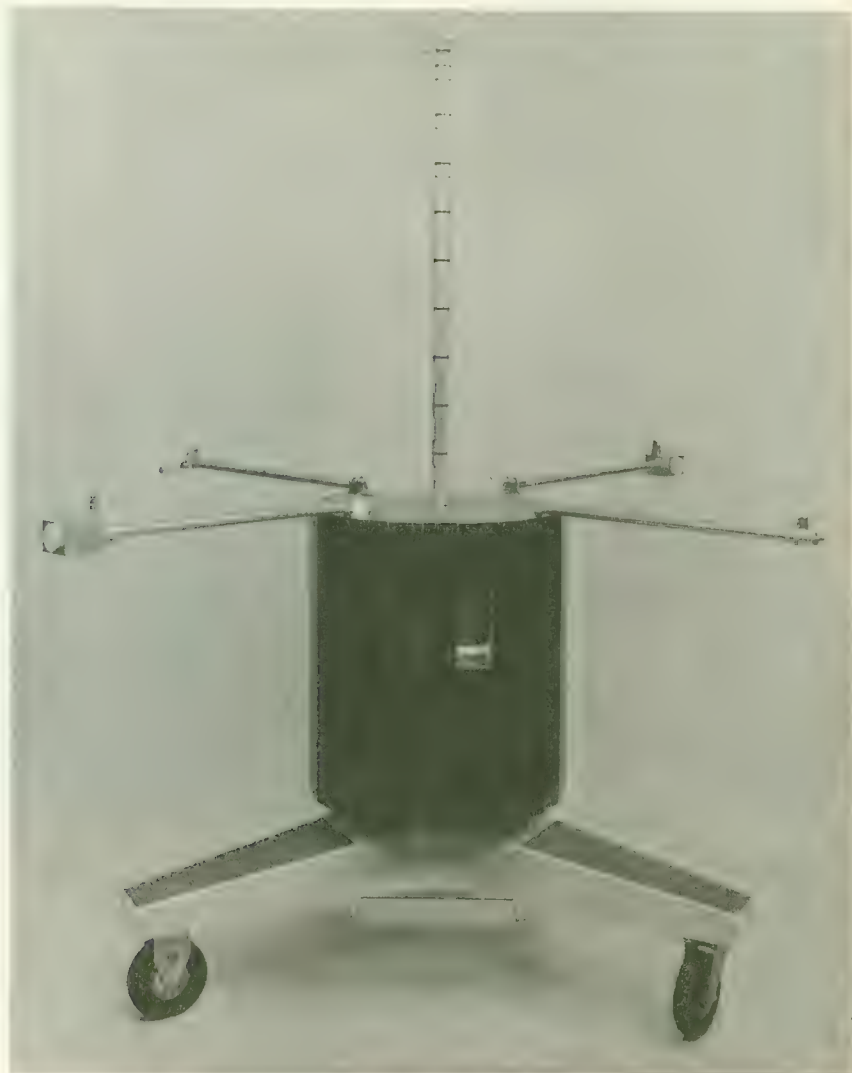


FIGURE 3-4.—Model of the Pioneer configuration proposed by STL in Mar. 1963. Note the four booms mounted at the top of the spacecraft. Earlier designs had no booms at all. (Courtesy of TRW Systems.)



FIGURE 3-5.—The Pioneer-6 spacecraft, showing final boom arrangement and the viewing band void of solar cells. Spacecraft is undergoing a spin test.

a fifth vehicle. For budgetary reasons the fifth spacecraft was dropped early in the program, but it was reinstated as Pioneer E in 1968.

With the substitution of a new array of experiments, several changes had to be made in the communications and electric power subsystems of the Block II spacecraft. During the latter part of the program, the payload capability of the Delta had increased to the point where an engineering experiment, a convolutional coder, could be added to Pioneers 9 and E.

The three Block-II flights carried piggyback TETR satellites as well as ballast.

All five Pioneers (6, 7, 8, 9, and E) were similar with only slight changes from spacecraft to spacecraft—a larger battery on Pioneer 8, an ultraviolet Sun sensor filter on Pioneer 9, etc., as shown in table 3-5. (See also figs. 3-4 and 3-5.) With this overview, the discussion can proceed to detailed descriptions of the spacecraft subsystems.

### REFERENCES

1. ANON.: Final Report on the Interplanetary Probe Study. Space Technology Laboratories, Redondo Beach, Aug. 15, 1962.
2. ANON.: Spacecraft and Associated Ground Equipment, Pioneer Specification A-6669. NASA Ames Research Center, Moffett Field, revised edition, Dec. 1, 1963; earlier version, released with RFP-A-6669, and later revisions exist.
3. ANON.: Proposal under RFP-A-6669 to Produce the Pioneer Spacecraft, Space Technology Laboratories, Proposal No. 1943.00, Redondo Beach, Mar. 4, 1963.
4. SHERGALIS, L. D.: A Magnetically Clean Pioneer. Electronics, vol. 38, Sept. 20, 1965, p. 131.



## The Spacecraft Subsystems

THE SEVEN PIONEER SPACECRAFT SUBSYSTEMS are defined by their various functions, such as communication, data handling, power generation, etc. (See table 1-2.) At the subsystem level in the Pioneer hierarchy of supersystem, system, and subsystem, the first engineering details begin to emerge. It is well known, however, that the subsystem engineer too often visualizes the spacecraft system as a collection of obscure black boxes dominated by the subsystem he is designing. The interface concept, discussed in the preceding chapter, helps dispel this myopia. Interfaces must be matched wherever signals, power, heat, and mechanical forces move from one subsystem to another. The following word portraits of the Pioneer subsystems and their interrelations will quickly dispel any thought that spacecraft subsystems can ever be independent black boxes. The solid lines separating the subsystems in the block diagram of figure 4-1 represent artificially constructed conceptual walls only.

### THE COMMUNICATION SUBSYSTEM

Compared with other interplanetary spacecraft—the U.S. Mariners and the Russian Veneras—the IQSY Pioneer spacecraft are factors of 5 and 20 lighter, respectively. Yet the much smaller Pioneers have done more than hold their own in the competition for honors in long-distance communication. It is impressive to be present in the Missions Operations room at Ames Research Center when several of the Pioneers are being worked simultaneously by DSN antennas that have the spacecraft in view from various locations around the world. Taking the Sun's pulse simultaneously from several locations across tens of millions of miles is a *tour de force* in communications engineering.

The basic problems in long-distance communication (ref. 1) are distance and natural radio noise. The inverse-square law cannot be circumvented and there is no way to turn off galactic and solar radio noise. Bigger spacecraft overcome these obstacles with a combination of high-power transmitters and high-gain, onboard paraboloidal antennas pointing directly at the Earth. Compared to most Earth satellites, the Pioneers have high-power transmitters for their weight class, but they cannot afford the added weight and complexity of paraboloids that can be pointed Earthward. Of course, the Pioneer high-gain Franklin-array antenna is pointed, in a sense,

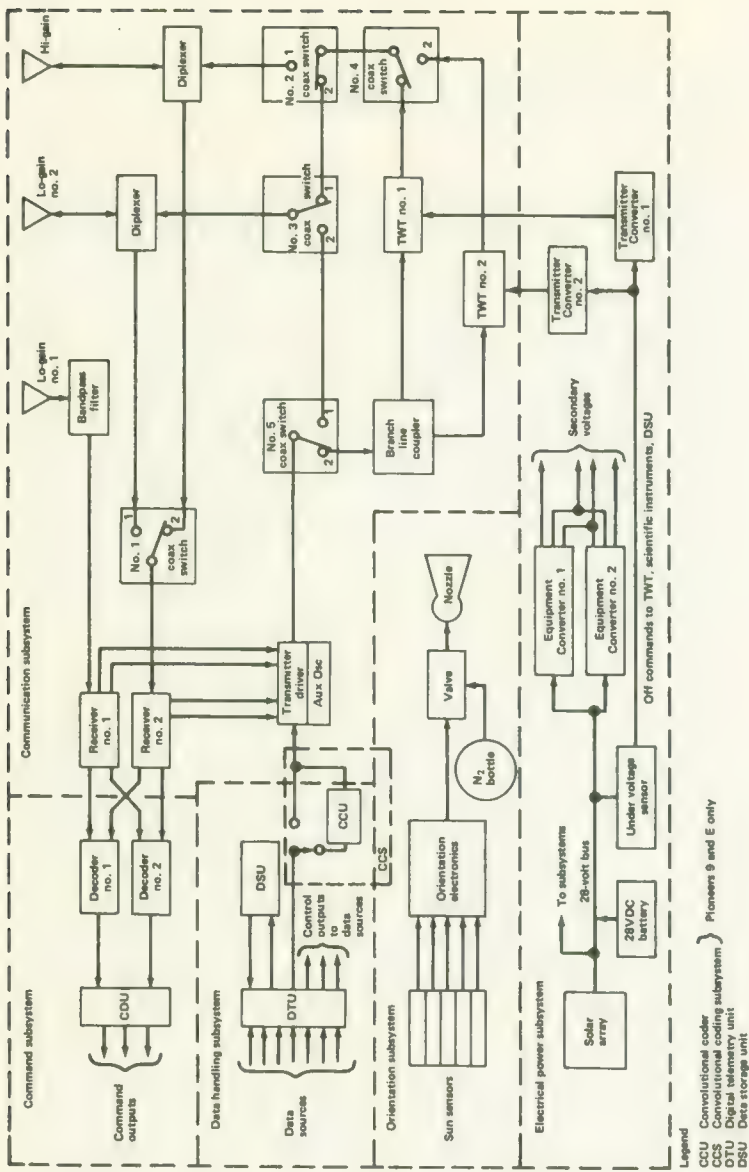


FIGURE 4-1.—Simplified block diagram showing the Pioneer spacecraft subsystems.

When the spacecraft's spin axis is oriented perpendicular to the plane of the ecliptic, the thin, disk-shaped beam intercepts the Earth. The gain of this type of antenna, however, is much lower than that of the pointable paraboloid.

Another factor entering the space communication picture is bandwidth. To transmit information rapidly, that is, attain a high bit rate, a wide-bandwidth is necessary—however, the wider the bandwidth the more power required by the spacecraft transmitter. Thus, transmitter power, bit rate, and antenna gains are all involved in the "communication trade-off." In the Pioneer concept transmitter power is fixed, but bandwidth and bit rate may be reduced by terrestrial command as the spacecraft recedes from Earth. In sum, the Pioneer spacecraft have relatively high transmitter power levels, moderate antenna gains, and variable bit rates; the last can be made very small (8 bits/sec) at extreme distances by command from Earth.

Telemetry of scientific data across the solar system is the most critical of the communication subsystem's functions. Two other communication functions greatly increase the spacecraft's value: the ability to receive commands from the Earth, and the transmission of signals that allow measurements of spacecraft radial velocity from the Doppler effect. The versatilities of the scientific experiments and the spacecraft equipment depend upon the ability to change modes of operation through commands from the Earth.

The final requirement placed upon the communication subsystem is maintaining communication with the spacecraft during the launch sequence, the coast period, and injection. After injection, the spacecraft must respond to commands that initiate the orientation maneuvers during which the entire spacecraft, carrying the rigidly mounted high-gain antenna, is torqued around so that its disk-shaped lobe intercepts the Earth. The high-gain antenna is useless for long distance communication until the completion of the orientation maneuvers. Prior to these maneuvers, communication is maintained between spacecraft and ground through two low-gain antennas, which have nearly isotropic reception patterns.

Once the launch pad umbilical cords are jettisoned, the communication subsystem interfaces first with the DSN 85-foot paraboloid at Johannesburg. As it ascends, other DSN antennas come into view. The DSN has been presented in earlier chapters as more than a communication interface. During the formulation of the Pioneer Program it also acted as a constraint upon the design of the communication subsystem. The JPL approach to interplanetary communication, with its phase-locked loops, phase-shift keying, and Doppler tracking was well-proven by the time the IQuS Pioneers reached the design stage. There was no reason to examine other schemes; the DSN was operational and it would have taken considerable time and money to implement any other communication scheme.

Just as the Delta exerted great influence upon the weight and volume of the spacecraft, the extant DSN dictated answers to the questions the space communications engineer usually asks at the beginning of a new spacecraft design. It should also be remembered that the spacecraft/DSN interface was not static. During the course of the Pioneer Program, the DSN improved its signal detection capability by a factor of about 10 dB, mainly through the introduction of the Goldstone 210-ft antenna (ch. 8). Furthermore, at the beginning of the Pioneer Program, the DSN was not fully operational as an S-band system.

The interfaces between the communication subsystem and the onboard spacecraft subsystems were less momentous. They are dealt with in table 4-1.

The major components of the communication subsystem are: one high-gain and two low-gain antennas, two receivers, a transmitter driver, two TWT power amplifiers, and five coaxial switches that can be activated from the ground to switch in redundant components should failures or anomalous operation occur (fig. 4-2). Although telemetry, commands, and tracking information are all handled by the communication subsystem, one cannot distinguish three separate, corresponding groups of

TABLE 4-1.—*Communication Subsystem Interfaces*

| Subsystem                            | Interface considerations  |
|--------------------------------------|---|
| Data handling                        | The communication subsystem receives telemetry words from the data handling subsystem and transmits them to Earth.  |
| Command                              | Uplink commands are received by the communication subsystem and passed on to the command subsystem.   |
| Electric power                       | The communication subsystem is the largest single user of electric power on the spacecraft.   |
| Orientation                          | A feedback control loop exists during the orientation maneuvers as the spacecraft is torqued via terrestrial commands into a position where signal strength received at a DSN station is maximum.   |
| Thermal control                      | The communication subsystem is also the largest producer of waste heat (primarily the TWT).   |
| Structure                            | This provides mechanical support of electronic packages and three antennas.   |
| Scientific instrument system         | The data handling subsystem acts as a buffer here. The spacecraft's end-mounted antennas do not compete for solid angle with instruments scanning the plane of the ecliptic. The magnetic interface with the TWT magnets is controlled by compensating magnets. |
| Tracking and data acquisition system | The electromagnetic interface and DSN constraints are discussed in chapter 8.   |
| Launch vehicle system                | A standard launch vehicle system is used.   |

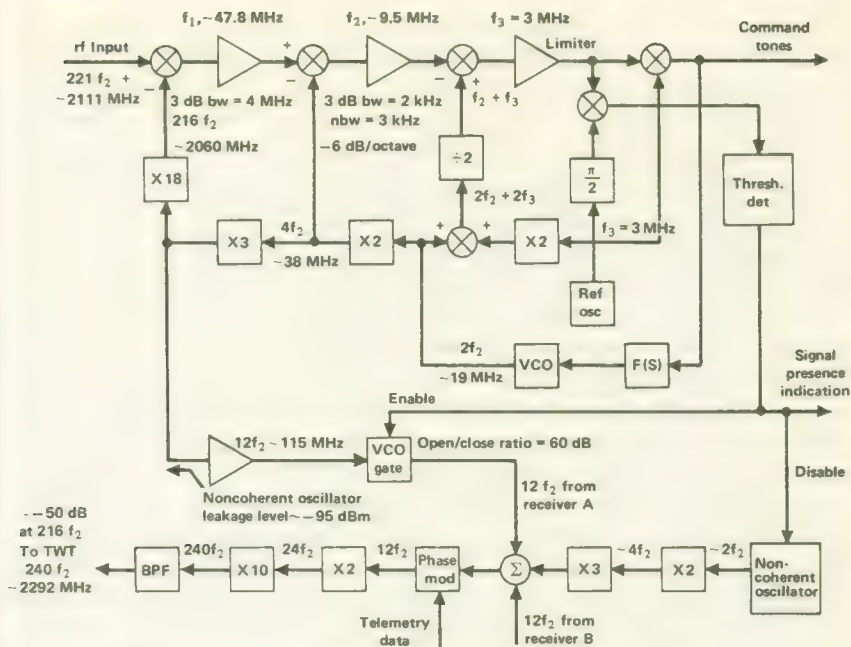


FIGURE 4-2.—Simplified receiver and transmitter driver block diagram.

subsystem components; they are all integrated into the basic subsystem.

To understand phase-lock loop operation, picture a Pioneer spacecraft 100 million miles or so ahead of the Earth in its orbit about the Sun. Assume first that the terrestrial DSN antennas are busy with some other spacecraft. In this situation, both spacecraft receivers are in a state of readiness for further instructions from Earth. The transmitter, however, still transmits any scientific and housekeeping information it receives from the data-handling subsystem even though no terrestrial antenna intercepts it. Thus, even if both spacecraft receivers should fail, DSN antennas can still acquire the spacecraft and record whatever data it transmits. During these periods, when the spacecraft is "on its own," the spacecraft transmitter frequency is controlled by an internal crystal-controlled oscillator. This is called the noncoherent mode of operation. This one-way Doppler tracking can be accomplished by merely listening to the spacecraft. The angular coordinates of the spacecraft can be measured accurately by the DSN antennas but, as explained in chapter 8, Doppler measurements suffer because the spacecraft oscillator frequency may drift slightly and introduce range-rate uncertainties. Only the functions of telemetry transmission and (limited) tracking can be performed during this type of operation.

Suppose, next, that a DSN antenna is swung around to point in the

direction where orbital computations predict the spacecraft will be. DSN receivers pick up (acquire) the weak telemetry signal and "lock on" to it. Lock is attained by means of a feedback loop involving a narrow bandpass filter and a voltage-controlled oscillator. A down-link lock exists when the voltage-controlled oscillator generates a signal at precisely the carrier frequency received from the spacecraft but with a 90° phase change. The feedback circuit in essence operates as a servomechanism to force the oscillator to match the spacecraft carrier frequency. Once a down-link lock has been established, the ground transmitter sends its own carrier in the direction of the spacecraft. Since the two spacecraft receivers are tuned to operate at different frequencies, the ground transmitter can select either one by using the proper carrier frequency. The presence of a signal in the spacecraft receiver automatically disconnects the spacecraft crystal-controlled oscillator and switches in a voltage-controlled oscillator that generates a frequency precisely 12/221 times that received from the DSN. This frequency is then multiplied by twenty in the transmitter driver. A phase-coherent transmitter signal with a frequency 240/221 times the frequency received from Earth is amplified in the operational TWT and dispatched to Earth via the high-gain antenna. The waiting DSN antenna locks onto this signal, which may be slightly different from that originally acquired because the spacecraft's crystal-controlled oscillator drifts slightly. Only when the spacecraft and DSN receivers are both locked on the signals received from Earth and spacecraft, respectively, can coherent, highly accurate, two-way tracking measurements be made.

While the spacecraft and DSN station are operating in phase-lock loop modes, telemetry signals are sent to Earth by phase-shift keying (PSK) of a 2048-Hz subcarrier that phase modulates (PM) the main carrier. Commands are sent up-link by using frequency-shift keying (FSK). Both commands and telemetry are pulse-code modulated (PCM). The Pioneer telemetry and command systems are therefore designated PCM/PSK/PM and PCM/FSK/PM, respectively. The information carried on the 2048-Hz subcarrier does not interfere with coherent Doppler measurements being made on the transmitter carrier which is in the 2290- to 2300-MHz range (part of the S-band).

The communication subsystem block diagram (fig. 4-2) shows five coaxial switches that give the subsystem appreciable flexibility should a failure or some anomalous event occur. Seven different coaxial switch commands comprise what is called the rf logic for Pioneer, as shown in table 4-2.

Note that one low-gain antenna can always receive commands regardless of switch positions or operability. Coaxial switches nos. 4, 5, and 2, however, must operate properly for the spacecraft to transmit telemetry. In other words, the coaxial switches are in line and essential to mission success.

TABLE 4-2.—*Switching Logic*

| Command number | Function                                  | Switching sequence |
|----------------|---|--------------------|
| 046            | Driver to low-gain antenna.....           | S3-2, S5-1*        |
| 047            | Operational TWT to high-gain antenna..... | S2-1               |
| 025            | Operational TWT to low-gain antenna.....  | S2-2, S3-1         |
| 015            | TWT no. 1 to operational status.....      | S4-1, S5-2, S3-1   |
| 022            | TWT no. 2 to operational status.....      | S4-2, S5-2, S3-1   |
| 033            | Receiver no. 2 to high-gain antenna.....  | S1-2               |
| 003            | Receiver no. 2 to low-gain antenna.....   | S1-1               |

\* S5-1 = Switch no. 5 commanded to position no. 1.

### Spacecraft Receiver

The two tasks assigned to the spacecraft receiver are:

- (1) To detect, demodulate, and amplify the commands impressed upon the carrier that is received from the DSN station working the spacecraft
- (2) To provide to the transmitter driver a phase-coherent signal 12/221 times the frequency of the received DSN carrier.

The up-link signal loss due to inverse-square-law attenuation and absorption is approximately 264.27 dB when a Pioneer is 100 million miles from Earth. To overcome this power loss, the spacecraft receiver can be made extremely sensitive; and the DSN stations, being ground-based, can afford to pump considerable power into a very narrow beam and point it directly at the spacecraft. In fact, the DSN station transmitter power is rated at 10 000 W compared with the spacecraft's 8 W. The seemingly easy up-link communication task is compounded by the necessity for making the command information more error-free than spacecraft telemetry. This is understandable because a spurious command could conceivably turn spacecraft off permanently by accident. Therefore, Pioneer up-link power budgets are calculated assuming the very low bit-error rate of  $10^{-5}$ . The power budget having an appropriate signal-to-noise ratio for this low bit-error rate is presented in table 4-3.

The small, lightweight Pioneer receiver was developed by STL and had already successfully flown on many spacecraft before it was adopted for the Pioneer spacecraft. A block diagram of the receivers and transmitter driver is presented in figure 4-2. Note that the threshold detector disables the on-board, crystal-controlled, noncoherent oscillator whenever an external signal from the DSN is detected. The coherent receiver then generates the phase-coherent signal that ultimately drives the TWT at 240/221 times the received frequency. There are, of course, many ways to build receivers to accomplish the tasks prescribed for the Pioneer receivers. An

TABLE 4-3.—*Uplink Power Budget*

| Requirement  | Value via<br>high-gain<br>antenna     | Value via<br>low-gain<br>antenna      |
|--|---------------------------------------|---------------------------------------|
| <b>Parameter</b>   |                                       |                                       |
| Total ground transmitter power (10 kW)-----  | 70.0 dBm                              | 70.0 dBm                              |
| Circuit loss (diplexer, switch, waveguide)-----                                      | 0.4 dB                                | 0.4 dB                                |
| Ground antenna gain (85-ft paraboloid)-----  | 51.0 dB                               | 59.0 dB                               |
| Space attenuation<br>(2110 MHz; $30 \times 10^6$ n. mi.)-----                        | 253.83 dB                             |                                       |
| Space attenuation<br>(2110 MHz; $100 \times 10^6$ n. mi.)-----                       | 264.27 dB                             |                                       |
| Polarization loss ( $1.0 \pm 0.5$ dB ellipticity)-----                               | 3.00 dB                               | 3.01 dB                               |
| Spacecraft antenna gain-----   | 10.5 dB                               | -1.0 dB                               |
| Spacecraft circuit loss-----   | 1.5 dB                                | 1.0 dB                                |
| Net transmission loss-----   | 207.68 dB                             | 208.24 dB                             |
| Total received power-----  | -137.68 dBm                           | -138.24 dBm                           |
| Receiver noise spectral density<br>(10 dB noise figure)-----                         | $-164.0 \frac{\text{dBm}}{\text{Hz}}$ | $-164.0 \frac{\text{dBm}}{\text{Hz}}$ |
| <b>Carrier loop performance</b>  |                                       |                                       |
| Carrier modulation loss<br>( $1.2 \pm 5$ percent radian peak deviation)-----         | 3.46 dB                               | 3.46 dB                               |
| Received carrier power-----  | -141.14 dBm                           | -141.70 dBm                           |
| Carrier loop noise bandwidth<br>( $2B_L = 25$ Hz at -141 dBm)-----                   | 14.0 dB                               | 14.0 dB                               |
| Threshold signal-to-noise ratio in $2B_L$ -----                                      | 6.0 dB                                | 6.0 dB                                |
| Threshold carrier power-----   | -144.74 dBm                           | -144.74 dBm                           |
| Performance margin<br>(low-gain antenna; $30 \times 10^6$ n. mi.)-----               |                                       | +3.0 dB                               |
| Performance margin<br>(high-gain antenna; $100 \times 10^6$ n. mi.)-----             | +3.6 dB                               |                                       |
| <b>Command data performance</b>  |                                       |                                       |
| Data modulation loss<br>( $1.2 \pm 5$ percent radian peak deviation)-----            | 3.04 dB                               | 3.04 dB                               |
| Received data power-----   | -140.72 dBm                           | -141.28 dBm                           |
| Data noise bandwidth ( $2.0 \pm 0.5$ Hz)-----  | 3.0 dB                                | 3.0 dB                                |
| Data threshold signal-to-noise ratio<br>(probability of bit error = $10^{-5}$ )----- | 13.4 dB                               | 13.4 dB                               |
| Degradation from theoretical-----  | 3.0 dB                                | 3.0 dB                                |
| Threshold data power<br>(0.25 dB limiter suppression)-----                           | -144.31 dBm                           | -144.31 dBm                           |
| Performance margin<br>(low-gain antenna; $30 \times 10^6$ n. mi.)-----               |                                       | +3.0 dB                               |
| Performance margin<br>(high-gain antenna; $100 \times 10^6$ n. mi.)-----             | +3.6 dB                               |                                       |

important feature of the STL design is that the frequencies of the phase detector and reference oscillator are not related in any simple way to the incoming frequency when divided by 221. This offset technique makes "self-lock" unlikely; that is, the receiver will not lock in error on a sub-harmonic of some frequency created in the receiver itself.

In constructing the Pioneer receivers, STL employed discrete circuits rather than the integrated circuits so common in more recent spacecraft. Integrated circuits were just coming into their own in 1963-64, and STL and NASA felt that they were not adequately proven to incorporate them in a spacecraft aiming at a 6-month life as a minimum. The circuit construction, like the design, was derived from previous STL space programs, notably the Able series and the "telebit" technology used on Explorer 6.

Perhaps the most critical transmitter and receiver components were the in-line coaxial switches (fig. 4-3). As mentioned earlier, these had to work after launch before all spacecraft functions could be consummated. During the component test program some of the coaxial switches proved unreliable, remaining stuck in the unproductive middle position. The cause was ultimately traced to a procedural problem in the supplier's plant, and corrected. Nevertheless, some concern always remained that when one of the coaxial switches was commanded to change its polarity it would stick in a middle position, disconnecting the antennas from the TWTs. Fortunately, this never happened in space; the Pioneer coaxial switches have perfect performance records.

The telemetry link from the spacecraft to the waiting DSN antenna possesses a power budget analogous to that for the uplink (table 4-4). Here,

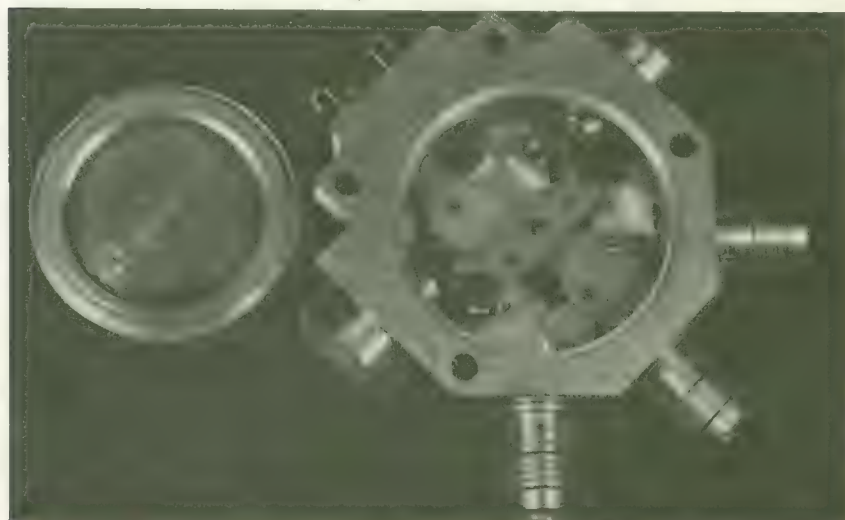


FIGURE 4-3.—One of the Pioneer coaxial switches. (Courtesy of TRW Systems.)

TABLE 4-4.—*Downlink Power Budget*

| Requirement  | Value                                 |
|--|---------------------------------------|
| <b>Parameter</b>   |                                       |
| Spacecraft transmitter power (7.7 W)   | 38.86 dBm                             |
| Circuit loss (diplexer, switch, coaxial cable)   | 1.7 dB                                |
| Spacecraft transmitting antenna gain   | 11.2 dB                               |
| Space attenuation (2292 MHz; $41.5 \times 10^6$ n. mi.)                                      | 257.36 dB                             |
| Polarization loss (including antenna pointing loss)  | 3.0 dB                                |
| Ground receiving antenna gain (85-ft paraboloid)   | 53.0 dB                               |
| Ground circuit loss (diplexer, switch, waveguide)  | 0.18 dB                               |
| Net transmission loss  | 198.04 dB                             |
| Total received power   | -159.18 dBm                           |
| Receiver noise spectral density ( $T_s = 55 \pm 10^\circ$ K)                                 | -181.2 $\frac{\text{dBm}}{\text{Hz}}$ |
| <b>Carrier loop performance</b>  |                                       |
| Carrier modulation loss (0.9 radian peak deviation, $\pm 5$ percent)                         | 4.12 dB                               |
| Received carrier power   | -163.30 dBm                           |
| Carrier loop noise bandwidth ( $2B_L = 23.5$ Hz)   | 13.71 dB                              |
| Signal-to-noise ratio in $2B_L$  | 4.2 dB                                |
| Threshold signal-to-noise ratio in $2B_{LO} = 12$ Hz   | 6.0 dB                                |
| Threshold carrier power  | -164.43 dBm                           |
| Performance margin   | +1.13 dB                              |
| <b>Data channel performance</b>  |                                       |
| Data modulation loss (0.9 radian peak deviation, $\pm 5$ percent)                            | 2.14 dB                               |
| Receiver i.f. and limiter degradation  | 0.95 dB                               |
| Receiver data power  | -162.27 dBm                           |
| Data noise bandwidth (8 Hz)  | 9.03 dB                               |
| Signal-to-noise ratio in data bandwidth  | 9.91 dB                               |
| Carrier loop degradation   | 1.03 dB                               |
| Sync and subcarrier loop degradation   | 1.0 dB                                |
| Adjusted data signal-to-noise ratio  | 7.88 dB                               |
| Data threshold signal-to-noise ratio <sup>a</sup><br>(probability of bit error = $10^{-3}$ ) | 7.3 dB                                |
| Performance margin   | +0.58 dB                              |

<sup>a</sup> Signal-to-noise ratio is defined as the ratio of average signal power to the noise power in a bandwidth equal to the bit rate. Noise power is computed using the single-sided noise spectral density.

again, the real technological burden is placed on the ground equipment instead of the spacecraft. The big high-sensitivity DSN paraboloids with their low-noise amplifiers are essential to long distance communication with the Pioneers. Despite terrestrial sophistication, the spacecraft must still generate considerable radio power, most of which is wasted because the Earth occupies only a small sector of the circular disk-like antenna pattern. The Pioneer transmitters generate about 8 W of radio-frequency

TABLE 4-5.—*Frequencies Assigned to the Pioneer Program*

| Link                    | Channel | Frequency (MHz) |
|-------------------------|---------|-----------------|
| Downlink telemetry----- | 6A *    | 2292.037037     |
|                         | 7A      | 2292.407407     |
| Uplink commands-----    | 6B      | 2110.584105     |
|                         | 7B      | 2110.925154     |

\* Channel 6A is also the nominal frequency of the on-board, crystal-controlled oscillator, which may drift slightly from the assigned frequency during non-coherent operation. In the coherent mode, either channels A or channels B may be used.

power compared to roughly 3 W radiated from Mariner 2's paraboloidal antenna.

### Spacecraft Transmitter (Driver and Power Amplifier)

The block diagram of the transmitter driver (fig. 4-2) shows three possible input signals, and a single output signal that drives the power amplifier connected to either the spacecraft high-gain or the low-gain antenna. The driver frequency, which becomes the spacecraft transmitter carrier frequency, is supplied by the receiver. The driver provides either the noncoherent signal from its crystal-controlled oscillator, or the phase-coherent signal that is 240/221 times the DSN carrier frequency. The signals from the data handling subsystem phase-modulate this carrier when they are present. The frequencies assigned to the Pioneer Program are listed in table 4-5.

The transmitter driver consists of a transistorized amplifier-modulator and a varactor multiplier (factor of 20).<sup>6</sup> The amplified signal of approximately 50 mW is fed next to the power amplifier, one of the most critical of all spacecraft components. The power amplifier must deliver about 8 W rf power to the spacecraft antenna with high reliability and high efficiency.

During STL's early studies of the Pioneer mission, four possible power amplifiers were examined: an all solid-state transmitter, the triode amplifier, the amplitron, and the TWT. The solid-state transmitter and triode amplifier were eliminated from consideration because of their low efficiencies. The amplitron, an rf amplifier tube similar to the magnetron, is very efficient—on the order of 50 percent for the power levels being considered for Pioneer. In fact, before the 1962 STL feasibility study, the amplitron was thought to be the best choice. But confidence in the amplitron waned with further study. A satisfactory operational lifetime had not been demonstrated for the amplitron in 1962. In addition, NASA and

<sup>6</sup> A varactor is a type of parametric amplifier.

STL engineers were concerned over the tendency of the amplitron to switch to a noisy mode of operation after a power supply transient, such as that expected when changing from coherent to noncoherent operation. The amplitron was also dirty from the magnetic standpoint. One test generated  $1700\gamma$  at 3 ft. TWTs seemed the only reasonable choice. Both Hughes Aircraft and Watkins Johnson had TWTs that very nearly met all Pioneer requirements for efficiency, weight, magnetic field, lifetime, and operating frequency. Ultimately the Hughes 349H TWT was selected for power amplification.

The performance of the Pioneer TWTs has been fairly good, but they have always been a source of concern. Hughes had difficulty in meeting the 30 percent efficiency goal; many TWTs had to be discarded before satisfactory tubes were found. NASA was concerned during the early Pioneer flights about the ruggedness of the TWT's hot filaments during the rigors of launch. For this reason, and to conserve the battery, the TWT filaments were not turned on during rocket ascent. A special automatic filament turn-on switch was installed so that the spacecraft could be acquired early by the Johannesburg tracking station. So far, the TWTs have not aborted any Pioneer mission, but shortly after the launch of Pioneer 7, the operational TWT began operating abnormally (its temperature changed, too), and the redundant TWT was switched in. The operational TWT on Pioneer 6 showed similar but less severe symptoms after over  $3\frac{1}{2}$  years of operation; however,  $3\frac{1}{2}$  years demonstrate a certain measure of reliability.

### Spacecraft Antennas

Three antennas serve the communication subsystem. Two are low-gain, multislot types with broad beamwidths. In the subsystems arrangement of coaxial switches (fig. 4-1) one of the low-gain antennas is permanently connected to one of the receivers. This arrangement guarantees that the spacecraft is always listening for commands, regardless of the operability of the coaxial switches. The other low-gain antenna may be connected to the second receiver by ground command. The low-gain antennas are essential during spacecraft acquisition and during the orientation maneuver when the high-gain antenna is being torqued into position. The high-gain antenna—the prominent mast atop the cylindrical Pioneer spacecraft (Figs. 1-4 and 4-4)—is critical to the whole Pioneer concept. Its gain is roughly 10 dB over an isotropic antenna. It contributes to Pioneer's long-range communication capability. The antenna is a colinear broadside array (a modified Franklin array) consisting of nine driven and nine parasitic elements. Commercial TV antennas use similar arrays because they also must focus rf energy into a flat, disk-like pattern, symmetric around  $360^\circ$  (fig. 4-4). More detailed antenna characteristics are presented in table 4-6.



FIGURE 4-4.—Closeup view of the spacecraft with top cover removed. Base of telemetry mast is supported by struts. Some test equipment is shown above the equipment platform.

The spacecraft antennas interface directly with the DSN antennas. All three spacecraft antennas emit linearly polarized electromagnetic waves; the high-gain antenna's plane of polarization is parallel to the spin axis, while the planes of both low-gain antennas are perpendicular to it. Usually, the DSN paraboloids are fitted with an "ultracone" which permits them to receive and transmit circularly polarized waves. The mismatching antenna polarizations result in a 3 dB loss in signal power. Between November 1968 and July 1969, however, "multifrequency" cones were installed in the DSN, enabling the antennas to receive linearly polarized signals without attenuation. In effect, matching the planes of polarization increases the potential communication distance by 40 percent.

A basic weakness in the Pioneer antenna patterns is that they all drop to very low values of gain in the directions viewed by the spacecraft spin axis (fig. 4-5). This causes no trouble when the spacecraft is properly oriented in deep space. However, situations can and do occur, as the spacecraft escapes the Earth's gravitational field and terrestrial antennas must look along the spacecraft axis, where the low-gain antenna sensitivity is so low that the reorientation maneuvers may be compromised by weak com-

TABLE 4-6.—*Spacecraft Antenna Characteristics*


---

|   |       |                                    |
|---|-------|------------------------------------|
| Single-frequency low-gain antenna (multi-slot)                      |       |                                    |
| <b>Uplink (2110 MHz)</b>  |       |                                    |
| Beamwidth   | ----- | 110° at -3 dB points               |
| Polarization  | ----- | Linear, perpendicular to spin axis |
| Gain  | ----- | -1.5 dB minimum                    |
| Downlink—not applicable   |       |                                    |
| <b>Dual-frequency low-gain antenna (multi-slot)</b>                 |       |                                    |
| <b>Uplink (2110 MHz)</b>  |       |                                    |
| Beamwidth   | ----- | 110° at -3 dB points               |
| Polarization  | ----- | Linear, perpendicular to spin axis |
| Gain  | ----- | -2.5 dB minimum                    |
| Downlink (2292 MHz)   |       |                                    |
| Beamwidth   | ----- | 85° at -3 dB points                |
| Polarization  | ----- | Linear, perpendicular to spin axis |
| Gain  | ----- | -0.5 dB minimum                    |
| <b>Dual-frequency high-gain antenna (collinear broadside array)</b> |       |                                    |
| <b>Uplink (2110 MHz)</b>  |       |                                    |
| Beamwidth   | ----- | 5° at -3 dB points                 |
| Polarization  | ----- | Linear, parallel to spin axis      |
| Gain  | ----- | +10 dB minimum                     |
| Downlink (2292 MHz)   |       |                                    |
| Beamwidth   | ----- | 5° at -3 dB points                 |
| Polarization  | ----- | Linear, parallel to spin axis      |
| Gain  | ----- | +10.7 dB minimum                   |

---

mand signals. The solution to this dilemma was a special maneuver termed "partial orientation," commanded from Johannesburg for Pioneer 6 and from Goldstone (where the normal orientation maneuver was commanded) for Pioneer 9. After partial orientation, the spacecraft is in such an attitude, with respect to terrestrial antennas, that commands dispatched from Goldstone can be heard easily by the spacecraft.

### THE DATA HANDLING SUBSYSTEM

The end product of most spacecraft, the Pioneers included, is information. Data flow not only between Earth and spacecraft but also among the various spacecraft subsystems. In the guises of telemetry, commands, and control signals, information is ubiquitous onboard a spacecraft. The data handling subsystem acts as a central clearing house where data are re-

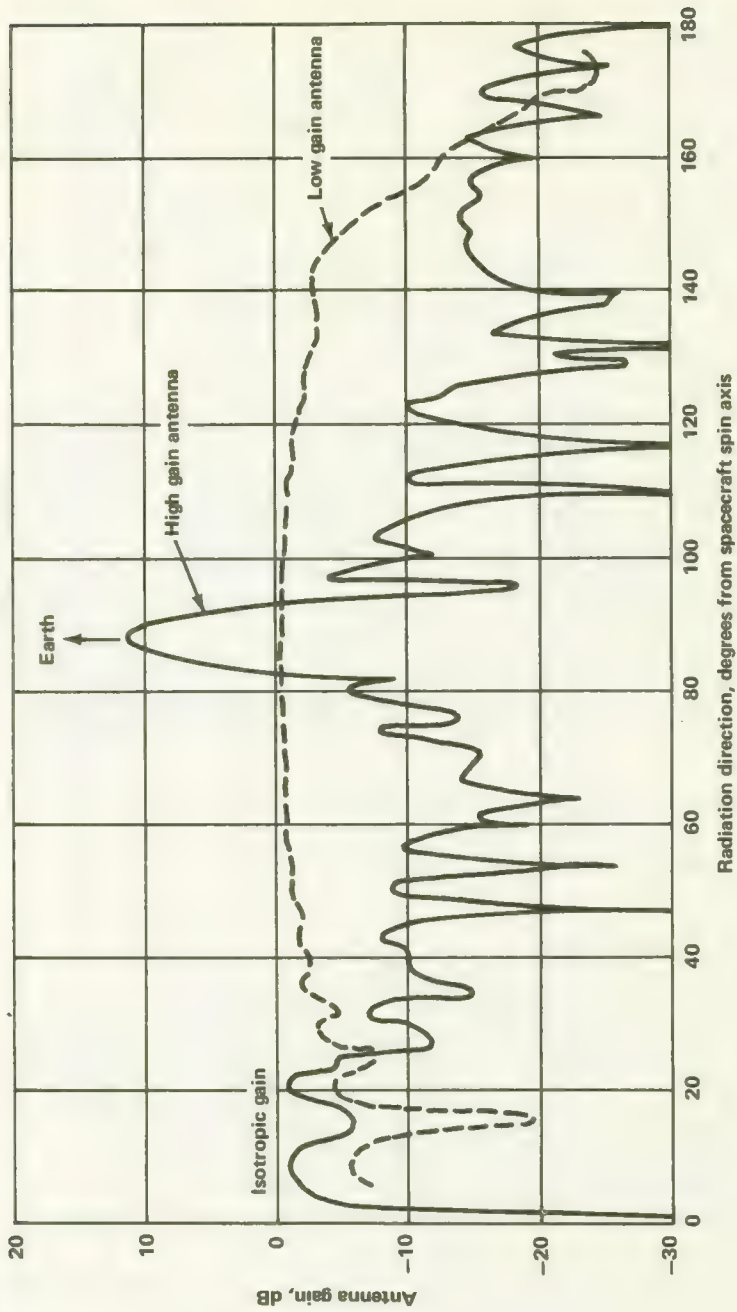


FIGURE 4-5.—Spacecraft antenna radiation patterns.

ceived, formatted, processed, stored, and sent back to Earth or to other Pioneer subsystems.

The functions of the data handling subsystem are:

(1) The sampling and encoding of analog and digital measurements taken by the scientific instruments (In special cases, the encoding is done by the scientific instrument.)

(2) The sampling and encoding of spacecraft engineering or house-keeping measurements

(3) The storage, upon command, of data, when DSN stations are not available to acquire spacecraft data

(4) The storage, upon command, of special data formats, when the spacecraft is communicating with the DSN

(5) The changing, upon command, of data bit rate and/or format as the spacecraft recedes and approaches the Earth (fig. 4-6 shows the impact of this feature on Pioneer-7 communication).

(6) The provision of sundry clock and control signals throughout the spacecraft, in effect forcing all spacecraft experiments and subsystems to work together in synchronism

Two units, or subsubsystems, make up the data handling subsystems: the digital telemetry unit (DTU), really the data processor, and the data storage unit (DSU), the spacecraft memory (fig. 4-7). A convolutional coder unit (CCU), which could be switched in-line from a standby status or vice versa, was added to Pioneers 9 and E on an experimental basis.

A look at the data handling subsystem as a black box reveals the following inputs:

(1) Scientific and engineering measurements

(2) Commands to change mode of operation

(3) Sun pulses from the Sun sensors to provide spacecraft attitude references

The outputs are only two:

(1) A PCM signal to the transmitter driver

(2) Timing and control signals to the rest of the spacecraft

The input-output view of the data handling subsystem oversimplifies the situation; it does not portray the great flexibility intrinsic in a commandable spacecraft. Commands from Pioneer Mission Control can change operational characteristics of the Pioneer data handling subsystem as follows:

(1) Bit rates available: 8, 16, 64, 256, and 512 bits/sec

(2) Transmission formats available: scientific format A, scientific format B, an engineering format, and a special-purpose format

(3) Modes of operation available: real-time mode, duty-cycle-store mode, telemetry mode, and memory readout mode

On Pioneers 9 and E, the convolutional coder can be switched in and out by ground command to provide another permutation. From the view-

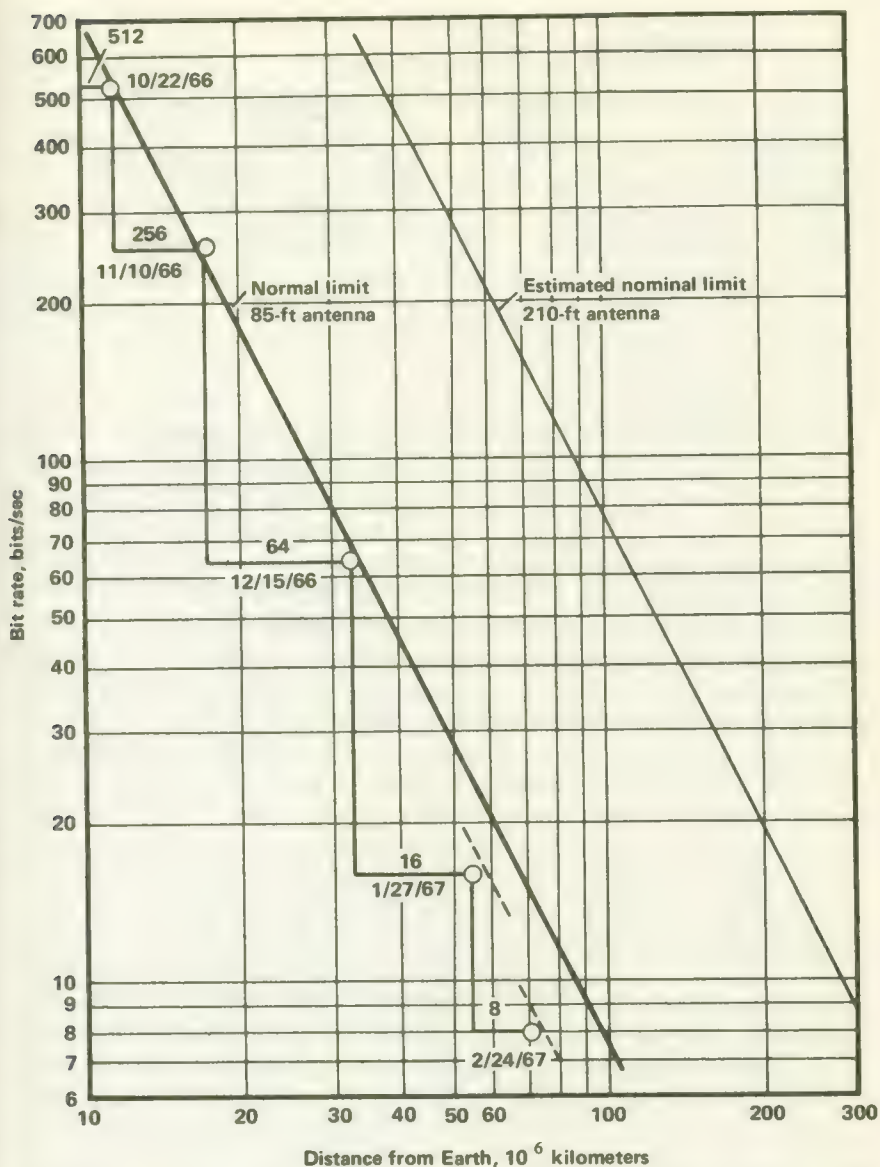


FIGURE 4-6.—Distance limitations for Pioneer 7, showing dates when telemetry bit rate was changed. Note the improved performance with the 210-ft antenna.

point of data acquisition and processing on the ground, Pioneer telemetry may arrive at a DSN antenna in any one of 80 varieties (160 for Pioneer 9), depending upon terrestrial commands. There is a definite need for these different formats and modes as will now be described.

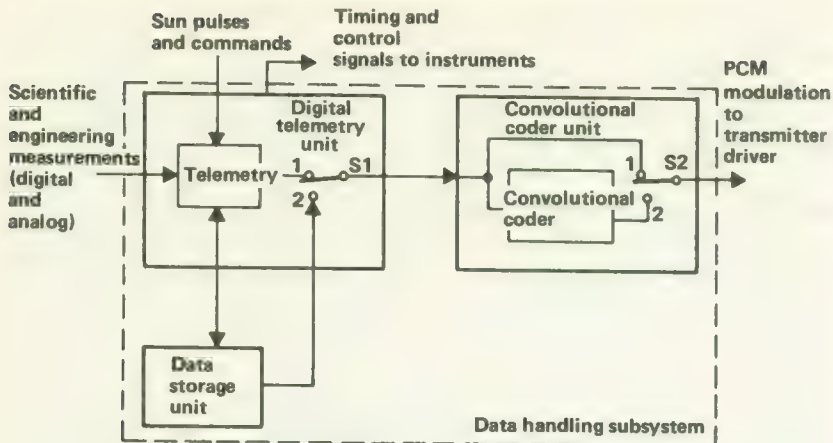


FIGURE 4-7.—Block diagram of the data handling subsystem.

The interfaces of the data handling subsystem are all internal to the spacecraft, since it "sees" the DSN only through the communication and command subsystems. The most important interface separates the data handling subsystem from the several scientific instruments. The design of this interface was controlled by the desire to make the spacecraft as useful as possible to the experimenters. A scientist on Earth looking at telemetry data from his instrument—which is far out in interplanetary space but still commandable at his discretion—wants to know, and be able to do, several things. He might pose the following questions: Where was the Sun when these data were taken? How can I turn my experiment on only when it points directly at the Sun? When the Sun shows signs of unusual activity, how can I record data more often, perhaps at a higher rate than the communication subsystem can handle? He might think his instrument more important during a solar flare than instrument X; however, he would like very much to know what instrument Y recorded at the time he recorded his data. All experimenters cannot be satisfied all of the time; NASA must set priorities and encourage cooperation. The basic reasons for a flexible data handling subsystem with the provision for data storage become apparent when the wishes of the experimenters are considered. And when the situation requires it, NASA mission controllers can alter priorities at will.

Each instrument (and experimenter) is different. Some instruments deliver digital data to the data handling subsystems; others send analog signals. The formats and word structures coming across the interface are also different. Besides being versatile in terms of what it does with the basic data, the data handling subsystem also must be generalized enough to accept a wide range of inputs and convert them all into standardized PCM

telemetry for the transmitter driver. It may be considered an "information melting pot."

### Reliability Considerations

Only the DTU of the data handling subsystem is permanently in-line; the DTU is absolutely critical to mission success at all times. All spacecraft telemetry must flow through the DTU; high reliability is as essential here as it is with the communication subsystem. According to figure 3-2, the early spacecraft reliability budget chart, the on-line portion of the data handling subsystem must achieve a reliability of 0.948. The DSU, on the other hand, is off-line; that is, it may be off-line if the proper switches are thrown by command from the Earth. Presumably, if the DSU should fail, it can be bypassed completely for the remainder of the mission, although this would reduce versatility by eliminating modes of operation involving data storage. The probability that both DSU and switch would fail together is negligible. The DSU reliability allocation of 0.897 was not figured into the overall reliability assessment for the spacecraft.

The basis for reliable design of both DTU and DSU was much the same as it was for the communication subsystem: employ conservative design practices, use proven techniques, apply redundancy judiciously, and select only well-qualified parts. Modular construction was also required here. In constructing the data handling subsystem, STL was once more able to draw upon many components, circuits, and techniques developed during prior military programs. Almost all subsystem components, for example, had already been qualified for a one-year lifetime in space.

### Codes, Words, and Formats

When the Pioneer Program was being formulated in 1962, there existed a general trend in the direction of PCM for space telemetry. The Mariner space probes, NASA's observatory series of satellites, and both the Gemini and Apollo Programs had adopted PCM. PCM has many advantages: unlimited accuracy (in principle), the existence of self-checking and error-correcting codes, and—far from the least—instant compatibility with computers. Because the Pioneers were going to interface with the DSN, with its already strong bias toward digital techniques, there were no overriding technical reasons not to follow the PCM trend.

The bits that constitute each PCM word can be communicated by any one of several two-valued properties of a modulated radio signal. Pioneer PCM bits are impressed upon the transmitter carrier by phase-modulating the 2048-Hz square-wave subcarrier; this follows JPL practice. More technically, the subcarrier is biphase modulated by a time-multiplexed train of bits, using a non-return-to-zero-mark (NRZ-M) format.<sup>7</sup>

<sup>7</sup> On Pioneers 9 and E, the non-return-to-zero-level (NRZ-L) format was introduced.

The basic unit of information in a telemetry message from a Pioneer spacecraft is a seven-bit word. The first six bits represent the instrument reading or datum, with the most significant bit (MSB) appearing first. The last, or seventh, bit is a parity bit based upon the first, third, and fifth bits in the preceding word. If the sum of these bits is odd, the parity bit will also be odd; i.e., one.

The parity bit represents a self-checking feature of the code. Words containing errors introduced during transmission and the many processing steps along the way can be identified and flagged in most instances by recomputing and checking the parity bit for the word that finally arrives at its terrestrial destination. The parity bit, as used in Pioneer telemetry, was worth roughly 2 dB in the sense that transmitted messages could be edited and made more accurate.

PCM words can be made as long as required by the spacecraft instruments. It is often said that PCM words can be made "infinitely accurate." However, the accuracy of much Pioneer scientific data is set by the capabilities of the analog-digital (A/D) converter, which is on the order of 2 percent. The six-bit length of Pioneer words gives the least significant bit (LSB) a value of 1/64—an accuracy greater than that of the A/D converters. The exceptions to the universal adequacy of the six-bit word were the Goddard Space Flight Center fluxgate magnetometers, the Minnesota cosmic-ray instruments, and the Ames plasma probes. The Goddard experiment, for example, needed eight-bit words and fabricated them by combining adjacent pairs of standard-length Pioneer words.

Four special-status words carry no parity bits. These are: (1) the frame-sync word and its complement, (2) the word identifying the telemetry mode being used, (3) the extended-frame counter word, and (4) the spin-rate word.

Just as bits are organized into words, the words themselves are ordered into frames consisting of 32 words each. The frames keep repeating one after the other, but the arrangement of words can be modified by command. This separation of words by interspersing them in the time dimension is called time multiplexing. In effect, each scientific and engineering instrument gets read periodically and the data are strung together in the 32-word frames (fig. 4-8). The flexibility of the formats represents one of the strong points of the Pioneer system design.

There is a problem in terminology. As indicated earlier, four fundamental Pioneer telemetry formats exist. There are, however, five lists of scientific and engineering words that are used in making up the four different telemetry formats that are commandable from the Earth. Pioneer literature often refers to these five lists as formats A through E, implying five Pioneer formats, when only four exist. To avoid semantic confusion, the five lists will be called "lists" A through E in this book. The four *bona fide* formats A, B, C, and D are described as follows:

|   |   |  |           |
|---|---|--|-----------|
| <b>1*</b><br>Frame synchronization<br><b>FS</b> | <b>2</b><br>Format identification         | <b>3</b><br>Scientific subcommutator<br>(16 words)   | <b>4</b>  |
| <b>5</b>  | <b>6</b>                                  | <b>7</b>   | <b>8</b>  |
| <b>9</b>  | <b>10</b>                                 | <b>11</b>  | <b>12</b> |
| <b>13</b>                                       | <b>14</b>                                 | <b>15</b>  | <b>16</b> |
| <b>17*</b><br><b>FS</b>                         | <b>18</b><br>Subcommutator identification | <b>19</b><br>Engineering subcommutator<br>(64 words) | <b>20</b> |
| <b>21</b>                                       | <b>22</b>                                 | <b>23</b>  | <b>24</b> |
| <b>25</b>                                       | <b>26</b>                                 | <b>27</b>  | <b>28</b> |
| <b>29</b>                                       | <b>30</b>                                 | <b>31</b>  | <b>32</b> |

\*Fixed Words

**FS** = complement of the frame synch word in position 1  
(i.e., ones are replaced by zeros and vice versa).

FIGURE 4-8.—Pioneer main telemetry frame, 32 words long.

(1) Format A, identical to list A (tables 4-7 and 4-8), is used primarily at bit rates of 512 and 256 bits/sec when the spacecraft is close to the Earth.

(2) Format B, identical to list B (tables 4-7 and 4-8), is used primarily at bit rates of 64, 16, and 8 bits/sec when the spacecraft is far from the Earth.

(3) Format C, identical to list C, except that list C has 64 words rather

TABLE 4-7.—*Lists A, B, and D for Pioneers 6 and 7<sup>a</sup>*

| Word | Scientific format A                        | Scientific format B                        | Special-purpose format D                   |
|------|--|--|--|
| 1    | Frame sync,<br>7 bits: 1110010             | Frame sync,<br>7 bits: 1110010             | Frame sync,<br>7 bits: 1110010             |
| 2    | Format/mode<br>identification              | Format/mode<br>identification              | Format/mode<br>identification              |
| 3    | Scientific<br>subcommutator<br>(16 words)  | Scientific<br>subcommutator<br>(16 words)  | Scientific<br>subcommutator<br>(16 words)  |
| 4    | Cosmic ray (Chicago)                       | Cosmic ray (Chicago)                       |  |
| 5    |  |  |  |
| 6    | Magnetometer<br>(Goddard)                  | Magnetometer<br>(Goddard)                  |  |
| 7    |  |  |  |
| 8    |  |  |  |
| 9    |  |  |  |
| 10   | Cosmic ray (Chicago)                       | Cosmic ray (Chicago)                       | Radio propagation<br>(Stanford)            |
| 11   |  |  |  |
| 12   | Cosmic ray (GRCSW) <sup>b</sup>            |  |  |
| 13   | Radio propagation<br>(Stanford)            |  |  |
| 14   |  | Plasma (MIT)                               |  |
| 15   | Plasma (MIT)                               |  |  |
| 16   |  |  |  |
| 17   | Frame sync complement<br>7 bits: 0001101   | Frame sync complement<br>7 bits: 0001101   | Frame sync complement<br>7 bits: 0001101   |
| 18   | Subcom identification<br>6-bit counter     | Subcom identification<br>6-bit counter     | Subcom identification<br>6-bit counter     |
| 19   | Engineering<br>subcommutator<br>(64 words) | Engineering<br>subcommutator<br>(64 words) | Engineering<br>subcommutator<br>(64 words) |
| 20   | Cosmic ray (Chicago)                       | Cosmic ray (Chicago)                       |  |

TABLE 4-7—Lists A, B, and D for Pioneers 6 and 7—Concluded.<sup>a</sup>

| Word | Scientific format A | Scientific format B             | Special purpose format D        |
|------|---------------------|---------------------------------|---------------------------------|
| 22   |                     | Magnetometer<br>(Goddard)       |                                 |
| 23   |                     |                                 |                                 |
| 24   |                     |                                 |                                 |
| 25   |                     |                                 |                                 |
| 26   | Plasma (Ames)       | Cosmic ray (GRCSW)              | Radio propagation<br>(Stanford) |
| 27   |                     |                                 |                                 |
| 28   |                     |                                 |                                 |
| 29   |                     | Radio propagation<br>(Stanford) |                                 |
| 30   |                     |                                 |                                 |
| 31   |                     | Plasma (Ames)                   |                                 |
| 32   |                     |                                 |                                 |

<sup>a</sup> Identical to formats A, B, and D mentioned in the text. See chapter 5 for experiment details.

<sup>b</sup> GRCSW = Graduate Research Center of the Southwest; later renamed Southwest Center for Advanced Studies (SCAS) and now known as The University of Texas at Dallas.

TABLE 4-8.—Lists A, B, and D for Pioneers 8 and 9<sup>a</sup>

| Word | Scientific format A                       | Scientific format B                       | Special-purpose format D                  |
|------|---|---|---|
| 001  | Frame sync,<br>7 bits: 1110010            | Frame sync,<br>7 bits: 1110010            | Frame sync,<br>7 bits: 1110010            |
| 002  | Format/mode<br>identification             | Format/mode<br>identification             | Format/mode<br>identification             |
| 003  | Scientific<br>subcommutator<br>(16 words) | Scientific<br>subcommutator<br>(16 words) | Scientific<br>subcommutator<br>(16 words) |
| 004  | Radio propagation<br>(Stanford)           | Radio propagation<br>(Stanford)           |   |
| 005  |   |   |   |
| 006  | Magnetometer                              | Magnetometer                              |   |
| 007  | Goddard on Pioneer 8                      |   |   |
| 008  | Ames on Pioneer 9                         |   |   |

TABLE 4-8—Lists A, B, and D for Pioneers 8 and 9—Concluded.<sup>a</sup>

| Word | Scientific format A                        | Scientific format B                        | Special purpose format D                   |
|------|--|--|--|
| 009  |  |  | Radio Propagation                          |
| 010  |  |  | (Stanford)                                 |
| 011  |  |  |  |
| 012  |  |  |  |
| 013  | Plasma (Ames)                              | Plasma (Ames)                              |  |
| 014  |  |  |  |
| 015  |  |  |  |
| 016  |  |  |  |
| 017  | Frame sync complement<br>7 bits: 0001101   | Frame sync complement<br>7 bits: 0001101   | Frame sync complement<br>7 bits: 0001101   |
| 018  | Subcom identification<br>6-bit counter     | Subcom identification<br>6-bit counter     | Subcom identification<br>6-bit counter     |
| 019  | Engineering<br>subcommutator<br>(64 words) | Engineering<br>subcommutator<br>(64 words) | Engineering<br>subcommutator<br>(64 words) |
| 020  | Cosmic ray (Minnesota)                     | Cosmic ray (Minnesota)                     |  |
| 021  |  |  |  |
| 022  | Magnetometer                               | Magnetometer                               |  |
| 023  | Goddard on Pioneer 8                       |  |  |
| 024  | Ames on Pioneer 9                          |  |  |
| 025  |  |  | Radio propagation                          |
| 026  |  |  | (Stanford)                                 |
| 027  | Cosmic ray (SCAS)                          | Cosmic ray (SCAS)                          |  |
| 028  |  |  |  |
| 029  |  |  |  |
| 030  |  |  |  |
| 031  | Cosmic ray (Minnesota)                     | Cosmic ray (Minnesota)                     |  |
| 032  |  |  |  |

<sup>a</sup> Identical to formats A, B, and D mentioned in the text.

than 32 and takes two frames (tables 4-9 and 4-10), consists mainly of engineering data and is used during special maneuvers (orientation) or when the spacecraft is in trouble.

(4) Format D, identical to list D (tables 4-7 and 4-8), consists of data from Stanford radio propagation experiment only, and is used during lunar occultations and other special events.

TABLE 4-9.—List C: Subcommutated Engineering Measurements for  
Pioneers 6 and 7

| Word | Bit <sup>a</sup> | State   |      | Identification <sup>b</sup>                 |
|------|------------------|---------|------|---|
|      |                  | 0       | 1    |   |
| 201  | 1-7              | No      | Yes  | Frame sync 1110010                          |
| 202  | 8                | No      | Yes  | Format A                                    |
|      | 9                | No      | Yes  | Format B                                    |
|      | 10               | No      | Yes  | Format C                                    |
|      | 11               | No      | Yes  | Format D                                    |
|      | 12               | No      | Yes  | Duty cycle store                            |
|      | 13               | No      | Yes  | Telemetry store                             |
|      | 14               | Yes     | No   | First 32 words of format C                  |
| 203  | 15-20            |         |      |   |
| 204  | 22-27            |         |      |   |
| 205  | 29               | No      | Yes  | Bit rate, 512 bps                           |
|      | 30               | No      | Yes  | Bit rate, 256 bps                           |
|      | 31               | No      | Yes  | Bit rate, 64 bps                            |
|      | 32               | No      | Yes  | Bit rate, 16 bps                            |
|      | 33               | No      | Yes  | Bit rate, 8 bps                             |
|      | 34               | Yes     | No   | Interlock switch to orientation electronics |
| 206  | 36               | Off     | On   | Battery power                               |
|      | 37               | ----    | ---- | Orientation pressure switch actuated        |
|      | 38               | Off     | On   | Orientation power                           |
|      | 39               | Yes     | No   | Undervoltage protection in effect           |
|      | 40               | No      | Yes  | Voltage below switch-trip level             |
|      | 41               | B       | A    | DTU redundancy                              |
| 207  | 43               | 2       | 1    | Antennas to TWT number                      |
|      | 44               | Low     | High | TWT to gain of antenna                      |
|      | 45               | Antenna | TWT  | Driver to                                   |
|      | 46               | Driver  | TWT  | Low-gain antenna to                         |
|      | 47               | Off     | On   | TWT 1 power                                 |
|      | 48               | Off     | On   | TWT 2 power                                 |
| 208  | 50               | Off     | On   | Converter 1, +16 V                          |
|      | 51               | Off     | On   | Converter 1, +10 V                          |
|      | 52               | On      | Off  | Converter 1, -16 V                          |
|      | 53               | Off     | On   | Converter 2, +16 V                          |
|      | 54               | Off     | On   | Converter 2, +10 V                          |
|      | 55               | On      | Off  | Converter 2, -16 V                          |
| 209  | 57               | No      | Yes  | Decoder 1 signal present                    |
|      | 58               | No      | Yes  | Decoder 2 signal present                    |
|      | 59               | Yes     | No   | Receiver 1 signal present                   |
|      | 60               | Yes     | No   | Receiver 2 signal present                   |
|      | 61               | Low     | High | Receiver 2 to gain of antenna               |
|      | 62               | Off     | On   | Coherent mode                               |
| 210  | 64               | No      | Yes  | Ordnance system armed                       |
|      | 65               | No      | Yes  | Third stage separated                       |
|      | 66               | Yes     | No   | Boom 1 (orientation) deployed               |
|      | 67               | Yes     | No   | Boom 2 (magnetometer) deployed              |

TABLE 4-9.—List C: Subcommutated Engineering Measurements for Pioneers 6 and 7 (Continued)

| Word | Bit <sup>a</sup> | State   |       | Identification <sup>b</sup>                 |
|------|------------------|---------|-------|---|
|      |                  | 0       | 1     |   |
| 211  | 68               | Yes     | No    | Boom 3 (wobble damper) deployed             |
|      | 69               | Yes     | No    | Stanford antenna deployed                   |
|      | 71               | On      | Off   | Experiment B power                          |
|      | 72               | -----   | ----- | Not assigned                                |
|      | 73               | -----   | ----- | Not assigned                                |
|      | 74               | On      | Off   | Experiment C power                          |
|      | 75               | No      | Yes   | Experiment C acquiring data                 |
| 212  | 76               | 2       | 1     | Experiment C mode                           |
|      | 78               | On      | Off   | Experiment A power                          |
| 213  | 79               | No      | Yes   | Telemetry store mode signal to experiment A |
|      | 80               | -----   | ----- | Not assigned                                |
|      | 81               | On      | Off   | Experiment G power                          |
|      | 82               | -----   | ----- | Not assigned                                |
|      | 83               | -----   | ----- | Not assigned                                |
|      | 85               | On      | Off   | Experiment D power, 28 V                    |
|      | 86               | No      | Yes   | Experiment D calibrate mode                 |
| 214  | 87               | Off     | On    | Experiment D dynamic range                  |
|      | 88               | No      | Yes   | Experiment D data overflow                  |
|      | 89               | Off     | On    | Experiment D power, 12 V                    |
|      | 90               | On      | Off   | Experiment E power                          |
|      | 92-97            | -----   | ----- | Not assigned                                |
|      | 215              | 99-105  | ----- | Spacecraft spin, rev /64 sec                |
|      | 216              | 106-111 | ----- | TWT 1 anode voltage                         |
| 217  | 113-119          | -----   | ----- | Frame sync complement 0001101               |
|      | 218              | 120-125 | ----- | Receiver 1 static phase error               |
|      | 219              | 127-132 | ----- | Receiver 2 static phase error               |
|      | 220              | 134-139 | ----- | Receiver 1 signal strength                  |
|      | 221              | 141-146 | ----- | Receiver 2 signal strength                  |
|      | 222              | 148-153 | ----- | Receiver 1 and 2 temperature                |
|      | 223              | 155-160 | ----- | TWT 1 helix current                         |
| 224  | 162-167          | -----   | ----- | TWT 1 cathode current                       |
|      | 225              | 169-174 | ----- | TWT 2 helix current                         |
|      | 226              | 176-181 | ----- | TWT 2 cathode current                       |
|      | 227              | 183-188 | ----- | TWT 1 temperature                           |
|      | 228              | 190-195 | ----- | TWT 2 temperature                           |
|      | 229              | 197-202 | ----- | TWT converter temperature                   |
|      | 230              | 204-209 | ----- | Driver temperature                          |
| 231  | 211-216          | -----   | ----- | DTU temperature                             |
|      | 232              | 218-223 | ----- | DSU temperature                             |
|      | 233              | 225-231 | ----- | Frame sync 1110010                          |
|      | 234              | 232     | No    | Format A                                    |
|      |                  | 233     | No    | Format B                                    |
|      |                  | 234     | No    | Format C                                    |
|      |                  | 235     | No    | Format D                                    |
|      |                  | 236     | No    | Duty cycle store                            |

TABLE 4-9.—List C: Subcommutated Engineering Measurements for Pioneers 6 and 7 (Concluded)

| Word | Bit <sup>a</sup> | State |       | Identification <sup>b</sup>                    |
|------|------------------|-------|-------|--|
|      |                  | 0     | 1     |  |
|      | 237              | No    | Yes   | Telemetry store                                |
|      | 238              | No    | Yes   | Last 32 words of format C                      |
| 235  | 239-244          | ----- | ----- | Experiment A, D <sup>4</sup> voltage           |
| 236  | 246-251          | ----- | ----- | Experiment A temperature                       |
| 237  | 253-258          | ----- | ----- | DTU A/D converter calibrate 1                  |
| 238  | 260-265          | ----- | ----- | DTU A/D converter calibrate 2                  |
| 239  | 267-272          | ----- | ----- | DTU A/D converter calibrate 1                  |
| 240  | 274-279          | ----- | ----- | Equipment converter +16-V bus                  |
| 241  | 281-286          | ----- | ----- | Equipment converter +10-V bus                  |
| 242  | 288-293          | ----- | ----- | Equipment converter -16-V bus                  |
| 243  | 295-300          | ----- | ----- | Equipment converter 1 and 2 temp               |
| 244  | 302-307          | ----- | ----- | Bus voltage                                    |
| 245  | 309-314          | ----- | ----- | Bus current                                    |
| 246  | 316-321          | ----- | ----- | Battery temperature                            |
| 247  | 323-328          | ----- | ----- | Battery current                                |
| 248  | 330-335          | ----- | ----- | TWT 2 anode voltage                            |
| 249  | 337-343          | ----- | ----- | Frame sync complement 0001101                  |
| 250  | 344-349          | ----- | ----- | Forward solar panel temperature                |
| 251  | 351-356          | ----- | ----- | Aft solar panel temperature                    |
| 252  | 358-363          | ----- | ----- | Platform temperature (no. 2)                   |
| 253  | 365-370          | ----- | ----- | Boom bracket temperature                       |
| 254  | 372-377          | ----- | ----- | High-gain antenna mounting bracket temperature |
| 255  | 379-384          | ----- | ----- | Louver actuator housing temperature            |
| 256  | 386-391          | ----- | ----- | Sun sensor A temperature                       |
| 257  | 393-398          | ----- | ----- | Platform temperature (no. 1)                   |
| 258  | 400-405          | ----- | ----- | Nitrogen bottle pressure                       |
| 259  | 407-412          | ----- | ----- | Nitrogen bottle temperature                    |
| 260  | 414-419          | ----- | ----- | Not assigned                                   |
| 261  | 421-426          | ----- | ----- | Not assigned                                   |
| 262  | 428-433          | ----- | ----- | Sun sensor C temperature                       |
| 263  | 435-440          | ----- | ----- | Platform temperature (no. 3)                   |
| 264  | 442-447          | ----- | ----- | Experiment B temperature                       |

<sup>a</sup> There are seven telemetry bits in each telemetry channel. Bits are numbered from 1 to 448 in the time order they are received from the spacecraft. Bit numbers missing in sequence refer to bits used to indicate parity (odd) for the first, third, and fifth bits. For analog and digital words, the first bit received is the MSB and assumes the largest weighted value in a word.

<sup>b</sup> Pioneer-6 experiments are identified by letters as follows:

A = Chicago cosmic-ray experiment

B = Goddard magnetometer

C = MIT plasma experiment

D = GRCSW cosmic-ray experiment

E = Stanford University radio propagation experiment

G = Ames plasma experiment

<sup>c</sup> Word not assigned when subcommutated.

TABLE 4-10.—List C; Subcommutated Engineering Measurements for  
Pioneers 8 and 9

| Word | Measurement <sup>a</sup>    |   | Word | Measurement <sup>a</sup> |   |
|------|-----------------------------|---|------|--------------------------|---|
| 001  | Frame sync, 7 bits: 1110010 |   | Y06  | Digital                  |   |
| 201  | Exp H frequency count       |   |      | Bit 1                    | Battery on                                    |
| 002  | Format/mode identification  |   |      | Bit 2                    | Change indicates orientation pulse            |
|      | Binary word                 | Indication  |      | Bit 3                    | Orientation power on and spacecraft separated |
|      | 001000X                     | RT <sup>b</sup>                                   |      | Bit 4                    | Undervoltage protection off                   |
|      | 001001X                     | MRO from TS <sup>b</sup>                          |      | Bit 5                    | CCU power on                                  |
|      | 101010X                     | MRO from DCS with format A <sup>b</sup>           |      | Bit 6                    | DTU redundancy A on                           |
|      | 011010X                     | MRO from DCS with format B <sup>b</sup>           |      | Bit 7                    | Parity bit                                    |
| 202  | Exp B overscale indicator   |   | Y07  | Digital                  |   |
| Y03  | Exp A internal temperature  |   |      | Bit 1                    | TWT 1 to antenna (S4-1)                       |
| Y04  | Digital                     |   |      | Bit 2                    | TWT to high-gain antenna (S2-1)               |
|      | Bit 1                       | Exp A power not on                                |      | Bit 3                    | Driver to TWT (S5-2)                          |
|      | Bit 2                       | Exp A not in flare mode                           |      | Bit 4                    | TWT to low-gain antenna (S3-1)                |
|      | Bit 3                       | Exp A not in flare mode sector                    |      | Bit 5                    | TWT 1 power on                                |
|      | Bit 4                       | Exp A detector B <sub>2</sub> not suppressed      |      | Bit 6                    | TWT 2 power on                                |
|      | Bit 5                       | Exp A detector B <sub>3</sub> not suppressed      |      | Bit 7                    | Parity bit                                    |
| Y05  | Digital                     |   | Y08  | Digital                  |   |
|      | Bit 1                       | 512 bps   |      | Bit 1                    | Equip. conv. 1, +16 V on                      |
|      | Bit 2                       | 256 bps   |      | Bit 2                    | Equip. conv. 1, +10 V on                      |
|      | Bit 3                       | 64 bps  |      | Bit 3                    | Equip. conv. 1, -16 V not on                  |
|      | Bit 4                       | 16 bps  |      | Bit 4                    | Equip. conv. 2, +16 V on                      |
|      | Bit 5                       | 8 bps   |      | Bit 5                    | Equip. conv. 2, +10 V on                      |
|      | Bit 6                       | Orientation power on and spacecraft not separated |      | Bit 6                    | Equip. conv. 2, -16 V not on                  |
|      | Bit 7                       | Parity bit  |      | Bit 7                    | Parity bit                                    |
| Y09  | Digital                     |   |      |                          |   |
|      | Bit 1                       | Decoder 1 signal present                          |      |                          |   |
|      | Bit 2                       | Decoder 2 signal present                          |      |                          |   |

TABLE 4-10.—List C: Subcommutated Engineering Measurements for Pioneers 8 and 9 (Continued)

| Word | Measurement <sup>a</sup>  | Word | Measurement <sup>a</sup>  |
|------|---|------|---|
| Y09  | Digital—Continued<br>Bit 3    Receiver 1 signal not present<br>Bit 4    Receiver 2 signal not present<br>Bit 5    Receiver 2 to high-gain antenna (S1-2)<br>Bit 6    Coherent mode enabled<br>Bit 7    Parity bit   | Y12  | Digital—Continued<br>Bit 3    Exp H power not on<br>Bit 4    Exp G power not on<br>Bit 5    Exp B sensor position indicator<br>(0 = normal,<br>1 = flip command)<br>Bit 6    Exp B change indicates flip command verification<br>(0 = normal,<br>1 = flip command)<br>Bit 7    Parity bit |
| Y10  | Digital<br>Bit 1    Ordnance system armed<br>Bit 2    Spacecraft separated from third stage<br>Bit 3    Boom 1 not deployed (orientation)<br>Bit 4    Boom 2 not deployed (magnetometer)<br>Bit 5    Boom 3 not deployed (wobble damper)<br>Bit 6    Stanford antenna not deployed<br>Bit 7    Parity bit                 | Y13  | Digital<br>Bit 1    Exp D power not on<br>Bit 2    Exp D calibrate on<br>Bit 3    Exp D low power mode on<br>Bit 4    Exp D slip mode on<br>Bit 5    Exp D aspect clock free running<br>Bit 6    Exp E power not on<br>Bit 7    Parity bit  |
| Y11  | Digital<br>Bit 1    Exp B power not on<br>Bit 2    Exp B calibrate on<br>Bit 3    Exp B channel switch flag (0=normal,<br>1=flipped)<br>Bit 4 }    { Exp. B<br>Bit 4 }    { Filter<br>Bit 6 }    { Freq<br>{ 001 = 512 bps<br>{ 010 = 256 bps<br>{ 011 = 64 bps<br>{ 100 = 16 bps<br>{ 101 = 8 bps<br>Bit 7    Parity bit | Y14  | Digital<br>Bits 1-4    Exp D measurements counter number<br>Bits 5-6    Exp D supercommutation number   |
| Y12  | Digital<br>Bit 1    Exp F power not on<br>Bit 2    Telemetry store mode on  | Y15  | Digital<br>Bits 1-7    Spin rate counter  |
|      |   | Y16  | TWT 1 anode voltage   |
|      |   | 017  | Frame sync complement, 7 bits:<br>0001101   |
|      |   | 217  | Exp H frequency count   |
|      |   | Y18  | Receiver 1 loop stress  |
|      |   | Y19  | Receiver 2 loop stress  |
|      |   | Y20  | Receiver 1 signal strength  |
|      |   | Y21  | Receiver 2 signal strength  |
|      |   | Y22  | Receiver 1 temperature  |
|      |   | Y23  | TWT 1 helix current   |

TABLE 4-10.—List C: Subcommutated Engineering Measurements for  
Pioneers 8 and 9 (Concluded)

| Word    | Measurement <sup>a</sup>           | Word    | Measurement <sup>a</sup>                       |
|---------|------------------------------------|---------|--|
| Y24     | TWT 1 cathode current              | Y44     | Primary bus voltage                            |
| Y25     | TWT 2 helix current                | Y45     | Primary bus current                            |
| Y26     | TWT 2 cathode current              | Y46     | Battery temperature                            |
| Y27     | TWT 1 temperature                  | Y47     | Battery current                                |
| Y28     | TWT 2 temperature                  | Y48     | TWT 2 anode voltage                            |
| Y29     | TWT converter temperature          | 049     | Frame sync complement, 7 bits:<br>0001101      |
| Y30     | Transmitter driver temperature     | 249     | Exp H freq count                               |
| Y31     | DTU temperature                    | Y50     | Solar panel 1 (upper)<br>temperature           |
| Y32     | DSU temperature                    | Y51     | Solar panel 2 (lower)<br>temperature           |
| 033     | Frame sync, 7 bits: 1110010        | Y52     | Mounting platform 2<br>temperature             |
| 233     | Exp H frequency count              |         |  |
| 034     | Format/mode identification         |         |  |
|         | Binary<br>word                     |         |  |
|         |                                    |         | Indication                                     |
| 001000X | RT <sup>b</sup>                    | 001001X | MRO from TS <sup>b</sup>                       |
|         |                                    | 101010X | MRO from DCS<br>with format A <sup>b</sup>     |
|         |                                    | 011010X | MRO from DCS<br>with format B <sup>b</sup>     |
| 234     | Exp D detector B temperature       |         |  |
| Y35     | Exp E 49-Hz signal amplitude       | Y53     | Exp H ramp-generator voltage<br>level          |
| Y36     | Receiver 2 temperature             | Y54     | Antenna mtg bracket (high gain)<br>temperature |
| Y37     | DTU inflight calibrate 1           | Y55     | Louver actuator housing<br>temperature         |
| Y38     | DTU inflight calibrate 2           | Y56     | Sun sensor "A" temperature                     |
| Y39     | DTU inflight calibrate 3           | Y57     | Mounting platform 1<br>temperature             |
| Y40     | Equip. conv., +16 V bus            | Y58     | Nitrogen bottle pressure                       |
| Y41     | Equip. conv., +10 V bus            | Y59     | Nitrogen bottle temperature                    |
| Y42     | Equip. conv., -16 V bus            | Y60     | Exp G electronics temperature                  |
| Y43     | Equip. conv 1 and 2<br>temperature |         |  |
|         |                                    |         |  |
|         |                                    | Y61     | Exp B sensor temperature                       |
|         |                                    | Y62     | Sun sensor "C" temperature                     |
|         |                                    | Y63     | Mounting platform 3<br>temperature             |
|         |                                    | Y64     | Not used (ground)                              |

<sup>a</sup> Pioneer-9 experiments are identified by letters as follows:

A = Minnesota cosmic ray  
 B = Ames magnetometer  
 D = SCAS cosmic ray  
 E = Stanford radio propagation  
 F = Goddard cosmic dust  
 G = Ames plasma  
 H = TRW electric field

<sup>b</sup> Telemetry modes are as follows:  
 RT = Real time

Formats A, B, and D each possess spaces for two subcommutated words. Words from the 64-word list C of engineering data are repeated one after the other, always in position 19, in successive frames of formats A, B, and D. When subcommutated in these formats, list C repeats every 64 frames compared to its repetition every two frames when format C is selected. This option permits the mission controllers to emphasize or de-emphasize engineering data as the situation requires.

List E (or format E) is always subcommutated in position 3 of formats A, B, and D. List E is only 16 words long (table 4-11) and consists primarily of lower-priority scientific data.

During the launch and reorientation maneuver, the spacecraft normally transmitted format C. While the spacecraft was still near the Earth, format A was usually employed. As the spacecraft receded from Earth, format B was adopted. If the trajectory of a Pioneer was favorable for lunar occultation, a command from Earth switched to format D. Out in the relatively calm reaches of deep space, the spacecraft transmits format B most of the time.

### Four Modes of Operation

Although variable bit-rate and telemetry format confer considerable flexibility, provision is needed for storing and thus delaying data transmission back to Earth. An important solar event could occur when one or more of the Pioneers is too far away to telemeter plasma-probe data rapidly enough to catch the details of the fast-breaking action. It would be like trying to make a movie of a high jumper with a movie camera taking only a frame or two per second; many details would be missed. The initial STL studies recognized the advantages of a small memory device in such situations. Data could be recorded at a high rate during the event and then retransmitted later at a bit rate compatible with the spacecraft's transmitter power and distance from the Earth.

The illustration above justifies three of the four Pioneer telemetry modes: (1) real-time operation, (2) telemetry store, and (3) memory readout. The fourth mode, the duty-cycle store mode, simply stores data in the memory when the spacecraft is not being worked by a DSN station.

---

MRO = Memory readout

TS = Telemetry store

DCS = Duty-cycle store

Notes:

For bit 7 of format/mode ID, X = 0 (zero) for the first 32 words of engineering subcommutator and X = 1 (one) for the last 32 words.

Word numbering system: 017 indicates main frame word 17.

217 indicates engr subcom word 17.

Y18 indicates can be either 018 or 218.

Statements indicated are for the true (one) state on digital words Y04 through Y13.

TABLE 4-11.—*Formats E (Lists E) for Pioneer Spacecraft<sup>a</sup>*

| Pioneers 6 and 7 |         |  | Pioneers 8 and 9 |         |  |
|------------------|---------|--|------------------|---------|--|
| Word             | Type    | Identification                               | Word             | Type    | Identification                               |
| 101              | Digital | Cosmic ray<br>(Chicago)                      | 101              | Digital | Cosmic ray<br>(Minnesota)                    |
| 102              | Analog  | Radio propagation<br>(Stanford)              | 102              | Analog  | Radio propagation<br>(Stanford)              |
| 103              | Digital | Unassigned                                   | 103              | Digital | Cosmic dust (Goddard)                        |
| 104              | Digital |  | 104              | Digital |  |
| 105              | Digital |  | 105              | Digital |  |
| 106              | Digital |  | 106              | Digital |  |
| 107              | Analog  | Radio propagation<br>(Stanford)              | 107              | Analog  | Radio propagation<br>(Stanford)              |
| 108              | Analog  | Plasma (Ames)                                | 108              | Analog  | Electric field<br>(Stanford/TRW)             |
| 109              | Digital | Cosmic ray (Chicago)                         | 109              | Digital | Cosmic ray<br>(Minnesota)                    |
| 110              | Digital | Plasma (MIT)                                 | 110              | Digital |  |
| 111              | Analog  | Radio propagation<br>(Stanford)              | 111              | Analog  |  |
| 112              | Analog  | Plasma (Ames)                                | 112              | Analog  | Electric field<br>(Stanford/TRW)             |
| 113              | Digital | Magnetometer<br>(Goddard)                    | 113              | Digital | Cosmic ray<br>(Minnesota)                    |
| 114              | Digital |  | 114              | Digital |  |
| 115              | Analog  | Radio propagation<br>(Stanford)              | 115              | Analog  |  |
| 116              | Digital | Bit rate code and<br>extended frame<br>count | 116              | Digital | Radio propagation<br>(Stanford)              |
|                  |         |  |                  |         | Bit rate code and<br>extended frame<br>count |

<sup>a</sup> Also called the "scientific subcommutator formats."

Any one of the four modes can be started with a specific command from Earth. Regardless of when the spacecraft receives the command, actual execution is delayed until the beginning of the next 32-word frame. Switching modes by command has its advantages, but if the data handling subsystem got stuck ("hung up") in the memory readout mode, when the 15 232 bits, (68 frames) worth of information in the memory came to an end, so would the mission. Consequently, all spacecraft modes automatically revert to the real-time mode whenever the DSU is filled or emptied, because the real-time mode is the most useful of the four.

There are some data-handling subtleties and restrictions that are best explained with a table (see table 4-12).

TABLE 4-12.—*More Details on Pioneer Telemetry Modes*

| Mode                           | Characteristics   |                              |                      |    |    |     |     |      |      |       |     |
|--------------------------------|---|------------------------------|----------------------|----|----|-----|-----|------|------|-------|-----|
| Real-time mode . . . . .       | This mode transmits any one of the four commandable formats continuously at any selected bit rate except for format D. When format D is selected, only 68 frames are transmitted before the subsystem automatically reverts to format B at 16 bits/sec. This precludes getting hung up on the Stanford radio propagation experiment. The 68 frames are stored in the memory as they are transmitted. This mode is employed during lunar occultation and other special scientific events.  |                              |                      |    |    |     |     |      |      |       |     |
| Telemetry-store mode . . . . . | The DSU is filled to 68-frame capacity (32-word frames) with format A, B, or C, whichever is commanded. The data are also transmitted in real time. When the DSU is filled, the subsystem reverts to format B at 16 bits/sec. This mode is useful for sampling data faster than real-time transmission permits.   |                              |                      |    |    |     |     |      |      |       |     |
| Duty-cycle mode . . . . .      | Frames in format A, B, or (rarely) C are filled at the 512 bits/sec rate and are stored in the DSU, one at a time, at one of four commandable rates given below:  |                              |                      |    |    |     |     |      |      |       |     |
|                                | <table> <thead> <tr> <th style="text-align: left;">Interval between frames, min</th> <th style="text-align: left;">Time to fill DSU, hr</th> </tr> </thead> <tbody> <tr> <td style="text-align: right;">17</td> <td style="text-align: right;">19</td> </tr> <tr> <td style="text-align: right;">8.5</td> <td style="text-align: right;">9.5</td> </tr> <tr> <td style="text-align: right;">4.25</td> <td style="text-align: right;">4.75</td> </tr> <tr> <td style="text-align: right;">2.125</td> <td style="text-align: right;">2.3</td> </tr> </tbody> </table> | Interval between frames, min | Time to fill DSU, hr | 17 | 19 | 8.5 | 9.5 | 4.25 | 4.75 | 2.125 | 2.3 |
| Interval between frames, min   | Time to fill DSU, hr  |                              |                      |    |    |     |     |      |      |       |     |
| 17                             | 19  |                              |                      |    |    |     |     |      |      |       |     |
| 8.5                            | 9.5   |                              |                      |    |    |     |     |      |      |       |     |
| 4.25                           | 4.75  |                              |                      |    |    |     |     |      |      |       |     |
| 2.125                          | 2.3   |                              |                      |    |    |     |     |      |      |       |     |
| Memory-readout mode . . . . .  | In other words, frames of data can be selected and stored for up to 19 hours. This mode is used primarily when the spacecraft is not being worked by the DSN. Following each eight frames of scientific data, format C (list C) is also stored. Data are also transmitted in real time but are, of course, not recoverable if the DSN is not working the spacecraft. When the DSU is filled, the subsystem reverts to format B at 16 bits/sec.  |                              |                      |    |    |     |     |      |      |       |     |
|                                | The contents of the DSU are transmitted at any selected bit rate. Data are read out only once because the process destroys the memory contents. Unfilled portions of the memory appear as is. At the end of memory readout, the subsystem reverts to the format and bit rate in use prior to the receipt of the readout command.  |                              |                      |    |    |     |     |      |      |       |     |

In summary, the variable bit rate, variable format, and variable mode permit the mission controller to tune the spacecraft and supporting systems to changing scientific requirements, emergency situations aboard the spacecraft, and the lengthening distance between the Earth and its automated outpost far out along the plane of the ecliptic.

### The Digital Telemetry Unit

The digital telemetry unit is not only the central clearing house for all spacecraft-generated data, it is also the spacecraft timer or synchronizer that keeps all spacecraft components operating in step. To do this and impose order upon the varied data requires a rather complex array of logic circuits, counters, and A/D converters (fig. 4-9).

The timing function is performed by a crystal-controlled-oscillator clock producing a 16 384-Hz output signal. This signal is then divided by 32, 64, 256, 1024, and 2048 to establish the five standard bit rates. (Note that these numbers are all powers of 2.) Armed with timing signals, the multiplexers and submultiplexers sample the various analog and digital outputs of the scientific and engineering instruments. All instruments are usually on at all times; and the only stimulus needed to make them provide a reading is an electronic "gate." (An exception is the Stanford radio propagation experiment, which is usually turned off at great ranges.) The multiplexers simply open and close gates leading to the instruments in the order specified by the last command from Earth. Electronic switches or gates are the mainstays of computers and other logic circuits. It is the spacecraft clock, of course, that ultimately drives all subsystem circuits.

Many instruments deliver digital information (bits) when the multiplexers open the gates. Others, particularly the engineering instruments, yield analog data. Such analog signals, really voltage levels between 0 and +3 V, must be converted into digital signals. This task falls to the A/D converter, another basic type of circuit in the data-handling subsystem.

Figure 4-9 also indicates that signals from the Sun sensors are counted in the DTU to establish a spin rate. Gas pulses from the orientation system are indicated by a one-bit toggle which switches between 0 and 1 or 1 and 0 for each pulse. Spin rate and orientation pulse data are dubbed into the telemetry stream as engineering data. The Sun pulses are sent to some experiments in order to turn them on to record data at certain azimuths, notably when pointed in the direction of the Sun.

All DTU components were essentially off-the-shelf, having been developed and qualified in commercial and military programs.

### The Data Storage Unit

The memory of the DSU is not large by terrestrial standards—only 15 232 bits—but this is sufficient for Pioneer's purposes in view of the very low data rates possible for transmission back to Earth. It takes over half an hour to read out a 15 232-bit memory at 8 bits/sec. Earth satellites, which generally have much larger memories, commonly carry tape recorders to store data until the memory can be read out over the next data-acquisition station. Tape recorders possess a high storage capacity but do not have the requisite reliability for a Pioneer mission. A solid-state mem-

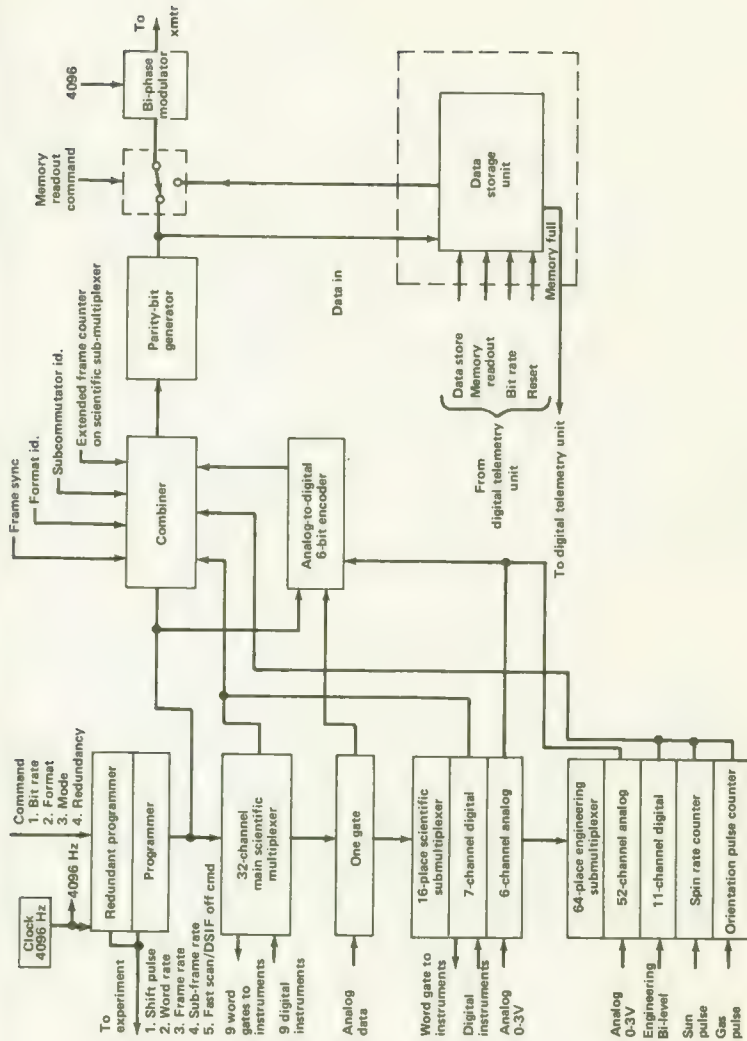
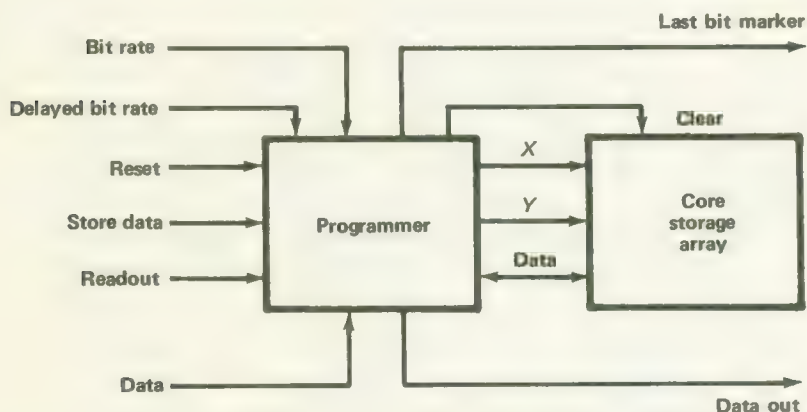


FIGURE 4-9.—Simplified block diagram of the digital telemetry unit.

ory, employing magnetic cores similar to those found in digital computers, was selected (fig. 4-10). The STL feasibility study and proposal had been based upon non-destructive memory readout, where each bit is reinserted into the memory immediately after being read out. But the power and weight penalties of this approach were too high, and destructive readout was chosen. The inevitable engineering tradeoff in this instance was that the DSN must be in downlink lock with the spacecraft and ready to accept data before the memory readout command can be transmitted. Memory readout can be terminated at any time by commanding a switch to the real-time mode, but the remaining data in storage are destroyed. In fact, if the data in the memory are not desired, the memory readout command followed immediately by a real-time mode command are collectively equivalent to a "memory clear" command. However, the real-time mode command can interrupt the telemetry-store mode, without the stored data's being destroyed. The DSU was built by Electronic Memories, Inc.

### The Convolutional Coder

Adding the parity bit in the standard Pioneer telemetry code is worth 2 dB of added gain; the parity bit enables the DSN to gather good data from greater distances than otherwise possible. The price paid for reducing the error rate, however, is additional spacecraft circuitry and the transmission time taken by the parity bits.



- Note:** Last bit marker causes DTU to generate a reset pulse
1. Following storage
  2. At the start of read out mode
  3. Following a read out mode. This reset pulse also is used by DSU programmer to generate a memory clear pulse.

FIGURE 4-10.—Simplified block diagram of the data storage unit.

The CCUs installed on Pioneers 9 and E, through more elaborate coding, reduce telemetry error rates by an amount equivalent to about 3 dB in overall system gain, perhaps as much as 3.9 dB (ref. 2). The price paid is 1.3 lb in the weight of the coder, plus the 1.3 W of power it draws when operating in-line, plus the bits added to the telemetry stream. With the Pioneer convolutional coder, every bit of telemetry information is matched by an extra bit from the coder, which in effect carries "information about information." The doubled bit stream created by the convolutional coder represents redundancy, which increases the accuracy of telemetry communication from a distant spacecraft.

The parity bit in the standard Pioneer code is computed from the three odd-numbered bits in the preceding telemetry word. If the sum of these three bits is odd, the parity bit is also odd, i.e., one. The parity bits in the convolutional coder are computed by directing the bit stream from the DTU into a 25-bit register. Each bit leaving the DTU moves into position 1 in the register, shifting the 25th bit out the other end. The bits in positions 1, 2, 4, 6, 8, 9, 12, 14, 15, 16, 20, 21, 22, 24, and 25 are then added; if the sum is odd, the parity bit associated with the first bit is also odd, i.e., one.<sup>8</sup> After the telemetry bit and its newly computed parity bit have been sent on, the entire group of bits moves up a position and a new one is added from the DTU. The process is repeated for each telemetry bit in the 7-bit Pioneer word, including the regular parity bit, so that the CCU gain of 3 dB is added to the 2 dB picked up from the normal parity bit. Each parity bit thus contains some intelligence regarding 15 bits in the 25-bit register (fig. 4-11). The register is reset to zero once each 32-word frame so that decoding can be done on a frame-for-frame basis.

The telemetry bit and its companion parity bit are phase-modulated onto the square wave subcarrier and sent on to the transmitter driver for relay to the Earth. On Pioneers 9 and E, the only spacecraft carrying the convolutional coder, the NRZ-L method of modulation was employed rather than the NRZ-M approach used in the earlier Pioneers.

Figure 4-7 illustrates how the convolutional coder was installed in the Pioneers 9 and E data handling subsystems on an experimental basis. It can be switched in or out, being an off-line element like the data storage unit. Flight experience on Pioneer 9 has been good. The 3-dB coding gain extended the maximum communication range of Pioneer 9 about 40 percent.

## THE COMMAND SUBSYSTEM

None of the flexibility and reliability gained through alternate modes of operation and redundancy can be realized without switches commandable from the Earth. To substitute a new TWT for one that falters,

<sup>8</sup> Technically, this parity bit is the "modulo-2 sum" of the 15 bits indicated.

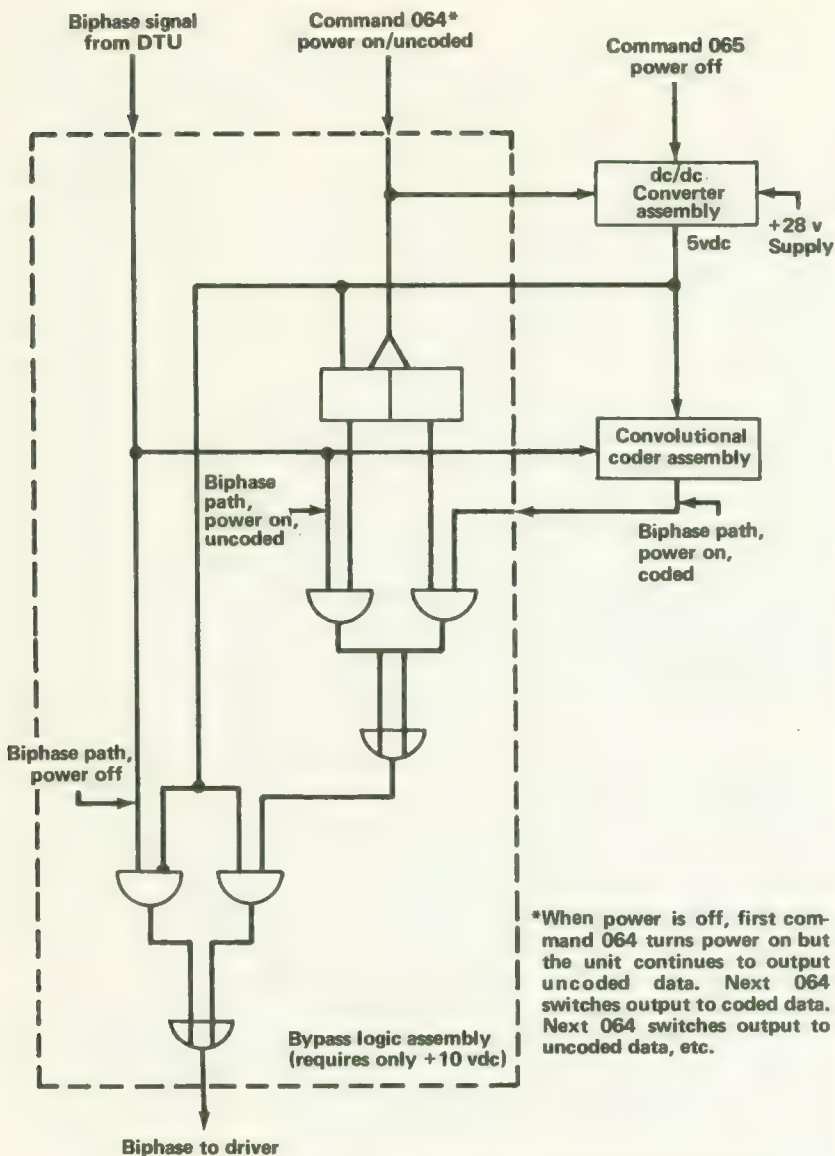


FIGURE 4-11.—Block diagram of the Pioneer convolutional coder unit.

or to change bit rate, the mission controller dispatches a command to the spacecraft directing a specific switch to open or close. The Pioneers employ between 57 and 67 commands (each spacecraft is slightly different) to activate the same numbers of spacecraft switches. About two-thirds of the commands pertain to spacecraft functions and the rest to experiments. The

number of Pioneer on-off switches corresponds roughly to the number of electric switches in a modern home, considering all the appliances. Thus while Pioneer has been presented as a relatively simple spacecraft in the preceding pages, it has almost  $2^{57}$  different operating permutations and can hardly be called primitive.<sup>9</sup>

Let us say that the mission controller at Ames Research Center wishes to change Pioneer 6's bit rate from 16 bits/sec to 8 bits/sec because the spacecraft is too far from Earth for the higher bit rate to be received without an excessive error rate. He constructs a 23-bit command word that is sent through JPL along NASA Communications Network (NASCOM) lines to the DSN station working Pioneer 6. The command is modulated onto the uplink carrier by frequency-shift keying. If a digital one is to be sent, a 240-Hz tone is phase-modulated on the DSN carrier; a 150-Hz tone represents a digital zero. The bit stream representing the command is thus a series of 23 beeps (in two pitches) on the DSN carrier.

The spacecraft communication subsystem possesses two frequency-addressable receivers; the carrier frequency selects the receiver once the PCM/PM/FSK signal reaches the spacecraft. The addressed spacecraft receiver demodulates the incoming signal and passes the series of tones on to two decoders. The command carries an address specifying only one of the redundant decoders; that decoder converts the tones into the 23-bit command and stores it in registers.

After checking the command for errors, the addressed decoder sends the command to the command distribution unit (CDU). The CDU selects the wire leading to the proper electronic switch, and the command is executed once the switch is thrown. If the switch is already in the commanded position no switching is changed.

### Command Format

The standard telemetry word is seven bits; the Pioneer command's 23-bit word is much longer. If only the command number were sent, seven bits would be sufficient. Pioneer 9, which used the most commands (67), barely needed seven bits. As figure 4-12 indicates, the basic Pioneer command number was actually seven bits long. Preceding the seven-bit segment, however, was a seven-bit complement of the command, in which the ones in the command number were replaced by zeros and vice versa. It is common spacecraft practice to promote high command accuracy by sending a considerable amount of redundant information. The consequences of a garbled command are too serious to settle for simple parity checks or even the more elaborate coding adopted in the convolutional coder.<sup>10</sup> While the

<sup>9</sup> Not all commands are mutually exclusive, so that  $2^{57}$  is indicative only.

<sup>10</sup> In some satellites, where transmission times are negligible, the spacecraft repeats the command it has received to the tracking station before executing it.

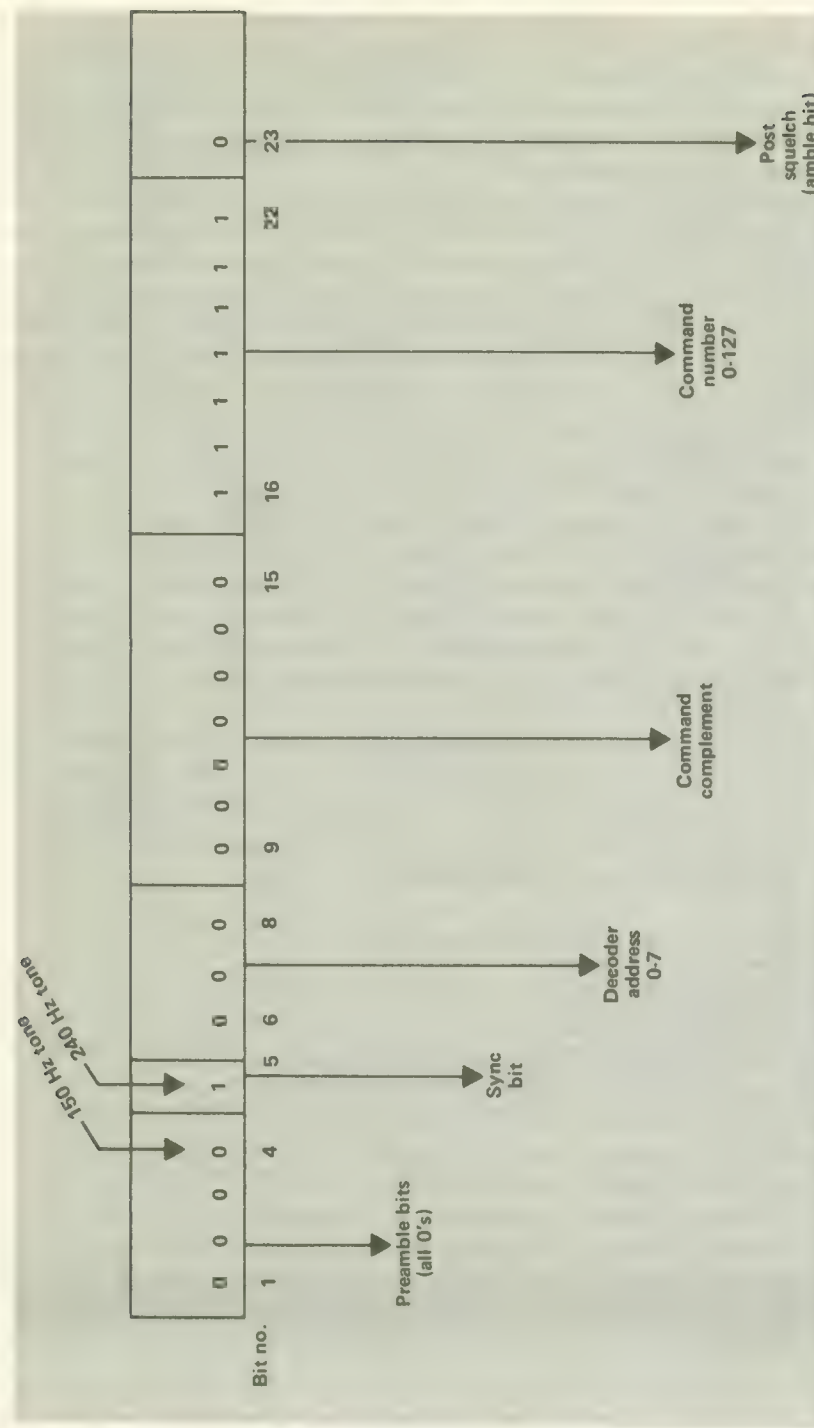


FIGURE 4-12.—Structure of the Pioneer command word.

23-bit command is in the decoder register, it is compared bit-by-bit with its complement. Complete correspondence is required before the command is released for execution. Incomplete or distorted commands are not executed. Loss of receiver lock also inhibits command execution.

The command number and its complement are preceded by the address that selects: (1) a specific Pioneer spacecraft, and (2) one of the two decoders on that spacecraft. Preceding the address is a sync bit and a series of four zeros at the beginning of the command word. The zeros, called a "preamble," aid command acquisition by the spacecraft decoder—in a sense, the zeros tell the decoder to prepare to receive a command. A post-squelch bit (or "amble" bit) follows at the end of the command word. The amble bit is always zero, and signals the end of the command. Physically, the function of the amble bit is to keep the decoder in operation; that is, it keeps the appropriate gates open until the command has been executed.

Command tones are modulated on the DSN carrier at the rate of only 1 bit/sec. It takes 27 sec to receive and execute a command aboard the spacecraft; this includes the time required for processing the command in the decoder and executing it. Pioneers are generally several light minutes away from Earth and are always "out of touch" to some degree, regardless of the low command rate.

The command numbers and their functions are listed in tables 4-13 and 4-14.

### The Command Decoder and Command Distribution Unit

The assigned task of the decoder is the delivery of a verified bit train to the CDU. The decoder block diagram shown in figure 4-13 illustrates how the incoming series of tones is detected by a filter-detector circuit. Once the filters sort out the tones by frequency and turn them into pulses, the bits move into the shift register described earlier. After checking the complement, the decoder transmits a series of pulses to a diode matrix that makes up the gating circuits within the CDU. The diode matrix sends an execute signal to the proper address within the spacecraft (fig. 4-14). Four different kinds of signals flow out of the CDU, each tailored for triggering a specific action—the end result of the command transmitted from Earth:

(1) Most command pulses are short ( $10 \mu\text{sec}$ ), low current (about 10 mA), at 10 V. These signals are sufficient to drive most Pioneer electronic circuits.

(2) Some devices, such as the coaxial switches, require somewhat longer pulses; the CDU provides a 160-msec, 28-V pulse for such devices.

(3) Where solid-state switches are inadequate because of the high currents involved, as in the case of the battery switch, the CDU activates relays.

TABLE 4-13.—*Command List for Pioneers 6 and 7, Grouped by Function*

| Command number | End function                    | Command number | End function               |
|----------------|---------------------------------|----------------|----------------------------|
|                | Communications                  |                | Telemetry (Continued)      |
| 001            | TWT 1 on                        | 037            | Format C                   |
| 003            | Receiver 2 to low-gain antenna  | 044            | DTU redundancy A           |
| 010            | TWTs off                        | 050            | Format D                   |
| 011            | TWT 2 on                        | 051            | Telemetry store            |
| 015            | TWT 1 to antenna/driver to TWT  | 052            | Memory readout             |
| 022            | TWT 2 to antenna/driver to TWT  | 053            | Duty-cycle store           |
| 025            | TWTs to low-gain antenna        | 060            | Real time                  |
| 030            | Coherent mode enabled           |                | Experiments                |
| 033            | Receiver 2 to high-gain antenna | 020            | All experiments off        |
| 043            | Non-coherent mode enabled       | 063            | Chicago cosmic ray         |
| 046            | Driver to low-gain antenna      | 070            | Calibrate                  |
| 047            | TWTs to high-gain antenna       | 076            | Normal mode                |
|                | Electrical                      | 055            | Power on                   |
| 000            | Undervoltage simulate           | 061            | Goddard magnetometer       |
| 017            | Battery on                      | 062            | Calibrate                  |
| 036            | Battery off                     | 013            | Flip sensor                |
| 107            | Undervoltage protection off     | 111            | MIT plasma                 |
| 110            | Undervoltage protection on      | 112            | Power on                   |
|                | Ordnance                        |                | Mode change no. 1          |
| 045            | Boom deployment (backup)        | 073            | Mode change no. 2          |
|                | Orientation                     | 100            | GRCSW cosmic ray           |
| 021            | Type-I restart                  | 101            | Dynamic range on           |
| 031            | Type-II clockwise               | 116            | Dynamic range off          |
| 040            | Type-II counterclockwise        |                | Calibrate                  |
| 041            | Power on                        | 071            | Power on                   |
| 042            | Power off                       | 077            | Stanford radio propagation |
|                | Telemetry                       |                | Calibrate                  |
| 004            | 512 bit rate                    | 054            | Power on                   |
| 005            | 256 bit rate                    | 072            | Ames plasma                |
| 006            | 64 bit rate                     | 113            | Calibrate                  |
| 016            | 16 bit rate                     |                | Mode change                |
| 024            | DTU redundancy B                |                | Spacecraft commands: 38    |
| 027            | 8-bit rate                      |                | Experiment commands: 19    |
| 034            | Format A                        |                |                            |
| 035            | Format B                        |                |                            |

TABLE 4-14.—*Command List for Pioneers 6 and 7, Grouped by Function*

| Command number | End function                      | Command number      | End function                       |
|----------------|-----------------------------------|---------------------|------------------------------------|
| 000            | Electrical Undervoltage simulate  | 033                 | Receiver 2 to high-gain antenna    |
| 017            | Battery on                        | 043                 | Noncoherent mode enabled           |
| 036            | Battery off                       | 046                 | Driver to low-gain antenna         |
| 107            | Undervoltage protection off       | 047                 | TWTs to high-gain antenna          |
| 110            | Undervoltage protection on        |                     | Experiments                        |
| 045            | Ordnance Boom deployment (backup) | 020                 | All experiments off                |
| 021            | Orientation Type-I restart        | 076                 | Minnesota cosmic ray Power on      |
| 031            | Type-II clockwise                 | 102                 | Arm                                |
| 040            | Type-II counterclockwise          | 103                 | Code                               |
| 041            | Power on                          | 104                 | Flare mode                         |
|                | Telemetry                         | 105                 | Sector flare mode                  |
| 004            | 512 bit rate                      | 111                 | Execute                            |
| 005            | 256 bit rate                      | 114                 | Disable detector D                 |
| 006            | 64 bit rate                       | 115                 | Select telescope T1                |
| 016            | 16 bit rate                       |                     | Ames magnetometer                  |
| 024            | DTU redundancy B                  | 013                 | Power on                           |
| 027            | 8 bit rate                        | 061                 | Calibrate and flip (if enabled)    |
| 034            | Format A                          | 062                 | Flip enable                        |
| 035            | Format B                          | 063                 | Spin demodulator select            |
| 037            | Format C                          | 070                 | Bandwidth change                   |
| 044            | DTU redundancy A                  | 073                 | SCAS cosmic ray                    |
| 050            | Format D                          | 101                 | High power mode on                 |
| 051            | Telemetry store                   | 113                 | Calibrate                          |
| 052            | Memory readout                    | 116                 | Low power mode on                  |
| 053            | Duty-cycle store                  |                     | Power on                           |
| 060            | Real time                         | 077                 | Stanford radio propagation         |
| 064            | CCU power on uncoded              | 071                 | Power on                           |
| 065            | CCU power off                     | 055                 | Calibrate                          |
|                | Communications                    | 112                 | Goddard cosmic dust                |
| 001            | TWT 1 on                          |                     | Power on                           |
| 003            | Receiver 2 to low-gain antenna    | 054                 | Ames plasma probe                  |
| 010            | TWTs off                          | 072                 | Power on                           |
| 011            | TWT 2 on                          | 074                 | Calibrate/sector delay mode select |
| 015            | TWT 1 to antenna/driver to TWT    | 100                 | Energy range select                |
| 022            | TWT 2 to antenna/driver to TWT    | 106                 | Suppression mode change            |
| 025            | TWTs to low-gain antenna          |                     | TRW electric field detector        |
| 030            | Coherent mode enabled             |                     | Power on                           |
|                |                                   | Pioneer             | 8 9                                |
|                |                                   | Spacecraft commands | 38 38                              |
|                |                                   | Experiment commands | 26 29                              |
|                |                                   | —                   | —                                  |
|                |                                   | 64                  | 67                                 |

<sup>a</sup> Pioneer 9 only.

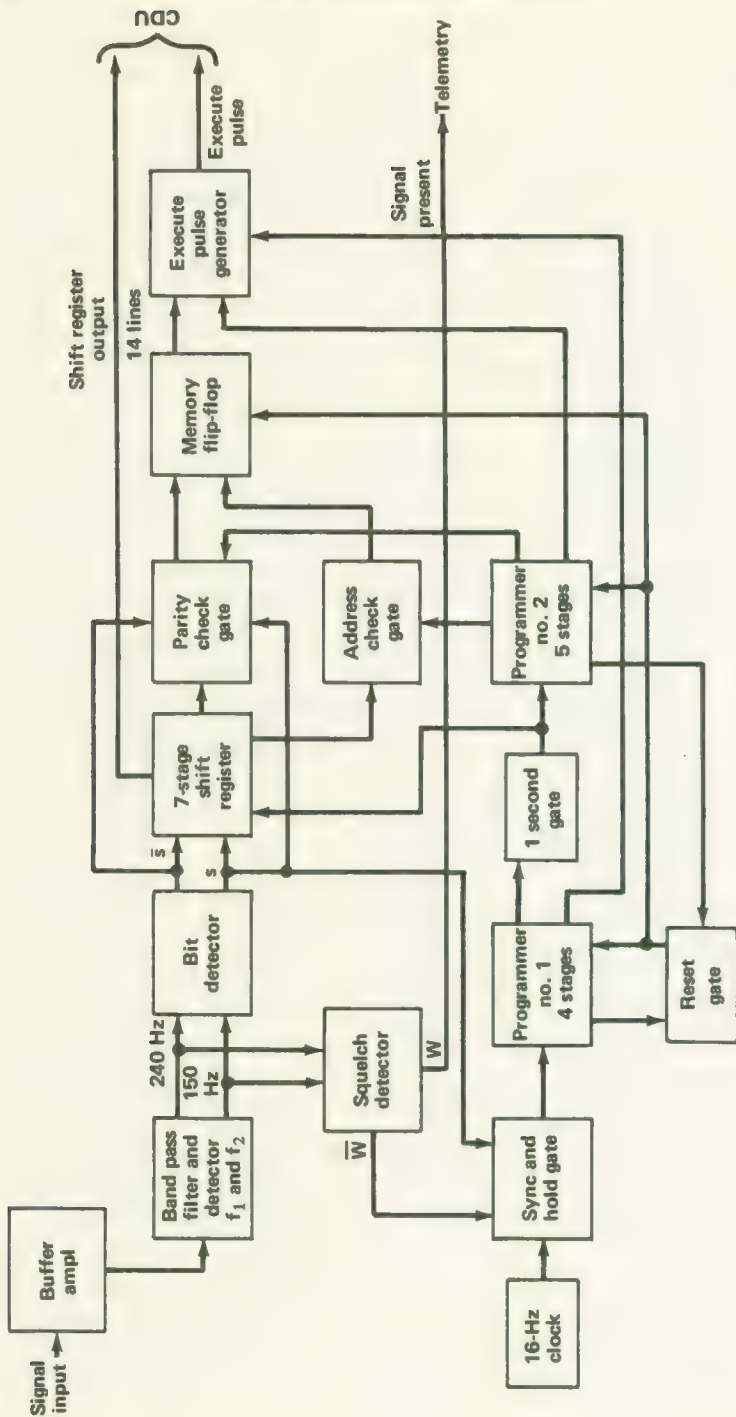


FIGURE 4-13.—Block diagram of the Pioneer command decoder.

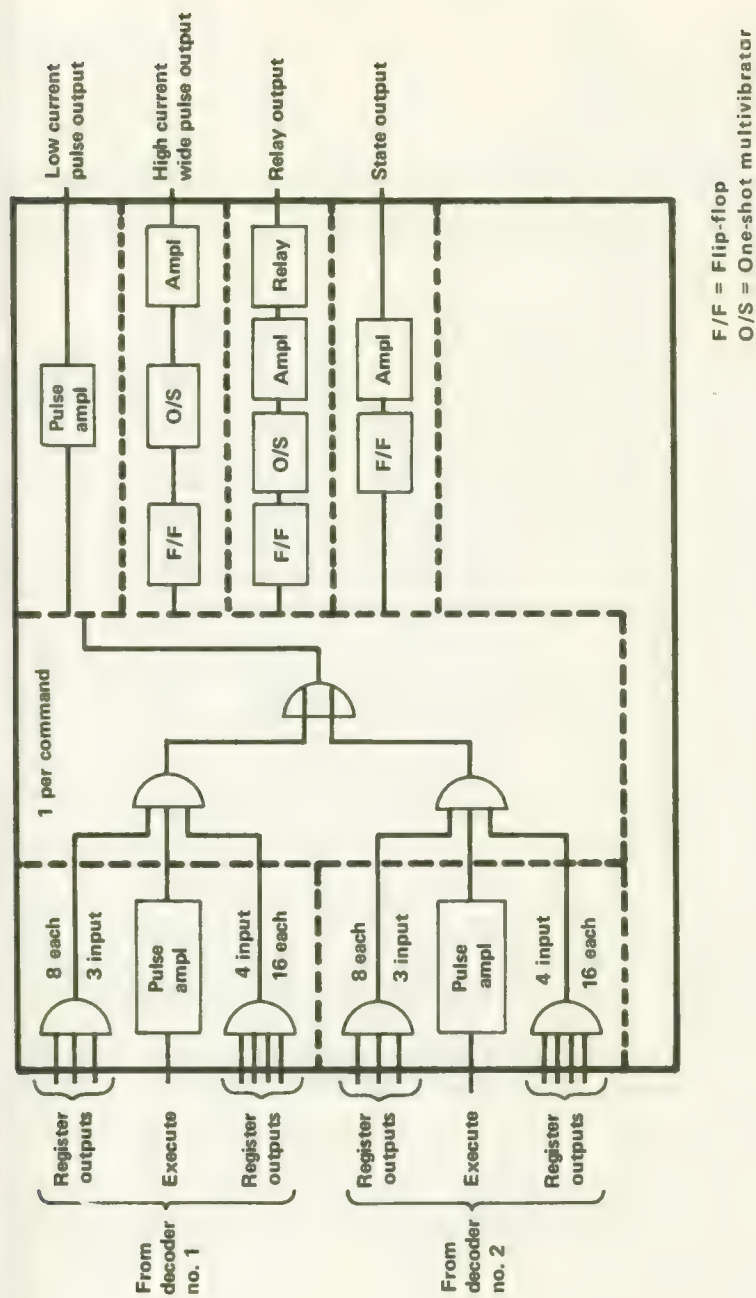


FIGURE 4-14.—Functional diagram of the command distribution unit.

F/F = Flip-flop  
O/S = One-shot multivibrator

(4) A "state" output (one of two voltage levels) is available for instrumentation. On the Pioneers, state commands were simply "voltage on" or "voltage off" commands.

Like the designs of much of Pioneer's electronic hardware, the command-decoder and CDU designs were derived from STL experience with Air Force aerospace programs. Solid-state components were employed throughout the command subsystem. In fabricating command subsystem hardware, STL employed welded modules, a reliable technique that has also proven to be very efficient in volume utilization.

### THE ELECTRIC POWER SUBSYSTEM

Once it leaves the Earth far behind, the Pioneer spacecraft is in full sunlight. The spacecraft can then convert solar energy into electricity to operate its scientific instruments and also to drive the subsystems that enable the vehicle to survive in outer space and maintain a communication link with the Earth. Without power, there can be no deep space mission. Only the conversion of solar energy into electromagnetic waves of a specific frequency makes the Pioneer stand out against the background of stars, planets, and other radio emitters on the celestial sphere.

The power picture is more complicated, however. A basic program ground rule states that the spacecraft must be flexible enough to operate between 0.8 and 1.2 AU without modification. Also, for purposes of acquisition, the spacecraft must be operable prior to escaping the Earth and breaking into full perpetual sunlight. The Pioneer shadow problem is a one-time affair, not repeating every few hours like that of an Earth satellite. Yet, the problem can be solved in the same way—with a battery serving as a reservoir of energy. In a satellite the battery is discharged and charged through several cycles each day; but with Pioneer, the battery becomes largely excess baggage once the Earth's shadow is traversed. Even in full sunlight, however, the spacecraft depends upon the battery for an assist in meeting sudden, brief surges in power demands during normal operation, due in particular to pneumatic valve pulses and, on Pioneers 6 and 7, the MIT experiment (fig. 4-15). The solar-cell array keeps the battery charged at a low level for this purpose.

The total electric power subsystem consists of (1) the solar array, the only source of new energy after launch; (2) the battery, which acts as a temporary source of power during the shadow period and as a reservoir to supply peak demands in space; (3) converters that change bus power into the voltages and current levels required by the TWTs and other spacecraft equipments;<sup>11</sup> (4) current and voltage sensors and protective devices; and (5) power switching and distribution equipment. The block diagram

<sup>11</sup> Individual experiments are supplied with converters to convert bus power to meet their specific requirements.

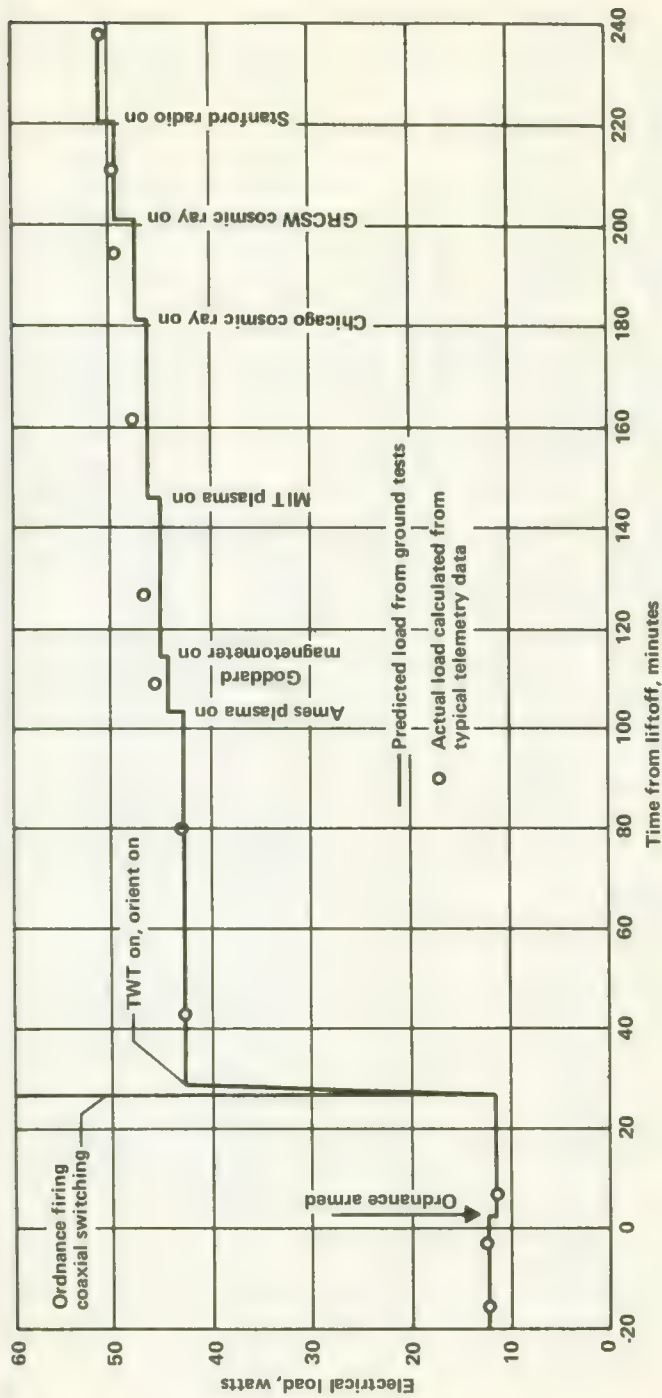


FIGURE 4-15.—Pioneer-6 power profile during the first 4 hr of flight. Superimposed upon the average power level are peak values up to 10 W from the MIT experiment and 7 and 8 W from the pneumatic valve solenoid in the orientation subsystem.

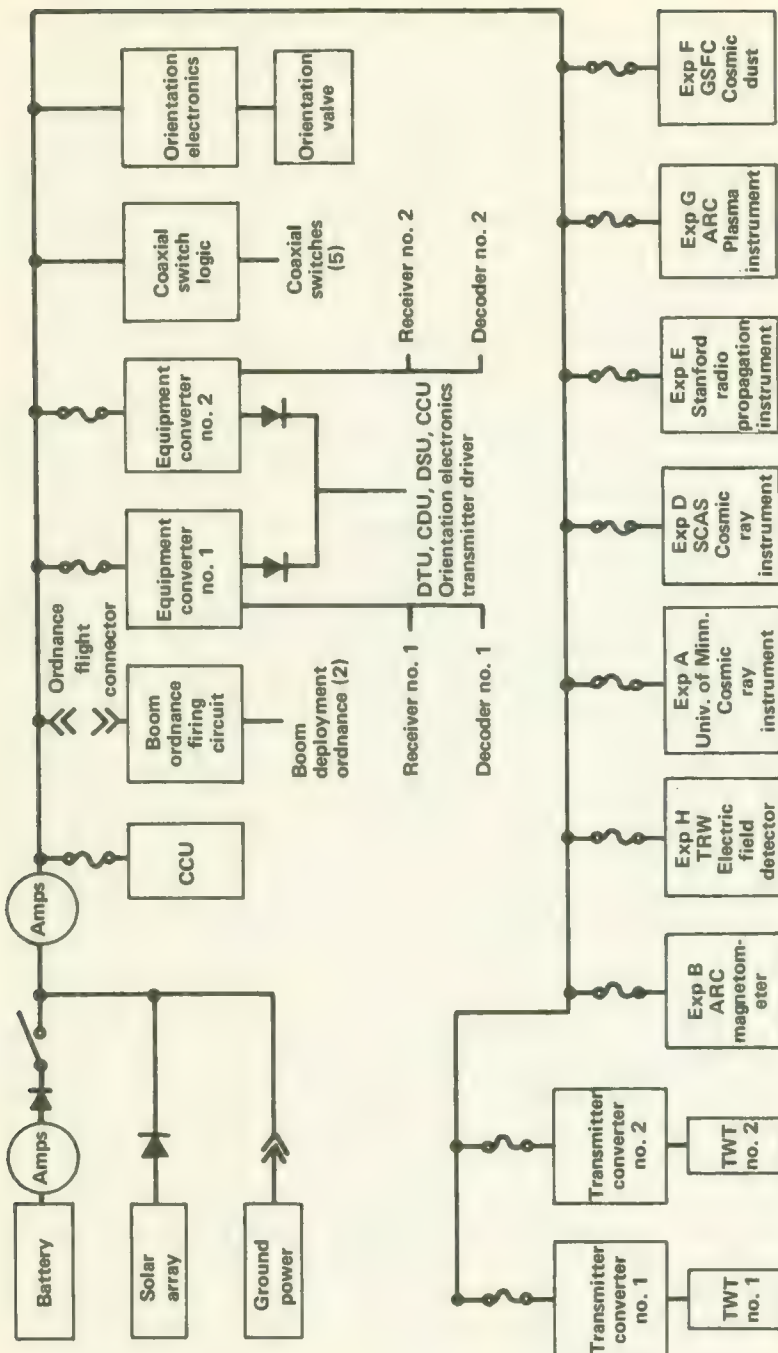


FIGURE 4-16.—Functional diagram of the Pioneer-9 electric power subsystem.

in figure 4-16 reflects the complexity added by items (3), (4), and (5); the power-conditioning, power-distribution, and protective equipment.

### The Electric Power Subsystem Interfaces

The preceding sections have dealt almost exclusively with electromagnetic and information interfaces—those associated with the brain and nervous system of the Pioneer man-machine system. In a biological analogy, the power subsystem must represent the heart and blood vessels of the spacecraft. Subsystems are completely dependent upon electrical power to do things, even the pyrotechnic stored-energy devices that effect boom deployment are detonated electrically. To illustrate the close relationship between action and power on Pioneer, one has only to examine the STL feasibility study and proposal. Early in the program, the CDU was considered part of the power subsystem rather than the command subsystem, because of the relationships between commands, energy, and physical action. The CDU was later consigned to the command subsystem because in reality it is a complicated control valve that permits pulses of power to flow to command-selected spacecraft equipment. The pulses, in turn, operate switches and fire ordnance. Thus, pulses of power animate the spacecraft while the steady bus power keeps the vital functions going.

Other interfaces are more straightforward. Because the power subsystem must sustain the spacecraft electrical load continuously and cannot depend upon the battery for anything but short bursts of power, the solar array must be kept directed toward the Sun as accurately as possible. Thus, the power subsystem imposes on the orientation subsystem the requirement that the spin axis be perpendicular to the Sun line within  $2^\circ$ . The shadowing or solid-angle interface with the spacecraft booms is the cause for the solar-cell-viewing band or bellyband around the girth of the cylindrical portion of the spacecraft. A thermal radiation interface exists between the solar array and the exhaust plume of the solid rocket motor comprising the final stage of the Delta launch vehicle. The plume fans out behind the motor to such an extent in a vacuum that the solar cells can obliquely "see" the hot gases. The thermal radiation can be particularly serious when the exhaust carries metal particles, as it does with newer high performance solid fuels. Fortunately, the solar cells on Pioneer were not compromised by the thermal plume.

The solar cells also interface directly with the solar electromagnetic and particulate radiation as well as the micrometeoroid flux prevailing between 0.8 and 1.2 AU. Solar thermal radiation raises the cell temperatures as the spacecraft swings in toward the Sun; this results in a drop of energy-conversion efficiency. The particulate radiation and hard electromagnetic radiation emitted by the Sun can damage the cells over a long period of

time. Glass covers are applied to reduce this effect. Figure 4-17 illustrates two of these considerations:

- (1) If the spacecraft ventures closer than 0.8 AU to the Sun, the solar array becomes "voltage-limited." Increases in solar power are more than offset by voltage losses due to overheating. Outward from 0.8 AU, the power subsystem is power-limited by the dwindling solar flux.
- (2) The predicted useful power generated drops about 10 W between 6 months and 3 years due to radiation damage of the solar cells.

Pioneer 9, an inward Pioneer, could not operate at 1.2 AU due to increased loads over the nominal Pioneer. The increases in electrical load came primarily from the instruments and the convolutional coder.

These interface forces obviously play a leading role in power subsystem design.

### The Design Approach

Flexibility and reliability were two critical design goals. Flexibility applied not only to the spacecraft's capacity to handle various scientific payloads, but also the ability to operate between 0.8 and 1.2 AU without the basic spacecraft design's being altered. The problem of the scientific instruments' differing from spacecraft to spacecraft was handled by the provision of a convenient bus voltage and placement of the burden of making further modifications upon experiment power converters.

By design, the bus voltage varied with distance from the Sun (fig. 4-17). The entire Pioneer power subsystem "floated" at a voltage determined by the solar-cell temperature. The spacecraft was overpowered intentionally on inward missions. The battery was provided with taps at lower voltages for use during the inward missions. Enough solar cells were added to the nominal spacecraft that it could operate at 1.2 AU; thus there were too many at 0.8 AU.

The pursuit of high subsystem reliability led to extensive paralleling or cross-strapping of critical components. The TWTs are fed by separate, independent converters, but much of the remainder of the spacecraft equipment receives power from two cross-strapped converters (fig. 4-16). Redundancy in the solar-cell array groups the 10 368 cells into 48 strings, each consisting of 216 cells. Each string is a series-parallel arrangement of four parallel groups of 54 cells in series. Fortunately, the Pioneer cells do not undergo the repetitive thermal cycling characteristic of cells on Earth satellites. Yet, one may expect a certain number of failures due to long-term thermal cycling as the spacecraft approaches and recedes from the Sun. The blocking diodes (needed to prevent cells on the sunlit side from sending current through those on the dark side) are also fallible elements. The impact of micrometeoroids—of large concern during the early days of the space effort—assumes negligible importance away from Earth. With

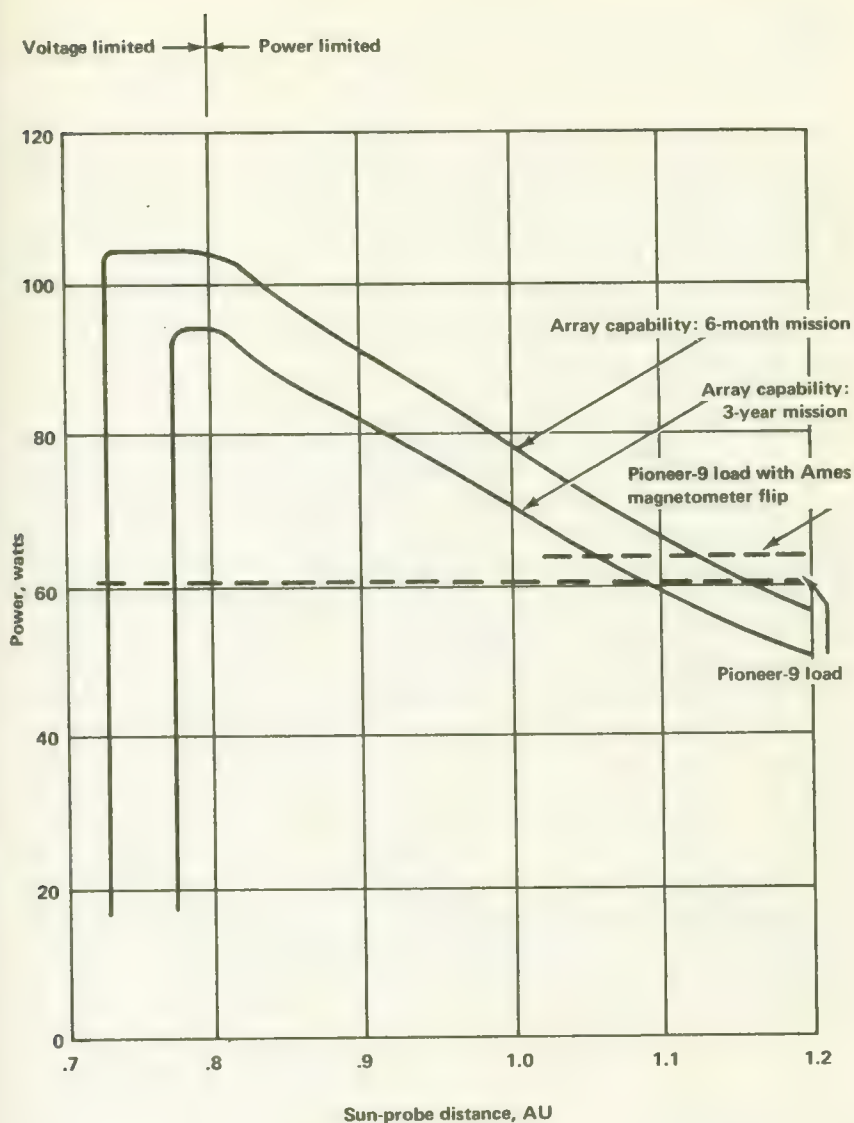


FIGURE 4-17.—Solar array power output vs. distance from the Sun, showing inverse-square-law and cell-heating effects.

these factors in mind, STL computed the reliability for the entire power subsystem to be a very high 0.9963 for a 6-month lifetime (fig. 3-1).

### Pioneer Power Budgets

Power requirements changed slightly from mission to mission. The largest change took place between the Pioneer 8 and 9 missions, when the convolutional coder was added and the Goddard magnetometer was replaced by one from Ames. These changes are summarized in table 4-15; these are, of course, average power levels, and the switching among the many spacecraft and experiment modes always created a varying power profile (fig. 4-15).

### The Solar Array

The Pioneer solar cell is a high efficiency, solderless, n-on-p type, with 1 to 3 ohm-cm base resistivity. Each cell is  $1 \times 2$  cm and is covered by a 0.15-mm glass slide for radiation protection. Early in the program, the average cell efficiency target was 12 percent; this was never achieved and the cells on the spacecraft averaged about 10.5 percent. Both suppliers, RCA and Texas Instruments, had considerable difficulty manufacturing cells to the demanding Pioneer specifications.

The individual cells were fabricated into two types of modules. In the first type, 12 cells were interconnected so that 3 were in series and 4 in parallel; in the second, there were 6 in series and 4 in parallel (figs. 4-18 and 4-19). A close look at figure 4-19 seems to show the cells "shingled" together along the long edges according to conventional practice. Actually each cell is soldered to metal connectors; this makes the modules both self-supporting and flexible. It was this flexibility that allowed the modules to be affixed with silicone rubber adhesive to a curved substrate conforming to the cylindrical spacecraft surface. The rather awkward faceted construction comprised of many small flat solar-cell modules originally proposed

TABLE 4-15.—*Pioneer Power Budgets*

| Average<br>electrical loads (W)      | Pioneer spacecraft |      |      |       |       |
|--------------------------------------|--------------------|------|------|-------|-------|
|                                      | 6                  | 7    | 8    | 9     | E     |
| Spacecraft system <sup>a</sup> ..... | 43.4               | 43.6 | 43.1 | 43.66 | 41.86 |
| Experiments.....                     | 9.2                | 8.2  | 12.3 | 17.57 | 17.80 |
| Total.....                           | 52.6               | 51.8 | 55.4 | 61.23 | 59.66 |

<sup>a</sup> Includes 30 W for the TWTs.

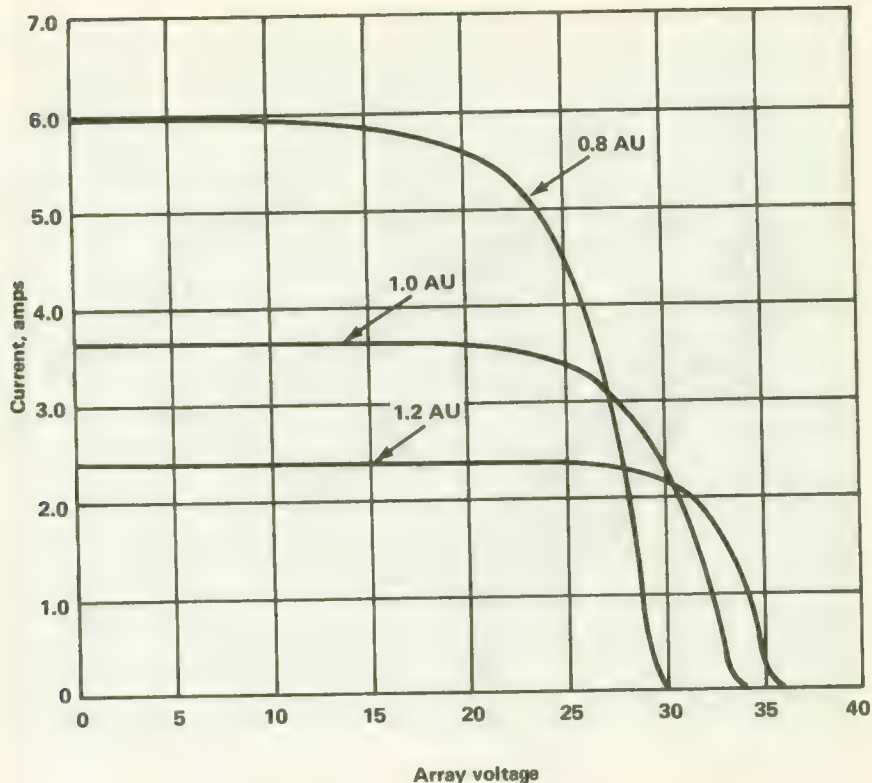


FIGURE 4-18.—Pioneer solar array output characteristics.

was thus eliminated. The self-supporting property did away with the usual module substrate (assumed in the STL proposal), reducing solar-cell-array weight. Instead, the modules were bonded to fiberglass face sheets separated by and bonded to an aluminum honeycomb core. The large curved panels created in this way were then attached to the spacecraft structure. These advances in array design and fabrication cut the array weight from 30 to 15 pounds.

Each of the 48 solar-cell strings was made from interconnected modules and a blocking diode. The diodes, in effect, permit power to flow out of, but not into, the strings. The strings cover a total area of 22.8 ft<sup>2</sup>; essentially this is all of the spacecraft's cylindrical surface except for the 7.5-inch viewing band—the locus of the heaviest boom shadowing. Solar cells along the edge of the bellyband are provided with shunt diodes arranged so that, even if they are shadowed, other cells in the string can still provide useful power to the spacecraft. The capability of the solar array is summarized in table 4-16.

The solar-cell strings are paralleled and attached to the bus feeding the

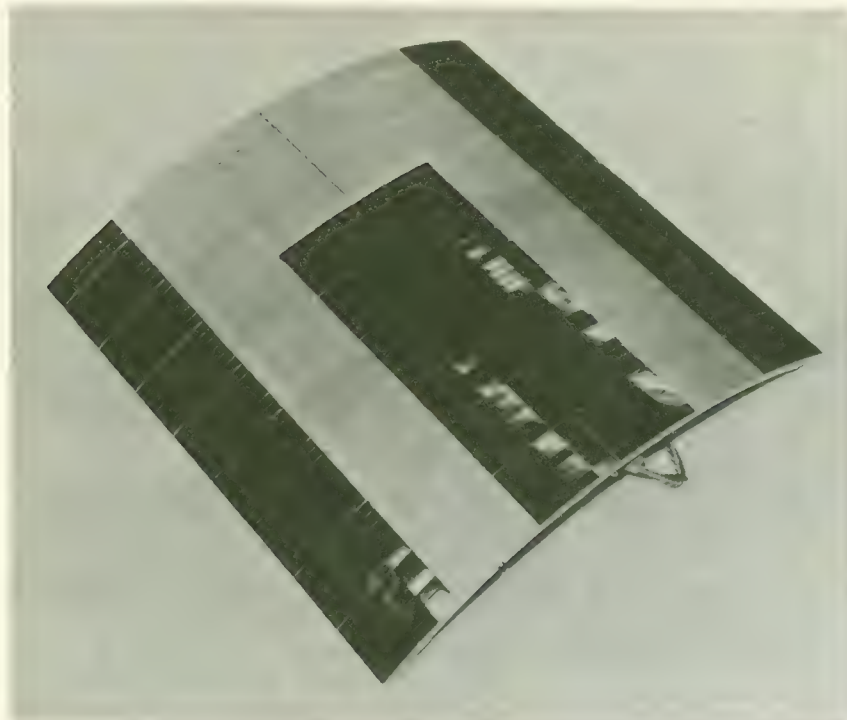


FIGURE 4-19.—One of the Pioneer solar panels, showing both 12- and 24-cell modules mounted on a curved substrate. (Courtesy of TRW Systems.)

spacecraft equipment and experiments. The bus voltage "floats" at the solar-cell array voltage. NASA specifications restricted the voltage swing of this bus to  $28 \pm 4$  volts for any load between 15.3 and 55.6 W in interplanetary space between 0.8 and 1.2 AU over the nominal lifetime of 6 months. These specifications were met satisfactorily.

### The Battery

A Pioneer is completely dependent upon its battery from the time ground power is severed on the launch pad until the fairing is jettisoned, and while the spacecraft is in the shadow cast by the Earth. During the latter period, the battery must supply about 12 W. After orientation, at the discretion of the mission controller back on Earth, the battery is left connected across the bus bar dominated by the solar-cell array voltage. The mission controller disconnects the battery by command if it begins to compromise the mission for some reason. Normally, the battery is left on for 6 to 12 months to accommodate any temporary power shortages or overloads. No power shortages have been known to occur in practice.

TABLE 4-16.—*Solar Array Capability*

|                                  |  |
|----------------------------------|--|
| Type of cell.....                | n/p  |
| Efficiency of bare cell.....     | 10.7 percent min.  |
| Cell internal resistance.....    | 0.46 ohm/cell  |
| Array configuration.....         | 48 strings in parallel (each string: 4 parallel, 54 series cells; total cells/array: 10 368) |
| Assembly losses.....             | 1 percent  |
| Glass losses.....                | 5.4 percent  |
| Losses due to proton damage..... | 0  |
| Diode losses.....                | 1.0 V max.   |
| Temperatures.....                | +116° F at 0.8 AU<br>+52° F at 1.0 AU<br>+4° F at 1.2 AU                                     |
| Range                            |  |
| Calc min.<br>net power           | 0.8 AU      1.0 AU      1.2 AU   |
| Bus volts.....                   | 24 25 26 24 26 27 29 27 28 29 30   |
| Watts.....                       | 103 89.5 63 79.6 81.4 79.7 62.3 59.7 60.5 60.6 57.3  |

Typical peak loads include instrument-power peaks, fault clearing, coaxial-switch operation, and pneumatic-valve operation. The battery is eventually disconnected when its age begins to make it a poor risk, sometimes as late as 18 months after launch.

Originally, a non-rechargeable battery was proposed for the spacecraft, but a study of the MIT plasma probe power requirements showed the need for a rechargeable battery that could meet the experiments' peak demands.

The battery finally chosen for Pioneer was of the sealed, silver-zinc type, which lends itself well to operation in the floating mode. The sealed case was made from fiberglass, a non-magnetic material. As already mentioned, the battery can be wired for inward and outward missions. Although it was built with 18 cells, taps were provided at 16, 17, and 18 cells, for the sake of mission flexibility. On the Block-I spacecraft, the usable battery capacity was about 1 A-h; on Block-II, it was increased to roughly 2 A-h. During normal mission operation, the battery was recharged only when the solar-cell-array voltage exceeded the battery voltage. However, the blocking diodes in the solar-cell array prevent battery current from flowing through the cells should the array voltage drop below that of the battery. In the event of a transient demand for more power than the solar cells can provide, the bus voltage drops until the battery level takes over. No battery charge-control devices exist on Pioneer, but the battery usually remained only partially charged. Battery volume was 44 in.<sup>3</sup>; weight, 2 lb; reliability, 0.99975 for 6 months' operation between 40° F and 80° F.

### The Converters

Three classes of power converters transform bus power into usable form for: (1) the TWTs, (2) the scientific instruments, and (3) the rest of the spacecraft equipment.

Each TWT has its individual converter. The TWT converters are similar to those used for the spacecraft equipment except for special output voltages, including 1000 V for the TWTs. The 1000-V line also must be regulated rather precisely:  $\pm 0.5$  percent over the  $28 \frac{+5}{-4}$  voltage swing of the bus bar. The TWT converters may be commanded on and off separately; but the switching logic is such that the TWTs cannot operate simultaneously. Furthermore, if the bus voltage falls below 23.5 V for more than 0.4 sec, an undervoltage command automatically shuts the TWTs off to preclude defocusing them or burning them out. Removal of the TWT load of approximately 30 W causes an immediate rise in bus voltage under normal operating conditions. Minimum efficiency specified for the TWT converters was 80 percent. Each converter weighs 2.35 lb and has a volume of 64.12 in.<sup>3</sup>.

As mentioned earlier, each scientific instrument possesses its own converter tied directly to the bus. All experiments are turned off simultaneously via a ground command or an undervoltage condition, but they may be turned on one at a time. Simultaneous turn-off permits quick diversion of power to spacecraft equipment in the event of an emergency. The instruments are also turned off by the same automatic undervoltage command that shuts down the TWTs.

The two equipment converters are packaged together, weigh 3.2 lb, and occupy a volume of 111.3 in.<sup>3</sup>. The units are identical, but their outputs are partially cross-strapped. Converter no. 1 supplies receiver no. 1 and decoder no. 1, while converter no. 2 provides power for receiver no. 2 and decoder no. 2; these power taps are not cross-strapped. All other outputs are cross-strapped and supply the CDU, DTU, DSU, the orientation subsystem, the transmitter driver, and the signal conditioner. The individual converters are fused separately and may thus be automatically removed from the circuit in the event of a short or some other fault that draws high current. However, the equipment converters cannot be turned on and off from the ground. The reason for this restriction is obvious; if both were turned off inadvertently, the spacecraft would be dead; without receivers it would no longer respond to commands.

### Power Control and Distribution

Power distribution within the spacecraft is commandable and automatic, with some provision for commandable override of the automatic. The solid-state logic for all power switching, and the switches themselves reside

in the CDU (fig. 4-14). The power-distribution portion of the CDU is illustrated in figure 4-20. Tables 4-13 and 4-14 show a large number of on-off commands that are really power-on/power-off commands that connect or remove components from the power source. With command 107, the mission controller can override the automatic undervoltage switch that disconnects the TWTs and experiments. Command 000, labelled "undervoltage simulate," is used if the TWTs and experiments must be disconnected all at once. Command 000 is then OR-gated with the undervoltage signal (which has not yet disabled the TWTs and experiments because the voltage is still within bounds), and the TWTs and experiments are turned off. Command 107 may also be employed to lock out command 000.

The undervoltage control senses the bus voltage from a voltage divider with a half-volt resolution. The trip point is adjustable and is usually set for 23.5 V. To prevent the inadvertent shutdown of the TWTs and experiments due to transients, the undervoltage control has a half-second time constant. Like all electronic circuits, the undervoltage control is fallible and might fail in a way that would shut down the spacecraft. The undervoltage override command was introduced primarily to prevent such an occurrence.

A number of current and voltage monitors report the operational condition of the electric-power subsystem to the mission controller back on Earth. These are listed in tables 4-9 and 4-10 with the other housekeeping telemetry words.

## THE ORIENTATION SUBSYSTEM

Only a small, spin-stabilized spacecraft could meet the cost, reliability, and launch-vehicle constraints of the Pioneer. For maximum utility, the Pioneers had to be oriented after launch so that their spin axes were perpendicular to the plane of the ecliptic. Only in this orientation would:

- (1) The scientific instruments be able to scan along the plane of the ecliptic
- (2) The disk-shaped antenna beam intercept the Earth, permitting greater communication range
- (3) The solar array power be maximized, eliminating the necessity of cumbersome, failure-prone solar paddles
- (4) The spacecraft's thermal control subsystem be able to radiate waste heat out the bottom of the spacecraft away from the Sun into cold space easily

The success of the Pioneer mission depended completely upon twisting the spacecraft's spin axis around after injection until its high-gain antenna pointed within 2° of the north ecliptic pole. The same orientation equipment performing this maneuver could also be used later in the mission to

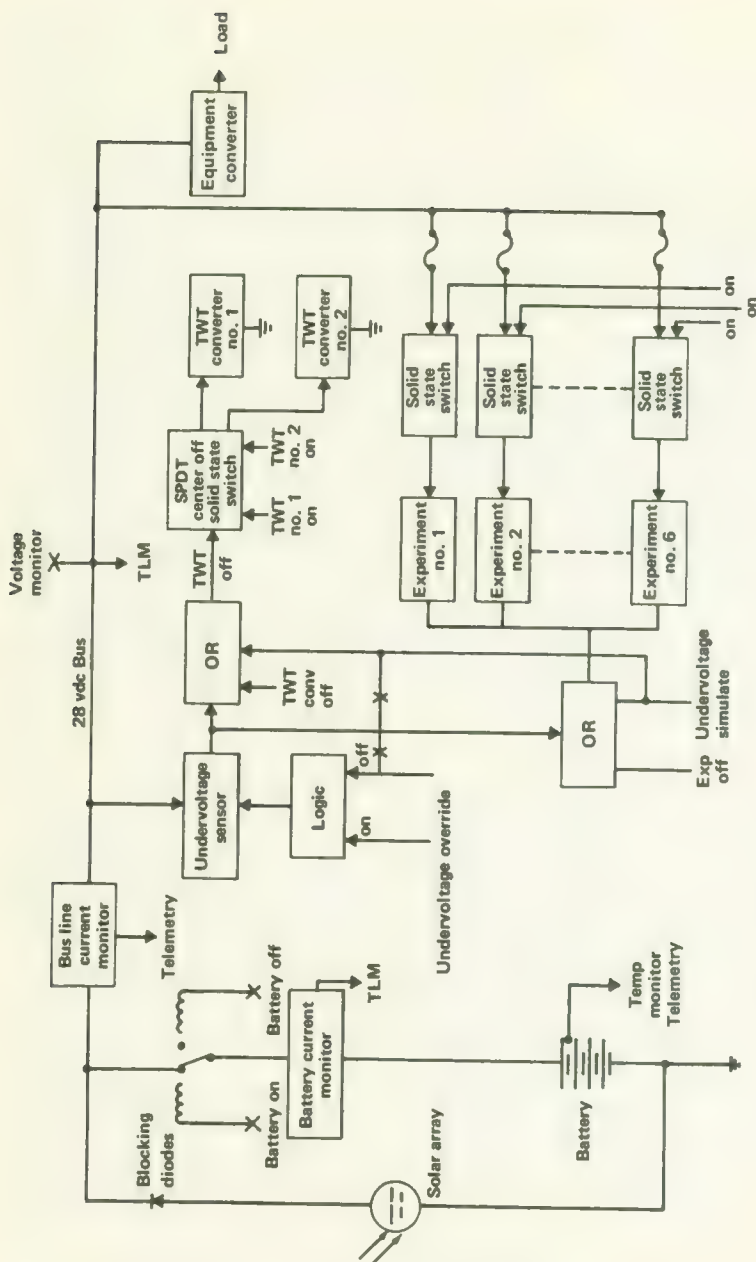


FIGURE 4-20.—A portion of the CDU showing how spacecraft power is controlled.

adjust spacecraft orientation if the axis drifted out of the  $90^\circ \pm 2^\circ$  attitude with respect to the plane of the ecliptic.

The most important components needed in such an orientation maneuver are: (1) a device to torque the angular momentum vector of the spacecraft, (2) sensors to control the direction of axis motion, (3) sensors to signal the status and, hopefully, the success of the orientation maneuver, and (4) a nutation wobble damper to dissipate nutation energy induced during the orientation. The small solar sail added at the tip of the high-gain antenna mast to offset any residual torque due to solar pressure<sup>12</sup> was not part of the original design.

The components will be covered in more detail later; first the orientation concept will be sketched out completely. After the spacecraft is injected into the plane of the ecliptic, two pairs of Sun sensors determine the attitude of the spacecraft with respect to a line joining Sun and spacecraft. The Type-I orientation maneuver commences automatically. The Sun sensors cause the nitrogen gas jet to fire and torque the spacecraft spin axis through the smallest angle until it is perpendicular (within  $\pm 0.5$  percent) to the spacecraft-Sun line.<sup>13</sup> At this point, thermal control is possible and the solar array generates full power. The Type-II orientation is commanded from the ground and is controlled by monitoring the strength of the spacecraft transmitter's signal strength. When it is maximized, the Pioneer spin axis is also perpendicular to the spacecraft-Earth line; the desired accuracy is  $\pm 1.0$  percent. If the spacecraft is perpendicular to both the spacecraft-Sun and spacecraft-Earth lines, it is also approximately perpendicular to the plane of the ecliptic. Orientation is now complete. Spin-axis orientation is maintained through spin stabilization at roughly 60 rpm (ref. 4).

Pioneer Specification A-6669 stipulated the performance of the orientation subsystem more precisely:

- (1) It had to function properly whenever the angle between the spacecraft spin axis and spacecraft-Sun line was  $10^\circ$  or greater.
- (2) It had to orient the spin axis to  $90^\circ \pm 1^\circ$  (changed later to  $90^\circ \pm 2^\circ$ ) from the spacecraft-Sun line.
- (3) It had to be able to turn the spin axis around the spacecraft-Sun line for up to 90 days after the orientation maneuvers.
- (4) It had to provide enough gas to turn the spin axis a total of  $225^\circ$ .
- (5) It had to provide a Sun reference pulse and indicate the orientation relative to the spacecraft-Sun line with a jitter of less than  $0.3^\circ$ .
- (6) It could not be deceived by sources of light other than the Sun.

<sup>12</sup> A net solar torque exists only when the center of pressure does not coincide with the center of mass. The addition of the Stanford antenna was the most significant change introducing asymmetry. The solar sail, of course, had nothing to do with the orientation maneuvers.

<sup>13</sup> The basic orientation concept was first proposed by T. G. Windeknecht in 1961 (ref. 3).

### The Sun Sensors

The sensitive elements of the Sun sensors were quad-redundant, photo-sensitive silicon-controlled rectifier (PSCR) chips, manufactured by Solid State Products, Inc. The chips were developed especially for the Pioneer Program. They delivered a signal to the orientation-control circuitry whenever the Sun was in view. However, the view of each Sun sensor was restricted by aluminum shades (fig. 4-21). On Pioneers 6 and 7 the light-sensitive chips were protected against space radiation damage by 20-mil quartz covers. Several months after launch, however, it was discovered that the Sun-sensor thresholds had changed. Laboratory testing implied that radiation damage was the primary cause, and the quartz covers on Pioneer 8 were made 100 mils thick. The trouble persisted. The real problem was discovered inadvertently at TRW Systems when the sensors were tested under ultraviolet light to see if it degraded the adhesives used in sensor construction. During these tests, it was discovered that the sensors were ultraviolet-sensitive. In space, the ultraviolet light from the Sun had caused the change in the sensor thresholds. Simple ultraviolet filters were added to 60-mil quartz covers; this cured the situation on Pioneers 9 and E.

The five Pioneer Sun sensors are mounted on the spacecraft with the fields of view specified in figure 4-22. Sensors A and C, located on the spacecraft bellyband, looking up and down respectively, help position the spacecraft during the Type-I orientation. As long as the spin axis does not point within  $10^\circ$  of the Sun, except for a small overlap of the field of view, sensors A and C will see the Sun once each revolution as the spacecraft spins. The Type-I orientation proceeds as sensor A or C, whichever one is illuminated, stimulates a succession of gas pulses from the jet on the end of the orientation boom. Each pulse lasts for  $45^\circ$  of spacecraft rotation and torques the spin axis around about  $0.15^\circ$  in the direction of the smallest angular displacement toward maneuver completion. The pulses cease when the other sensor finally sees the Sun. When both sensors see the Sun at the same time, the spin axis will be perpendicular to the spacecraft-Sun line within about  $\pm 0.5^\circ$ . The original design of the orientation subsystem provided a deadband, rather than overlapping fields of view for sensors A and C. Presumably, the gas pulses would cease when neither sensor saw the Sun. Analog simulation, however, demonstrated that this arrangement was unstable, due mainly to the presence of residual wobble. The simple changes in logic and sensor fields of view solved the problem.

The Type-II orientation employs sensors B and D, also located on the spacecraft bellyband, but with  $20^\circ$  fields of view centered on the spacecraft meridian plane. These sensors do not exercise complete control over the gas pulses that torque the spin axis during Type-II orientations; they only time the pulses. Sensor B, for example, triggers the gas pulse at just the right time for clockwise rotation of the spin axis around the spacecraft-Sun



FIGURE 4-21.—The Pioneer Sun sensors: A or C (top); B or D (middle); and E (bottom).

line. (Note that through Type-I orientation, the spacecraft is already in a position perpendicular to the spacecraft-Sun line; it retains this attitude during Type-II orientation.) Sensor D times the gas pulses for counter-clockwise torquing of the spin axis. Thus, sensors B and D control the direction and pulse duration but not the extent of the rotation about the spacecraft-Sun line.

The magnitude of the angle of rotation is determined solely by carrier strength of the spacecraft at a DSN station (usually Goldstone); when the

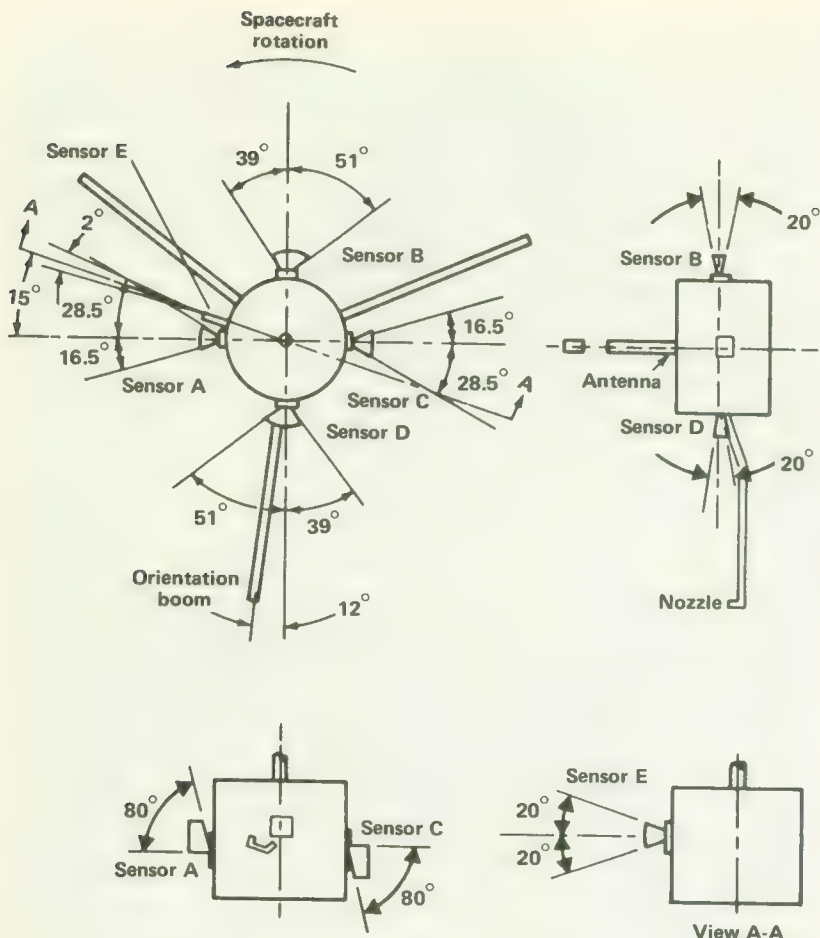


FIGURE 4-22.—Sun-sensor locations and fields of view.

carrier strength is "loudest" (after taking the spacecraft's inclination to the plane of the ecliptic into account), Type-II orientation is complete. During this maneuver, the side lobes of the spacecraft antenna pattern (fig. 4-4) give the mission controller clues about the spacecraft attitude. In practice the maximum is usually overshot a few degrees intentionally to insure that a true maximum has been found and to help calibrate the effectiveness of the gas pulses. Backtracking to the maximum then occurs. (The potential for success of this maneuver was a controversial subject early in the program.) The DSN station senses the relative orientation of the spacecraft antenna mast and then sends signals initiating gas pulses. The seat of control is on the spacecraft during Type-I orientation and at the DSN station during Type-II orientation.

Sensor E establishes the reference position of the spacecraft with respect to the Sun and sends signals to the scientific experiments. Sensor E is also mounted on the viewing band of the spacecraft. It possesses only a 2° field of view that provides short, sharp pulses, as it sees the Sun roughly once each second. Because the field of view is only 40° in the other direction (fig. 4-22), Sun pulses appear only when the spin axis is within 20° of being perpendicular to the spacecraft-Sun line. The appearance of Sun pulses also indicates that the Type-I orientation is proceeding successfully and near its end.

### The Pneumatics Assembly

Short bursts of cold nitrogen gas from the pneumatics assembly change the spacecraft angular-momentum vector. Gyroscopes, hot-gas jets, small pyrotechnic devices, and miniature rockets have all been used on Earth satellites for purposes of attitude control. The cold-gas system chosen for Pioneer is simple and extremely reliable. It had already been well proven on other space missions when Pioneer was being designed.

The pneumatic assembly is a titanium alloy pressure vessel containing about 0.9 lb of nitrogen at 3250 psi (fig. 4-23), a pressure regulator, a solenoid valve, a pressure switch, and a nozzle. The nitrogen had to be very dry to preclude the valve's icing at low temperatures. An electrical signal opens the solenoid valve for a moment, releasing a burst of gas at about 50 psi which provides the desired impulse. The solenoid valve and nozzle are located on the end of a 62-in. boom to increase the angular impulse and isolate the iron core in the valve solenoid from the magnetometer (fig. 4-24). Originally the nozzle was on the tip of the high-gain-antenna mast, but it was displaced by the magnetometer during the evolution of the spacecraft. Finally, both were placed on booms.

Simple as the pneumatic assembly is, it was the source of concern on Pioneers 6 and 7. Although the basic missions were not compromised, gas leaks did reduce the amount of spin-axis torquing possible. After a study of the declining gas supply on Pioneer 6 and simulations of the failure in the laboratory, a tuning fork spring was installed under the pressure-vessel regular assembly to cushion it against the shock and vibration of the launch. The problem persisted on Pioneer 7, though greatly reduced in magnitude, and pressure-system seals were tightened beyond the supplier's recommendations on subsequent spacecraft. No important leaks occurred on Pioneers 8 and 9.

### Orientation Subsystem Electronics

The function of the orientation subsystem electronics is to deliver the pulses that activate the solenoid valve upon signal from the Sun sensors and command from the Earth. The electronic block diagram is shown in figure 4-25.

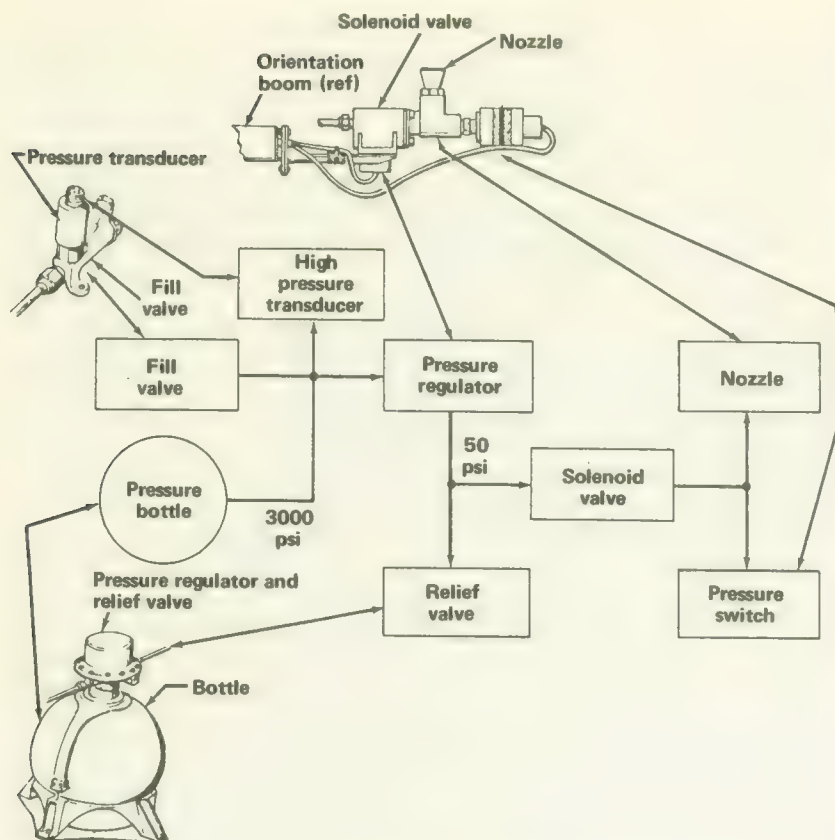


FIGURE 4-23.—Components and block diagram of Pioneer pneumatic equipment.

Whenever the orientation subsystem electronics are switched on by terrestrial command, a Type-I orientation is automatically set into motion. The first Type-I orientation, however, begins automatically when any one of the booms is properly deployed and locked into position, closing a microswitch. In other words, the first Type-I orientation transpires without ground command and without intervention from any other spacecraft subsystem—it is that important a maneuver. The pneumatic valve is pulsed until Sun sensors A and C are both illuminated. A subsequent Type-I orientation begins whenever the electronics are turned on and always precedes a Type-II orientation. But, once the electronics are on, Type-II commands can be given indefinitely.

During a Type-II orientation, a command from the Earth enables either sensor B or D to signal a respective clockwise or counterclockwise angular impulse. The Sun sensor provides only the precise timing necessary; the

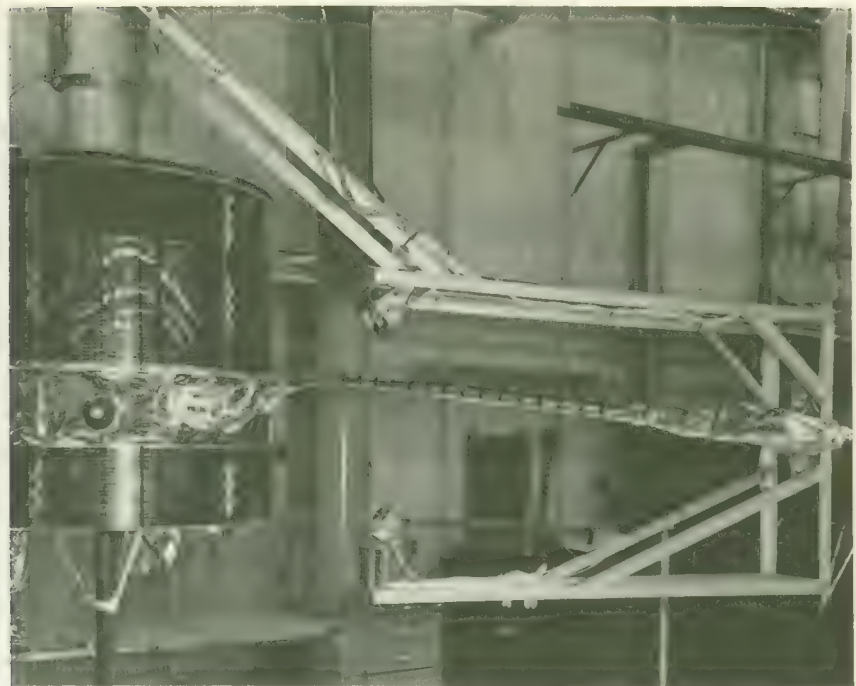


FIGURE 4-24.—The Pioneer orientation boom, shown on Pioneer C during thermal-vacuum test. (Spacecraft is upside down.)

terrestrial command starts the chain of events leading up to the gas pulse. A command from Earth is needed for each Type-II gas pulse; there may be hundreds during a complete maneuver.

### The Wobble Damper

Spin-axis nutation may result from the orientation maneuver, from injection and third-stage separation forces, or possibly from an external cause, such as a meteoroid impact (an unlikely event). If the wobble is excessive, it can compromise the scientific experiments and interfere with the Type-I orientation maneuver. A Type-I orientation maneuver usually begins before the wobble damper can remove all of the wobble. The maneuver proceeds until Sun sensors A and C both are illumined. Suppose that the maneuver is moving along satisfactorily with gas pulses slowly torquing the spin axis into position. If the spacecraft is wobbling excessively, however, the unilluminated Sun sensor (A or C) will see the Sun momentarily during one of the wobbles before it should; the maneuver is then terminated automatically, prior to actual completion. The average

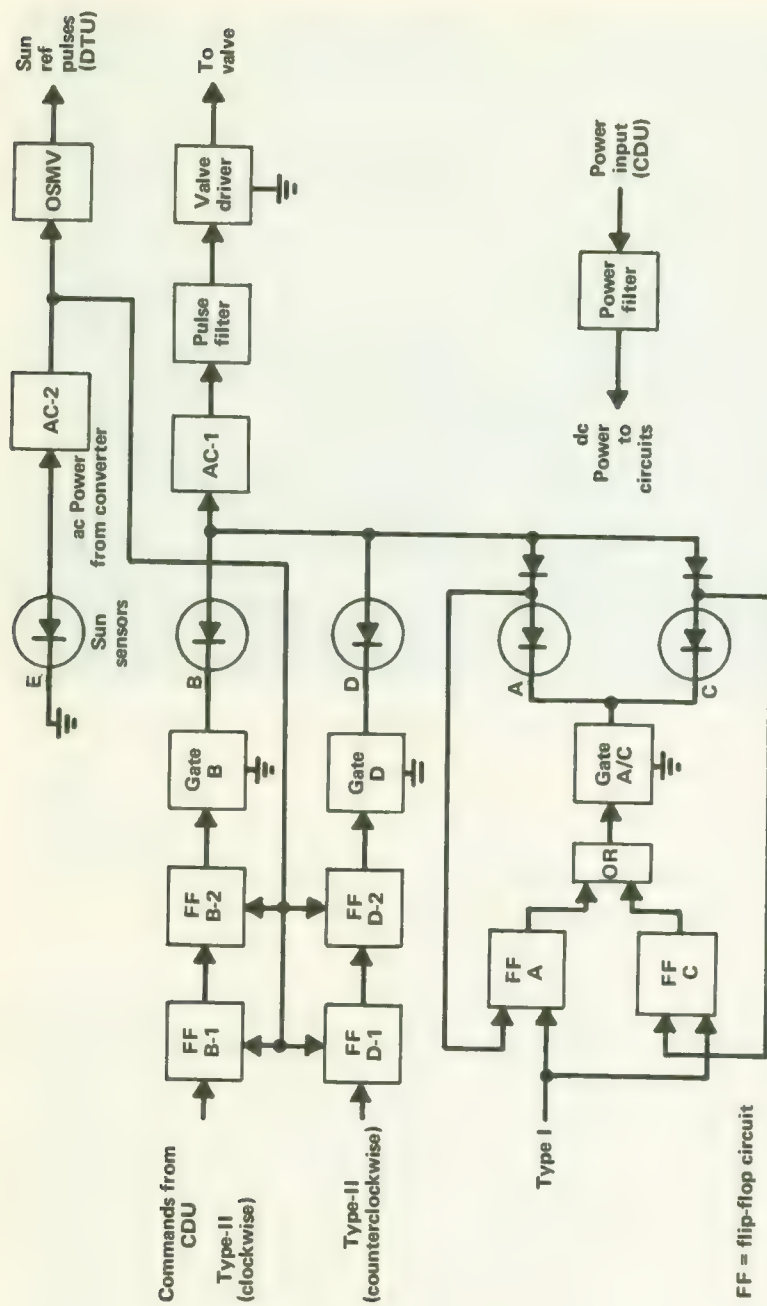


FIGURE 4-25.—Block diagram of the orientation subsystem electronics.

pointing error will equal the peak amplitude of the wobble. Even with a severe wobble, this degree of orientation achieved will probably be sufficient for thermal control and nearly full power production. The spacecraft will be self-sustaining and not dependent upon the battery. Thus there will be time for a wobble damper to suppress the residual wobble. After this occurs, the orientation electronics can be turned on again, automatically initiating another Type-I orientation to trim the spacecraft attitude more finely. In fact, the accuracy of the orientation can be checked by noting whether the gas jet fires upon the initiation of a Type-I maneuver. If nothing happens or if only one pulse is detected, the spacecraft is oriented precisely enough for sensors A and C both to see the Sun.

Most wobble dampers in use on satellites and other spacecraft remove wobble energy by dissipating it as friction-generated heat. On the Pioneer spacecraft, the energy of nutation was dissipated by beryllium-copper balls rolling inside and impacting at the ends of a pair of tubes located at the end of the 62-in. boom. Rolling friction and inelastic collisions at the ends of the tubes extracted the energy of nutation, converting it to heat. Originally, the tubes were to be filled with gas to provide hydrodynamic friction, but it was found that the gas was unnecessary. The damper was built by STL.

### Weight, Reliability, and Power Drain

The entire orientation subsystem weighs only 6.5 lb, including about 0.9 lb of nitrogen. This figure includes almost completely redundant parts (with voting circuits) in the electronics and Sun sensor assemblies. The pneumatic equipment is not redundant, although this was seriously considered early in the program. Even so, the reliability of the entire subsystem was calculated as 0.980 for a 6-month lifetime in space. When the orientation subsystem is in a standby mode (as it is most of the time), it consumes roughly 0.6 W. Maximum power is drawn when the gas valve is firing: about 6.3 W.

## THE THERMAL CONTROL SUBSYSTEM

The task of the thermal-control subsystem is keeping the spacecraft cool enough (under 90° F) on the inward missions and warm enough (over 30° F) on those swinging away from the Sun to 1.2 AU. The solar heat flux varies from 690 to 307 Btu/hr-ft<sup>2</sup> between 0.8 and 1.2 AU; and Pioneer ground rules stipulated that these conditions be handled without spacecraft design changes for inward and outward missions. The internal heat loads also vary as electrical equipment is switched on and off. These load changes are small, however, roughly a swing of 12 W or about 20 percent compared to the greater than 2:1 fluctuation in solar flux.

NASA and STL engineers also had to examine several transient events

or situations that occurred before the spacecraft broke into full sunlight following launch:

(1) The launch-pad environment—the spacecraft-determined air-conditioning requirements had to be examined.

(2) Aerodynamic heating of the shroud during launch and the consequent transfer of heat to the spacecraft—this was controlled by adding thermal insulation (chargeable to spacecraft payload) to the shroud in quantities dependent upon the specific trajectory selected (ch. 7).

(3) Aerodynamic heating of the spacecraft at very high altitudes after shroud ejection—analysis showed that no problem existed here.

(4) Radiant heating of the bottom of the spacecraft by the third-stage rocket plume—the switch to the X-258 third stage, which used aluminum oxide additives in the rocket grain, stimulated concern over excess radiation; a special STL study determined that a thermal shield was needed to block the solar array's view of the plume.<sup>14</sup>

(5) Cooling during eclipse of the Sun by the Earth during ascent—this period, which would last at the most 30 min, would not be long enough to allow the spacecraft to cool excessively. (Actually, the dark side of the Earth contributes considerable thermal radiation to the spacecraft during eclipse.)

In summary, analysis of the transient events from launch pad to solar orbit resulted only in the addition of a radiation shield for the thermal louver actuators and varying amounts of thermal insulation to the shroud. The long cruise around the Sun controlled the major aspects of spacecraft thermal design.

So far, only the thermal control of the spacecraft interior has been mentioned. The solar cells, Sun sensors, antenna mast, and booms must be maintained within operating limits, too. Because they are spacecraft extremities, the thermal control techniques applying to the interior of heat-generating spacecraft may not apply to them.

### Coping With Variability

Passive thermal control, employing no moving parts, would have been the simplest and most reliable approach in the Pioneer program. However, the more than 2:1 variation in solar flux and changing internal heat loads ruled out passive control. To illustrate, a passive thermal control subsystem that provided a 60° F spacecraft interior at the Earth's orbit would have permitted the temperature to rise to 142° F and fall to 40° F at 0.8 and 1.2 AU, respectively. The changing internal loads and varying heat leakage through the solar cells and down the antenna mast swung the

<sup>14</sup> This contract (NAS2-1642) was let July 23, 1963, while the main spacecraft contract was being written. The final report, issued in 1964, was entitled "Study of the Effects of X-258 on Pioneer Spacecraft."

internal heat load by 50 percent at these extreme points in the mission spectrum. Active thermal control was the best solution, even though the addition of moving parts would detract from overall spacecraft reliability.

The whole Pioneer mission concept depended upon the concept of a spin-stabilized spacecraft with a spin axis normal to the plane of the ecliptic. The curved sides of the cylinder receive essentially all solar radiation, while the ends point toward cold space. This situation is ideal for a thermally insulated spacecraft with active thermal control. Insulation around the sides of the structure allows only a small portion of the solar heat load to reach the inside of the spacecraft. Insulation on the top leaves the bottom as the only possible exit for heat (fig. 4-26). This heat leakage, which varies depending on the distance from the Sun, can be radiated out the spacecraft bottom along with the variable internally generated heat load. The variability is handled by changing the effective radiating area of the bottom of the spacecraft. Mechanization of the concept consists of a set of Venetian-blind-like louvers that varies the effective radiating area, increasing it as the internal temperature rises and reducing it when the inside of the spacecraft becomes too cool (fig. 4-27). The setting of the louvers is controlled by bimetallic thermal actuators sensitive to the internal temperature. When the Pioneer program began, STL was also applying this basic concept to the OGO, which, though much larger than Pioneer, was fully stabilized in orbit and had many of the same thermal problems. The louvers used on Pioneer came directly from OGO technology. (STL was also the OGO spacecraft prime contractor.) Other space probes and stabilized Earth satellites have also used the same approach as Pioneer.

The thermal insulation covering the spacecraft sides and top thermally isolate the antenna mast, the booms, the Sun sensors, and the solar array from the volume that is temperature-controlled by the louvers. As we shall see below, the components just listed can tolerate the harsher outside environment. Their temperatures can be regulated adequately by passive thermal coatings applied specifically for conditions anticipated on each mission. In reality, then, two thermal control schemes were applied to the Pioneer spacecraft: active control inside, and passive control for the extremities.

In the discussions of the other Pioneer subsystems, the subject of interfaces, particularly information interfaces, has always been high on the list of priorities. The Pioneer thermal control subsystem, however, cannot be commanded from Earth; it is completely automatic. Temperature readings at various locations around the spacecraft are monitored and telemetered, (table 4-17) but if they prove anomalous the only solution is to disconnect electrical loads. Electrical power is not required by the thermal control subsystem. It is a simple subsystem, but just as critical to mission success as subsystems with thousands of electronic parts. STL engineers believed that

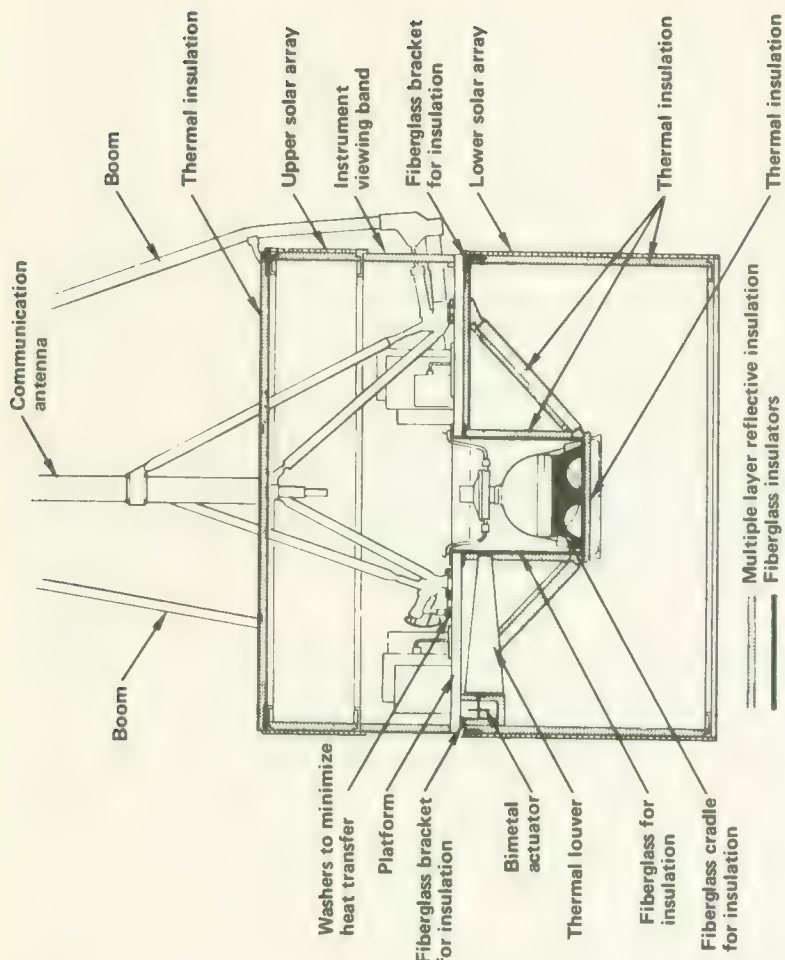


FIGURE 4-26.—Diagram of the components affecting thermal control.

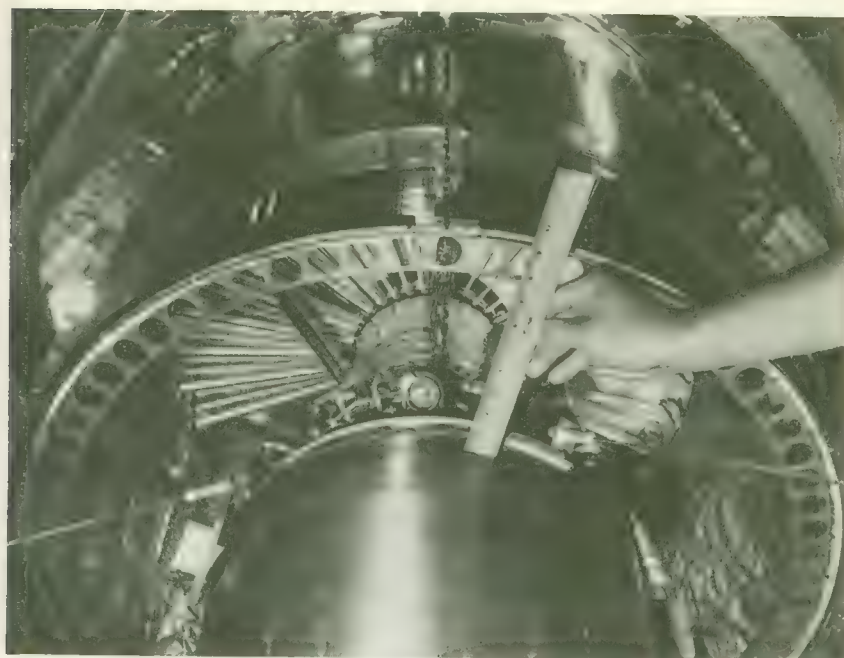


FIGURE 4-27.—Bottom view of the Pioneer spacecraft with the third-stage motor in place. The thermal louvers, covering two-thirds of the equipment platform, are shown in an open position.

the basic spacecraft thus protected could venture between 0.55 and 2.0 AU without thermal control modifications, although contractually they were committed to only 0.8 and 1.2 AU.

#### Spacecraft Thermal Analysis

Spacecraft thermal equilibrium results if the sum of the internally generated heat power and the heat power leaking in through the insulation and the structures that pierce it exactly equals the heat power radiated through the louver assembly. STL used two analytical thermal models in its computations. The first model assumed that the spacecraft was located 1.0 AU from the Sun. The temperatures at various locations within the spacecraft were then computed. In the second model, the spatial temperature distribution computed in the first model was assumed fixed; that is, relative temperatures remained the same, but absolute temperatures would rise or fall (by the same amount) throughout the spacecraft interior. With this greatly simplified model, the effects of distance from the Sun and internal power loads were calculated. The actual analysis was rather involved and cannot be pursued here.

TABLE 4-17.—*Thermal-Sensor Locations*

| Thermal-sensored equipment              | Thermal-sensor location   |
|---|---|
| Receivers 1 and 2                       | On receivers, near voltage-controlled oscillator  |
| TWTs 1 and 2                            | At juncture of mounting screw and platform  |
| TWT converter                           | Exterior of converter top cover   |
| Transmitter driver                      | On platform close to driver   |
| Digital telemetry unit                  | At juncture of mounting screw and platform  |
| Data storage unit                       | At base of data storage unit  |
| Equipment converters 1 and 2            | At base of equipment converter  |
| Battery                                 | Internal to battery   |
| Upper solar panel and lower solar panel | Approximately 30° to right (top view) of orientation boom. Between substrate and insulation (insulated from compartment). |
| Platform 2                              | On platform position 2  |
| Antenna mounting bracket                | Midway on bracket, within compartment   |
| Louver actuator housing                 | Between insulation and housing  |
| Sun sensor A                            | In head of sensor   |
| Platform 1                              | On platform position 1  |
| Nitrogen bottle                         | Epoxied directly to bottle  |
| Sun sensor C                            | In head of sensor   |
| Platform 3                              | On platform position 3  |
| Magnetometer sensor (Ames) 4            | Internal to boom-mounted magnetometer sensor  |
| Magnetometer, electronics (Ames) 4      | Internal to instrument  |
| Plasma, electronics (Ames) 5            | Internal to instrument  |
| Cosmic ray (SCAS) 6                     | Internal to instrument  |
| Cosmic ray (Minn.) 1                    | Internal to instrument  |

Because complex geometry and the manifold heat paths make spacecraft thermal analyses so difficult, it is customary to build a thermal mockup or model of the spacecraft. Heat sources and sinks as well as all significant spacecraft structures are usually simulated physically rather than mathematically. Temperatures are measured and compared with those computed. In the Pioneer analysis STL built a thermal model and simulated space conditions between 0.8 and 1.2 AU using their cryogenic vacuum chambers. Different internal loads and solar fluxes were approximated. Agreement between computations and thermal model measurements was good. Inflight performance has also verified the accuracy of the original analysis.

### Spacecraft Thermal Design

The back of the solar array, the interstage structure, and the top of the spacecraft (fig. 4-27) are all covered with multiple-layer, aluminized-Mylar thermal insulation. All interruptions in the layers of insulation, the places where antenna, boom, and solar-array supports pierce it, are made

high heat impedances with fiberglass mountings to minimize heat leaks into the interior. On the other hand, heat paths from internal components to the bottom of the equipment platform are designed with high conductivity in mind. The spacecraft's instrument platform and the boxes mounted on it were made thermally "black" to encourage temperature equalization. Other "inside" surfaces, such as the top cover and spacecraft sides, were either aluminum or aluminized Mylar. The equipment platform is an aluminum honeycomb panel constructed with the "starved" bonding technique to insure good thermal conductance through it to the radiating surface on the bottom.

The louver system (fig. 4-27) consists of 20 individual louvers, each actuated independently by a spiral-wound, bimetallic spring. Springs are insulated so that they are responsive only to local temperatures. The open radiating area was approximately 3 ft<sup>2</sup>. One-third of the platform area, the portion directly under the magnetometer electronics, does not require thermal louvers. Instead, it is covered with aluminized-Mylar insulation. The louver blades themselves were made highly reflective and specular to infrared radiation to minimize radiation from them back to the equipment platform when they were in the full open position. They are also good thermal insulators, so that when closed they help retain heat within the spacecraft. The bottom of the equipment platform is the emitting surface for all waste heat.

Protection of the spacecraft from thermal-plume heating during injection consisted of applying aluminum foil around the top of the Delta third stage and aluminized-Mylar insulation around the interstage ring. The plume heating, however, was not so severe as expected.<sup>15</sup>

### Controlling Extremity Temperatures

The spacecraft extremities, including the solar cells, possess no internal energy sources which receive electrical power except the boom-mounted magnetometer and the pneumatic valve. The solar array and each boom and mast were subjected to thorough thermal analysis to determine their approximate temperatures at various distances from the Sun. Thermal coatings were applied to the booms and Sun-sensor shades. If the same thermal coatings are applied for both inward and outward missions, the temperatures of externally exposed components at 0.8 AU will be 1.118 times those at 1.0 AU and 0.913 times lower at 1.2 AU. The application of a different thermal coating may raise or lower the absolute values of the temperatures, but the ratios remain fixed. However, it is little trouble to change the coatings for inward and outward missions, and this was done to a limited extent for the various Pioneer flights.

<sup>15</sup> In 1964, an Argo D-4 sounding rocket was fired from Wallops Island carrying an experiment to measure plume heating. Unfortunately the flight was a failure.

### Thermal Control Subsystem Reliability

The thermal coatings, thermal insulation, and thermal conduction paths in the Pioneer spacecraft present no reliability problems. The only moving parts are the individually actuated thermal louvers. Catastrophic failure of several louvers in the neighborhood of a large source of thermal energy is highly unlikely. In fact, the use of individual actuators for the louvers makes the probability of acceptable operation over a 6-month lifetime very high, roughly 0.999.

## THE STRUCTURE SUBSYSTEM

The structure subsystem, like the thermal control subsystem, is a largely passive, but critical, subsystem. Spacecraft have rather complex structure subsystems which must be analyzed as painstakingly as the communications subsystem or any other subsystem. The Pioneer structure (figs. 4-28 through 4-30) consists of the following major sections:

- (1) The interstage ring and cylinder
- (2) The equipment platform and struts
- (3) High-gain antenna mast supports
- (4) Solar-array substrate and supports
- (5) Boom dampers
- (6) The booms and associated deployment and locking equipment
- (7) The Stanford experiment antenna

### Overall Configuration

Spacecraft structure is highly variable. In orbit about the Earth are cylinders, spheres, boxes, even tetrahedrons and other polyhedrons. Subsystem functions and program ground rules determine spacecraft geometry. In the case of Pioneer, axial symmetry was the direct result of the choice of spin stabilization—an essential ingredient of the whole Pioneer concept.

Spin-stabilized spacecraft need not be cylindrical in shape; only symmetry about a spin axis is required. Spheres, for example, also lend themselves to spin stabilization. With Pioneer, however, there was good reason to choose a cylinder. The spacecraft was to be oriented with its spin axis perpendicular to the plane of the ecliptic. Thus, body-mounted solar cells would always be perpendicular to sunlight once each revolution (roughly once per second). Axis perpendicularity was a condition for maximum power generation and obviously a factor enhancing the whole Pioneer concept. Pioneer depended upon several highly dependent, interlocking ideas (ch. 3). The cylindrical body of Pioneer, with the long high-gain antenna mast atop it, is the logical consequence of the Pioneer ground rules of simplicity and low cost, and the Delta payload capability.

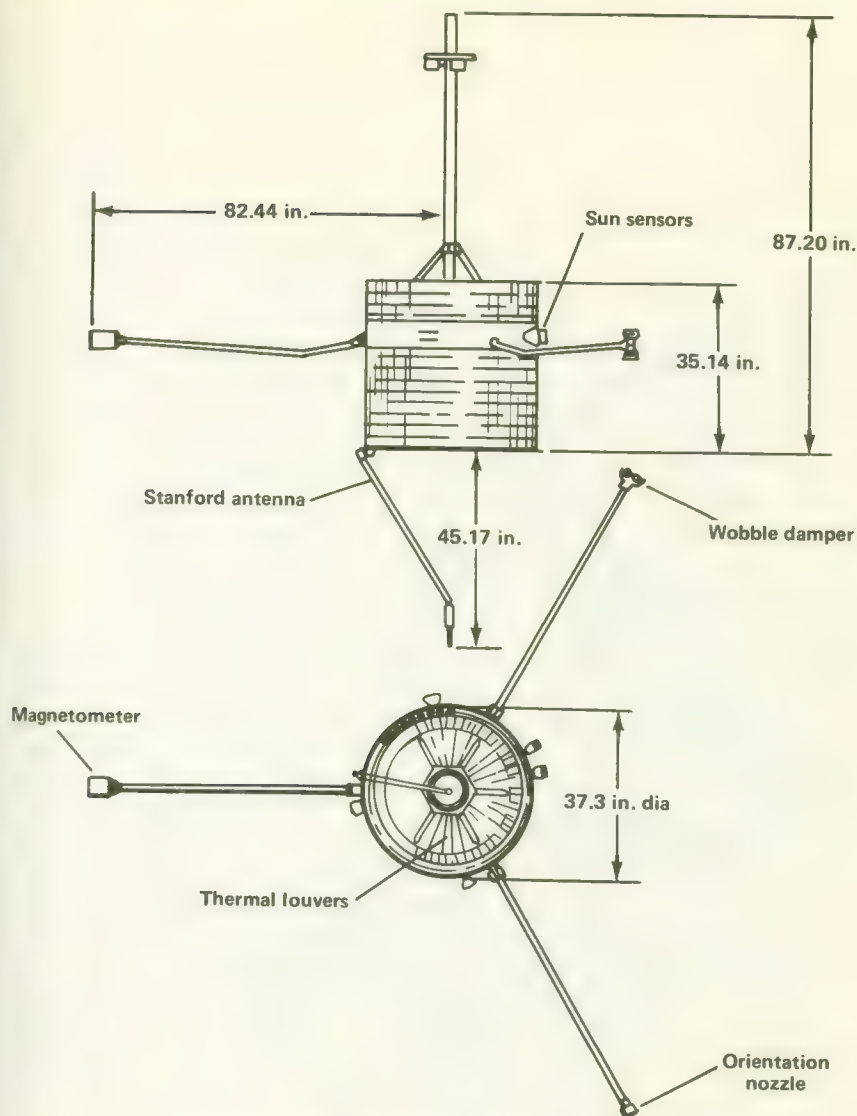


FIGURE 4-28.—Spacecraft external dimensions.

The Pioneer spacecraft sketched out in the feasibility study had no booms at all. Booms were added for three reasons:

(1) With the magnetometer at the top of the antenna mast, as it was in the original concept, spin stability was marginal. The addition of booms, one with the magnetometer at its end, assured stability. Spin stability depends upon a moment of inertia along the spin axis that is greater than those moments along the other axes.)

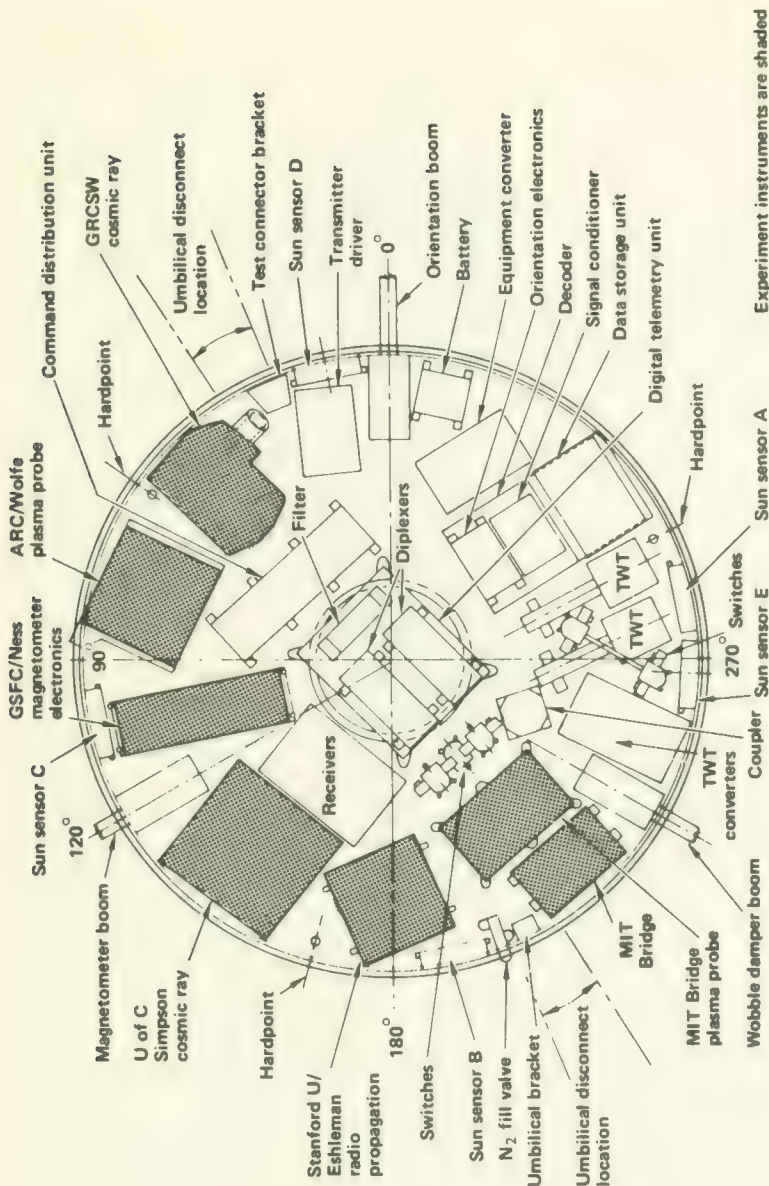


FIGURE 4-29.—Equipment platform layout for Pioneers 6 and 7. Layouts for the Block-II Pioneer were very similar.

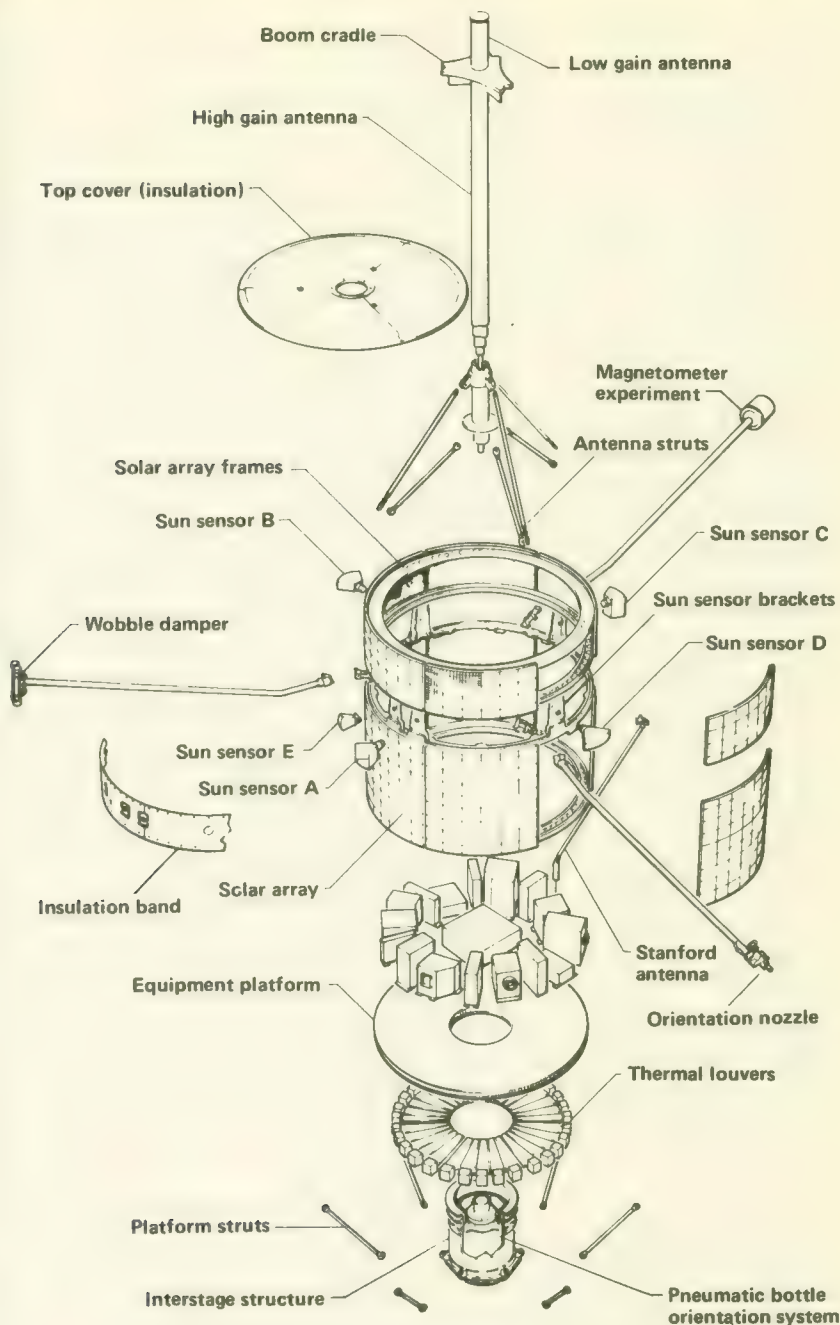


FIGURE 4-30.—Exploded view of the Pioneer spacecraft.

(2) The booms provide magnetic isolation for the magnetometer and exile the orientation nozzle solenoid and the wobble damper, both of which pose magnetic cleanliness problems.

(3) The effectivenesses of the orientation nozzle and wobble damper are increased by placing them on the ends of booms.

The decision to add deployable booms to the spacecraft was most critical from the structures standpoint. Booms are moving parts that must be stowed in a launch configuration and then unfolded and locked in position after the launch vehicle fairing has been jettisoned. Other scientific satellites, such as OGO 1, have been compromised by boom failures. In the case of Pioneer, the advantages of using booms far outweigh their potential liability.

Externally, the Pioneers are cylinders 37.3 in. in diameter and 35.14 in. long, with three booms 120° apart extending 82.44 in. from the spin axis (fig. 4-28). The Stanford experiment antenna projects downward when deployed, and in appearance and complexity is a fourth boom. The high-gain antenna mast projects roughly 53 in. above the top edge of the cylinder. Pioneer, therefore, presents appendages in all directions, in contrast to the relatively clean configuration first suggested by STL (ref. 5).

Internally, the major requirements were support for scientific instrumentation and spacecraft subsystems and, once again, spin-axis symmetry. Symmetry must be taken here to mean the judicious placement of mass around the spin axis to preclude the spacecraft's wobbling. The farther components were located from the spin axis, the greater the spin stability; that is, the better the spinning spacecraft could resist destabilizing influences. The internal configuration (fig. 4-29) follows general spacecraft practice—the major structural element is a strong equipment platform. This platform supports all internal components, the three radial booms, and the high-gain antenna mast. The equipment platform is the internal skeleton. The cylindrical shell, which is rigidly attached to the equipment platform, is constructed of aluminum honeycomb with fiberglass face sheets; it is the structural skin that forms the base of the solar array. Sun sensors and the Stanford antenna are attached to the equipment platform. The major structural elements are the equipment platform, appendages, and cylindrical shell.

### Structural Details

The most important structural loads are impressed during the launch process. The acceleration, vibration, and shock loads that dictate much of the spacecraft structure are stipulated in some detail in chapter 7. Once the spacecraft is injected into solar orbit, applied loads fall far below those imposed by the Delta launch vehicle.

An 8.75-in. fiberglass thrust cylinder carries the launch vehicle forces

from the aluminum interstage ring to another ring attached to the bottom of the equipment platform. The nitrogen pressure vessel supplying the orientation subsystem nests within this cylinder. Six struts link the platform with the bottom of the thrust cylinder, providing additional rigidity. The equipment platform supports the rest of the spacecraft (fig. 4-30). Three aluminum-mast struts absorb side loads transmitted by the antenna mast. The top cover, which is made of an aluminized-Mylar blanket, bears no loads. The original cover was an aluminum sheet, but it was discarded to save weight. The bottom of the "can" is really the equipment platform, although the solar-array skirt continues downward for another 20 in.

The equipment platform is an aluminum honeycomb sandwich, 0.75-in. thick with 0.016-in. aluminum face sheets. The material weighs 3.1 lb/ft<sup>3</sup>. It carries the loads transferred from interstage cylinder and struts to the booms, antenna mast, solar array, etc. The thermal louvers are mounted on two-thirds of the lower surface of the platform. An insulation blanket covers the remaining one-third of the surface. On the top surface, the spaces between mounted equipment are covered with black paint.

Aluminum-honeycomb sandwich material was also used for the solar-array substrates. The inner and outer face sheets are "prepreg" fiberglass sheets. The substrate panels are attached to the equipment platform by fiberglass brackets around the lower ring of solar panels and through the Sun sensor brackets around the upper ring. Support rings at the top and bottom ends complete this part of the structure. Upper panels are interchangeable among themselves, as are those in the lower ring. The 6.75-in. band between upper and lower rings was left bare because the boom shadows would have rendered solar cells useless in that area anyway. This band is closed thermally with an aluminized Mylar blanket. The booms are hinged in this "bellyband."

The 62-in. radial booms, which isolate the orientation nozzle, wobble damper, and magnetometer from the spacecraft proper, are made from thin-walled aluminum tubing. During launch, a reefing line holds these booms in a stowed position around the antenna mast. Immediately after third-stage separation, redundant pyrotechnic cable cutters free the booms, allowing centrifugal force to spread them outward. Piston-type boom dampers, somewhat like those on heavy doors, prevent them from snapping into position too rapidly. A leaf-type spring and pawl lock the booms into position permanently.

The Stanford experiment antenna is similar to the radial booms in construction. However, it has two hinges: one controls the kinematics of the entire assembly, and the other permits the unfolding of the high frequency element of the antenna until it lies along the spin axis. Brackets on the magnetometer boom hold the Stanford antenna in its stowed position until the magnetometer boom has deployed about 40°. Microswitches on each boom indicate successful deployment and locking.

### Other Structures Tests and Analysis

STL performed the stress analysis of the Pioneer spacecraft. The studies involved static analysis and examination of such dynamic factors as balance, moments of inertia, rigidities, limitations of vibratory response, spacecraft spinup and separation, and attitude stability and damping. The dynamics of appendage deployment were of particular concern because of past difficulties with booms. This concern led to a special test apparatus which was built to check deployment under close-to-actual conditions (see ch. 7). Spin tests, vibration tests, and the other related tests described in chapter 7 were extensive. They required the construction of a special "structural model" of the spacecraft, wherein the major structures either duplicated those in the intended flight model or, in the case of electronic equipment, simulated them in weight.

Structural reliability analysis is not as advanced as it is for electronics equipment; nevertheless, some estimates can be made. STL calculated that the overall structure reliability would be 0.998 for launch, boost, injection, and free flight. This estimate was based upon tests performed upon cable cutters and deployable booms built for OGO and other space programs. Of course, such estimates based on moving parts assume that no failures of static structural members occur. The use of factors of safety during the stress analysis gives this assumption some foundation. Pioneer structural studies assumed a yield factor of 1.35 and an ultimate safety factor of 1.50.

The possible effects of the space environment upon the spacecraft were also analyzed carefully. The analysis showed:

- (1) Solar heat flux was controlled by the louvers and thermal coatings discussed previously under thermal control.
- (2) Solar particulate radiation, which has a potential for degrading material structures, was several orders of magnitude below damage thresholds.
- (3) Micrometeoroids in deep space (many times less prevalent than in Earth orbit) were deemed to be of negligible structural import to vehicles this side of the asteroid belt.
- (4) Space vacuum may result in the sublimation of materials with high vapor pressures and the cold-welding of moving parts. Of the Pioneer structural materials, magnesium has the highest vapor pressure, but the loss over a year's time was computed to be negligible. The only spacecraft moving parts that must operate successfully throughout the mission are the thermal louvers. These are lubricated with a low-vapor-pressure solid grease developed for the OGO program.

### OVERALL WEIGHT BREAKDOWN

The subsystem weight breakdown for the entire spacecraft is presented in table 4-18 for the two blocks of IQUY Pioneer spacecraft.

TABLE 4-18.—*Block-I and Block-II Spacecraft Weight Breakdowns*

| Equipment                           | Block I <sup>a</sup> | Block II <sup>b</sup> |
|-------------------------------------|----------------------|-----------------------|
| Communication subsystem             | 14.35 lb             | 14.33 lb              |
| Receivers (2)                       | 6.14                 | 6.14                  |
| Transmitter driver                  | 1.31                 | 1.29                  |
| TWTs (2)                            | 1.89                 | 1.89                  |
| Attenuators and supports            | 0.12                 | 0.12                  |
| Branch line coupler                 | 0.24                 | 0.25                  |
| Diplexers (2)                       | 1.39                 | 1.38                  |
| Bandpass filter                     | 0.25                 | 0.25                  |
| Coaxial switches (5)                | 1.00                 | 1.00                  |
| High-gain antenna                   | 2.01                 | 2.01                  |
| Data handling subsystem             | 10.65                | 10.78                 |
| Digital telemetry unit              | 8.57                 | 8.64                  |
| Data storage unit                   | 1.73                 | 1.75                  |
| Signal conditioner                  | 0.35                 | 0.39                  |
| Command subsystem                   | 10.72                | 11.47                 |
| Command decoder                     | 5.60                 | 6.15                  |
| Command distribution unit           | 5.12                 | 5.32                  |
| Electric power subsystem            | 36.54                | 38.03                 |
| Solar cells, substrate, glass, etc. | 13.98                | 13.41                 |
| Support rings and brackets          | 2.96                 | 2.96                  |
| Battery                             | 2.19                 | 3.16                  |
| Equipment converter                 | 3.02                 | 2.99                  |
| TWT converters (2)                  | 4.52                 | 4.49                  |
| Cabling and connectors              | 9.87                 | 11.02                 |
| Orientation subsystem               | 6.68                 | 6.95                  |
| Nitrogen bottles and supports       | 1.54                 | 1.75                  |
| Nitrogen gas                        | 0.87                 | 0.93                  |
| Solenoid valve                      | 0.44                 | 0.40                  |
| Regulator                           | 0.99                 | 1.00                  |
| Nozzle                              | 0.01                 | 0.01                  |
| Pressure transducer                 | 0.21                 | 0.21                  |
| Sun sensors                         | 0.86                 | 0.87                  |
| Pressure switch                     | 0.12                 | 0.12                  |
| Plumbing and supports               | 0.46                 | 0.46                  |
| Logic circuits                      | 0.98                 | 1.00                  |
| Fill valve                          | 0.20                 | 0.20                  |
| Thermal control subsystem           | 6.80                 | 7.00                  |
| Louvers                             | 0.48                 | 0.48                  |
| Structure and actuators             | 1.64                 | 1.64                  |
| Thermal insulation                  | 4.68                 | 4.88                  |
| Structure subsystem                 | 17.46                | 18.10                 |
| Equipment platform                  | 7.01                 | 7.03                  |
| Interstage structure                | 0.99                 | 0.99                  |
| Interstage support ring             | 0.18                 | 0.18                  |
| Payload fitting                     | 0.97                 | 0.97                  |
| Antenna supports and fittings       | 1.03                 | 1.03                  |
| Wobble damper                       | 0.46                 | 0.46                  |
| Booms (3)                           | 1.47                 | 1.57                  |

TABLE 4-18.—*Block-I and Block-II Spacecraft Weight Breakdowns (Continued)*

| Equipment  | Block I <sup>a</sup> | Block II <sup>b</sup> |
|--|----------------------|-----------------------|
| Magnetometer boom flange                           | 0.05                 | 0.07                  |
| Hinge fitting structure                            | 1.50                 | 1.50                  |
| Boom dampers (3)                                   | 0.57                 | 0.57                  |
| Boom tie-down                                      | 0.79                 | 0.79                  |
| Solar sail   | 0.06                 | 0.06                  |
| Hardware   | 1.18                 | 1.25                  |
| Inertia weights (on boom)                          | 0.12                 | 0.55                  |
| Platform struts                                    | 1.08                 | 1.08                  |
| Total spacecraft weight without experiments        | 103.20               | 106.66                |
| Experiments  | 34.74                | 40.54                 |
| Magnetometer (Goddard/Ames)                        | 5.81                 | 7.74                  |
| Cosmic ray detector (Chicago)                      | 4.71                 | —                     |
| Cosmic ray detector (GRCSW)                        | 4.39                 | 5.55                  |
| Plasma probe (MIT)                                 | 6.13                 | —                     |
| Plasma probe (Ames)                                | 6.33                 | 5.92                  |
| Stanford radio propagation experiment <sup>c</sup> | 7.37                 | 7.01                  |
| Cosmic dust (Goddard)                              | —                    | 4.29                  |
| Cosmic ray (Minnesota)                             | —                    | 7.91                  |
| Electric field (TRW)                               | —                    | 0.87                  |
| Convolutional coder                                | —                    | 1.25                  |
| Total spacecraft weight with experiments           | 137.94               | 147.20 <sup>d</sup>   |

<sup>a</sup> Reported spacecraft weights vary slightly for each spacecraft depending upon the data source. The weights shown in this column are for Pioneer 6; taken from "Monthly Informal Technical Progress Report, Pioneer Spacecraft Program," Period 1 December to 31 December 1965, TRW Systems Report 8400.3-247, January 10, 1966.

<sup>b</sup> For Pioneer 9. Taken from "Monthly Informal Technical Progress Report, Pioneer Spacecraft Project," Period 1 November to 30 November 1968, TRW Systems Report, December 9, 1968.

<sup>c</sup> Includes balance compensation weights of 1.33 and 0.63 lb, respectively.

<sup>d</sup> Actual weight 146.82 lb when the assembled parts were weighed en masse.

## REFERENCES

1. KRASSNER, G. N.; AND MICHAELS, J. V.: Introduction to Space Communication Systems. McGraw-Hill Book Co., Inc., 1964.
2. LUMB, D. R.; AND HOFFMAN, L. B.: An Efficient Coding System for Deep Space Probes with Specific Application to Pioneer Missions. NASA TN D-4105, 1967.
3. WINDEKNECHT, T. G.: A Simple System for Sun Orientation of a Spinning Satellite. IAS/ARS Joint Meeting, 1961.
4. MASSEY, W. A.: Pioneer 6 Orientation Program System Design Survey: NASA/ERC Design Criteria Program, Guidance and Control. NASA CR-86193, 1968.
5. ANON.: Proposal under RFP-A-6669 to Produce the Pioneer Spacecraft. Space Technology Laboratories Proposal No. 1943.00, Redondo Beach, Mar. 4, 1963.

## Scientific Instruments

### SCIENTIFIC OBJECTIVES

THE PIONEERS are multidisciplinary spacecraft. From the scientific standpoint they are very close relatives of the Interplanetary Monitoring Platforms (IMPs) orbited around the Earth and Moon from 1963 on. In fact, many IMP experimenters are also Pioneer experimenters, and their instruments are similar on both series of spacecraft. This is not surprising, as both types of spacecraft were designed to measure the same important facets of the interplanetary medium: the plasma, cosmic rays, magnetic fields, cosmic dust, electric fields, and space propagation properties. The IMPs, however, center on the Earth-Moon system, while the Pioneers are Sun-centered.

The scientific objectives of the Pioneer spacecraft are to measure the above-named facets of the interplanetary field. In 1962 virtually nothing was known of what transpired in interplanetary space. In particular, Earth-bound scientists had little feel for how plasma, cosmic rays, etc., varied spatially and in the time and energy dimensions. The Pioneer scientific objectives were sharpened in three ways:

(1) The spacecraft were launched at intervals that permitted the solar cycle to be covered from minimum to maximum. (The long lifetimes of the Pioneers has extended this coverage well beyond the 1969-1970 maximum.)

(2) Pioneers were launched on inward and outward missions so that some precede and some lag the Earth, giving scientists synoptic coverage over much of the plane of the ecliptic.

(3) The outward launches (Pioneers 7 and 8) were sent in backward-curving arcs that took them far out into the Earth's "tail" or geomagnetic wake (fig. 5-1). Thus, measurements were acquired in this poorly understood shadow zone; the zone is the subject of considerable controversy concerning its length and structure.

It is this extensive spatial and temporal coverage of the interplanetary medium that makes the Pioneers especially valuable scientifically. The scientific results and their interpretations are presented in Volume III. Only experimental hardware is covered in this chapter.

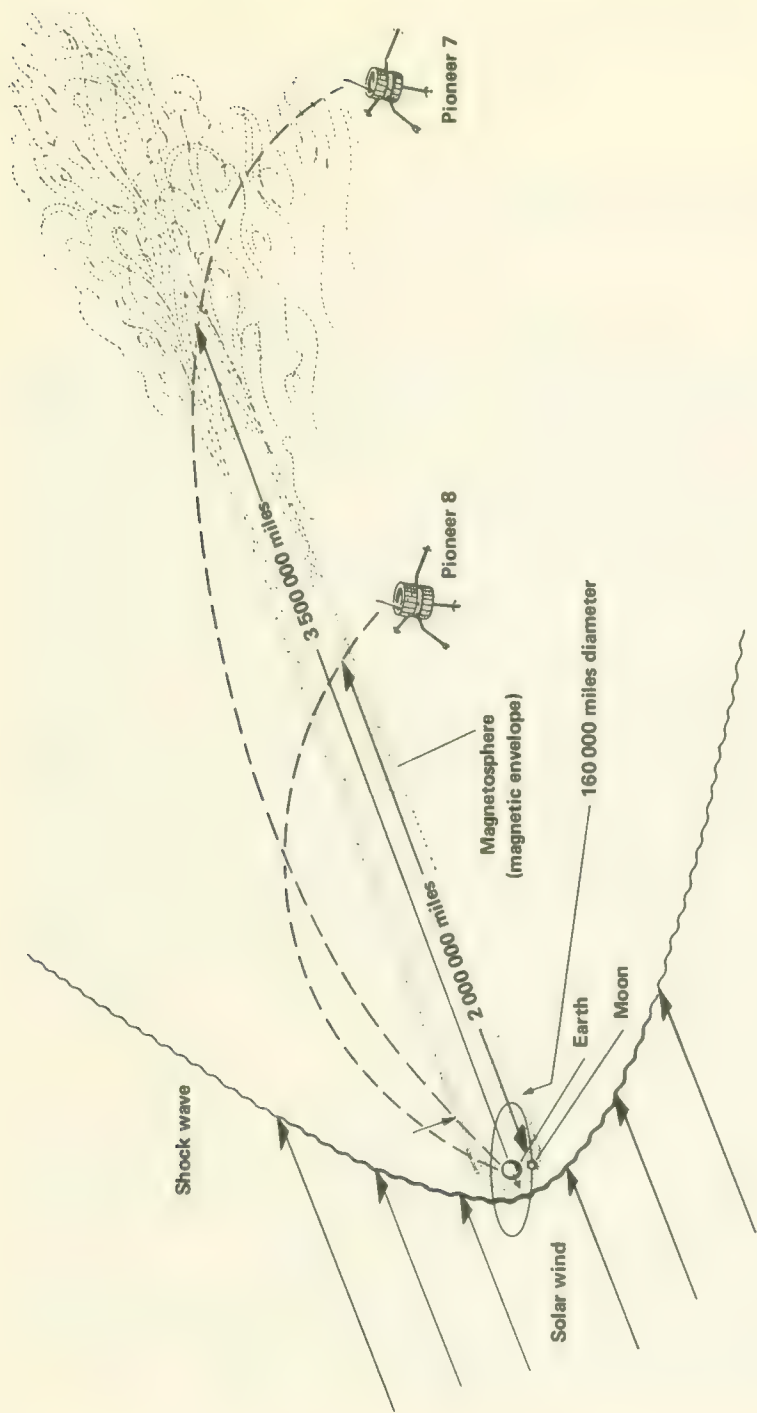


FIGURE 5-1.—Trajectories of Pioneers 7 and 8 through the Earth's magnetic tail.

## APPLICATIONS OF PIONEER DATA

In 1962 and 1963, the Pioneers would hardly have been called "applications" spacecraft, so firmly were they directed toward satisfying scientific curiosity. Solar events, however, have wide repercussions, jiggling magnetometers on Earth, disrupting long-distance communication, and the like. Pioneers 8 and 9, cruising well behind the Earth in its path around the Sun, can radio warnings to the Earth of solar radiation storms which will soon catch up with the Earth. Since the Sun rotates once each 28 days and drags its plasma and radiation streams around with it, the Pioneers lagging the Earth are well-situated to forecast interplanetary weather for the Earth several days in advance. These data are now sent to the Environmental Science Services Administration, which then distributes them to about a thousand users (see Vol. III).

Thus, Pioneer instrumentation has practical applications not foreseen at the beginning of the program. On the later Pioneers, instrument selection and design were affected to some extent by this new dimension of the program.

## INSTRUMENT INTERFACES AND SPECIFICATIONS

In Pioneer terminology, the scientific instruments are considered a separate system rather than a subsystem of the spacecraft. The forces exerted on the scientific instruments are considered to be similar to those encountered by the spacecraft subsystems. The most important are the mechanical loads imposed during launch, the heat from the Sun, the magnetic and electromagnetic environments extending from the other subsystems, and the information interface enforced by the data handling subsystem. These spacecraft subsystems are defined in detail in chapter 4.

To provide the experimenters with a view of the interfaces as seen by their instruments, Ames Research Center prepared a series of specifications and interface documents. The first, "Scientific Instrument Specification," No. A-7769, was issued December 31, 1963, for the purpose of acquainting experimenters with the spacecraft test requirements, the ground-support equipment, documentation requirements, and the responsibilities levied on the experimenters. A series of more detailed documents describing the spacecraft/scientific instrument interfaces followed. The reader should consult the references at the end of this volume for a complete list of Pioneer specifications. The interface documents were double-edged—both engineers and scientists working on the spacecraft could use them as definitive descriptions of the scientific instruments written in hardware language with dimensions, weights, electrical-connector-pin assignments, and the like, spelled out.

It is worth while to review the main points covered in the instrument

interface specifications to reemphasize the extra dimensions involved in instrument design for space research. The following considerations were necessary:

- (1) Mechanical interfaces—dimensions, weights, mounting orientations and view angles
- (2) Electrical interfaces—power levels, voltages, transients, connectors and cabling
- (3) Information interfaces—word lengths, bit rates, formats, and timing signals
- (4) Thermal interfaces—operating temperatures and surface coatings
- (5) Electromagnetic interfaces—interference, shielding and grounding

The factors mentioned above are discussed in chapter 4.

In addition to matching spacecraft interfaces, each scientific instrument had to mesh with the interfaces presented by ground-support equipment. Before even reaching the launch pad, instruments had to be qualified (usually through prior flights on sounding rockets or satellites) and then tested according to the standards described in chapter 6.

A number of military specifications were also applied to the Pioneer spacecraft and its cargo of instruments. One of the most critical was MIL-I-26600, "Interference Control Requirements, Aeronautical Equipment," highlighting the fact that the electromagnetic environment had to be shared with other spacecraft as well as a host of other aerospace equipment at Cape Kennedy prior to and during launch. Finally, the presence of radioactive sources for instrument calibration meant that federal and state laws governing the use and transport of radioactive materials also applied.

The scientists flying instruments on Pioneer (or any spacecraft, for that matter) had to deal with managerial controls, with specifications more restrictive than those encountered in the terrestrial laboratory, and with rather rigorous testing and qualification regimens. The specific details may be found in the other chapters referenced above and in the documents listed at the end of this chapter (refs. 1 and 2).

## INSTRUMENT SELECTION

The instruments selected for the Pioneer flights had to promote the mission's scientific objectives, as well as match spacecraft interfaces and meet management criteria such as the cost and schedule limitations set forth in chapter 1. NASA has a well-defined procedure for choosing experiments and experimenters. When a mission has been delineated well enough to permit some hard thinking about experiments, NASA solicits the scientific community by letter, telegram, or (more commonly today) a solicitation entitled "Opportunities to Participate in Space Flight Experi-

ments." Experiments for Pioneers A and B were solicited by letter in early 1963; for Pioneers C and D, in late 1963 and early 1964.

When experiment proposals have been received, they are evaluated at NASA Headquarters with the assistance of the Space Sciences Steering Committee. The members of the Committee and its several subcommittees are appointed from scientists in NASA, other Government agencies, universities, and non-profit organizations. In the case of Pioneer, the following four subcommittees were involved: Astronomy, Solar Physics, Ionospheres and Radio Physics, and Particles and Fields. The Pioneer Project Office also reviewed experiment proposals from the standpoints of engineering feasibility, cost, and compatibility with the spacecraft.

Usually NASA receives more proposals for experiments than the spacecraft can carry. Therefore, the Space Sciences Steering Committee must choose those experiments that meet the minimum requirements and then assign priorities. For example, 18 proposals were evaluated in depth for Pioneers A and B, 15 for Pioneers C and D; but only 7 and 8 experiment flew on these two blocks of spacecraft, respectively. The general criteria employed in the selection process are: (1) scientific merit, (2) ability of the instrument to make the desired measurement, (3) development status of the instrument, and (4) understanding and experience of the experimenters. The criteria specific to Pioneer that were employed are: (1) pertinence to Pioneer mission, weight, data rate, power, etc.; and (2) pertinence with respect to the solar minimum.

The Summary Minutes of the meeting of the Space Sciences Steering Committee, dated July 22, 1963, typify the selection procedure. Pioneer A and B experiments were divided into two categories as follows:

- (1) Firm payload, including magnetic fields, plasma, cosmic-ray gradients, and radio propagation
- (2) Tentative or backup experiments, including cosmic-ray anisotropy and plasma

It was also recommended that the cosmic-ray anisotropy experiment be rocket-tested prior to the Pioneer launch. Within the "firm payload" group, the radio propagation experiment was given the lowest priority should subsequent spacecraft and instrument developments require weight reduction.

The above list for Pioneers A and B includes no cosmic dust or micro-meteoroid experiment. A cosmic dust experiment was proposed for the Block-I Pioneers by Ames Research Center, but development problems precluded its inclusion. Thus, one of the major parameters of interplanetary space had to be neglected on the early Block-I flights. When experiments were solicited for Pioneers C and D, no cosmic dust proposals were received. Trying to make up for this deficiency, NASA specifically solicited several scientists by telegram, asking if they would be interested in building cosmic-dust experiments for the Pioneer interplanetary mission. Three proposals

were received; and ultimately the one submitted by Goddard Space Flight Center was selected for the Pioneer C and D payloads.

When it was decided to combine the parts left over from Pioneers A through D and assemble Pioneer E, the question of experiment selection was revived. During the fall of 1965, however, NASA decided to retain the Pioneer C and D payload rather than making extensive modifications to the spacecraft parts on hand.

Some of the proposed experiments did not fall within the mission scope suggested by NASA. For example, a proposal submitted by Space/Defense Corporation was aimed at investigating the influence of electromagnetic and gravitational fields on diurnal rhythm. Interesting as such an experiment would have been, it would not have measured parameters related to the other investigations.

The experiments finally selected for the five Pioneer spacecraft are presented in table 5-1.

### THE GODDARD MAGNETOMETER (PIONEERS 6, 7, AND 8)

The interplanetary magnetic field is created by the Sun and modulated by the streams of plasma that spiral out into the space between the planets. Magnetic field measurements, particularly those that record transients following solar activity, are critical to our understanding of the space surrounding the Sun.

The spin-stabilized Pioneers permitted the use of a unique magnetometer design whereby all three components of the magnetic field could be measured with a single-axis sensor (ref. 3). If the sensor axis is mounted at an angle of  $54^{\circ}45'$  to the spin axis, and if the sensor is sampled at three equally spaced intervals during the rotation of the spacecraft, the experimenter receives three independent measurements of three orthogonal components of the magnetic field.

The sensor of the single-axis fluxgate magnetometer employed in the Goddard experiment is a saturable inductance driven by a gating magnetic field applied in a winding. The flux induced in the saturable core is modified by the presence of the external magnetic field in such a way that the contribution of the external field can easily be extracted and quantified.<sup>16</sup> The Pioneer magnetometers were developed and manufactured for Goddard by the Schonstedt Instrument Company.

The fluxgate sensor is mounted on one of Pioneer's three booms, at a distance of 2.1 m from the spin axis, in a canister employing passive thermal control. An unusual feature of this experiment is the explosive-actuated indexing device, which permits the experimenter back on Earth to flip the sensor over by  $180^{\circ}$  so that magnetic fields created by the space-

<sup>16</sup> For a more complete description of how the various instruments used in space science work, see: W. R. Corliss, *Scientific Satellites*, NASA SP-133, 1967.

TABLE 5-1.—*Experiments Aboard the Pioneers*

| Instrument                          | Pioneer spacecraft |   |   |   |   |
|-------------------------------------|--------------------|---|---|---|---|
|                                     | 6                  | 7 | 8 | 9 | E |
| Single-axis fluxgate magnetometer * | X                  | X | X |   |   |
| Triaxial fluxgate magnetometer *    |                    |   |   | X | X |
| Faraday-cup plasma probe            | X                  | X |   |   |   |
| Plasma analyzer                     | X                  | X | X | X | X |
| Cosmic ray telescope                | X                  | X |   |   |   |
| Cosmic-ray anisotropy detector      | X                  | X | X | X | X |
| Cosmic-ray gradient detector        |                    |   | X | X | X |
| Radio propagation experiment        | X                  | X | X | X | X |
| Electric-field detector             |                    |   | X | X | X |
| Cosmic dust detector                |                    |   | X | X | X |
| Celestial mechanics                 | X                  | X | X | X | X |

\* The triaxial fluxgate magnetometer was originally scheduled to fly on Pioneers C and D, but because it could not make the launch date, the single-axis fluxgate magnetometer was substituted on Pioneer C.

craft can be taken into account. The Goddard sensor is rotated by a spring-driven escapement mechanism. Because of their high reliability, eleven pairs of small explosive charges were used to activate the escapement mechanism. Thus, eleven sensor flip-overs are possible by remote control.

The spacecraft Sun sensor triggered the Goddard experiment once each rotation of the spacecraft. Beginning with this signal, the experiment electronics generated three equally spaced sampling gates which permitted analog readings from the fluxgates to enter analog/digital converters. These data were then converted into digital words. Each magnetometer measurement required eight bits. Measurements were stored in a 24-bit data buffer until all three measurements were completed; then, they were transferred to the spacecraft data handling subsystem (fig. 5-2). As noted in chapter 4, the Goddard telemetry word is longer than the standard Pioneer 6-bit word. Consequently, four spacecraft words were required to transmit three Goddard experiment words.

Another important component of the experiment was the analog/digital converter, which converted the analog voltage measurements provided by the sensor into eight-bit words. The time-average computer, also shown in figure 5-2, averaged sensor readings during those periods of the mission when the spacecraft was far from Earth and the telemetry rates were less than the rate at which data accumulated from the experiment.

Magnetic interference is a critical problem for the experimenter flying a magnetometer in interplanetary space. The fields are usually less than  $10\gamma$  and may be overwhelmed by the fields generated by the spacecraft.

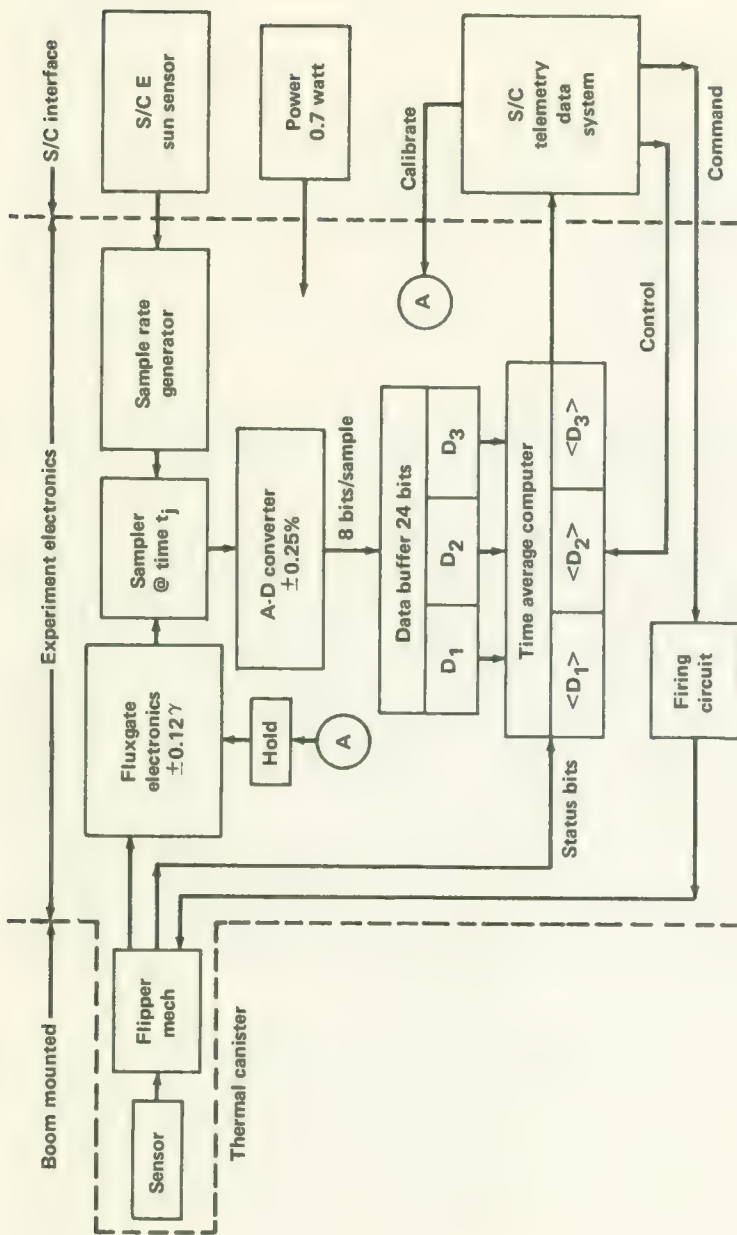


FIGURE 52.—Block diagram of the Goddard magnetic field experiment.

For this reason, the Pioneers were made as magnetically clean as possible (ch. 4), and the magnetometer sensor was located on a spacecraft boom 2.1 m from the spacecraft spin axis. Detailed mapping indicated that the magnetic interference from the spacecraft was less than  $0.125\gamma$ ,  $0.35\gamma$ , and  $0.2\gamma$  on Pioneers 6, 7, and 8, respectively. The Pioneers were among the magnetically cleanest spacecraft ever built. The data telemetered to Earth have, therefore, been of great utility in mapping the magnetic structure of solar disturbances and, during the first few hours of flight, the Earth's magnetic tail.

The overall characteristics of the Goddard magnetometer are tabulated in table 5-2. Originally, the magnetometer was to be located at the end of the axial high-gain telemetry antenna, but this proved impractical and it was mounted on a boom (fig. 1-4). The location of the experiment electronics on the spacecraft equipment platform is shown in figure 4-29.

### THE AMES MAGNETOMETER (PIONEERS 9 AND E)

The Ames magnetometer instrumentation consists of a fluxgate-sensor package located at the end of one of the 62-in. spacecraft booms and an electronics package mounted on the spacecraft equipment platform. Like the Goddard magnetometer, the Ames instrument is based on the fluxgate saturable inductance sensor; but it employed three sensors mounted along

TABLE 5.2.—*Characteristics of the Goddard Magnetometers*

| Characteristic                    | Pioneers            |  |  |
|-----------------------------------|---------------------|--|--|
|                                   | 6                   | 7  | 8                                      |
| Weight                            |                     |  |  |
| Electronic assembly               | 4.5 lb              | 4.5 lb                                       | 5.0 lb                                 |
| Boom assembly                     | 0.7 lb              | 0.7 lb                                       | 0.7 lb                                 |
| Power required                    | 0.7 W               | 0.7 W  | 0.9 W                                  |
| Input voltage<br>(spacecraft bus) | $28^{+5}_{-4}$ V dc | $28^{+5}_{-4}$ V dc                          | $28^{+5}_{-4}$ V dc                    |
| Range                             | $\pm 64\gamma$      | $\pm 32\gamma$                               | $\pm 32\gamma$<br>■ $\pm 96\gamma$     |
| Thermal calibration               |                     |  |  |
| Electronics                       |                     | $-25^\circ \text{C}$ to $+55^\circ \text{C}$ |  |
| Sensor                            |                     | $-75^\circ \text{C}$ to $+75^\circ \text{C}$ |  |
| Resolution (sensitivity)          | $\pm 0.25\gamma$    | $\pm 0.125\gamma$                            | $\pm 0.125\gamma$<br>$\pm 0.375\gamma$ |

\* An automatic switch was added on Pioneer 8. High magnetic fields switched the magnetometer to the higher range.

mutually orthogonal axes rather than a single sensor like the Goddard instrument. One fluxgate axis is parallel to the spacecraft spin axis and a second oriented radially. The Ames experimenters hoped that their three-axis magnetometer would provide a better measure of the interplanetary magnetic field during disturbances involving large, rapid magnetic fluctuations.

The permalloy-core fluxgate sensors were built by Honeywell, Inc., and supplied to Philco-Ford, the magnetometer prime contractor, as Government-furnished equipment (ref. 4). The general construction of the basic sensor is portrayed in figure 5-3. A 6144-Hz drive signal of approximately 1.5 V rms applied to the toroidally wound drive winding modulates the permeability of the sense-winding core. The sense winding provides the signal that indicates the direction and strength of the ambient magnetic field. The feedback winding generates a signal that helps to minimize nonlinearities. The three sensors comprise two packages: one single-axis fluxgate is located in a package mounted so that the sensor axis is parallel to the spacecraft boom axis; the second package contains two orthogonally mounted fluxgates with both axes perpendicular to the boom axis. The Ames instrument includes a flipping mechanism, but it is powered by two resistance-heated bimetallic motors rather than a pyrotechnic device, such as that used by the Goddard magnetometer. The motors on the Ames instrument flip the dual sensor assembly 90° upon command from Earth. One motor flips the sensors clockwise; the other counterclockwise. The Ames magnetometer sensors can be flipped again and again and are not limited to the number of pyrotechnic charges launched with the spacecraft (the Goddard instrument has 11 flips); however, an additional burden is placed upon the spacecraft power supply by the resistance heaters in the motors.

The electronics package (fig. 5-4) has these major functions:

- (1) Provision of the 6144-Hz drive signals, which must have a negligible second-harmonic content
- (2) Selection, amplification, and demodulation of the second harmonic signal obtained from the sense windings
- (3) Analog-to-digital conversion of the analog signals from the sense winding
- (4) Spin demodulation of the signals received from the two sensors in the spacecraft spin plane
- (5) Digital filtering to match the five allowable spacecraft bit rates
- (6) Periodic sampling of data in the buffer storage

Once safely in space, the Ames instrument is commanded each day into a self-calibrate sequence. Sinusoidal currents are injected into the feedback windings to establish calibration fields. The calibration sequence is often repeated after the dual-sensor package has been commanded into the flipped position. This interchange of sensor positions, of course, permits

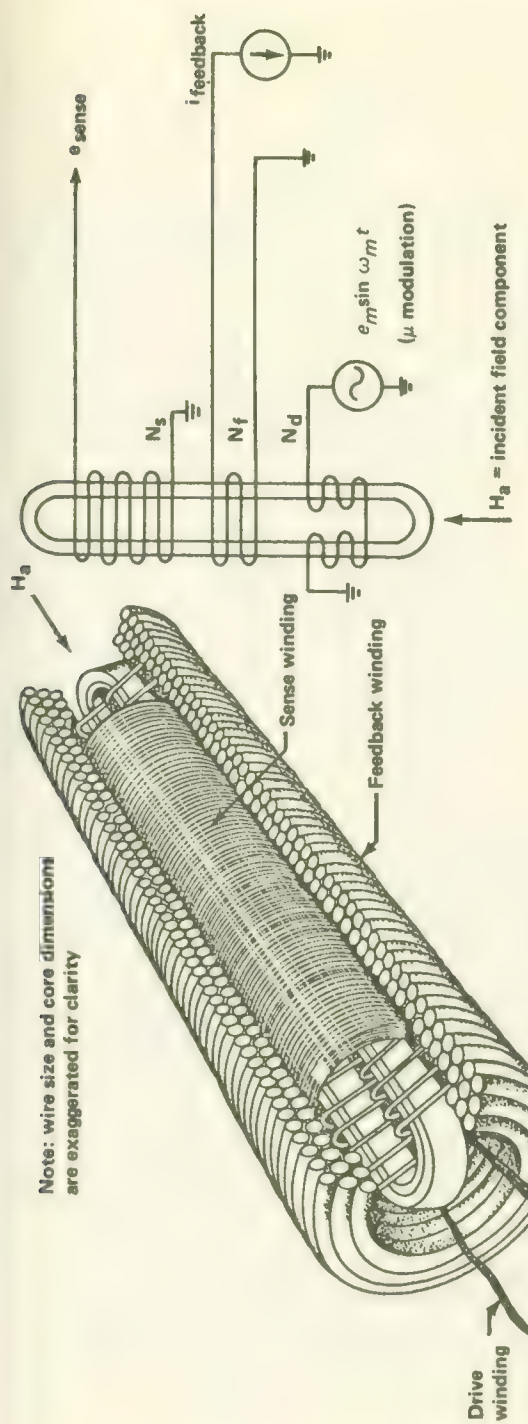


FIGURE 5-3.—Construction of the Ames fluxgate sensor.

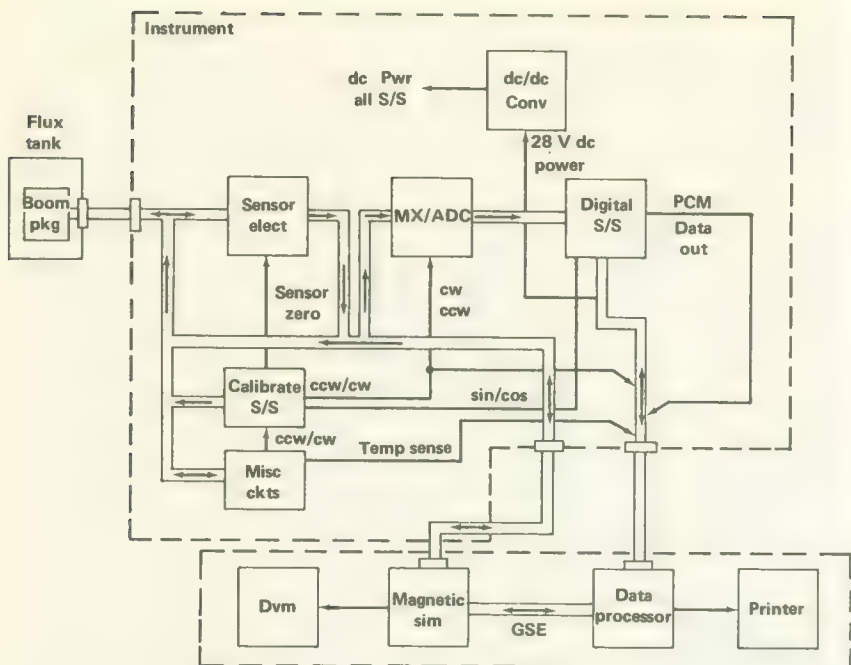


FIGURE 5-4.—Simplified block diagram of the Ames fluxgate magnetometer.

periodic measurement of the zero level of the sensor aligned with the spacecraft spin axis.

The overall instrument parameters—as originally specified and ultimately attained—are presented in table 5-3. The table indicates a change in dynamic range from  $\pm 200\gamma$  to  $\pm 50\gamma$  after it became apparent from deep space measurements from the Mariners and Block-I Pioneers that  $\pm 50\gamma$  was more than adequate.

The Ames magnetometer was designed and fabricated by Philco-Ford's Space and Reentry Systems Division. The contract was awarded by NASA in December 1965. The memory system was procured from Electronic Memories, Inc.; the fluxgate sensors were supplied through NASA from Honeywell, Inc. The initial program goal was the provision of a flight-qualified instrument for Pioneer 8 but this date could not be met. As a consequence, the Goddard magnetometer flew on Pioneer 8, and the Ames instrument was deferred to Pioneer 9.

#### MIT FARADAY-CUP PLASMA PROBE (PIONEERS 6 AND 7)

By 1965, plasma probes flown on several Earth satellites and planetary probes had confirmed that the interplanetary plasma originates in the Sun's corona and flows outward toward the planets at about 300 km/sec,

TABLE 5-3.—*Ames Magnetometer Specifications*

| Parameter                  | Specifica-<br>tion | Design<br>value       | Realized parameters |                         |                         |
|----------------------------|--------------------|-----------------------|---------------------|-------------------------|-------------------------|
|                            |                    |                       | Proto-<br>type      | Flight<br>unit<br>no. 1 | Flight<br>unit<br>no. 2 |
| Weight (lb)                |                    |                       |                     |                         |                         |
| Boom package               | 0.7                | 0.85<br>( $\pm 0.1$ ) | 0.815               | —                       | 0.837                   |
| Instrument                 | 4.6                | 6.8<br>( $\pm 0.3$ )  | 5.85                | 5.79                    | 5.87                    |
| Power requirement (W)      |                    |                       |                     |                         |                         |
| Normal                     | 3.0                | 5.6                   | 5.72                | 5.5                     | 5.3                     |
| Calibrate                  | —                  | 8.0                   | 9.16                | 8.7                     | 8.65                    |
| Flip calibrate             | 6.36               | 8.3                   | 8.24                | 8.3                     | 7.8                     |
| Reliability prediction     | 0.75               | @10 000 hr            |                     |                         |                         |
| Instrument dynamic range   |                    |                       |                     |                         |                         |
| Prototype and flight no. 2 | $\pm 50\gamma$     | $\pm 50\gamma$        |                     |                         |                         |
| Flight no. 1               | $\pm 200\gamma$    | $\pm 200\gamma$       | $\pm 50\gamma$      | $\pm 200\gamma$         | $\pm 50\gamma$          |
| Resolution                 |                    |                       |                     |                         |                         |
| Prototype and flight no. 2 | $\pm 0.05\gamma$   | $\pm 0.05\gamma$      | $\pm 0.05\gamma$    | $\pm 0.2\gamma$         | $\pm 0.05\gamma$        |
| Flight no. 1               | $\pm 0.02\gamma$   | $\pm 0.2\gamma$       |                     |                         |                         |
| Repeatability              | $\pm 0.2\gamma$    | $\pm 0.1\gamma$       | $\pm 0.2\gamma$     | $\pm 0.2\gamma$         | $\pm 0.1\gamma$         |
| Accuracy (percent)         | $\pm 0.35$         | $\pm 0.35$            | $\pm 0.5$           | $\pm 0.5$               | $\pm 0.35$              |
| DC offset                  | $\pm 0.2\gamma$    | —                     | $0.3\gamma$         | $\pm 0.4\gamma$         | $\pm 0.4\gamma$         |
| Step response (percent)    | <1                 | —                     | 1                   | 1                       | <1                      |
| Cross coupling             | < $2\gamma$        | —                     | < $2\gamma$         | < $2\gamma$             | < $2\gamma$             |

remaining ionized out to several AU. Further, this plasma is electrically conducting and interacts in complex ways with solar and planetary magnetic fields. The scientific objective of the MIT plasma probes was to measure the following characteristics of this interplanetary plasma:

- (1) Positive ion flux as a function of energy and direction
- (2) Electron flux as a function of energy and direction
- (3) The temporal and spatial variations of the above physical quantities
- (4) Correlation of plasma measurements with magnetic field measurements

MIT scientists had flown Faraday-cup plasma probes on the IMP and OGO series of Earth satellites prior to the Pioneer 6 and 7 flights. The Pioneer instruments were basically similar to these flight-proven plasma probes. The Pioneer sensors, the Faraday cups, are 6 in. in diameter, with the open sides normal to the spacecraft spin axis so that they sweep out the plane of the ecliptic as the spacecraft spin (ref. 5). At the bottom of the cup, two halves of a split collector intercept those electrons and positive ions that are able to pass through a modulator grid which electrically

sorts out the particles in the external plasma according to species and energy. The split in the collector is parallel to the spacecraft equatorial plane to provide directional information about the plasma fluxes in the meridian plane.

The energy spectra of the plasma ions and electrons are measured by applying square waves at different voltage amplitudes to the modulator grid directly in front of the split collector. For example, an 1800-Hz square wave varying between  $V_1$  and  $V_2$  admits only those particles in the plasma with energies between  $V_1$  and  $V_2$  electron volts. Further, the square wave modulates the stream of particles impinging on the collectors so that the currents collected and resultant signals delivered to the electronics section of the experiment varies at 1800 Hz, a signal that can be amplified and filtered conveniently. The amplitude of the square wave is varied between 100 and 10 000 V in 14 contiguous intervals to scan the positive ion spectrum and between 100 and 2000 V in four intervals for the electron spectrum.

The instrument's sensor is sampled once during each of the 32 equal  $11.25^\circ$  angular increments that the Faraday-cup sees in one complete rotation of the spacecraft. Since the interplanetary plasma flows outward from the Sun, samples from the eight segments within  $\pm 45^\circ$  of the Sun line are always used to make up a data frame. Five additional samples taken during a spacecraft revolution complete the 13 data samples that comprise the "fine" measurements. Each of these represents the highest flux measurement from the four ( $11.25^\circ$ ) segments in each of the five ( $45^\circ$ ) sectors comprising the remainder of the complete rotation. Although all 32 ( $11.25^\circ$ ) segments are examined during each rotation, only 13 plasma measurements are recorded. The 13 samples are then digitized as six-bit words and stored temporarily in a core memory with a 256-word capacity.

During each complete spacecraft revolution, the square-wave amplitude is held constant. Then, the entire sampling procedure is repeated—on alternate revolutions of the spacecraft—for another square-wave amplitude, until all of the 14 positive ion and one of the four electron energy groups have been scanned at all azimuths. Instrument calibration and engineering data are placed in the core during a sixteenth revolution. During the other sixteen interlaced revolutions, no data are taken; rather, the square-wave amplitude is changed during these revolutions. Thus, a complete data "mode" requires 32 spacecraft revolutions. All 14 positive ion-energy groups are scanned each revolution, but the four electron-energy groups are subcommutated, with a different group being scanned during each data-taking revolution (fig. 5-5).

During the sampling procedure described above, the currents measured by the two halves of the collector are summed to make the basic data words. These words represent the instrument's "fine" data, but, because

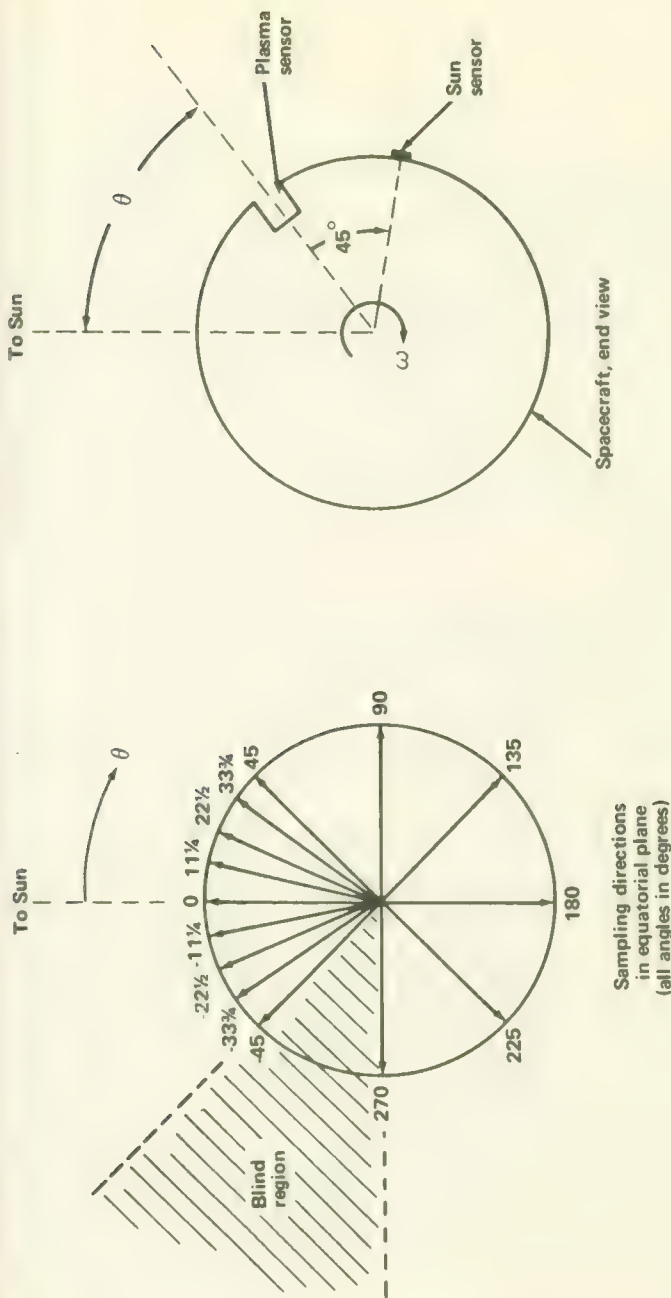


FIGURE 5-5.—Sampling interval of the MIT plasma probe.

of the summing operation, fine data indicate plasma characteristics only in the spacecraft equatorial plane. "Coarse" data are obtained by processing the current collected by a single half of the split collector. The largest of the 32 measurements taken from this collector during a spacecraft revolution comprises the coarse data word. Comparison of coarse and fine data words yields a measure of plasma direction in the spacecraft meridian plane; that is, the shadowing effect of the Faraday-cup walls combined with the view angles of the split collectors permits some coarse resolution of plasma fluxes arriving from above and below the plane of the ecliptic.

To summarize, a complete data mode of 256 words consists of 15 frames made up of 13 fine data words, 1 coarse data word, 1 coarse angle word (indicating which of the 32 angular segments provided the coarse data word) and 1 high voltage calibration word. The sixteenth frame comprises 16 words of engineering data. When the 256-word memory is completely filled—as it is at the end of a data mode—power is shut off to portions of the electronics, and the entire memory is read out to the spacecraft data handling subsystem. Then a new mode begins. The power drain of the MIT plasma probe therefore varies in a cyclic fashion, as mentioned in the last chapter.

The block diagram of the electronic circuits required to accomplish the experiment's formidable switching tasks is shown in figure 5-6.

Angular resolution of the MIT instrument is better than  $5^\circ$  in the equatorial plane of the spacecraft, which is approximately parallel to the plane of the ecliptic. The useful flux range is between  $10^6$  and  $4 \times 10^9$  singly charged particles per  $\text{cm}^2$  per sec.

#### AMES PLASMA PROBE (PIONEERS 6, 7, 8, 9, AND E)

When the angular distributions of the ions and electrons comprising the interplanetary plasma are not well known, the response of the Faraday-cup probe is often hard to interpret. The so-called curved-surface electrostatic plasma analyzers provide more detail, but they are correspondingly more complex. Plasma analyzers work on a different principle. They separate the plasma components into different energy-per-unit-charge ( $E/q$ ) groups and also into much smaller solid angles. In other words, their  $E/q$  and solid-angle discriminations are better.

The theory of operation of the curved-surface plasma analyzers has been described in detail in other publications. They work by the application of stepped voltages to a pair of curved plates (fig. 5-7). Positively charged particles in the plasma are deflected toward one plate, negatively charged particles toward the other. Depending upon the voltage difference across the plates, only those particles within a narrow range of energy-to-charge ratio and within a narrow solid angle will reach the particle collector at the end of the curved plates. In effect, the curved plates form a filter that

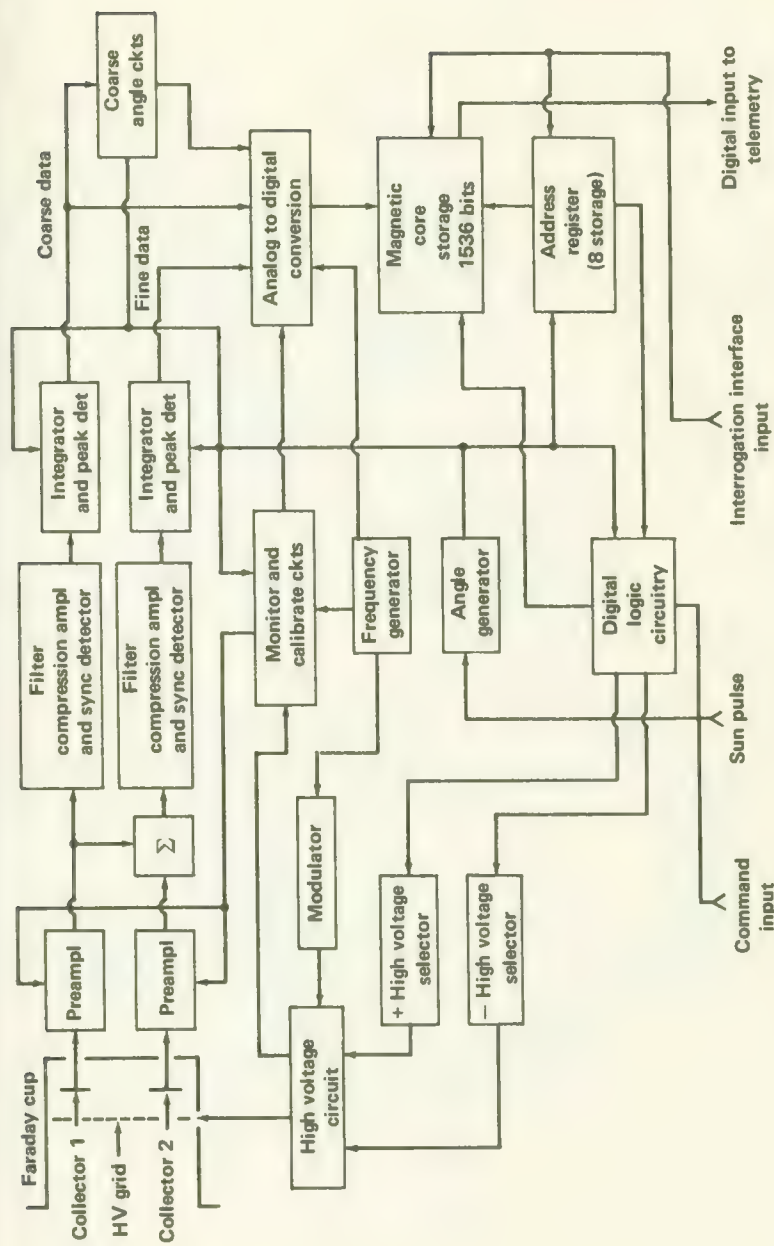


FIGURE 5-6.—Block diagram of the MIT plasma probe.

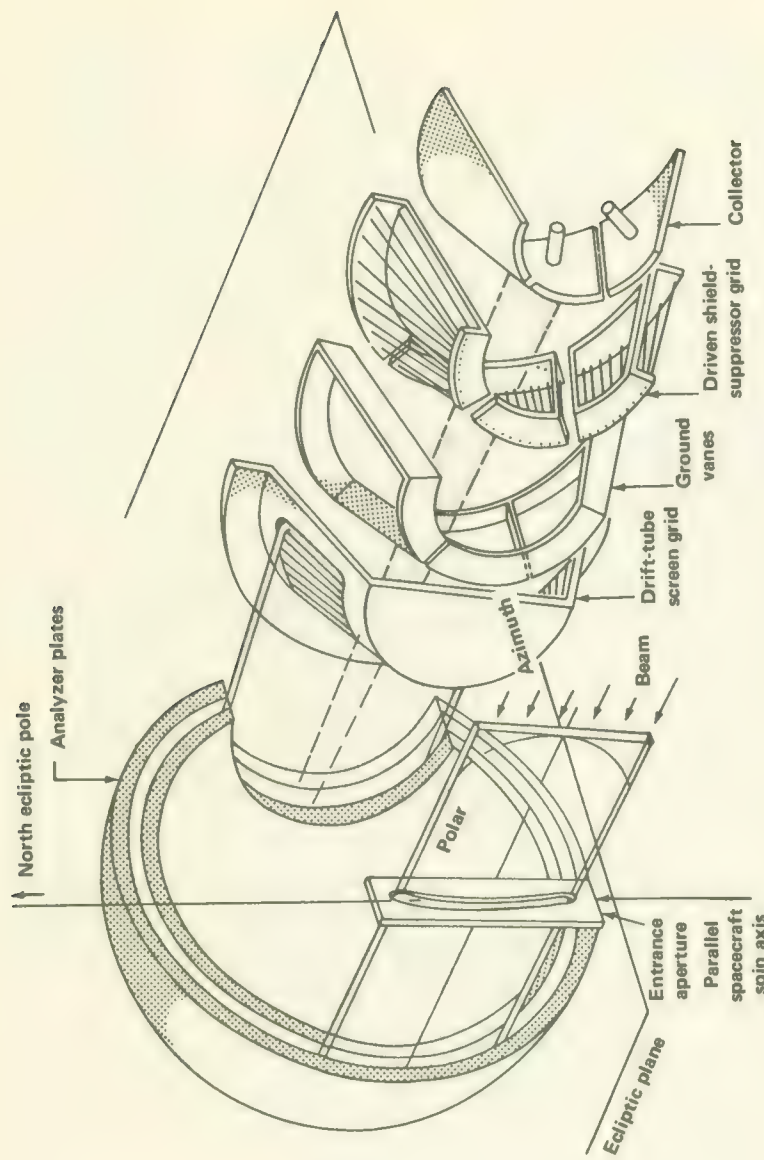


FIGURE 5-7.—Arrangement of the electron optics in the Block-II Ames plasma probe.

passes only a certain range of energy-to-charge ratios. If the plates are made portions of spherical surfaces and the collectors are segmented, the plasma flux arriving from different directions can be analyzed. If the applied voltages are stepped, energy-to-charge spectrum scanning is possible. Through the use of a mass spectrometer as the particle detector, particles with different masses, but within the same energy-to-charge-ratio group, can be extracted, but this was not part of the Pioneer experiment.

When the Pioneer payload was being formulated, the Ames Research Center group had flown quadrispherical plasma analyzers on OGO 1 and the IMP Earth satellites and was therefore in a good position to propose the similar instruments for the Pioneer series.

Although their basic principles of operation were the same, the plasma analyzers flown on the Block-I Pioneer spacecraft were significantly different from those on Block-II spacecraft. These differences are summarized below:

#### Block-I Instruments

Quadrисpherical plates  
8 current collectors  
16 positive ion groups between 200 and 10 000 eV  
8 electron groups between 0 and 500 eV

#### Block-II Instruments

Truncated hemispherical plates  
3 current collectors  
30 positive ion groups between 150 and 15 000 eV  
14 electron groups between 12 and 1000 eV

#### **Block-I Instruments**

An entrance slit on the instrument face, figure 5-8, permits electrons and positive ions in the interplanetary plasma to pass into the space between the quadrисpherical plates. The amplitude and phase of the voltage applied to these plates are varied through 24 steps, dividing the plasma into the 16 positive ion and eight electron groups mentioned above. The ions and electrons that pass all the way around the curved plates are collected by eight identical targets located in a semicircle at the lower end of the quadrisphere. Each of the targets is connected to an electrometer amplifier. Currents detected by the instrument vary between  $10^{-14}$  and  $10^{-10}$  amperes. The magnitudes of the currents measured, when combined with the knowledge of the instantaneous position of the entrance slit with respect to the Sun line as the spacecraft spins, determine the angular distribution of the interplanetary plasma flux.

The basic timing signals for the instrument are the Sun pulses, which arrive approximately once per sec. A sector programmer locks onto the Sun pulse frequency and divides the interval between the pulses into 1024 equal segments. Sector pulses are then generated that divide the azimuthal

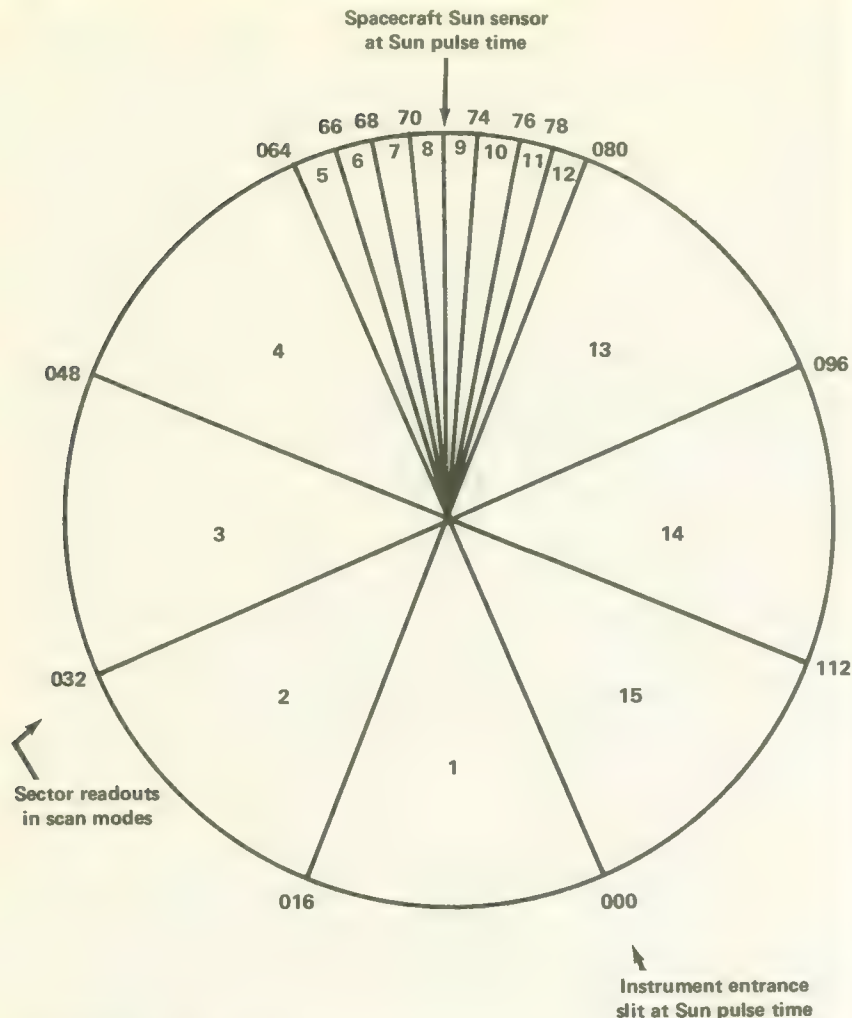


FIGURE 5-8.—Sector division and orientation for the Block-I Ames plasma probe.

plane into 128 equal segments and ultimately into the 15 sectors diagrammed in figure 5-8.

The Block-I instrument is capable of three separate modes of operation:

(1) Full Scan (FSM)—All 15 sectors are scanned during one spacecraft revolution at a specific energy step, for one specific collector. The second scan is at the same energy step and same collector but in the MFM mode described below. For the third scan the energy step is changed. The fourth scan is another MFM scan. This is repeated until all 24 energy steps have been utilized. Then, the process begins over again but for a different one of the eight collectors. This continues until all eight collectors (or channels)

have been measured for all 24 energy steps, in all 15 sectors. This mode is employed when the bit rate is 512 bits/sec. Spacecraft format A is used.

(2) Short Scan (SSM)—This mode is identical to the FSM mode except that only the eight small selectors clustered around the Sun line, as shown in figure 5-8, are read out. SSM is used at 256 bits/sec, format A.

(3) Maximum Flux (MFM)—In this mode, the eight collectors or channels are not scanned in sequence. The measurement read out in this mode is the maximum flux measured during each spacecraft revolution. The specific sector and channel where this measurement was made are identified in the telemetry. As with the other modes the plate voltage remains the same during each spacecraft revolution and is stepped when a new revolution commences. MFM is used at the 8, 16, and 64 bits/sec rates, format B.

### Block-II Instruments

The Block-II instrument configuration is basically hemispherical, with the entrance aperture defined by a slit, as shown in figure 5-7. A series of grids and ground vanes are interposed between the analyzer plates and the three current-collectors, which are located so that they can monitor particles arriving from above and below as well as from along the plane of the ecliptic. Fluxes within  $\pm 80^\circ$  of the plane of the ecliptic can be monitored. The detectable range of current is  $10^{-14}$  to  $10^{-9}$  amperes.

A sector programmer once again is employed to divide the time between Sun pulses into equal parts; 2048 timing intervals are used to divide the azimuthal plane into 128 equal sectors. During one of the scan modes, the 23 shaded sectors shown in figure 5-9 are selected for current measurements. Most of these favored sectors lie near the Sun line. A comparison of figure 5-8 with figure 5-9 shows the differences in sector widths, especially away from the Sun line.

The types of operation for the Block-II instrument differed markedly from those of Block I:

(1) Polar Scan (PS)—The instrument identifies the sector at which the flux amplitude is maximum during each spacecraft rotation. The fluxes are measured for each of the three collectors at this sector.

(2) Azimuthal Scan (AS)—Only the flux reaching the center collector is measured and, then, only at the 23 sectors defined in figure 5-9.

(3) Maximum Flux Scan (MFS)—Only the maximum flux seen by the center collector and the sector during which it occurs is measured.

When the spacecraft is close to Earth and the two highest bit rates can be used (512 and 256 bits/sec), polar and azimuthal scans are made alternately. One PS and one AS is made for each of the 30 high-voltage steps in each positive ion subcycle; 15 steps are used in the electron subcycle. A complete high-bit-rate cycle consists of seven ion subcycles followed by one electron subcycle.

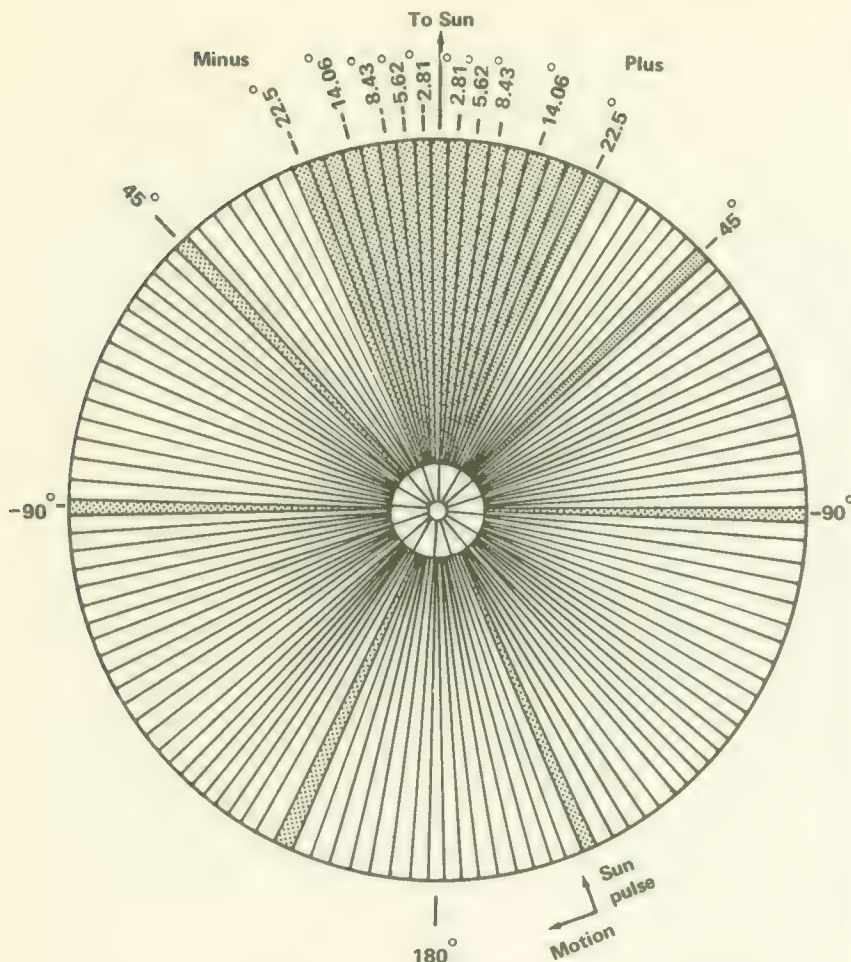


FIGURE 5-9.—Sector division and orientation for the Block-II Ames plasma probe.

At low bit rates (8, 16, and 64 bits/sec), an MFS is made for each of the 30 positive ion steps. Then, the voltage is set at the step where the maximum flux was detected, and one PS and one AS are made. In the electron mode, an MFS is made for each of the 15 levels followed by a PS and an AS as the voltage level of the seventh step. A complete low-bit-rate cycle also consists of seven ion subcycles followed by one electron subcycle.

A functional block diagram of the Block-II plasma probe is presented in figure 5-10 and the external view is shown in figure 5-11.

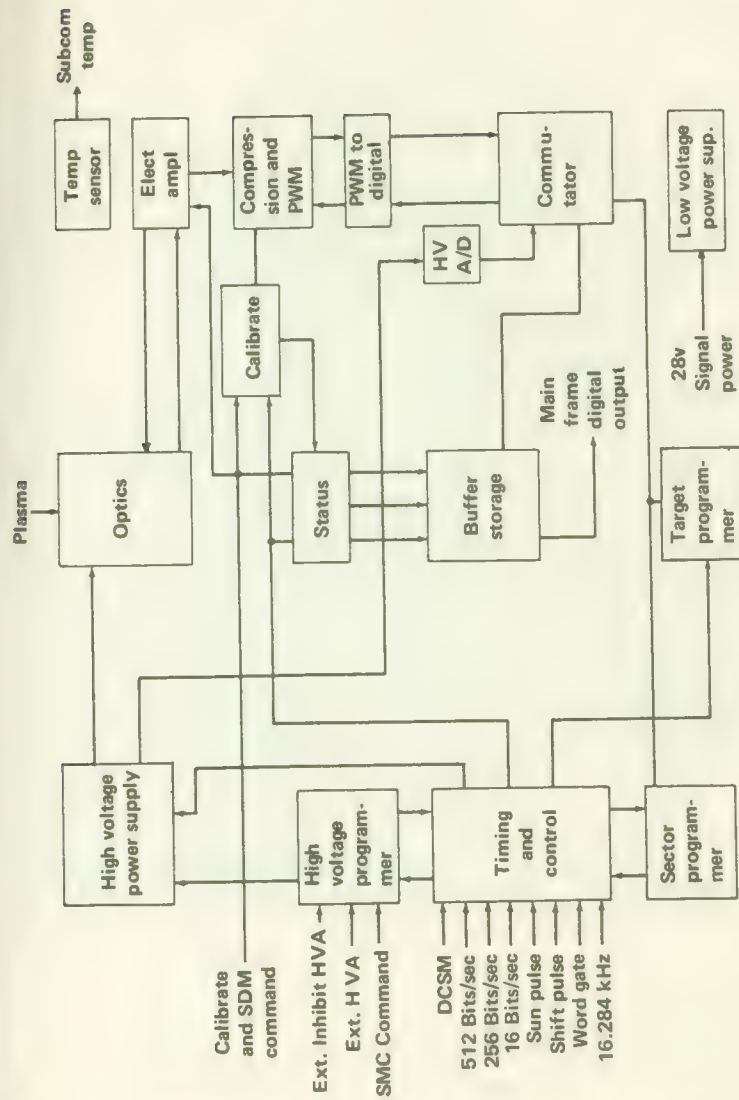


FIGURE 5-10.— Functional block diagram of the Block-II Ames plasma probe.

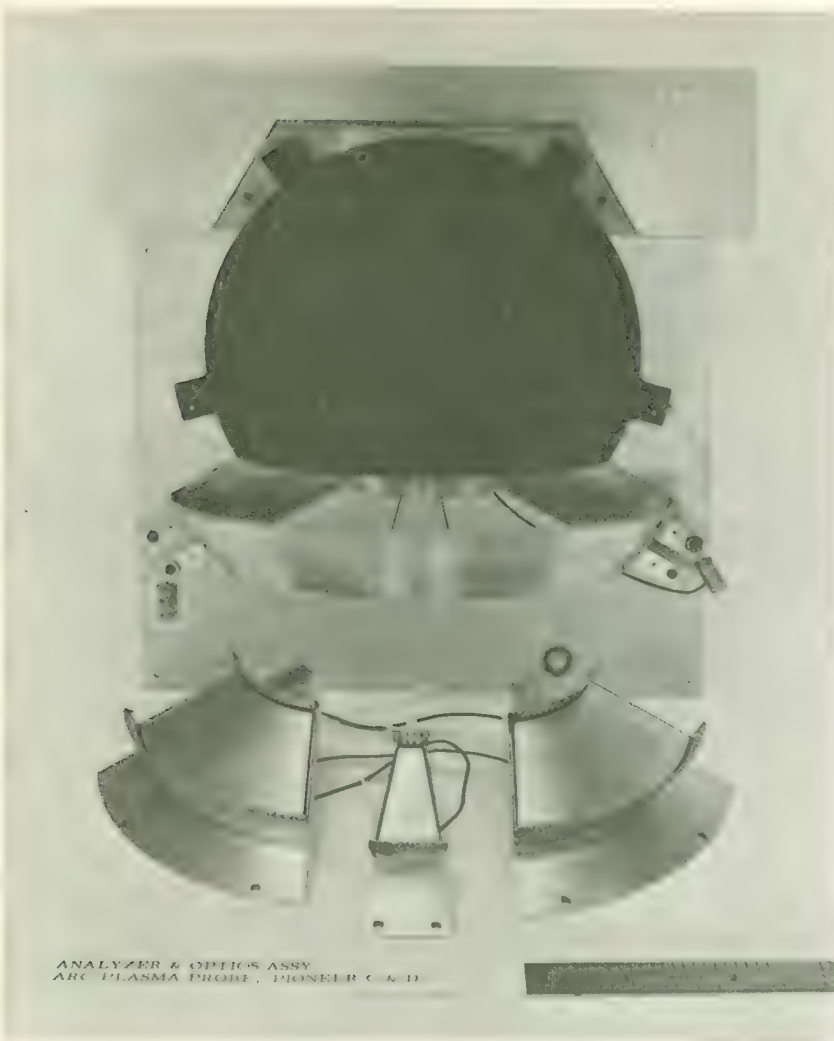
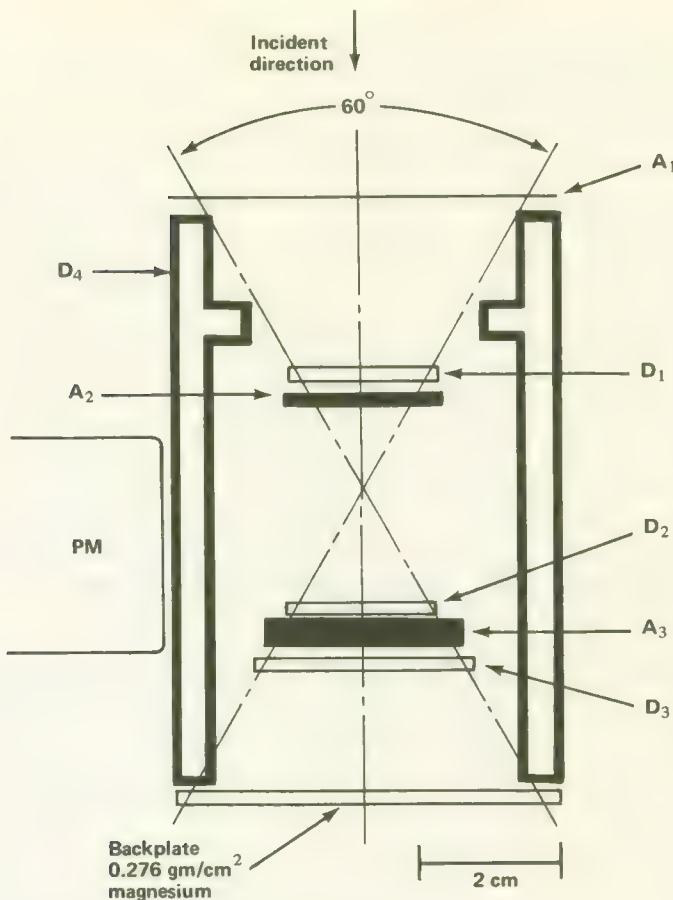


FIGURE 5-11.—External view of the Block-II Ames plasma probe.

#### THE CHICAGO COSMIC RAY EXPERIMENT (PIONEERS 6 AND 7)

The scientific objective of the Chicago cosmic ray experiment was the measurement of the heliocentric, radial gradient of the proton and alpha-particle fluxes in various energy ranges. Such information is useful in evaluating various models of the interplanetary magnetic field that modulates solar cosmic rays.

The basic instrument is a four element, solid-state, cosmic ray telescope

**Legend**

|                      |   |                      |   |
|----------------------|---|----------------------|---|
| <b>A<sub>1</sub></b> | Aluminized Mylar window 0.5 mg/cm <sup>2</sup>          | <b>D<sub>2</sub></b> | Lithium drift silicon detector 0.230 gm/cm <sup>2</sup> |
| <b>D<sub>1</sub></b> | Lithium drift silicon detector 0.122 gm/cm <sup>2</sup> | <b>A<sub>3</sub></b> | Platinum absorber 8.46 gm/cm <sup>2</sup>               |
| <b>A<sub>2</sub></b> | Aluminum absorber 0.103 gm/cm <sup>2</sup>              | <b>D<sub>3</sub></b> | Lithium drift silicon detector 0.22 gm/cm <sup>2</sup>  |
|                      |   | <b>D<sub>4</sub></b> | Plastic scintillator                                    |
|                      |   | <b>PM</b>            | Photomultiplier tube                                    |

FIGURE 5-12.—Arrangement of detectors and absorbers in the Chicago cosmic-ray telescope.

(fig. 5-12) (ref. 6). Three telescope elements (D<sub>1</sub>, D<sub>2</sub>, and D<sub>3</sub>) are lithium-drifted silicon-semiconductor wafers. These detectors are surrounded by a plastic scintillator (D<sub>4</sub>), which defines the 60° acceptance cone for incident charged particles. A photomultiplier tube monitors the plastic scintillator. The silicon wafers, and of course the photomultiplier tube, are all sensitive

to sunlight; this makes a light-tight enclosure a necessity. Particle absorbers between the telescope elements define the response of the elements to various particles at various energies.

The analysis of the pulses generated in the four telescope elements is complex, as indicated by the supporting electronic circuitry (figure 5-13). Ignoring for the moment the significance of pulses indicating the passage of particles from the four detectors, let us look at the 6 six-bit words that the experiment feeds into the spacecraft data handling subsystem. Five of these words are displayed on the main scientific data frames while the sixth appears twice in subcommutated scientific data (ch. 5). The Chicago experiment constructs six "spacecraft" words from five "experiment" words, which are labeled Aa, Ab, Ac, Ad, and Ae. The 18-bit word Ab is composed of three contiguous six-bit spacecraft words that are derived from the following experiment components: seven bits from the pulse-height analyzer associated with D1 and five bits from the D3 pulse-height analyzer; four more bits of information concerning the quadrant in which arriving particles were detected; one bit indicating the counting rate of coincidences from all four detectors (D1D2D3D4); and one bit showing whether the experiment is in a normal or calibrate mode.

Words Aa and Ac each contain three bits from each of the two counting-rate scalers that indicate counting rates for the following coincidence-anticoincidence situations:  $\overline{D1D2D4}$ ;  $D1\overline{D2D3D4}$ ;  $\overline{D1D2}\overline{D3D4}$ ; and  $D1\overline{D2}D3D4$ .<sup>17</sup> The sixth (six-bit) word is subcommutated twice and is labelled Ad and Ae. This word contains five bits of rate information for the four quadrants of spacecraft rotation for the  $D1D2\overline{D3D4}$  logic, plus a quadrant flag-indicator bit.

Now, consider particles entering the instrument through the solid angle defined by the plastic scintillator. The particles pass through D1, producing pulses with heights proportional to the amount of energy lost in transit through the silicon wafer. The energy-loss response of D1 is plotted in figure 5-14. The detectors D2 and D3 have the same general characteristics. Armed with knowledge of the energy-loss characteristics of the absorbers placed between D1, D2, and D3, and pulse-height analysis, the experimenters can deduce considerable information about the cosmic-ray environment seen by the instrument as it scans the plane of the ecliptic.

The energy-discriminating capabilities of the experiment (when pulse-height analysis is employed) are summarized below:

*For protons:* 6 to 8 MeV and 80 to 190 MeV

*For alpha particles:* 8 to 80 MeV per nucleon and 80 MeV per nucleon to relativistic energies

*For electrons:* 1 to 20 MeV in the mode  $D1D2\overline{D3D4}$  and in excess

<sup>17</sup> A bar over a detector designation signifies anticoincidence. For example  $D1\overline{D2}$  logic means that detector D1 detects a particle at a given instant in time but D2 does not.

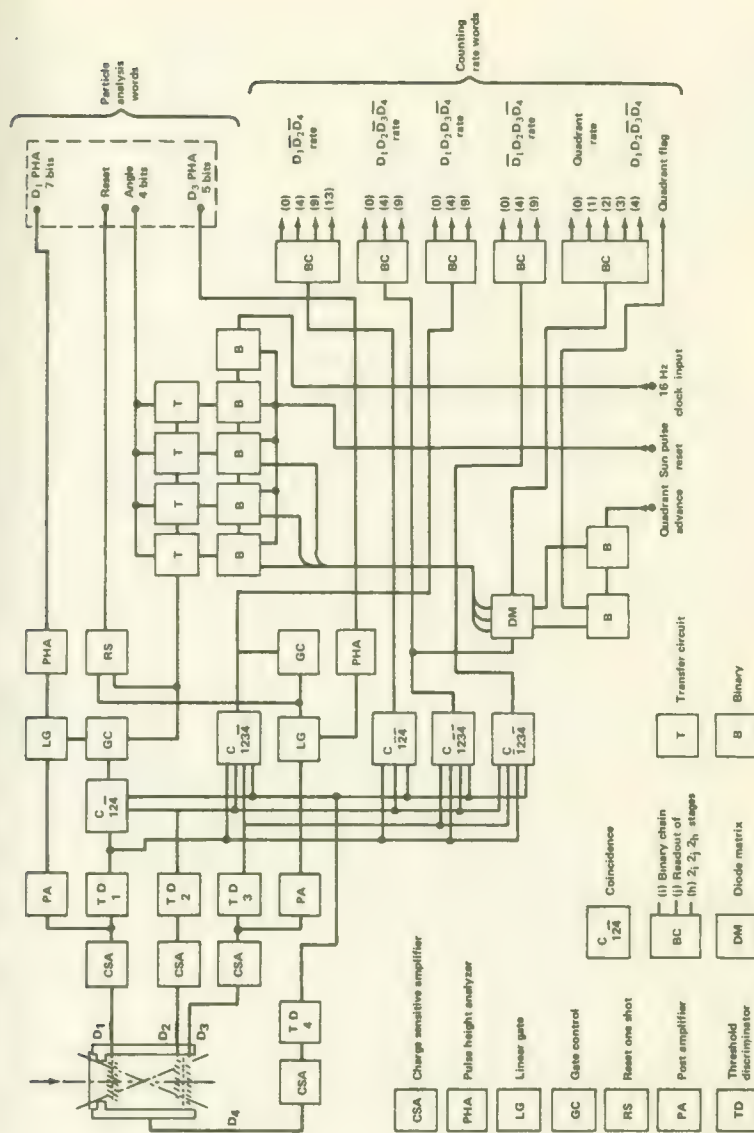


FIGURE 5-13.—Block diagram of the Chicago cosmic-ray telescope electronics.

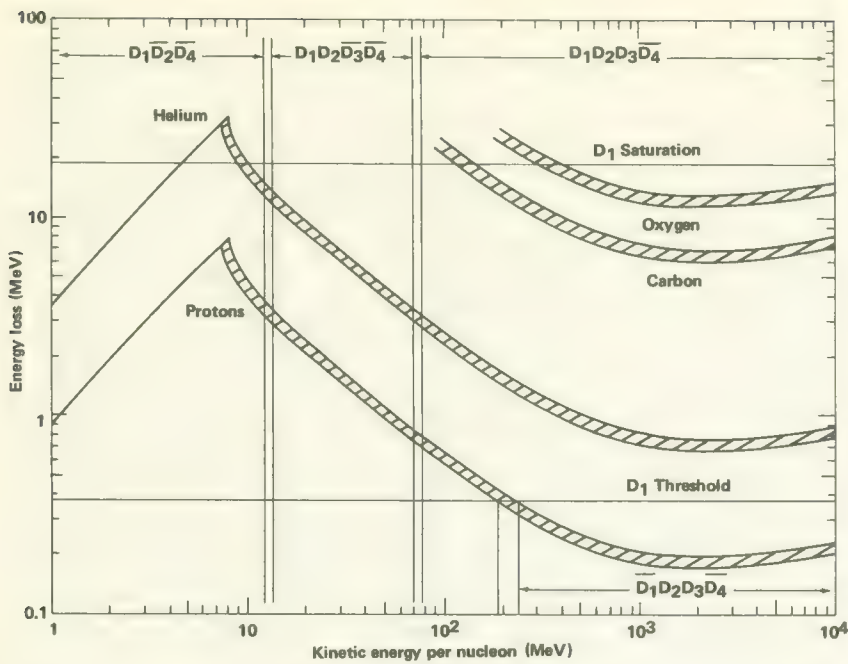


FIGURE 5-14.—D1 detector energy loss vs. particle energy, Chicago cosmic-ray telescope.

of 160 keV when D1 counts are considered alone. Electrons can be distinguished in the pulse-height analysis of D1 signals because they cause mainly low-amplitude pulses. Counting rates alone—that is, without pulse-height analysis—can also provide significant energy-and-particle discrimination in themselves. Two examples follow:

*For protons plus alphas:*

D1D2D4 logic provides counts in the 0.8 to 8 MeV per nucleon range.

*For protons and alphas:*

D1D2D3D4 logic yields counts between 8 and 80 MeV per nucleon.

The direction of particle arrival can be determined to within less than 60° with respect to the Sun line. As figure 5-9 indicates, the spacecraft Sun pulse signals are employed as references to establish the quadrant data mentioned above.

The final layout of the spacecraft instrument platform was such that the Chicago instrument was shadowed by the magnetometer boom. To compensate, the entire telescope assembly was rotated 10° with respect to the housing. The first instrument supplied to Ames was too heavy (by 300 g)

and also violated magnetic cleanliness specifications. Consequently, major redesign work was carried out at the University of Chicago in July 1964 to bring the experiment within specifications. Weight was shaved off the final design by such stratagems as the use of hollow mounting screws, the elimination of unused pins on plugs, and the milling of the magnesium structures.

An operational problem cropped up at Cape Kennedy because the Chicago experiment used—for the first time—large-area lithium-drifted silicon wafers, which required stringent humidity control. The experiment had to be flushed with dry nitrogen while it was on the launch pad at Cape Kennedy until the last possible moment. Ames Research Center provided the control system for the nitrogen flushing apparatus.

### THE GRCSW COSMIC RAY EXPERIMENTS (PIONEERS 6, 7, 8, 9, AND E)<sup>18</sup>

The Earth-based study of cosmic-ray anisotropy has always been hampered by the presence of the Earth's magnetic field and atmosphere. Even scientific satellites do not get far enough away from the Earth to avoid its magnetic field completely. The crucial test of one theory that describes the motion of cosmic rays within the solar system depends upon the careful measurement of cosmic-ray anisotropy at energies below 1000 MeV. For such measurements, the instruments must be carried well away from the Earth. The Pioneer probes were ideal for this purpose.

GRCSW instruments were part of all five Pioneer payloads, but those on Pioneers 8, 9, and E (Block II) represented a second generation of equipment (refs. 7 and 8). The later equipment was more sophisticated because additional low-energy measurements were made in, above, and below the plane of the ecliptic.

In both Block-I and Block-II generations of equipment, the principal cosmic-ray detector consisted of a flat cylindrical CsI(Tl)-scintillator crystal (detector C) contained within a cup-like cylindrical container of scintillating polytoluene (detector D), which functioned as a guard detector. On all five Pioneers the CsI(Tl) and plastic scintillators were connected in anticoincidence so that the detector was directional with an acceptance cone of about 107°. Particles with energies greater than 90 MeV/nucleon were also eliminated because, even if they entered the instrument's aperture, they passed right through the CsI(Tl) scintillator and activated the guard scintillator. Separate photomultiplier tubes watched the two scintillators (fig. 5-15). A 10-nanocurie americium-241 radioactive source was attached to each of the CsI(Tl) scintillators for purposes of

<sup>18</sup> GRCSW = Graduate Research Center of the Southwest; later renamed Southwest Center for Advanced Studies (SCAS) and now known as The University of Texas at Dallas.

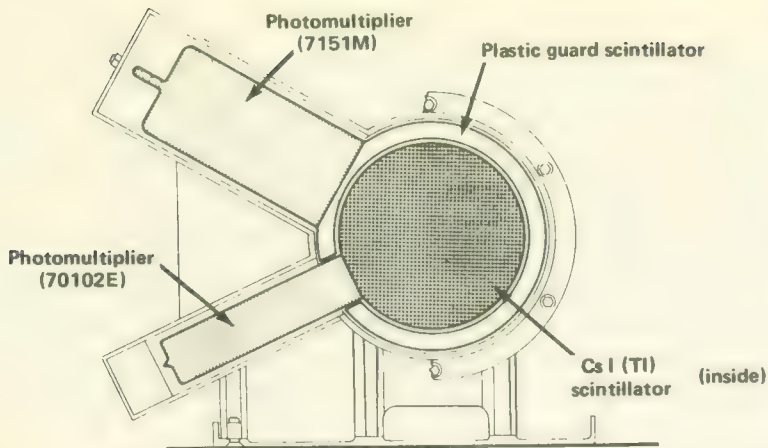


FIGURE 5-15.—Axial view of the GRCSW cosmic-ray telescope, Block-I Pioneers. The detector dimensions and positions were changed for the Block-II flights; see text.

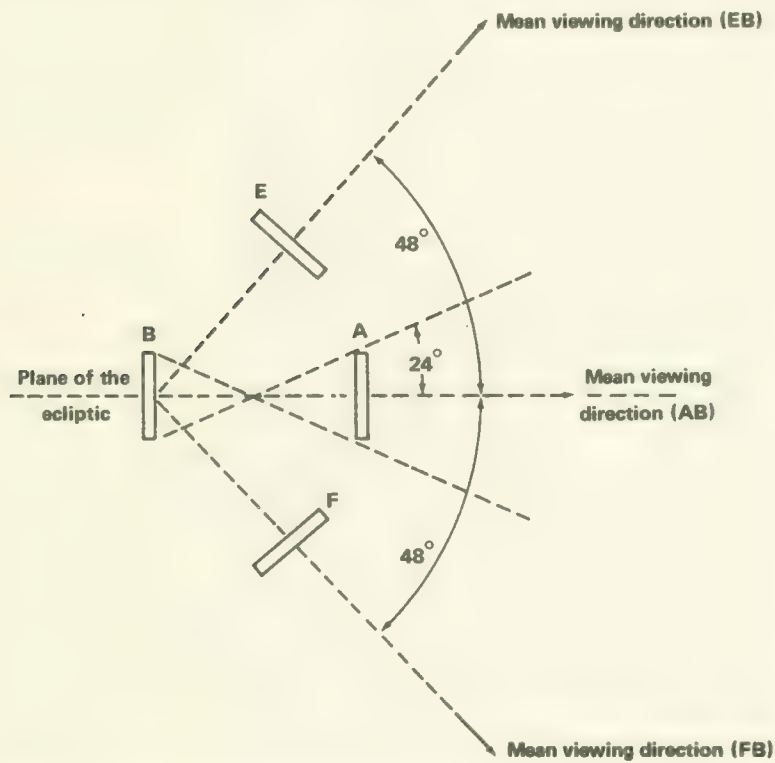


FIGURE 5-16.—Viewing angles of the Block-II GRCSW cosmic-ray experiment's solid-state detectors.

instrument calibration. Two sheets of 0.0005-in. aluminized-Mylar covered each plastic cup and protected the detectors from light, heat, and micro-meteoroids.

The same basic scintillator arrangement was employed for the Block-II flights, but it was supplemented with a three-way coincidence telescope consisting of four 100-micron, totally depleted silicon, surface-barrier detectors arranged and labeled as shown in figure 5-16. EB-coincidence logic counts particles within the energy range 0.5 to 5.0 MeV/nucleon arriving from  $48^\circ$  above the plane of the ecliptic. AB logic permits monitoring the plane of the ecliptic, while BF logic keeps track of particles arriving from  $48^\circ$  below the plane of the ecliptic.

The detectors scan the plane of the ecliptic as the spacecraft spins. In the Block-I instruments, additional directional discrimination is provided by four electronic quadrant gates ( $Q_1$ ,  $Q_2$ ,  $Q_3$ , and  $Q_4$  in fig. 5-17) which are opened by electronic gates in sequence during each revolution following a Sun pulse. Quadrants 1 and 3 look away from and toward the Sun, respectively; quadrants 4 and 2 look fore and aft along the spacecraft's orbit, respectively.

The goal of the experiments was the study of cosmic ray anisotropies as small as  $10^{-3}$  of the mean cosmic-ray flux. Consequently, the count-accumulation times for the four quadrant-registers had to be identical to at least one part in  $10^4$  to provide meaningful experimental results. A unique and critical part of the experiment, therefore, was the precision, crystal-controlled aspect clock that controlled the gating pulses.

The primary modes of operation of the Block-I experiment are listed below:

(1) Dynamic range off—The length of each of the four time periods is almost one-fourth of a spacecraft revolution. This is used when the Sun is relatively quiet.

(2) Dynamic range on—Each of the four periods is approximately  $\frac{1}{32}$  of a revolution. This is used when the Sun is active.

(3) Slip mode—The quadrant time periods are shifted by  $45^\circ$  to help obtain better angular resolution with only four basic time sectors. The slip mode was used only on Pioneer 7.

(4) Calibrate mode—The built-in americium-241 source was used to calibrate the instrument.

The desire for finer directional discrimination in the Block-II instruments led to the development of a more sophisticated method of scanning the azimuthal plane as well as the four surface-barrier detectors already mentioned. The electronic equipment supporting the Block-II instruments is correspondingly more complex (see fig. 5-18). Signals generated by the passage of cosmic rays in the six detectors are selected for pulse-height analysis by an array of linear switches. The pulse-height analyzers establish energy windows for the particle-produced signals. In the case of the ani-

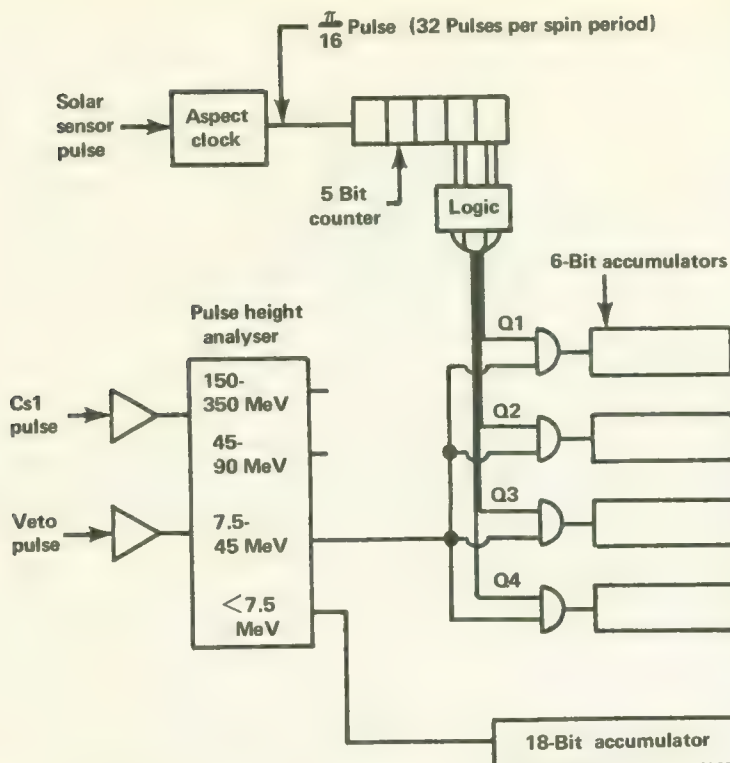


FIGURE 5-17.—Greatly simplified block diagram of the electronics associated with a single channel of the GRCSW cosmic-ray experiment, Block-I instruments only.

sotropy pulse-height analyzer, a pulse from detector B must fall within the energy window and also be coincident with a signal from A, E, or F. In this way, particles are divided into three groups that accumulate counts from particles arriving above, below, and within the plane of the ecliptic. The logic for detectors C and D is the same as it was for the Block-I instruments.

Rather than the Block-I approach to quadrant division—use of the Sun pulses and aspect clock—the Block-II experiments employ octant-division circuitry. An azimuth computer accurately divides the plane of the ecliptic into 32 equal parts plus a short “dead time” to allow for variations in the spacecraft spin rate. The slip mode used on Block-I Pioneers was not necessary because of the finer spatial discrimination of the Block-II electronics.

Five spacecraft telemetry words (a total of 30 bits) were assigned to the Block-II instruments. Nine bits were assigned to each of three experiment data accumulators. The remaining three bits were associated with the

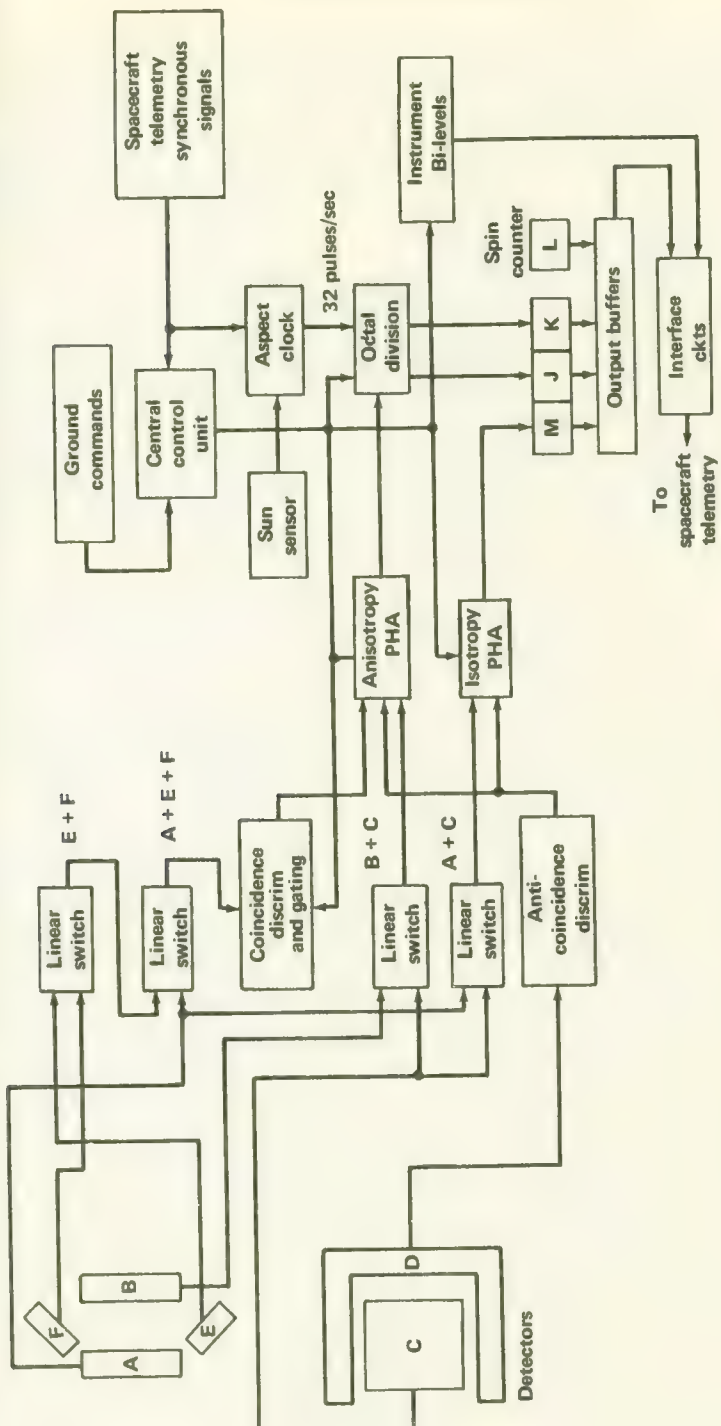


FIGURE 5-18.—Block diagram of the electronics associated with the Block-II GRCSW cosmic-ray experiment.

experiment's spin counter. To conserve power, the output buffer—a serial shift register—was limited to only 21 bits. During readout of the experimental data, as soon as 13 bits are shifted out of the buffer into the telemetry stream, nine bits from the isotropy data accumulator are dumped into the buffer to complete the 30-bit message. Because the experiment counting rate often exceeds the storage capacity of the nine-bit accumulators, a form of logarithmic storage was employed which allowed 2752 counts to be stored in the nine-bit format.

The additional sophistication of the Block-II instruments increased experiment weight from 4.4 to 5.6 lb; the average power drain went from 1.6 to 1.8 W. During the hardware development of the experiment, it was discovered that commercially supplied photomultiplier tubes normally contained so much magnetic Kovar alloy that the magnetic cleanliness standards could not be met. Tubes with the Kovar replaced by a nonmagnetic nickel alloy (Alloy 180) were built especially for the experiment. Standards could not be met. Special tubes with the Kovar replaced by a nonmagnetic nickel alloy (Alloy 180) were built especially for the experiment.

### MINNESOTA COSMIC RAY DETECTOR (PIONEERS 8, 9, AND E)

The Minnesota cosmic ray experiment had a purpose entirely different from that of the GRCSW instrument. The experiment objectives listed below reflect the lack of high precision cosmic ray experiments flown on spacecraft prior to the spring of 1964:

- (1) To measure the quiet-time energy spectrum of protons, alphas, and heavier nuclei up to a charge of 14 over a wide energy range with better energy and background discrimination than previously obtained
- (2) To measure the variations in these spectra, including the features of Forbush decreases as well as the 11-year variation during the solar cycle
- (3) To measure the radial and azimuthal cosmic-ray gradients existing in interplanetary space during quiet and disturbed periods on the Sun
- (4) To measure comprehensively the charge, isotropic composition, and energy spectrum of solar cosmic rays

The Minnesota instrument incorporates seven separate detectors (fig. 5-19), which are, in effect, electronically arranged into five different telescopes via commands from the Earth (ref. 9). Detector G is a two-piece guard counter made of Pilot B plastic; it is viewed by a photomultiplier tube. Detector D, at the bottom of the telescope, is a 1-cm-thick piece of synthetic sapphire and functions as a Cerenkov counter. Another photomultiplier tube views this detector. The remaining five detectors— $B_{1A}$ ,  $B_{1B}$ ,  $B_2$ ,  $B_3$ , and C—are all of the semiconductor type. The coincidence-anticoincidence conditions that electronically create five different telescopic arrangements are listed in table 5-4 along with the ranges and particles which they can detect.

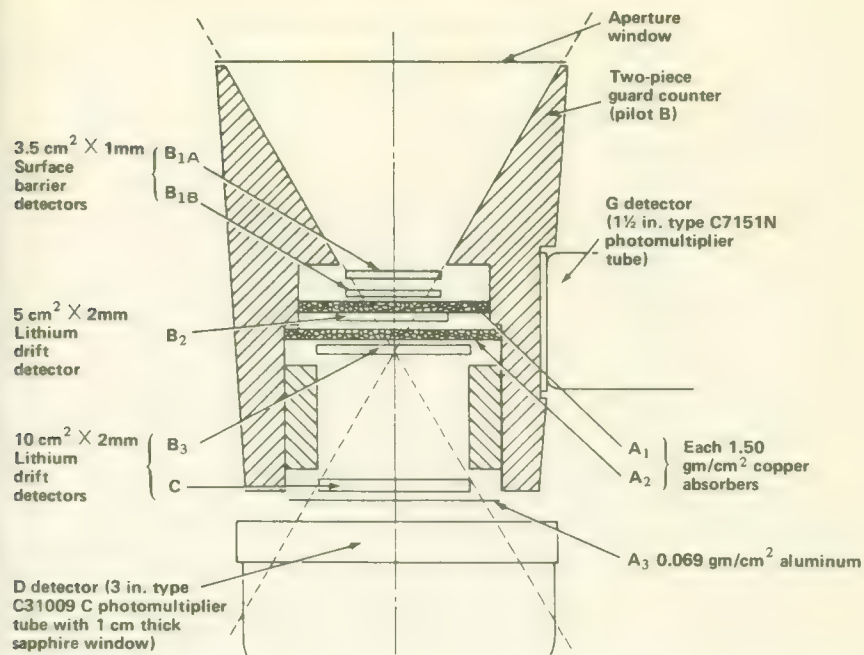


FIGURE 5-19.—Arrangement of detectors and absorbers in the Minnesota cosmic-ray telescope.

Telescope T5 is essentially omnidirectional and samples the particles in the cosmic-ray flux with energies greater than 14 MeV per nucleon. Electrons greater than 0.6 MeV are also detected. In telescope T4, however, the guard scintillator G is in anticoincidence and only particles entering the aperture are counted. Detector B<sub>2</sub> sets the range energy. The pulses from T4 are pulse-height-analyzed into nine energy groups. In telescope T3, the geometry is established by B<sub>1A</sub>, B<sub>1B</sub>, B<sub>2</sub>, and G. The energy range is set by detectors G and C. Here, the signals from B<sub>2</sub> and B<sub>3</sub> are summed and pulse-height-analyzed into three energy groups. Telescopes T1 and T2 are differentiated by the following condition: If D > B<sub>3</sub> - B<sub>1</sub>, the event is defined as a T1 event; if D < B<sub>3</sub> - B<sub>1</sub>, it is a T2 event. The reader is referred to Lezniak's thesis for details about all five telescopes (ref. 10).

Figure 5-20 presents a functional block diagram of the electronic circuitry supporting the experiment. The entire experiment weighed approximately 8.0 lb and required 3.1 W of spacecraft power.

### THE STANFORD RADIO PROPAGATION EXPERIMENT (PIONEERS 6, 7, 8, 9, AND E)

The Stanford experiment<sup>19</sup> measured the integrated electron density

<sup>19</sup> Actually a joint project of Stanford University and Stanford Research Institute.

TABLE 5-4.—*Minnesota Cosmic-Ray Telescope Arrangements*

| Telescope | Coincidence-anticoincidence requirements                           | Charge and energy ranges of the particles detected |   |
|-----------|--|--|---|
| T1, T2    | $B_{1A} \cdot B_{1B} \cdot B_2 \cdot B_3 \cdot C$                  | $Z \geq 1$   | $E \gtrsim 64$ MeV per nucleon  |
|           |  | $e^\pm$  | $E \gtrsim 8.4$ MeV   |
| T3        | $B_{1A} \cdot B_{1B} \cdot B_2 \cdot \bar{C} \cdot \bar{G}$        | $e^\pm$  | $4.2 \text{ MeV} \leq E \leq 8.4 \text{ MeV}$                           |
|           |  | ${}_1H^1$  | $39.6 \text{ MeV} \leq E \leq 64.3 \text{ MeV}$                         |
|           |  | ${}_2He^4$   | $39.4 \text{ MeV per nucleon} \leq E \leq 64.1 \text{ MeV per nucleon}$ |
| T4        | $B_1 \cdot \bar{B}_2 \cdot \bar{G}$<br>( $B_1 = B_{1A} + B_{1B}$ ) | $e^\pm$  | $0.34 \text{ MeV} \leq E \leq 4.3 \text{ MeV}$                          |
|           |  | ${}_1H^1$  | $3.5 \text{ MeV} \leq E \leq 39.7 \text{ MeV}$                          |
|           |  | ${}_2He^4$   | $6.6 \text{ MeV per nucleon} \leq E \leq 39.7 \text{ MeV per nucleon}$  |
| T5        | $B_{1A} \cdot B_{1B}$  | $Z \geq 1$   | $E \gtrsim 14$ MeV per nucleon  |
|           |  | $e^\pm$  | $E \gtrsim 0.6$ MeV   |

along the radio transmission path between the Earth and spacecraft (ref. 11). For successful operation the experiment required that a dual-channel, phase-locked-loop receiver in the spacecraft lock onto signals transmitted from the 150-ft parabolic antenna located on the Stanford campus. When the experiment is in progress, two modulated coherent carriers of approximately 49.8 and 423.3 MHz are sent to the spacecraft from the 150-ft Stanford antenna. The spacecraft receiver measures the relative phase change between the modulation envelopes. Since the higher frequency is relatively unaffected by the presence of ionization, the comparison provides the information needed to compute the integrated electron-number density, or the total number of electrons per square meter between Earth and spacecraft. The rate of phase change of one signal with respect to the other is also measured to very high precision to determine the time variation of the integrated electron number density. The experiment also measures the strength of the signals sent from Earth.

Both the 49.8- and 423.3-MHz transmissions to the spacecraft originate at the Stanford computer-controlled "Big Dish." The 49.8-MHz signal is fed to a crossed, folded dipole and a reflector that are located just below the focal point of the 150-ft dish (fig. 5-21). This signal is generated in a 300-kW linear amplifier transmitter. The high frequency signal, 423.3 MHz, is radiated directly from the horn of the dish. A 30-kW klystron transmitter generates the signal. Some additional transmitter information is listed in table 5-5.

The transmitting system block diagram (fig. 5-22) begins with the 1-MHz crystal oscillator common to both transmitted frequencies. The circuits

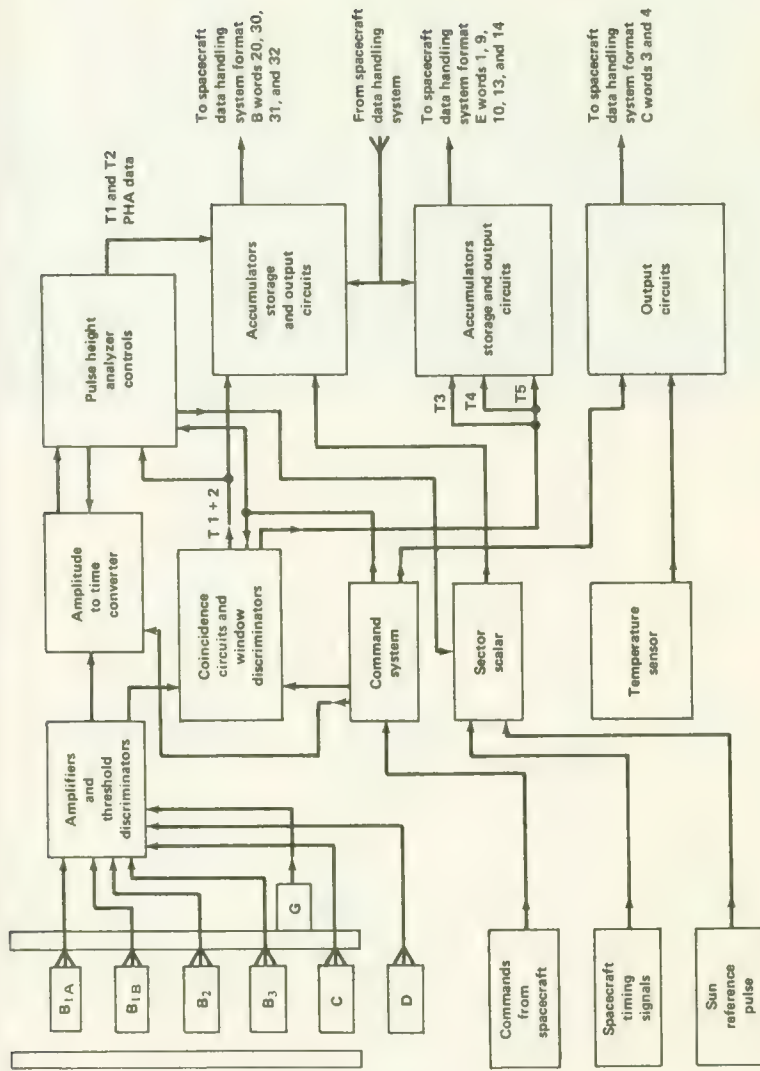


FIGURE 5-20.—Data flow diagram for normal-mode operation, Minnesota cosmic-ray experiment.



FIGURE 5-21.—The 150-ft dish at Stanford University, Palo Alto, Calif. This antenna is used in the radio propagation experiment.

TABLE 5-5.—*Stanford Experiment Transmitter Characteristics*

| Characteristic                            | Channel 1                            | Channel 2           |
|---|--------------------------------------|---------------------|
| Transmitter frequency                     | 49.8 MHz                             | 423.3 MHz           |
| Type of transmitter                       | Triode linear amplifier              | Klystron            |
| Power output for Pioneer experiment       | 300 kW<br>84.0 dBm                   | 30 kW<br>74.7 dBm   |
| Antenna type                              | 150-ft-diameter parabolic dish       |                     |
| Antenna gain, $\eta = 1$                  | 25 dB                                | 42 dB               |
| 3-dB beamwidth                            | 8.0°                                 | 1.2°                |
| Antenna efficiency, $\eta$ (est.)         | 0.50                                 | 0.50                |
| Polarization                              | Left-hand elliptical                 | Right-hand circular |
| Polarization loss                         | Varying with Faraday rotation        | 3 dB                |
| Area of receiving dipole on spacecraft    | 4.7 m <sup>2</sup>                   | 0.65 m <sup>2</sup> |
| Modulation frequency                      | 7.692 or 8.692 kHz                   |                     |
| Modulation phase                          | Continuously adjustable through 360° | Fixed               |
| Fraction of power in modulation sidebands | 0.5                                  | 0.5                 |

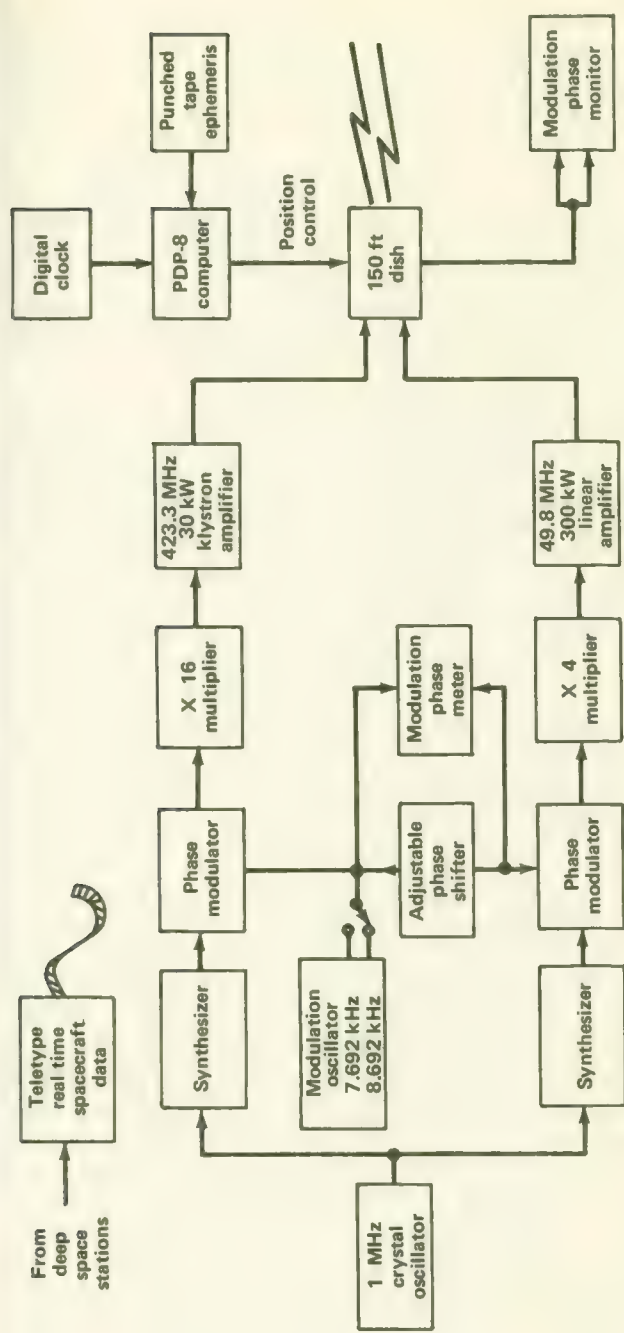


FIGURE 5-22.—Block diagram of the Stanford Earth-based transmitter used in the Pioneer radio-propagation experiment.

following then set the 423.3-MHz carrier at exactly 17/2 times the 49.8-MHz carrier. Both carriers are modulated at either 7.692 or 8.692 kHz for differential group path measurement. Real-time teletype data are sent to Stanford from the DSN showing the operating point of the spacecraft phase meter. This information is used to keep the spacecraft phase meter on its positive slope.

Both carriers from the Earth are received by the Stanford spacecraft antenna (fig. 5-23) and sent to the dual-channel receiver, which consists of two separate coherent phase-locked receivers (fig. 5-24). The main reasons for the phase-lock design are: (1) to increase the sensitivity of the receiver, and (2) to detect the difference in radio frequency cycles between the 49.8 MHz and the 2/17 harmonic of the 423.3-MHz carrier. Additional receiver data are presented in table 5-6.

Because the Stanford experiment must have transmitter operators at Stanford in the loop during its operation, real-time teletype data are relayed directly from JPL's SFOF to Stanford (ch. 8). Teletyped parameters include the modulation phase-difference measurements and the rf-difference counts. The Stanford operator uses this information to adjust the transmitter frequencies, powers, and modulation phase offset for best operation. At the experiment design range of 300 000 000 km, it takes about 33 min for the effects of transmitted changes to be seen in the teletype messages from JPL.

Minor changes were made in the experiment during the program and these are reflected in the slight weight change between Block-I and Block-II Pioneers. The spacecraft portion of the Stanford experiment weighed 6.0 and 6.3 lb for Blocks I and II, respectively. Power consumption was approximately 1.6 W for all flights.

#### THE TRW SYSTEMS ELECTRIC FIELD DETECTOR (PIONEERS 8, 9, AND E)

The Stanford and TRW Systems experiments are closely related. In fact, the TRW Systems experiment makes direct use of the Stanford antenna (ref. 12). The purpose of the radio propagation experiment—measuring integrated electron density over long distances—is essentially macroscopic in nature, whereas the TRW Systems experiment is microscopic in design. Its purpose is the detection of charge differences over small distances in interplanetary space through the electric fields they create along the Stanford antenna. Plasma waves and other cooperative actions in the 100- to 100 000-Hz vlf range of charged particles in collisionless interplanetary space can be detected with the instrument.

The decision to add the Electric Field Detector was made well after the Block-II payload was selected. Six spare words from the Pioneer telemetry format were made available. The weight, 0.9 lb, and power drain, 0.5 W,

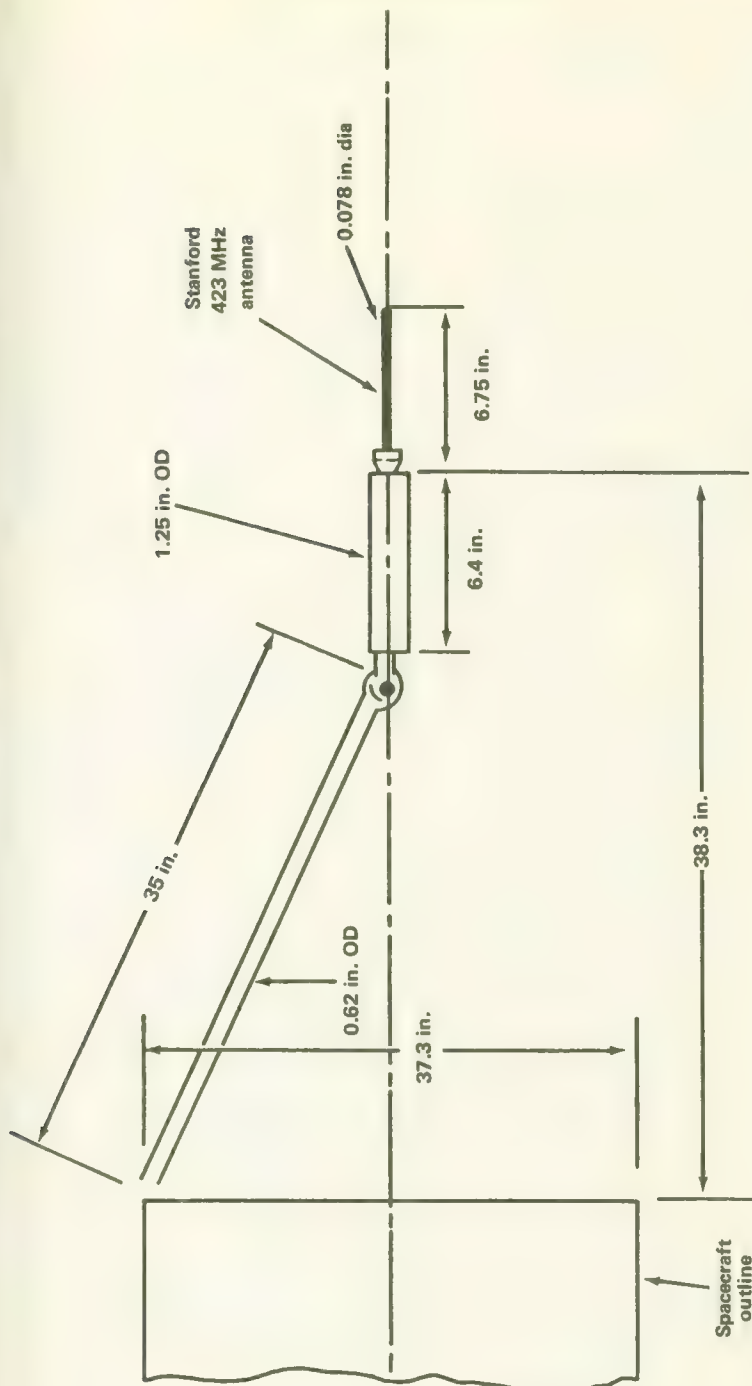


FIGURE 5-23.—Dimensions of the spacecraft antenna used in the Stanford radio-propagation experiment (not to scale).

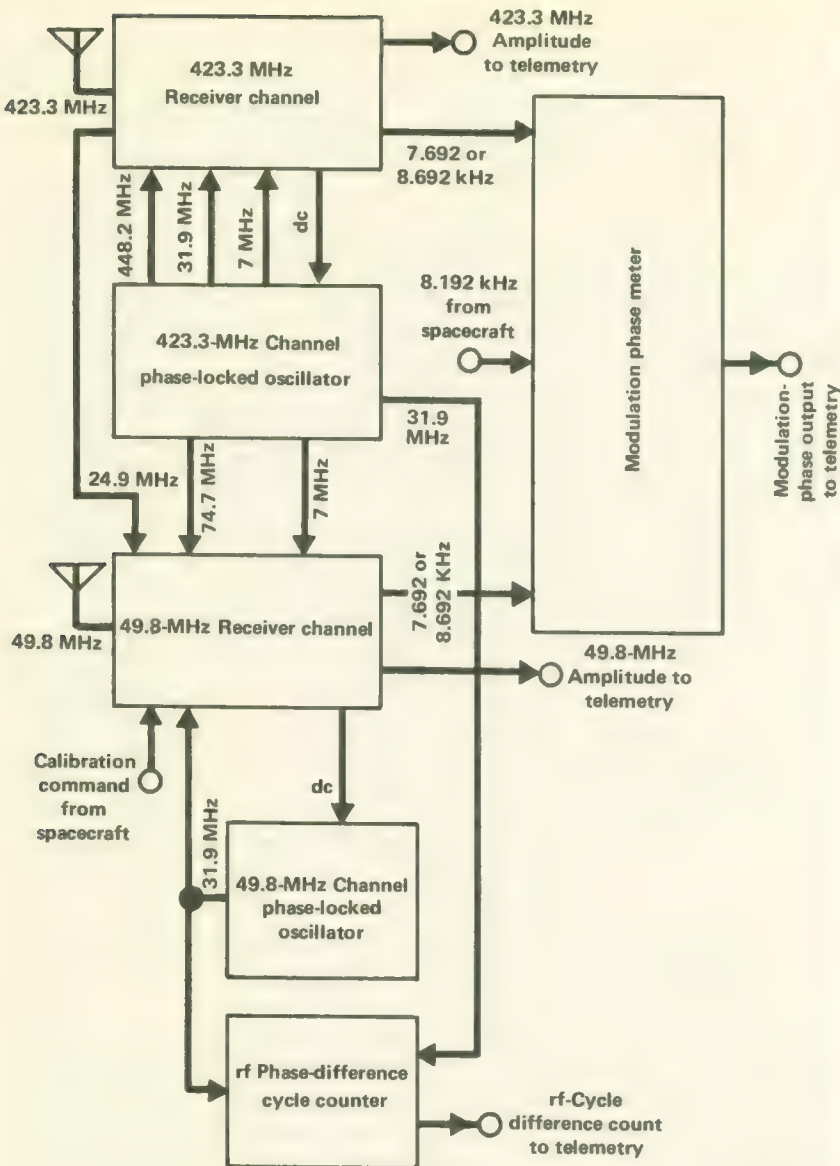


FIGURE 5-24.—Block diagram of the Stanford dual-channel spacecraft receiver.

made it possible to squeeze this experiment onto the spacecraft without major changes (particularly since it could use the Stanford antenna). In a sense, it is an addendum to the Stanford experiment, and it is often treated thus in the literature.

The electric field experiment makes use of the short (6.4 in.) 423.3-MHz

TABLE 5-6.—*Stanford Experiment, Receiver Parameters*

| Frequency  | 49.8 MHz           | 423.3 MHz  |
|--|--------------------|--|
| I.F. bandwidths  |                    |  |
| 3-dB bandwidth   | 40 kHz             | 40 kHz   |
| Noise bandwidth  | 45 kHz             | 45 kHz   |
| Receiver input noise (including image)                         |                    |  |
| Noise figure   | 3 dB               | 3 dB   |
| Noise temperature  | 300° K             | 290° K   |
| Cosmic noise (in a dipole with axis parallel to galactic axis) | 8000° K            | 100° K   |
| Spacecraft noise plus cosmic noise for Pioneer 7               |                    |  |
| Noise temperature  | 17 000° K          | 400° K   |
| Modulation frequencies for phase meter                         | 7.692 or 8.692 kHz |  |
| Modulation phase accuracy                                      |                    | Digitized to approximately 3.15° per digit; additional error estimated to be +2° |
| Differential phase path  |                    | Quantized to 1 Hz of rf phase difference at 49.8 MHz                             |

segment of the Stanford antenna (fig. 5-23) as a capacitively coupled sensor with which local plasma waves can be detected. The sensor is relatively insensitive, but adequate for the purposes of the experiment. A number of Earth satellites have carried similar vlf radio receivers for the same purpose.

The availability of only six subcommutated telemetry words restricted the experiment's capability to survey a wide range of plasma waves in interplanetary space. Even when the spacecraft transmits at the highest bit rate of 512 bits/sec, the TRW Systems experiment sends only two words every 7 sec, and the four others every 28 sec. The portion of the wave spectrum to be studied was selected carefully in advance on the basis of limited knowledge of plasma waves in space. The high frequency channel selected was at 22 kHz for Pioneer 8 and 30 kHz for Pioneers 9 and E. The low frequency channels were at 400 Hz and 100 to 100 000 Hz (for the broadband survey) on all Block-II spacecraft.

Referring to the experiment block diagram, figure 5-25, the two band-pass channels are sampled every seven seconds when the spacecraft transmits at 512 bits/sec. The remaining four telemetry words carry data from the broadband portion of the broadband pulse-height experiment. As analysis proceeds, positive pulses per unit time that exceed preset trigger levels are counted. The trigger level is changed in a programmed sequence of 16 or 8 steps. (See table 5-7 for differences between Pioneer 8 and 9 instrumentation.) The pulse-frequency count is read out before the trigger level is changed to the next step. At the 512 bits/sec rate, the entire broad-

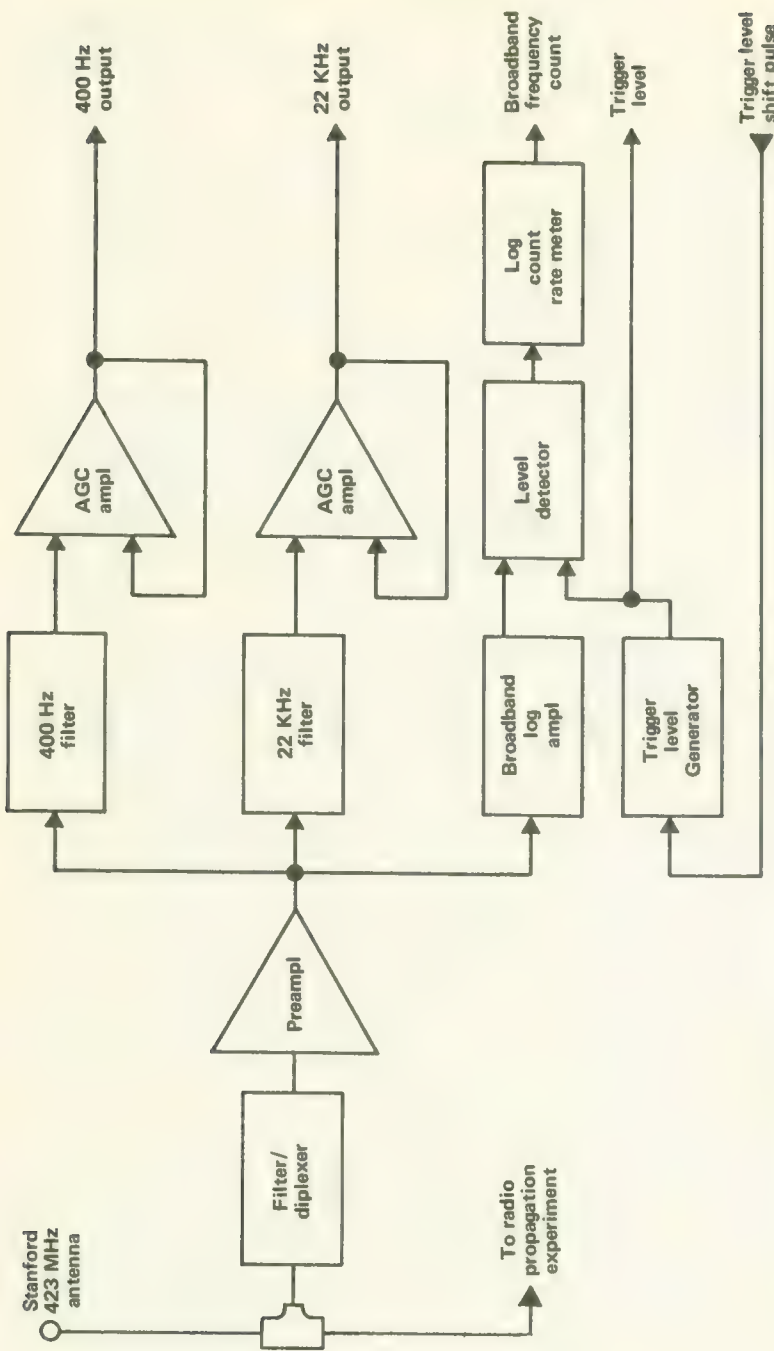


FIGURE 5-25.—Block diagram of the TRW Systems electric-field instrumentation, showing the use of the Stanford antenna.

TABLE 5-7.—*Differences Between TRW Experiments*

| Difference                                     | Pioneer 8                   | Pioneers 9 and E         |
|--|-----------------------------|--------------------------|
| Engineering words for frequency count-----     | 2                           | 4                        |
| Engineering words for step number-----         | 2                           | 1                        |
| Number of steps-----                           | 16                          | 8                        |
| Frequency readings before step is changed----- | 2                           | 1                        |
| Time for broadband scan-----                   | 7.47 min for<br>16 channels | 56 sec for<br>8 channels |

band scan is repeated every 7.47 min on Pioneer 8 and every 56 sec on Pioneer 9.

### THE GODDARD COSMIC DUST EXPERIMENT (PIONEERS 8, 9, AND E)

As related at the beginning of this chapter, no cosmic dust experiments were initially proposed for the Block-II Pioneers, and the Block-I experiment proposed by Ames Research Center was not far enough along in development to make the Block-I flights. The Block-II Goddard cosmic dust experiment described below is the result of a specific solicitation of likely experimenters in this field by NASA Headquarters. The following discussion is adapted from Berg and Richardson (ref. 13).

The experiment objectives were four in number:

- (1) To measure the cosmic-dust density in the solar system well away from the Earth
- (2) To determine the distribution of cosmic-dust concentrations (if any) in the Earth's orbit
- (3) To determine the radiant flux density and speeds of particles in meteor streams
- (4) To perform an in-flight determination of the reliability of the microphone as a cosmic-dust detector

The last objective reflected the growing disenchantment with microphone micrometeoroid detectors due to the possibility of spurious data arising from thermal effects in Earth orbit.

The instrument consists of two film-grid sensor arrays spaced 5 cm apart, followed by an acoustical impact plate (microphone) upon which the last film is mounted. Three types of cosmic dust particles were considered in the design of the experiment:

- (1) High-energy, hypervelocity particles ( $> 1.0 \text{ erg}$ )
- (2) Low-energy, hypervelocity particles ( $< 1.0 \text{ erg}$ )
- (3) Relatively large high-velocity particles ( $> 10^{-10} \text{ grams}$ ).

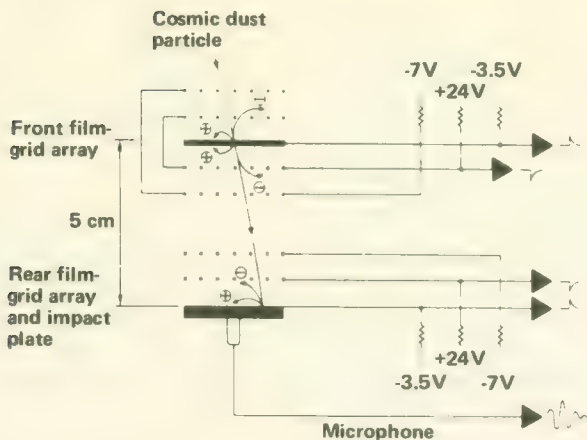


FIGURE 5-26.—Schematic diagram of the Goddard micrometeoroid sensor.

As a *high-energy, hypervelocity particle* pierces the front film sensor (fig. 5-26), some of its kinetic energy generates ionized plasma at the front, or "A" film. The electrons in the plasma are collected on the positively biased grid (+24 V); this creates negative pulses, as shown. The positive ions in the plasma are collected on the negatively biased film (-3.5 V); this produces a positive pulse that is pulse-height-analyzed to measure the particle's kinetic energy. The same thing occurs at the rear sensor, or "B" film; this generates a second set of plasma pulses. Impact on the plate produces an acoustical pulse. A peak-pulse-height analysis is performed on the acoustical sensor output as a measure of the particle's remaining momentum.

A *low-energy, hypervelocity particle* will yield all of its kinetic energy at the "A" film. A pulse-height analysis measures the particle's kinetic energy. A high-energy hypervelocity particle may be erroneously registered as a low-energy hypervelocity particle if, because of its angle of entry, it fails to hit the "B" film. If a *relatively large, high-velocity particle* enters, it may pass through the front and rear film arrays without generating detectable plasma because of its relatively low velocity; but it may still impart a measurable impulse to the acoustical sensor. An electronic "clock" registers the times of flight of particles. The time lapses between positive pulses from the "A" and "B" films are used to derive particle speeds.

The time-of-flight sensor is one of 256 similar sensors that comprise the portion of the Pioneer instrument measuring particle speed and direction. Figure 5-27 is an exploded schematic view of the overall experiment. It shows the four vertical film strips crossed by four horizontal grid strips that create 16 front and 16 rear film sensor arrays (each  $2.5 \times 2.5$  cm) or 256 total combinations. Each grid strip and film strip connects to a

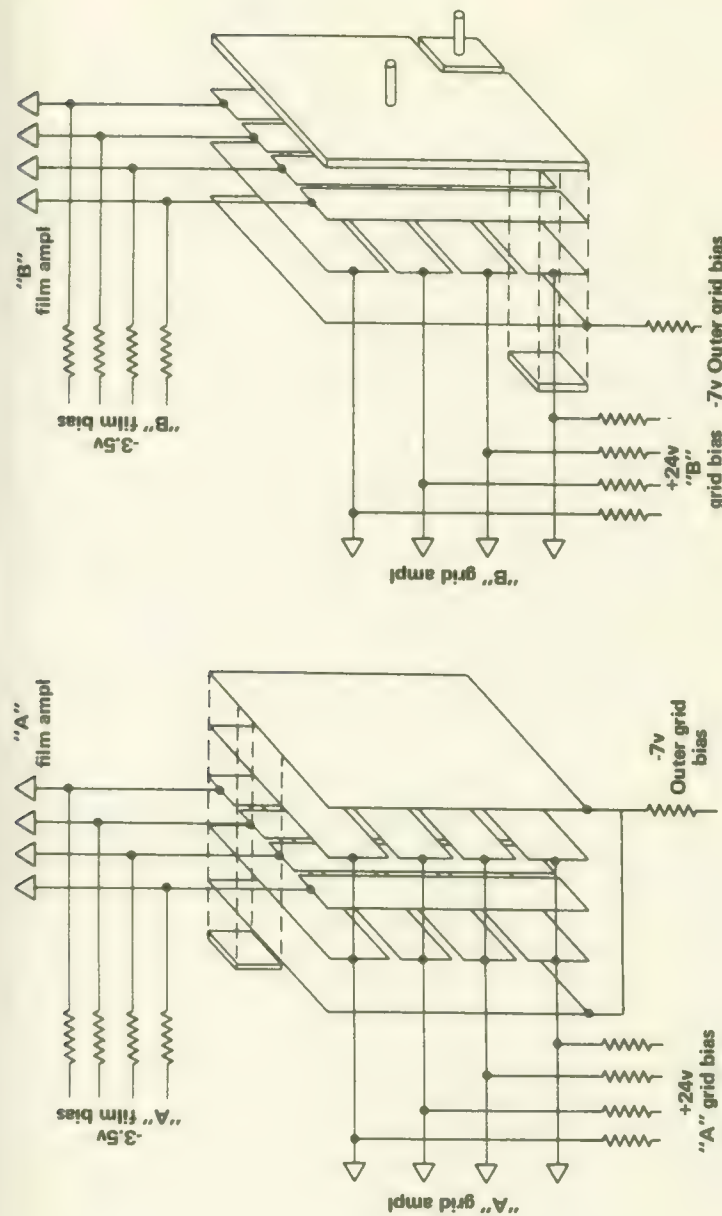


FIGURE 5-27.—Geometry of the sensor arrays in the Goddard cosmic-dust experiment.

separate output amplifier. The output signals from these amplifiers are used to determine the segment in which an impact occurred. Thus, by knowing the front film-grid segments penetrated and the rear film-grid segment affected by the impact, one can determine the direction of the incoming particle with respect to the sensor axis and the spacecraft attitude. The solar-aspect sensor determines the Sun line at the time of an impact.

Each of the four vertical films of the front sensor array, as shown in figure 5-27 is a composite of the eight layers shown in the exploded view (fig. 5-28). Ideally, a thin copper foil ( $500 \text{ \AA}$ ) could be used alone for the vertical strips of the front sensor array, but the foil is very fragile and subject to corrosion. Therefore, the nickel grid, the parylene substrate, and the parylene encapsulation are used as supports and anti-corrosion covering for the metal film deposits. The aluminum layers, which serve only as fabrication aids during the preparation of the composite film, reflect the intense heat generated by copper evaporation upon the parylene substrate. Each of the rear sensor array film strips is a  $60\text{-}\mu$  molybdenum sheet cemented to a quartz acoustical sensor plate.

Extensive calibrations were made using a 2-MeV electrostatic accelerator. Unfortunately the particles used for calibration have been limited to high-density, hard spheres of iron ( $10^{-13} \text{ g} < \text{mass} < 10^{-9} \text{ g}$ ) with velocities merely approaching the low end of the meteoroid velocity spectrum (2 to  $10 \text{ km/sec}$ ).

The plasma sensors respond nearly linearly to the particle's kinetic energy over the limited particle parameter range specified above for the

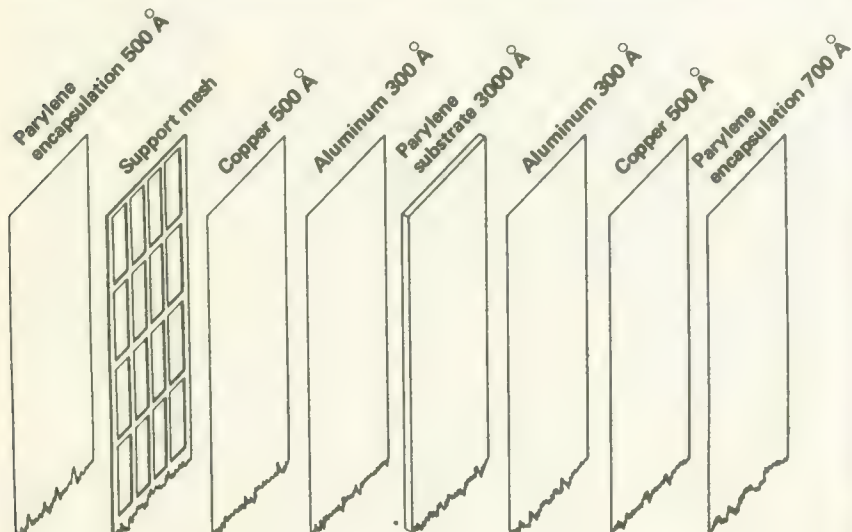


FIGURE 5-28.—Construction of a front film sensor in the Goddard cosmic-dust experiment.

laboratory simulator. The acoustical sensors respond to the particle's momentum for that same particle range.

The threshold sensitivity of the front film sensor array to laboratory particles is 0.6 erg. Time-of-flight is registered for laboratory particles having kinetic energies of 1.0 erg or greater. The electronics of the time-of-flight sensor are limited to particles with velocities ranging from 2 to 72 km/sec.

Figure 5-29 shows a block diagram of the experiment. A summing amplifier receives the positive pulse from each "A" film strip. After a gain of unity, the pulse travels two separate paths. On one path it is amplified 15 times; its pulse height is analyzed; and its amplitude is recorded in the storage register. On the other path it is amplified 1000 times and fed into a threshold one-shot multivibrator. The output pulse performs three functions:

- (1) Its origin identification is impressed directly upon the storage register.
- (2) It passes through the NOR gate and initiates a time-of-flight measurement.
- (3) It is gated back to the threshold one-shot multivibrator to inhibit any other "A" film pulse until the measurement has been completed.

An inhibit signal to the other three films is necessary to avoid capacitative crosstalk for high-energy impact signals. The "A" film pulse is pulse-height-analyzed and the results are stored in the register to await readout.

Positive pulses from the "B" film follow similar, but separate, electronic paths with the following two exceptions: (1) no pulse-height analysis is performed on the "B" film pulses, and (2) the pulse is used to stop the time-of-flight clock. If no "B" film pulse follows an "A" film pulse, the time-of-flight register goes to the full (63-bit) state and remains full until another event occurs.

Negative pulses from each of the "A" and "B" grids are amplified via separate units and are registered by identification (ID) as shown. For simplicity, only one set of collector amplifiers is shown in figure 5-29.

The output signal from the crystal sensor on the impact plate is a ringing sinusoidal wave that increases to a maximum and then decays. After amplification in a tuned amplifier, the peak signal amplitude is used to advance the microphone accumulator, start the register reset (readout of register data), and record the amplitude of the impulse imparted to the microphone sensor plate. The one-shot multivibrator and inhibit block shown in the microphone circuit inhibit further processing of subsequent microphone pulses until after the final pulse is placed in the storage register.

Pulses from the control microphone (not shown in the block diagram) follow a similar, but separate, electronic course with the exceptions that no pulse-height analysis is performed and they do not trigger the register reset.

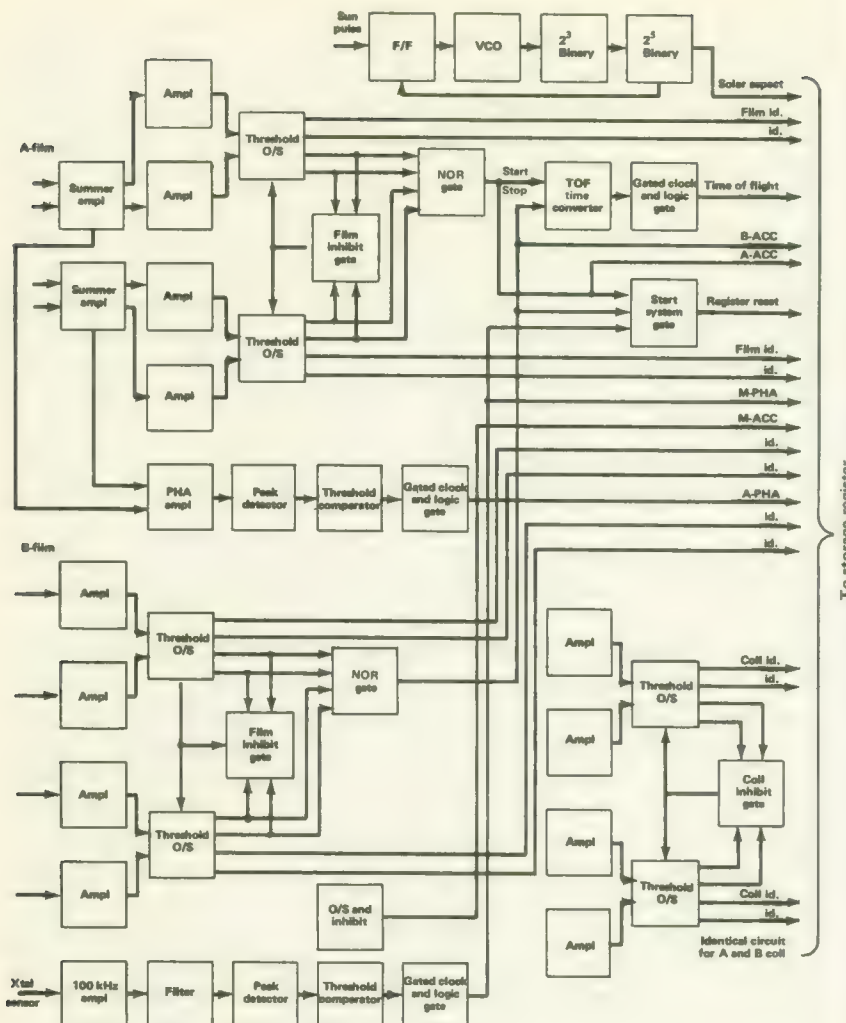


FIGURE 5-29.—Block diagram of the Goddard cosmic-dust experiment.

The data are displayed as 48 bits in four (six-bit) words. This is accomplished by alternately displaying the data in the two formats known as the "0" frame and "1" frame. The first bit in each frame identifies the frame. The next eight bits in the "0" frame identify the "A" film strip and "B" grid column affected by a cosmic dust particle impact. Bits 10 and 11 record the number of events measured by the control microphone. Six bits are assigned to time-of-flight for projectiles in the velocity range of

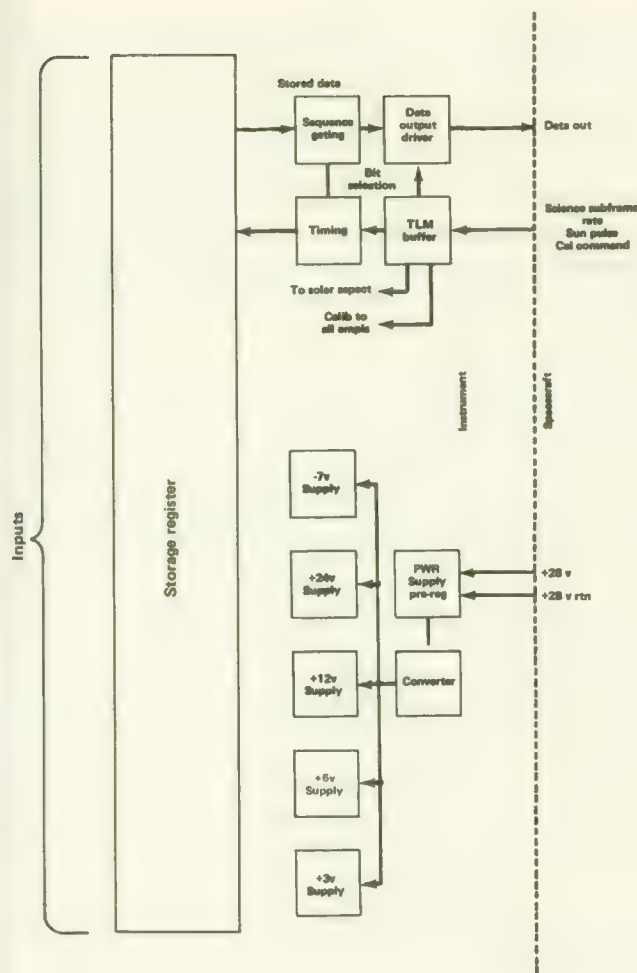


FIGURE 5-29.—Concluded.—Block diagram of the Goddard cosmic-dust experiment.

2 to 72 km/sec, which corresponds to a time-of-flight range of  $2.5 \times 10^{-5}$  to  $7 \times 10^{-7}$  sec. Any "A" film event initiates the start of a 4-MHz clock that is stopped by either a "B" film event or a filled register of 63 bits. A solar-aspect counter uses the next six bits of frame "0". This device starts its count upon each revolution of the spacecraft at a time when the Sun sensor sees the Sun. The last bit in frame "0" provides an experiment parity check.

The next eight bits following frame identification in frame "1" are used for "B" film strip and "B" grid column identification for the rear sensor array. A single bit is used to indicate signal noise that may have occurred during pulse-height analysis of any "A" film event or microphone event. Bits 11 and 12 of frame "1" register the total number of main-microphone events; bits 13 and 14 register the accumulated number of "B" film events. The "A" film pulse-height analysis and microphone pulse-height analysis are registered on the next six bits. The remaining four bits are assigned to the display of accumulated "A" film hits. All of the data on both formats remain, and are repetitively displayed, until an event occurs involving the "A" film, the "B" film, or the microphones.

### THE JPL CELESTIAL MECHANICS EXPERIMENT (PIONEERS 6, 7, 8, 9, AND E)

The celestial mechanics experiment required no special equipment on the spacecraft or at the tracking stations (ref. 14). The tracking data provided by the DSN (ch. 8) were sufficiently accurate to support the following primary objectives:

- (1) To obtain better measurements of the masses of the Earth and Moon and of the Astronomical Unit
- (2) To improve the ephemeris of the Earth
- (3) To investigate the possibility of testing the Theory of Relativity using Pioneer tracking data

The methods employed in the analysis of the tracking data are discussed in Volume III, where the results from all experiments are presented.

### REFERENCES

1. ANON.: Spacecraft/Scientific-Instrument Interface Specifications. Ames Research Center PC-121.00 through PC-121.8, 1965.
2. ANON.: Spacecraft/Scientific-Instrument Interface Specifications. Ames Research Center PC-122.00 through PC-122.08, 1967.
3. SCEARCE, C. S.; ET AL.: Magnetic Field Experiment, Pioneers 6, 7 and 8. Goddard Space Flight Center X-616-68-370, 1968.
4. ANON.: Final Report, Pioneer Magnetometer. Philco-Ford Corp. Rept. TR-DA-2117, 1969.
5. ANON.: Final Engineering Report for the M.I.T. Plasma Experiment on Pioneer 6 and Pioneer 7. MIT Rept., 1967.
6. ANON.: Final Engineering Report on University of Chicago Cosmic Ray Telescope for Pioneer 6 and 7. Univ. Chicago Rept., 1968.
7. BARTLEY, W. C.; McCACKEN, K. G.; AND RAO, U. R.: Pioneer VI Detector to Measure Degree of Anisotropy of Cosmic Radiation in Energy Range 7.5-90 MeV/Nucleon. Rev. Sci. Inst., vol. 38, Feb. 1967, p. 266.
8. BUKATA, R. P.; KEATH, E. P.; AND YOUNSE, J. M.: Technical Report on Cosmic Ray Particle Detectors Designed for Interplanetary Studies Utilizing the Pioneers 8, 9, and 10 Spacecrafts. Univ. Tex. Rept. N70-13082, 1969.

9. LEZNIAK, J. A.; AND WEBBER, W. R.: *Astrophysical J.*, vol. 156, 1969, p. 173.
10. LEZNIAK, J. A.: Ph.D. Thesis, Univ. of Minn., 1969.
11. KOEHLER, R. L.: *Interplanetary Electron Content Measured Between Earth and the Pioneer 6 and 7 Spacecraft Using Radio Propagation Effects*. Stanford Univ. SU-SEL-67-051, 1967.
12. SCARF, F. L.; ET AL: *Initial Results of the Pioneer 8 VLF Electric Field Experiment*. TRW Systems 10472-6002-RO-00, 1968.
13. BERG, O.; AND RICHARDSON, F. F.: *The Pioneer Cosmic Dust Experiment*. NASA TN D-5267, 1969.
14. ANDERSON, J. D.; AND HILT, D. E.: *Improvement of Astronomical Constants and Ephemerides from Pioneer Radio Tracking Data*. AAS Paper 68-130, 1968.



## The Pioneer Test and Ground Support Program

**T**HE SCIENTIFIC UTILITY of the Pioneer spacecraft rested ultimately upon: (1) their high intrinsic reliability, (2) their ability to withstand the rigors of the space environment, and (3) their "clean" experimental environments—that is, low magnetic field, lack of electromagnetic interference, and favorable temperatures. These attributes did not arise automatically. Experience and good design were vital; so was a deep-searching, comprehensive test program.

The Pioneer test program began at the material and component level and continued until the final moments before launch. The magnitude of the test program, as blocked out in figure 6-1,\* is impressive, particularly considering that the Pioneers are relatively small spacecraft. The tests that logically fall within the scope of this volume are those that begin with the component manufacturer, continue at TRW Systems, and end with the preship review and final dispatch of the spacecraft and instruments to Cape Kennedy (far right of fig. 6-1). The prelaunch activities and countdown at the Cape are mainly relegated to Volume III, except the electrical ground support equipment (EGSE) tests and the integrated system tests (ISTS), which are essentially the same as the EGSE tests and ISTs at TRW Systems, the spacecraft contractor.<sup>20</sup>

While the test program delineated in figure 6-1 shows the spacecraft and instrument systems being tested in parallel, Pioneer-unique equipment at Cape Kennedy—the EGSE; and at the tracking stations—the ground operational equipment (GOE) also undergo their own battery of tests before they are committed to a mission. Similarly the DSIF and the Delta launch vehicle systems undergo their own series of tests and checkout.

The highlights of the Pioneer test program—indeed, of almost every spacecraft test program—are the qualification and acceptance tests, and the integrated system tests. Along the way, many special tests are the rule rather than the exception. For example, magnetic testing was much more important in the Pioneer program than in most other spacecraft programs. Boom deployment in space was considered a potential source of difficulty;

\* See foldout at end of book.

<sup>20</sup> For a detailed description of the tests performed by TRW Systems—the great bulk of all Pioneer spacecraft tests—see the TRW Final report: *Pioneer Spacecraft Project, Final Project Report*. TRW Systems, 8830-28, 1969.

so a special ground test was devised to simulate conditions during deployment. Thus, the primary testing sequence is embellished by many special checks not portrayed in figure 6-1. Some of the more critical tests of this type are covered below.

### TEST SPECIFICATIONS

Just what constitutes a successful test of a Pioneer component or even the entire spacecraft? Test specifications constitute the standards against which all tests are measured. In view of all of the forces exerted on a Pioneer spacecraft and the abundant interfaces, it is not surprising to find the test specifications rather voluminous (ref. 1). The Pioneer test specifications delineate the 11 classes of tests defined in table 6-1. Test specifications include requirements placed upon the test facilities employed and stipulate exactly how the tests will be made and witnessed, and the documentation required of the contractor. A typical development test matrix is given in table 6-2.

### SPACECRAFT MODELS

Throughout tables 6-3 through 6-6, certain spacecraft "models" are mentioned; for example, the "prototype model" of the spacecraft. Likewise, figure 6-1 shows the parallel paths of acceptance and qualification spacecraft models. The flight models are the spacecraft actually intended for flight. They are identical in almost every respect to the prototype model. The flight models are subjected to the milder acceptance tests, while the prototype must survive the stiffer qualification tests. It is proper to look upon the prototype model as a machine the engineers could work with, a machine much like the prototype automobiles the car manufacturers subject to grueling tests and design modifications before they commit a design to the production line.

During the entire Pioneer program, TRW Systems built one prototype and five flight models. Originally, Ames Research Center had adopted the philosophy that a backup spacecraft would be prepared for each flight, but this was soon dropped as too costly. In fact, the Pioneer program could be characterized as austere from the few spares and minimum extra hardware ordered from manufacturers. Pioneer E, which was not part of the original Block-II procurement under which TRW Systems built Pioneers C and D, was assembled from spares and other extra hardware.

A spacecraft program rarely moves directly from the design stage into a completely instrumented prototype. Instead, a succession of cruder models precedes the prototype. During the development stage, when some of the critical engineering questions have not been answered, it is desirable to have various engineering models available to test ideas and to try different arrangements of components and different kinds of materials. These engi-

TABLE 6-1.—*Classes of Tests Used in the Pioneer Program*

| Type of test                    | Description  |
|---------------------------------|--|
| Parts, materials, and processes | Outgassing tests and magnetic properties tests were used.  |
| Development                     | Performance verification of breadboards, engineering models, subsystems, etc.—see table 6-2 for a typical test matrix.   |
| Life                            | Tests conducted to establish failure modes, wearout characteristics, and their effect on spacecraft reliability—many spacecraft parts were subjected to thermal-vacuum tests for over 6 months.  |
| Fabrication                     | Assemblies and subassemblies were checked during fabrication to assure functional integrity.   |
| Integration                     | During spacecraft assembly, compatibility was established by electrical continuity tests, rf interference tests, etc.  |
| Assembly qualification          | Tests conducted on all spacecraft assemblies * under forces usually more severe than those anticipated during launch and interplanetary flight—generally qualification tests were 1.5 times more severe than expected conditions. As indicated in figure 6-1, equipment subjected to qualification testing did not fly. (See table 6-3 for details.) |
| Spacecraft qualification        | Similar to assembly qualification tests, the purpose of these tests was to demonstrate the ability of the spacecraft to meet all performance requirements under conditions much more stringent than those expected during flight. (See table 6-4 for details.) They were conducted on a prototype spacecraft model not intended for flight.          |
| Assembly flight acceptance      | Similar to but less severe than the qualification tests, these tests had conditions closely duplicating those expected on the mission; their purpose was to locate latent defects in material and workmanship; assemblies passing these tests might be employed on the flight spacecraft. (See table 6-5 for details.)                               |
| Spacecraft flight acceptance    | Flight models of the spacecraft were subjected to forces actually expected during mission. (See table 6-6 for details.)  |
| Preflight                       | Conducted at Cape Kennedy, this test included spacecraft functional tests and spacecraft launch vehicle electrical interface tests. (See Vol. III for details.)  |
| Launch vehicle compatibility    | Fit and interface checks were made at the Cape. (See Vol. III for details.)  |

\* A spacecraft assembly occupies the level of complexity immediately below the subsystem. An assembly performs some distinctive function in the operation of the overall spacecraft system.

TABLE 6-2.—*Development Test Matrix, Electric Power Subsystem*

| Characteristics              | System | Solar array | Battery | Battery-current monitor | Battery-temperature monitor | Load-current monitor | Bus-voltage sensor | Battery-voltage sensor | Filter network | Undervoltage circuitry | TWT converter | Equipment converter |
|------------------------------|--------|-------------|---------|-------------------------|-----------------------------|----------------------|--------------------|------------------------|----------------|------------------------|---------------|---------------------|
| Voltage-current              |        | X           |         |                         |                             |                      |                    |                        |                |                        |               |                     |
| Power output                 |        | X           | X       | X                       |                             |                      |                    |                        |                |                        |               |                     |
| Impedance                    | X      | X           | X       |                         |                             |                      |                    |                        |                |                        |               |                     |
| Magnetic effects             | X      | X           | X       | X                       | X                           | X                    | X                  | X                      | X              | X                      | X             | X                   |
| Charge-discharge             |        |             | X       |                         |                             |                      |                    |                        |                |                        |               |                     |
| Ampere-hour capability       |        |             | X       |                         |                             |                      |                    |                        |                |                        |               |                     |
| Floating mode                |        |             | X       |                         |                             |                      |                    |                        |                |                        |               |                     |
| Switching capability         | X      |             | X       |                         |                             |                      |                    |                        |                |                        |               |                     |
| Dynamic range                |        |             |         | X                       | X                           | X                    | X                  | X                      | X              |                        |               |                     |
| Resolution                   |        |             |         | X                       | X                           | X                    | X                  | X                      | X              |                        |               |                     |
| Power input                  |        |             |         | X                       | X                           | X                    | X                  | X                      | X              |                        | X             | X                   |
| Noise generation             | X      | X           | X       | X                       | X                           | X                    | X                  | X                      | X              | X                      | X             | X                   |
| Charge requirements          |        |             | X       |                         |                             |                      |                    |                        | X              |                        |               |                     |
| Dropout voltage              |        |             |         |                         |                             |                      |                    |                        | X              |                        |               |                     |
| Sensitivity                  |        |             |         |                         | X                           | X                    | X                  | X                      | X              |                        | X             |                     |
| Time delay                   |        |             |         |                         |                             | X                    | X                  | X                      | X              |                        | X             |                     |
| Operation after undervoltage |        |             | X       |                         |                             |                      |                    |                        |                |                        | X             |                     |
| General operation            |        |             | X       |                         |                             |                      |                    |                        |                |                        | X             |                     |
| Noise susceptibility         |        |             | X       |                         |                             |                      |                    |                        |                |                        | X             |                     |
| Solar array operating point  | X      | X           |         |                         |                             |                      |                    |                        |                |                        |               |                     |
| Loads                        |        | X           |         |                         |                             |                      |                    |                        |                |                        |               |                     |
| Beat notes                   |        | X           |         |                         |                             |                      |                    |                        |                |                        |               |                     |
| Ground loops                 | X      | X           | X       | X                       | X                           | X                    | X                  | X                      | X              | X                      | X             | X                   |

neering models vary in sophistication depending upon their purpose. During the Pioneer program the following types of engineering models were fabricated: (1) a structural model, (2) a thermal model, (3) an electrical development model,<sup>21</sup> and (4) an antenna model. These models were, in effect, specialized mockups of the spacecraft. Instruments and other components were simulated (where necessary) by inert pieces of

<sup>21</sup> The electrical development model was commonly called the "engineering model" during the program. Its accomplishments included the establishment of overall spacecraft electrical compatibility, spacecraft/EGSE compatibility, DSIF compatibility, spacecraft/computer program evaluation, and others.

TABLE 6-3.—*Assembly Qualification Test Details*

| Type of test   | Description  |
|----------------|--|
| Humidity       | This test aimed at preventing damage from humidity during shipping and storage; performance of assemblies was not to be degraded by 24 hr in humidity chamber at: $86 \pm 5^{\circ}$ F; humidity, $95^{+8}_{-5}$ percent.  |
| Vibration      | Assemblies were vibrated in each of the three orthogonal axes. The specific frequencies, durations, etc., are too lengthy to list here; they included both sinusoidal and random-vibration test schedules.   |
| Acceleration   | Thrust was 1.5 times the maximum acceleration expected in powered flight. (See ch. 7 for Delta characteristics.) Spin was 185 rpm, as compared to the 60 rpm expected during normal cruise.  |
| Thermal-vacuum | Pressure was less than $10^{-5}$ torr; temperature was $25^{\circ}$ F above the predicted maximum and $25^{\circ}$ F below the predicted minimum; during the 24-hr exposure, cold-start capability had to be demonstrated at least three times for cyclically operated components. |
| Shock          | Three shocks of $50 \pm 5$ g peak for $6^{+1}_{-0}$ msec were applied in each of the three orthogonal directions.  |
| Magnetic       | See chapter 3.   |
| Solar array    | Calculated performance figures were verified in sunlight at the JPL Table Mountain facility and facilities at Palm Springs.  |

TABLE 6-4.—*Spacecraft Qualification Test Details*

| Type of test                                 | Description  |
|--|--|
| Balance                                      | Prototype spacecraft in spinup configuration was dynamically balanced at $150 \pm 5$ rpm; spin balance weights were added to meet balance specifications.  |
| Spin   | Spacecraft was: (1) spun at rate varying linearly between 150 and 190 rpm for period of 20 sec, (2) spun at $80^{+5}_{-0}$ rpm for sufficient time so that at least one frame of telemetry was received for each ground command mode.                            |
| Weight, center of gravity, moment of inertia | These factors were measured and compared with design requirements.   |
| Humidity                                     | This test was the same as the assembly qualification humidity test. (See table 6-3.)   |
| Vibration                                    | This test was similar to the assembly qualification vibration test. (See table 6-3.)   |
| Acceleration                                 | The objective was to test for 3 minutes at 1.5 times the maximum acceleration expected during powered flight (see ch. 7), but this value was never attained during the acceleration tests. Critical stresses on booms were simulated by the addition of weights. |

TABLE 6-4.—*Spacecraft Qualification Test Details (Concluded)*

| Type of test                                    | Description  |
|---|--|
| Thermal-vacuum                                  | The spacecraft was tested in thermal-vacuum chamber at pressures less than $5 \times 10^{-5}$ torr, with simulated solar radiation and with chamber walls cooled to $-305 \pm 15^\circ F$ ; insulation was simulated between the values expected at 0.8 and 1.2 AU; test duration was at least 9 days; spacecraft was spun fast enough to stabilize temperatures of solar array; and the solar wind was simulated. (These thermal-vacuum tests were not carried out on the prototype model of the spacecraft.) |
| Magnetic properties                             | Magnetic measurements were made at 34 specified operating modes. (See ch. 3 for magnetic cleanliness philosophy.) Four types of magnetic tests were conducted on the prototype spacecraft: Type I—spacecraft magnetic field mapping; Type II—spacecraft stray field; Type III—solar array mapping; and Type IV—solar-array stray fields.   |
| Electromagnetic compatibility                   | Systems performance tests were to assure that no subsystems were adversely affected by the operation of the rest of the subsystems.  |
| Boom deployment                                 | These tests under near-zero-g conditions at expected spin rates were to see if all booms deployed satisfactorily; a structural model was used rather than the prototype.   |
| Subsystem qualification                         | Some of the more critical subsystems were qualification-tested separately.   |
| Spacecraft/solar-array electrical compatibility | Compatibility of complete spacecraft with flight power supply was tested during simulated operational conditions.  |

metal or other material. In a sense, these models paralleled the customary "breadboarding" of electrical assemblies, but at the spacecraft level.

## TEST FACILITIES

Extensive test facilities are essential to the success of any spacecraft development program. In the case of Pioneer, most of the requisite facilities were located at TRW Systems. A few of the more important facilities are described briefly below.

To duplicate the interplanetary environment accurately, the TRW Systems 30-ft thermal-vacuum test chamber (fig. 6-2) was used for Pioneers A through C and their 22  $\times$  45-ft chamber (fig. 6-3) for Pioneers D and E. The 30-ft chamber's inside diameter is 28 ft. The temperature limits are  $-320$  to  $+440^\circ F$ , easily meeting the Pioneer qualification test requirements (table 6-3). The pressure within this chamber can be pumped down to about  $10^{-6}$  torr, again exceeding the Pioneer test requirements. The

TABLE 6-5.—*Assembly Acceptance Test Details*

| Type of test             | Description   |
|--------------------------|---|
| Vibration.....           | Similar to qualification tests except that only sinusoidal vibration schedule used; levels not exceeding expected flight levels |
| Thermal-vacuum.....      | Tests conducted within maximum and minimum expected temperatures only for 12 hr; otherwise similar to qualification tests       |
| Magnetic properties..... | Same as qualification tests (table 6-3)   |
| Solar array.....         | Same as qualification tests (table 6-3)   |

TABLE 6-6.—*Spacecraft Acceptance Test Details*

| Type of test         | Description  |
|----------------------|--|
| Initial balance..... | Similar to qualification tests, except that degree of balance had to be within 1.5 times the values specified  |
| Vibration.....       | Similar to qualification tests; random and sinusoidal vibration schedules used   |
| Thermal-vacuum.....  | Similar to qualification tests, except test lasted only 7 days (table 6-4)   |
| Final balance.....   | Balanced prior to shipment to Cape Kennedy and (for Pioneer 6 only) again before mating with live third-stage motor; balance weights added to bring degree of balance within stipulated values |

chamber walls are cooled cryogenically to simulate the blackness of space away from the Sun. In the 22 × 45-ft chamber the Sun was simulated by a large reflector and a high-power xenon arc.

Because the Pioneers each carried plasma probes to measure the plasma stream outward from the Sun, it was thought advisable to bombard the spacecraft with an artificial plasma beam to see how the probes would respond. These tests were carried out while the spacecraft was spinning in the thermal-vacuum chamber. A Kaufman ion source was used to generate positive ions which were then mixed with electrons to form a neutral plasma (ref. 2).

The magnetic cleanliness campaign required special test equipment (ref. 3). Fortunately, the Pioneer spacecraft is rather small and it was possible to employ the 6.5-m-diameter Fanselau coil system located at Malibu, California (fig. 6-4). With the Fanselau coils, the ambient field can be nulled out completely so that the permanent field of the spacecraft can be measured directly. Once the permanent field has been measured,

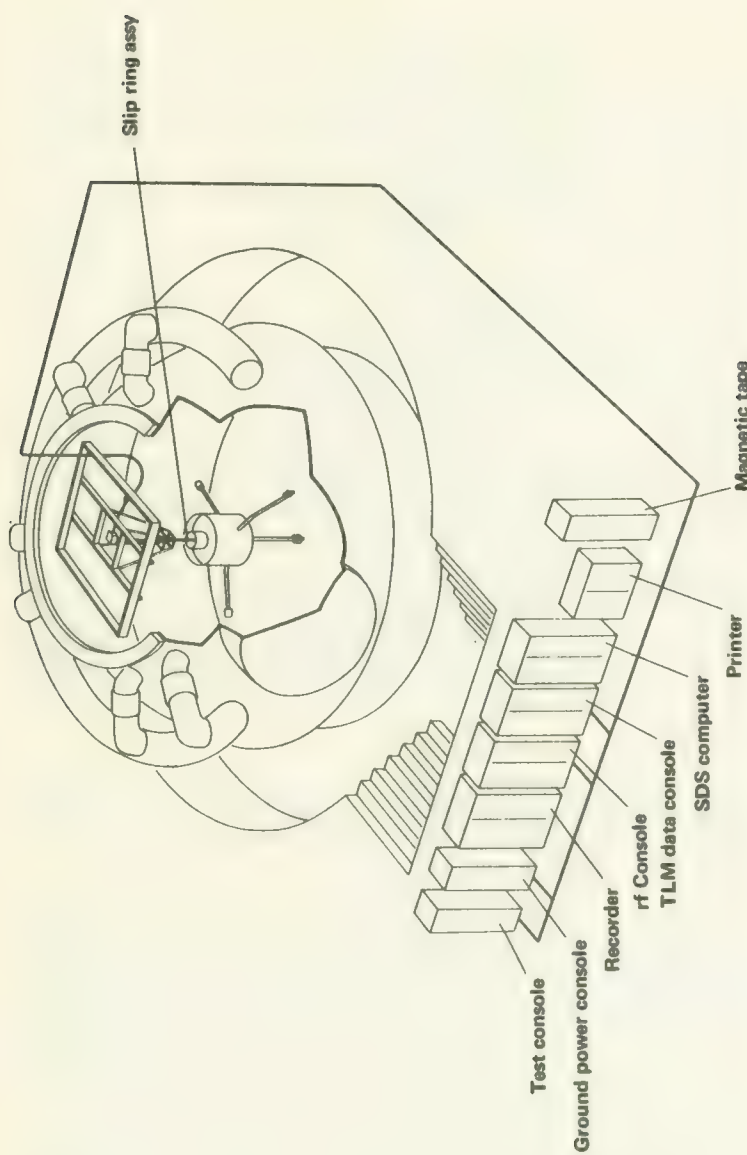


FIGURE 6-2.—Configuration of equipment around the TRW Systems 30-ft thermal-vacuum chamber during tests of Pioneers A, B, and C.

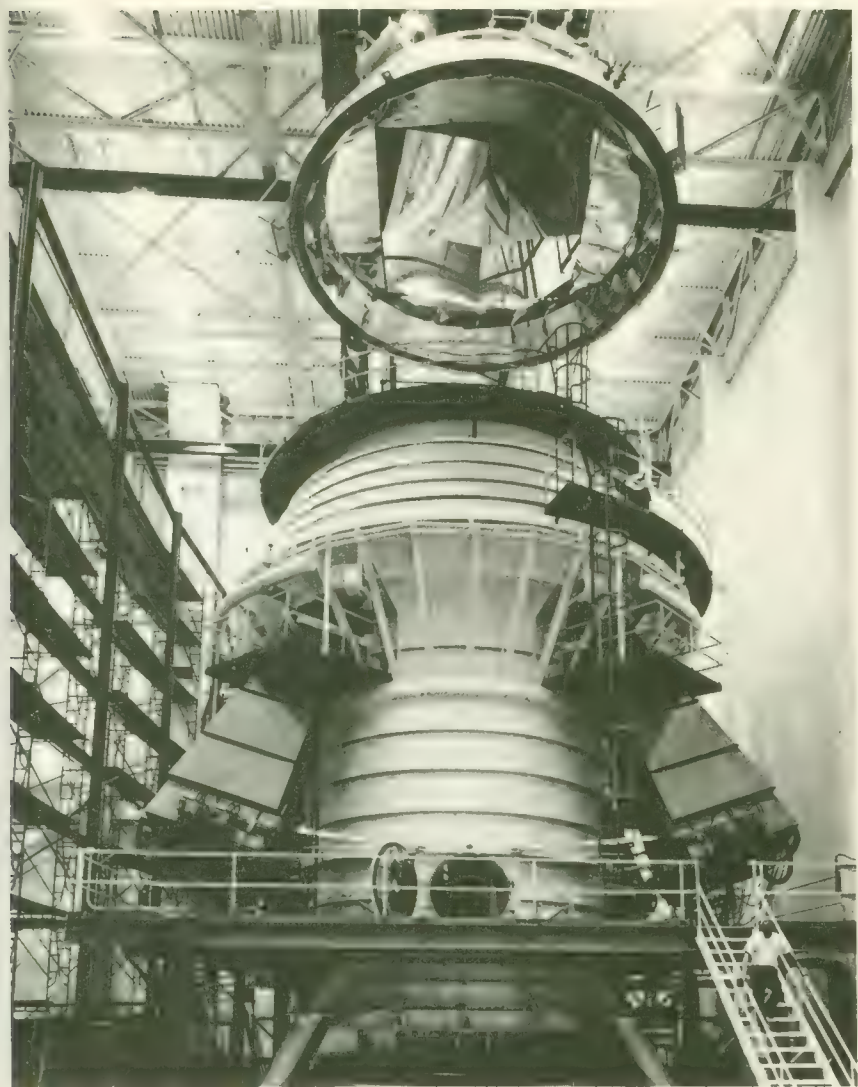


FIGURE 6-3.—The TRW Systems 22 × 45-ft thermal-vacuum chamber and solar simulator used during the tests of Pioneers D and E. (Courtesy of TRW Systems.)

known fields can be applied along each axis to determine induced fields. (See the discussion of magnetic cleanliness in ch. 3.) Testing was done at night to avoid the daytime variations in the Earth magnetic field.

The Pioneer vibration test configuration is shown in figure 6-5. These tests employed a standard shake table made available at the TRW Systems Structural Test Laboratory. Another piece of pertinent equipment at this

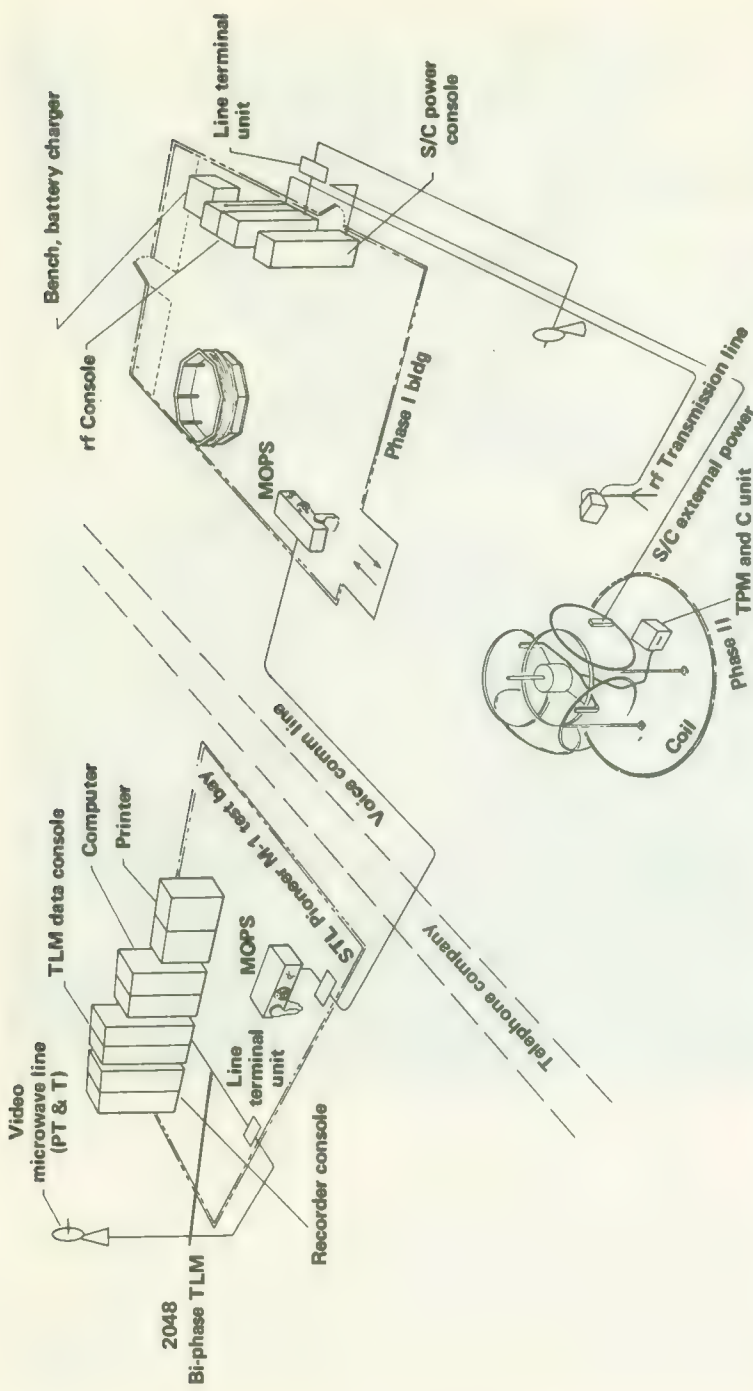


FIGURE 6-4.—Configuration of equipment during Pioneer-A magnetic-field tests at Malibu, Calif. The microwave and telephone links were not used on subsequent spacecraft tests.

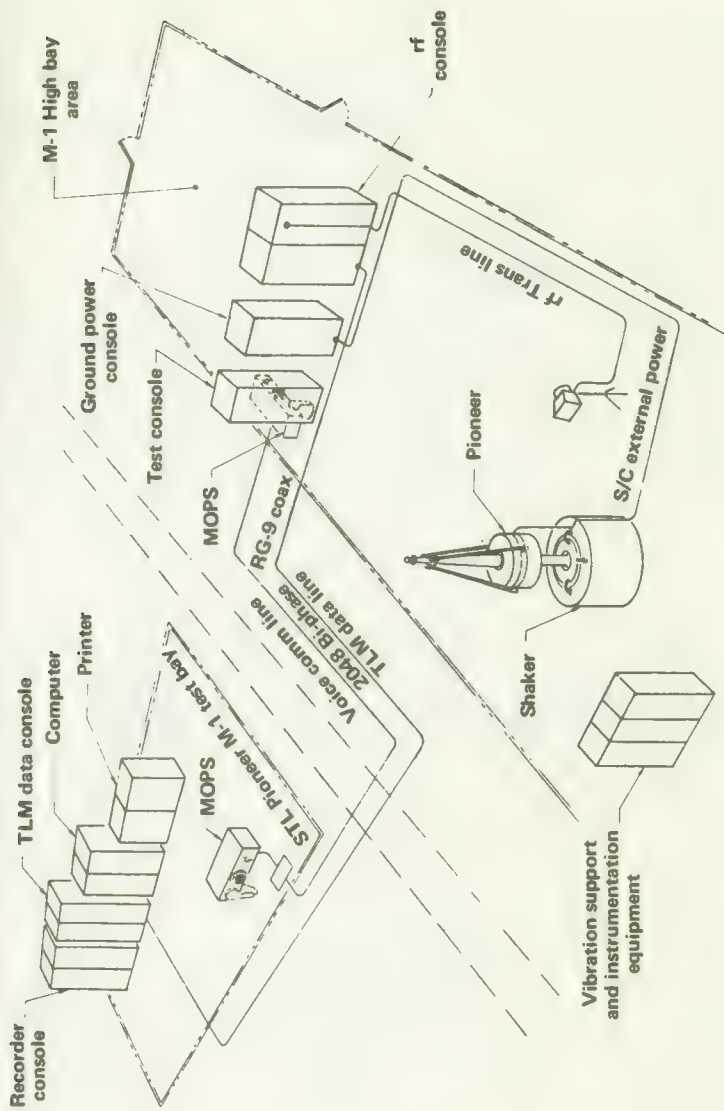


FIGURE 6-5.—Configuration of equipment during Pioneer spacecraft vibration tests.

laboratory was a dynamic balancing machine upon which degree of balance and moments of inertia could be measured.

To test the boom deployment sequence under simulated space conditions, the spacecraft was first spun up to about 110 rpm on a spin table, as shown in figure 6-6. Zero-g conditions were then simulated by a vertical lift of the entire spinning spacecraft (ref. 4). During the coast phase, the booms were deployed. Deployment was observed visually to check the smoothness of the operation, and the possible introduction of spacecraft wobble. A nine-channel telemetry system transmitted additional information on joint angles and stresses during deployment. The entire deployment scheme was a worrisome point during the program. Fortunately, these tests showed that the design was sound.

The solar array was also subjected to a special series of tests (ref. 5). A special outdoor test fixture was constructed that could accept either engineering model panels or the complete solar array. The test fixture consisted of a rotating dummy spacecraft, a simulated electronic load, temperature and power output monitoring devices with sliprings, and a large collimating tube plus standard-cell mount that could be pointed at the Sun (fig. 6-7). The initial test was set up at the JPL Table Mountain site in California; the rest of the panels were tested at Palm Springs.

## SPACECRAFT INTEGRATION AND TEST PROCEDURES

The test cycle begins with spacecraft component tests and continues through a graduated series of production tests to final assembly. Each assembly undergoes the complete regimen of environmental and functional tests described earlier. Figure 6-1 shows the overall plan on a broad scale. Upon completion of the assembly tests, subsystems can begin to be integrated into the spacecraft. The spacecraft-integration-and-test phase is that portion of the test program that begins with the receipt of accepted hardware from bonded store and goes through all spacecraft tests to launch. (See sheet 2 of fig. 6-1.) A summary of the tests performed during this phase is presented in table 6-7. Figure 6-8 presents a typical test history from spacecraft integration to the launch pad.

A "building block" philosophy is utilized during subsystem integration to ensure mutual compatibility and proper operation of each subsystem (ref. 6). Basically, there are two kinds of tests: (1) those that evaluate the assembly or subsystem as a unit, and (2) those that explore its interactions with other assemblies and subsystems. As the spacecraft was built up piece by piece, tests were repeated to verify that newly added subsystems (including the instruments) did not interfere with or degrade the performance of those already installed.

The Integrated System Tests are so important that a separate discussion is warranted. The ISTs provide an overall spacecraft performance baseline

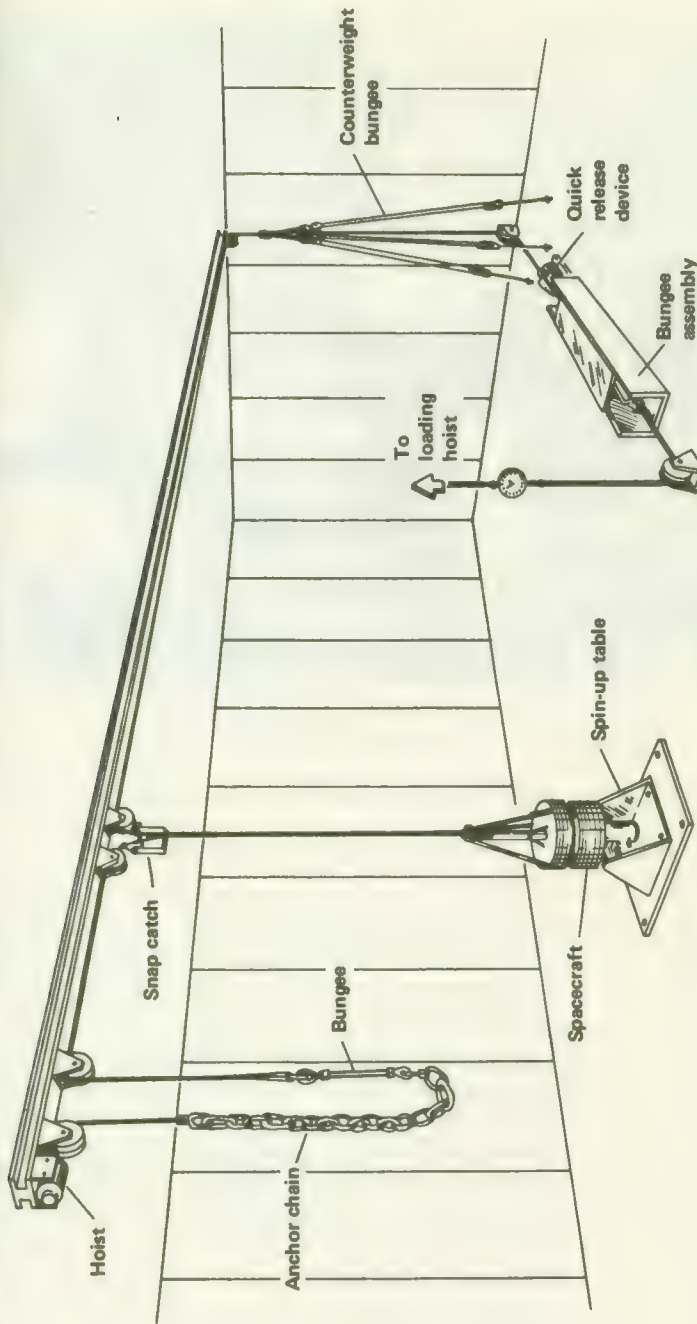


FIGURE 6-6.—The vertical-lift equipment and spin table used during boom deployment test.



FIGURE 6-7.—Solar-array outdoor test setup.

TABLE 6-7.—*Tests Performed During Spacecraft Integration*

| Type of test                     | Description   |
|----------------------------------|---|
| Electromagnetic compatibility    | The spacecraft, including the instruments, was operated in all proper operating modes within an rf-shielded enclosure; interference and susceptibility tests were performed on the integrated spacecraft. |
| Telemetry calibration            | Projected telemetry outputs were compared with actual signal measurements.  |
| Power profile                    | Spacecraft load currents were measured under varying input voltages for different spacecraft operating modes.   |
| Subsystem performance            | These tests made various parameter checks that could not be ascertained during the Integrated System Test, such as receiver sensitivity, solar-array back emf, and Sun sensor and DTU threshold checks.   |
| Integrated system test           | See body of text.   |
| Physical and magnetic properties | These tests verified weight, center of gravity, moments of inertia, and magnetic cleanliness, as described earlier.   |
| Detailed equipment test          | Each scientific instrument was tested in detail, with all other instruments and all spacecraft subsystems operating.  |

whereby changes in performance throughout the test program can be detected. Deviations between the prototype and various flight models can also be checked. The IST was repeated frequently so that engineers could see trends that might develop due to subsystem degradation. The ISTs measured the most important system-wide parameters with the spacecraft as near flight configuration as possible. Some of the parameters measured during the IST are listed below:

- (1) Each receiver was frequency-addressed and its performance verified. The quality of the demodulated command signals fed to the decoder was verified.
- (2) The rf power radiated from the spacecraft was verified in various spacecraft modes.
- (3) The CDU operation was verified in all spacecraft modes, including ordnance-control circuitry and undervoltage output signals.
- (4) Simulated Sun pulses were inserted and the pneumatic pressure switch was monitored to check the operation of the pneumatic equipment.
- (5) Bit rates, bit formats, and the quality of the data transmitted were monitored to check the DTU and the DSU.
- (6) Spacecraft bus current was monitored continuously and compared with the nominal power profile.
- (7) Each scientific instrument was tested to verify performance during typical operation.

In a sense, the IST was a thorough physical examination for the complete operating spacecraft. The IST was repeated at least twice for each spacecraft when it reached the launch pad.

### ELECTRICAL GROUND SUPPORT EQUIPMENT

Although the operations at Cape Kennedy prior to launch are covered in Volume III, it is pertinent here to describe the EGSE, installed specifically to carry out prelaunch spacecraft tests, especially the "on stand" IST.

The EGSE contains the command generators, the telemetry acquisition equipment, and the necessary data processing, display, and recording equipment to carry out ISTs. A block diagram of the EGSE is shown in figure 6-9.

The prime communication path between the EGSE and the spacecraft was an rf link; this made the tests before launch as realistic as possible. A few hardlines were employed to transmit certain simulation and fault-isolation signals—for example, Sun-sensor signals; but these did not compromise the validity of the tests.

The system test station at the Cape consisted of the equipment racks and associated peripheral equipment shown in figure 6-10. The functions of the various consoles were as follows:

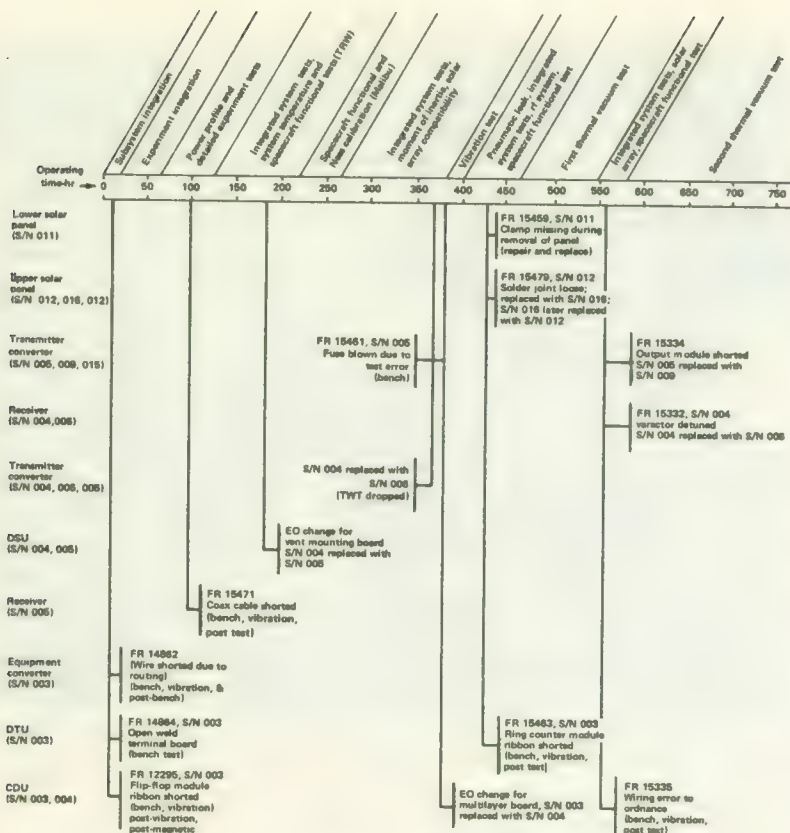


FIGURE 6-8.—Pioneer A spacecraft test history.

(1) Radio frequency console contained command transmitting and data receiving equipment; viz, command encoder, command transmitter, ramp generator, antenna, and telemetry receiver.

(2) Telemetry data console contained equipment which collected, processed, displayed, and recorded the telemetry data received. An SDS-910 computer controlled the data handling, and established frame synchronization and other similar functions.

(3) Recorder console consisted of an instrument patch panel, a strip chart recorder, and a magnetic tape recorder.

(4) Test console was used to support detailed subsystem performance tests. The three major assemblies were a test-point monitor and control assembly, a Sun sensor simulator, and a Sun sensor stimulator.

(5) Ground power console provided primary power to the spacecraft during tests.

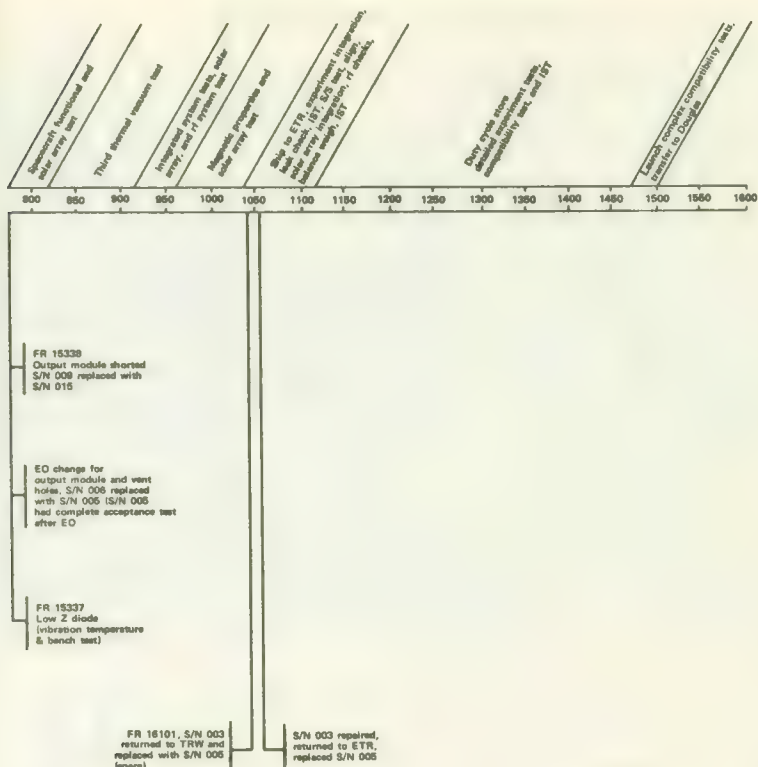


FIGURE 6-8.—Concluded.—Pioneer-A spacecraft test history.

### TYPICAL TEST RESULTS

The purpose of any test program is to improve the probability that the spacecraft will perform satisfactorily in space for the desired design lifetime. Since the four Pioneers that were successfully launched have greatly surpassed their nominal 6-month design life, the test program must have been singularly successful in weeding out incipient failures and in pinpointing design weaknesses.

Some of the feedback from the test program into spacecraft engineering is shown in figures 6-11 and 6-12. The electronic subsystems and assemblies required the greatest rework and redesign. The coaxial switches were of particular concern to the engineers.

Another view of the overall test program is shown in figure 6-11. The acceptance portion of the program is shown to be the most important in

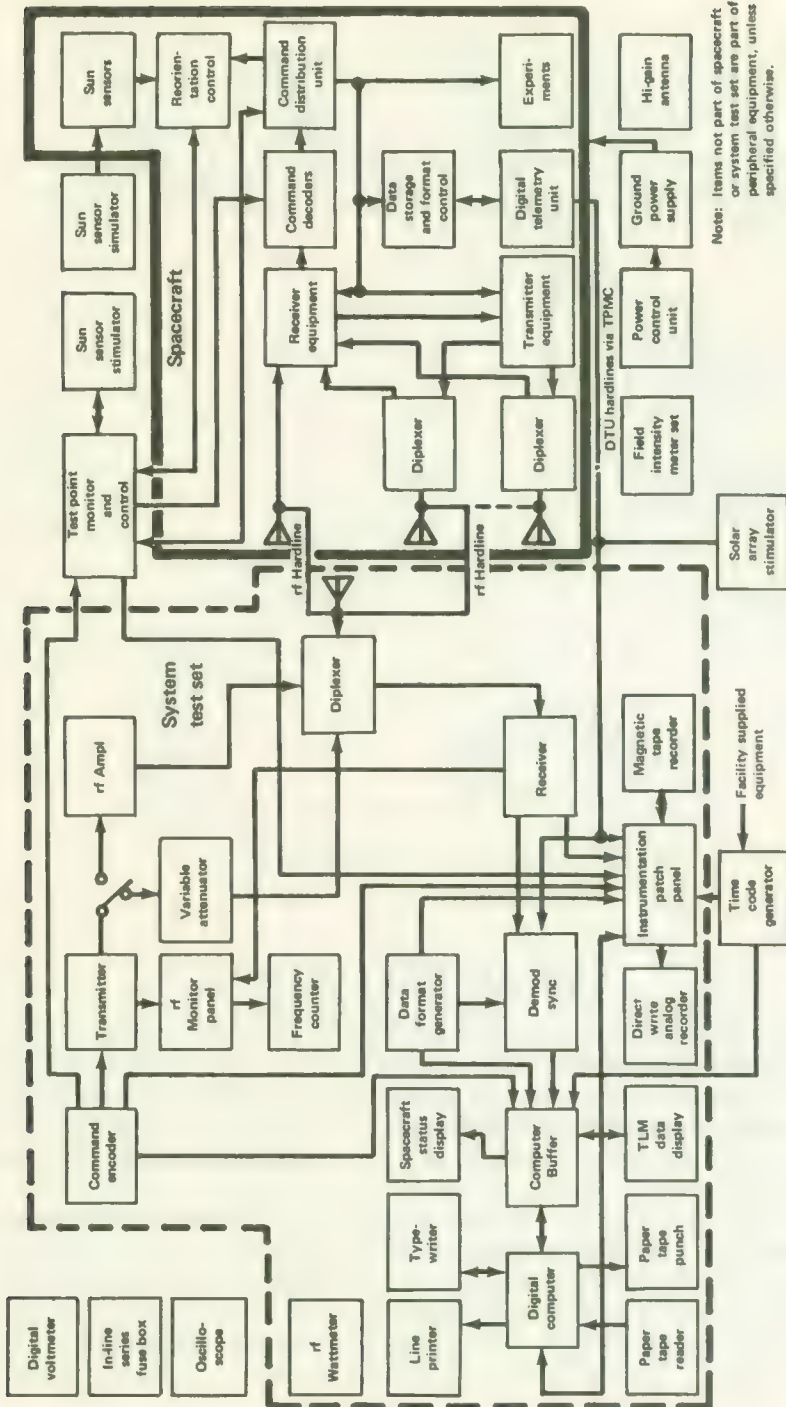


FIGURE 6-9.—Block diagram of the EGSE.

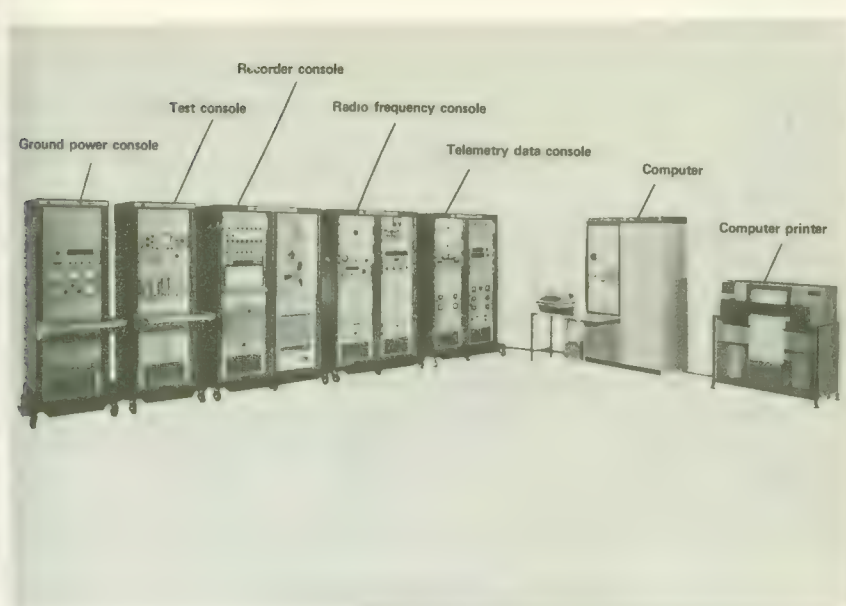


FIGURE 6-10.—Electrical ground support equipment (EGSE) consoles.



FIGURE 6-11.—Percentage of test-program failures by subsystem.

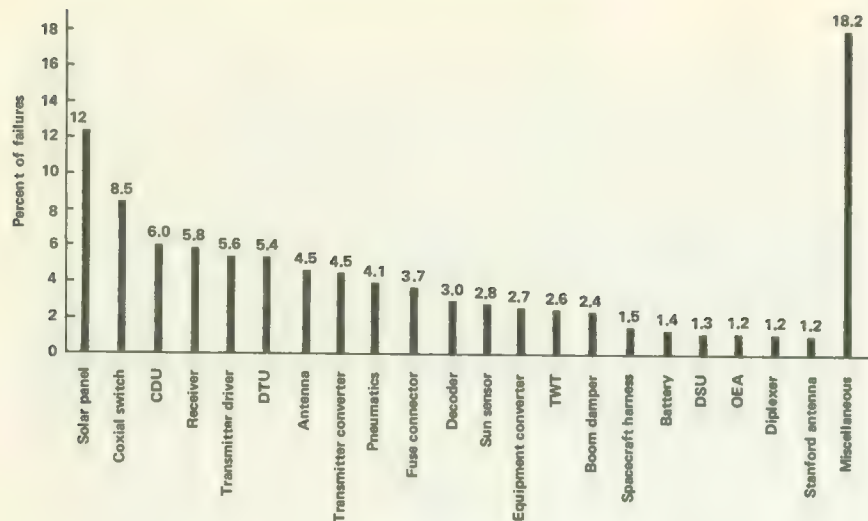


FIGURE 6-12.—Percentage of test-program failures by unit.

terms of detecting failures. It is rather surprising that the qualification tests, which were more severe than the acceptance tests, did not encounter more failures. A possible explanation of the difference lies in the fact that the qualification tests were made only on qualification units, while all flight units, plus the spares, had to pass the acceptance tests.

## REFERENCES

1. ANON.: Spacecraft and Associated Ground Equipment, Specification A-6669, NASA, Ames Research Center, 1963; and subsequent revisions.
2. KEMP, R. F.; AND SELLEN, J. M., JR.: Solar Wind Simulation with the Pioneer Spacecraft. AIAA Paper 66-153, 1966.
3. GLEHHORN, G. J.; AND LINDNER, J. W.: Magnetic Considerations in the Design and Testing of the OGO and Pioneer Spacecraft. 16th Intl. Astronaut. Congr., 1965.
4. GLUCK, R.; AND GALE, E. H.: Motion of a Spinning Satellite During the Deployment of Asymmetrical Appendages. J. Spacecraft, vol. 3, Oct. 1966, p. 1963.
5. BARON, W. R.: The Solar Array for the Pioneer Deep Space Probe. Electronics and Power, vol. 14, Mar. 1968, p. 105.
6. SCHUMACHER, C. E.: Pioneer Spacecraft Test and Support Program. AIAA Paper 65-247, 1965.

## CHAPTER 7

# The Delta Launch Vehicle

### WHY THE DELTA?

THE DELTA LAUNCH VEHICLE, or Thor-Delta, has been one of NASA's most successful launch vehicles (fig. 7-1). As of July 1, 1970, 71 Delta launches have succeeded, with only 7 failures noted on the record books. This remarkable dossier was not available to NASA mission planners in 1961, when the IGSY Pioneers were first brought under discussion. Up to July 1, 1961, the Delta had successfully launched Echo 1, Tiros 2, and Explorer 10, while failing only on its first try (Echo A-1, May 13, 1960). A 75 percent success record was extremely good in 1961. Thus, the planners of Pioneer selected a launch vehicle of high promise.

The Delta had several other points in its favor. It was a low-cost launch vehicle derived largely from previously developed military and Vanguard Program hardware. Its payload capability for the escape mission was something over 100 lb, roughly what NASA wanted for its "precursor" Pioneer. The Delta was also considered NASA's very own launch vehicle, because it had not been obtained through military channels. However, NASA had procured the earlier Thor first stages directly from the U.S. Air Force and then turned them over to the Delta prime contractor, McDonnell-Douglas, who had built them in the first place. NASA was anxious to create its own "stable" of launch vehicles at this point—another plus favoring the choice of the Delta. Further, if history is a valid measure of the future, the Delta was an auspicious choice because Pioneers 1, 2, and 5 had been launched by the Thor-Able launch vehicle, the progenitor of Delta. In particular, the highly successful Pioneer 5 probe had been placed in a solar orbit like those planned for the new series of Pioneers by the Delta-like Thor Able II.

The use of the Delta was thus one of the basic ground rules established for the Pioneer Program in 1961. In the final analysis, it was the only reliable all-NASA launch vehicle capable of doing the job, that would be available for the projected 1964 launch date.

### THE EVOLUTION OF THE DELTA

NASA did not develop the Delta as an entirely new launch vehicle; rather, the first Deltas were much-modified Able-II Space Test Vehicles



FIGURE 7-1.—The Pioneer-7 launch from Complex 17A at Cape Kennedy. Delta 40 was a thrust-augmented improved Model E launch vehicle.

(STVs), which, in turn, grew out of the Able-II Precisely Guided Reentry Test Vehicle (PGRTV) Program. The precise genealogy becomes confusing here because there were Ables I, II, and IV as well as many other combinations of similar space hardware on the scene. Basically, the Delta rocket owes its first stage to the Thor IRBM;<sup>22</sup> while its second and third stages were based on the Vanguard second and third stages.

<sup>22</sup> IRBM = Intermediate range ballistic missile

Almost as soon as it was created on October 1, 1958, NASA began to plan its stable of launch vehicles. The favorable record of the Able-II STV led NASA to sign a \$24 million contract with Douglas Aircraft on April 29, 1959, for the design and manufacture of 12 Able-based launch vehicles. Originally, the Deltas were intended only as interim launch vehicles for the 1960–1961 period—something to fill the gap while bigger boosters were being developed. As it turned out, the later Deltas could easily and very reliably orbit satellites weighing up to almost 500 lb. This payload was more than ample for most NASA scientific missions. The “interim Delta” did not fade away but became instead a workhorse that has propelled more than three-score spacecraft into orbit around the Earth or Sun.

The Delta is basically a three-stage rocket. The liquid first and second stages are topped by a small solid-propellant third stage (fig. 7-2). The first-stage core is the venerable Thor military rocket, burning a hydrocarbon fuel similar to kerosene (RP-1, RJ-1, etc.) with liquid oxygen. This stage is manufactured by the McDonnell-Douglas Astronautics Company. The three first-stage engines are made by the Rocketdyne Division of North American Rockwell. The solid, thrust-augmentation rockets strapped on the first stages of later models are Castor rockets, usually produced by the Thiokol Chemical Corporation. The fuel for the much smaller second stage is unsymmetrical dimethyl hydrazine (UDMH), which is oxidized by inhibited red fuming nitric acid (IRFNA). The second stage is also a product of McDonnell-Douglas Corporation. It employs an Aerojet-General engine. The third-stage solid rockets have been manufactured by various concerns during the evolution of the Delta: Allegheny Ballistics Laboratory (ABL), United Technology Center (UTC), and Thiokol Chemical Corporation (see table 7-1). The Delta is one of NASA’s smaller launch vehicles (first-stage thrust, about 175 000 lb; plus about 160 000 lb from solid strap-ons on later models).

No launch vehicle that has seen as much use as the Delta remains fixed or inflexible for very long. Almost every launch vehicle is different, at least in some minor detail, because the interface with each payload is different. More significant changes arise when rocket motors are uprated, propellant tank sizes are changed, and solid-fuel rockets are strapped on for first-stage augmentation. The Delta has gone through over a dozen of these upratings and improvements as described by the different model numbers in table 7-1.

The Delta variations in physical configuration and terminology are rather confusing to the uninitiated. The following list should relieve this semantic problem:

- (1) *Delta* is the basic name for this series of launch vehicles; it is used interchangeably with Thor-Delta. In 1970, the name Delta, used without qualification, meant a TAID. (See below.)
- (2) *Thor-Delta* is used interchangeably with Delta.
- (3) *Thrust-Augmented Delta* (*TAD*) employs three or more strapped-on

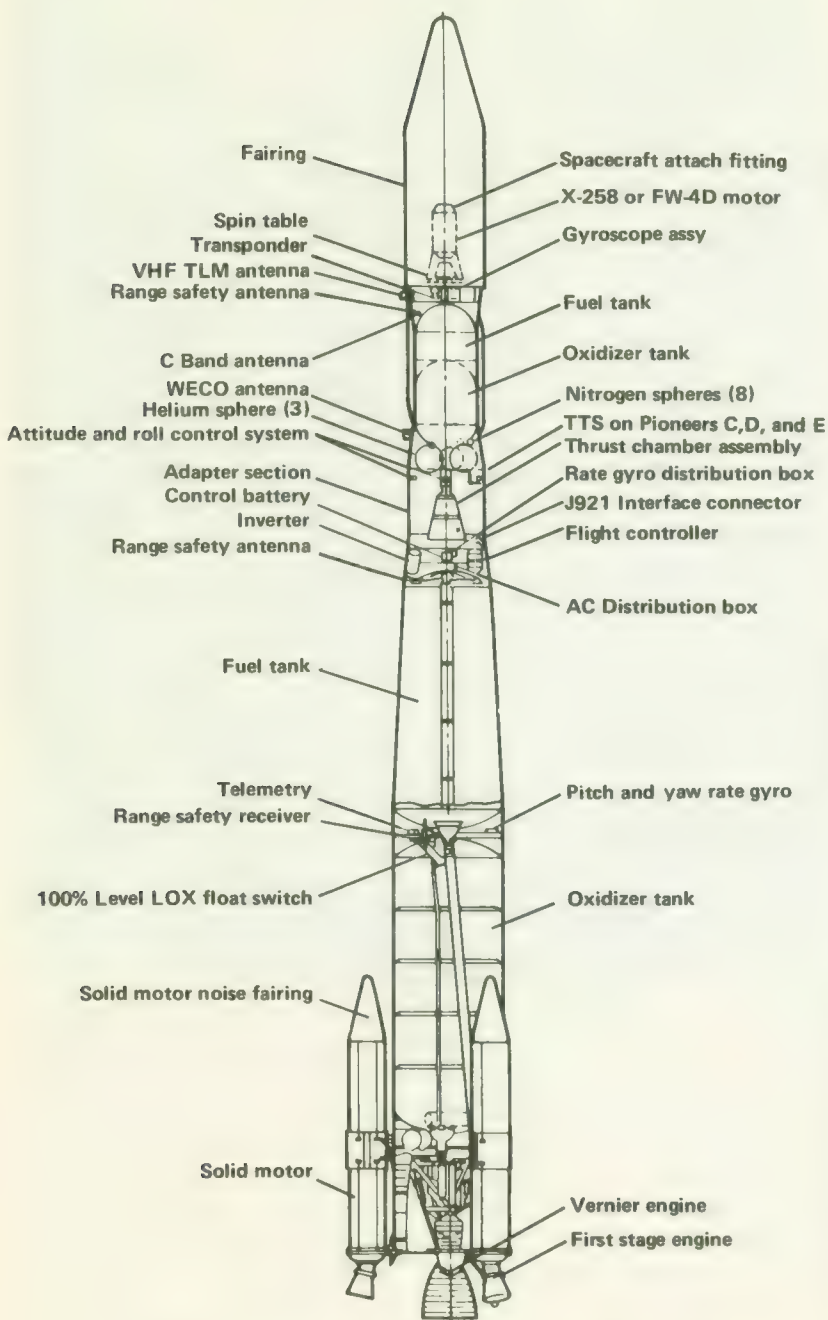


FIGURE 7-2.—The thrust-augmented improved Delta (TAID).

TABLE 7-1.—Nomenclature of Various Delta Configurations

| Vehicle model number<br>MDC | NASA    | MDC designation | Firststage propulsion<br>Engine (Rocketdyne) | Second-stage propulsion<br>(Aerojet-General) | Third-stage propulsion | Popular name           | Pioneer flights    |
|-----------------------------|---------|-----------------|--|--|------------------------|------------------------|--------------------|
| DM-19                       | Delta A | DM-19           | MB-3, Block I                                | None   | AJ10-118               | NPP X-238              | Delta              |
| DSV-3A                      | Delta B | DM-21           | MB-3, Block II                               | None   | AJ10-118               | NPP X-238              | Delta              |
| DSV-3B                      | Delta C | DSV-2A          | MB-3, Block II                               | None   | AJ10-118A              | NPP X-248              | Delta              |
| DSV-3C                      | Delta D | DSV-2A          | MB-3, Block II                               | None   | AJ10-118D              | ABL X-258              | Delta              |
| DSV-3D                      | Delta E | DSV-2C          | MB-3, Block III                              | 3 Castor I                                   | AJ10-118D              | UTC FW-4S<br>ABL X-258 | TAD                |
| DSV-3E                      | Delta F | DSV-2C          | MB-3, Block III                              | 3 Castor I/II                                | AJ10-118E              | ABL X-258              | TAID               |
| DSV-3F                      | Delta G | DSV-2C          | MB-3, Block III                              | None   | AJ10-118E              | UTC FW-4D              | TAID               |
| DSV-3G                      | Delta H | DSV-2C          | MB-3, Block III                              | 3 Castor I/II                                | AJ10-118E              | UTC FW-4D              | Imp. Delta         |
| DSV-3H                      | Delta J | DSV-2C          | MB-3, Block III                              | None   | AJ10-118E              | None                   | TAID               |
| DSV-3J                      | Delta L | DSV-2L-1B       | MB-3, Block III                              | 3 Castor I/II                                | AJ10-118E              | TCC TE-364-3           | Imp. Delta         |
| DSV-3L                      | Delta M | DSV-2L-1B       | MB-3, Block III                              | 3 Castor II                                  | AJ10-118E              | TCC FW-4D              | TAID               |
| DSV-3L                      | Delta N | DSV-2L-1B       | MB-3, Block III                              | 3 Castor II                                  | AJ10-118E              | TCC TE-364-3           | Long tank<br>Delta |
|                             |         |                 |  |  | None                   | Long tank<br>Delta     | Long tank<br>Delta |

Notes:

MDC = McDonnell-Douglas Astronautics Company  
 NPP = Naval Propellant Plant  
 ABL = Allegheny Ballistics Laboratory

UTC = United Technology Center  
 TCC = Thiokol Chemical Corporation  
 TAD = Thrust-Augmented Delta  
 TAID = Thrust-Augmented Improved Delta

solid rockets for first-stage augmentation; most of the later models were TADs.

(4) *Improved Delta* is a delta with the "fat-tank" second stage but no first-stage augmentation.

(5) *Thrust-Augmented Improved Delta (TAID or ITAD)* is a Delta "improved" in the mid-1960s by increasing the diameter of the second-stage tank from 32 to 54 in. The burning time of the second stage "fat-tank" Delta was increased from about 160 to about 400 sec.

(6) *Long-Tank Delta* consisted of a Delta with the first-stage tank lengthened by 14.5 ft (fig. 7-3). The first-stage burn time was increased from 150 sec (Pioneer 8) to 221 sec (Pioneer E).

Future changes may involve the adoption of the Titan-III transstage engine and introduction of the Delta Inertial Guidance System (DIGS). The latter would improve the injection accuracy of the first and second stages.

Changes in the third-stage solid rocket motor did not lead to overall name changes, but the model designations did change as the original

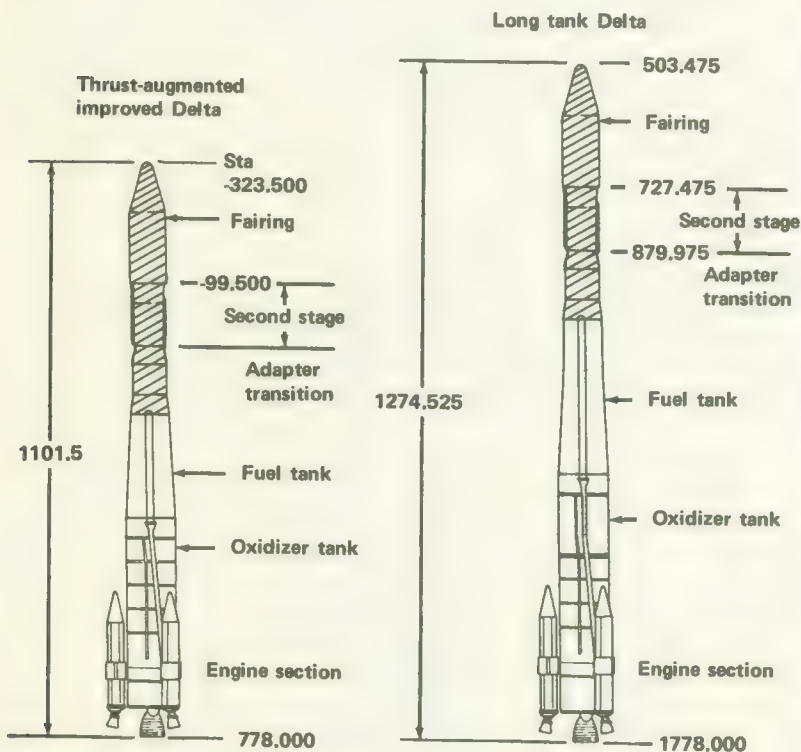


FIGURE 7-3.—Comparative outboard profiles of the TAID and long-tank Delta. (Dimensions are in inches.)

X-248 was replaced by the X-258, which, in turn, was displaced by the FW-4D, etc., as indicated in table 7-1.

The Delta models applied to the Pioneer Program are specified and described in more detail in table 7-2. The Pioneer Deltas came from five points along the evolutionary history of the Deltas, but only four significantly different models were employed:

- (1) Pioneer 6: Delta E, TAID with X-258 and Castor I augmentation
- (2) Pioneers 7 and 8: Delta E, TAID with FW-4D and Castor I augmentation
- (3) Pioneer 9: Delta E, TAID with FW-4D and Castor II augmentation
- (4) Pioneer E: Delta L, a long-tank Delta with FW-4D and Castor II augmentation.

## THE DELTA-SPACECRAFT INTERFACE

The spacecraft-to-launch-vehicle interface is more subtle than one might suppose. Voluminous documents detail the design restraints that affect spacecraft design. These design restraints are essentially detailed descriptions of the mechanical, spatial, electrical, and thermal interfaces that the spacecraft designer must match if his spacecraft is to fit on the rocket and survive the heat and other forces applied during the launch process.

The hardware manifestations of interface matching are attach fittings, fairings, thermal insulation, and shrouds. Much of the interface matching between spacecraft and launch vehicle occurs where the bottom of the spacecraft physically meets the top of the third stage. Pioneer 6 was launched by a Delta with an X-258 third stage, but the remaining four in the series had to be matched to the FW-4D stage.

A brief description of the FW-4D defines the general physical environment at the top of the Delta. The FW-4D is essentially an encased solid-propellant grain engine with a nozzle at the bottom. The spacecraft attach-fitting (not considered part of the motor) is at the top. The motor proper weighs 663.5 lb before firing and only 58.5 lb afterward. Length and diameter are 59.25 and 19.6 in. respectively. The solid propellant consists of polybutadiene acrylic acid/acrylonitrile (PBAN) binder, ammonium perchlorate oxidizer, and aluminum. From the top down: the attach flange is aluminum; the motor case is made from fiberglass and epoxy resin; a composite material comprises the nozzle; the interstage fittings are aluminum. At an ambient temperature of 75° F, the motor burns for 30.8 sec, with a maximum thrust of 6800 lb, producing a total impulse of 172 700 lb-sec.

### Attach Fittings

The Delta Project at Goddard Space Flight Center has developed a wide inventory of attach fittings of various sizes to accommodate different space-

TABLE 7-2.—*Physical Characteristics of the Pioneer Deltas<sup>a</sup>*

| Characteristic           | Pioneer 6                      | Pioneer 7 | Pioneer 8 | Pioneer 9 | Pioneer E       |
|--------------------------|--------------------------------|-----------|-----------|-----------|-----------------|
| Delta popular name       | TAID                           | TAID      | TAID      | TAID      | Long-tank Delta |
| Delta model number       | E                              | E         | E         | E         | L               |
| Delta launch number      | 35                             | 40        | 55        | 60        | 73              |
|                          |                                |           |           |           |                 |
| First stage              | Model Height with adapter (ft) | DSV-2C    | DSV-2C    | DSV-2C    | DSV-2C          |
|                          | Diameter (ft)                  | 60.4      | 60.4      | 60.4      | 60.4            |
|                          | Weight (lb)                    | 8         | 8         | 8         | 8               |
|                          | Sea-level thrust (lb)          | 186 000   |           |           |                 |
|                          | 175 600                        | 175 600   | 175 600   | 175 600   | 172 000         |
|                          |                                |           |           |           |                 |
| First stage augmentation | Model Height with nozzle (ft)  | Castor I  | Castor I  | Castor I  | Castor II       |
|                          | Diameter (ft)                  | 24.3      | 24.3      | 24.3      | 24.3            |
|                          | Weight (lb)                    | 2.6       | 2.6       | 2.6       | 2.6             |
|                          | Sea-level thrust (lb)          | 29 600    |           |           |                 |
|                          | 161 700                        | 161 700   | 161 700   | 156 450   | 156 450         |
|                          |                                |           |           |           |                 |
| Second stage             | Height (ft)                    | 13        | 13        | 13        | 13              |
|                          | Diameter (ft)                  | 5.8       | 5.8       | 5.8       | 5.8             |
|                          | Weight (lb)                    | 14 000    | 14 000    | 14 000    | 14 000          |
|                          | Sea-level thrust (lb)          | 7400      | 7400      | 7400      | 7400            |
|                          |                                |           |           |           |                 |
| Third stage              | Model                          | X-258     | FW-4D     | FW-4D     | FW-4D           |
|                          | Height (ft)                    | 5         | 5         | 5         | 5               |
|                          | Diameter (ft)                  | 1.7       | 1.7       | 1.7       | 1.7             |
|                          | Weight (lb)                    | 735       | 663       | 663       | 663             |
|                          | Vacuum thrust (lb)             | 6200      | 5600      | 5600      | 5600            |
|                          |                                |           |           |           |                 |
| Total launch vehicle     | Height with shroud (ft)        | 92        | 92        | 92        | 92              |
|                          | Weight (lb)                    | 150 000   | 150 000   | 150 000   | 150 000         |
|                          | Date                           | 12-16-65  | 8-17-66   | 12-13-67  | 11-8-68         |
|                          |                                |           |           |           |                 |
| Space-craft              | Nominal weight (lb)            | 138       | 138       | 147       | 147             |
|                          |                                |           |           |           |                 |

<sup>a</sup> Thrust and weight figures are approximate.

craft, particularly the larger satellites that can be launched with the more powerful versions of the Delta. The relatively small Pioneer spacecraft however, were attached to the FW-4D and X-258 by a small 9 × 8 in, conical attach fitting (fig. 7-4). A two-piece marmon-type clamp secured by two bolts held the spacecraft in the attach fitting. In flight, the spacecraft were separated from the attach fitting by ordnance cutters that severed both bolts (the severing of one bolt is actually sufficient). Separation springs imparted relative velocities of 6 to 8 ft/sec to the spacecraft.



FIGURE 7-4.—The 9 × 8-in. conical attach fitting used on Delta Pioneer launches.

## Fairings and Payload Envelopes

During launch, spacecraft were protected from buffeting and aerodynamic heating by a thin-walled fiberglass fairing or shroud. All five Pioneers used the so-called "standard" Delta fairing (fig. 7-5). This protective shell is 224 in. long, 65 in. in diameter, and weighs roughly 535 lb exclusive of any thermal insulation the spacecraft may need.

Once the sensible atmosphere had been breached, the two halves of the fairing were freed by firing explosive bolts. Spring-loaded latches then pushed the fairing halves aside and the spacecraft, plus the second and third stages, proceeded unencumbered.

The interface between the fairing and spacecraft is primarily spatial; that is, the spacecraft must fit within the envelope defined in figure 7-6. Some of the Pioneers required thin layers of thermal insulation on the fairing nose; the amount depended upon the trajectory selected and the resultant heating.

## Spacecraft Mechanical Loads During Launch

The rocket motors propelling the Pioneer spacecraft into escape trajectories generate what is termed the "launch environment" for the spacecraft; that is, the sinusoidal, random, acoustic, and shock loads induced during launch affected spacecraft design. The low-frequency sinusoidal excitations occurred mostly at liftoff, during transonic flight, and just prior to first-stage cutoff. Maximum random and acoustic excitations occurred at liftoff and during transonic flight. Shocks were transmitted to the spacecraft when explosive bolts and other pyrotechnic devices detonated. Finally, acceleration or g-loads stressed the spacecraft structure during all phases of powered flight.

The time histories of these mechanical forces vary for each Delta model. The Delta restraint documents specify the payload mechanical environments in detail for each model (ref. 1). A few representative curves presented here should give the reader a feeling for the "dynamic" mechanical interface (figs. 7-6 to 7-9). The Delta restraint graphs are translated into spacecraft design and test specifications (ref. 2). The Pioneer test program is covered in ch. 6 in this volume.

The tests employed shake tables, spin tables, and other equipment that simulates the dynamic environment created by the Deltas. The dynamic forces impressed on the spacecraft during test normally exceeded those stipulated in the Delta restraint publications.

Several of the general design specifications in Pioneer Specification A-6669 were derived from Delta-produced forces. For example:

3.1.10 *Static Balance.* The spacecraft center of gravity shall not be displaced from the spacecraft centerline by a distance greater than 0.015 in.

- 3.1.11 *Inertial Axes.* The spacecraft principal axes of inertia shall be perpendicular and parallel to the spacecraft centerline within an angle of 0.001 rad.
- 3.1.12 *Rigidity.* Rigidities of the spacecraft in the launch configuration shall be such as to make all resonant frequencies of the entire structure and/or assemblies greater than 5 cycles per second.
- 3.2 *Load Factors.* The following critical load factors expressed in gravity units will exist at the spacecraft center of gravity during launch. The side loads are caused by both translational and pitching accelerations.

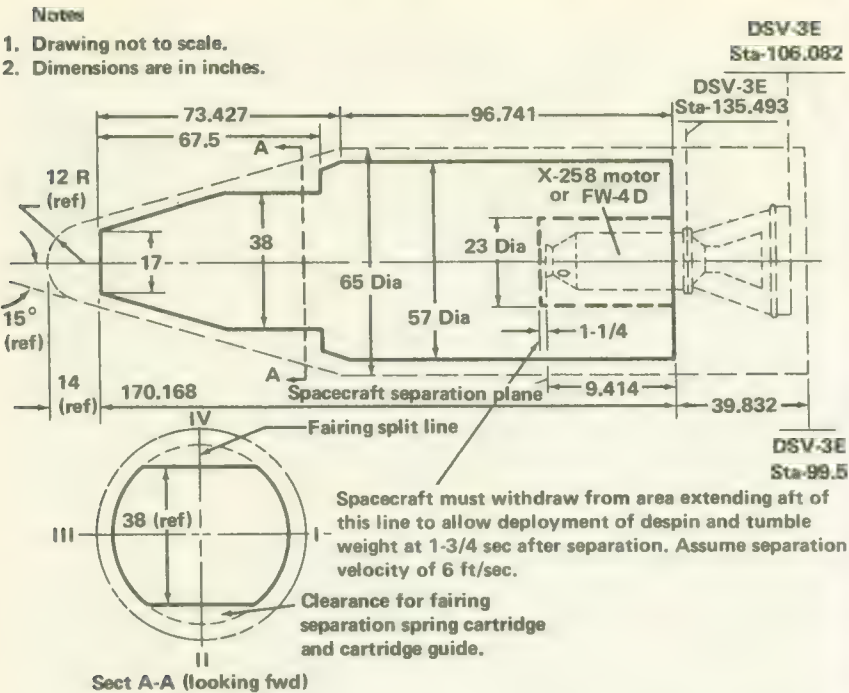
| Condition                             | Axial load factor (g)                    | Side load factor (g) |
|---------------------------------------|--|----------------------|
| 120 sec after ignition of first stage | 6.20                                     | 1.05                 |
| First-stage burnout                   | 14.00                                    | 0.70                 |
| Third-stage spinup                    | 0  | 0                    |
| Third-stage ignition                  | 6485                                     | 0                    |
|                                       | $587 + (\text{spacecraft weight in lb})$ |                      |
| Third-stage burnout                   | 6770                                     |                      |
|                                       | $77 + (\text{spacecraft weight in lb})$  |                      |

The specifications above are taken from NASA-ARC Specification A-6669.07, dated November 13, 1964. Both specifications and launch vehicle restraints changed frequently during the history of the spacecraft program.

Specifications numbered 3.1.10 and 3.1.11 introduce another mechanical force felt by the spacecraft as it ascends from the Earth—centrifugal force. The Pioneer spacecraft were spin-stabilized and, each in the company of a Delta third stage, were “spun up” during third-stage burn to provide dynamic stability, much as rifle bullets are stabilized by spinning. The entire third stage and its spacecraft payload were mounted on a spin table located on the top of the second stage (fig. 7-10). After the fairing had been jettisoned, and prior to third-stage ignition, small rockets mounted with thrust axes tangential to the circular spin table ignited and started the spin table spinning after the fashion of a Fourth-of-July cartwheel. Spinup required dynamic symmetry of the payload around the spin axis, as expressed in specifications 3.1.10 and 3.1.11.

### Fairing Heating

As mentioned earlier, the Delta fairing heated up as it ascended through the sensible atmosphere at high velocities. The temperature history of the



Access to the spacecraft attach fitting must be provided to install clamp, torque bolts, and to install and checkout all pyrotechnics.

FIGURE 7-5.—Payload envelope of the improved Delta shroud. From: Specification A-6669.07, fig. 3.1.2.

inside of the fairing shows that the temperature varied from point to point and depended upon the actual launch vehicle trajectory. If the inside of the fairing exceeded 500° F, outgassing might have occurred to the detriment of both fairing and payload. Lower temperatures could damage the spacecraft components. It was the responsibility of the launch-vehicle contractor to apply enough insulation to the outside of the fairing to prevent damage. Fairing insulation was a critical matter because some fraction of each pound added—usually 2 to 3 percent—had to be subtracted from the spacecraft weight.

The general approach to this problem in the Pioneer Program was the specification of a reference trajectory and the temperature history of the inside of the fairing without insulation. Figures 7-11 and 7-12 present the trajectory and temperatures stipulated for Pioneer spacecraft. Insulation was applied on the Delta third stage and fairing where needed.

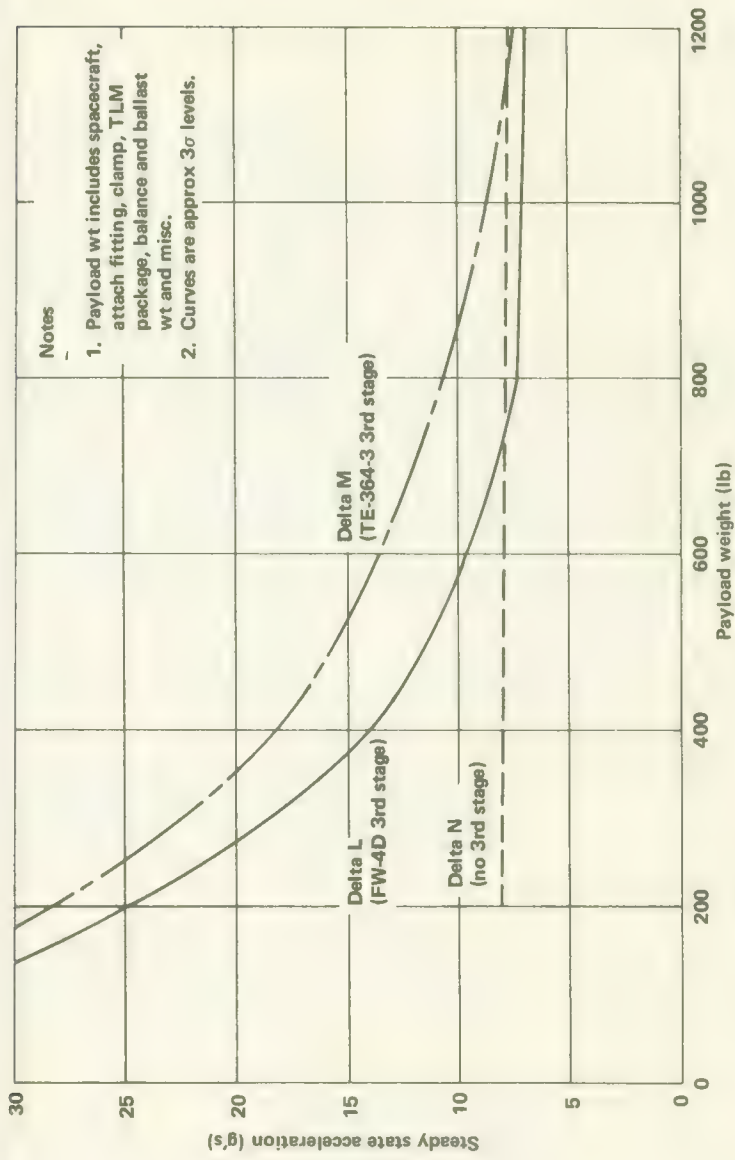


FIGURE 7-6.—Acceleration vs. payload weight for long-tank Deltas.

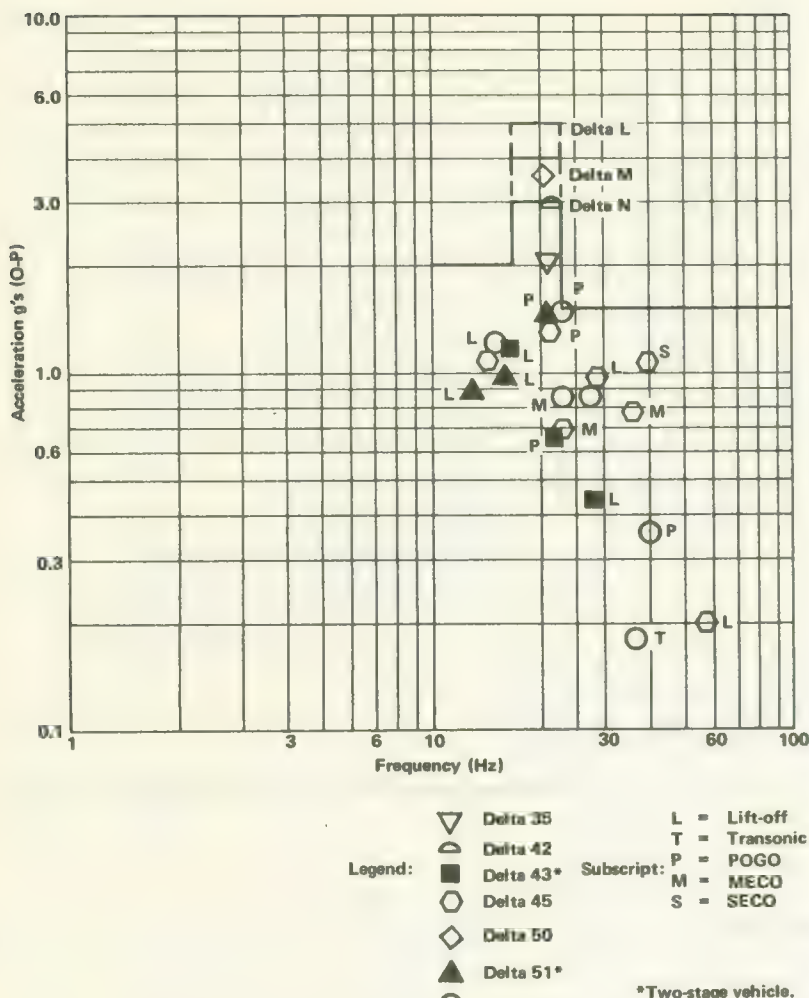


FIGURE 7-7.—Sinusoidal vibrations measured along thrust axis on Models L, M, and N.

### OTHER INTERFACES

The other category of interfaces included all the electrical connections that had to be made between the consoles in the blockhouse, through Delta umbilical wiring, to the spacecraft. The spacecraft was checked out and provided with electrical power while on the launch pad, through these wires.

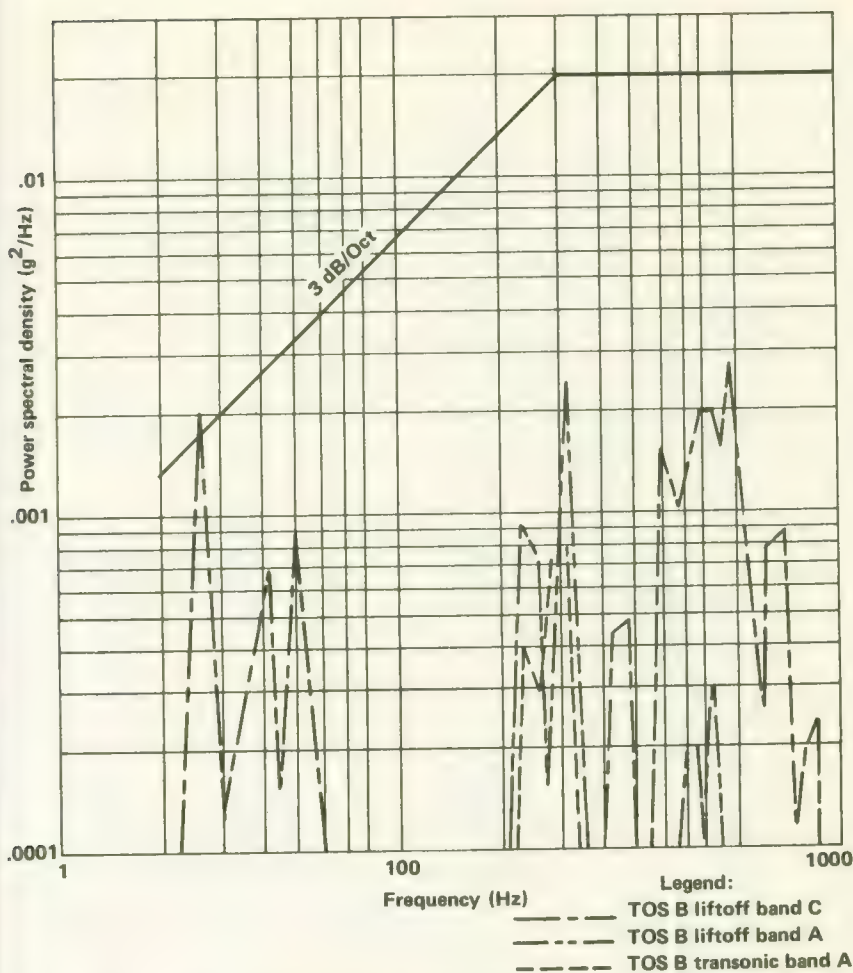


FIGURE 7-8.—Random vibration levels measured along the thrust and lateral axes of Delta L and M vehicles.

### TRAJECTORY DESIGN

Each Pioneer launch trajectory was different. The following factors precluded identical trajectories:

- (1) The Delta launch vehicle has evolved with the later versions capable of placing much larger payloads into orbit.
- (2) Pioneers 6 and 9 were inward-bound (toward the Sun), while Pioneers 7 and 8 were outward-bound.

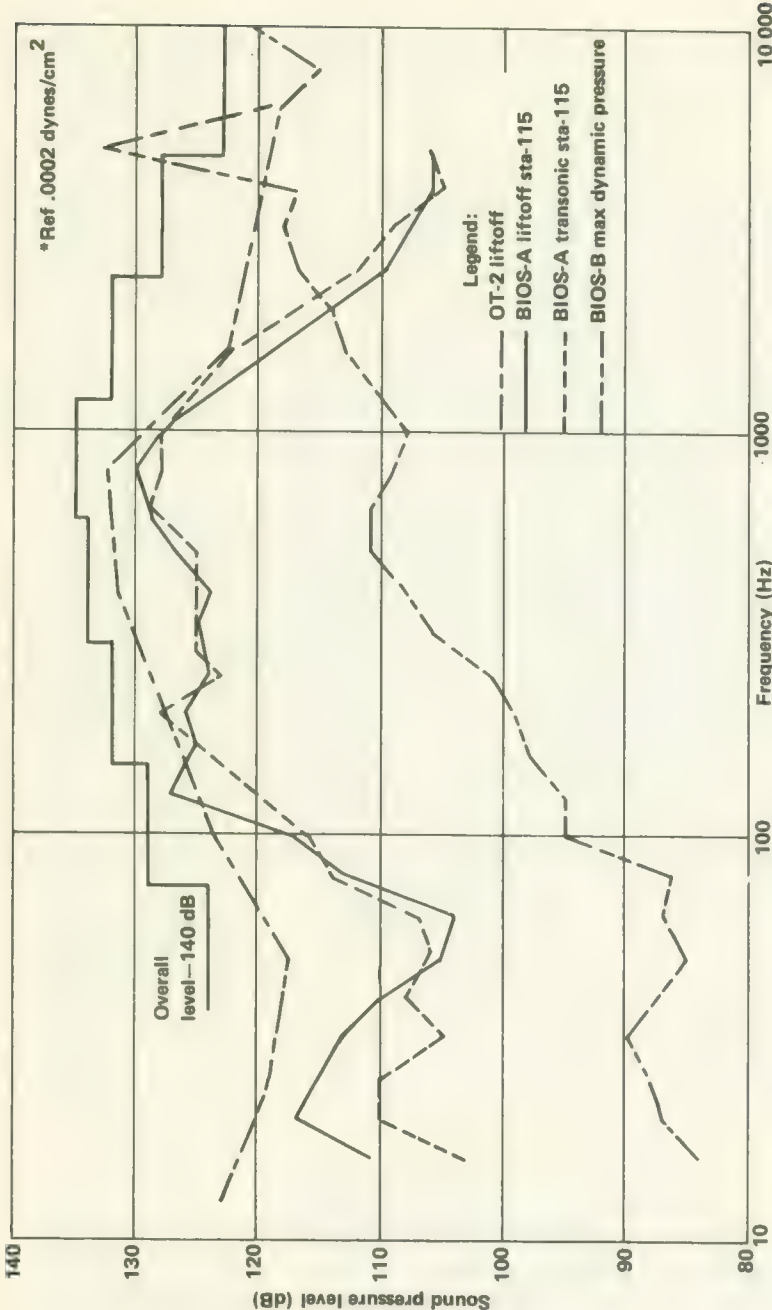


FIGURE 7-9.—Acoustic noise flight levels predicted for the Delta.

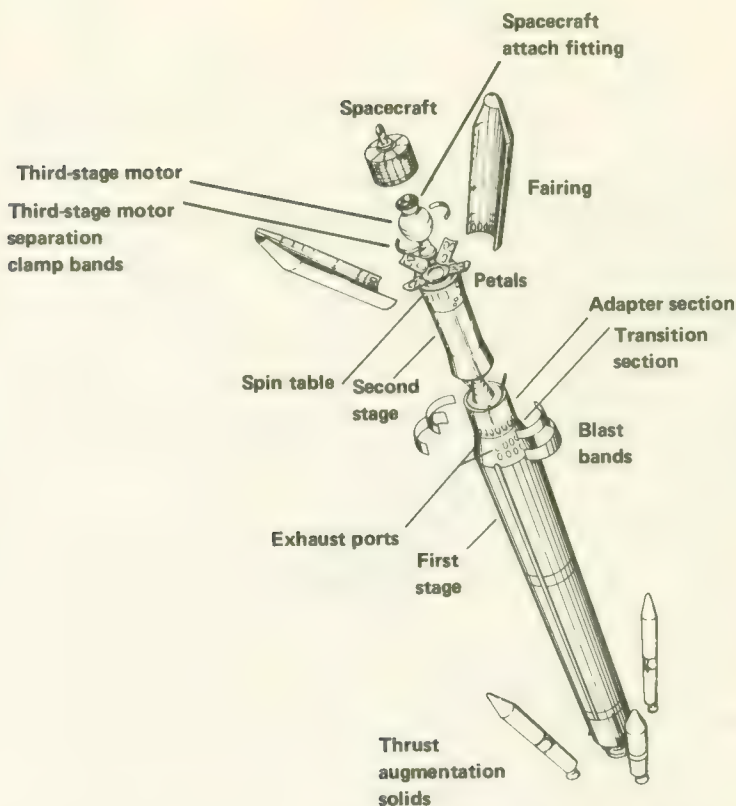


FIGURE 7-10.—Delta staging and separation events, shown here for an Applications Technology Satellite launch.

(3) TETRs were carried "piggyback" on the second stage on the Pioneer 8, 9, and E launches.

In addition to these major factors, the Pioneer payload weights varied slightly.

In very general terms, the Pioneer-carrying Deltas were all launched southeastward from Cape Kennedy along the Eastern Test Range (fig. 7-13). During the coast phase, the Delta passed over Ascension, and the NASA tracking stations in the vicinity of Johannesburg, Republic of South Africa. Roughly 520 sec after liftoff, the second stage cut off and the Delta third stage plus the spacecraft were in orbit over the Indian Ocean during the coast phase. Here, the TETR piggyback satellites were ejected from the second stage on flights 8 and 9.<sup>23</sup> Some several hundred seconds after

<sup>23</sup> The Pioneer Flight E carried a TETR but it was destroyed by the Range Safety Officer soon after liftoff on Aug. 27, 1969.

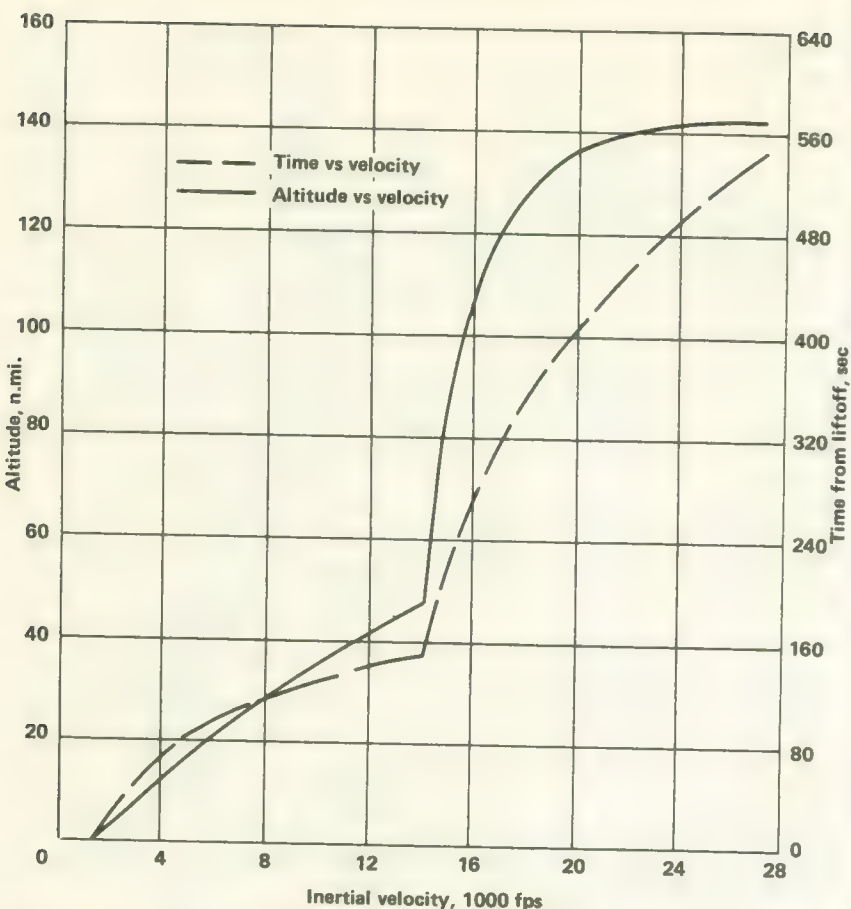


FIGURE 7-11.—The reference trajectory specified by NASA for Pioneer launches.

orbital injection, when the Delta third stage plus spacecraft drifted close to the plane of the ecliptic, the third stage fired, propelling the spacecraft out of Earth orbit into orbit around the Sun. For inward solar orbits, the spacecraft had to be injected antiparallel to the Earth's direction of motion about the Sun; that is, the spacecraft was given an orbital velocity around the Sun smaller than the Earth's. (See ch. 2.) As the inward Pioneers (6 and 9) fall toward the Sun, they pick up speed and eventually pull farther and farther ahead of the Earth. Conversely, Pioneers 7 and 8, the outward Pioneers, were injected parallel to the Earth's direction of motion and now lag the Earth by ever-greater distances.

The actual trajectories flown by the Deltas during the Pioneer launches are described in Volume III. Here, the objective is to show the impact of

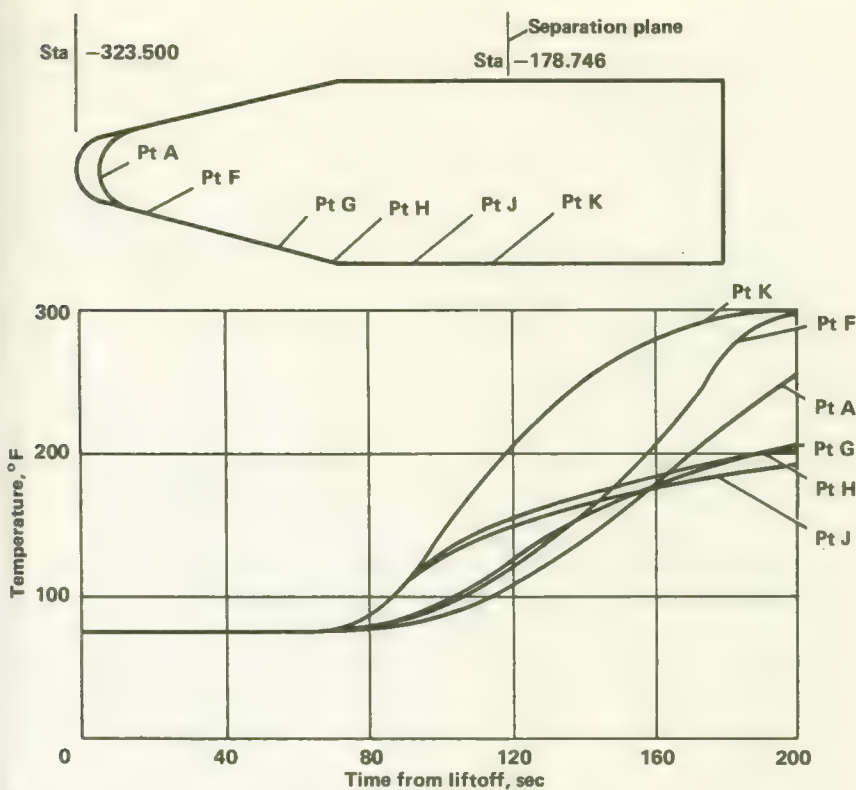


FIGURE 7-12.—Internal temperature histories specified for Delta shroud. Insulation had to be added to meet these specifications on several Pioneer launches.

mission objectives on the launch vehicle and trajectory and the interfaces between the several systems that must work in harmony for a successful launch.

### PRIMARY LAUNCH OBJECTIVES

The primary Pioneer launch objective was the successful injection of the spacecraft into an orbit around the Sun. However, the orbital parameters and the shape of the trajectory taking the spacecraft into orbit had to be carefully designed to meet conditions arising from the scientific objectives, tracking requirements, secondary payload objectives, etc. These factors are discussed in more detail in chapter 2.

In addition to meeting the mission objectives, launch trajectories also had to meet stringent range safety requirements at Cape Kennedy, as well as a set of conditions called (in Cape Kennedy jargon) "WECO look-angle

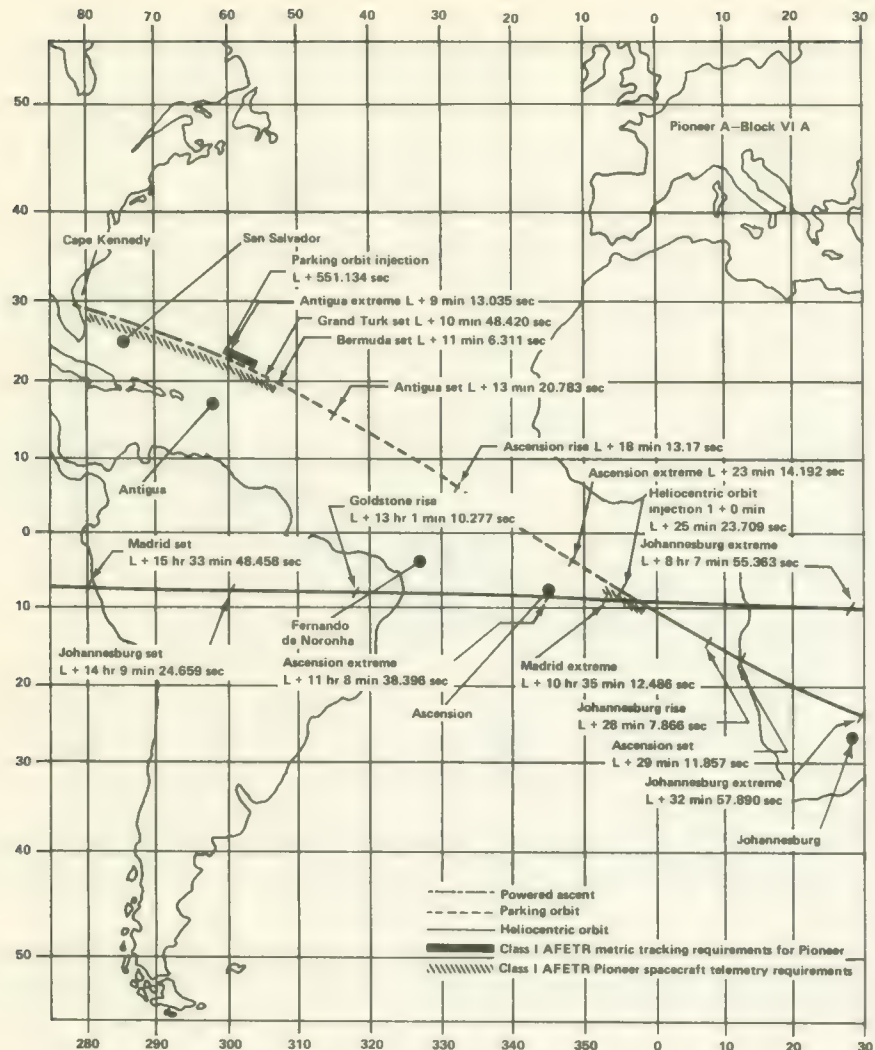
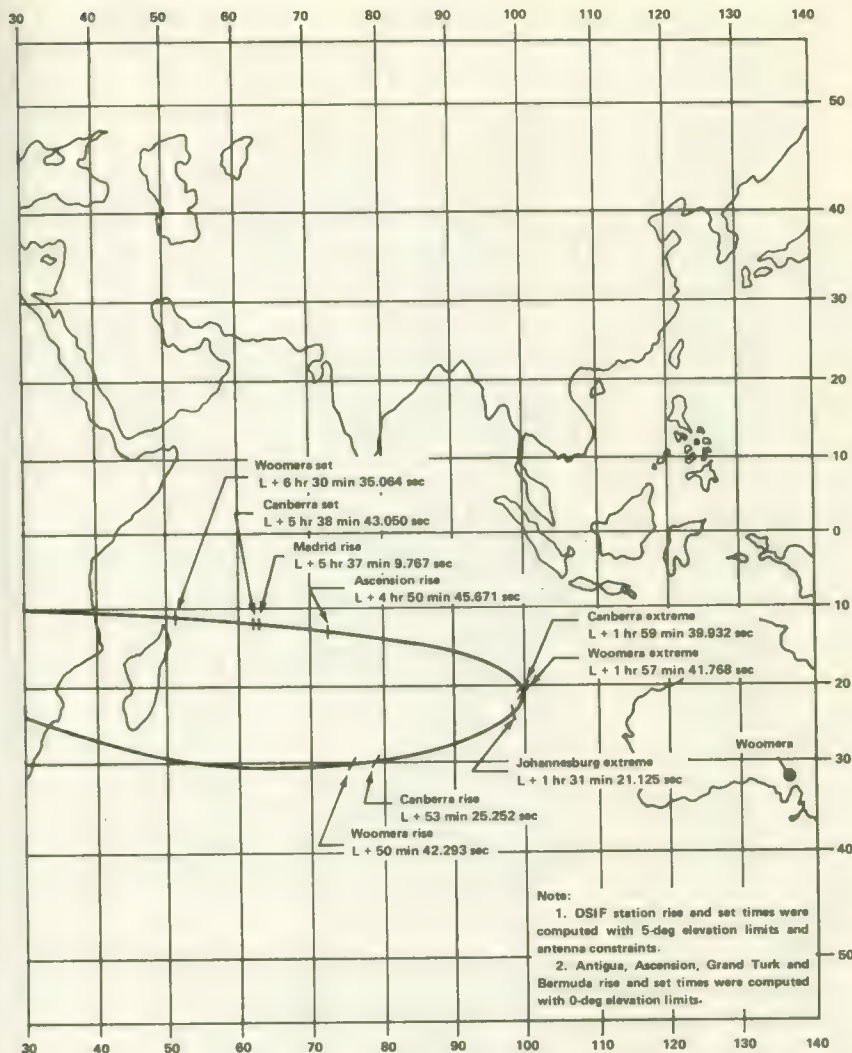


FIGURE 7-13.—Earth track of Pioneer 6 showing DSIF involvement during flight. As the spacecraft escaped from Earth, the Earth turned under it, giving rise to apparent retrograde motion.

constraints.” (WEKO refers to Western Electric Company, the manufacturer of the radar-controlled guidance equipment employed on all Delta Pioneer launches.) For the guidance equipment to function properly, the launch trajectory had to remain within the radar’s field of view (look angle) for a stipulated period of time.



### THE LAUNCH SEQUENCE

For the Pioneer-9 launch, which will be used to illustrate the entire series, two launch blocks of time were selected, and within each block, a prime launch day. The Pioneer-9 blocks were November 1 through November 22, 1968, and November 27 through December 22, 1968; the prime launch days were November 6 and December 18, respectively.

The length of time that the third-stage-spacecraft combination has to coast in Earth orbit to reach the plane of the ecliptic varies slightly from

TABLE 7-3.—*Events Planned in Pioneer-9 Trajectory Sequence*

| Time (sec)                      | Event                               |  |
|---------------------------------|-------------------------------------|--|
| 0.000                           | Stage-1 liftoff                     |  |
| 2.000                           | Begin stage-1 roll program          |  |
| 3.670                           | End stage-1 roll program            |  |
| 4.000                           | Begin stage-1 pitch program         |  |
| 9.670                           | End first pitch rate—stage 1        |  |
| 10.000                          | Begin second pitch rate—stage 1     |  |
| 38.190                          | Solid motors burnout                |  |
| 64.670                          | End second pitch rate—stage 1       |  |
| 65.000                          | Begin third pitch rate—stage 1      |  |
| 70.000                          | Jettison solid motor casings        |  |
| 89.670                          | End third pitch rate—stage 1        |  |
| 90.000                          | Begin fourth pitch rate—stage 1     |  |
| 130.000                         | End stage-1 pitch program           |  |
| 150.531                         | Main engine cutoff                  |  |
| 154.531                         | Stage-2 ignition signal             |  |
| 154.531                         | Start VCS * channel 1               |  |
| 155.581                         | Stage-1 separation                  |  |
| 156.331                         | Stage-2 90 percent chamber pressure |  |
| 159.531                         | Begin stage-2 pitch program         |  |
| 166.531                         | End first pitch rate—stage 2        |  |
| 167.531                         | Begin second pitch rate—stage 2     |  |
| 169.531                         | Jettison fairing                    |  |
| 460.000                         | End VCS channel 1                   |  |
| 460.000                         | Start VCS channel 2                 |  |
| 534.352                         | End VCS channel 2                   |  |
| 534.352                         | Second-stage engine cutoff command  |  |
| 534.352                         | End stage-2 pitch program           |  |
| 534.721                         | Final cutoff—stage 2                |  |
| 561.531                         | Begin coast-phase pitch program     |  |
| First firing      Second firing |                                     |  |
| block                           | block                               |  |
| 696.531                         | 734.531                             | End coast-phase pitch program                                |
| 735.531                         | 735.531                             | Begin coast-phase yaw program                                |
| 760.531                         | 760.531                             | End coast-phase yaw program                                  |
| 1201.531                        | 1349.531                            | Start stage-3 ignition time-delay relay<br>Fire spin rockets |
| 1203.531                        | 1351.531                            | Jettison stage 2, activate retro system                      |
| 1216.531                        | 1364.531                            | Stage-3 ignition   |
| 1247.331                        | 1395.331                            | Stage-3 burnout  |
| 1263.531                        | 1411.531                            | Pioneer separation   |
| 1300.531                        | 1448.531                            | TETR separation from stage 2                                 |

\* VCS = Velocity cutoff system.

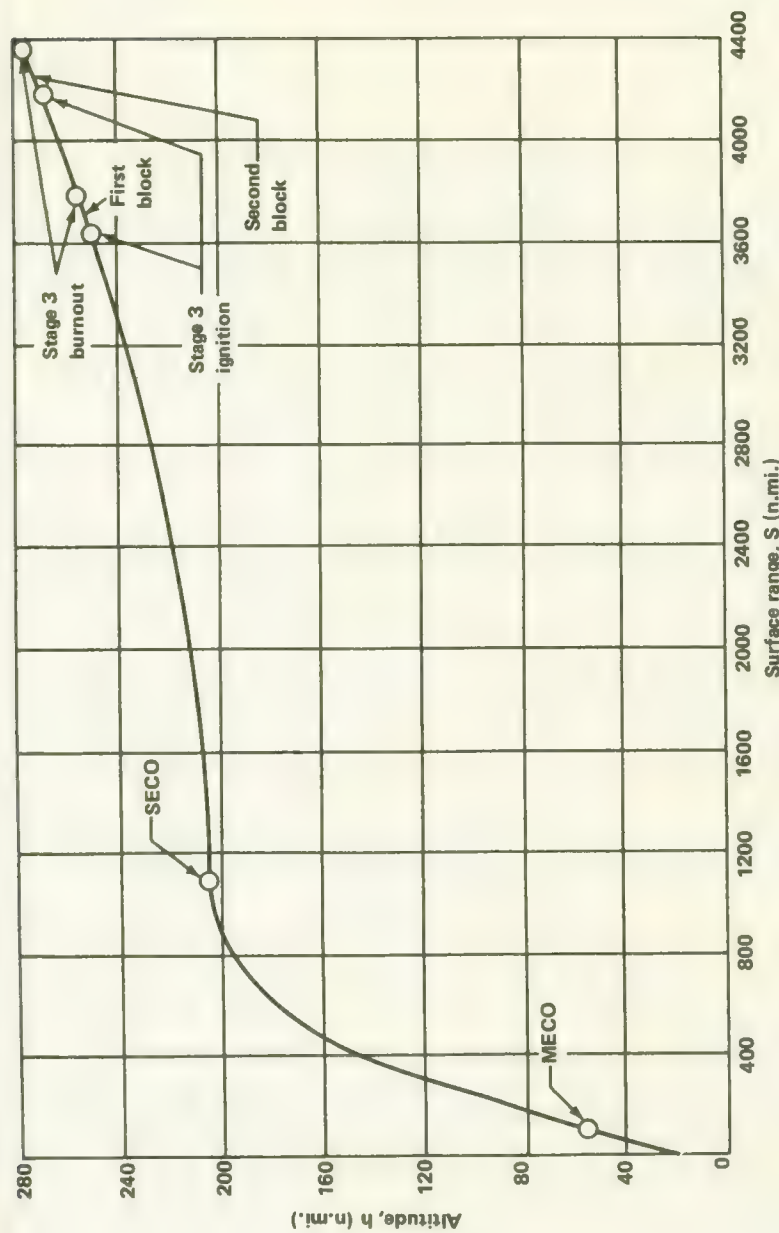


FIGURE 7-14.—Altitude vs. surface-range history planned for Pioneer-D launch.

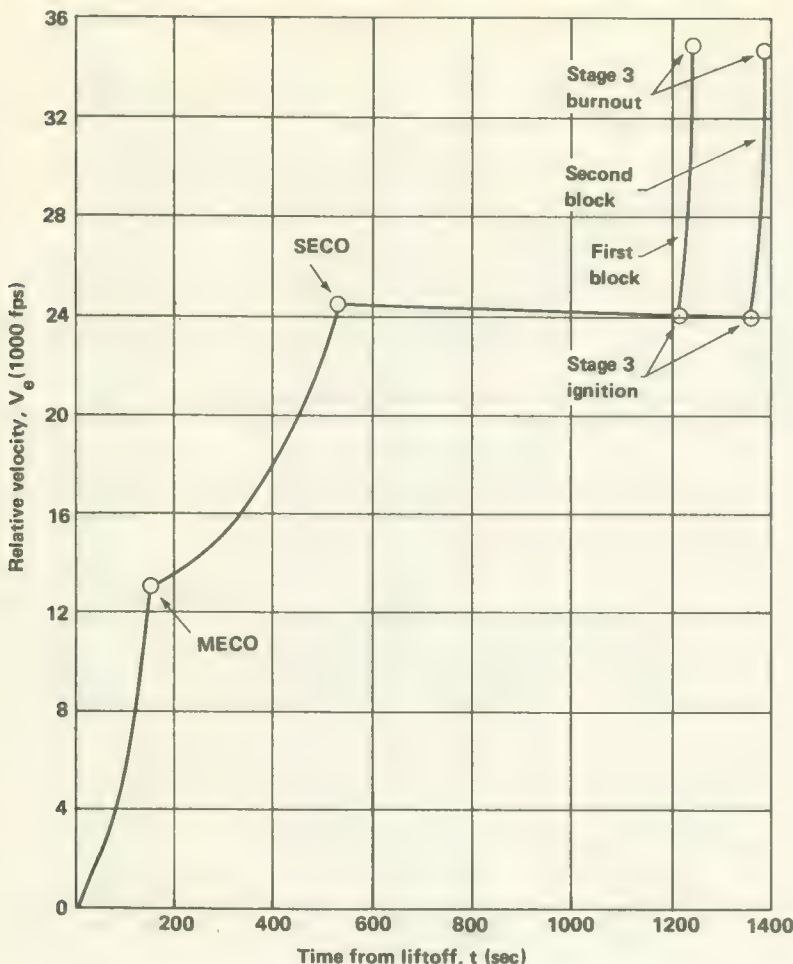


FIGURE 7-15.—Relative-velocity history planned for Pioneer-D launch.

day to day and even more from block to block. From the launch of Pioneer 9 to a planned orbit  $502 \times 203$  n. mi., the trajectories were identical regardless of day of launch within each block of days, as noted in the launch sequence listed in table 7-3. The coast periods, however, are 682 and 830 sec, respectively, for the November and December launch blocks.

The trajectory planned for Pioneer 9 is illustrated crudely by figures 7-14 and 7-15. In this computer-assisted age, trajectory and orbit details are customarily presented at great length by computer printouts. From the moment of liftoff to 1000 days later, the critical rocket and spacecraft parameters for the Pioneer 9 flight were printed out (in some 330 pages)

by the Delta contractor (ref. 3). Printouts such as this were prepared for each Pioneer flight. Detailed scenarios were also prepared for each flight telling each member of the launch team what to do and when to do it. (See Vol. III.)

### A TYPICAL WEIGHT BREAKDOWN

The object of all these tables and computer printouts, of course, is the injection of the small spacecraft, weighing only about 1 percent as much as the launch vehicle on the pad, into orbit around the Sun. Since this chapter focuses on the Delta, it will be instructive to see how 99 percent of the launch vehicle weight is applied to the 1 percent payload (table 7-4).

TABLE 7-4.—*Typical Pioneer Launch-Vehicle Weight Breakdown*

| Item   | Weight (lb) |
|--|-------------|
| Launch vehicle at liftoff                            | 152 153     |
| Vented liquids and gases                             | -39         |
| Fuel and oxygen burned, stage 1                      | -26 316     |
| Solid propellants burned, augmentation               | -24 786     |
| Launch vehicle at solid motor burnout                | 101 012     |
| Vented liquids and gases                             | -49         |
| Fuel and oxygen burned, stage 1                      | -20 898     |
| Burned-out solid motor                               | -4 803      |
| Launch vehicle after jettison of solid motor         | 75 262      |
| Vented liquids and gases                             | -129        |
| Fuel and oxygen burned, stage 1                      | -52 791     |
| Launch vehicle at MECO                               | 22 342      |
| MECO (151.56 sec)                                    |             |
| Main-engine stop losses                              | -66         |
| Fuel and oxygen burned, vernier engine               | -42         |
| Launch vehicle before stage-1 separation             | 22 234      |
| Vernier engine fuel and oxygen available for impulse | -63         |
| Residual propellants, stage 1                        | -200        |
| Trapped liquids and gases                            | -846        |
| Dry stage 1 (DSV-3E-1) jettisoned                    | -7001       |
| Launch vehicle after stage-1 separation              | 14 124.10   |
| Interstage structure jettisoned                      | -180.55     |
| Launch vehicle at stage-2 ignition                   | 13 943.55   |
| Fuel and oxidizer lost during startup transients     | -19.60      |
| Usable pressurized nitrogen                          | -3.15       |

TABLE 7-4.—*Typical Pioneer Launch-Vehicle Weight Breakdown (Continued)*

| Item  | Weight (lb) |
|---|-------------|
| Fairing jettisoned  | -539.45     |
| Fuel and oxidizer consumed  | -10 313.33  |
| Launch vehicle at second-stage engine cutoff command (SECOM)                                    | 3068.02     |
| Fuel and oxidizer consumed and lost during engine stop transients                               | -26.50      |
| Residual propellants  | -294.91     |
| Trapped propellants and gases   | -65.15      |
| Spin table jettisoned   | -82.06      |
| Dry stage 2 (DSV-3E-3) jettisoned   | -1665.51    |
| TETR satellite released   | -58.00      |
| Launch vehicle at stage-3 ignition  | 875.89      |
| Start losses, stage 3   | -0.05       |
| Inert loss during burning, stage 3  | -4.30       |
| Propellant consumed, stage 3  | -606.90     |
| Launch-vehicle and third-stage burnout  | 264.64      |
| Stage-3 motor, ballast, balance weights, support rings, beacon,<br>and telemetry kit jettisoned | -46.62      |
| Stage-3 motor case jettisoned   | -54.45      |
| Spacecraft attach fitting jettisoned  | -16.01      |
| Spacecraft injected into solar orbit  | 147.56      |

## REFERENCES

1. ANON.: Delta Spacecraft Design Restraints. McDonnell-Douglas Astronautics Co. DAC-61687, Oct. 1968 (one of series of updated Delta restraint documents).
2. ANON.: Pioneer Program, Specification A-6669.00. NASA, Ames Research Center, Rev. no. 7, Jul. 28, 1966.
3. ANON.: Detailed Test Objectives for Improved Delta Launch Vehicle. Spacecraft: Pioneer D, McDonnell-Douglas Astronautics Co. DAC-61696, Oct. 1968. (A similar report exists for each Pioneer flight.)

# Tracking and Communicating with Pioneer Spacecraft

## TRACKING THE FIRST PIONEERS

THE FIRST GROUP OF PIONEER SPACE PROBES (Pioneers 1 through 5) were launched in the direction of the Moon between 1958 and 1960. The tracking and data acquisition theories and hardware developed by JPL to support these flights ultimately developed into the present DSN. The DSN, managed by JPL for NASA, tracks NASA's unmanned spacecraft launched toward the Moon, the planets, and deep space.

The basic problem that JPL had to solve in tracking and acquiring data from spacecraft beyond Earth orbit involved the immense distances of interplanetary flight. Ten thousand miles posed little difficulty, but at tens of millions of miles spacecraft signals faded away amid the radio noise of interplanetary space. The Minitrack radio interferometer stations that the Naval Research Laboratory (NRL) had installed around the world during 1956 and 1957 for the IGY could work near-Earth satellites, but they could not detect faint signals from deep space with their low-gain antennas. Conventional radars could not track spacecraft much beyond 1000 miles. Therefore, new techniques were needed for deep space tracking.

Three fundamental concepts permit the successful tracking of very distant spacecraft by the DSN:

(1) The concept of a high-gain, highly directional, paraboloidal antenna with a large diameter —high gain permits reception of very weak spacecraft signals; high directionality provides the accurate angular bearings needed for tracking. Big-dish antennas have been in the radio astronomer's repertoire since a radio amateur named Grote Reber built a small one in his backyard in 1937.

(2) A radio ranging technique, utilizing pseudorandom noise, allowed ground observers to measure the transit time and Doppler shifts of radio signals between Earth and spacecraft and back again. Spacecraft distance and radial velocity come from these measurements.

(3) The JPL phase-lock-loop, conceived by JPL's Eberhardt Rechtein during the 1950s, was adopted by the DSN and later by the Manned Space Flight Network (MSFN) for its Unified S-Band tracking during the Apollo Program. The phase-lock-loop concept is fundamental to the

detection of signals by the DSN, but it is independent of the pseudorandom noise approach to tracking.

JPL put its tracking and data acquisition concepts into practice prior to October 1958, while it was still under U.S. Army sponsorship. Explorers 1 through 5 were tracked by a handful of JPL phase-lock-loop, Microlock stations as well as the NRL Minitrack Network. By late 1958, as the first Pioneers were launched, JPL had established tracking stations at Cape Canaveral, Puerto Rico, and Goldstone Lake, California. The biggest dish in the embryonic network was the 85-foot paraboloid at the Goldstone Pioneer Site (fig. 8-1). Smaller dishes were located at Cape Canaveral, Florida, and near Mayaguez, Puerto Rico. A 60-ft, Department of Defense dish in Hawaii and the famous 250-ft antenna at Jodrell Bank, England, cooperated with the JPL stations during the early Pioneer launches.

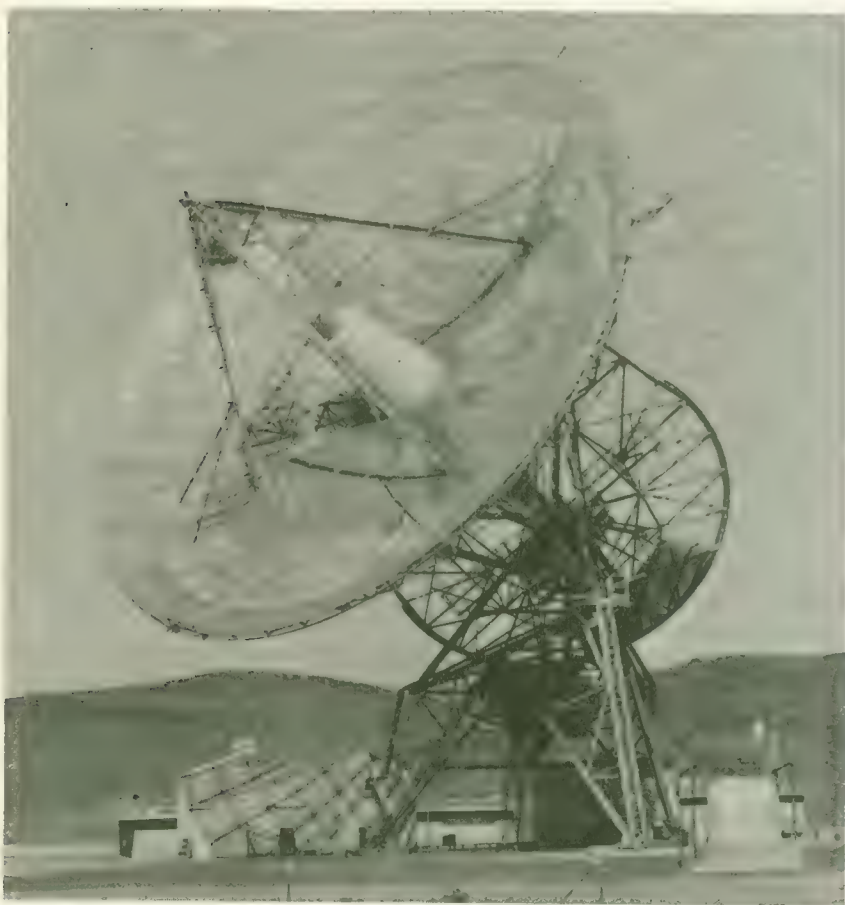


FIGURE 8-1.—The first 85-ft paraboloidal antenna installed at Goldstone (Pioneer site).

DSN evolution since 1960 has been expressed primarily in terms of physical size (antenna diameter and new stations), electronic sophistication (masers, lower antenna noise temperatures, etc.). The 85-ft dishes, the hallmark of the DSN, are now found near Madrid, Johannesburg, Woomera, and Canberra, as well as Goldstone. A 210-ft paraboloid was added at Goldstone in 1966; others are under construction at Madrid and Canberra.

When the Pioneer Program began in late 1961, there was no question about network choice. The DSN was the only one of NASA's three networks that could track and communicate with a deep-space probe. Like the Delta launch vehicle, the DSN became a basic, general-purpose pillar of the Pioneer Program—but a pillar already in place that could be altered very little for any specific mission. Even more than the Delta's, the basic capabilities of the DSN helped shape the Pioneer spacecraft design.

### SOME GENERALITIES ABOUT TRACKING AND DATA ACQUISITION

The three basic functions performed by terrestrial ground-support equipment during the Pioneer missions were:

(1) Tracking—Spacecraft position was measured with high precision from liftoff at the launch pad to injection into parking orbit, through the coast phase, to injection into heliocentric orbit, and as far out in deep space as possible—several hundred million miles and more if possible. Out to about 10 000 miles this function was accomplished by the Near Earth Phase Network, which consists of MSFN and U.S. Air Force precision radars; beyond 10 000 miles, the DSN performed this function.

(2) Communication or data acquisition—Scientific and housekeeping data were detected and acquired from the spacecraft, and routed from the worldwide network stations to a central location for evaluation and processing.

(3) Command—Commands were dispatched from a centralized control center to the network station working the spacecraft and, then, to the spacecraft itself.

Obviously the Pioneer spacecraft could not be designed independently of the DSN and its relatively fixed roster of equipment. As described in chapter 4, the spacecraft communication subsystem had to be matched in terms of power level and frequency to the specific DSN receiving equipment expected to be operational at the time of launch. The same was true for the uplink that carried commands to the spacecraft.

The DSN was not a static facility. Its capabilities improved markedly over the 5-year Pioneer launching schedule. These improvements were not due to fundamental changes in the DSN but rather to continual upgrading and improvement, much like the collective changes that so greatly in-

creased the Delta's payload capacity during the same period. In addition to the evolutionary improvements, some of the 85-ft MSFN antennas adjacent to the DSN antennas for redundancy during Apollo flights were pressed into service tracking Pioneers while they were still relatively close to the Earth. With the Apollo, Mariner, and Pioneer Programs, NASA had so many active spacecraft in deep space that it pooled its big antennas to achieve optimum coverage.

In general terms, the DSN carries out its three basic functions using three distinct facilities (ref. 1):

(1) The Deep Space Instrumentation Facility (DSIF) consists of the DSN tracking and data acquisition stations shown in table 8-1.

(2) The Space Flight Operations Facility (SFOF) is located at JPL, in Pasadena, California; it monitors all spacecraft data, issues commands, and performs all necessary mission calculations.

(3) The Ground Communication Facility (GCF) ties all DSIF stations to the SFOF with high-speed, real-time communications. The bulk of DSN communication traffic is carried via NASA's global communication system, NASCOM, which contributes circuits to the GCF.

One other network of equipment crucial to the Pioneer mission is the Eastern Test Range (ETR) run by the U.S. Air Force. ETR radars, optical instruments, and other tracking equipment follow all launches from Cape Kennedy down range past Ascension Island, over Africa, into orbit, where NASA networks assume the full tracking load. They are considered

TABLE 8-1.—*The DSN Stations*

| DSS<br>no. | Location                                     | Dish<br>size | Primary during<br>Pioneer flight |   |   |   |   |
|------------|--|--------------|----------------------------------|---|---|---|---|
|            |  |              | 6                                | 7 | 8 | 9 | E |
| 11         | Goldstone, Cal. (Pioneer) <sup>a</sup> ----- | 85-ft        |                                  |   | X | X |   |
| 12         | Goldstone, Cal. (Echo)-----                  | 85-ft        | X                                | X | X | X |   |
| 13         | Goldstone, Cal. (Venus) <sup>b</sup> -----   | 85-ft        |                                  |   |   |   |   |
| 14         | Goldstone, Cal. (Mars) <sup>c</sup> -----    | 210-ft       | X                                | X | X | X |   |
| 41         | Woomera, Australia-----                      | 85-ft        |                                  |   |   | X |   |
| 42         | Canberra, Australia <sup>d</sup> -----       | 85-ft        | X                                | X |   |   | X |
| 51         | Johannesburg, South Africa-----              | 85-ft        | X                                | X | X | X | X |
| 61         | Madrid, Spain (Robledo) <sup>a</sup> -----   | 85-ft        |                                  |   |   | X | X |
| 62         | Madrid, Spain (Cebreros)-----                | 85-ft        |                                  |   | X | X |   |
| 71         | Cape Kennedy, Fla.-----                      | 4-ft         | X                                | X | X | X | X |

<sup>a</sup> MSFN Apollo Wing located here was used during some Pioneer flights.

<sup>b</sup> Used primarily for research and development.

<sup>c</sup> Used on "extended" Pioneer missions.

<sup>d</sup> Also called Tidbinbilla.

part of the Near Earth Phase Network during the early portions of the Pioneer missions.

To complete the picture of the DSN, JPL engineers often visualize the three facilities just described as vertical sinews interwoven with six horizontal sinews representing the groups of equipment that accomplish the tracking, data acquisition, and command functions as well as those of simulation, monitoring, and operational control (fig. 8-2).

When Pioneers 1 through 5 headed for deep space, they were the only active spacecraft beyond Earth orbit. The few trackers in existence could find and follow these space probes readily, though without great precision and not very far. It was a "simple" picture in 1960. Today, however, NASA has stationed almost a score of 85-ft dishes and one 210-ft dish at various spots on the globe and filled the adjacent buildings with advanced electronic gear. It is possible to listen to, track and command spacecraft 200 million miles away from Earth. Because of many currently active spacecraft, DSN priorities have to be assigned to each spacecraft; and each tracking station, being only a part of a tremendously complex machine, operates on a rigorous schedule. The DSN is a world-wide data collector for scientists.

## GENERAL DEEP SPACE NETWORK CAPABILITIES

After the Pioneer Program was officially approved by NASA Headquarters on November 9, 1962, spacecraft design and mission planning commenced at Ames Research Center. The capabilities of the Delta launch vehicle helped fix the weight and volume of the spacecraft, while the DSN—as it was projected for the 1965–1969 period—had considerable influence over spacecraft antenna design, frequency selection, telemetry bit rates, type of telemetry, and many other facets of spacecraft communication and command.

### The Deep Space Instrumentation Facility

In tracking language, the DSIF is the Earth-based portion of a two-way, phase-coherent,<sup>24</sup> precision tracking and communication system capable of providing position tracking, telemetry, and command for spacecraft more than 10 000 miles from the Earth. Each DSN station feeds acquired tracking measurements (two angles and range rate) to the Ground Communications Facility (GCF) which relays it to the SFOF in near real time (i.e., almost instantaneously). Pioneer telemetry data are partially processed in real time by on-site computers. Data are then teletyped or airmailed to the SFOF at

<sup>24</sup> "Phase-coherent" signifies fixed frequency and phase relationships between transmitted and received signals.

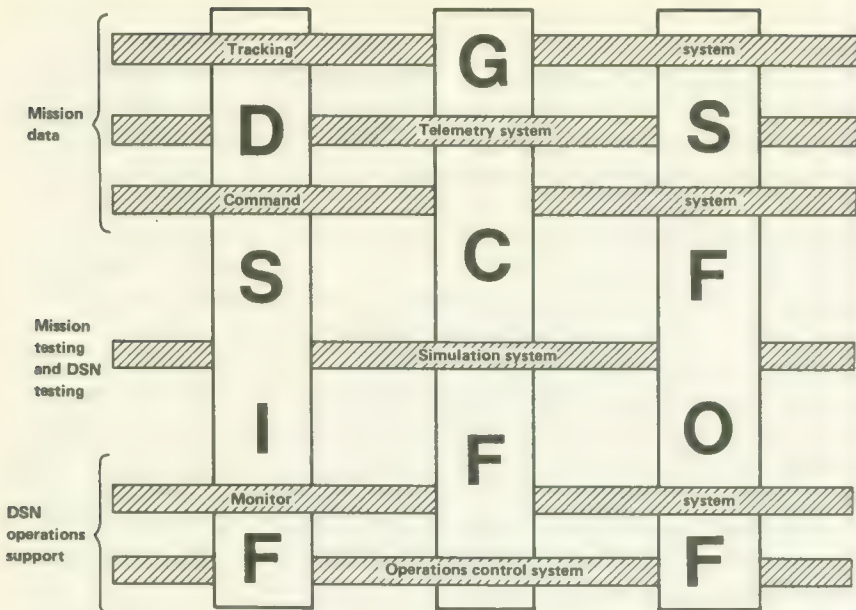


FIGURE 8-2.—The Deep Space Network can be visualized as three facilities (DSIF, GCF, and SFOF) interwoven with six systems.

JPL. The spacecraft must carry a phase-coherent transponder for the DSN to track the spacecraft satisfactorily.

The DSN stations listed in table 8-1 were deliberately placed about 120° apart in longitude in a band between 40° north and 40° south latitude. Overlapping sky coverages result with the 85-ft dishes (figs. 8-3 and 8-4). Although local conditions cause slight variations in building arrangements, the DSN stations appear essentially identical to a spacecraft across the electromagnetic and information interfaces.

Pioneer Earth-to-spacecraft transmissions occur at 2110 MHz; spacecraft-to-Earth at 2292 MHz. For coherent two-way Doppler tracking measurements, several pairs of channels are selected with a frequency ratio of 221/240. (See ch. 4 for a discussion of phase-lock receivers and their use in the Pioneer Program.)

Two-way Doppler measurements are made by first transmitting an S-band signal from a DSN site to the spacecraft. The spacecraft, using phase-coherent frequency multiplication, converts the received signal into one of higher frequency and transmits it back to Earth. Measurements of time and Doppler shift provide range and range rate. In the Pioneer Program, only Doppler range is used in pinpointing spacecraft locations. DSN precision Doppler measurements are usually made with this closed,

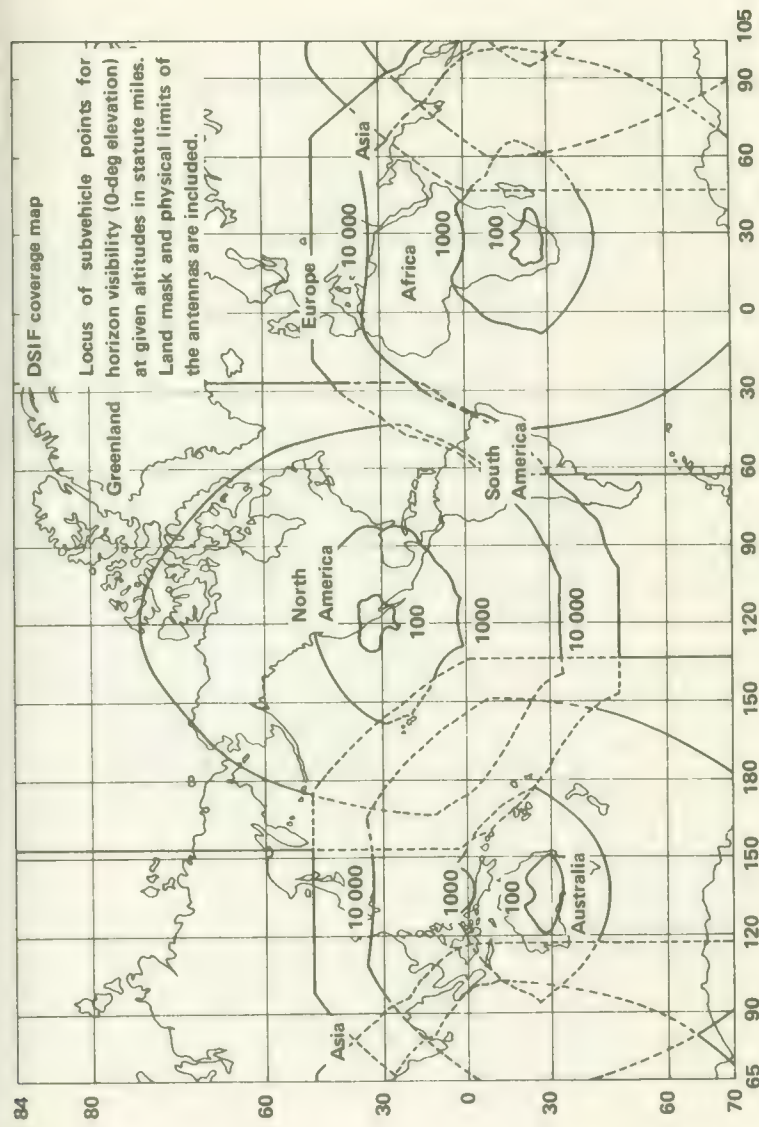


FIGURE 8-3.—Station coverages for the three polar-mounted 85-ft DSIF antennas at Goldstone, Woomera, and Johannesburg.

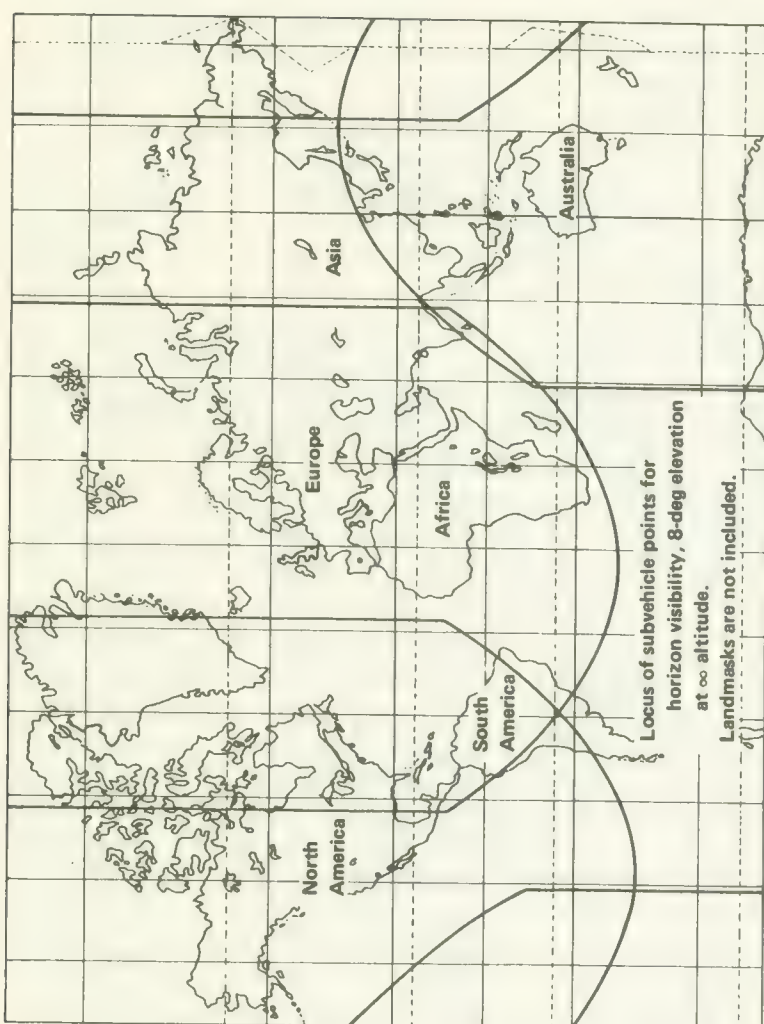


FIGURE 8-4.—Station coverages for the three polar-mounted 85-ft DSIF antennas at Goldstone, Madrid, and Canberra.

two-way, phase-locked mode. A less accurate one-way Doppler mode is sometimes used by stations that are merely listening to the spacecraft transmissions. Drifting of the spacecraft crystal-controlled oscillator limits the precision when the spacecraft receiver is not locked onto the Earth transmitter's frequency. When two separate but intercommunicating DSN stations have the spacecraft in view, three-way modes are possible, with one station in a two-way mode and the other in a one-way mode. The accuracy of DSN ranging is approximately  $\pm 15$  m one way (three-sigma value). Range rate accuracy varies with the magnitude of the Doppler shift.

The standard DSN site with its 85-ft dish depends upon 14 subsystems (ref. 1). See figure 8-5. A few important features are:

(1) Antenna mechanical subsystem—Most of the 85-ft dishes are S-band, Cassegrain feed, and monopulse in operation. The antennas point with an accuracy of  $0.02^\circ$  in a 45-mph wind.

(2) Antenna microwave subsystem—Some of the most critical and sophisticated DSIF components are included here: Cassegrain simultaneous lobing feeds, traveling-wave masers, and parametric amplifiers. Beamwidths to the half-power points are  $0.32 \pm 0.03^\circ$  and  $0.36 \pm 0.03^\circ$  for receive and transmit modes, respectively.

Acquisition-aid subsystem—DSN stations 11, 41, 42, and 51 are equipped with S-band antennas with beamwidths of  $16^\circ$  to help lock the 85-ft antennas, with their much narrower beamwidths, onto the spacecraft.

The Goldstone Mars station (DSS-14) is equipped with a 210-ft dish on an azimuth-elevation mount. This big antenna is more sensitive than the 85-ft dishes and is essential for the tracking of Pioneer spacecraft over 100 million miles away. The nominal beamwidths to the half-power points of the 85-ft dishes are  $0.135^\circ$  and  $0.145^\circ$  for receive and transmit, respectively. During Pioneer operations the beamwidths have appeared to be about  $0.20^\circ$ . Pointing accuracy is 50 arcseconds.

### The Ground Communications Facility

NASCOM consists of those circuits, terminals, and switching centers that link the dispersed stations of all three NASA networks together and to their respective control centers. NASCOM is a real-time network; that is, the stations and control centers can exchange data, teletype, and voice messages almost instantaneously.<sup>25</sup> The Pioneer Mission Operations Center at Ames Research Center (fig. 8-6) can, for example, dispatch commands in real time to any one of the Pioneer spacecraft as long as a DSN antenna somewhere in the world is in contact with it.

The GCF utilizes NASCOM for its long-distance traffic (fig. 8-7). Except for the Goldstone-JPL information flow, DSN traffic converges

<sup>25</sup> Limited mainly by the finite speed of light.

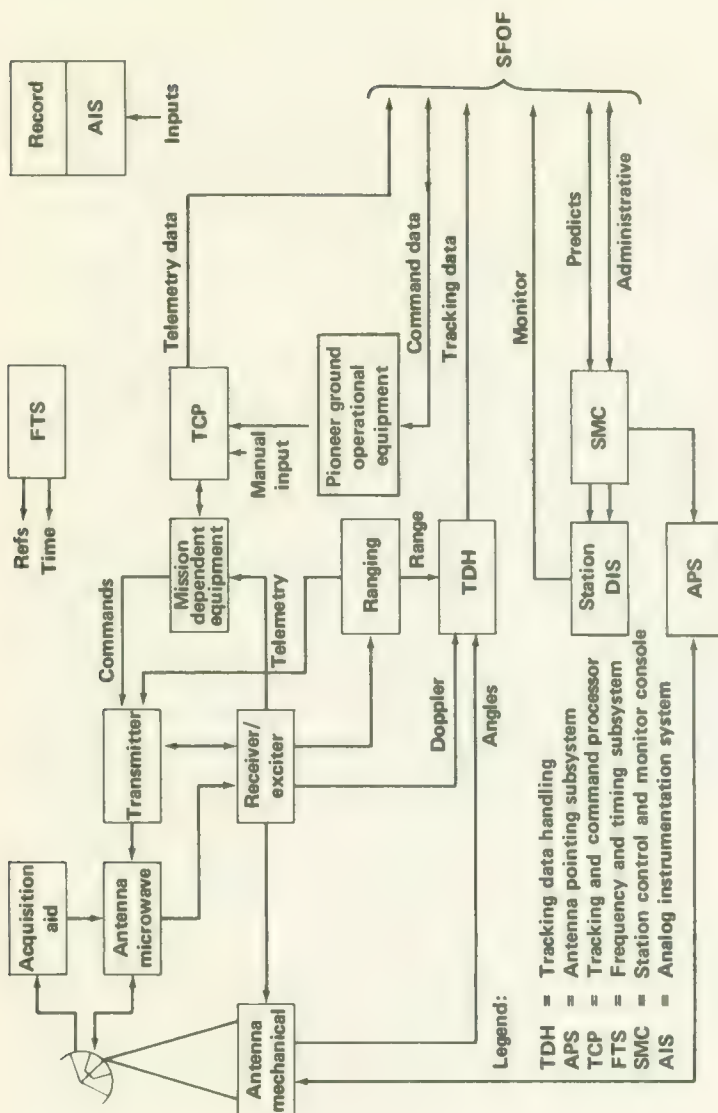


FIGURE 8-5.—Block diagram of the DSIF subsystems.



FIGURE 8-6.—Pioneer Mission Operations Center at Ames Research Center.

first on several NASCOM overseas switching centers, which in turn route it to the central computer-controlled switching center at Goddard Space Flight Center, Greenbelt, Maryland. From Goddard, the traffic is directed to the address indicated on the message. In the case of Pioneer, the SFOF at JPL is the major addressee, although individual DSIF stations can address one another. Goddard Space Flight Center manages NASCOM, but JPL has operational control of the circuits it is using at any given moment.

The five subsystems of the GCF are: (1) inter-station transmission, (2) SFOF communications terminal, (3) DSS communications terminal, (4) DSIF internal communications, and (5) SFOF internal communications (fig. 8-8). In other words, the GCF includes considerable terminal equipment not considered part of NASCOM proper. As figure 8-9 indicates, tracking data flow back to the SFOF primarily by teletype. Most scientific data are recorded on tape and airmailed to the SFOF, where the tapes are verified and then shipped to Ames Research Center for further processing (ch. 9).

The voice circuits are used primarily for coordination and control between the SFOF and the DSN stations. The high-speed data circuits transmit up to 2400 bits/sec with time delays only slightly greater than the

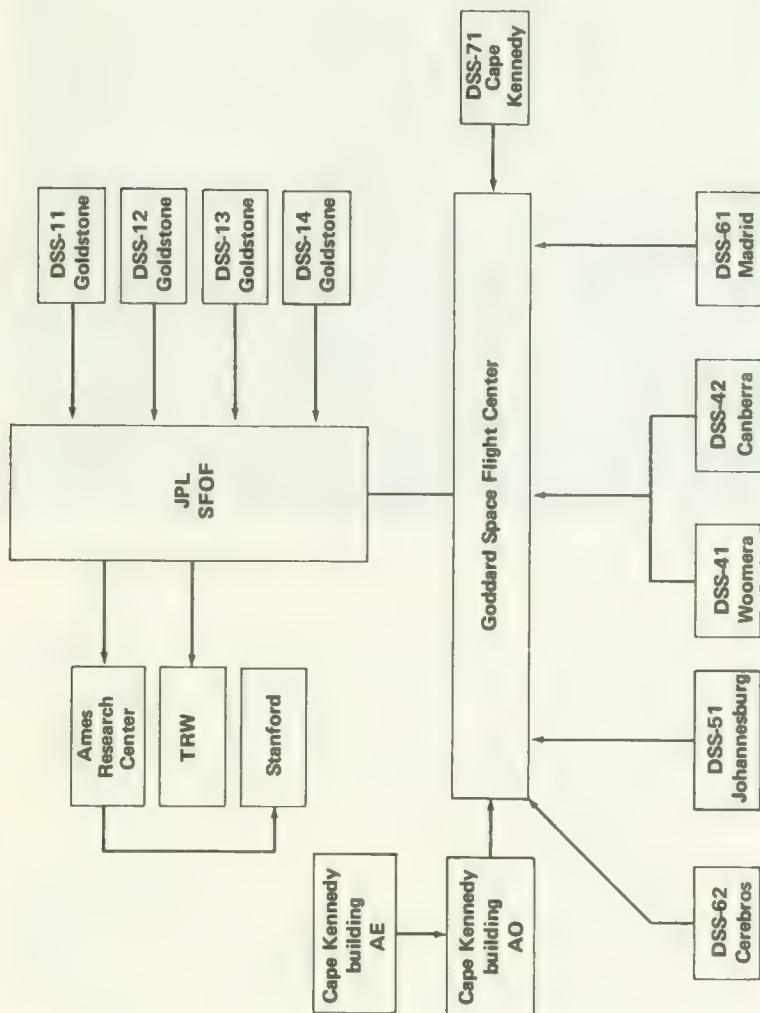


FIGURE 8-7.—Generalized communication traffic routing diagram for GCF. Overseas stations are handled by Goddard's NASCOM lines.

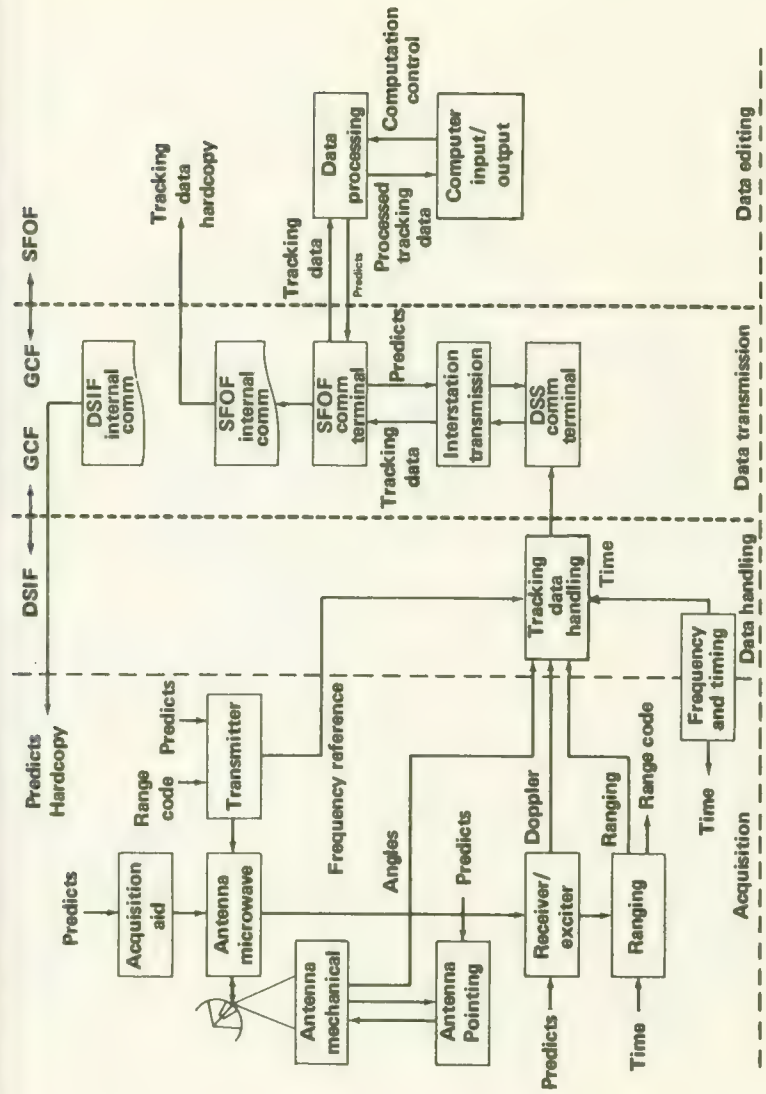


FIGURE 8-8.—Interface diagram for the DSIF, GCF, and SFOF showing the five GCF subsystems.

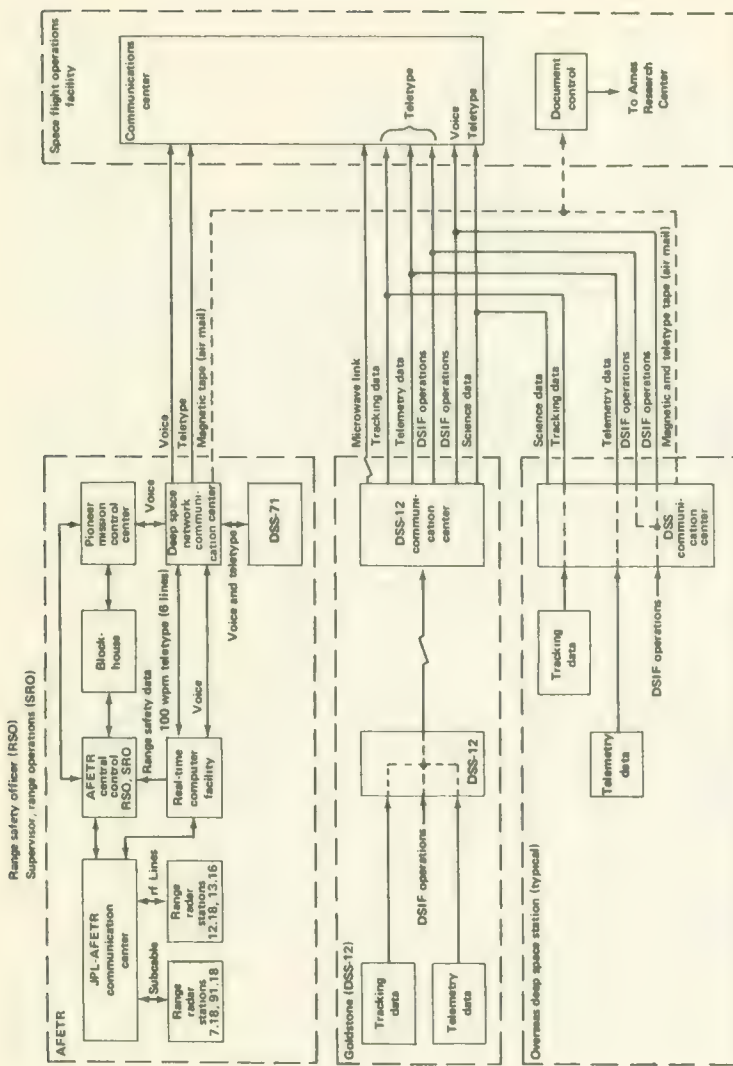


FIGURE 8 9.—Telemetry- and tracking-data flow from the ETR and DSIF to the SFOF and Ames Research Center. Tapes are sent first to the SFOF for verification and then to Ames.

time it would take light to travel the same distance. In effect, "real time" means delays of only tenths of a second at most. The teletype circuits, however, are a little slower, with  $\frac{1}{4}$ -sec delays at each control point (up to a maximum of three control points). The site communication's processors, however, introduce delays of 30 to 120 sec. During the early parts of its flight, a Pioneer often transmits at its maximum rate of 512 bits/sec, which is greater than the teletype rate of 60 words/min. During this time it is possible to call up selected blocks of data via the teletype circuits in order to assess the condition of the spacecraft.

### The Space Flight Operations Facility

The focal point of DSN activity is a modernistic four-story building at JPL, in Pasadena; this building is the SFOF. The SFOF terminal of the GCF occupies part of the basement. Above are the computers, displays, controls, and facilities for mission control, a major part of which involves DSN control.

Brief descriptions of the eight subsystems that make up the SFOF follow:

(1) Data Processing Subsystem (DPS)—The function of the DPS is the ingestion of DSIF tracking data and its subsequent processing into the formats required for display and control. General-purpose digital computers are the mainstay of the DPS.

(2) Computer Input/Output (I/O) Subsystem—Consoles, printers, and plotters provide one interface between the Data Processing Subsystem and SFOF users.

(3) Data Processing Control and Status (DPCS) Subsystem—Three consoles are used here to monitor and control the Data Processing Subsystem.

(4) Telemetry Processing Subsystem (TPS)—The TPS performs real-time and non-real-time processing of all telemetry except that received on teletype. The TPS carries DPS processing several steps further, depending upon the desires of the mission controllers and experimenters.

(5) Timing Subsystem—This SFOF subsystem generates, distributes, and displays accurate time signals throughout the SFOF.

(6) Display Subsystem—This subsystem drives the automatic displays, the Mission Display Board, and the orbital parameters display in the SFOF. It provides one more interface between the SFOF user and the spacecraft and DSN.

(7) Simulation Data Subsystem—The Simulation Data Subsystem supplies simulated telemetry and tracking data during network tests and training exercises.

(8) Operations Support Subsystem—This subsystem is a catchall for such SFOF activities as document control, transmitting services, support planning, etc.

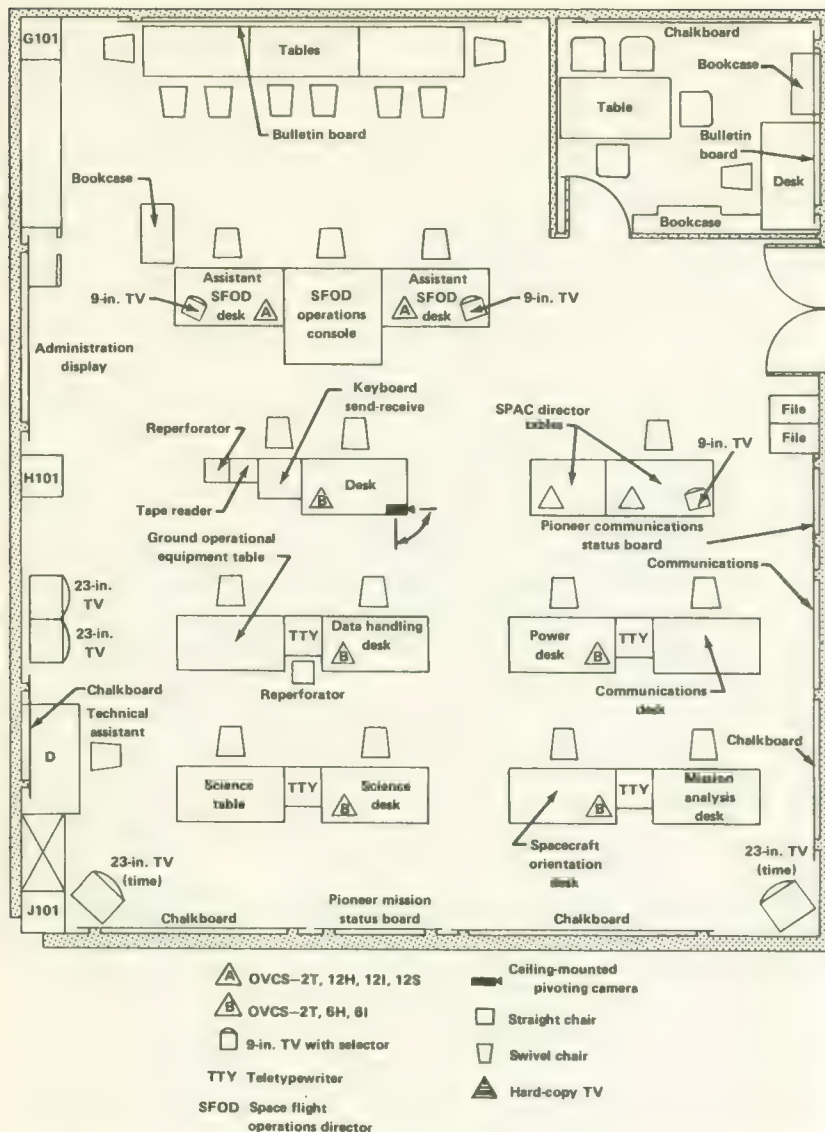


FIGURE 8-10.—Floor plan of the Pioneer mission support area at the SFOF.

Ames personnel controlled the spacecraft from the Pioneer Mission Support Area at the SFOF during critical portions of the flights (fig. 8-10). Spacecraft/orientation maneuvers, however, were controlled from Goldstone and, in the case of the partial orientation maneuver of Pioneer 6, from Johannesburg.

### Special Pioneer Requirements Placed on the DSN

The DSN was better equipped during the launches of the Block-II Pioneers than it was when Pioneers 6 and 7 first probed deep space. With the 210-ft Goldstone antenna in operation, the DSN could track and communicate with spacecraft most of the way around the Sun—the Pioneers are some 150–200 million miles away before the Sun's radio noise overwhelms their telemetry signals. As success followed success in the Pioneer Program, scheduling the tracking time of the big DSN dishes and those borrowed from the MSFN became a more difficult task. The swelling number of manned and unmanned lunar spacecraft added to the tracking burden.

The finite resources of the DSN dictates careful planning to avoid supersaturation. The Office of Tracking and Data Acquisition, at NASA Headquarters in Washington, serves as a focal point where requirements, priorities, and resources are weighed for all NASA missions and all three NASA networks. A standard yet rather flexible procedure has developed. The project requiring tracking and data acquisition support issues a "requirements document" called a SIRD (for Support Instrumentation Requirements Document). The SIRD collects priorities, requirements, and other important factors for all Pioneers in space and those being readied for the launch pad. In response to each SIRD, JPL issues an NSP (or NASA Support Plan) relating how it plans to meet the requirements. Goddard Space Flight Center does the same for MSFN support. Each document must be the result of considerable negotiation and balancing of priorities. The SIRDs are updated frequently to reflect changing demands. For example, the launching of a new Pioneer or the loss of signal from an old one might be significant enough to require SIRD updating.

Requirements set forth in the Pioneer SIRDs over the years have been voluminous. In the interest of brevity, only portions of the Pioneer SIRD issued prior to the launch of Pioneer E are summarized in tables 8-2 through 8-6 (ref. 2). These tables do reveal the complexity and magnitude of the tracking and data acquisition tasks for a spacecraft of moderate size, as do figures 8-11 and 8-12. The conditional nature of assigning tracking and data acquisition is revealed in the following list of priority-requirements criteria:

*Priority I (Emergency).*—This priority applies only to coverage required to investigate or correct a spacecraft or scientific-instrument anomaly if prompt action is necessary to safeguard achievement of primary mission objectives.

*Priority II (Critical).*—These requirements are mandatory for attaining primary mission objectives.

(1) Launch plus 30 days, continuous coverage from DSN stations with GOE

TABLE 8-2.—*Critical Pioneer Mission Operations Involving the DSN*

| Operation  | Orbit phase   | Operation period   | Purpose   |
|--|---|--|---|
| 1. Separation from third stage   | 58.5 sec after third-stage burnout  |  | Separate spacecraft from spent third-stage; Mission Control: JPL/SFOF   |
| 2. Orient spacecraft spin axis normal to the spacecraft-Sun line (Type-I orientation maneuver) | Automatically initiated at separation from third stage  | Nominally 0–10 min   | Orient spacecraft for maximum solar energy to provide spacecraft power utilizing the on-board solar array; Mission Control: JPL/SFOF  |
| 3. Initial acquisition by DSN  | Acquisition of downlink telemetry before launch plus one hour   | Approximately 15 min   | Acquire spacecraft during transfer to heliocentric orbit and assess spacecraft health; Mission Control: JPL/SFOF  |
| 4. Spacecraft data-mode changes and experiment turnon  | Commanded from ground after uplink lock and assessment of spacecraft health and orbit                                   | Approximately 6 hr after acquisition   | Prepare spacecraft for scientific data collection; Mission Control: JPL/SFOF  |
| 5. Orient spacecraft spin axis normal to plane of ecliptic (Type-II orientation maneuver)      | Commanded from DSS-12 with other DSS stations as alternates within several days of launch                               | One complete DSS pass takes approximately 8–10 hr  | Establish final reference orientation of spacecraft spin axis; Mission Control: DSS-12 (Goldstone); except for partial Type-II orientation maneuver for Pioneer 6 made from Johannesburg    |
| 6. Cruise phase (nominal mission)  | Begins upon injection into heliocentric orbit and upon completion of experiment turnon and Type-II orientation maneuver | Continuous tracking coverage for first month after launch; two tracking missions coverage per day through nominal lifetime; dependent on schedule conflicts, and with high-priority DSN, | Collect scientific data; major coverage provided by DSS containing Pioneer GOE for assessment and analysis of real-time science and engineering data; Mission Control: Ames Research Center |

|   |   |  |   |
|---|---|--|---|
| 7. Cruise phase (extended mission)                        | Begins upon completion of cruise phase of nominal mission   | One tracking mission coverage per day; tracking missions to be provided by the DSN 210-ft antenna at Goldstone, Cal.; extended mission to continue until spacecraft cannot provide useful science data or when spacecraft is beyond DSN capability   | Collect scientific data; Mission Control: Ames Research Center                    |
| 8. Solar-flare coverage phase                             | Begins when Mission Operations Manager requests coverage for reported Class-II-Bright or above solar flare during cruise phase  | Nominal mission: continuous coverage for 30 to 50 hr; extended mission: within capability of 210-ft antenna system net to provide coverage over a 50-hr period Continuous coverage from syzygy-minus-5-days to syzygy-plus-15 days   | Collect maximum scientific data in spacecraft vicinity during high solar activity |
| 9. Geomagnetospheric tail analysis (Pioneers 7, 8, and E) | Nominal period of analysis established prior to launch, actual required coverage period provided upon analysis of the resultant trajectory  | Continuous coverage from entrance minus 10 hr to exit plus 10 hr   | Define boundaries and characteristics of the geomagnetospheric tail               |
| 10. Lunar occultation (Pioneers 7 and E)                  | The probability of a lunar occultation indicated from analysis of the nominal trajectory; definite times established upon detailed analysis of resultant trajectory; simultaneous view periods from Stanford University and Goldstone necessary | Provide lunar occultation analysis utilizing the Stanford University on-board instrument in conjunction with the Stanford 1.50-ft tracking system and DSS-12 and DSS-14 at Goldstone, Cal.; coverage also required from other stations (Australia, Spain, or South Africa) if period occurs during overlap view with Goldstone and Stanford University |   |

TABLE 8-2.—*Critical Pioneer Mission Operations Involving the DSN (Continued)*

| Operation  | Orbit phase  | Operation period  | Purpose  |
|--|--|---|--|
| 11. Superior conjunction or analysis of Sun's corona during solar occultation (Pioneers 6, 7, 8, 9, and E) | Part of the extended mission and to be fixed to a given period upon analysis of resultant heliocentric orbit | Continuous coverage within the capabilities of the 210-ft antenna beginning one month prior to and ending one month following solar occultation           | Provide analysis of Sun's corona characteristics during superior conjunction   |
| 12. Reorientation maneuvers during cruise phase  | As determined by the Mission Operations Manager  | During a complete tracking pass at DSS-12 Goldstone.  | Possibility of Mission Control's being moved to DSS-12 during this maneuver; to provide spacecraft spin axis orientation as determined by the Mission Operations Manager |
| 13. Spacecraft anomalies   | As determined by the Mission Operations Manager  | Continuous coverage until anomaly has been corrected or it has been decided that it cannot be corrected, as determined by the Mission Operations Manager. | Possibility of Mission Control's being moved to JPL/SFOF or remaining at NASA/ARC as determined by the Mission Operations Manager  |

TABLE 8-3.—General Pioneer Tracking Requirements as of March 1969<sup>a</sup>

| Pioneer | Nominal mission  |
|---------|--|
| 6       | DSS-14 daily coverage 4-8 hr/day; absolute minimum, DSS-14 daily coverage 3 hr/day   |
| 7       | DSS-14 daily coverage; 4-8 hr/day; absolute minimum, DSS-14 daily coverage 3 hr/day  |
| 8       | DSS-12, -42, -51, -62 and DSS-11, -42, -61: continuous coverage; absolute minimum, DSS-12, -42, -51, -62 and DSS-11, -41, -61; two tracking missions/day for a total of 16 hr/day          |
| 9       | DSS-12, -42, -51, -62; continuous coverage; absolute minimum, DSS-12, -42, -51, -62 and DSS-11, -41, -61 and MSFN; two tracking missions/day for a total of 16 hr/day, with 1 hour overlap |
| E       | DSS-12, -42, -51, -62; continuous coverage; absolute minimum, DSS-12, -42, -51, -62 and DSS-11, -41, -61 and MSFN; two tracking missions/day for a total of 16 hr/day                      |

<sup>a</sup> These requirements vary with time, of course. This table is illustrative only.

(2) Thirty-first day to end of mission, two passes per day (coverage period 16 hr or greater)

(3) For duration of mission, at least one horizon-to-horizon two-way-Doppler tracking mission per week not to be on same day of the week

(4) Coverage of specific scientific events that offer single time periods within the flight mission when the data may be retrieved; when in effect, this requirement to take priority over all those noted above

(5) Solar-flare coverage, 30-50 hr from flare initiation for Class-II Bright or greater; upon occurrence, this requirement to take priority over all previously stated requirements above

The above requirements are reduced to 3-4 hr per day to end of mission because of spacecraft-Earth distance, spacecraft- and ground-antenna characteristics, or because only one 210-ft antenna is available for operational support.

*Priority III (Critical).*—These requirements are time-sensitive for other-than-primary mission objectives:

(1) Two final operational readiness tests.

(2) Countdown for launch.

The requirements stated under Priority II above may, during brief periods, be reduced to Priority III to insure optimum use of the DSN resources in the best interests of NASA. This upgrading of priority classification can only be made by the Pioneer Project Manager or the Pioneer Mission Operations Manager.

*Priority IV (Non-critical).*—These requirements are mandatory for attaining primary mission objectives with no risk:

TABLE 8-4.—*Typical Tracking Requirements for a Pioneer Flight*

| Time/distance coverage  | Data required   | Data presentation  |
|---|---|--|
| Class-I requirement <sup>a</sup>  | Time, azimuth,<br>elevation, range  | The data to be converted for<br>presentation in NRT by<br>teletype to the SFOF as<br>follows:  |
| A. Launch-vehicle second-stage<br>engine cutoff (SECO)<br>to SECO-plus-60 sec<br>(fig. 8-11).   | Data points per sec:<br>$\frac{1}{10}$ minimum,<br>$\frac{1}{6}$ desired,<br>$\frac{1}{3}$ maximum <sup>b</sup> | (a) Decimal raw-data<br>format   |
| B. Launch-vehicle third-<br>stage burnout to third-<br>stage spacecraft separa-<br>tion (minimum of 60<br>sec of data if available).  |   | (b) Orbital elements and<br>injection conditions of<br>parking orbit   |
| Class-II requirement <sup>a</sup>   |   | (c) Orbital elements and<br>injection conditions of<br>transfer orbit assuming<br>nominal third-stage burn   |
| A. SECO to SECO plus 180<br>sec.  |   | (d) Orbital elements and<br>injection conditions of<br>transfer orbit based on<br>actual third-stage burn  |
| B. Ascension (ETR Station<br>12) rise to Ascension set.   |   |  |
| Class-III requirement <sup>a</sup>  | Acceleration  | Voice link and/or single-<br>sideband data link in NRT;<br>initially launch plus approxi-<br>mately 2 hr, and as<br>required to meet accuracy<br>requirements <sup>c</sup> |
| SECO to third-stage ignition;<br>third-stage spinup to third-<br>stage burnout; DSS<br>tracking coverage sufficient<br>to define the free-flight<br>orbit (figs. 2-6 through<br>2-9). |   |  |

<sup>a</sup> See table 8-4 for priority definitions.

<sup>b</sup> These orbital criteria are stated to fulfill project orbital determination requirements only; they in no way reflect the tracking requirements established by the celestial mechanics experiment of J. Anderson. The celestial mechanics experiment will use as a data source the standard DSN two-way Doppler tracking data with the capability for 60-sec readout.

<sup>c</sup> The accuracy of the orbit based upon tracking data received from Deep Space Stations will be as follows:

Injection: 10 km and 2-Hz two-way Doppler

Injection-plus-10 days: 200 km and 5-Hz two-way Doppler

Injection-plus-180 days: 1000 km and 5-Hz two-way Doppler

- (1) Thirty-first day to end of mission, continuous coverage
- (2) For duration of mission, one horizon-to-horizon two-way-Doppler tracking mission every 4 days
- (3) Coverage of specific solar events of high scientific value unrelated to specific flares
- (4) Station time required to investigate a specific spacecraft characteristic or an operational hardware or software anomaly.

TABLE 8-5.—Pioneer Telemetry Data-Acquisition Requirements

| Channel | No. | Frequency       | No. of segments  | Data rates  | Recording interval and accuracy   |
|---------|-----|-----------------|--|---|---|
|         | 6A  | 2292.037037 MHz | Transmitted in a 7 binary-bit data word on a 2048-Hz square wave, which is biphase-modulated with a time-multiplexed PCM bit train, using a non-return-to-zero-mark format. Telemetry data are formatted into 32-word main frames. | 512, 256, 64, 16, and 8 bps selectable by ground command; when the convolutional coder is operating, a parity bit will be transmitted with each data bit; this will have the effect of doubling the transmitted bit rate to obtain the same data rates noted above (fig. 8-23). | Telemetry data are received, demodulated, synchronized, recorded and transmitted to an on-site SDS-920 computer. The computer decommutes and formats the telemetry data and outputs a portion of this data on teletype to the Ames Mission Operations Center. The aforementioned takes place at stations having Pioneer GOE during a tracking mission. At stations not having GOE, the output of the ground receiver is recorded during a tracking mission. During noncoverage tracking periods the telemetry data will be stored onboard for later readout. This mode is selectable by ground command. |
|         | 7A  | 2292.407407 MHz |  |   |   |

<sup>a</sup> DSS-12 only.

TABLE 8-6.—*Pioneer Ground Command Requirements*

| Coverage   |
|--|
| Time or phase of orbit   |
| Rise to set of DSS equipped with Pioneer mission-dependent GOE.  |
| DSN stations   |
| DSS-12—Echo, Goldstone, Cal.   |
| DSS-42—Tidbinbilla, Australia  |
| DSS-62—Cebreros, Spain   |
| DSS-51—Johannesburg, South Africa  |
| DSS-71—Cape Kennedy, Fla. (launch checkout only)   |
| Signal   |
| Frequency  |
| Receiver 1, Channel 6B 2110.584105 MHz   |
| Receiver 2, Channel 7B 2110.925154 MHz   |
| Modulation   |
| FSK /PM  |
| Coding   |
| 150-Hz and 240-Hz tones representing 0 and 1, respectively   |
| Required transmitter power   |
| Variable; depends on spacecraft receiver signal strength which is dependent on range of 10-kW transmitter at a spacecraft signal strength threshold of -150 dBm  |
| Transmission time required to execute commands   |
| Transmission time equals the transit light time to the spacecraft plus 23 sec; the transit light time varies with spacecraft range relative to Earth; the command message is 23 bits in length transmitted at 1 bit per sec.         |
| Format   |
| 23-bit word (See ch. 4 for details.)   |
| Special equipment  |
| Pioneer mission-dependent GOE  |
| Command encoder: produces encoded commands; indicates verification in DSS TCP computer and transmits 23-bit command message  |
| Computer buffer: provides connection for GOE and special-purpose equipment with the DSS TCP computer; provides serial input of command message from command encoder to DSS TCP computer  |
| DSS TCP computer operational program tapes: provide computer program to supply real-time processed data to NASA/ARC Mission Operations Center; also provides alarm and verifies information for command activity and Mission Control |
| Permissive command tapes: provide computer with allowable commands for transmission.   |
| DSS Mission-independent equipment  |
| DSS TCP computer: SDS-910/920 computer verifies command prior to transmission and checks bit-by-bit during transmission; provides stop signal on any non-permissive or non-verified command during transmission.                     |

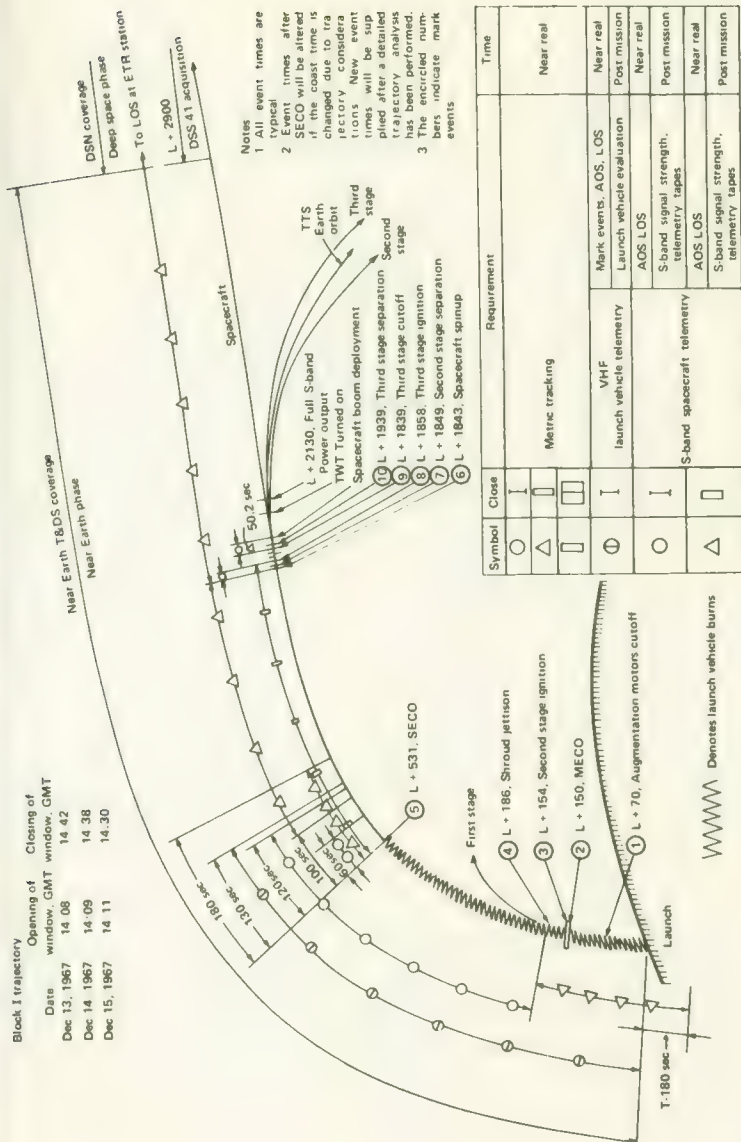


FIGURE 8-11.—Near-Earth tracking and telemetry requirements for the Pioneer 8 flight. From:  
JPL Rept. 607-90, P. 40.

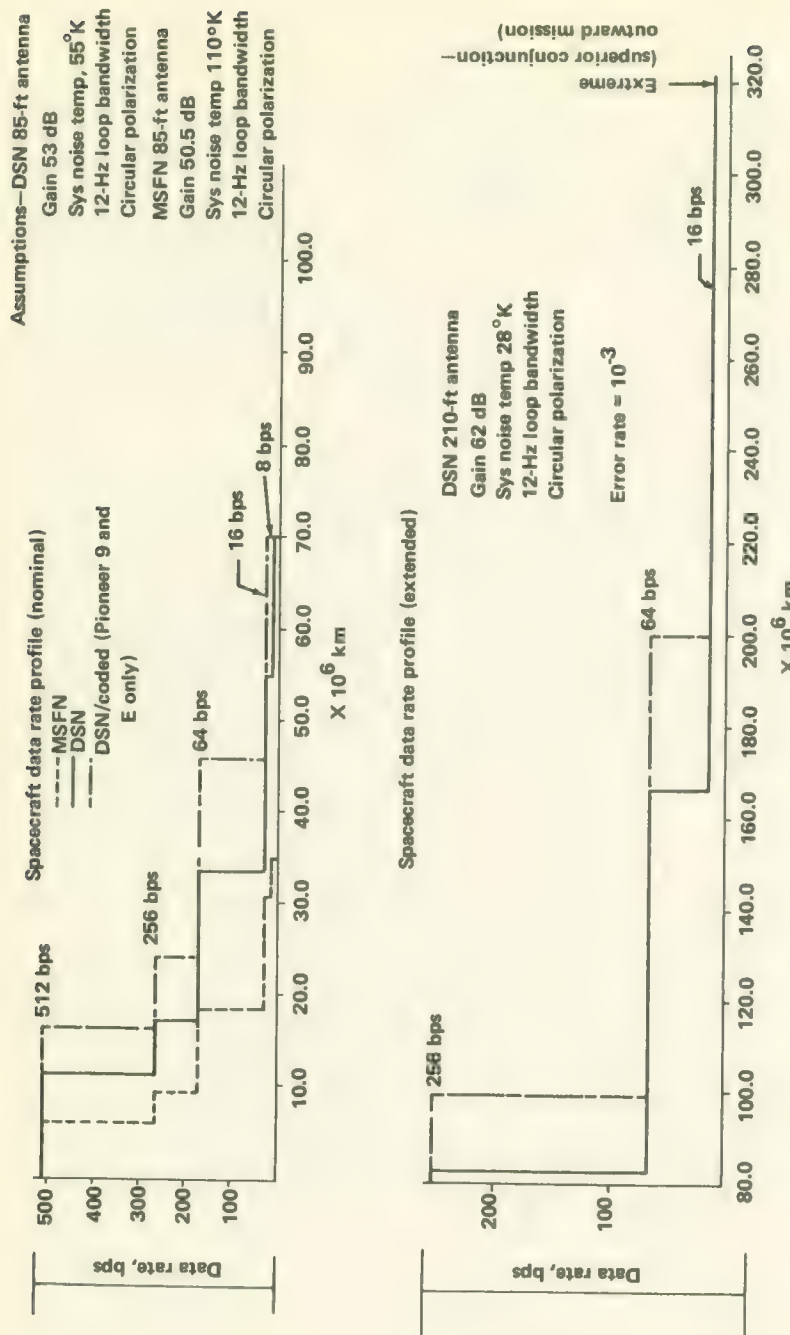


FIGURE 8-12.—Pioneer data rate profiles as functions of distance from Earth. From: SIRD-69, p. 510.

The above requirements are reduced to 6–8 hr per day to end of mission because of spacecraft/Earth distance, spacecraft- and ground-antenna characteristics, or because only one 210-ft antenna is available for operational support.

*Priority V (Non-critical).*—These requirements are not mandatory for attaining primary mission objectives:

- (1) Any tracking coverage in excess of 24-hr coverage
- (2) Operational integration testing
- (3) Station time required to test a proposed modification to operational hardware or software.

## SPECIFIC PIONEER NETWORK CONFIGURATIONS

The terrestrial facilities that NASA pooled to meet the requirements of the Pioneer flights consisted of parts of the following facilities:

1. The DSN, which included the DSIF, GCF, and SFOF
2. The MSFN, which provided 85-ft-dish support on occasion
3. NASCOM, which contributed many circuits to the DSN's GCF
4. The AFETR (Air Force Eastern Test Range), which supplied much of the ground environment from the launch pad downrange 5000 miles to Ascension Island, i.e., the Near-Earth Phase Network

Each Pioneer flight could be divided logically into two main phases: near-Earth phases and deep-space phases. The successful injection of the spacecraft into a heliocentric orbit was the event that effectively separated the two phases (fig. 8-11). At this point, somewhere over the Indian Ocean, the spacecraft would be handed over completely to the DSN and cooperating MSFN stations. Each phase of tracking required a different configuration of tracking, data acquisition, command, and ground communication equipment (ref. 3).

### Near-Earth-Phase Network Configurations

The equipment committed to the Pioneer Program varied slightly from flight to flight, as detailed in table 8-7. The stations along the AFETR had the primary responsibility for tracking (or "metric data") during the launch and Earth-orbit portions of the flights. Cape Kennedy has many radars, radio interferometers, and a great variety of optical tracking equipment. AFETR and MSFN downrange stations and Range Instrumentation Ships (RIS) also possess impressive complements of tracking radars and telemetry receiving equipment. Data are fed back to Cape Kennedy via submarine cables and radio links.

The DSN station at the Cape (DSS-71) was an integral part of all DSN configurations supporting Pioneer flights during the near-Earth passes. JPL also maintains a field station at Cape Kennedy that provides an

TABLE 8-7.—*Configuration of Tracking and Data Acquisition Stations During Near-Earth Phases*

| Station number | Location                                    | Tracking radars            | Telemetry   | Use during Pioneer flights |   |   |   |
|----------------|---|----------------------------|-------------|----------------------------|---|---|---|
|                |   |                            |             | 6                          | 7 | 8 | 9 |
| AFETR 1        | Cape Kennedy-----                           | FPQ-6<br>FPS-16,<br>TPQ-18 | vhf, S-band | X                          | X | X | X |
| 3              | Grand Bahama-----                           | FPS-16,<br>TPQ-18          | vhf         | X                          | X | X | X |
| 7              | Grand Turk-----                             | TPQ-18                     | vhf         | X                          | X | X | X |
| 91             | Antigua                                     | FPQ-6                      | vhf, S-band | X                          | X | X | X |
| 12             | Ascension-----                              | FPQ-18,<br>FPS-16          | vhf, S-band | X                          | X | X | X |
| 13             | Pretoria-----                               | MPS-25                     | vhf, S-band | X                          | X | X | X |
| —              | <i>Twin Falls</i> (ship)-----               | FPS-16                     |             | X                          | X | X | X |
| —              | <i>Coastal Crusader</i> (ship)-----         |                            |             | X                          | X | X | X |
| MSFN 1         | Bermuda-----                                | FPS-16,<br>FPQ-6           | vhf         | X                          | X | X | X |
| 2              | Ascension-----                              |                            |             | X                          | X | X | X |
| 3              | Tananarive, Malagasy----                    | Capri                      | vhf         | X                          | X | X | X |
| 4              | Carnarvon, Australia-----                   | FPQ-6                      | vhf         | X                          | X | X | X |
| 5              | Goddard Space Flight Center, Greenbelt, Md. |                            |             | X                          | X | X | X |
| 6              | Guam-----                                   |                            |             | X                          | X | X |   |
| 7              | Hawaii-----                                 |                            |             | X                          | X | X |   |
| DSN 71         | Cape Kennedy-----                           |                            |             | X                          | X | X | X |

TABLE 8-7.—*Configuration of Tracking and Data Acquisition Stations During Near-Earth Phases—Concluded*

| Station number | Location                  | Tracking radars | Telemetry | Use during Pioneer flights |   |   |   |
|----------------|---------------------------|-----------------|-----------|----------------------------|---|---|---|
|                |                           |                 |           | 6                          | 7 | 8 | 9 |
| 72             | Ascension                 |                 |           | X                          | X | X | X |
| 51             | Johannesburg              |                 |           | X                          | X | X | X |
| —              | SFOF, Pasadena            |                 |           | X                          | X | X | X |
| —              | Building AO, Cape Kennedy |                 |           | X                          | X | X | X |

operational interface between the SFOF, in Pasadena, and the Air Force and Goddard Space Flight Center groups. In view of the manifold operations at Cape Kennedy, their complex interactions, and the immense detail required for effective coordination, such interface groups are essential. The JPL field station also contains an Operations Center with abundant displays of different types to help JPL personnel operate range instrumentation under their control. Critical tracking and telemetry data are also routed to the SFOF through the field station.

All launches from Cape Kennedy are under the direct control of the Air Force until the spacecraft leave ETR jurisdiction somewhere beyond Ascension. Because it is responsible for range safety, the Air Force monitors launch vehicle status data and tracking information. Commands to terminate the mission through the destruction of the launch vehicle are also an Air Force prerogative—one which was exercised during the launch of Pioneer E on August 27, 1969.

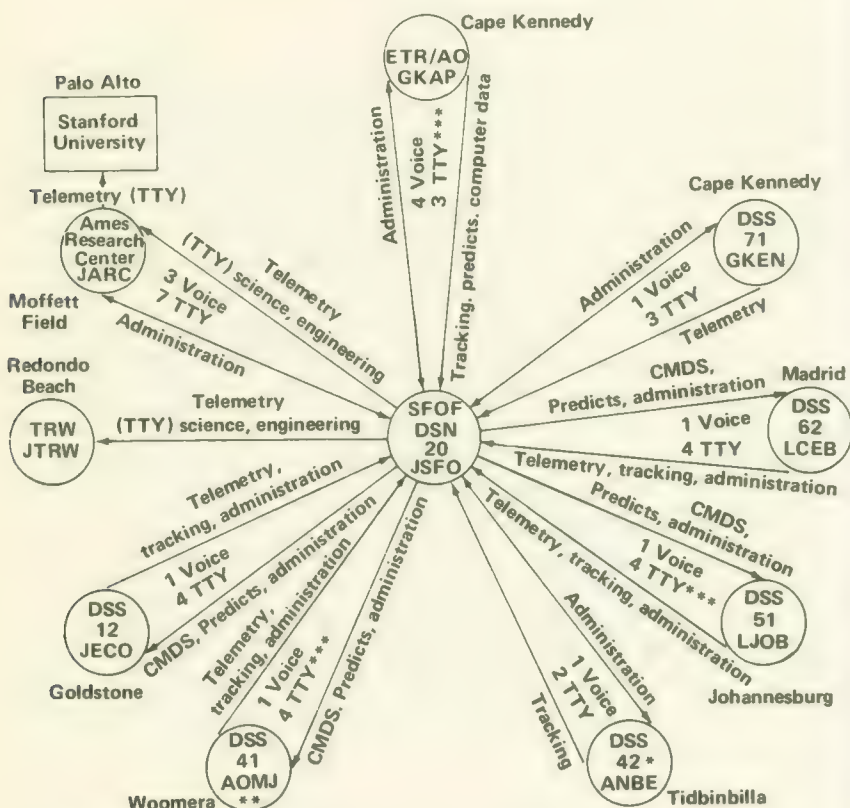
In summary, the near-Earth phase of a Pioneer flight is scrutinized by dozens of radars, theodolites, and interferometers from Cape Kennedy to South Africa. Telemetry and tracking data flow back to the Cape and the SFOF where they are monitored by the Air Force, NASA, and JPL personnel. Operational control rests with the Air Force during the launch phase and is handed over to NASA when the Pioneer spacecraft has been injected into heliocentric orbit.

### Deep-Space-Phase Configuration

After leaving Earth orbit, the Pioneer spacecraft quickly ascended beyond the 500- to 1000-mile ranges of the AFETR and MSFN tracking radars. From then on, they were tracked, communicated with, and com-

manded by the primary DSS stations listed in table 8-1. MSFN and other DSIF stations worked the Pioneer spacecraft on an as-needed basis. Communication traffic flowed back to the SFOF and NASA/ARC over GCF lines; commands, of course, moved in the opposite direction (fig. 8-13).

Each of the primary DSS stations was outfitted with so-called "mission-dependent" equipment that accommodated general-purpose DSIF machinery to specific Pioneer requirements. In Pioneer vernacular, the DSS gear was called Ground Operational Equipment (GOE). No special equipment was installed at the SFOF, although a general-purpose mission-support area was reconfigured for the Pioneer missions (fig. 8-10). Additional mission-dependent equipment was installed at Ames Research Center (fig. 8-6). Since the presence of Pioneer mission-dependent equipment constituted the major difference between a DSS station in the Pioneer



\* DSS 42 backup for DSS 41

\*\* DSS 41 prime acquisition station

\*\*\* These TTY circuits (using CP) are to have hardwire backup.

FIGURE 8-13.—GCF channels established for Pioneer 8.

configuration and any other mission-dependent configuration, a few details are in order.

The Pioneer GOE was designed to make maximum use of the general-purpose DSS equipment, particularly the Telemetry and Command Processor (TCP) equipment (the SDS-910 and SDS-920 computers) (fig. 8-14). Type-I GOE, consisting of five racks of electronic hardware, plus a module tester, a test transponder, and an instructor control set, was installed only at the Goldstone site. The primary overseas DSS stations received Type-II GOE, consisting of three racks only. The two extra racks at Goldstone were the recorder and display racks employed during the spacecraft Type-II orientation maneuver. The Woomera site (DSS-41) possesses no GOE equipment. The specific pieces of equipment in both types of GOE are indicated in the labels on figures 8-15 and 8-16. As the block diagram, figure 8-14, indicates, the GOE was actually specialized interface between the antenna and the DSS equipment.

## TELEMETRY CAPABILITIES

Telemetry capabilities were provided as follows:

- (1) Provided up to 120 frames of continuous spacecraft telemetry data for near-real-time teletype transmission to the SFOF (TCP)
- (2) Provided selected spacecraft engineering data for near-real-time teletype transmission to the SFOF (TCP)
- (3) Provided local typewriter printout in real time at each DSN station of selected spacecraft engineering data periodically and upon request (This capability accommodates operational requirements during spacecraft initial acquisition as well as routine orbital operations.) (TCP)
- (4) Drove local DSIF displays for spacecraft parameters necessary for uplink acquisition and verification of spacecraft receiver lock (TCP)

## COMMAND CAPABILITIES

Command capabilities were provided as follows:

- (1) Encoded manually inserted commands in a 23-bit format compatible with the Pioneer spacecraft command system (GOE)
- (2) Generated an FSK signal suitable for exciting the DSIF S-band transmitter phase modulator at a rate of 1 bit per sec (GOE)
- (3) Established a means for preventing the transmission of any command not entered in the "permissive command list" (TCP)
- (4) Verified that the transmitted command corresponded to the manually inserted command and terminated transmission of commands in which errors are detected (TCP)
- (5) Provided a typewriter printout of spacecraft command status, a notation of the transmitted commands and their time of transmission.

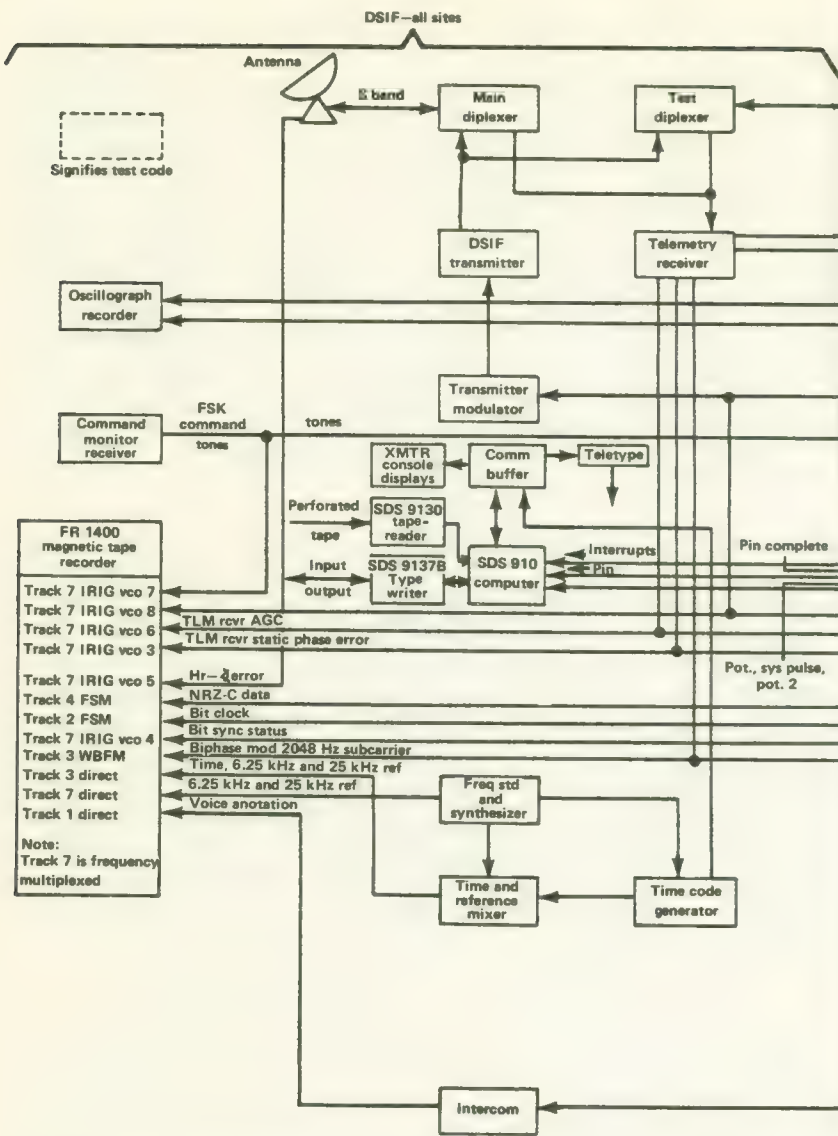


FIGURE 8-14.—Functional block diagram of Pioneer GOE at the DSIF sites.

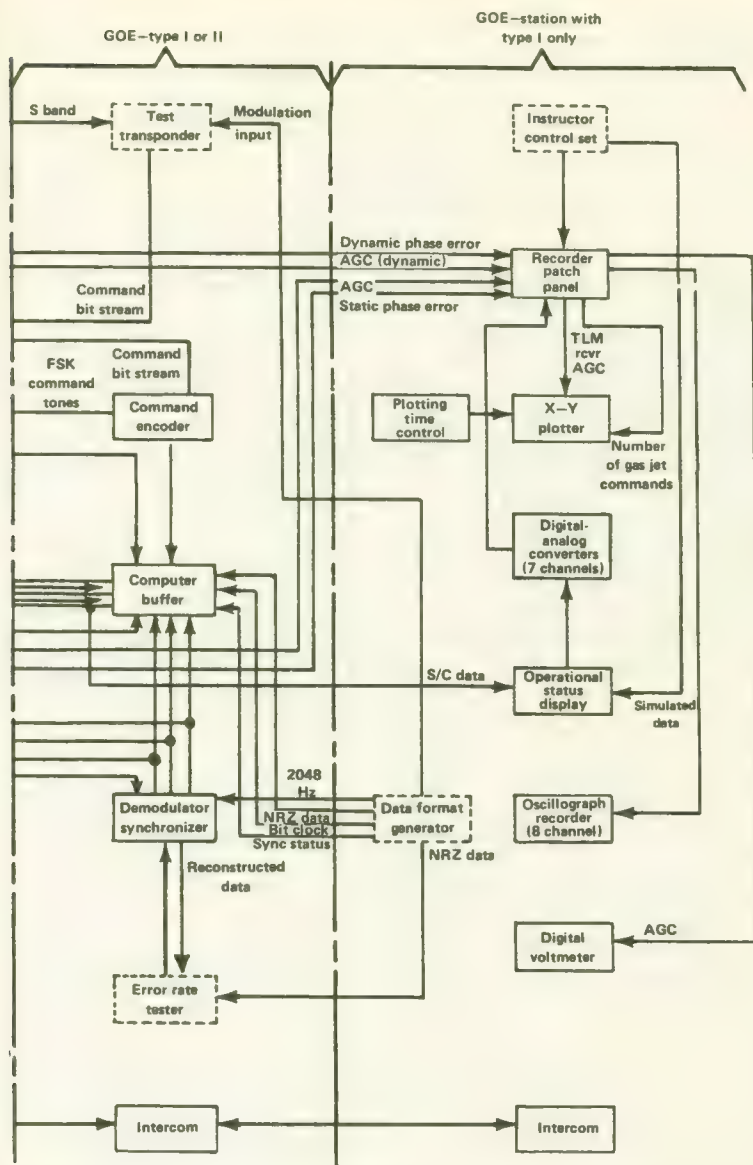


FIGURE 8-14.—Concluded.—Functional block diagram of Pioneer GOE at the DSIF site.

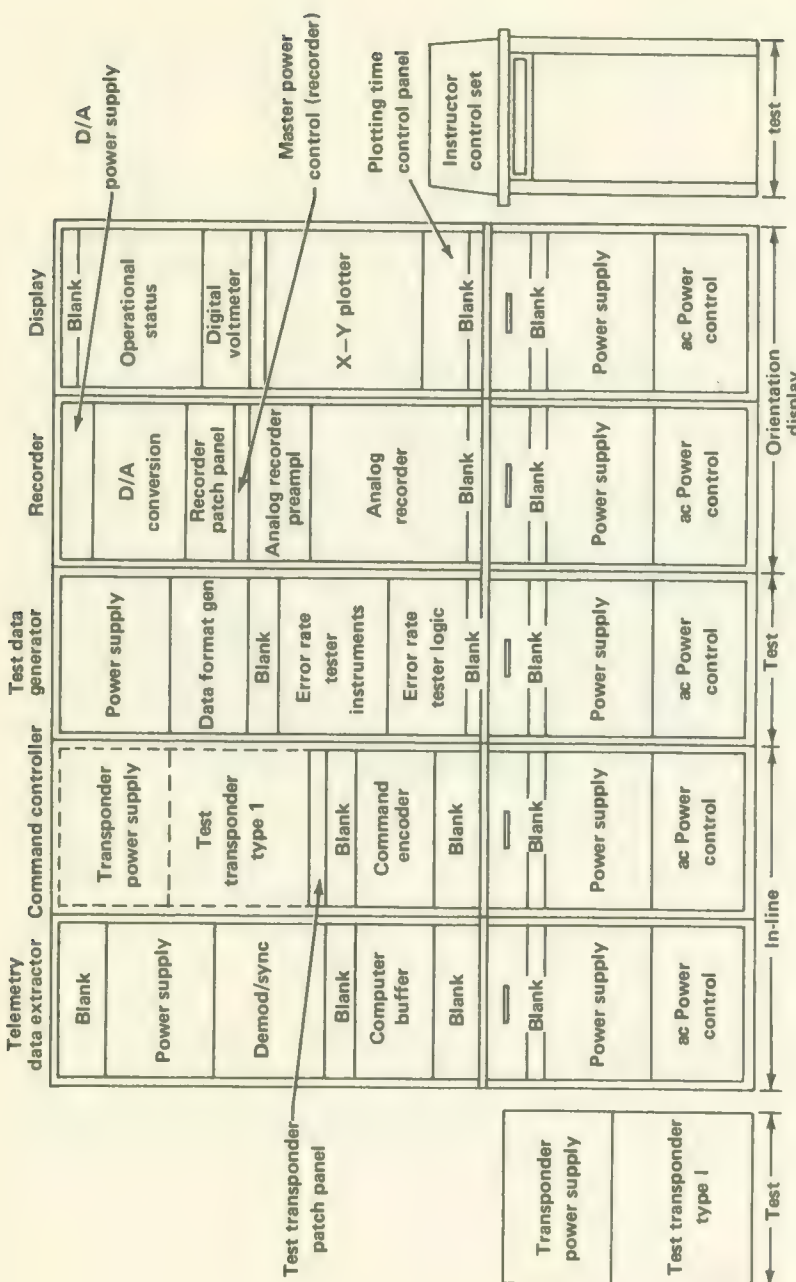


FIGURE 8-15.—The five racks of Type-I GOE at Goldstone.

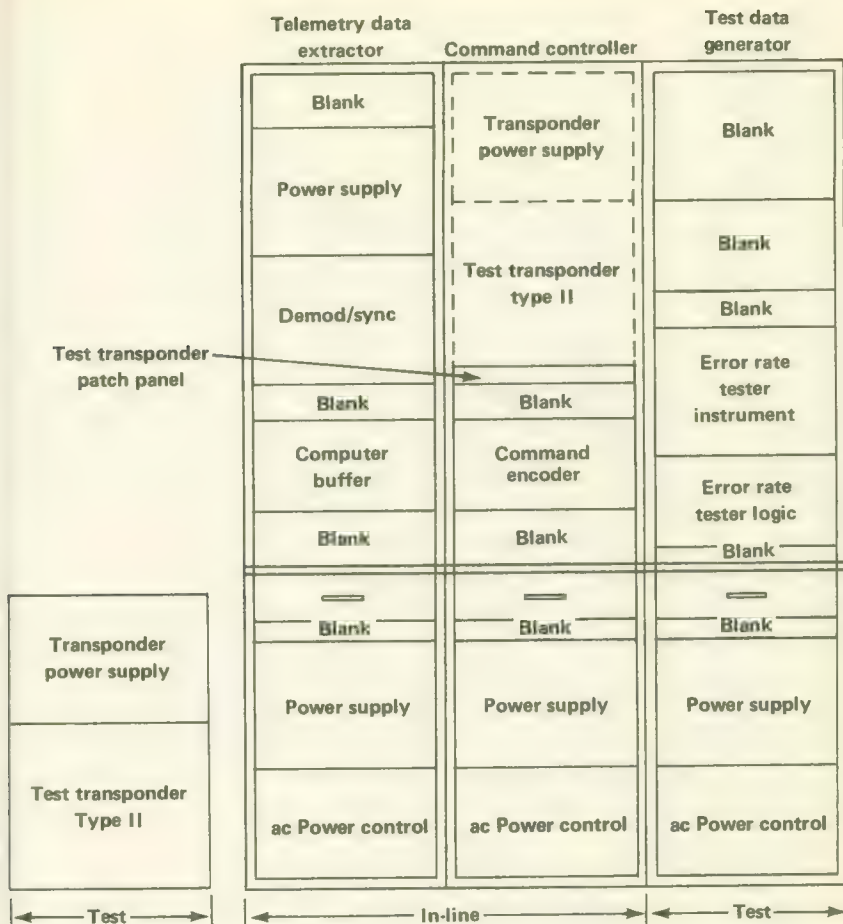


FIGURE 8-16.—The three racks of Type-II GOE at overseas DSIF stations.

(Verification that the command had been executed on the spacecraft was done by the controller at the Pioneer Mission Operations Center at Ames Research Center.) (TCP)

(6) Organized command data and command status into a format suitable for near-real-time teletype transmission to the SFOF (Again, command verification was done at Ames.) (TCP)

The second DSN facility that assumed specific configurations especially tailored for the Pioneer mission was the Ground Communications Facility. The configurations varied from flight to flight and even during the same mission. It is impractical to catalog all these changes; the arrangement for Pioneer 8 was rather typical, and it is reproduced in figure 8-17.

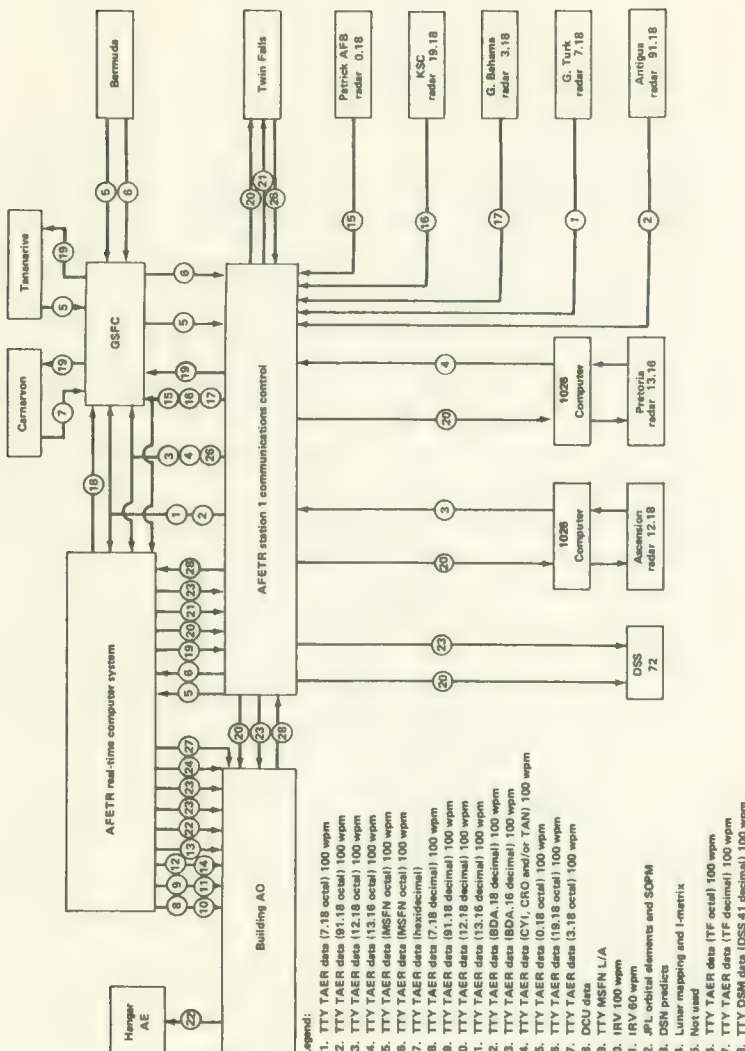


FIGURE 8-17.—Flow diagram for near-Earth-phase tracking data for the Pioneer 8-mission.

A similar situation existed with the SFOF; it is another general-purpose facility that was modified to accommodate Pioneer requirements. A Pioneer Mission Support Area was set up at JPL's SFOF for use as an operational control center during the launch phases of Pioneer flights when activity was high. Spacecraft performance and scientific data analyses were also carried out there. One of the special SFOF Mission Control Rooms and an associated Flight Path Analysis Area were made available to the Pioneer Project during critical phases of each mission. A data flow diagram (fig. 8-18) illustrates the routing of data within and without the SFOF during the Pioneer Program. The dispatch of data packages to Ames Research Center (fig. 8-18) completed the DSN role in data processing and handling. Ames processed data tapes and passed scientific data on to the experimenters, completing the data link from spacecraft to scientist.

Cruise portions of the flights were controlled at Ames where spacecraft and instrument expertise were readily available. SFOF space was used for control only during the launch phase or in the event of extremely critical periods.

#### REFERENCES

1. ANON.: DSN Capabilities and Plans, Vol. I. Description of Deep Space Network Capabilities as of 1 July 1968. JPL Rept. 801-1, 1968.
2. ANON.: Support Instrumentation Requirements Document, Pioneers 6, 7, 8, 9, and E. NASA, Mar. 1969.
3. RENZETTI, N. A.: Tracking and Data System Final Support for the Pioneer Mission, Pioneer 6 Pre-Launch to End of Nominal Mission. JPL Rept. TM 33-426, 1970. (A similar report exists for each Pioneer flight.)

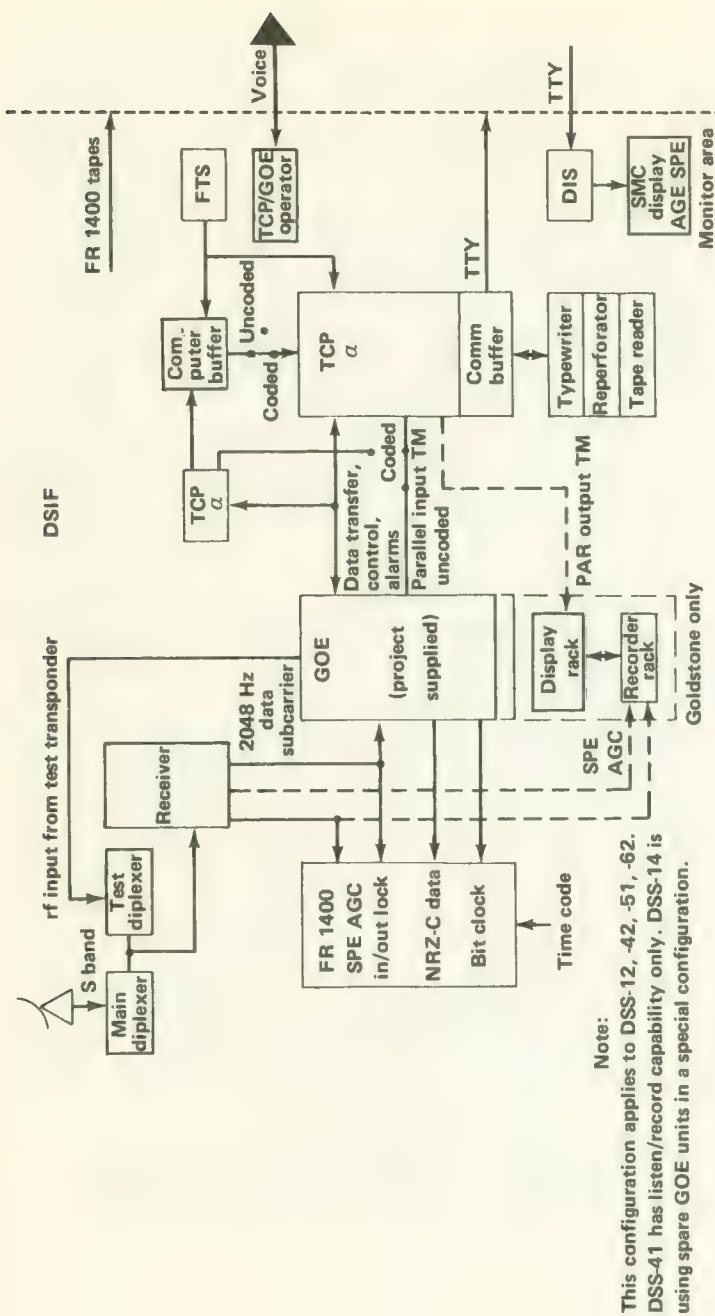


FIGURE 8-18.—DSN telemetry configuration.

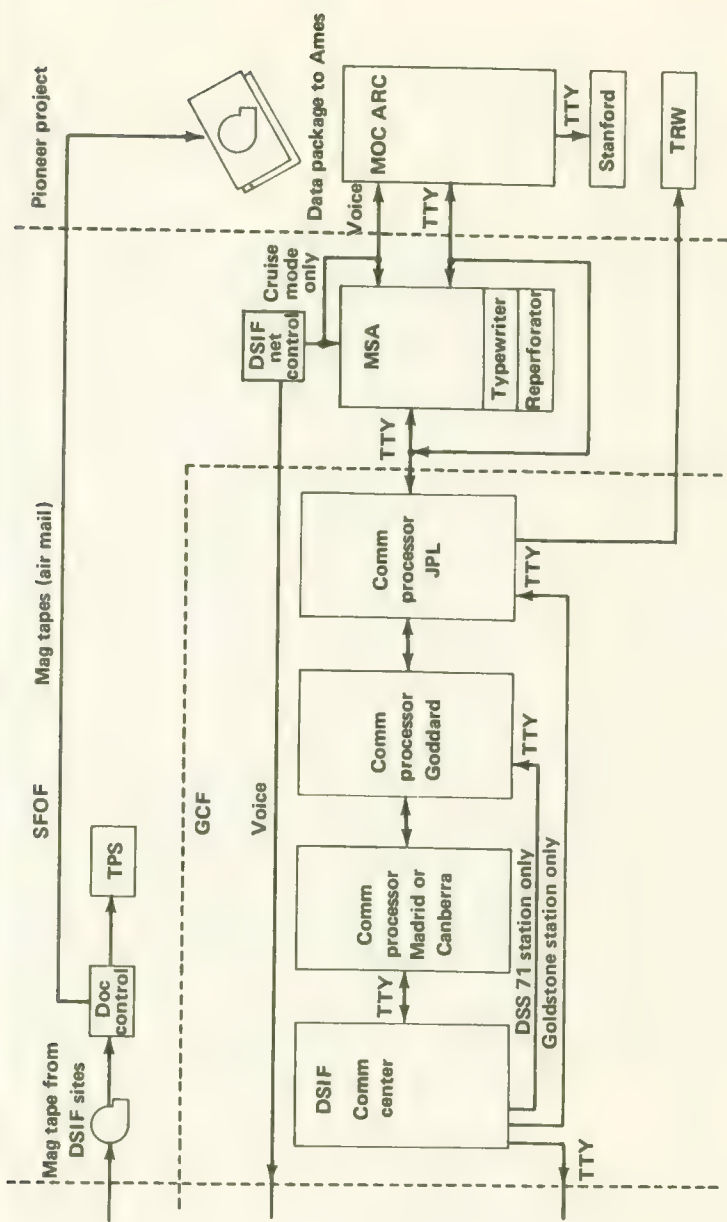
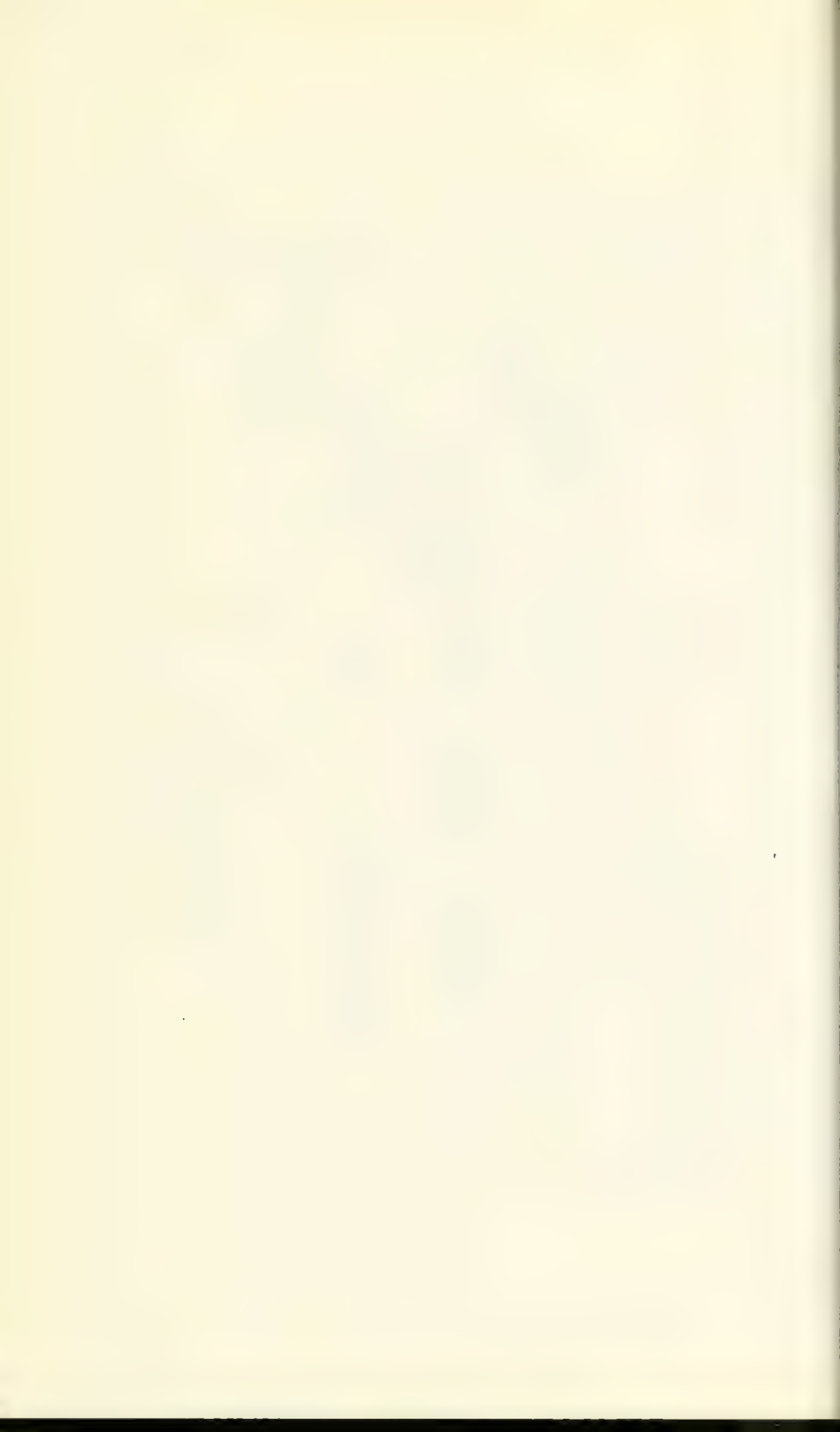


FIGURE 8-18.—DSN telemetry configuration.—Concluded.



## Pioneer Data-Processing Equipment

PIONEER SPACECRAFT radioed back to Earth two kinds of data: (1) scientific data for the several Pioneer experimenters, and (2) engineering data to permit the mission controllers to assess the operational condition of the spacecraft. Referring to figure 8-18, one sees that the telemetry data follow two paths between the DSN stations, which receive it directly from the spacecraft, and the experimenters and Pioneer project personnel. Pioneer telemetry data are recorded directly on magnetic tape as they arrive from deep space at the DSN stations and airmailed to JPL for verification and then to Ames Research Center. This is the first route, and all data follow it. At Ames, they are processed on the Pioneer Off-Line Data-Processing System (POLDPS) for subsequent transmission to the experimenters on digital magnetic tapes in formats compatible with their computer facilities. Some of the telemetry data, however, also follow a second route. These are dispatched immediately from the DSN to Ames Research Center via teletype through JPL's SFOF. These are called "quick look" data; they are used for checking the scientific instruments and for retransmission (after some processing) to ESSA to help forecast solar activity. Data from the Stanford radio propagation experiment are handled differently. As described in chapter 5, proper operation of this experiment requires the near-real-time feedback to Stanford of information on the Stanford receiver status. This information is relayed by teletype from Ames Research Center to Stanford a few miles away. In addition, engineering data flow via teletype from the DSN station to the SFOF and thence to both Ames and TRW Systems for analysis. At Ames, these engineering data are used to assess the condition of the spacecraft and help make operational decisions.

The data-processing facilities at Ames and TRW Systems are described below.

### PIONEER OFF-LINE DATA-PROCESSING SYSTEM

In 1964 when JPL computers were heavily loaded, the decision was made to construct the processing line at Ames Research Center. Bids from ten companies were received in late 1964 as a result of NASA solicitation. Computer Sciences Corporation (CSC) received the prime POLDPS contract on January 7, 1965. Astrodata, Inc., was the subcontractor respon-

sible for building the POLDPS hardware. By the summer of 1965, POLDPS was ready for operation.

Magnetic tape represented the only practical way to transmit the bulk of the data from the active Pioneer spacecraft—teletype facilities could not handle the volume. At each DSN station, two Ampex FR-1400 tape recorders operating in parallel prepared analog tapes of the transmissions received from the Pioneers. Tape loading times for each machine were staggered to avoid the loss of data. One set of tapes containing all recorded data were selected and shipped first to JPL for verification to ensure the quality of reproduction (fig. 9-1). The tapes were then sent to the Pioneer Off-Line Data Processing System at Ames Research Center.

During 1969, Pioneer tape shipments averaged 400 (9200-ft) tapes per month, each containing 4 hr worth of data with half-hour overlaps. POLDPS processed and sorted out these data, preparing an average of 400 (2400-ft) tapes per month for the experimenters. The preparation of over 15 experimenter tapes per working day indicates that POLDPS was extremely active during 1969, when four Pioneers were transmitting data back to Earth (fig. 9-2).

The input to POLDPS consists of the FR-1400 magnetic tapes received by airmail from DSS sites around the world. The following seven channels are recorded on these tapes at 5.5 in./sec:

- (1) Voice (containing station events)
- (2) Bit clock data from the DSS demodulator/bit synchronizer
- (3) Universal time and 6.25- and 25-kHz reference signals
- (4) NRZ-C data (see ch. 4)
- (5) The biphase-modulated 2048-Hz subcarrier containing the time-multiplexed PCM-data bit train
- (6) Spare channel
- (7) Various DSS data, such as static phase error, sync status, antenna error, command tones, etc.

POLDPS processes these tapes in a two-level system. (fig. 9-3) The first level, called the tape processing station (TPS), produces a multifile digital tape that serves as the input to the second level of processing, which consists of the Pioneer off-line direct-coupled system (POLDCS). POLDCS generates separate experimenter tapes that are IBM-compatible and in the formats and densities desired by the individual Pioneer experimenters.

## TAPE PROCESSING STATION

The TPS consists of an FR-1400 Tape Recorder-Reproducer, an STL Bit Synchronizer/Demodulator, an SDS-910 computer, Astrodatal interface hardware, and the necessary software to control the equipment and process the input data into a multifile digital tape acceptable to POLDCS (ref. 1). Data recorded at any DSS can be processed even if the station does

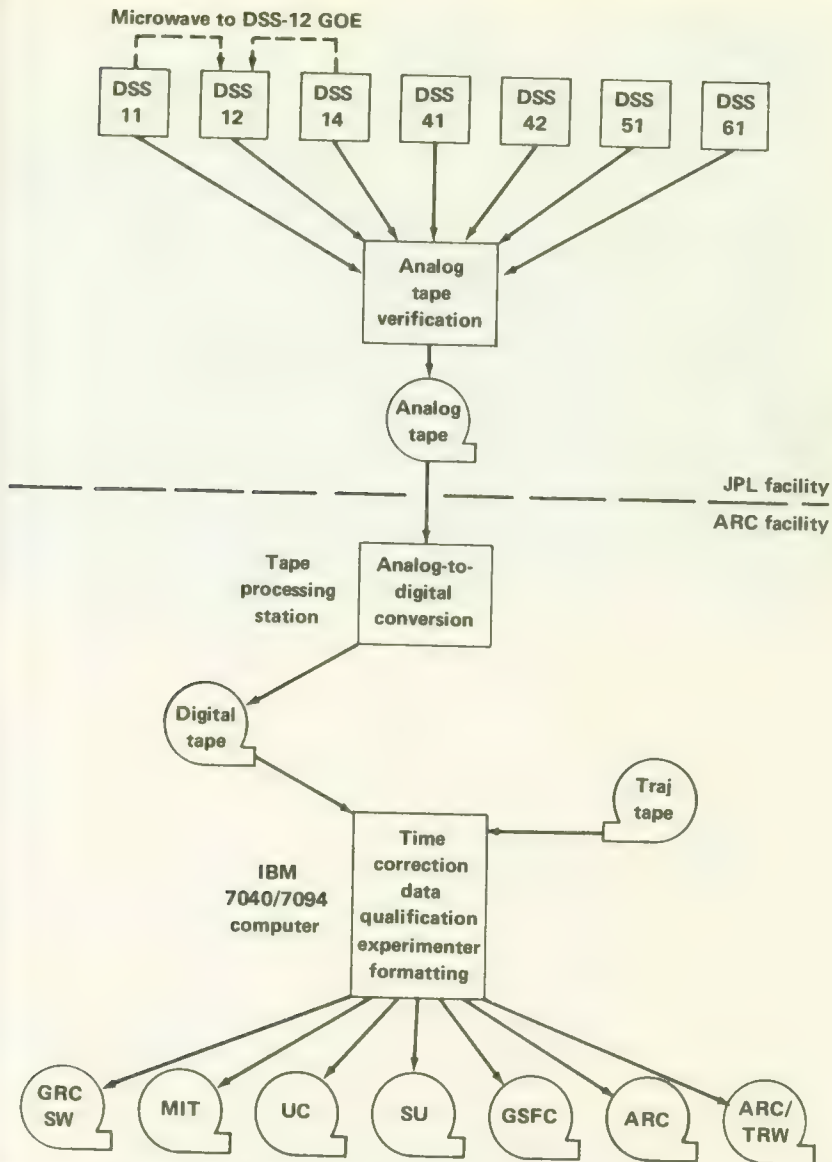


FIGURE 9-1.—The Pioneer off-line data processing station showing data flow paths.

not possess the Pioneer-unique GOE described in chapter 8. The TPS performs the following functions:

- (1) Establishes frame and word synchronization of the telemetry data from either the NRZ bit stream or the biphase-modulated subcarrier
- (2) Provides a bit clock from the recorded signal or the output of the bit



FIGURE 9-2.—Pioneer Off-Line Data Processing System (POLDPS) at Ames Research Center.

#### synchronizer

- (3) Generates time information (in days, hr, min, sec, and msec) from the bit-clock channel
- (4) Demodulates PCM signals and sync information from the raw data
- (5) Digitizes analog functions
- (6) Converts the FSK command data into digital format
- (7) Records the above information on IBM-compatible computer tapes at 556 characters per in.

All TPS operations are performed automatically except for the handling of tape reels, patch-board wiring, installation of plug-in units, and TCP control.

#### PIONEER OFF-LINE DIRECT-COUPLED SYSTEM

POLDCS digests the TPS output tapes and performs the following functions:

- (1) Selects the "best" telemetry data from multiple input sources
- (2) Evaluates the quality of the telemetry data
- (3) Converts ground station time into spacecraft time
- (4) Calibrates the engineering data
- (5) Decommoduates the evaluated telemetry data

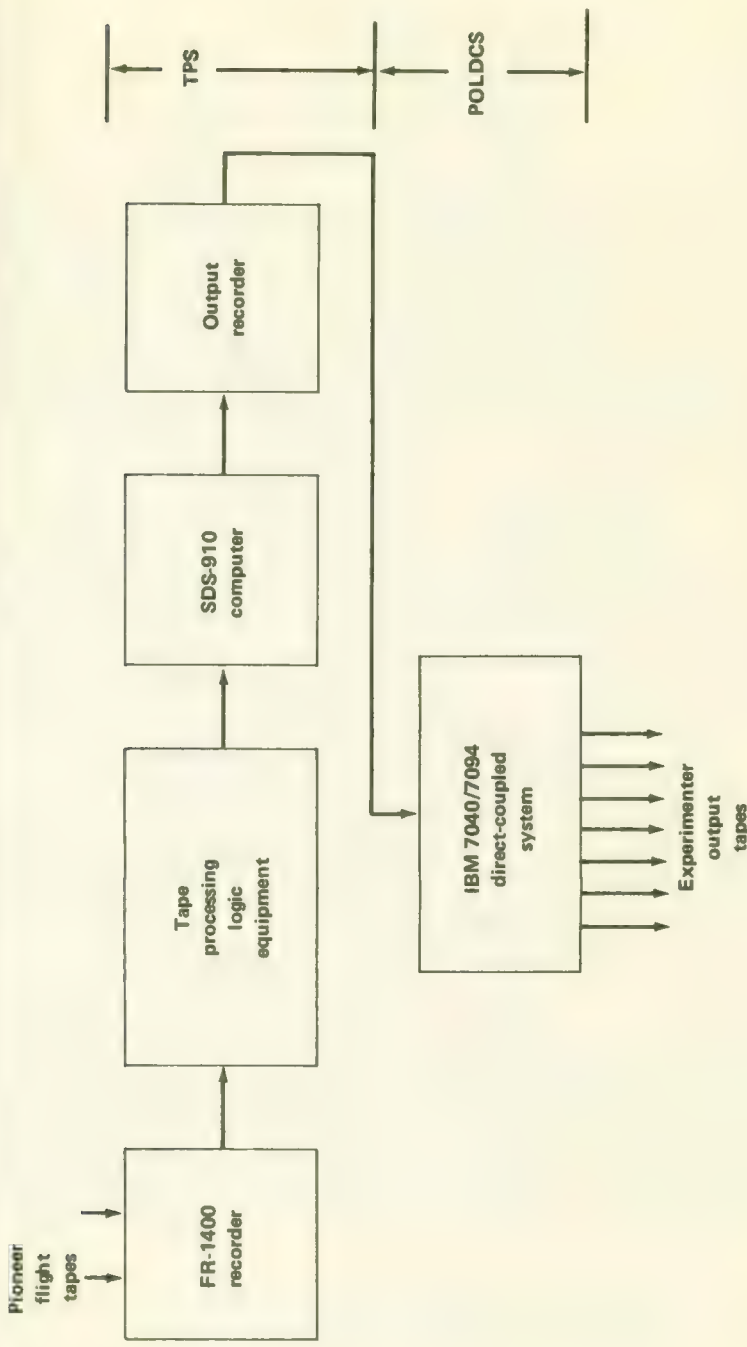


FIGURE 9-3.—Block diagram of Pioneer off-line tape processing.

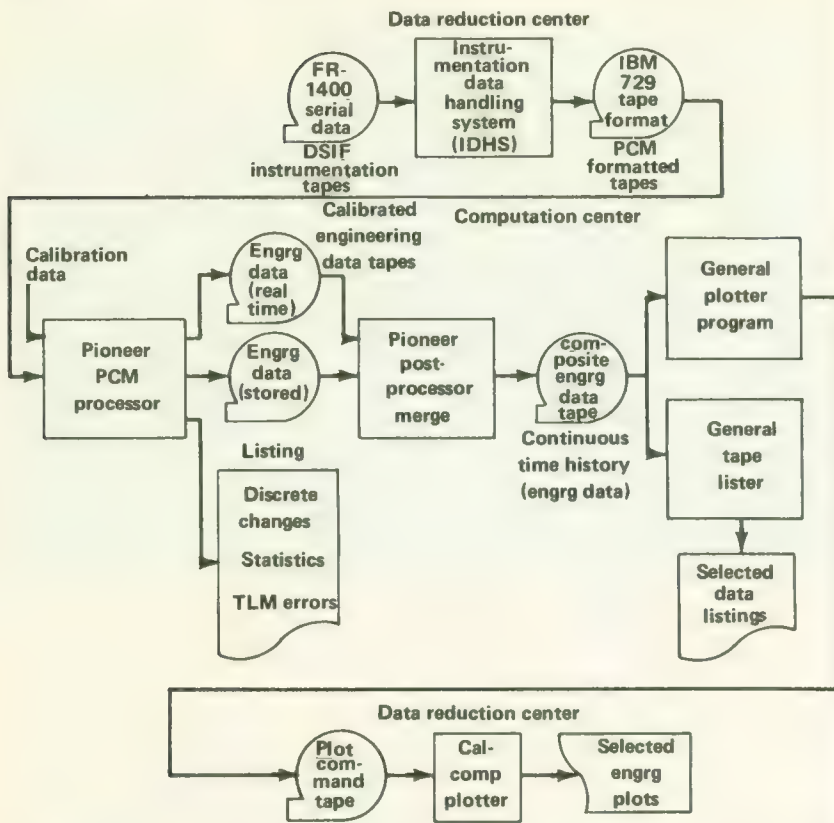


FIGURE 9-4.—Block diagram of data processing line at TRW Systems used on occasion for Pioneer tapes.

(6) Prepares the magnetic tapes for the individual Pioneer experimenters

Because the Pioneer data rates are usually very low (in comparison to those from scientific satellites, for example) NASA felt that some indication of data quality ought to be added to the experimenter tapes. The so-called data condition indicator (DCI) was established, using information from Channel 7 of the analog tapes received at Ames. A numerical code added to the experimenter tapes indicated the following conditions for each spacecraft word:

- 40 Filled word
- 36 Replaced value (known words only)
- 22 FSK command inserted
- 20 Command from another DSS station

- 10 DSS receiver out of lock
- 04 Bit error probability in excess of  $10^{-3}$
- 02 DSS bit synchronizer out of lock
- 01 Parity error
- 00 Good data

The experimenter tapes are supplemented by trajectory tapes giving the spacecraft position as a function of time. The basic trajectory tapes are prepared at JPL, but Ames reprocesses them to put them in the formats and densities requested by the experimenters.

POLDPS has remained substantially the same throughout the Pioneer program. The only significant change was made for Pioneer 9, which carried the convolutional coder designed to improve the quality of Pioneer data. The effects of the addition of the convolutional coder upon Pioneer telemetry are described in chapter 4.

### DATA PROCESSING AT TRW SYSTEMS

TRW Systems receives copies of the FR-1400 analog tapes made at the DSS stations for the first 4 days following a launch. As spacecraft prime contractor, TRW Systems was primarily interested in the engineering data on these tapes. The output from the TRW Systems data-processing line consists mainly of tabulated engineering data and automatically plotted engineering parameters suitable for assessing spacecraft performance as a function of time (fig. 9-4).

The FR-1400 tapes are first formated at the TRW Systems Data Reduction Center by the Instrumentation Data Handling System (IDHS). Formating prepares them for an IBM 7094, which next edits, sorts, and calibrates the data. In addition, the Pioneer General Data Processing Program performs the following operations:

- (1) Prepares statistics in the form of minima, maxima, and averages for each engineering parameter
- (2) Summarizes those telemetry errors detected
- (3) Monitors digital data

The computer prints out tabular data and prepares a magnetic tape for input to a CalComp Plotter, which draws the graphs of desired engineering parameters.

The TRW Systems processing line described above was not used on a regular basis.

### REFERENCE

1. ANON.: Pioneer Off-Line Data Processing System—System Manual. Computer Sciences Corp. Rept., 1965.



# Bibliography

**I**NCLUDED HERE ARE all engineering reports and papers of significance dealing with the four Pioneer systems: spacecraft, instruments, launch vehicle, and tracking and data acquisition. Because a great deal of Pioneer descriptive information is available only in the program specifications, a comprehensive list of these follows this bibliography. Volume III includes the bibliography covering Pioneer operations and scientific results.

- ANON.: Pioneer. TRW Spacelog, vol. 4, no. 18, Fall 1964.
- ANON.: Pioneer Off-Line Data Processing System—Systems Manual. Computer Sciences Corp. Rept., 1965.
- ANON.: Description of the Deep Space Network, Operational Capabilities as of January 1, 1966. JPL Rept. 33-255, 1966.
- ANON.: Pioneer B Mission, Manned Space Flight Network Post Mission Report. Goddard Space Flight Center X-552-66-543, 1966.
- ANON.: Pioneer Systems Capabilities. TRW Systems, 1966.
- ANON.: Single-Purpose Concept Credited with Pioneer 6 Success. Aviation Week, Apr. 1966.
- ANON.: DSIF Development and Operations. JPL Space Programs Summary. JPL Rept. 37-43, vol. IV, Jan. 1967, p. 17; and subsequent issues.
- ANON.: Final Engineering Report for the M.I.T. Plasma Experiment on Pioneer 6 and Pioneer 7. MIT Rept., 1967.
- ANON.: The Pioneer Spacecraft. NASA Facts NF-31, 1967.
- ANON.: Tracking and Navigational Accuracy Analysis. JPL Space Programs Summary. JPL Rept. 37-44, vol. III, Mar. 1967, p. 3.
- ANON.: Communications Systems Research: Sequential Decoding, Supporting Research and Advanced Development. JPL Rept. N69-16491, 1968, pp. 171-175.
- ANON.: DSN Capabilities and Plan. Vol. I—Description of Deep Space Network Capabilities as of July 1968. JPL Rept. 801-1, 1968.
- ANON.: Final Engineering Report on University of Chicago Cosmic Ray Telescope for Pioneer 6 and 7. Univ. Chicago Rept., 1968.
- ANON.: Goddard Space Flight Center Network Operations Plan (GSFC NOP) for Pioneer S-Band Support. Goddard Space Flight Center, 1968.
- ANON.: Pioneer Handbook 1965-1969. TRW Systems, 1968.
- ANON.: Detailed Test Objectives for Long Tank Delta Launch Vehicle, Spacecraft: Pioneer-E-Launch Block 1. McDonnell-Douglas Corp. Rept. DAC-61830, 1969.
- ANON.: Final Report, Pioneer Magnetometer. Philco-Ford Corp. Rept. TR-DA-2117, 1969.
- ANON.: Pioneer Project/MSFN/DSN Tracking and Data Acquisition Support Interface Document. JPL, 1969.
- ANON.: Pioneer Spacecraft Project, Final Project Report. TRW Systems Rept. 8830-28, 1969.

- ANON.: Technical Manual for Ames Research Center Plasma Probe. Marshall Laboratories Rept. ML/TN 2200-106.
- BALL, J. E.: The Effect of the Gas Leak on the Pioneer VI Orbit. *JPL Space Programs Summary*. JPL Rept. 37-41, vol. III, Sept. 30, 1966, p. 62.
- BARON, W. R.: The Solar Array for the Pioneer Deep Space Probe. *Electronics and Power*, vol. 14, Mar. 1968, p. 105.
- BARTLEY, W. C.; McCACKEN, K. G.; AND RAO, U. R.: A Digital System for Accurate Time Sector Division of a Spin-Stabilized Vehicle. *IEEE Trans., AES-3*, Mar. 1967, p. 230.
- : Pioneer VI Detector to Measure Degree of Anisotropy of Cosmic Radiation in Energy Range 7.5-90 MeV/Nucleon. *Rev. Sci. Inst.*, vol. 38, Feb. 1967, p. 266.
- BARTLEY, W. C.; ET AL.: GRCSW Final Technical Report on Cosmic Ray Anisotropy Detectors Flown on Pioneer VI and VII. Southwest Center for Advanced Studies, Rept. DASS-66-12, 1966.
- BARTLEY, W. C.; ET AL.: Recent Advances in Cosmic Ray Payloads for Interplanetary and Planetary Spacecraft. *Natl. Telem. Conf.*, 1968, pp. 238-244.
- BAUERNSCHUB, J. P., JR.: Nonmagnetic Explosive-Actuated Indexing Device. NASA TN D-3914, 1967.
- BERG, O. E.: The Pioneer 8 Cosmic Dust Experiment. NASA TN D-5267, 1969. Also: *Rev. Sci. Inst.*, vol. 40, Oct. 1969.
- BINGHAM, R. C.; ET AL.: Two Satellite-Borne Cosmic Radiation Detectors. *IEEE Trans., NS-13*, Feb. 1966, p. 478.
- BOLTON, R. C., JR.: The Present Technology in Space Communications Equipment in Deep Space Probes. *IEEE Conv. Rec.*, vol. 4, 1968, p. 586.
- BRIGGS, D. C.; ET AL.: Silicon Solar Cells for Near-Sun Missions. NASA TM-X-59774, 1967.
- BUKATA, R. P.; KEATH, E. P.; AND YOUNSE, J. M.: Final Technical Report on Cosmic Ray Particle Detectors Designed for Interplanetary Studies Utilizing the Pioneers 8, 9, and 10 Spacecrafts. Univ. Texas Rept. N70-13082, 1969.
- CANTARANO, S. C.; ET AL.: Magnetic Field Experiment, Pioneers 6, 7, and 8. NASA TM-X-63395, 1968.
- CHANAY, D.; CURKENDALL, D. W.; AND MOTSCH, R.: Pioneer VI High Frequency Data Analysis. *JPL Space Programs Summary*, JPL Rept. 37-41, Sept. 30, 1966, p. 57.
- CROOK, G. M.; ET AL.: Instrument Report, TRW Electric Field Detector. TRW Systems Rept. 07194-6004-R000, 1968.
- CULL, B. D.: Flight Report for Delta Vehicle S/N 20222, Delta Program Mission No. 60, Spacecraft: Pioneer-D. McDonnell-Douglas Rept. DAC-61695, 1969.
- CURKENDALL, D. W.: Pioneer Project Support. *JPL Space Programs Summary*, JPL Rept. 37-41, Vol. III, p. 56, Sept. 30, 1966; and 37-42, vol. III, p. 21, Nov. 30, 1966.
- DUGAN, D. W.: A Preliminary Study of the Solar Probe Mission. NASA TN D-783, 1961.
- EBERHARD, C. A.; AND LINDNER, J. W.: Control of Magnetic Properties of Scientific Spacecraft, NASA N68-85537, 1967.
- EDGAR, R. B.; AND MORRISON, J. M.: Magnetic Moment Control for Spacecraft Electronics. *Space/Aero.*, vol. 44, Sept. 1965, p. 94.
- ERICKSON, M. D.; AND MATTHEWS, H. F.: The NASA Advanced Pioneer Mission, NASA TM X-54039, 1964.
- GALE, E. H.; AND GLUCK, R.: Motion of a Spinning Satellite during the Deployment of Asymmetrical Appendages. *J. Spacecraft*, vol. 3, Oct. 1966, p. 1463.
- GALLAGHER, J. F.: Pioneer B Trajectory Dispersions and DSN Initial Acquisition. *JPL Space Programs Summary*. JPL Rept. 37-41, vol. III, Sept. 30, 1966, p. 59.
- GLEGHORN, G. J.; AND LINDNER, J. W.: Magnetic Considerations in the Design and Testing of the OGO and Pioneer Spacecraft. 16th Int'l. Astronaut. Congr., 1965.

- GUNN, C. R.: Delta—A Scientific and Application Satellite Launch Vehicle. Goddard Space Flight Center X-470-69-406, 1969.
- HALL, C. F.; NOTHWANG, G. J.; AND HORNBY, H.: A Feasibility Study of Solar Probes. IAS Paper 62-21, 1962.
- HALL, C. F.; AND MICKELWAIT, A. B.: Development and Management of the Interplanetary Pioneer Spacecraft. NASA TM X-60564, 1967. Also in Proc., 18th. Intl. Astronaut. Congr., vol. 2, M. Lunc, ed., Pergamon Press, Oxford, 1968.
- HALLUM, C. E.; AND WEBSTER, P. W.: New Functional Redundancy Approaches for Attitude Control Thruster Systems. NASA CR-73231, 1968.
- IUFER, E. J.: Magnetic Program for Pioneer and Its Scientific Payload. Proc. Magnetic Workshop, JPL, 1965.
- KEMP, R. F.; AND SELLEN, J. M., JR.: Solar Wind Simulation with the Pioneer Spacecraft. AIAA Paper 66-153, 1966.
- KERWIN, W. J.: Solar Wind Measurement Techniques. Part I—An Improved Magnetometer for Deep Space Use. NASA/ARC Rept.
- KOEHLER, R. L.: Interplanetary Electron Content Measured Between Earth and the Pioneer VI and VII Spacecraft Using Radio Propagation Effects. Stanford Univ., 1967.
- : A Phase Locked Dual Channel Spacecraft Receiver for Phase and Group Path Measurements. Stanford Univ. Rept. SU-SEL-65-007, 1965.
- LINDBERG, R. G., ED.: Feasibility Study for Conducting Biological Experiments Aboard a Pioneer Spacecraft. NASA CR-73178, 1968.
- LUMB, D. R.; AND HOFMAN, L. B.: An Efficient Coding System for Deep Space Probes with Specific Application to Pioneer Missions. NASA TN D-4105, 1967.
- LUMB, D. R.: A Study of Codes for Deep Space Telemetry. IEEE Intl. Conf. and Exhibit, 1967.
- : Test and Preliminary Flight Results on the Sequential Decoding of Convolutional Encoded Data from Pioneer IX. IEEE ICC Conf. Publ., vol. 5, 1969, pp. 39-1 to 39-8.
- MASSEY, W. A.: Pioneer 6 Orientation Control System Design Survey: NASA/ERC Design Criteria Program, Guidance and Control. NASA CR-86193, 1968.
- MATTHEWS, H. F.; AND ERICKSON, M. D.: The NASA Advanced Pioneer Mission. SAE Paper 857D, 1964.
- MICKELWAIT, A. B.; AND SPANGLER, E. R.: Dolling Up a Space Probe. Electronics, vol. 37, Mar. 23, 1964, p. 80.
- MICKELWAIT, A. B.: The Pioneer 6 Spacecraft. Raumfahrtforschung, vol. 10, July-Sept. 1966, p. 138.
- : The Pioneer Spacecraft. Symp. on Moon and Interplanetary Space, 1966.
- MUÑOZ, R.: The Ames Magnetometer. 1966 Natl. Telem. Conf., 1966.
- NEWELL, D. H.: Navigation for Spin Stabilized Deep Space Planetary Spacecraft. Proc. 3rd Space Congr., 1966, pp. 656-686.
- NUNAMAKER, R. R.; HALL, C. F.; AND FROSOLONE, A.: Solar Weather Monitoring—Pioneer Project. AIAA Paper 68-36, 1968.
- NUNAMAKER, R. R.; DICKERSON, L. W.; AND HALL, C. F.: Pioneer Project—1965-1970. 1970.
- ORBISON, J.: Flight Project Support. JPL Space Programs Summary. JPL Rept. 37-40, Vol. III, July 31, 1966, pp. 101-103; and subsequent issues.
- PESCHEL, A. H.; AND ELLIS, R. B.: Pioneer D (IX) Trajectory and Orientation Analysis. TRW Systems Rept. 3432.8-5, 1968.
- PISZKIN, F. M.: Delta Launch Vehicle Performance Capabilities. Goddard Space Flight Center X-470-68-006, 1968.

- REIFF, G. A.: Interplanetary Spacecraft Telecommunication Systems. IEEE Spectrum, April 1966.
- : The Pioneer Spacecraft Program. AAS Paper, 1969.
- : Evolution of Deep Space Communications—1958 to 1968. IEEE Conv. Rec., vol. 4, 1968, p. 570.
- SCEARCE, C. S.; ET AL.: Magnetic Field Experiment Pioneers 6, 7, and 8. NASA TM-X-63395, 1968.
- SCHUMACHER, C. E.: Pioneer Spacecraft Test and Support Program. AIAA Paper 65-247, 1965.
- SELWEN, H.: Study of Pioneer Spacecraft Oscillator Stability. NASA CR-73307, 1968.
- SHERGALIS, L. D.: A Magnetically Clean Pioneer. Electronics, vol. 38, Sept. 20, 1965, p. 131.
- SPANGLER, E. R.; AND THIEL, A. K.: Temperature Control of Unmanned Satellites Remote from Earth. VDI Zeitschrift, vol. 108, 1966, p. 712.
- : Structural Design of Unmanned Space Vehicles. VDI Zeitschrift, vol. 108, 1966, p. 573.
- STAMBLER, I.: The New Pioneer Satellites. Space/Aeronaut., vol. 40, Nov. 1963, p. 58.
- STONE, I.: Six-Month Lifetime Predicted for Pioneer. Aviation Week, vol. 80, Jan. 27, 1964, p. 69.
- THIEL, A. K.: Spacecraft Development in the Next Decade. In *Saturn V/Apollo and Beyond*. AAS (Tarzana), 1967.
- WINDEKNECHT, T. G.: A Simple System for Sun Orientation of a Spinning Satellite. IAS/ARS Joint Meeting, 1961.

# Pioneer Specifications

THE TWO A-SERIES SPECIFICATIONS were first used during the solicitation of spacecraft and instrument proposals. They were updated frequently later. Specification A-6669 was updated with almost every modification of the contract with TRW Systems. P-series specifications were issued early in the program and replaced by the PC-series. The PC numbers under 100 apply to Block I; numbers between 100 and 199 apply to Block II. Specifications were frequently updated and revised.

- A-6669 Spacecraft and Associated Ground Equipment (12-1-63)
- A-7769 Scientific Instrument Specifications (12-31-64)
  - P-1 Documentation Procedures (1-2-64)
  - P-2 Amendments to NASA Quality Publications (12-1-63)
  - P-3 Amendment to MSFC-PROC-158B (6-19-64)
  - P-4 Project Development Plan
  - P-5 Launch Vehicle Performance Analysis for the Pioneer Program (12-1-64)
  - P-6 Classification Guide for Project Pioneer (12-15-64)
  - P-8 An Analysis of the Effects of the Spacecraft Systems and TAD Launch Vehicle on the Pioneer Trajectories (8-1-64)
  - P-9 Simulator Description (8-12-64)
  - P-10 Pioneer Time Resolution of Telemetry (8-28-64)
  - P-11 Procedures for the Preparation and Processing of Range Documentation (2-15-65)
  - P-12 Pioneer Canberra GOE ARC/STL Acceptance Test Results, July 1, 1965 (7-1-65)
  - P-13 Pioneer Johannesburg GOE ARC/STL Acceptance Test Results, July 1, 1965 (7-1-65)
  - P-14 Pioneer Ascension GOE ARC/STL Acceptance Test Results, July 1, 1965
  - P-15 Pioneer Goldstone GOE ARC/STL Acceptance Test Results, July 1, 1965 (7-1-65)
  - P-16 Pioneer Goldstone GOE Approved Engineering Configuration (9-1-65)
  - P-17 Engineering Configuration Pioneer GOE Serial 002 (Canberra) (9-1-65)
  - P-18 Engineering Configuration Pioneer GOE Serial 003 (Johannesburg) (9-1-65)
  - P-19 Engineering Configuration Pioneer GOE Serial 004 (Cape Kennedy)
  - P-20 Engineering Configuration Pioneer GOE Serial 005 (Ascension) (9-1-65)
  - P-21 Preliminary Evaluation of Pioneer Compatibility with CKAFS Facilities (8-6-65)
- PC-1 Spacecraft/Scientific-Instrument Interface Specification (3-6-64)
- PC-2 Spacecraft/DSIG/GOE Interface Specification (8-3-64)
- PC-003 Project Development Plan (11-16-64)
- PC-010 S/C & Associated Ground Equipment (A-6669) (renumbered)
- PC-011 General Instrument Specification (A-7769) (renumbered)
- PC-013 Pioneer GOE Specification (8-3-65)
- PC-020 Pioneer Solar Array Checkout at Table Mountain (6-5-64)

- PC-021 Spacecraft/Scientific-Instrument Interface Specification  
PC-023 Spacecraft/Launch Vehicle Interface Specification (7-19-65)  
PC-025 Scientific Instrument Integration Activities (8-1-64)  
PC-030 GOE Installation, Integration and Compatibility (4-19-65)  
PC-046 Pioneer Flight Operations (2-19-65)  
PC-047 Flight Operations Test Plan (8-2-65)  
PC-050 Procedures for Pioneer-A Flight Operations Test (11-24-65)  
PC-051 Pioneer A Flight Operations—Detailed Task Sequence  
PC-052 Pioneer A Flight Operations—Detailed Task Sequence for Participating Groups  
PC-053 Pioneer A Flight Operations, Stanford Procedures (11-15-65)  
PC-054 Pioneer-B Flight Operations  
PC-060 Pioneer Off-Line Data Processing System at ARC (8-28-64)  
PC-062 Pioneer Permissive Command Tape Program (10-20-67)  
PC-064 Pioneer-6 and 7 DSIF Operational Computer Program Requirement Specification (5-23-68)  
PC-070 Pioneer Solar Array Checkout at Table Mountain (PC-070) (renumbered)  
PC-071 Activities at the Air Force Eastern Test Range (6-19-64)  
PC-072 Scientific Instrument Integration Activities  
PC-073 Pioneer Spacecraft/DSS-71/GOE Compatibility Test Specifications (8-12-65)  
PC-080 Tests of Scientific Instruments at ARC  
PC-081 Scientific Instrument Test Requirements (1-29-65)  
PC-083 Experiment Tests at Malibu Coil Facility—Master Test Procedures (3-31-65)  
PC-084 Procedure for GOE/DSIF Compatibility Tests (5-18-65)  
PC-085 Pioneer Spacecraft/DSIF-71/GOE On-Stand Compatibility Test Procedures (5-27-66)  
PC-090 Pioneer-A Trajectories  
PC-091 Pioneer-B Trajectories  
PC-092 Pioneer GOE-DSIF User's List (6-14-65)  
PC-093 Maintenance and Configuration Control (11-1-65)  
PC-094 Data Format Generator, Type II—Operation and Maintenance Manual Ground Operational Equipment (5-16-66)  
PC-111 Pioneer Instrument Specification (12-23-64)  
PC-121 Spacecraft/Scientific-Instrument Interface Specification (1-22-65)  
PC-122 Spacecraft/Scientific-Instrument Interface Specification (4-5-67)  
PC-123 Spacecraft/Convolutional Coder Unit Interface Specification (10-25-67)  
PC-130 GOE/Convolutional Coder Installation, Integration and Compatibility Specifications  
PC-146 Pioneer Space Flight Operations (7-67)  
PC-147 Flight Operations Test Plan (7-13-67)  
PC-148 Pioneer D Test Plan (8-20-68)  
PC-152 Pioneer-C Flight Operations (Sequence of Events)  
PC-153 Pioneer D Space Flight Operations—Procedures  
PC-154 Pioneer-E Flight Operations  
PC-155 Pioneer-C Flight Operations  
PC-160 Pioneer C/E Off-Line Data Processing System at ARC (3-15-68)  
PC-161 EGSE Computer Programming Specifications for the Scientific Instruments (10-21-66)  
PC-162 Simulation Operation Program (7-67)  
PC-163 EGSE Computer Program Required for CCU  
PC-164 Pioneer VIII and Pioneer D DSIF Operation Computer Program Requirement Specification (6-20-68)  
PC-165 Pioneer Space Weather Program

- PC-166 Pioneer VIII and IX Operational Computer Program Requirement Specification (11-29-69)
- PC-167 Pioneer 9 Operational Decoder (5-69)
- PC-168 TPS/Convolutional Coder Modification Interface Specification (5-20-68)
- PC-171 Activities at the Air Force Eastern Test Range (5-24-67)
- PC-173 Pioneer Spacecraft/DSS-71/GOE Compatibility Test Specification (8-9-68)
- PC-174 ETR/Pioneer Compatibility Test Plan (7-12-67)
- PC-180 Tests of Scientific Instruments at ARC
- PC-181 Scientific Instrument Test Requirements for Systems Tests of Pioneer C/D/E
- PC-182 SPAC and POLDPS Checkout Magnetic Recordings (9-27-67)
- PC-183 Convolutional Coder Test Requirements
- PC-184 Procedure for GOE/CCU Installation and Checkout
- PC-186 ETR/Pioneer Compatibility Test Procedure
- PC-187 Spacecraft Dolly Proof Load Procedure
- PC-188 Pioneer VI and VII DSIF Operational Computer Program Test Procedure (4-1-67)
- PC-190 Pioneer Trajectories
- PC-191 Pioneer D Trajectory Characteristics
- PC-192 Pioneer E Trajectory
- PC-193 GOE/Maintenance and Configuration Control Specification (8-25-67)
- PC-194 Pioneer-C RF Equipment and Trajectory Information
- PC-195 CCU Description and GOE Modifications
- PC-196 Pioneer-D RF Equipment and Trajectory Information
- PC-197 Pioneer-E RF Equipment and Trajectory Information (4-18-69)
- PT-1 Pioneer Trajectory Group Computer Report I, Coordinate Transformation Programs (8-16-65)



## Reliability and Quality Assurance<sup>1</sup>

**R**ELIABILITY CONTROLS used as a function of program phasing are shown in figure A-1 with a time line at the top indicating the approximate number of months on each phase through the first launch and the controls applied during each phase. What is considered to be the more significant of these controls will be described in the following three figures.

Figure A-2 describes the organization designed around the major controls with specific tasks listed. A particular individual within the reliability area was assigned to each of these disciplines. In the case of design reviews this individual was required to schedule, define package content, prepare and distribute minutes, see that action items were accomplished on schedule, and provide the best reviewers possible. In the area of specifications, the responsibility was for preparation of environmental specifications and signoff on all other specifications. Of utmost importance should be that the callouts in the specifications are realistic, not too tight, but adequate to account for drift.

For manufacturing and test surveillance two individuals were assigned. These individuals covered floor problems and attended all problem area meetings held by the functional activity. They were responsible for monitoring changes that affected their area and had an input as to the disposition of material that failed. The test surveillance monitor reviewed the test procedures and reviewed all test setups prior to the start of testing.

In the area of failure reporting, instruction was given as to the use of forms and pickup points where the forms were to be deposited. A failure review board was established which was responsible for failed part analysis and for appropriate and timely fixes. In addition to the involved specialists at TRW, this board had as members the system engineer and reliability engineer from NASA/ARC.

Reliability design tradeoffs were made throughout the initial phase of the program. Emphasis was given in particular to the use of proven designs

---

<sup>1</sup> Because of the great importance of long spacecraft life in the exploration of deep space, this appendix is devoted to a detailed description of the Reliability and Quality Assurance Program employed by NASA and the spacecraft contractor, TRW Systems. This text is extracted from the paper "Interplanetary Pioneer Success Story," prepared for the IEEE WINCON 70 meeting, by T. M. Lough (TRW Systems), J. Mulkern (NASA Ames), and B. Roseman (TRW Systems). These individuals had important roles in formulating the program and it is appropriate here to use their own words in describing it.

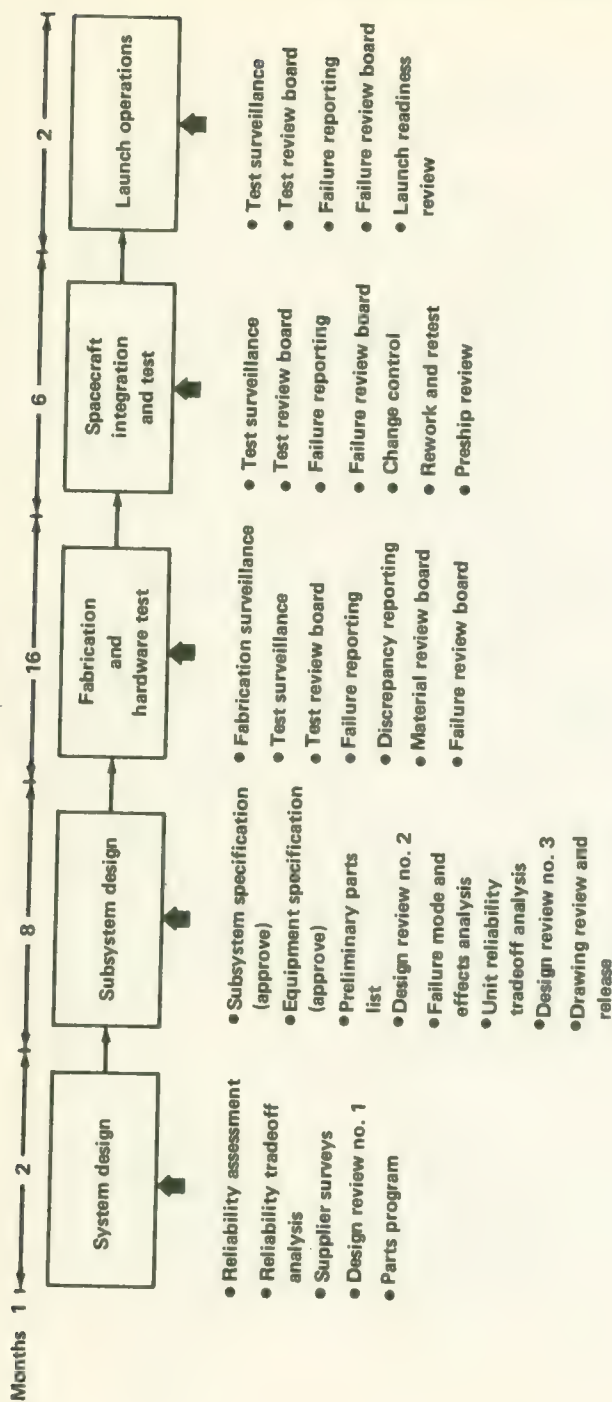


FIGURE A-1.—Pioneer A-E reliability controls.

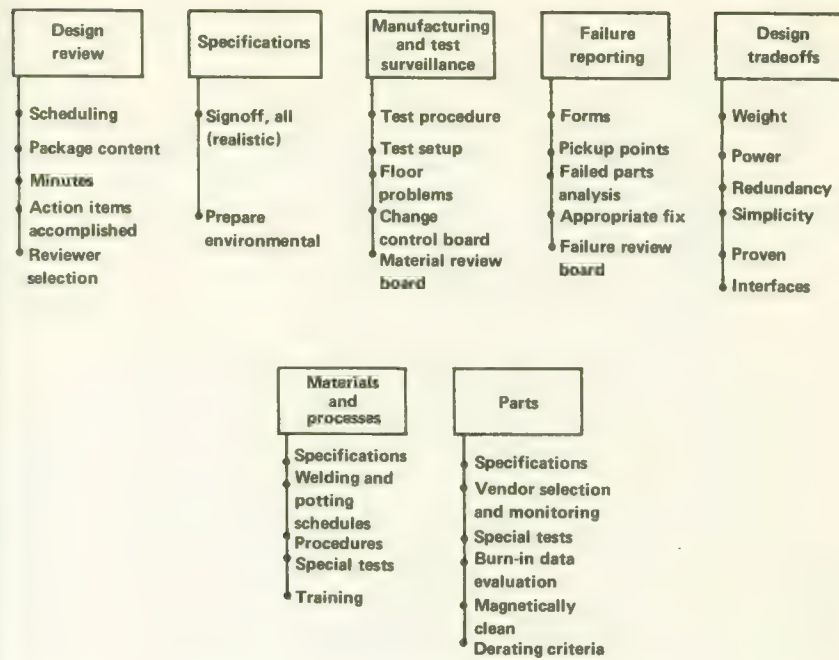


FIGURE A-2.—Reliability organization and functions.

and knowledge of interface parameters. Types of redundancy were evaluated, with consideration continually being given to weight and power.

Materials and processes personnel provided specifications and welding and potting schedules. They were continually involved in special testing and training when problem areas occurred.

Parts discipline has one of the greatest impacts on reliability and therefore this area was given considerable emphasis. The area was managed by a parts engineer assigned to the reliability program. He was responsible for the parts list and deviations to the parts list, high reliability part specifications, special tests and in-house receiving tests, evaluation of burn-in data, and for obtaining magnetically clean parts that were reliable.

Table A-1 describes the significant reliability elements associated with the design phase of the program. Part types used were limited. That is, the designer had to select his parts from a prepared list. This allowed for a better selection of high quality vendors and made vendor control simpler. This program started when the Minuteman program was in full swing and approximately \$20 million had been spent with parts vendors on a high reliability parts program. Consequently all our part specifications were written new and were based on Minuteman criteria and wherever possible certified Minuteman vendors were used. Reliability engineers were assigned

TABLE A-1.—*Significant Reliability Elements (Design)*


---

|                                |   |
|--------------------------------|---|
| General                        |   |
|                                | Part specifications based on Minuteman criteria               |
|                                | Reliability engineer assigned to each major design area       |
|                                | Redundancy selected on greatest improvement/lb                |
| Design reviews                 |   |
|                                | Kept small (12 to 25 knowledgeable engineers, including NASA) |
|                                | Data packages, concise and early                              |
|                                | Separate reviews for drawings (producibility)                 |
| High reliability parts program |   |
|                                | 100 percent burn-in (100 to 250 hr)                           |
|                                | Parameter drift screening                                     |
|                                | 100 percent environmental and life test sampling              |
|                                | No new types, processes or production lines                   |
|                                | Part types limited (Parts Deviation Board)                    |

---

TABLE A-2.—*Significant Reliability Elements (Manufacturing and Test)*


---

|                           |   |
|---------------------------|---|
| General                   |   |
|                           | Reliability surveillance during manufacturing and test                              |
|                           | Environmental test evaluation criteria established for each equipment               |
| Failure evaluation system |   |
|                           | Failure reporting forms simple, drop stations convenient                            |
|                           | Cause of failure defined rapidly (dissection, X-ray, etc.)                          |
|                           | Determine and implement corrective action   |
|                           | Concurrency by Failure Review Board (TRW and NASA participants)                     |
| Test philosophy           |   |
|                           | Equipment tests—development, life, qualification, acceptance                        |
|                           | System tests—development, qualification, integration, acceptance (space simulation) |
|                           | Maximum test time possible (minimum 1000 hr/system)                                 |

---

to each major design area to give assurance that tradeoffs were performed with reliability in mind. Redundancy was selected primarily on the basis of the greatest improvement per lb. Eighteen lb of redundancy theoretically brought the reliability from approximately 0.6 to 0.9 for 6 months in space. Specification review and approval and responsibility for the environmental test specifications were assigned to reliability engineers.

We learned early in our design review program to keep the number of persons in attendance small, that is, between 12 and 25 persons; to select knowledgeable and outspoken engineers for design evaluation, to have data packages that were concise and were distributed early enough that reviewers had time to digest the material contained. Finally . . . separate reviews for drawings [were needed] since in the general overall design review there was not time to go over drawings in sufficient detail. This

particular discipline contributed to seeing that the producibility of the equipment was at an acceptable level.

The high reliability parts program was considered of major importance and contained 100 percent burn-in, that is, burn-in of all parts from 100 to 250 hr depending on the part type. It also included parameter drift screening; i.e., monitoring the drift of various parameters over the interval the part was in burn-in, and 100 percent environmental and life test sampling. No new types of parts were allowed with one exception which will be discussed later. Table A-2 describes the significant reliability elements associated with the manufacturing and test phase of the program. Manufacturing and test surveillance was provided by two reliability engineers. This consisted primarily of assembly and test setup procedure evaluation, evaluation of test procedures to determine that the environmental test criteria for each equipment was correctly assigned to disclose design weaknesses, participation in the disposition of failed material, and control of changes as well as assignment of test requirements following a failure. Preship and prelaunch evaluation of flight scheduled equipment consisted of reviewing each equipment's history carefully before it was assigned to flight status. In the area of failure evaluation, failure report forms were kept simple and drop stations were located convenient to the manufacturing and test stations. Failure definition was determined expeditiously (within 2 days normally) by means of dissection, x-ray, etc. These results were used to assign fixes and served the Failure Review Board in making their decision.

The Pioneer program test philosophy was very simple. The equipment was made to operate; therefore let it operate as much as practical. A minimum of 1000 operating hours were accrued per system prior to each launch. On occasion at the Cape, when the launch was postponed for launch vehicle reasons, the spacecraft was turned on and left operating in one case for as long as a week. The test program for equipment included development, life, qualification and acceptance testing. System tests included development, qualification, integration and acceptance; the system acceptance tests culminating in a space simulation of 7-day duration.

This describes in brief detail the type of reliability program utilized. Now, what was the result of this program and where could the program have been improved? Figure A-3 shows that design areas were the major problem contributors indicating added emphasis needed to be placed on design reviews. Notice the combination of circuit, packaging and test set design accounts for approximately 50 percent of the total problems. The other major contributors were processes, procedures, and visual aids, which accounted for approximately 35 percent of the major problems.

Figure A-4 shows the areas in which major problems were detected. It is somewhat disconcerting to see the large number of problems, 23 percent, that were not detected until integration test. This would indicate that

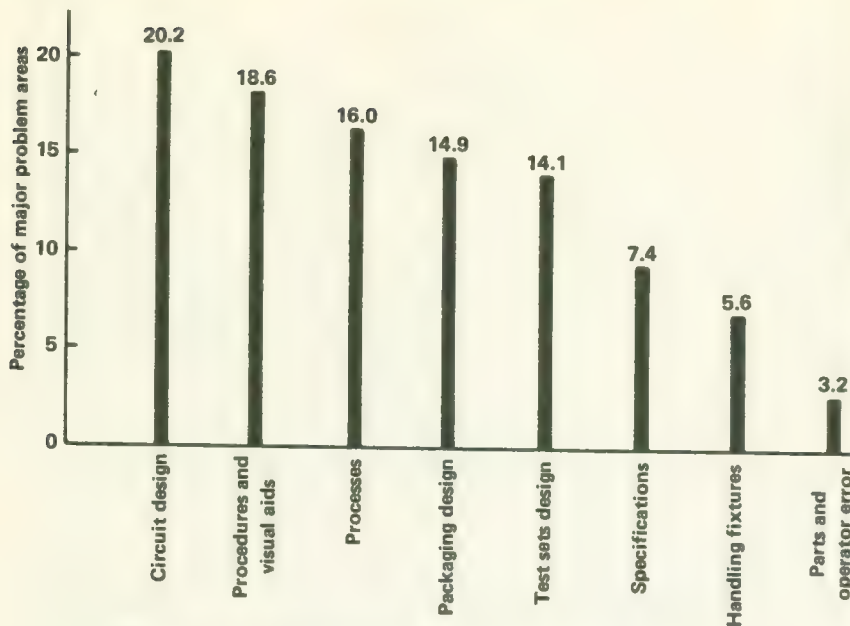


FIGURE A-3.—Causes of major problem areas (prelaunch).

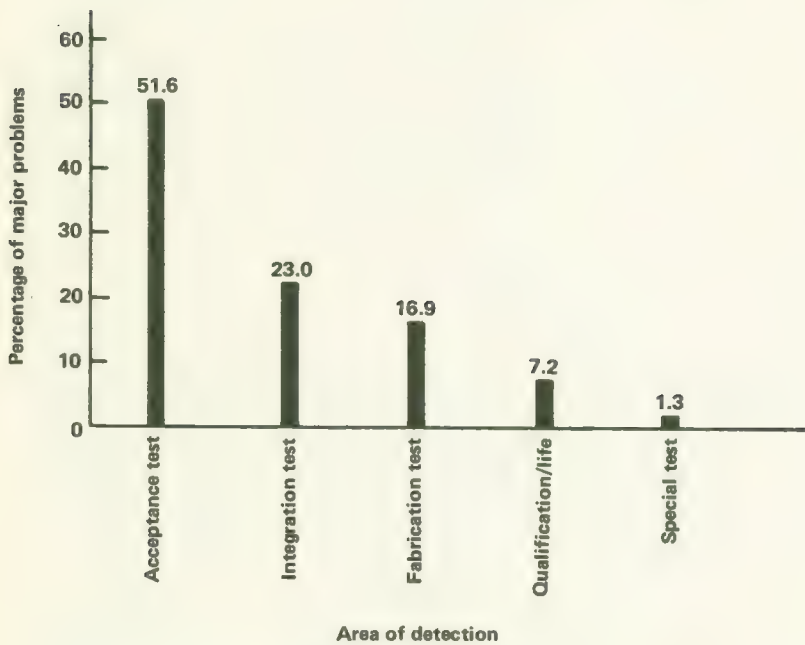


FIGURE A-4.—Percentage of major problems by area detected.

TABLE A-3.—*Post-launch Anomalies*

|  |
|--|
| Six anomalies noted in eleven spacecraft years of operation                      |
| One anomaly degraded mission   |
| Cause—New innovation device (PSCR Sun sensor)                                    |
| Threshold sensitive to ultraviolet radiation                                     |
| Experiment viewing direction lost on Pioneer 7 (two experiments of little value) |
| Fix (ultraviolet filter) included on Pioneer 9                                   |
| Five anomalies produced no mission degradation because                           |
| Redundancy available by ground command (1)                                       |
| Self-heal (2)  |
| Function not required following orientation (2)                                  |

probably the test sets did not satisfactorily simulate interface conditions. Another major fault of the reliability program can therefore be assigned to not including test equipment in the design review program. The final chart, table A-3 in the Pioneer A-E discussion, shows that there were six anomalies noted in 11 spacecraft years of operation. Only one of these failures caused degradation to the mission, and this was because of the use of an unproven device, something that a good reliability engineer should avoid if at all possible. The reason for using this device, a photo silicon control rectifier, as a Sun sensor was to save approximately three-quarters of a lb in weight. The viewing direction during spin has been lost on Pioneer 7 which makes two of the experiments of little value. A study subsequently revealed the threshold of this device to be sensitive to ultraviolet radiation and since a fix could not be implemented until Pioneer 9 it is anticipated that Pioneers 6 and 8 will fail in a like manner. Five other anomalies have been noted, none of which have degraded the mission. It is entirely possible that the self-heal anomalies will reoccur again as failures.



# Index

- Aerojet-General Corp., 213, 215  
Allegheny Ballistics Laboratory, 213, 215  
Ames magnetometer, 136, 149  
  design, 145–148  
  telemetry, 76–78, 86  
Ames plasma probe, 136  
  design, 152–160  
  telemetry, 76–78, 86, 157, 158  
Ames Research Center, 2, 8, 9, 11, 27, 55,  
  95, 139, 141, 146, 155, 165, 181, 192,  
  241, 245, 247, 254, 255, 256, 259, 260,  
  266, 273, 277, 278, 280, 282, 283, 293  
  (*See also* Ames magnetometer, Ames  
  plasma probe)  
Anderson, J., 258  
Antennas, spacecraft, 12–13, 55, 57, 66–  
  69, 132, 133, 194  
Antennas, tracking. *See* Deep Space  
  Network.  
Astrodata, Inc., 277  
  
Booms, spacecraft, 131–132, 133, 134,  
  191–192, 202  
  
Cape Canaveral (Cape Kennedy), 140,  
  165, 191, 193, 205, 229, 238, 240, 263,  
  265  
Castor motors, 213, 215, 217  
Chicago cosmic-ray experiment, 136  
  design, 160–165  
  telemetry, 76–78, 86, 162  
Command Distribution Unit (CDU). *See*  
  Command subsystem.  
Command subsystem, Command Distribu-  
  tion Unit (CDU), 93, 95–100, 103,  
  112, 135, 205  
command format, 93–95  
command lists, 96–97  
  design, 91–100  
  functions, 7  
Communication subsystem, antennas, 12–  
  13, 55, 57, 66–68  
  bit rates, 40, 57  
  design, 55–68, 135  
  distance capabilities, 71  
  functions, 7  
  interfaces, 58  
  phase-lock operation, 59–60, 61, 63  
  power budget, 62, 64  
  receiver, 61–65  
  reliability, 14–46  
  transmitter, 65–66  
Computer Sciences Corp., 277  
Constraints, system, 3, 39  
Convolutional Coder Unit (CCU). *See*  
  Data handling subsystem.  
Cosmic dust detector. *See* Goddard cosmic  
  dust experiment.  
Cosmic ray experiments. *See* Chicago  
  cosmic ray experiment, GRCSW  
  cosmic ray experiment, Minnesota  
  cosmic ray experiment.  
  
Data handling subsystem, Convolutional  
  Coder Unit (CCU), 70, 90–91, 92,  
  136, 283  
Data Storage Unit (DSU), 70, 86, 87,  
  88–90, 205  
  design, 68–91, 135  
Digital Telemetry Unit (DTU), 70, 88,  
  89, 205  
feasibility study of, 16–17  
formats, 72, 73–85, 86, 87  
functions, 7, 68, 70  
modes of operation, 85–87  
modulation techniques, 60, 93

- reliability, 46, 73  
 word structure, 74, 91  
**Data processing**, 259, 277–283  
**Data Storage Unit (DSU)**. *See* Data handling subsystem.  
**Deep Space Instrumentation Facility (DSIF)**. *See* Deep Space Network.  
**Deep Space Network (DSN)**, 3, 9, 11, 15, 40, 41, 55, 57, 58, 61, 63, 64, 65, 67, 70, 85, 87, 90, 93, 95, 115, 116, 176, 191, 194, 277, 278  
 antennas, 245  
 design, 237–273  
**DSIF**, 241–245  
 station configurations for Pioneer, 264, 274–275  
 station list, 240  
 tracking requirements, 21, 253–263  
 tracking functions, 59–60, 239, 242–243  
*(See also Space Flight Operations Facility)*  
**Delta launch vehicle**, 3, 9, 11, 14, 40, 41, 52, 58, 103, 127, 191, 239, 240, 241  
 configurations, 215, 218  
 description, 211–236  
 interfaces, 217–225  
 launch requirements, 21  
 launch sequence, 231–235  
 Pioneer-9 launch description, 27–29  
 trajectory design, 225–229, 230, 232  
 weight breakdown, 235–236  
**Digital Telemetry Unit (DTU)**. *See* Data Handling subsystem.  
**DSIF**. *See* Deep Space Network.  
**DSN**. *See* Deep Space Network.  
  
**Eastern Test Range**, 240, 258, 263, 264  
**EGSE**. *See* Electrical Ground Support Equipment.  
**Electrical Ground Support Equipment (EGSE)**, 191, 194, 205–206, 208, 209  
**Electronic Memories, Inc.**, 90, 148  
**Electric-power subsystem**, battery, 104, 108–109  
 design, 100–111, 135  
 functions, 7  
 interfaces, 103–104  
 power requirements, 106  
 reliability, 47  
 solar array, 49, 103–108, 109, 202, 204  
 test matrix, 194  
  
**Environmental Science Service Administration (ESSA)**, 2, 139, 277  
**ESSA**. *See* Environmental Science Service Administration.  
**Experiments**. *See* specific experiments.  
  
**Feasibility study**, 8–11, 14, 15–17, 18, 39, 44, 47, 48, 49, 90, 103, 129  
  
**Goddard cosmic dust experiment, design**, 135, 181–188  
 selection, 141–142  
 telemetry, 76–78, 86, 186, 187, 188  
**Goddard magnetometer, design**, 136, 142–145, 146  
 telemetry, 76–78, 86, 143  
**Goddard Space Flight Center (GSFC)**, 74, 217, 265  
*(See also Delta launch vehicle, Goddard cosmic dust experiment, Goddard magnetometer)*  
**GOE**. *See* Ground Operational Equipment.  
**GRCSW cosmic ray experiment, design**, 136, 165–170  
 telemetry, 76–78, 86, 168, 170  
**Ground Operational Equipment (GOE)**, 191, 253, 260, 266–271, 279  
  
**Honeywell, Inc.**, 146, 148  
**Hughes Aircraft**, 66  
  
**IGY**. *See* International Geophysical Year.  
**Instruments, design**, 137–190  
 interfaces, 139–140  
 list of, 143  
 selection of, 140–142  
 specifications for, 139–140  
*(See also Goddard magnetometer, etc.)*  
**Interfaces**, spacecraft, 6, 8, 55, 58, 103–104, 139–140, 217–225  
**International Geophysical Year (IGY)**, 1  
**International Quiet Sun Year (IQSY)**, 1  
**IQSY**. *See* International Quiet Sun Year.  
  
**Jet Propulsion Laboratory (JPL)**, 3, 27, 57, 73, 176, 202, 237, 238, 241, 245, 251, 253, 254, 256, 263, 265, 273, 277, 278, 283 *(See also Deep Space Network, JPL celestial mechanics experiment)*  
**JPL**. *See* Jet Propulsion Laboratory.  
**JPL celestial mechanics experiment**, 188

- Launch requirements, 14, 26-27  
Launch vehicle. *See* Delta launch vehicle.  
Launch windows, 26-29  
Lifetime, spacecraft, 14, 40  
(*See also* Reliability)
- Magnetic cleanliness, 7, 39, 40, 42, 44, 47-49, 144-145  
tests for, 196, 197-198, 200, 204
- Magnetometers, 48, 49, 129  
(*See also* Ames magnetometer, Goddard magnetometer)
- Manned Space Flight Network, 237, 239, 240, 253, 257, 263, 264
- McDonnell-Douglas Astronautics Co., 27, 211, 213, 215
- Minnesota cosmic ray detector, design, 136, 170-171, 172, 173  
telemetry, 76-78, 86
- Mission objectives, 1-3, 19-20
- MIT Faraday-cup plasma probe, design, 101, 136, 148-153  
telemetry, 76-78, 86, 100, 109, 150, 152
- NASA Communications Network (NASCOM), 93, 240, 245-251, 263
- NASA Headquarters, 8, 181, 241, 253
- NASCOM. *See* NASA Communications Network.
- Naval Propellant Plant, 215
- Naval Research Laboratory (NRL), 237, 238
- North American Rockwell, 213
- Orbital characteristics, 26, 29, 34  
table of, 36
- Orientation, partial, 68  
Type I maneuver, 21, 37, 46, 113, 114, 115, 116, 117, 118, 119, 121, 254  
Type II maneuver, 37, 113, 114, 115, 116, 118, 119, 254, 267
- Orientation subsystem, design, 111-121, 135  
functions, 7, 111  
pneumatics assembly, 117, 118  
reliability, 46  
requirements, 35, 37, 111, 113  
Sun sensors, 114-117  
wobble damper, 119-121
- Phase-lock loop operation, 59-60, 61, 63, 237, 238
- Philco-Ford, 146, 148
- Pioneer mission operations center, 245, 247, 259, 260, 271
- Pioneer A. *See* Pioneer 6.
- Pioneer B. *See* Pioneer 7.
- Pioneer C. *See* Pioneer 8.
- Pioneer D. *See* Pioneer 9.
- Pioneer E, 23, 52, 142  
launch vehicle, 217  
scientific objectives, 20, 255, 256, 265  
tracking requirements, 253
- Pioneers 1-4, 211, 237, 241
- Pioneer 5, 12, 211, 237, 241
- Pioneer 6, 52, 101, 130, 299  
gas leak, 177  
launch trajectory, 230  
launch vehicle, 217  
scientific objectives, 19, 256  
test history, 206-207
- Pioneer 7, 130, 138, 299  
gas leak, 117  
launch, 22, 212  
launch vehicle, 217  
scientific objectives, 19-20, 255, 256
- Pioneer 8, 138, 266, 271, 272, 299  
launch vehicle, 217  
scientific objectives, 20, 255, 256
- Pioneer 9, 102, 283, 299  
launch sequence, 231-235  
launch vehicle, 217  
scientific objectives, 20, 256  
trajectory analysis, 25, 27-34
- Plasma probes. *See* Ames plasma probe, MIT Faraday-cup plasma probe.
- Power supply. *See* Electric-power subsystem.
- Quality assurance, 44, 293-299
- Radio Corporation of America (RCA), 106
- Radio propagation experiment. *See* Stanford radio propagation experiment.
- Rechtin, E., 237
- Reliability, 39, 40, 41-47, 128, 134, 293-299
- Rocketdyne Division of North American Rockwell, 213-215
- Schonstedt Instrument Co., 142
- Scientific objectives, 1, 137
- SFOF. *See* Space Flight Operations Facility.

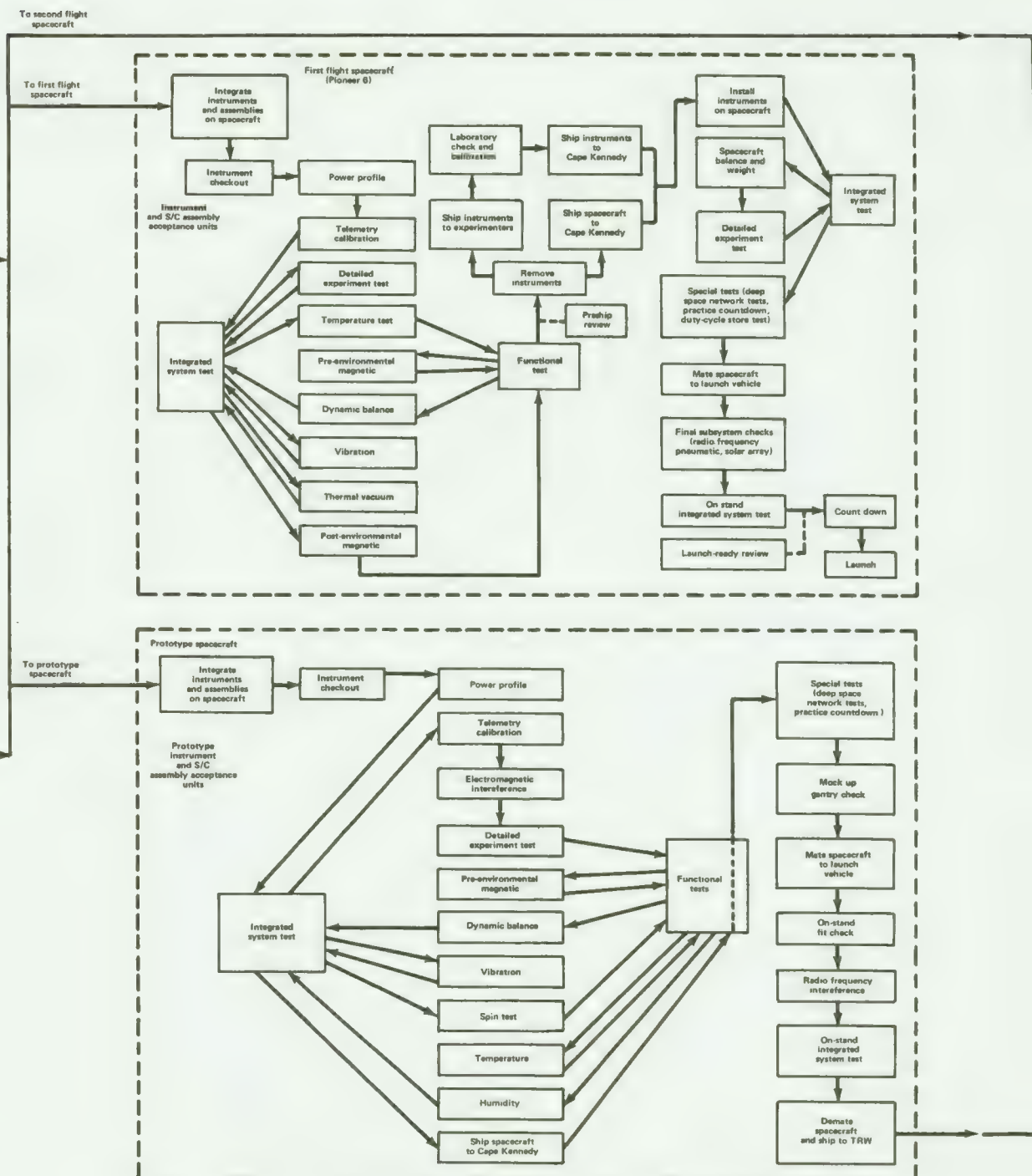
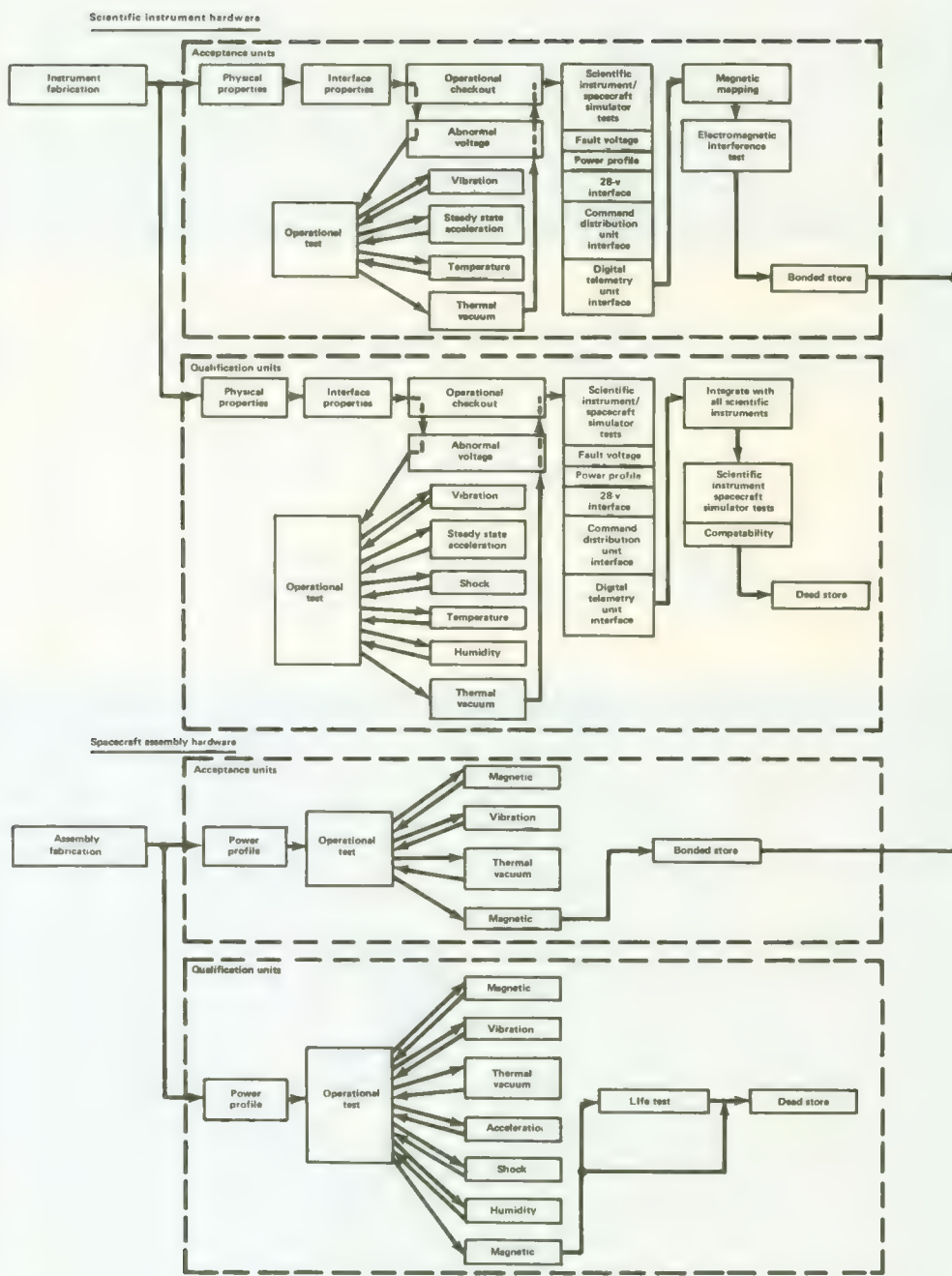
- Solar array. *See* Electric power subsystem.
- Spacecraft design philosophy, 3, 39-44
- Spacecraft evolution, 48-53
- Space disturbance forecasts, 2, 34, 139, 277
- Space Flight Operations Facility (SFOF), 3, 176, 240, 241, 242, 256, 258, 263, 265, 266, 267, 273, 277
- Space Science Steering Committee, 17, 141
- Space Technology Laboratories (STL). *See* TRW Systems.
- Stabilization, 12, 41, 129, 132  
*(See also* Orientation subsystem)
- Stanford radio propagation experiment, 13, 80, 87, 88, 132, 133, 255, 277
- design, 136, 171-176, 177, 179
- telemetry, 76-78, 86
- Structure subsystem, booms, 131, 132, 133, 134
- design, 135, 128-136
- dimensions, 129, 132
- functions, 7
- reliability, 134
- STL. *See* TRW Systems.
- Sun sensor, degradation, 49, 114
- design, 114-117, 118, 119, 121, 127
- functions, 143
- System and subsystem definition, 3-8, 9, 55, 56
- Telemetry. *See* Communication subsystem.
- Test program, 44, 134, 191-210
- facilities, 196-202
- Test and Training Satellite (TETR), 21, 41, 53, 227
- Texas Instruments, 106
- Thermal control subsystem, design, 15, 121-128, 135
- functions, 7
- requirements, 121-122
- Thiokol Chemical Corp., 213, 215
- Tracking. *See* Deep Space Network.
- Trajectory, constraints, 20-21, 225-229, 230, 232
- design, 20
- launch phase, 21-22, 225-229, 230, 232
- Pioneer 9, 27-34
- TRW Systems, 8, 11, 12, 42, 45, 50, 51, 63, 65, 66, 85, 90, 100, 103, 107, 121, 122, 123, 125, 126, 134, 191, 192, 196, 198, 199, 277, 278, 282, 283, 293, 296
- TRW Systems electric field detector, design, 136, 176-181
- telemetry, 76-78, 86, 176, 179
- Type I and Type II maneuvers. *See* Orientation.
- Unified S-Band, 238
- United Technology Center, 213, 215
- U.S. Air Force, 239, 263, 264, 265
- U.S. Army, 238
- Watkins Johnson, 66
- Weight, spacecraft, 23, 39, 40, 41
- detailed breakdown, 134-136
- evolution, 48, 49
- Wobble damper, 12

SP-280

ARY

RY

ON



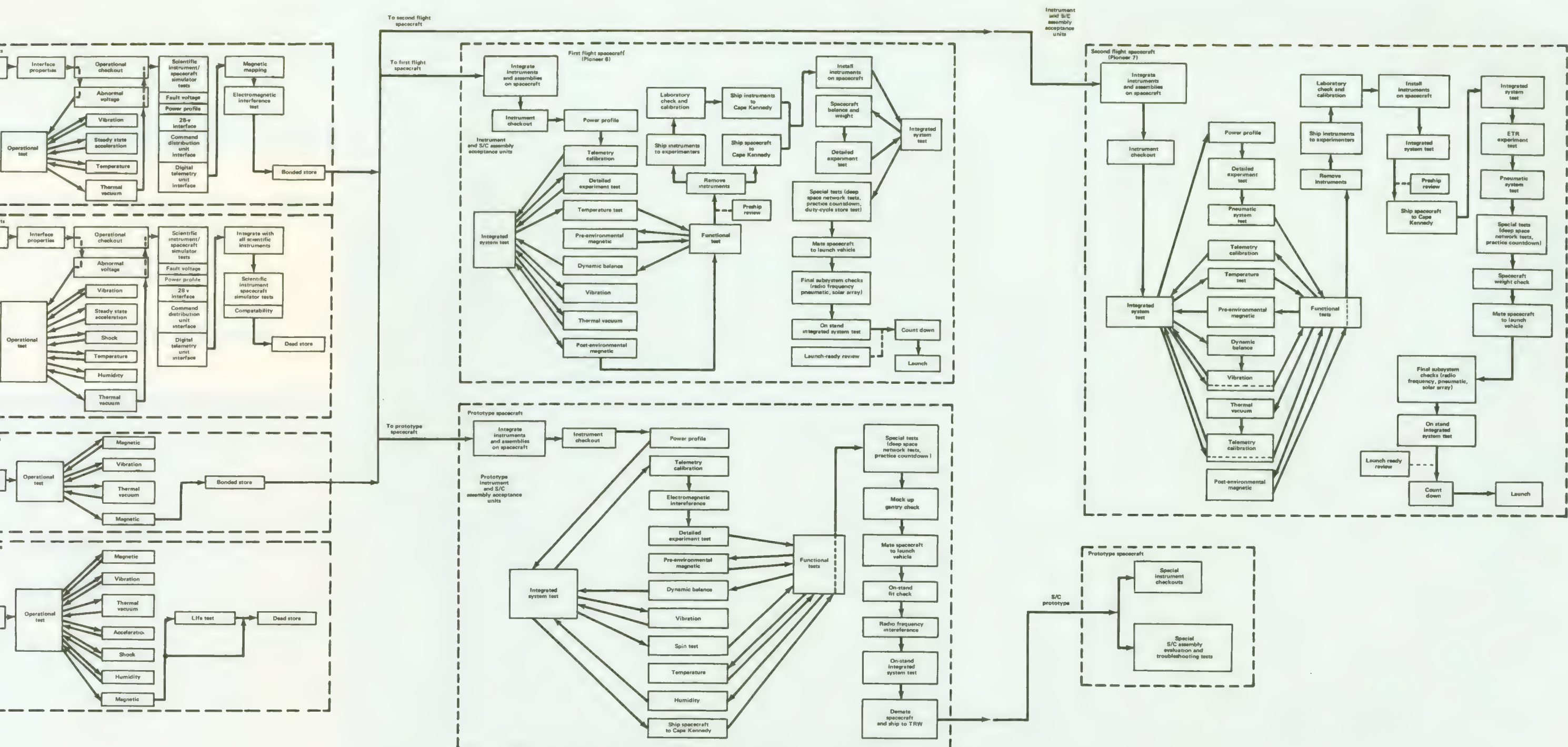


FIGURE 6-1.—Pioneers 6 and 7 test program.

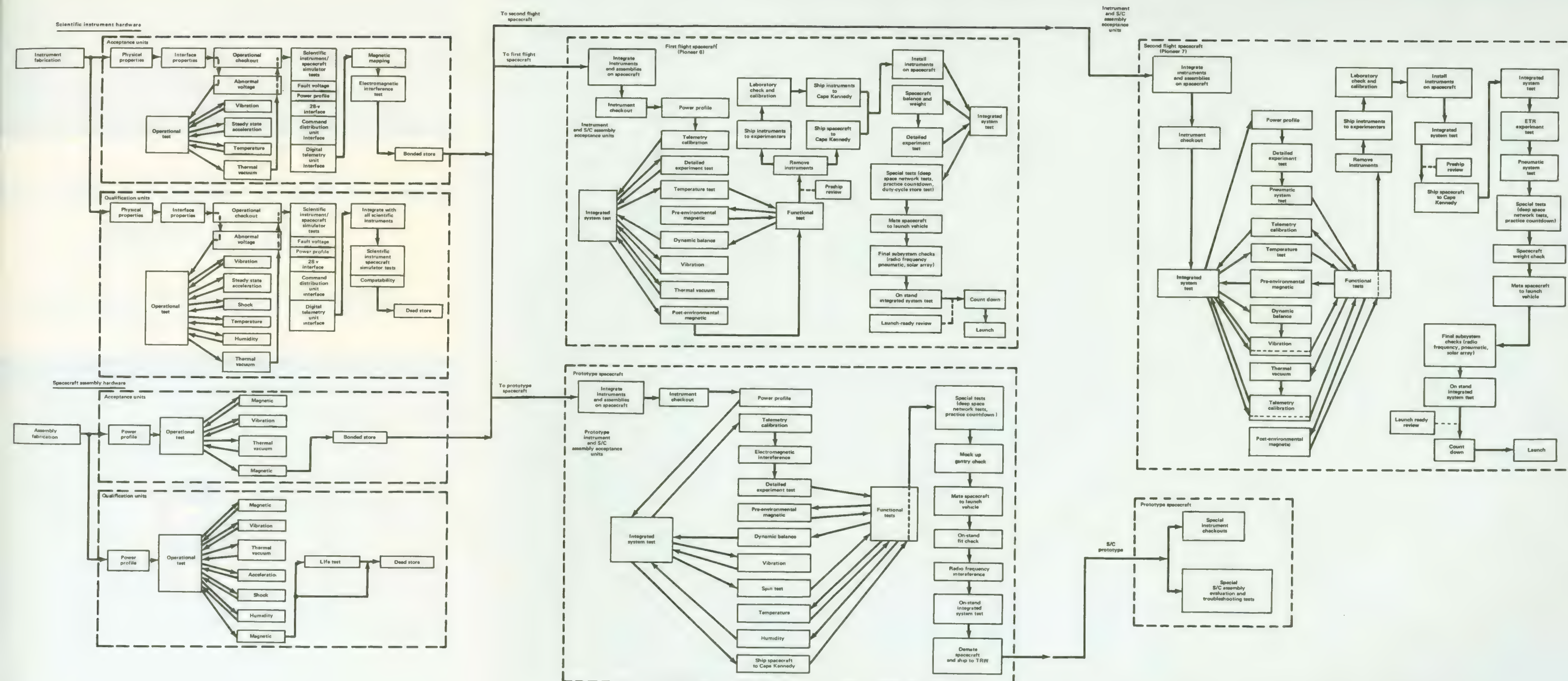


FIGURE 6-1.—Pioneers 6 and 7 test program.

TECHNOLOGY  
FEDERAL

NASA SP-280

SEATTLE PUBLIC LIBRARY

MAY 8 1973

# THE INTERPLANETARY PIONEERS

## VOLUME III: OPERATIONS



NATIONAL AERONAUTICS AND SPACE ADMINISTRATION



# THE INTERPLANETARY PIONEERS

## VOLUME III: OPERATIONS

by

William R. Corliss



Scientific and Technical Information Office  
NATIONAL AERONAUTICS AND SPACE ADMINISTRATION  
Washington, D.C.

1972

---

For sale by the Superintendent of Documents,  
U.S. Government Printing Office, Washington, D.C. 20402  
Price \$1.75 domestic postpaid or \$1.50 GPO Bookstore, Stock Number 3300-0451  
*Library of Congress Catalog Card Number 74-176234*

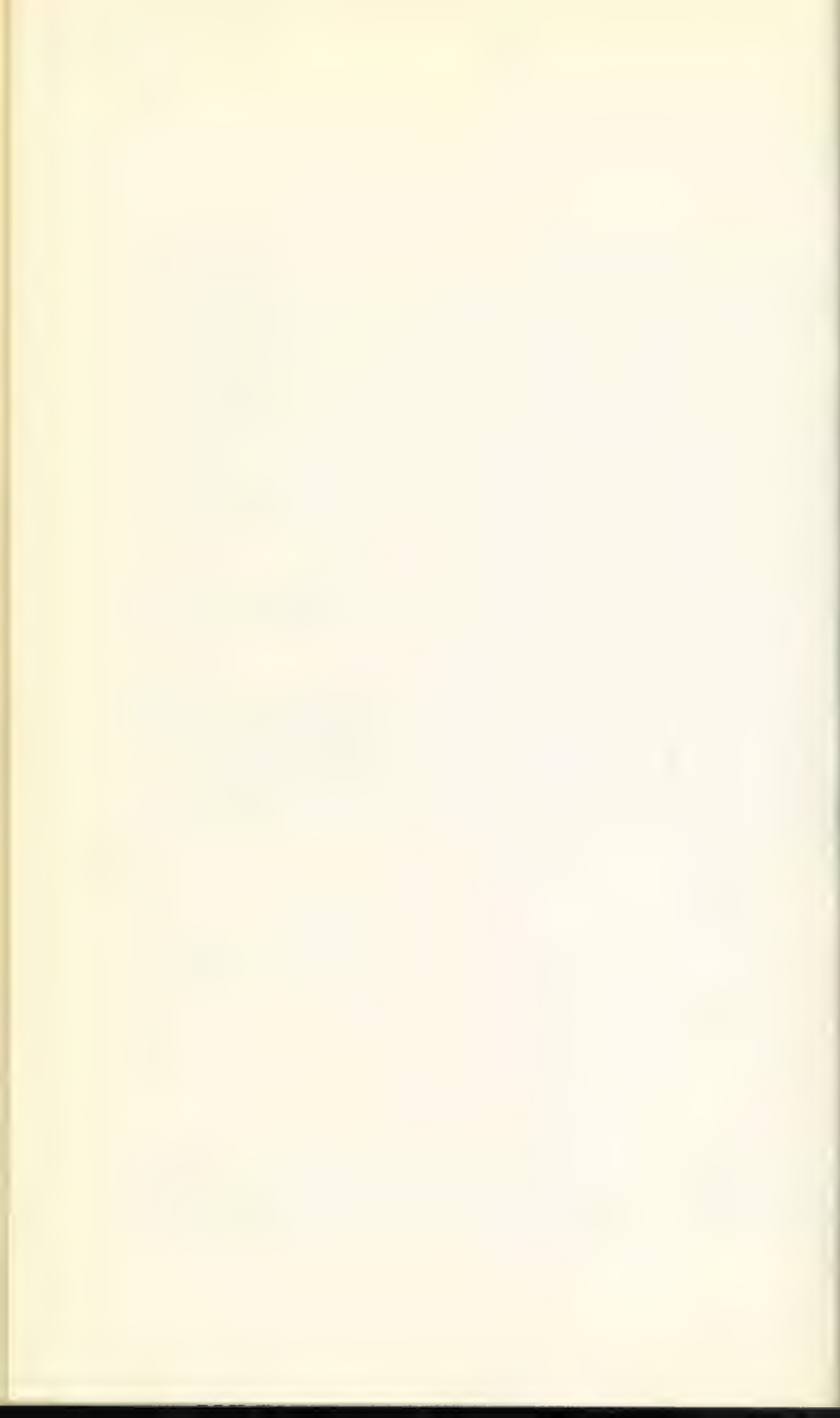
# Foreword

SOME EXPLORATORY ENTERPRISES start with fanfare and end with a quiet burial; some start with hardly a notice, yet end up significantly advancing mankind's knowledge. The Interplanetary Pioneers more closely fit the latter description. When the National Aeronautics and Space Administration started the program a decade ago it received little public attention. Yet the four spacecraft, designated Pioneers 6, 7, 8, and 9, have faithfully lived up to their name as defined by Webster, "to discover or explore in advance of others." These pioneering spacecraft were the first to systematically orbit the Sun at widely separated points in space, collecting information on conditions far from the Earth's disturbing influence. From them we have learned much about space, the solar wind, and the fluctuating bursts of cosmic radiation of both solar and galactic origin.

These Pioneers have proven to be superbly reliable scientific explorers, sending back information far in excess of their design lifetimes over a period that covers much of the solar cycle.

This publication attempts to assemble a full accounting of this remarkable program. Written by William R. Corliss, under contract with NASA, it is organized as Volume I: Summary (NASA SP-278); Volume II: System Design and Development (NASA SP-279); and Volume III: Operations and Scientific Results (NASA SP-280). In a sense it is necessarily incomplete, for until the last of these remote and faithful sentinels falls silent, the final word is not at hand.

HANS MARK  
*Director*  
*Ames Research Center*  
*National Aeronautics and*  
*Space Administration*



# Contents

|   | <i>Page</i> |
|---|-------------|
| <b>Chapter 1. PIONEER OPERATIONS</b>  | 1           |
| <b>Chapter 2. PRELAUNCH ACTIVITIES</b>                                      | 3           |
| Facilities Involved in Pioneer Prelaunch Activities                         | 3           |
| Organizations and Their Responsibilities                                    | 4           |
| Significant Events in the Pioneer Prelaunch Phase                           | 9           |
| Prelaunch Schedules—Planned and Actual                                      | 13          |
| The Actual Prelaunch Phases and How They Compared                           | 17          |
| <b>Chapter 3. LAUNCH TO DSS ACQUISITION</b>                                 | 25          |
| Performance of the Delta Launch Vehicle                                     | 26          |
| Tracking and Data Acquisition   | 36          |
| Spacecraft Performance  | 44          |
| <b>Chapter 4. FROM DSS ACQUISITION TO THE BEGINNING OF THE CRUISE PHASE</b> | 45          |
| Sequence of Events  | 45          |
| Pioneer Operations—Acquisition to Cruise Phase                              | 49          |
| <b>CHAPTER 5. SPACECRAFT PERFORMANCE DURING THE CRUISE PHASE</b>            | 55          |
| Pioneer-6 Performance   | 55          |
| Pioneer-7 Performance   | 68          |
| Pioneer-8 Performance   | 73          |
| Pioneer-9 Performance   | 74          |
| References  | 75          |
| <b>Chapter 6. PIONEER SCIENTIFIC RESULTS</b>                                | 77          |
| The Goddard Magnetic Field Experiment (Pioneers 6, 7, and 8)                | 78          |
| The MIT Plasma Probe (Pioneers 6 and 7)                                     | 85          |
| The Ames Plasma Probe (All Pioneers)  | 90          |
| The Chicago Cosmic-Ray Experiment (Pioneers 6 and 7)                        | 97          |
| The GRCSW Cosmic-Ray Experiment (All Pioneers)                              | 102         |
| The Minnesota Cosmic-Ray Experiment (Pioneers 8 and 9)                      | 111         |
| The Stanford Radio Propagation Experiment (All Pioneers)                    | 115         |
| Radio Propagation Experiments Using the Spacecraft Carrier (All Pioneers)   | 124         |

|   | <i>Page</i> |
|---|-------------|
| TRW Systems Electric Field Experiment (Pioneers 8 and 9) . . . . .  | 127         |
| The Goddard Cosmic Dust Measurements (Pioneers 8 and 9) . . . . .   | 135         |
| The Pioneer Celestial Mechanics Experiment (All Pioneers) . . . . . | 138         |
| Solar Weather Monitoring . . . . .                                  | 141         |
| References . . . . .  | 142         |
| <b>BIBLIOGRAPHY</b> . . . . .                                       | <b>147</b>  |
| <b>INDEX</b> . . . . .  | <b>151</b>  |

## CHAPTER 1

# Pioneer Operations

**T**HIS VOLUME DESCRIBES the long chain of events that began with the arrival, checkout, and launch of the Pioneer spacecraft at Cape Kennedy and culminated in the publication of results in the scientific journals. There were five major links in the chain, each beginning and ending with a critical event:

Phase 1. *Prelaunch Operations*—Began with the arrival of the spacecraft at the Cape and ended with the launch

Phase 2. *Launch to DSS Acquisition*—Spacecraft usually acquired first by Deep Space Station (DSS) at Johannesburg

Phase 3. *Near-Earth Operations*—Commenced with DSS acquisition and ended with completion of all orientation maneuvers

Phase 4. *Nominal and Extended Cruise*—From completion of orientation maneuvers to end of useful spacecraft life

Phase 5. *Presentation of Scientific and Engineering Results*—Began as soon as the scientific instruments were turned on and ended only when the data became superseded

Scientific data may remain viable for decades, with information of value still being extracted after the spacecraft itself has stopped transmitting.

The operational histories of the five Pioneer spacecraft could be related separately, although this would result in five highly repetitive chapters, and the comparison of spacecraft performance and cooperative spacecraft activities would be difficult. The descriptions of spacecraft operations, therefore, are organized with a chapter assigned to each of the five phases established above.

A Pioneer launch required the coordination of thousands of people located not only at the launch site but also at the tracking stations around the world and at the communication focal points at the Jet Propulsion Laboratory's Space Flight Operations Facility (SFOF) and the Ames Research Center. Some measure of organization had to be superimposed on these people and the operations they performed with the Pioneer spacecraft, the Delta launch vehicle, and the Deep Space Network. Ames Research Center, as the overall program manager, established principles and general specifications for all operational phases. The two most significant of the Ames specifications were:

- (1) PC-046—Pioneer Flight Operations (for Block I)
- (2) PC-146—Pioneer Space Flight Operations (for Block II)

These specifications spelled out—in some 6 in. of documentation for each block of Pioneers—the operational requirements for each facility and the many participating organizations. Also defined were critical technical terms and the interfaces between the organizations involved. Mutual understanding of what was to be done, and by whom, were the goals of these documents. In addition, they were supplemented by separate Ames operations specifications for each mission as well as by more detailed definitions of critical organizational interfaces.

In themselves, the Ames specifications were too broad to provide the second-by-second directions required by the launch teams at the Cape from Ames, Goddard, JPL, the Air Force, McDonnell-Douglas, TRW Systems, and other participating organizations. After a spacecraft was launched successfully, day-by-day instructions were needed by DSS crews working the spacecraft. At the working level then, a host of countdown documents, operations directives to downrange stations, and other schedules translated the broad, general Ames specifications into working documents.

Documentation seems a rather dull aspect of such a fascinating topic as the scientific exploration of deep space. Spacecraft, however, are launched and operated by people, even though machines (particularly computers) now make more and more of the routine decisions. People work in concert only when they all understand an activity in the same terms and work from a detailed schedule. Without question a major accomplishment of the space program has been its blending of people and equipment into a smoothly functioning global apparatus. The Pioneer program has been an effective part of this larger machine.

## Prelaunch Activities

THE SUCCESSFUL COMPLETION of spacecraft preship review signaled the beginning of prelaunch activities. The spacecraft was carefully packed and shipped to Cape Kennedy by air. Its arrival at the Cape initiated a 6- to 10-week series of tests and checkout procedures to assure the readiness of the spacecraft and its compatibility with the Delta launch vehicle, the Deep Space Network (DSN), and equipment along the Air Force's Eastern Test Range. If all went well, the pieces did fit together, and the spacecraft was launched successfully. Of course, the real picture was more complicated.

Basically, one must view Cape Kennedy as a production line where spacecraft and launch vehicles meet, are tested, and fired. Such a complex enterprise requires rigorous scheduling and definition of responsibilities, leading, in this case, to the launches of the Pioneer spacecraft within their narrow launch windows.

### FACILITIES INVOLVED IN PIONEER PRELAUNCH ACTIVITIES

More people and facilities participated during the Pioneer prelaunch and launch activities than at any other time in the mission. Although Cape Kennedy and the Eastern Test Range's downrange stations were the focal points during this phase of operations, the DSN and SFOF were all involved in various tests and during various checkout procedures. As the moment of launch approached, more and more of the NASA and Air Force general-purpose facilities "came on the line" for the launch. Radars, optical instrumentation, and telemetry antennas at the Cape and downrange were all, in effect, waiting for the Delta and its Pioneer payload during the minutes before launch. Likewise, critical antennas at some of the DSN's Deep Space Stations broke off from tracking Mariners and Pioneers already out in space and swung toward the points where the new Pioneer was expected to come over the horizon.

The major facilities concerned with a Pioneer launch are described in some detail in Vol. II. Here, only the major functions are reiterated.

*Cape Kennedy.*—The Cape provided facilities for spacecraft tests, checkout, and integration. Facilities were also provided for mating of spacecraft with launch vehicle and for launch vehicle assembly and launch. The Pioneer Electrical Ground Support Equipment (EGSE)

provided an interface between the spacecraft and the launch pad environment. Figure 2-1 shows Launch Complex 17, from which all five Pioneers were launched. The AE, AM, AO, and M buildings are seen in the aerial view presented in figure 2-2. Figure 2-3 was taken from inside the Mission Director's Center.

*USAF Eastern Test Range (ETR)*—This facility provided tracking and data acquisition services from launch through nominal DSS acquisition at Johannesburg.

*The Deep Space Network (DSN)*—The DSN supplied tracking, data acquisition, and transmission of command signals to the spacecraft. Included in the DSN is the Deep Space Instrumentation Facility (DSIF) which encompasses all of the DSSs, the SFOF, and the Ground Communications Facility (GCF). For further information see Ch. 8, Vol. II. The Pioneer Ground Operational Equipment (GOE) at selected DSS stations provided an interface between the spacecraft and the generalized DSS equipment.

### ORGANIZATIONS AND THEIR RESPONSIBILITIES

Hundreds of people from government and industry applied their talents and training during the testing and checkouts that led to a Pioneer launch. They operated the facilities listed above, or they were part of the launch crews associated with the Delta and the spacecraft.



FIGURE 2-1.—Aerial view of Launch Complex 17 at Cape Kennedy.



FIGURE 2-2.—Aerial view of part of the Cape Kennedy complex. The buildings in the foreground are, from left to right, M, AO, AM, and AE.

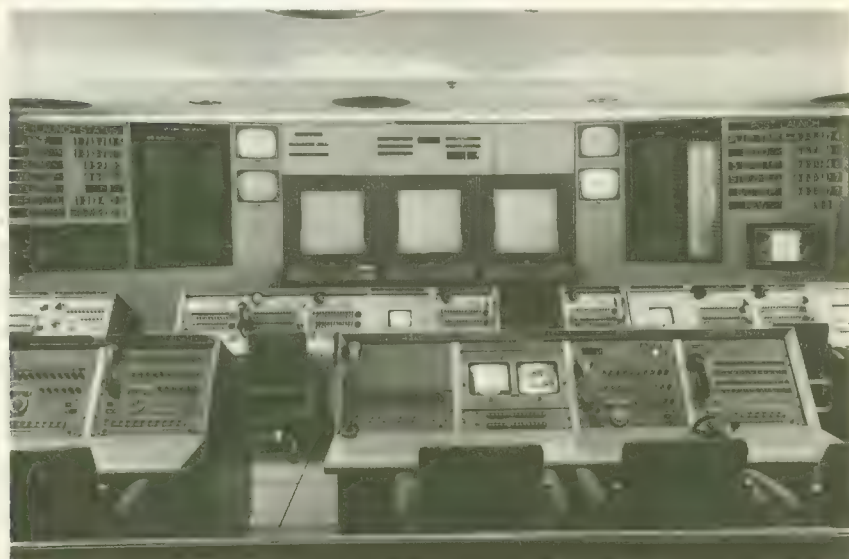


FIGURE 2-3.—The Mission Director's Center at Launch Complex 17.

They also had to be given directions and schedules. Ames Research Center, as the arm of NASA managing the Pioneer Program, provided both. The Pioneer Flight Operations Specifications issued by Ames<sup>1</sup> established the prelaunch-phase responsibilities as follows.

#### **Ames Research Center Prelaunch Responsibilities**

1. Plan and document the Pioneer space flight operations.
2. Prepare and document a Pioneer space flight operations test plan.
3. Plan and schedule acceptance, integration, and operational readiness tests.
4. Determine requirements and initiate tasks and procurements required to provide the necessary aids and materials used during tests, such as tapes containing simulated spacecraft telemetry and tracking data.
5. Participate in equipment preparation, acceptance, integration, and operational readiness tests.
6. Direct conduct of, monitor, and review acceptance, integration, and operational readiness tests.
7. Prepare and update procedures for mission-dependent activities to be performed during the flight operations.
8. Plan for and initiate tasks and procurements required to provide the necessary GOE, the communications net between the stations supporting the mission, the mission-dependent displays, and the off-line data-processing system.
9. Develop procedures for flight operations associated with mission-dependent equipment for handling on-line and off-line data, for the analysis of spacecraft, experiment, and GOE performance, and for disseminating information to the spacecraft contractor and experimenters.

#### **Jet Propulsion Laboratory Prelaunch Responsibilities**

1. Manage and coordinate activities of DSN.
2. Provide personnel to operate mission-independent equipment and Pioneer GOE (except during Type-II orientation) during acceptance, integration, and operational readiness tests, and during flight operations at DSIF.
3. Provide personnel to operate mission-independent equipment during acceptance, integration, and operational readiness tests at SFOF.

---

<sup>1</sup>The basic documents are Pioneer Specifications PC-046, for Block-I Pioneers, and PC-146, for Block-II Pioneers. See Bibliography in Vol. II. Many of these activities, particularly those involving planning, occurred prior to the shipment of the spacecraft to the Cape. The actual equipment preparations and tests prior to launch are covered in detail in the next section.

4. Coordinate communications at SFOF to and from the Pioneer Mission Operations Area and to and from Ames, TRW Systems,<sup>2</sup> and Stanford.
5. Provide and maintain mission-independent equipment at DSIF and SFOF required to support the Pioneer mission.
6. Maintain and repair Pioneer GOE at DSIF sites.
7. Prepare space flight operations plan for use by DSN personnel.
8. Prepare Tracking Instruction Manual.
9. Prepare data as required pertinent to DSN operations for use in the preparation of procedures and training aids to be used during acceptance, integration, and operational readiness tests.
10. Provide data as required pertinent to DSN operations for inclusion in Ames operational documents.
11. Prepare and maintain the Mission Control Center in SFOF to support the Pioneer Project during tests simulating operations from launch to the completion of Type-II orientation maneuvers.
12. Participate in the review of acceptance, integration, and operational readiness tests.

#### TRW Systems Prelaunch Responsibilities

1. Provide data for and review plans and procedures prepared by Ames for equipment preparation, acceptance, integration, and operational readiness tests and flight operations.
2. Provide data for and review specifications prepared by Ames for test aids, such as magnetic tapes and teletype paper tapes containing simulated spacecraft telemetry data.
3. Provide test aids, such as magnetic tapes and teletype paper tapes containing simulated spacecraft telemetry data.
4. Provide two field engineers at DSS-12 and SFOF to aid Ames in training DSN personnel in operational procedures. Participate in reviewing the telemetry data and command system acceptance tests.
5. Provide as required systems and subsystem engineers at SFOF, knowledgeable in the preparation and operations of the spacecraft and GOE, to participate in acceptance, integration, and operational readiness tests.
6. Provide four field engineers at DSS-12, knowledgeable in the operations of the spacecraft telecommunications and orientation subsystems, the GOE, and the flight dynamics of the spacecraft, to participate in all tests in which the Type-II orientation maneuver is exercised.

---

<sup>2</sup> Spacecraft contractor.

### **Experimenters' Prelaunch Responsibilities**

1. Provide data for plans and procedures prepared by Ames for experiment preparation, acceptance, integration, operational readiness tests, and flight operations.
2. Provide requirements for use by Ames in the preparation of weekly and daily operations plans and in the conduct of the mission as it pertains to the scientific instruments.
3. Stanford must provide a field crew as required to operate the transmitter at Stanford University during equipment preparation, acceptance, integration, operational readiness tests and during flight operations of the Pioneer spacecraft.

### **NASA Headquarters Prelaunch Responsibilities**

1. Review operations readiness of the Pioneer Project prior to launch.
2. Advise the Public Information Office on procedures to be followed for Pioneer.
3. Participate in launch operations at ETR.
4. Participate in flight operations at SFOF.

### **Goddard Space Flight Center Prelaunch Responsibilities**

1. Prepare and submit the Pioneer operations requirements to ETR.

### **Kennedy Space Center Prelaunch Responsibilities**

1. Plan the launch operations.
2. Provide technical direction and implementation of the launch operation.
3. Coordinate activities between NASA, contractors, and ETR groups.

### **McDonnell-Douglas<sup>3</sup> Prelaunch Responsibilities**

1. Prepare planning, reference, and predictive powered-flight trajectories.
2. Review technical documents that relate to launch operations and that have been prepared by other elements within the Pioneer Program.
3. Prepare launch countdown documentation.

### **Eastern Test Range (USAF) Prelaunch Responsibilities**

1. Review technical requirements and documents that relate to launch operations and that have been prepared by other elements within the Pioneer Program.

---

<sup>3</sup>Delta contractor.

2. Provide crews as required to operate ETR stations supporting the Pioneer Program during integration and operational readiness tests and during the launch countdown and powered-flight phase of the Pioneer mission.

From these assignments of responsibility came detailed schedules of procedures telling individuals in all organizations involved what they should do and when. Although the proliferation of plans, task assignments, and schedules may seem overly complex, it is this kind of paperwork that permits large groups of people from diverse organizations to function successfully.

### SIGNIFICANT EVENTS IN THE PIONEER PRELAUNCH PHASE

The prelaunch phase of activities consisted of many hundreds of separate items and events; so many, in fact, that the checkout and countdown lists were printed by computers. In addition to the extensive planning activities just described, two other groups of processes and events stand out as important:

- (1) Training in operational procedures
- (2) Preparation and testing of the spacecraft, launch vehicle, and other mission-dependent hardware

Training in operational procedures was most important during the preparations for the launch of Pioneer A in 1965, when the Pioneer Program was new to ETR and DSN personnel. The Delta, of course, was a familiar sight at the Cape; and the ETR and DSN had already handled spacecraft more complex than the Pioneers. Some of the "different" aspects of the Pioneer launches were:

- (1) The unusual orientation maneuvers following launch
- (2) The narrow launch window associated with injecting the spacecraft into an orbit roughly parallel to the plane of the ecliptic
- (3) The ejection of the Test and Training Satellites (TETR) from Block-II Pioneers
- (4) The occultations and flights through the Earth's magnetic tail

The orientation maneuvers, especially, required careful training at the Goldstone DSS site and, in the case of Pioneers 6 and 9, at Johannesburg and Goldstone, respectively, where "partial" Type-II orientation maneuvers were carried out.

The prelaunch preparation and testing of the spacecraft, launch vehicle, and associated hardware commenced with the arrival of the spacecraft at the Cape. These highly important checks and double-checks were performed primarily by Ames, TRW, Goddard, and Ken-

nedy personnel. Although the actual operations varied slightly from mission to mission, the following list of major tasks is representative.<sup>4</sup>

### Pioneer Prelaunch Tasks

- Task 1. Receipt, unpacking, and inventorying of spacecraft and associated equipment at hangar
- Task 2. Verification of mechanical condition of the spacecraft, ground handling equipment, and EGSE
- Task 3. Validation of EGSE
- Task 4. Spacecraft pneumatic system leak test
- Task 5. Spacecraft alignment checks
- Task 6. Solar-array performance test
- Task 7. Performance checks of critical unit parameters not accessible during an Integrated Systems Test (IST)
- Task 8. Integrated System Test (see discussion below)
- Task 9. Preparation of spacecraft for mating with third stage
- Task 10. Mating of spacecraft to inert third stage
- Task 11. Installation of EGSE in blockhouse and its validation
- Task 12. Mating of spacecraft and third stage to rest of launch vehicle at the launch pad
- Task 13. Preliminary spacecraft on-stand electrical and radio-frequency tests
- Task 14. Verification of spacecraft/launch vehicle compatibility with the range
- Task 15. Nose fairing fit check
- Task 16. Preliminary on-stand Integrated Systems Test
- Task 17. Flight readiness demonstration with a spacecraft/launch-vehicle practice countdown
- Task 18. Replacement of inert third stage with a live third stage and final spacecraft preparations
- Task 19. Verification that the experiments are operating to the satisfaction of the experimenters
- Task 20. Spacecraft radio-frequency subsystem test
- Task 21. Integrated Systems Test
- Task 22. Final spacecraft check prior to dynamic balancing (entails moving spacecraft back to hangar)
- Task 23. Spacecraft dynamic balance check
- Task 24. Mating of spacecraft with live third stage
- Task 25. Dynamic balance test of spacecraft and third stage
- Task 26. Reinstallation of EGSE in blockhouse and revalidation

<sup>4</sup>TRW Space Technology Laboratories: Test Program Plan, Pioneer Spacecraft Program, Aug. 1964.

Task 27. Mating of spacecraft and live third stage to launch vehicle on pad

Task 28. Spacecraft on-stand electrical and radio-frequency tests

Task 29. Final launch vehicle/spacecraft/range radio-frequency compatibility test

Task 30. Final on-stand Integrated Systems Test

Task 31. Preparation of spacecraft for pre-terminal count (includes installation of live pyrotechnics)

Task 32. Perform joint launch vehicle/spacecraft/range pre-terminal count

Task 33. Terminal count and launch

The Integrated Systems Test, or IST, was performed at least twice for each spacecraft at the Cape. This test (actually a check for launch readiness) was described in Ch. 6, Vol. II. Each spacecraft was subjected to at least one IST before it left the TRW Systems plant for the Cape. A successful IST demonstrated that the spacecraft met all spacecraft performance requirements. It provided a baseline upon which to gage spacecraft operational condition—a background against which to spot trends. It was because of this diagnostic value that the IST was repeated twice or more before launch. The final IST was “on-stand;” that is, carried out when the spacecraft was mated to the Delta rocket on the launch pad. The on-stand IST was the final comprehensive spacecraft check before launch. Recapitulating the IST description in Vol. II, the IST was as close to a realistic operational test as one could get prior to launch and yet be independent of the Delta, the ETR, and the SFOF. A minimum of hardlines were used; radio links were used instead to simulate actual communication links (fig. 2-4). Sun-sensor pulses were also simulated. Basically, a successful IST was a vote of confidence in the spacecraft, even though interfaces with the Delta and DSN were not tested.

The operational readiness tests were dress rehearsals that demonstrated that all personnel, equipment, and facilities participating in a Pioneer launch were ready to support the mission. While the IST was a spacecraft test, the operational readiness test encompassed the entire Pioneer supersystem; that is, the spacecraft and its instruments, the Delta, and the DSN (fig. 2-5). The events and tasks performed and simulated were representative of the actual mission events. The most critical “dry runs” were those simulating the Type-II orientation maneuver in conjunction with the Goldstone DSS. Another simulated situation brought Stanford University into the system, permitting operators there to practice with the spacecraft and ground equipment under realistic conditions. Of course, the normal mission was simulated too, via ersatz commands and telemetry sent over NASA’s worldwide communication system (NASCOM) and along ETR communication channels.

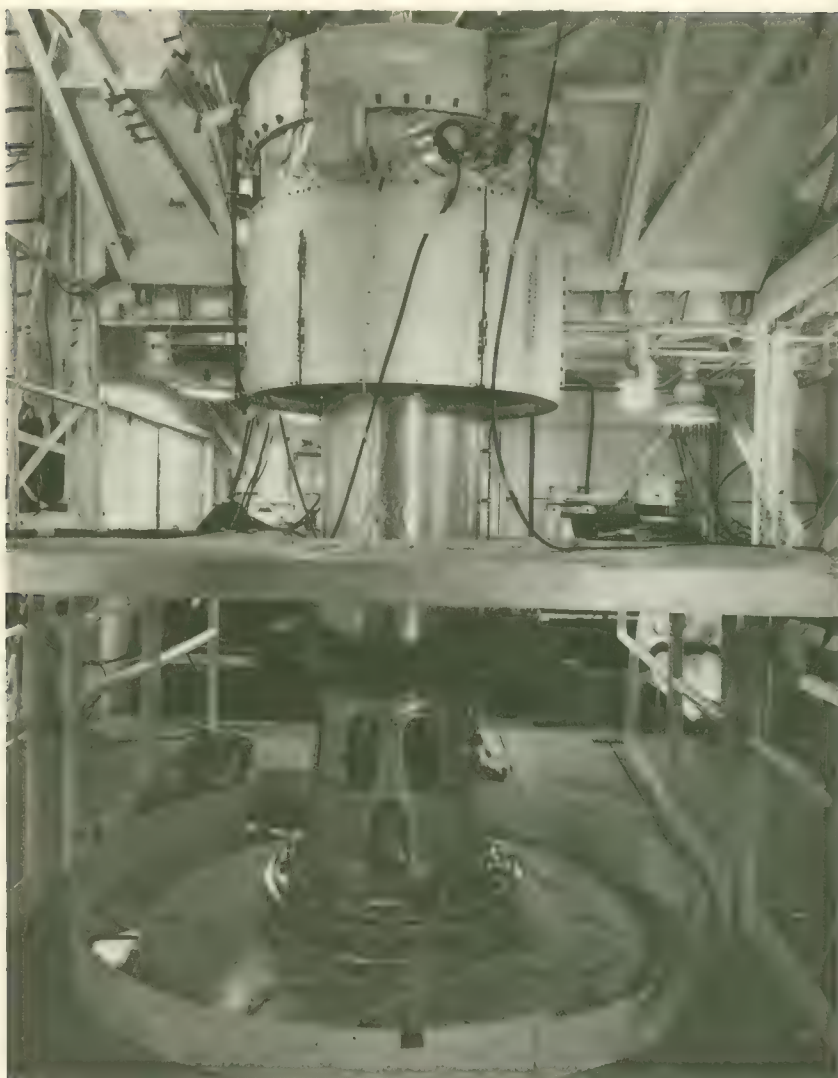


FIGURE 2-4.—Pioneer E wired for on-stand checkout at the Cape.

Two operational readiness tests were planned for each prelaunch phase. With Pioneer 6, for example, the first operational readiness test was scheduled for 48-hr duration, with 4 hr devoted to Cape and ETR activities, 13 hr for first-pass events at Johannesburg, and 9 hr for the Type-II orientation maneuver commanded from Goldstone. For Pioneers 6 and 9 the partial Type-II orientation maneuver was simulated at Johannesburg. Normal cruise operations were simulated at all stations. The second operational readiness test just before liftoff was a



FIGURE 2-5.—Scene in control room at SFOF in Pasadena, Calif., during Pioneer-B operational readiness test.

repeat of the first, except that everything was to be compressed into a 24-hr period. If all systems passed the second operational readiness test, a launch readiness review was held by the Pioneer Mission Director (fig. 2-6). The "go/no-go" decision was made at this final meeting. If the decision was "go," the actual countdown began.

#### PRELUNCH SCHEDULES—PLANNED AND ACTUAL

The Pioneer spacecraft arrived at the Cape 6 to 10 weeks prior to the planned launch. As the various tests were successfully passed, events multiplied crescendo-like as the day of launch approached. F-2, F-1, and F-0 days were filled with critical tests. The Pioneer project prepared schedules to lend some order to these events. The first "working" schedule of importance was the Detailed Task Sequence prepared by Ames Research Center a few months before the spacecraft was shipped to Cape Kennedy. The Detailed Task Sequence was published as a Pioneer specification. In the case of Pioneer D, which is used as an example here, Specification PC-153 contains the Detailed Task Sequence shown in table 2-1. Although the Detailed Task Sequence was presented

NATIONAL AERONAUTICS AND SPACE ADMINISTRATION  
 AMES RESEARCH CENTER MOFFETT FIELD, CALIFORNIA

Mission Readiness Review  
Pioneer C

Date: December 8, 1967  
 Place: E & O Building Conference Room 116  
 Time: 0930 EST.  
 Chairman: Charles F. Hall, ARC Pioneer Project Manager

AGENDA

| <u>Time, EST.</u> | <u>Item</u>                        |  |
|-------------------|------------------------------------|--|
| 0930              | Introduction                       | C. F. Hall/ARC                                 |
| 0945              | Mission Objectives                 | C. F. Hall/ARC                                 |
| 1000              | Launch Operations Status           | J. Nielon/ULO                                  |
| 1020              | Launch Vehicle Status              | W. McCall/ULO                                  |
| 1100              | COFFEE BREAK                       |  |
| 1115              | Launch Vehicle/TTS Status          | J. Tomasello/<br>T. Longo/GSFC<br>P. Burr/GSFC |
| 1135              | TTS Spacecraft Status              |  |
| 1205              | LUNCH                              |  |
| 1305              | Summary of Pioneer Cape Activities | R. W. Holtzclaw/ARC                            |
| 1325              | Pioneer Spacecraft Status          | B. O'Brien/TRW                                 |
| 1410              | Pioneer Instrument Status          | J. Lepetich/ARC                                |
| 1440              | COFFEE BREAK                       |  |
| 1455              | Pioneer Post Launch Activities     | C. F. Hall/ARC                                 |
| 1515              | T & DS Support                     | J. Thatcher/JPL                                |
|                   | ETR                                | R. Norman/ULO                                  |
|                   | MSFN                               | D. Bonnell/GSFC                                |
|                   | DSN                                | J. Thatcher/JPL                                |
|                   | NASCOM                             | J. Thatcher/JPL                                |
| 1600              | Interstation Conference            |  |
|                   | Station Reports                    | J. Thatcher/JPL                                |
| 1645              | Summary of Mission Status          | C. F. Hall/ARC                                 |
| 1705              | Pioneer Program Office Comment     | J. Mitchell/<br>M. Aucremanne/HQ               |

FIGURE 2-6.—Reproduction of the schedule for the Pioneer-C Mission Readiness Review held at the Cape.

on a time base and was much more detailed than the general Block-II specifications, PC-146, it was not a working schedule in the sense that it specified who, what, when, and where.

The Detailed Task Sequence was next rendered into more specific schedules. It is impractical to reproduce the item-by-item details, but the reader can get a "feel" of these working-level schedules from the Pioneer-D F—2, F—1, and F—0 day schedules in tables 2-1 and 2-2. Detailed descriptions of the tasks to be performed—in terms of switches to be thrown, meters to be read, calibrations to be made, etc.—had to accompany these schedules.

TABLE 2-1.—*Planned Pioneer-D Typical Detailed Task Sequence*<sup>a</sup>

| Date                              | Location   | Task  |
|-----------------------------------|------------|---|
| Oct. 1                            | SFOF       | Flight path analysis and command group acceptance test                                  |
| Oct. 1                            | SFOF       | Spacecraft performance analysis area/science analysis and command group acceptance test |
| Oct. 2                            | SFOF       | SFOF integration test   |
| Oct. 9                            | ETR        | DSS hangar and on-stand compatibility test  |
| Oct. 16                           | ETR        | Practice on-stand IST   |
| Oct. 24                           | SFOF       | First operational readiness test  |
| Oct. 25                           | ETR        | Preliminary electrical and radio-frequency checks                                       |
| Oct. 28                           | ETR        | DSS hangar and on-stand compatibility test  |
| Oct. 31                           | SFOF       | Second operational readiness test   |
| Oct. 31                           | ETR        | Practice countdown (pre-fairing installation)   |
| Nov. 1                            | ETR        | Practice countdown (post-fairing installation)  |
| Nov. 4 (major F—2 day milestones) |            |   |
| 0725 EST                          | ETR        | Countdown initiation  |
| 0730                              | Delta      | Task 2, engine checks   |
| 0730                              | Spacecraft | Task I, preparations and spacecraft checks  |
| 0900                              | Delta      | Task 3, electrical systems checks   |
| 1120                              | Spacecraft | Task II, pneumatic pressure and fill valve lead check                                   |
| 1210                              | Delta      | Task 5, stray voltage checks  |
| 1320                              | Spacecraft | Task III, service magnetometer  |
| 1440                              | Delta      | Task 6A, class B ordnance installation and hookup                                       |
| 1440                              | Spacecraft | Ordnance installation   |
| 1710                              | Delta      | Task 6B, squib installation   |
| 1840                              | ETR        | Built-in hold (8 hr, 15 min)  |
| Nov. 5 (major F—1 day milestones) |            |   |
| 0700 EST                          | Spacecraft | Task V, remove Red Tag items and protective covers                                      |
| 0725                              | ETR        | Countdown initiation  |
| 0730                              | Delta      | Task 7B, second-stage final preparations  |
| 0730                              | Delta      | Task 9A, Second-stage propellant servicing setup  |
| 0830                              | Delta      | Task 7A, fairing erection   |
| 1130                              | Delta      | Task 6C, FW-4 (third stage) hookup  |
| 1200                              | Delta      | Task 7B, fairing installation   |
| 1330                              | Spacecraft | Task III, umbilical checks  |
| 1400                              | Delta      | Task 9B, second-stage propellant servicing  |
| 1730                              | Delta      | Task 7C, blast-band installation  |
| 1745                              | Delta      | Task 10, first-stage fueling  |
| 1900                              | Delta      | Task 60, ordnance checks  |
| 2015                              | ETR        | Built-in hold (4 hr, 35 min)  |
| Nov. 6 (major F—0 day milestones) |            |   |
| 2349 (Nov. 5)                     | Spacecraft | Task VII, spacecraft radio-frequency checks   |
| 0224                              | ETR        | Countdown initiation  |
| 0229                              | Delta      | Task 11, launch-vehicle radio-frequency checks  |
| 0309                              | Spacecraft | Spacecraft standby status checks  |
| 0319                              | Delta      | Task 12, class-A ordnance installation and hookup                                       |
| 0319                              | Spacecraft | Task IX, ordnance arm   |
| 0404                              | Spacecraft | Task IX, sustained operation  |

TABLE 2-1.—*Planned Pioneer-D Typical Detailed Task Sequence—Continued*

| Date        | Location   | Task   |
|-------------|------------|--|
| 0549        | Delta      | Tasks 13 to 15, launch-vehicle final preparation and tower removal |
| 0549        | Spacecraft | Task X, spacecraft terminal count                                  |
| 0649        | Delta      | Task 16A, liquid oxygen setup                                      |
| 0749        | Delta      | Task 17, beacon checks   |
| 0809        | ETR        | Built-in hold (57 min)   |
| During hold | Delta      | Task 16B, liquid oxygen fill                                       |
| During hold | Delta      | Task 13, second-stage pressure fill                                |
| 0847        | ETR        | End of hold  |
| 0937        | ETR        | Built-in hold (5 min)  |
| 0942        | ETR        | End of hold  |
| 0947        | ETR        | Liftoff  |

<sup>a</sup> Adopted from Pioneer Specification PC-153.00. Cross checks between actual working schedules and the actual sequence of events at the Cape for Pioneer D reveal several minor changes in plans. Arabic task numbers apply to the launch vehicle; Roman numerals are assigned to spacecraft tasks. These tasks are defined in great detail in Goddard and Ames documents. Pioneer Specification PC-153.00 covered only flight operations; preparation of the spacecraft, launch vehicle, and other hardware are typified in Figure 2-7.

TABLE 2-2.—*Spacecraft Countdown Detailed Schedule<sup>a</sup>*

| Time                                      | Countdown time | Task  |
|---|----------------|---|
| <b>F—2 day schedule</b>                   |                |   |
| 0420 EST                                  | T—2430         | All personnel report to Hangar AM.                                |
| 0450                                      | T—2400         | Area-17 personnel report to Spacecraft Coordinator in blockhouse. |
| 0505                                      | T—2385         | Area-17 personnel report to Levels 8B and 9.                      |
| 0550                                      | T—2340         | Start Task I, preparations and spacecraft and experiment checks.  |
| 1110                                      | T—2020         | Complete Task I.  |
| 1110                                      | T—2020         | TRW personnel not required in Task II report to blockhouse.       |
| 1110                                      | T—2020         | Begin Task II, final pneumatics pressurization.                   |
| 1310                                      | T—1900         | Task II complete.   |
| 1310                                      | T—1900         | Begin Task III, magnetometer service.                             |
| 1430                                      | T—1820         | Task III complete.  |
| 1430                                      | T—1820         | Begin Task IV, ordnance installation and checks.                  |
| 1530                                      | T—1760         | Complete Task IV.   |
| End of F—2 day activity, secure Level 8B. |                |   |
| <b>F—1 day schedule</b>                   |                |   |
| 0040 EST                                  | T—1550         | Crew arrives at blockhouse 30 min prior to start of Task V.       |
| 0110                                      | T—1520         | Begin Task V, Red Tag removal and final preparations.             |

TABLE 2-2.—*Spacecraft Countdown Detailed Schedule—Continued*

| Time                    | Countdown time | Task  |
|-------------------------|----------------|---|
| 0340                    | T—1370         | Complete Task V.  |
| 0340                    | T—1370         | TRW and NASA observers on stand as required.                  |
| 0950                    | T—1000         | Task VI preparations; spacecraft crew reports to blockhouse.  |
| 0950                    | T—1000         | Begin Task VI, umbilical checks.                              |
| 1010                    | T—980          | Task VI complete.   |
| 1040                    | T—950          | End of F—day activity, secure Level 8B.                       |
| <b>F—0 day schedule</b> |                |   |
| 1855                    | T—525          | Crew arrives at blockhouse 10 min prior to start of Task VII. |
| 1905                    | T—515          | Begin Task VII, spacecraft systems checks.                    |
| 2205                    | T—335          | Complete Task VII.  |
| 2205                    | T—335          | Begin Task VIII, spacecraft standby status preparations.      |
| 2215                    | T—325          | Complete Task VIII.   |
| 2215                    | T—325          | Begin Task IX, ordnance Connection and final secure.          |
| 2235                    | T—305          | Arm ordnance.   |
| 2255                    | T—285          | Secure.   |
| 2300                    | T—280          | Complete Task IX.   |
| 2300                    | T—280          | Spacecraft sustained operation.                               |
| 0035                    | T—185          | Stand personnel required for Task X report to road block.     |
| 0045                    | T—175          | Start Task X, terminal countdown.                             |
| 0045                    | T—175          | Tower removal preparations.                                   |
| 0200                    | T—100          | Tower removal.  |
| 0215                    | T—85           | RF checks (receiver 2).                                       |
| 0240                    | T—60           | RF checks (receiver 1).                                       |
| 0255                    | T—45           | Receiver 1 and 2 final frequency report.                      |
| 0305                    | T—35           | Built-in hold (60 min).                                       |
| 0405                    | T—35           | Begin terminal count.   |
| 0430                    | T—10           | Spacecraft to internal power.                                 |
| 0435                    | T—5            | Built-in hold (5 min).  |
| 0440                    | T—5            | Resume count.   |
| 0442                    | T—3            | Spacecraft go/no-go report.                                   |
| 0445                    | T—0            | Liftoff.  |

<sup>a</sup> As issued to spacecraft launch team at Cape Kennedy for the launch of Pioneer D, Delta, DSN, and ETR events not shown, although they participate in some tests, such as the operational readiness test.

### THE ACTUAL PRELAUNCH PHASES AND HOW THEY COMPARED

Each of the five prelaunch phases had its own inventory of anecdotes and special circumstances that made it slightly different from the others. Of course, the spacecraft, the Delta, the DSN, and the ETR all evolved between Pioneer flights so that the ingredients were somewhat different for each launch. A brief narrative for each launch follows with emphasis on events not appearing on the planners' charts in tables 2-1

|   | F days | Date | Procedure      | 23 | 22 | 21 | 20 | 19 | 18 | 17 | 16 | 15 | 14 | 13 | 12 | 11 | 10 | 9 |
|---|--------|------|----------------|----|----|----|----|----|----|----|----|----|----|----|----|----|----|---|
| Receive EGSE/MGSE and inventory         |        |      | PP-S-68 N/C    |    |    |    |    |    |    |    |    |    |    |    |    |    |    |   |
| Pressurize pneumatics cart              |        |      | N/A            |    |    |    |    |    |    |    |    |    |    |    |    |    |    |   |
| Receive spacecraft                      |        |      | N/A            |    |    |    |    |    |    |    |    |    |    |    |    |    |    |   |
| Fit check S/C to DAC 3rd stage          |        |      | N/A            |    |    |    |    |    |    |    |    |    |    |    |    |    |    |   |
| Inspect spacecraft                      |        |      | PP-S-68 NC     |    |    |    |    |    |    |    |    |    |    |    |    |    |    |   |
| Validate EGSE and IST preps             |        |      | PP-S-67A       |    |    |    |    |    |    |    |    |    |    |    |    |    |    |   |
| Proof load dolly                        |        |      | N/A            |    |    |    |    |    |    |    |    |    |    |    |    |    |    |   |
| Set up and check mass spectrometer      |        |      | PP-7S-03 NC    |    |    |    |    |    |    |    |    |    |    |    |    |    |    |   |
| Pressurize spacecraft                   |        |      | PP-7S-03 NC    |    |    |    |    |    |    |    |    |    |    |    |    |    |    |   |
| Leak check (mass spectrometer)          |        |      | PP-7S-03 NC    |    |    |    |    |    |    |    |    |    |    |    |    |    |    |   |
| IST                                     |        |      | PP-S-71B       |    |    |    |    |    |    |    |    |    |    |    |    |    |    |   |
| Integrate flight decoder                |        |      | PP-0S-11 S.IVA |    |    |    |    |    |    |    |    |    |    |    |    |    |    |   |
| DSIF compatibility                      |        |      | PP-S-53B       |    |    |    |    |    |    |    |    |    |    |    |    |    |    |   |
| Practice on-stand IST                   |        |      | PP-S-74 NC     |    |    |    |    |    |    |    |    |    |    |    |    |    |    |   |
| Practice countdown and test review      |        |      | PP-S-75 NC     |    |    |    |    |    |    |    |    |    |    |    |    |    |    |   |
| ETR experiment tests and exp burnin     |        |      | PP-16S-34/41   |    |    |    |    |    |    |    |    |    |    |    |    |    |    |   |
| Decoder troubleshooting and eng tests   |        |      | N/A            |    |    |    |    |    |    |    |    |    |    |    |    |    |    |   |
| Squib checks                            |        |      | PP-0S-13 NC    |    |    |    |    |    |    |    |    |    |    |    |    |    |    |   |
| Leak check (Delta P) in hanger          |        |      | PP-7S-03 NC    |    |    |    |    |    |    |    |    |    |    |    |    |    |    |   |
| IST                                     |        |      | PP-S-71B       |    |    |    |    |    |    |    |    |    |    |    |    |    |    |   |
| S/C inspection and mech cleanup         |        |      | 104800         |    |    |    |    |    |    |    |    |    |    |    |    |    |    |   |
| Ship to spin bldg and mate to 3rd stage |        |      | N/A            |    |    |    |    |    |    |    |    |    |    |    |    |    |    |   |
| Balance S/C/3rd stage                   |        |      | N/A            |    |    |    |    |    |    |    |    |    |    |    |    |    |    |   |
| Install blockhouse GSE and check out    |        |      | N/A            |    |    |    |    |    |    |    |    |    |    |    |    |    |    |   |
| Fairing cable check                     |        |      | N/A            |    |    |    |    |    |    |    |    |    |    |    |    |    |    |   |

FIGURE 2-7—Pioneer-C prelaunch activities. (a) November.

|  | F days      | Date | Procedure | December |   |    |    |    |    |    |    |    |    |    |    |    |    |    |    |
|--|-------------|------|-----------|----------|---|----|----|----|----|----|----|----|----|----|----|----|----|----|----|
|  |             |      |           | 8        | 9 | 10 | 11 | 12 | 13 | 14 | 15 | 16 | 17 | 18 | 19 | 20 | 21 | 22 | 23 |
| Mate to Delta                              | N/A         |      |           |          |   |    |    |    |    |    |    |    |    |    |    |    |    |    |    |
| Preliminary elec and rf checks             | PP-S-32B    |      |           |          |   |    |    |    |    |    |    |    |    |    |    |    |    |    |    |
| S/C press. and Delta P leak check on stand | PP-7S-03 NC |      |           |          |   |    |    |    |    |    |    |    |    |    |    |    |    |    |    |
| DSIF compatibility (on-stand)              | PP-S-53B    |      |           |          |   |    |    |    |    |    |    |    |    |    |    |    |    |    |    |
| IST preps                                  | N/A         |      |           |          |   |    |    |    |    |    |    |    |    |    |    |    |    |    |    |
| Solar array checks                         | PP-14S-03B  |      |           |          |   |    |    |    |    |    |    |    |    |    |    |    |    |    |    |
| On-stand IST                               | PP-S-74A    |      |           |          |   |    |    |    |    |    |    |    |    |    |    |    |    |    |    |
| Fairing installation (cable check)         | N/A         |      |           |          |   |    |    |    |    |    |    |    |    |    |    |    |    |    |    |
| LV all systems test and rfi                | PP-S-27A    |      |           |          |   |    |    |    |    |    |    |    |    |    |    |    |    |    |    |
| Practice countdown (post-fairing)          | PP-S-75 NC  |      |           |          |   |    |    |    |    |    |    |    |    |    |    |    |    |    |    |
| Remove fairing                             | N/A         |      |           |          |   |    |    |    |    |    |    |    |    |    |    |    |    |    |    |
| Practice countdown (pre-fairing)           | PP-S-75 NC  |      |           |          |   |    |    |    |    |    |    |    |    |    |    |    |    |    |    |
| Launch readiness review and ORT            | N/A         |      |           |          |   |    |    |    |    |    |    |    |    |    |    |    |    |    |    |
| Countdown                                  | PP-S-75 NC  |      |           |          |   |    |    |    |    |    |    |    |    |    |    |    |    |    |    |
| Launch                                     | N/A         |      |           |          |   |    |    |    |    |    |    |    |    |    |    |    |    |    |    |

FIGURE 2-7.—Pioneer-C prelaunch activities—Concluded. (b) December.

and 2-2. A typical schedule of actual prelaunch events is presented in figure 2-7.

### Pioneer-A Prelaunch Narrative

Both the prototype and flight models were sent to the Cape. The prototype arrived October 1, 1965, and was used for practicing pre-launch operations. When the prototype model and an inert Delta third stage were mated to the launch vehicle (Delta 35) on November 29, it was discovered that the umbilical wiring was improperly connected. Modifications were made to correct this.

The Pioneer-A flight model was delivered for mating with the Delta third stage on December 5. During preliminary alignment checkout, a Total Indicator Runout of 0.25 in. was noted, indicating a physical mismatch. The attach fitting was shaved down to bring the alignment within tolerance. Tests and checkouts proceeded normally through F-1 day ("normally" meaning only minor, easily corrected problems).

December 15, F-0 day, was relatively calm with visibility of only 0.125 to 2 miles. Countdown commenced 30 min early at 1630. Everything went smoothly until T-90 min when the second-stage umbilical plug was inadvertently pulled, causing loss of power to the Delta second stage and the spacecraft itself. No one was certain what would happen if the plug were reinserted, and it was considered possible that some unforeseen signal could cause serious damage by firing some of the ordnance. The spacecraft and the Delta were revalidated. The built-in 60-min hold and ultimately the launch window had to be extended while further checks were made. The terminal count resumed at 0145, December 16, at T-35 min.

At T-2 min an abnormality in the radio guidance equipment caused another hold. The situation seemed to correct itself, and the count was recycled to T-8 min. Liftoff occurred at 0231:20 EST, December 16, 1965 (fig. 2-8).

### Pioneer-B Prelaunch Narrative

The prelaunch operations for Pioneer B were comparatively uneventful. The flight spacecraft arrived at Building AM on July 17, 1966. On August 9, it was discovered that, when the Chicago cosmic-ray experiment warmed up, a connection opened, partially disabling the experiment. As a result, the experiment indicated a non-existent low radiation level at all times. The experiment flew in this condition.

On F-2 day, August 15, a receiver lockup problem was encountered on the two S-band uplinks. Ultimately, the trouble was traced to an antenna on Building AM that was not pointed toward the launch pad.

F-0 day, August 17, had superb weather, with 5-knot winds and



FIGURE 2-8.—The launch of Pioneer A on Delta 35.

a visibility of 10 miles. The countdown proceeded normally to T - 3 min, when a hold was called due to the loss of communications down-range on the ETR. Communications were restored after 2 min, and liftoff occurred at 1020:17 EST.

#### Pioneer-C Prelaunch Narrative

Pioneer C was the first of the Block-II spacecraft. In addition, this flight was the first to carry a TETR mounted in the Delta second stage. The Pioneer-C flight model was received at Building AM on November 11, 1967. The IST of November 15 identified a faulty decoder which was replaced. On November 22, the Ames plasma probe was removed to correct a wiring error.



FIGURE 2-9.—Pioneer E arriving by air-freight from the West Coast.

F—2 day, December 11, was plagued by bad weather which forced personnel to clear the pad twice. At 1520, the electrical power was lost for 25 min, causing some concern because the spacecraft air conditioning was also lost. On F—1 day, the fairing had to be removed to repair wiring to the third-stage velocity meter. Terminal count began at 0543, December 13, and Pioneer C was launched successfully at 0908:00 on December 13, 1967.

### Pioneer-D Prelaunch Narrative

This spacecraft was the first to incorporate the convolutional coder experiment and the Ames magnetometer. Pioneer D arrived at Building AM on October 6, 1968. The beginning of the countdown was delayed for 2 days while tests and adjustments were made to the second-stage programmer. As soon as the programmer was accepted for flight, F—2 day activities commenced. The countdown proceeded smoothly to 0900 EST when anomalies appeared in the experimental data and experimental performance. Holds were called to investigate these problems which were found to be due to radio and electrical interference from the launch vehicle. No troubles were encountered during F—1 day countdown activities. At 1850 EST, November 7, 1968, F—0 day checks began. Spacecraft power was turned on at 1920. Spacecraft systems checks (Task VII) ran ahead of schedule, and a 20-min hold was called at 2015 to give the spacecraft receiver additional time to warm up. The terminal count began at 0050, November 8. Following a hold of 9.5 min due to high sheer winds aloft, the Delta lifted off at 0446:29.

### Pioneer-E Prelaunch Narrative

On July 18, 1969, the Pioneer-E spacecraft was received at Cape Kennedy (fig. 2-9). There were no unusual prelaunch events. A study of the launch vehicle test summary indicates a normal sequence of pre-launch events although a number of minor problems arose—as they usually do—and were corrected. Nothing in the prelaunch tests and checkout presaged the failure of the launch vehicle after liftoff.

Spacecraft and radio-frequency checks, Task VII, began at 0835 EDT on F—0 day, August 27, 1969. Except for a thunderstorm that temporarily delayed work, weather was excellent, with a visibility of 8 miles and light winds. The terminal countdown was uneventful. Liftoff was at 1759:00 EDT, August 27, 1969.



## Launch to DSS Acquisition

THE PHASE OF PIONEER OPERATIONS stretching from launch to DSS acquisition lasted less than 1 hr, but it was the only time when all four Pioneer systems operated together. Even this observation is a forced one because the spacecraft and scientific instrument systems were essentially passive during powered flight and the coast phase. Only housekeeping data were telemetered, and all scientific instruments were off. The spacecraft came to life only when the Travelling Wave Tubes (TWTs) were switched on, the booms were deployed, and the Type-I orientation maneuver was initiated. By this time, the spacecraft had been spun up and had separated from the Delta third stage. The ground-based DSN was involved in a configuration called the Near-Earth Phase Network which, during this phase, incorporated some facilities from the Air Force Eastern Test Range and the NASA Manned Space Flight Network (MSFN). Figure 3-1 illustrates the chronology and terminology involved in this phase of the mission.

It is best to view Pioneer operations from several vantage points so that the operations of all four systems can be appreciated. First, the sequence of events is portrayed schematically in figure 3-2. The nominal time frame for one of the launches is added to the picture in table 3-1. Of course, the timing of the critical events varied from mission to mission because the burn and coast times changed with each launch, and the Delta rocket was upgraded during the program. The nominal time frame, with its critical events, provides a yardstick against which to measure the success of this portion of the launch. Altitude and distance downrange are also important diagnostic parameters. However, the DSN stations waiting downrange tend to see the picture as having an additional spatial dimension (fig. 3-3). This is not surprising because the tracking of spacecraft in orbit or far out in space is essentially four-dimensional (including time), whereas range tracking, as on the ETR, was more nearly three-dimensional in character; that is, altitude, range, and time. In fact, one of the critical displays at the Cape is an impact point predictor—a two-dimensional display. "Handover" from the Near-Earth Phase Network to the DSN was facilitated by "predicts" sent ahead to DSS-51 (Johannesburg) to tell its acquisition-aid antennas where to look in the western sky. Once the acquisition aid had the spacecraft, the 85-ft. parabolic antenna was slewed to it.

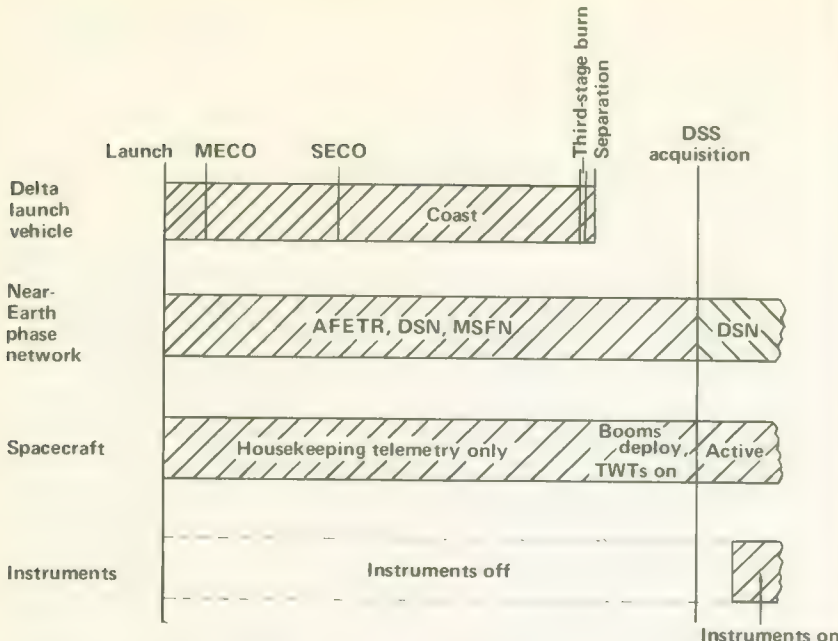


FIGURE 3-1.—Status of the four Pioneer systems from launch through DSS acquisition.

### PERFORMANCE OF THE DELTA LAUNCH VEHICLE

The Delta launch vehicle performed superbly during the first four Pioneer launches. The fifth mission, Pioneer E, had to be aborted by the Range Safety Officer when the vehicle began to stray off course. It would be repetitious to narrate each launch in detail. Instead, tables 3-2 and 3-3 summarize Delta "mark events" and stage performance, respectively. A series of figures (figs. 3-4 to 3-7) portrays the Delta overall metric performance for the four successful missions. Of course, none of the flights was flawless, but the deviations were all minor compared to the failure on the final flight. These perturbations are summarized below along with a description of the loss of Pioneer E.

#### Pioneer-6 Launch Vehicle Performance

All mission objectives were achieved and vehicle flight was well within the "three-sigma" limits.<sup>5</sup> All liquid engines and solid motors performed satisfactorily, including the spinup rockets. Second-stage thrust misalignment in pitch was excessive, however, and alignment procedures were to be modified on future Delta flights. Another minor deviation

<sup>5</sup>Theoretically, the "three-sigma" limits encompass 99.86 percent of all observations.

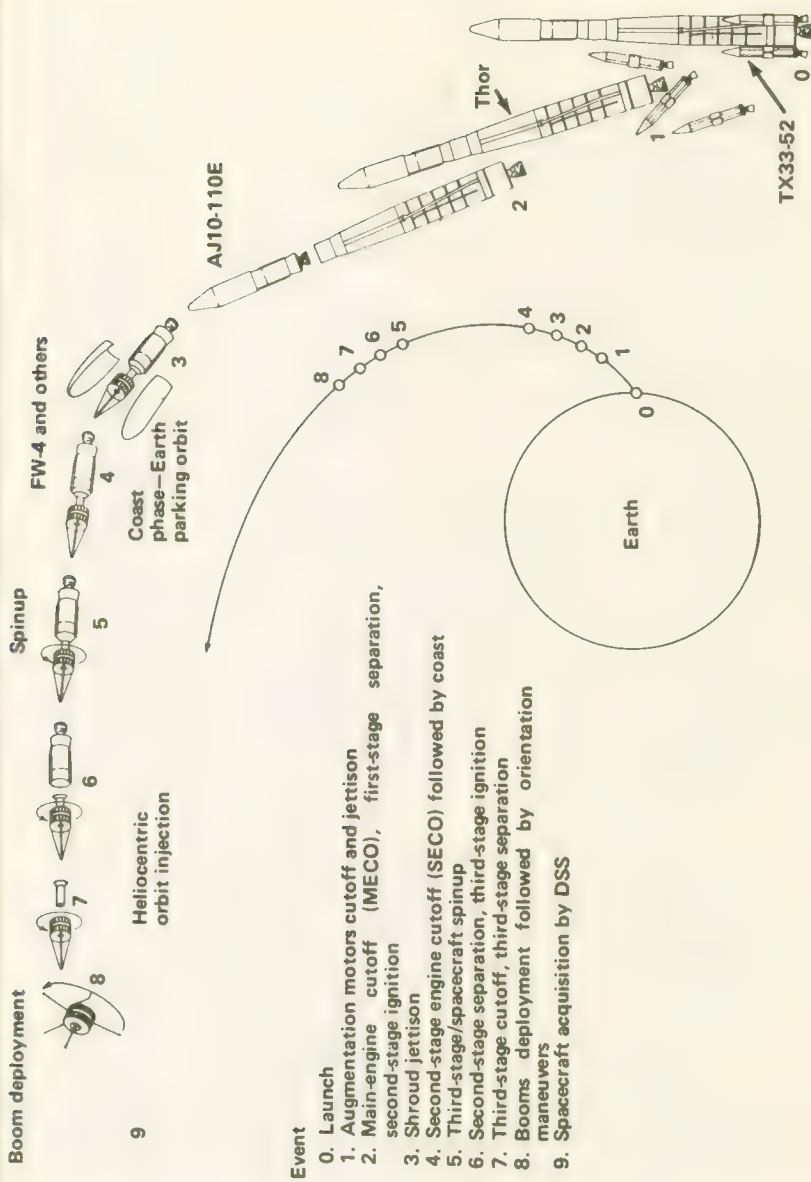


FIGURE 3-2.—A typical Pioneer launch sequence.

TABLE 3-1.—*Pioneer-6 Nominal "Mark Events," Launch to DSS Acquisition*

| Mark event  | Nominal time from launch, sec |
|---|-------------------------------|
| Liftoff   | 0                             |
| Solid motor burnout (thrust augmentation)                     | 43.0                          |
| Grand Bahama rise (ETR station)                               | 56.0                          |
| Solid motors jettisoned                                       | 70.0                          |
| Main engine cutoff  | 149.2                         |
| Second-stage ignition   | 153.2                         |
| First-stage jettisoned  | 153.4                         |
| Fairing jettisoned  | 179.2                         |
| Second-stage engine cutoff                                    | 551.1                         |
| Control transferred from SFOF to Johannesburg                 | 1200.0                        |
| Third-stage spinup  | 1486.2                        |
| Second-stage jettisoned                                       | 1488.2                        |
| Third-stage ignition  | 1501.2                        |
| Third-stage burnout   | 1523.7                        |
| Spacecraft separation   | 1583                          |
| Type-I orientation begins automatically                       | 1583                          |
| Booms and Stanford antenna deployed                           | 1584                          |
| TWT 1 turned on and switched to low-gain antenna              | 1584                          |
| Johannesburg rise (DSS acquisition can occur after this time) | 1688                          |

from normal performance was caused by the asymmetric ejection of the nozzle closure ring on the second-stage engine. As a result, a redesign of the nozzle closure diaphragm was recommended. These minor departures from perfect performance are common in any operation involving sophisticated machines.

### Pioneer-7 Launch Vehicle Performance

The launch vehicle performed even better on this flight than it did on Pioneer 6. The only failure of even minor significance concerned the third-stage air-inlet-adapter primary-loop lanyard, which failed during liftoff. The adapter was successfully released by a secondary lanyard.

### Pioneer-8 Launch Vehicle Performance

Pioneer 8 and the TETR-1 satellite were launched successfully. All flight parameters were well within the three-sigma limits. Unexplained moments in the pitch and yaw planes were noticed just after second-stage engine cutoff, but they did not affect the mission. Some circuit anomalies occurred after second-stage separation. These were caused when the second-stage engine burned some wire insulation on the jettisoned first stage.

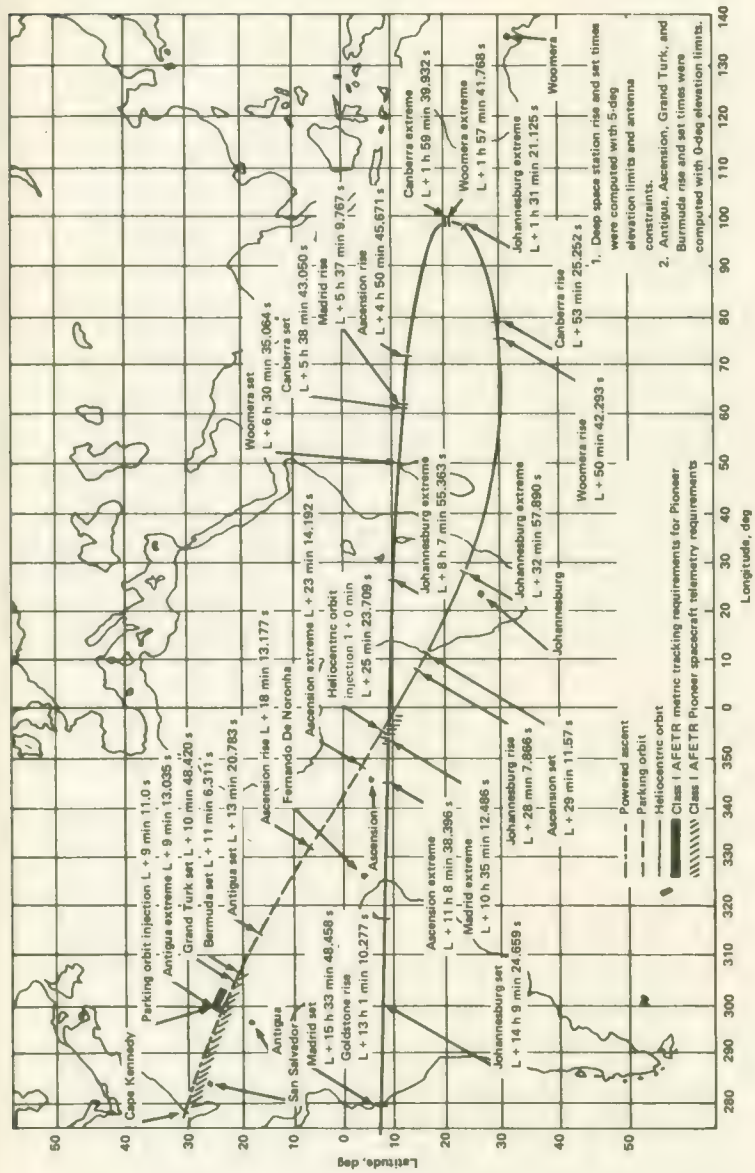


FIGURE 3-3.—Pioneer-6 ground track showing tracking station coverage.

TABLE 3-2.—Summary of Critical Nominal and Actual Launch Events

| Event                              | Pioneer 6a    |         | Pioneer 7b    |         | Pioneer 8c    |         | Pioneer 9d   |         | Pioneer Ee    |        |
|------------------------------------|---------------|---------|---------------|---------|---------------|---------|--------------|---------|---------------|--------|
|                                    | Nominal       | Actual  | Nominal       | Actual  | Nominal       | Actual  | Nominal      | Actual  | Nominal       | Actual |
| Liftoff (sec)                      | 0             | 0       | 0             | 0       | 0             | 0       | 0            | 0       | 0             | 0      |
| Solid motor burnout                | 43.00         | 42.23   | 42.65         | 41.60   | 41.90         | 42.25   | 38.19        | 39.4    | 70.00         | 69.8   |
| Solid motors jettisoned            | 70.00         | 69.97   | 70.00         | 70.79   | 70.00         | 70.3    | 70.00        | 69.94f  | 220.0         | 215.4  |
| Main engine cutoff                 | 149.21        | 148.01  | 149.52        | 148.10  | 149.75        | 149.45  | 150.53       | 151.35  | 224           | 224    |
| Second-stage ignition              | 153.21        | 152.03  | 153.52        | 152.13  | 153.75        | 153.50  | 154.53       | 155.42  | 229           | 229.1  |
| Fairing jettisoned                 | —             | 178.84  | 175.52        | 174.74  | 185.75        | 186.16  | 169.53       | 171.01  |               |        |
| Second-stage engine cutoff command | 551.13        | 531.44  | 529.32        | 527.89  | 530.93        | 536.73  | 534.35       | 539.01  |               |        |
| Third-stage spinup                 | 1486.21       | 1485.03 | 1575.52       | 1474.12 | 1842.75       | 1842.42 | 1201.53      | 1202.40 |               |        |
| Second-stage jettisoned            | 1488.21       | 1487.03 | 1477.52       | 1476.12 | 1844.75       | 1844.43 | 1203.53      | 1204.37 |               |        |
| Third-stage ignition               | 1501.21       | 1496.94 | 1490.52       | 1488.98 | 1857.75       | 1857.98 | 1216.53      | 1218.54 | —             | —      |
| Third-stage burnout                | 1523.71       | 1520.74 | 1521.34       | 1519.80 | 1888.55       | 1888.78 | 1247.33      | 1249.34 | —             | —      |
| TETR separation                    | —             | —       | —             | —       | 1904.75       | 1904.25 | 1263.53      | 1264.4  | —             | —      |
| Actual launch date                 | Dec. 16, 1965 |         | Aug. 17, 1966 |         | Dec. 13, 1967 |         | Nov. 8, 1968 |         | Aug. 27, 1969 |        |
| Actual launch time                 | 0231:20 EST   |         | 1020:17 EST   |         | 0908:00 EST   |         | 0446:29 EST  |         | 1739:00 EST   |        |

<sup>a</sup> McDonnell-Douglas Corp.: Flight Report for Improved Delta Vehicle S/N 460/20202/20202, Delta Program—Mission No. 35, Spacecraft: Pioneer A, Rept. SM-48998, 1966, pp. 44-46.

<sup>b</sup> McDonnell-Douglas Corp.: Flight Report for Delta Vehicle S/N 462/20204/20207, Delta Program—Mission No. 40, Spacecraft: Pioneer B, Rep. DAC-58324, 1966, pp. 30-31.

<sup>c</sup> McDonnell-Douglas Corp.: Flight Report for Delta Vehicle S/N 20216, Delta Program—Mission No. 55, Spacecraft: Pioneer C, Rept. DAC-58726, 1968, pp. 45-47.

<sup>d</sup> McDonnell-Douglas Corp.: Flight Report for Delta Vehicle S/N 20222, Delta Program—Mission No. 60, Spacecraft: Pioneer D, Rept. DAC-61695, 1969, pp. 35-37.

<sup>e</sup> First-stage hydraulic pressure lost at 214 sec. Destruction by Range Safety Officer at 483.9 sec.

<sup>f</sup> For one motor; the other two augmentation motors were jettisoned at 69.992 sec.

TABLE 3-3.—Summary of Delta Performance Factors<sup>a</sup>

|  | Pioneer 6 |         | Pioneer 7 |         | Pioneer 8 |         | Pioneer 9 |         |
|--|-----------|---------|-----------|---------|-----------|---------|-----------|---------|
|  | Nominal   | Actual  | Nominal   | Actual  | Nominal   | Actual  | Nominal   | Actual  |
| Overall weight (lb)                              | 149,977   | 149,904 | 150,084   | 149,560 | 149,537   | 149,468 | 151,765   | 151,875 |
| First-stage liquid-engine thrust (lb)            | 186,889   | 188,567 | 186,525   | 187,803 | 186,967   | 187,502 | 185,888   | 185,432 |
| First-stage liquid-engine specific impulse (sec) | 273.12    | 273.13  | 279.39    | 279.58  | 281.16    | 280.98  | 281.72    | 281.72  |
| MECO inertial velocity (ft/sec)                  | 14,141    | 14,153  | 12,941    | 13,020  | 14,049    | 14,093  | 14,331    | 14,242  |
| MECO inertial flight path elevation angle (deg)  | 16.9      | 16.9    | 17.23     | 17.02   | 20.34     | 20.31   | 19.38     | 19.32   |
| MECO inertial flight path azimuth angle (deg)    | 100.9     | 101.0   | 107.31    | 107.41  | 107.22    | 107.15  | 107.31    | 107.24  |
| MECO range (n. mi.)                              | 91.1      | 90.8    | 92.7      | 92.7    | 87.9      | 87.9    | 92.4      | 92.4    |
| MECO altitude (n. mi.)                           | 48.3      | 48.1    | 51.0      | 51.3    | 54.9      | 54.4    | 55.9      | 55.4    |
| Second-stage thrust (lb)                         | 7369.0    | 7384.8  | 7553.5    | 7485.2  | 7572.6    | 7502.2  | 7527.3    | 7371.3  |
| Second-stage specific impulse (sec)              | 268.9     | 269.1   | 271.34    | 274.41  | 272.3     | 279.4   | 275.2     | 267.8   |
| SECO inertial velocity (ft/sec)                  | 26,348    | 26,279  | 26,056    | 26,035  | 25,342    | 25,216  | 25,677    | 25,715  |
| SECO inertial flight path elevation angle (deg)  | 0.033     | 0.087   | -0.61     | -0.86   | 0.97      | 0.75    | 0.10      | -0.06   |
| SECO inertial flight path azimuth angle (deg)    | 110.6     | 111.1   | 115.96    | 116.12  | 115.69    | 115.83  | 115.91    | 115.73  |
| SECO range (n. mi.)                              | 118.5     | 111.9   | 110.91    | 111.1   | 1063.1    | 1079.8  | 1099.5    | 1108.0  |
| SECO altitude (n. mi.)                           | 149.7     | 149.2   | 149.9     | 145.8   | 205.9     | 205.5   | 202.9     | 202.5   |
| Third-stage burn time (sec)                      | 22.5      | 23.8    | 30.82     | 30.82   | 30.80     | 30.80   | 30.80     | 30.80   |
| Third-stage impulse (lb-sec)                     | 139,761   | 140,496 | 172,160   | 171,896 | 172,696   | 172,418 | 172,481   | 172,354 |
| TSB inertial velocity (ft/sec)                   | 35,542    | 35,593  | 35,869    | 35,898  | 35,185    | 35,383  | 36,225    | 36,208  |
| TSB inertial flight path elevation angle (deg)   | 1.6       | 1.7     | 2.44      | 2.01    | 0.00      | -0.55   | 2.00      | 2.22    |
| TSB inertial flight path azimuth angle (deg)     | 119.2     | 119.3   | 129.51    | 129.81  | 114.60    | 114.35  | 124.33    | 124.53  |
| TSB range (n. mi.)                               | 4913.8    | 4898.5  | 4952.0    | 4980.1  | 5984.8    | 6025.3  | 3794.6    | 3794.5  |
| TSB altitude (n. mi.)                            | 301.7     | 304.6   | 230.2     | 204.0   | 314.7     | 262.3   | 251.5     | 251.8   |

<sup>a</sup>Same references as those cited in table 3-2.<sup>b</sup>MECO = Main Engine Cutoff; SECO = Second-stage Engine Cutoff; TSB = Third Stage Burnout.

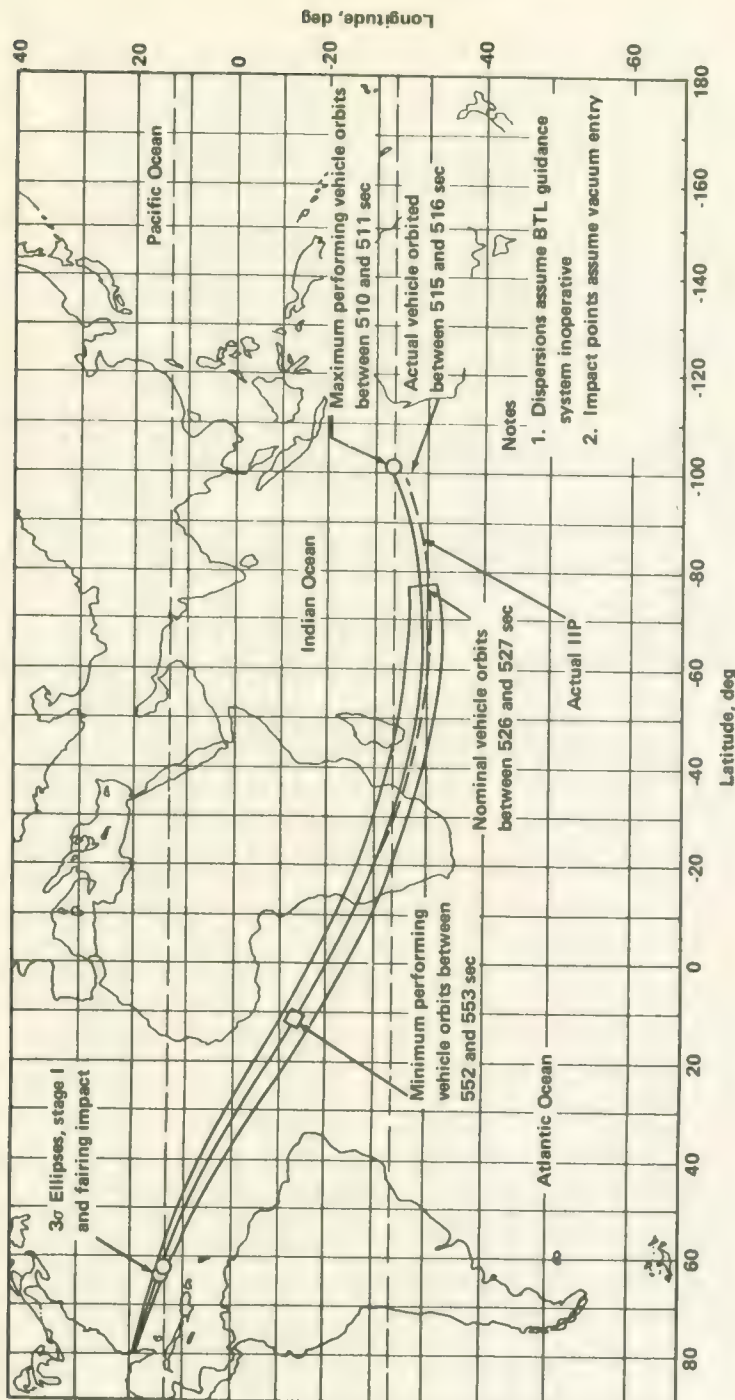


FIGURE 3-4.—The Pioneer-6 trajectory, showing the  $3\sigma$  limits.

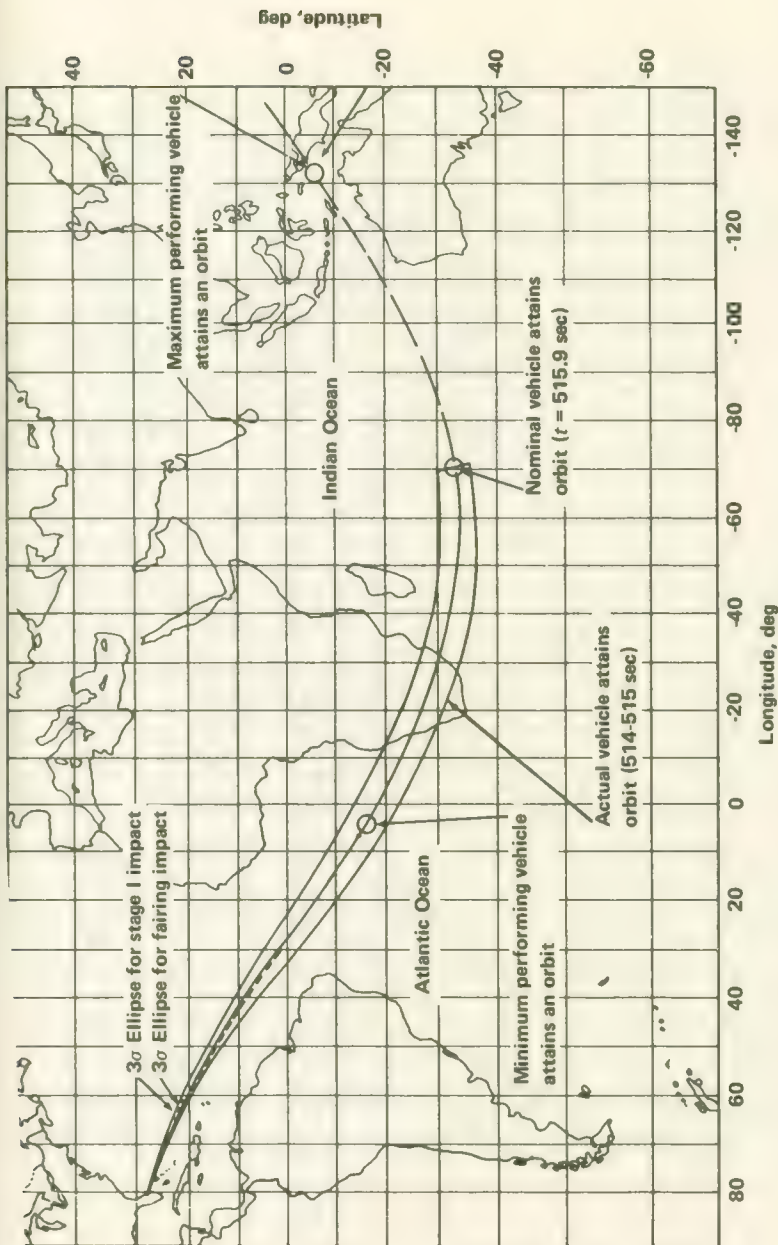


FIGURE 3-5.—The Pioneer-7 trajectory, showing the  $3\sigma$  limits.

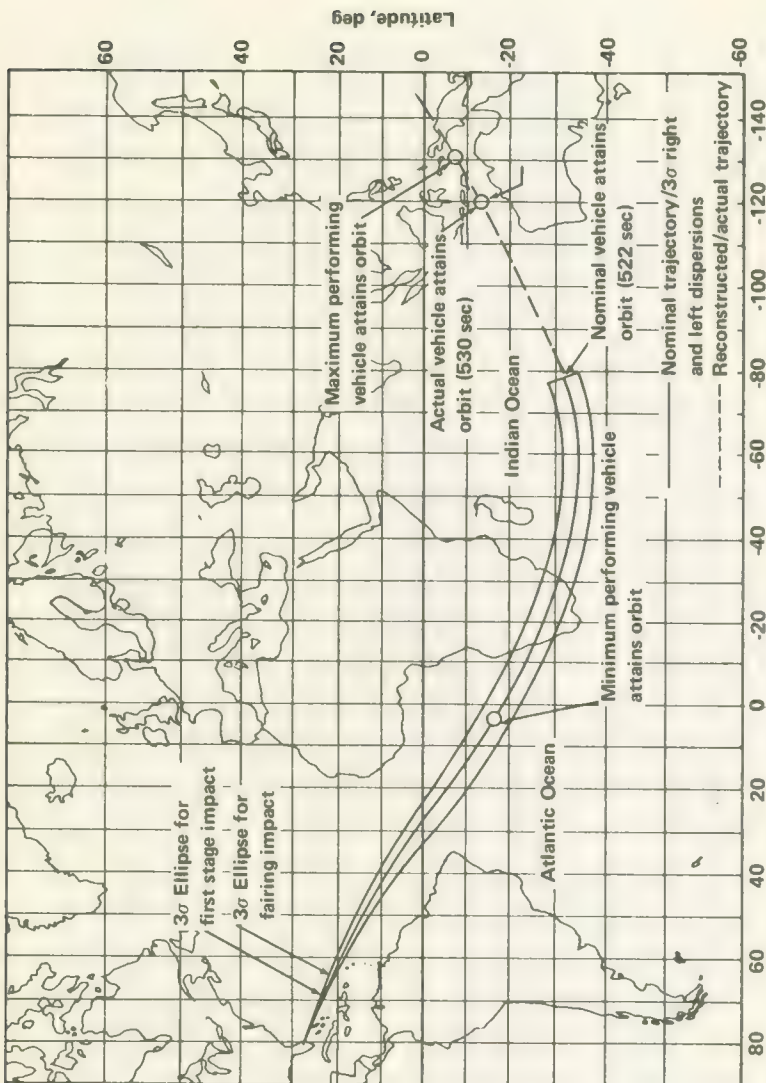


FIGURE 3-6.—The Pioneer-8 trajectory, showing the 3 $\sigma$  limits.

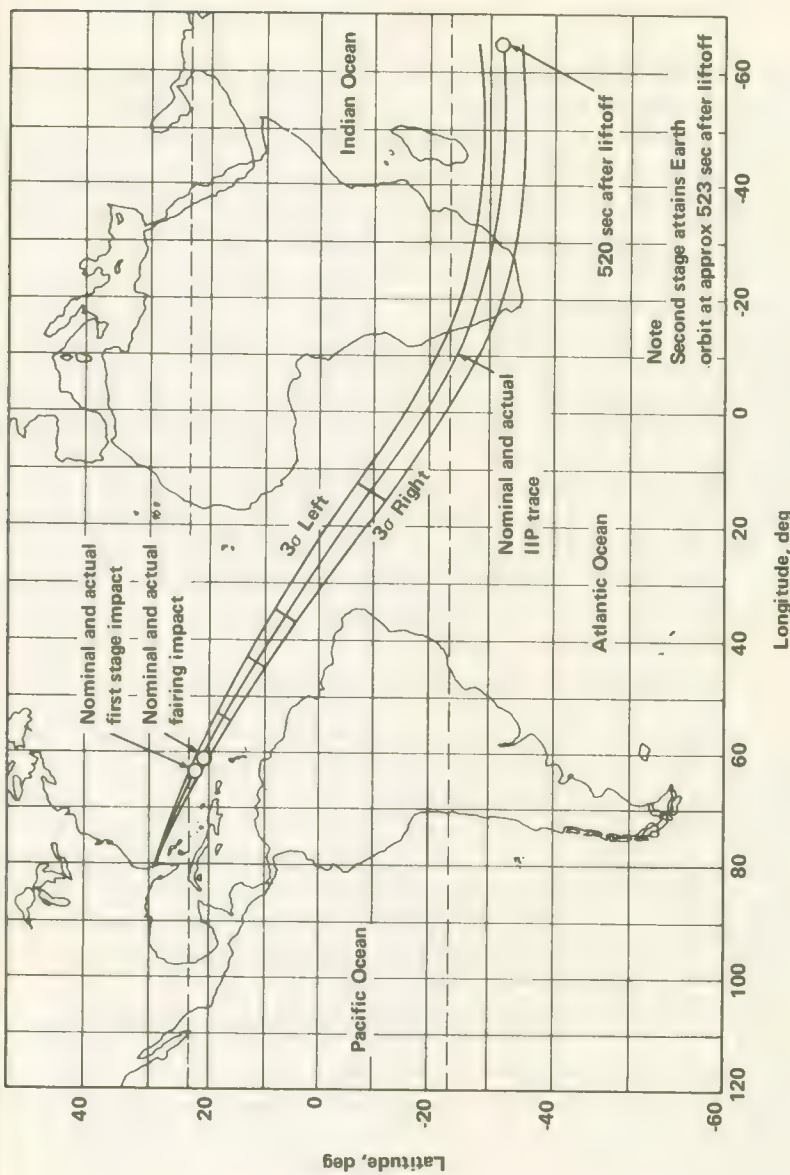


FIGURE 3-7.—The Pioneer-9 trajectory, showing the  $3\sigma$  limits.

### Pioneer-9 Launch Vehicle Performance

This was essentially a perfect launch from the Delta viewpoint.

### Pioneer-E Launch Vehicle Performance

Ignition and liftoff were normal. The three solid, thrust-augmentation engines operated properly and were jettisoned simultaneously and at the proper moment. At 63 sec into the flight, the first-stage hydraulic pressure decreased from 3150 to 3000 psia. Then the pressure began fluctuating. At 213 sec, the pressure dropped to zero, and all first-stage control was lost. Telemetered propulsion parameters began to indicate violent vehicle maneuvers.

With the first-stage hydraulic pressure lost, the main engine pitched down, yawed left, and rolled counterclockwise. As a result, the second-stage gyros were driven out of their limits during second-stage ignition and separation. The ignition and initial performance of the second-stage engine were approximately normal, but the damage was done, and the second stage was far off course.

After main engine cutoff, the predicted impact point on the plotboard began to move at a 45° angle to the right and downrange. The Range Safety Officer sent "arming" commands to downrange stations to ensure they had the capability for vehicle "destruct." At 483.9 sec, the deviation from the planned course was too great, and the vehicle was destroyed.

## TRACKING AND DATA ACQUISITION

As a Pioneer spacecraft and its launch vehicle rose from the launch pad at Cape Kennedy, they were tracked downrange by a variety of radio and optical tracking devices. Until the spacecraft was "handed over" to the Johannesburg DSS station, the pooled radars, optical trackers, guidance equipment, and telemetry receivers of the Air Force ETR and some stations of NASA's DSN and MSFN were crucial to mission success. We examine now how these resources were put together and how they functioned during this phase of each Pioneer mission.

### Tracking and Data Acquisition Requirements and Station Configurations

Tracking and telemetry data are needed to assess the performance of both the launch vehicle and the spacecraft and also for ensuring range safety. All of the "mark events" and launch vehicle positions, velocities, and headings described in the preceding section are obtained through tracking and analysis of telemetry data.

The facilities assigned to each of the Pioneer missions from launch through DSS acquisition are listed in table 3-4. The ETR was the pri-

TABLE 3-4.—*Tracking and Data Acquisition Support Stations Through DSS Acquisition*

| Range/network | Station                                 | Used during Pioneer flights |   |   |   |    |   |
|---------------|---|-----------------------------|---|---|---|----|---|
|               |   | 6                           | 7 | 8 | 9 | 10 | E |
| AFETR         | 1. Cape Kennedy and Patrick AFB         | x                           | x | x | x | x  | x |
|               | 3. Grand Bahama I.                      | x                           | x | x | x | x  | x |
|               | 7. Grand Turk I.                        | x                           | x | x | x | x  | x |
|               | 9.1 Antigua I.                          | x                           | x | x | x | x  | x |
|               | 12 Ascension I.                         | x                           | x | x | x | x  | x |
|               | 13 Pretoria, S.A.                       | x                           | x | x | x | x  | x |
|               | <i>Twin Falls</i> (ship)                | x                           | x | x | x | x  | x |
|               | <i>Coastal Crusader</i> (ship)          | x                           | x | x | x | x  | x |
|               | <i>Sword Knot</i> (Ship)                | x                           | x | x | x | x  | x |
|               | Merritt I.                              | x                           | x | x | x | x  | x |
| MSFN          | Bermuda                                 | x                           | x | x | x | x  | x |
|               | Grand Bahama                            |                             |   |   |   |    |   |
|               | Antigua                                 |                             |   |   |   |    |   |
|               | Ascension I.                            | x                           | x | x | x | x  | x |
|               | Tanannative, Malagasy Rep.              | x                           | x | x | x | x  | x |
|               | <i>Vanguard</i> (ship)                  |                             |   |   |   |    |   |
|               | DSS-71, Cape Kennedy                    | x                           | x | x | x | x  | x |
| DSN           | DSS-72, Ascension I.                    | x                           | x | x | x | x  | x |
|               | DSS-51, Johannesburg, S.A.              | cx                          | x | x | x | x  | x |
|               | DSS-41, Woomera, Australia <sup>b</sup> |                             |   | x | x | x  | x |
|               |   |                             |   |   |   |    |   |

<sup>a</sup>Scheduled, but not actually used due to abort.<sup>b</sup>The "primary" DSN acquisition station for Pioneer 8.<sup>c</sup>Commanded partial Type-II orientation. This maneuver was commanded from Goldstone on Pioneer 9.

mary agency responsible for providing metric (tracking) data during this phase of operations. The MSFN stations, listed in table 3-4, provided redundant radar support. Metric requirements were met by tracking the C-band beacon aboard the Delta and the S-band telemetry signal from the spacecraft. From liftoff to 5000-ft altitude, ETR optical equipment provided additional metric data.

During this "powered" phase of flight, telemetry came primarily from the first and second stages of the launch vehicle. These were PDM/FM/FM links operating at 228.2 and 234.0 MHz, respectively. ETR stations 1, 3, 9.1, 12, 13, and the Range Instrumentation Ships (RIS) acquired this telemetry.

The ETR Real Time Computer Facility (RTCF) at the Cape, which used CDC 3600 and 3100 computers during the Pioneer flights, processed the metric data flowing back from downrange sites and converted them into "predicts" for stations which had not yet acquired the spacecraft and/or launch vehicle stages.

During the Pioneer flights, Building AO (fig. 3-8) contained joint JPL-AFETR facilities that were vital to mission analysis and control. Briefly, these facilities were:

(1) A joint operations center consisting of status displays, a timing system, and consoles. During the early portion of the Pioneer mission, control was transferred to the SFOF.

(2) A joint communication center, which provided the local terminals and interfaces for voice, teletype, and data circuits to and from Cape facilities, the SFOF, and the ETR.

### Flight Operations—Tracking and Data Acquisition

The scenarios of tracking and data acquisition activities vary slightly for each launch. Short narratives rather than tables seem in order here.

*Pioneer 6.*—Liftoff occurred at 0731:20 GMT, December 16, 1965. Grand Bahama rise was at 0732:15, but its receiver was in and out of lock until 0737:33. At 0751, control was transferred from the SFOF to DSS-51, Johannesburg, for the planned partial Type-II orientation. The Johannesburg acquisition aid antenna acquired the spacecraft at 0759. Initial telemetry indicated that the automatic Type-I orientation was underway. At 0804:14, the spacecraft signaled that the Type-I orientation was complete. At 0807, the Johannesburg receiver was transferred from the acquisition aid antenna to the 85-ft dish.

There were some minor problems with telemetry coverage during this flight. Stations did not acquire and lock onto the spacecraft signal as early as predicted; however, the signal was tracked longer than anticipated (fig. 3-9). This anomalous performance was scheduled for later investigation. The first and only indication of third-stage ignition

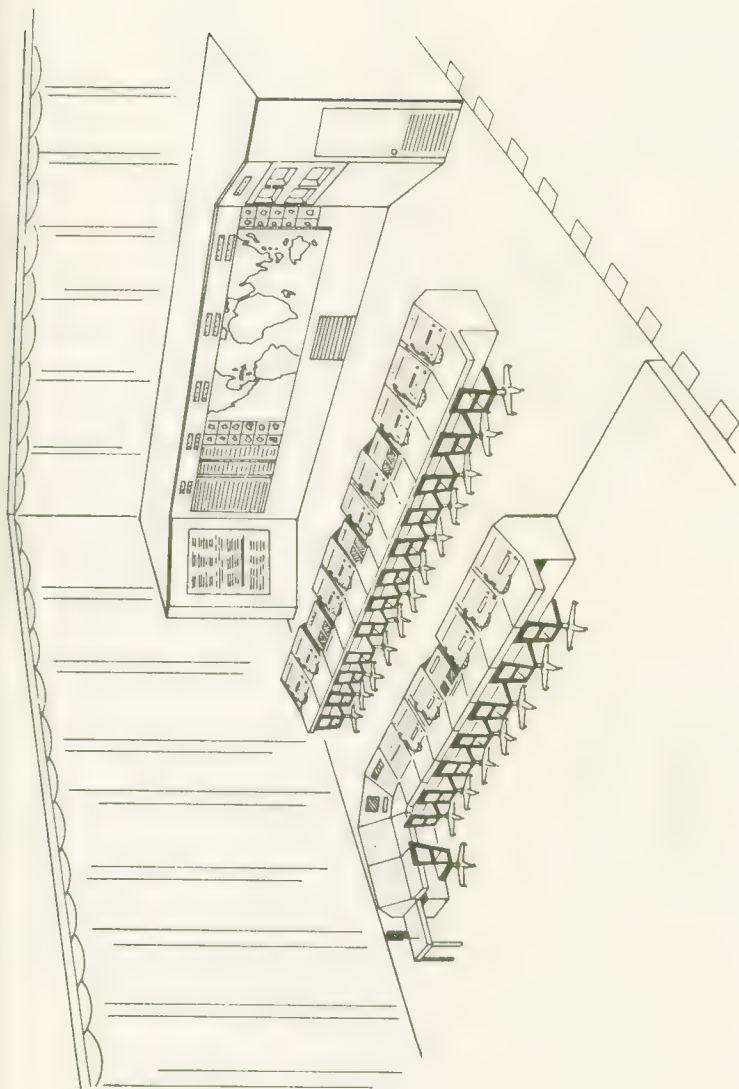


FIGURE 3-8.—Sketch of the JPL-AFETR Operations Center in Building AO at Cape Kennedy.

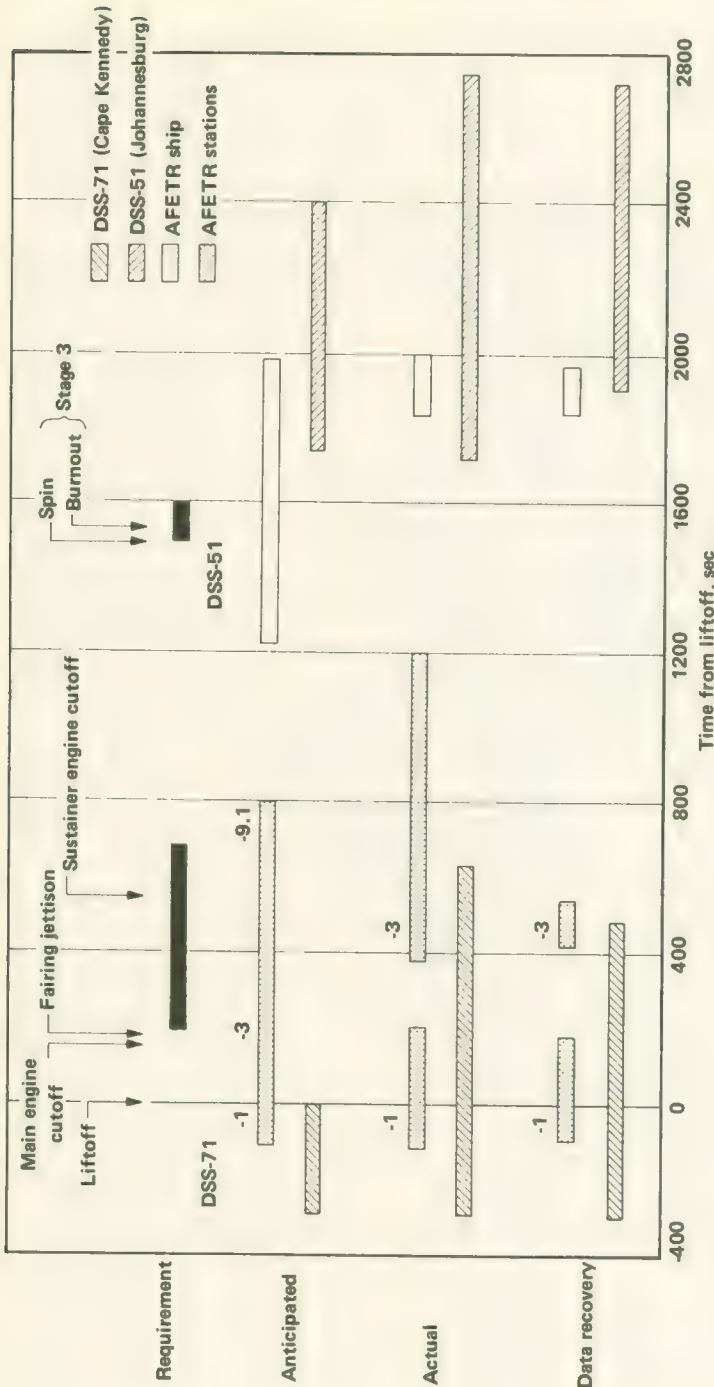


FIGURE 3-9.—Pioneer-6 telemetry coverage from launch through DSS acquisition.

in near real time was the dropout of vhf telemetry as the third-stage plume engulfed the second stage. RF propagation problems precluded receipt of real-time data from Ascension Island. When a report was finally received, it indicated only a 50-percent burn time. All other tracking and telemetry data, however, indicated a normal third-stage burn. Later, it was found that someone had read the wrong scale on the Doppler plot at Ascension. Finally, the *Coastal Crusader* obtained no Doppler data from either the 136-MHz Delta beacon or the spacecraft S-band carrier due to equipment problems. The parking orbit parameters computed from downrange tracking data are tabulated in table 3-5.

*Pioneer 7*.—This mission's launch window opened at 1518; liftoff was at 1520:17, August 17, 1966. Grand Bahama rose at 1521. Nominal Johannesburg rise was 1547, but acceptable two-way Doppler was not achieved until 1558:24. Telemetry indicated that the Type-I orientation had been completed and had required 28 gas pulses.

Near-Earth tracking was generally excellent, except for some drop-outs as indicated in figure 20a. Due to an operator error aboard the *Sword Knot*, the spacecraft separation mark event was not recorded. This error was attributed to the fact that the *Sword Knot* did not receive mission instructions until F—1 day. Early in the launch phase, the spacecraft S-band telemetry signal was some 20 dB higher than expected.

*Pioneer 8*.—Under an overcast sky, liftoff occurred at 1408:00 GMT, December 13, 1967. The flight appeared to be on time until 480 sec into the flight, when the African Destruct Line was crossed 6 to 8 sec later than predicted. At DSS-51 (Johannesburg), only one-way downlink contact was made to check the spacecraft status, which was normal. Because of the short pass and excessive tracking rates at Johannesburg caused by the location of the trajectory, DSS-41 (Woomera) was considered the primary station for first acquisition. Woomera rise and acquisition were at 1455:42. Two-way lock was established at 1510:52. Telemetry indicated that the Type-I orientation had been completed successfully. The first command to the spacecraft was sent at 1535.

A special third-stage telemetry system was flown on this mission. It provided better data on the events from third-stage spinup through spacecraft separation. The third stage proved difficult to track because it apparently began tumbling after spacecraft separation. The parking orbits given in table 3-5 were computed from Antigua data. Predicts for DSS-51 and DSS-41 were also generated from Antigua data with the addition of nominal third-stage burn parameters.

*Pioneer 9*.—Liftoff occurred at 0946:29, November 8, 1968. At 0948:40, DSS-71 (Cape Kennedy) and ETR station reported they had lost the

TABLE 3-5.—Earth Parking Orbit Parameters

| Parameter         | Pioneer 6 |         | Pioneer 7 |         | Pioneer 8 |        | Pioneer 9 |        |
|-------------------|-----------|---------|-----------|---------|-----------|--------|-----------|--------|
|                   | Nominal   | Actual  | Nominal   | Actual  | Nominal   | Actual | Nominal   | Actual |
| Eccentricity      | 0.07632   | 0.07181 | 0.05883   | 0.05479 | 0.0213    | 0.0139 | 0.0424    |        |
| Inclination (deg) | 30.168    | 30.196  | 32.915    | 33.005  | 32.91     | 32.90  | 32.9      | 32.876 |
| Period (min)      | 101.375   | 100.604 | 97.6      | 97.4    |           |        | 98.4      | 98.1   |
| Apogee (n. mi.)   | 743.1     | 704.8   | 533       | 552     | 324       | 267    | 502       | 525    |
| Perigee (n. mi.)  | 150       | 149.1   | 145       | 137     | 165       | 166    | 203       | 202    |

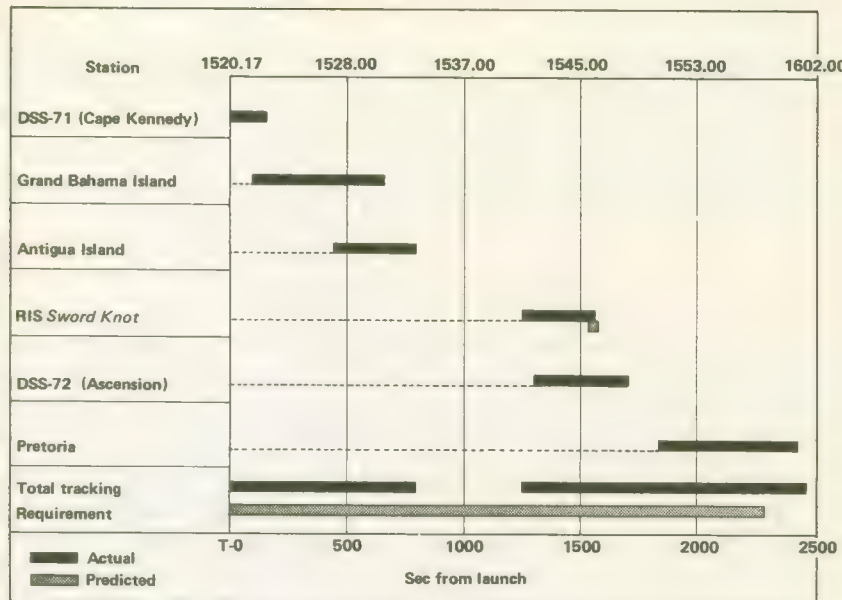


FIGURE 3-10.—Pioneer-7 tracking coverage along the ETR.

spacecraft's S-band signal. The supposition was that the vibration of the launch had thrown the spacecraft into a nonstandard position, but a subsequent investigation failed to determine the exact cause. At 1012:32, DSS-51 (Johannesburg) reported a momentary signal; this was about 10 min later than the predicted acquisition time, and the signal was 16 dB low. Two-way lock was established at 1030:18. The first command was sent at 1045:23. The spacecraft transmitter power level later rose to normal levels.

Cape Kennedy radar coverage terminated early in order to provide a phasing slot for another radar. The Antigua radar lost track for 5 sec due to an unexplained power fluctuation. Generally, though, the radar coverages exceeded expectations.

The vhf telemetry support also exceeded predictions. Grand Bahama lost 18 sec of data when the antenna slewed away from the vehicle during a switchover. The *Coastal Crusader* could not produce real-time data on two VHF links due to the failure of a recorder.

*Pioneer E.*—Following a brief thunder shower, liftoff took place at 2159:00, August 27, 1969. Mainland radars followed the flight through destruct, which was commanded at 482 sec, to 1136 sec. Radars at ETR stations 3 and 7 provided additional coverage from 85 to 1257 sec. Other ETR downrange stations did not acquire the vehicle. The launch ve-

hicle, the Pioneer-E spacecraft, and the TETR-C impacted in the Atlantic at  $11^{\circ}30.23'N$ ,  $55^{\circ}42.1'W$ .

During the period following main engine cutoff, the radars tracked something that veered off at a  $45^{\circ}$  angle to the right of the vehicle trajectory. The identity of this object could not be determined.

Analysis of telemetry from ETR stations, DSS-71 (Cape Kennedy), and downrange MSFN stations indicated that the spacecraft was operating normally at the time the destruct command was sent.

### SPACECRAFT PERFORMANCE

The spacecraft were nearly dormant during the so-called "powered-flight" stages. About 5 min before launch, the spacecraft was put on internal power, that is, the battery. The spacecraft low-gain antenna 2 was connected to the transmitter driver rather than one of the TWTs in order to conserve battery power. Consequently, only about 40 mW of signal power was broadcast until the TWT was switched on. Housekeeping telemetry during launch was set at 64 bps—a relatively low rate—in order to increase the likelihood of obtaining good diagnostic data at a low power level if the TWT failed to turn on properly.

As soon as the spacecraft separated from the Delta third stage, the booms and Stanford antenna automatically deployed and locked into position. Power was applied to the TWT and the orientation subsystem, again automatically. The Type-I orientation maneuver then began and proceeded in the manner described in Ch. 4, Vol. II. When the low-gain antenna was switched from the transmitter driver to the TWT, the telemetry signal from the spacecraft faded for about a minute while the TWT warmed up. By the time Johannesburg rose, the spacecraft was transmitting about 7W. It was fully operational and had completed one Type-I orientation maneuver. Upon acquisition, the first commands generally sent were: (1) switch to 512 bps, and (2) repeat the Type-I orientation maneuver.

Pioneers 6 through 9 successfully went through the above sequence of events with the exception of Pioneer 9 which experienced the switching problem described earlier.

## CHAPTER 4

# From DSS Acquisition to the Beginning of the Cruise Phase

### SEQUENCE OF EVENTS

THE PERIOD OF SEVERAL HOURS between the initial acquisition of the spacecraft by one of the DSSs and the beginning of the cruise phase encompassed several events crucial to the success of the mission:

- (1) Two types of orientation maneuvers
- (2) Experiment turn ons
- (3) The first thorough assessment of spacecraft operational condition in flight
- (4) The first passes over all participating DSSs.

Prior to DSS acquisition, the spacecraft automatically went through the Type-I orientation maneuver. This event was started by micro-switches triggered when the deploying appendages locked into position. By the time the spacecraft was acquired by DSS, spacecraft power was on and the transmitter was sending telemetry. In addition, the spin axis was almost perpendicular to the Sun line by virtue of the automatic Type-I orientation maneuver.

The first command dispatched after a two-way lock had been established was usually that which changed the telemetry bit rate from Format C, 64 bps, to Format C, 512 bps. Next, a command initiating the Type-I orientation maneuver was sent to refine the alignment made automatically prior to acquisition and, more important, to preclude the possibility that the automatic orientation sequence may have terminated prematurely. The third in the series of preparatory commands was Undervoltage Protection On, but this was sent only if analysis by the Spacecraft Analysis and Command (SPAC) Group (located at the SFOF during launch) was confident that the spacecraft power level was normal and that the spacecraft was operating properly. Following the spacecraft's execution of Undervoltage Protection On, the Pioneer was ready for experiment turn on and the all-important Type-II orientation maneuvers.

#### Experiment Turn-On

The Pioneer scientific instruments were turned on by command during the first pass over Johannesburg (DSS-51). The planned

sequences for the Block-I and Block-II spacecraft are indicated below. Usually, experiment turn-ons were separated by other spacecraft status commands, instrument calibration commands, and, in the case of Pioneer 6, the partial Type-II orientation commands. The actual events are described later for each mission in chronological order.

#### Experiment Turn-On Sequences

| Block I                    | Block II                   |
|----------------------------|----------------------------|
| Ames plasma                | Goddard cosmic dust        |
| Goddard magnetometer       | Ames plasma                |
| MIT plasma                 | Ames magnetometer          |
| Chicago cosmic ray         | TRW electric field         |
| GRCSW cosmic ray           | GRCSW cosmic ray           |
| Stanford radio propagation | Stanford radio propagation |

The reasoning behind the above sequences was that those instruments measuring important near-Earth phenomena, particularly in the transition region as the spacecraft passed through the magnetosphere, should be turned on and calibrated first. Generally, about 20 min were scheduled between each experiment turn on. The Stanford Radio Propagation Experiment, which required the transmission of signals from Stanford University at Palo Alto, was usually not turned on until just before the first Goldstone (DSS-12) pass.

#### Orientation Maneuvers

The purpose of the Type-II maneuver was the rotation of the spacecraft spin axis about the Sun line until the spin axis was perpendicular to the plane of the ecliptic. As explained more fully in Vol. II, this maneuver was normally controlled from Goldstone where the Operations Orientation Director (OOD) maximized the telemetry signal received from the Pioneer's high-gain telemetry antenna. Generally, hundreds of Type-II orientation commands were relayed to the spacecraft, each giving rise to a pulse of gas from the orientation subsystem. Usually, there was some jockeying back and forth across the peak in the signal-strength-reception curve. On occasion, the normal Type-II orientation process was interrupted for another Type-I maneuver to remove any spin-axis misalignment inadvertently introduced by cross coupling during Type-II maneuvers. Often, orientation maneuvers were commanded even after the beginning of the cruise phase to "trim" spacecraft altitude and correct for drift, solar pressure effects, and other perturbations.

Preliminary trajectory analysis in the cases of Pioneers 6 and 9 indicated that the so-called "partial Type-II orientation" would be desir-

able early in the flight to preclude an unfavorable spacecraft orientation later in the flight. As discussed in Ch. 4, Vol. II, the low-gain omnidirectional antenna used for communication early in the flight had a very low gain within a 10° cone aft along the spin axis. During the partial Type-II orientation maneuver, the gas pulses torqued the spin axis sufficiently so that Goldstone antennas would not be looking up this cone at the spacecraft during the final Type-II orientation maneuver.

The partial Type-II orientation maneuvers were performed during the first passes of the spacecraft. For Pioneer 6, Johannesburg (DSS-51) was responsible for this special maneuver (table 4-1). But on the Pioneer-9 flight, it was decided to wait 4 hr until the spacecraft had been acquired by Goldstone (DSS-12), where the OOD and his team were already situated for the final Type-II orientation maneuvers, which customarily took place a pass or two later over Goldstone.

The final Type-II orientation maneuvers were always directed from Goldstone. Special equipment for this task as well as the OOD and his team were positioned here. The OOD began this maneuver when control was transferred to him from the Space Flight Operations Director (SFOD). His first commands were: (1) Format C, 512 bps, which provided maximum engineering telemetry to check spacecraft status and (2) Type-I orientation, to trim the orientation with respect to the Sun line. If all seemed to be going well, the command was given to reduce the engineering telemetry rate to 16 bps so that no data would be lost if the high-gain antenna was switched on and it happened to have Goldstone in one of the minima of its lobed gain pattern. (See antenna patterns in Ch. 4, Vol. II.) Next, the OOD commanded the spacecraft

TABLE 4-1.—*Deep Space Stations Participating in Orientation Maneuvers*

| Orientation maneuvers                   | Pioneer 6           | Pioneer 7 | Pioneer 8 | Pioneer 9 |
|---|---------------------|-----------|-----------|-----------|
| Initial acquisition                     | DSS-51 <sup>a</sup> | DSS-51    | DSS-41    | DSS-51    |
| Initial Type-I orientation <sup>b</sup> | DSS-51              | DSS-51    | DSS-41    | DSS-51    |
| Partial Type-II orientation             | DSS-51              | —         | —         | DSS-12    |
| Final Type-II orientation               | DSS-12              | DSS-11    | DSS-12    | DSS-12    |

<sup>a</sup> DSS-11, Goldstone; DSS-2, Goldstone; DSS-41, Woomera; DSS-51, Johannesburg.

<sup>b</sup> The first Type-I orientation is automatic and occurs before and during DSS acquisition.

to switch from the low-gain omnidirectional antenna to the high-gain directional antenna. This antenna had to be used if telemetry was to be received from deep space. The spacecraft was now ready for the final Type-II orientation commands.

By direction of the OOD, blocks of Type-II orientation commands were transmitted to the spacecraft. Because each separate command released a single gas pulse which torqued the spin axis only about  $0.3^\circ$ , blocks of up to 30 commands had to be used to achieve noticeable changes in the signal strength detected by the Goldstone station. In practice, each block of commands was followed by a short period of analysis, during which primary interest was focused on the plot of received signal strength versus the number of Type-II commands transmitted. As further blocks of commands were sent, the plots would show definite minima and maxima characteristic of the Pioneer high-gain antenna. The major lobe was usually easy to recognize by its size. Nevertheless, further commands were issued beyond this peak until the signal strength had been roughly halved. This procedure insured that the main lobe had truly been found, and it permitted the OOD's engineers to compute the number of commands between the maximum and half-power point. It was then possible to return to the maximum by transmitting a fixed number of commands.

Interspersed with the above sequence of blocks of commands were occasional Type-I orientation commands which, as mentioned earlier, were necessary to reduce the effects of cross-coupling between the two degrees of freedom. These Type-I maneuvers were commanded only at maxima in the antenna pattern where the spacecraft telemetry could be safely switched to 512 bps. Only at 512 bps was status data transmitted faster than the automatically generated Type-I gas pulses.

A few reversals of the Type-II torquing sequence were also commanded to insure the OOD that the entire orientation subsystem was working satisfactorily. It would have been disastrous to reach the half-power point on the other side of the signal-strength maximum and find that backtracking to the maximum was impossible.

Usually, the Type-II maneuvers were interrupted several times for a half hour or more in order to assess the performance of the scientific instruments. Format B and the highest bit rate commensurate with the spacecraft signal strength were commanded during these periods.

Upon the successful completion of the Type-II orientation maneuver, the Type-I orientation command was given once more. Then, the spacecraft was placed in its cruise mode, with a telemetry bit rate of 512 bps, Format B. Spacecraft status was checked a final time, and, to terminate the maneuvers, the OOD sent the Orientation Power Off command. The

OOD then transferred mission control to SFOD at the SFOF, and the cruise phase began.

The Pioneer orientation maneuvers were unique. Despite considerable initial skepticism about the feasibility of the whole concept, the maneuvers proved relatively easy to carry out and control in practice. Other small and moderately sized spacecraft, American and foreign, have adopted similar altitude-control strategies.

### Predicts

Upon acquisition, the SPAC group at the SFOF in Pasadena began to generate orbital data. The first orbit based on data from the first acquisition station was usually available about 1.5 hr after launch. Orbital data were teletyped to Ames Research Center where station look angles were computed for DSS-41, DSS-51, and DSS-12. Earth-spacecraft-Sun angle computations were also computed and teletyped to the SFOD and the OOD at Goldstone.

## PIONEER OPERATIONS—ACQUISITION TO CRUISE PHASE

The Pioneer flights generally adhered to the scenario just described. Each, however, was different in several ways. The best technique to describe these specific differences and, in addition, convey the flow of events, is by chronologically recording the highlights of each flight from DSS acquisition to the beginning of the cruise phase. Tables 4-2 to 4-5 assemble these important events. For the purpose of illustration, Pioneer 6 events are presented in more detail than the other three flights.

TABLE 4-2.—*Highlights of the Pioneer-6 Flight:  
Acquisition to Cruise*

| Date,<br>GMT  | Event and remarks  |
|---------------|--|
| Dec. 16, 1965 |  |
| 0759          | Initial downlink acquisition by DSS-51.  |
| 0800          | First telemetry signals indicated that the Type-I orientation was in progress and spacecraft normal.   |
| 0804          | Type-I orientation completed. An estimated $386 \pm 6$ gas pulses were required, corresponding to a rotation of $64.1^\circ \pm 1.0^\circ$ .   |
| 0813          | Type-I orientation command given. No gas pulses indicated by telemetry inferring that the automatic Type-I maneuver had been successful.   |
| 0824          | Undervoltage Protection On command transmitted.  |
| 0825          | Initial downlink acquisition at DSS-42.  |
| 0835          | The signal received from the spacecraft began to fade rapidly and "lock" was lost by the computer. Telemetry indicated that a signal was present in both receivers. Although both spacecraft failure and poor spacecraft orientation |

TABLE 4-2.—*Highlights of the Pioneer-6 Flight:  
Acquisition to Cruise—Continued*

| Date,<br>GMT  | Event and remarks   |
|---------------|---|
|               | were suspected at first, the problem was finally attributed to a normal but unforeseen phenomenon of coherent operations.   |
| 0851          | First of 33 counterclockwise Type-II orientation commands sent from DSS-51 as part of partial Type-II orientation maneuver. No change in signal strength was noted. The inference from the spacecraft antenna pattern was that the spin axis had changed either from 125° to 135° or from 60° to 70° with respect to the North Ecliptic Pole. |
| 0914          | Ames Plasma Experiment turned on.   |
| 0931          | First of 32 additional Type-II orientation commands sent.   |
| 0957          | MIT Plasma Experiment turned on. Received signal strength increased 2 dB, assuring the OOD that the first change had been from 125° to 135°. With the spacecraft axis now between 140° and 150°, the partial Type-II orientation maneuver was terminated.   |
| 1013          | Format-A command executed.  |
| 1031          | Chicago Cosmic-Ray Experiment turned on.  |
| 1050          | GRCSW Cosmic-Ray Experiment turned on.  |
| 1110          | Stanford Radio Propagation Experiment turned on.  |
| 1130          | Type-I orientation command sent. Single gas pulse indicated.  |
| 1255          | Spacecraft penetrated magnetosphere 12.8 radii from Earth.  |
| 1710          | Earth-solar wind bow shock penetrated at 20.5 Earth radii.  |
| 1912          | First Stanford radio propagation data on teletype.  |
| 2003          | First acquisition by DSS-12.  |
| 2100          | First command link transfer, DSS-51 to DSS-12.  |
| Dec. 17, 1965 |   |
| 2008          | Second acquisition by DSS-12.   |
| 2120          | Control transferred from SFOF to DSS-12 for completion of Type-II orientation maneuver. Also, first data sent to experimenters from Ames Tape Processing Station.   |
| 2128          | Type-I orientation command sent. Seven gas pulses counted.  |
| 2130          | Telemetry changed to 16-bps mode.   |
| 2137          | Spacecraft commanded to Format C, 16 bps.   |
| 2158          | Spacecraft transmitter switched to high-gain antenna.   |
| 2210          | Block of 33 counterclockwise Type-II orientation commands sent 1 min apart.   |
| 2250          | Telemetry bit rate changed to 512 bps.  |
| 2254          | Type-I orientation command given to correct for cross coupling. Four pulses noted from spacecraft telemetry.  |
| 2321          | Block of 67 counterclockwise Type-II orientation commands dispatched 1 min apart.   |
| Dec. 18, 1965 |   |
| 0031          | Ten more Type-II commands sent.   |
| 0048          | Four gas pulses noted when Type-I orientation sequence was repeated.  |
| 0114          | Block of 15 counterclockwise Type-II orientation commands sent.   |
| 0137          | Only one gas pulse counted when Type-I orientation sequence was repeated.   |

**TABLE 4-2.—*Highlights of the Pioneer-6 Flight:  
Acquisition to Cruise—Concluded***

| Date,<br>GMT | Event and remarks  |
|--------------|--|
| 0144         | Block of 3 clockwise Type-II orientation commands sent to assure OOD that backtracking to maximum antenna lobe was possible. |
| 0148         | Open-ended block of counterclockwise Type-II orientation commands started. A total of 27 were sent.                          |
| 0220         | Three gas pulses noted as Type-I orientation sequence was repeated.  |
| 0223         | Block of 10 clockwise Type-II orientation commands sent.   |
| 0345         | Second block of 10 clockwise Type-II orientation commands sent.  |
| 0409         | One gas pulse noted when Type-I orientation sequence was repeated.   |
| 0411         | Orientation Electronics Off command executed.  |
| 0413         | Format-A command executed.   |
| 0424         | Mission Control returned to SFOF. Orientation maneuvers over; cruise phase began.  |

**TABLE 4-3.—*Highlights of the Pioneer-7 Flight:  
Acquisition to Cruise***

| Date,<br>GMT  | Event and remarks  |
|---------------|--|
| Aug. 17, 1966 |  |
| 1548          | Initial acquisition by DSS-51. First telemetry indicated that Type-I orientation maneuver was in progress and that the spacecraft was functioning normally.          |
| 1557          | Coherent, two-way lock established by DSS-51.  |
| 1600          | Bit rate commanded from 64 to 512 bps.   |
| 1611          | First acquisition by DSS-42.   |
| 1621          | Signal received from spacecraft dropped rapidly.   |
| 1625          | Due to ground station problems at DSS-51, the command link was transferred to DSS-42. Apparently, DSS-51 was tracking Pioneer 7 on a sidelobe of the ground antenna. |
| 1702          | Spacecraft entered Earth's shadow as indicated by bus-voltage telemetry.   |
| 1739          | Spacecraft emerged from Earth's shadow.  |
| 1746          | Battery on spacecraft turned off for 11 min due to high charging current overheating partially discharged battery.   |
| 1810          | Undervoltage Protection On command transmitted.  |
| 1815          | Experiment turn ons began. Completed at 2015.  |
| Aug. 18, 1966 |  |
| 0426          | First acquisition by DSS-11. (DSS-12 was engaged in tracking other space-craft.)   |
| Aug. 19, 1966 |  |
| 0429          | Second acquisition by DSS-11. Type-II orientation maneuvers commanded from DSS-11 during second pass. Required 191 Type-II commands.                                 |

TABLE 4-4.—*Highlights of the Pioneer-8 Flight:  
Acquisition to Cruise*

| Date,<br>GMT  | Event and remarks   |
|---------------|---|
| Mar. 29, 1968 |   |
| 1443          | DSS-51 acquired first spacecraft telemetry. Telemetry indicated that all spacecraft subsystems were performing normally.  |
| 1455          | Initial acquisition at DSS-41.  |
| 1457          | DSS-41 acquired one-way lock.   |
| 1535          | Spacecraft commanded from 64 to 512 bps.  |
| 1538          | Telemetry indicated periodic fluctuation in primary bus voltage.  |
| 1550          | Goddard Cosmic Dust Experiment turned on. By 2030, all experiments were on.<br>Orientation power turned on during third pass over DSS-12.   |
| April 1, 1968 |   |
| 1900          | Orientation power on.<br>Type-I orientation maneuver performed automatically. Twenty-eight gas pulses noted.  |
| 1945          | Type-I orientation maneuver commanded. Two valve pulses noted.  |
| 2000          | Another Type-I orientation maneuver commanded. Only one valve pulse this time.  |
| 2030          | Type-II orientation counterclockwise command sent. No valve pulse recorded.   |
| 2045          | Type-II orientation clockwise command sent. One valve pulse recorded, as expected.  |
| 2100          | Again a counterclockwise valve pulse was attempted, and again the telemetry showed that none actually occurred.   |
| 2115          | Type-II orientation counterclockwise command sent through other spacecraft decoder. Still the valve did not pulse. The implication was that the Sun-sensor thresholds had degraded just as they had on Pioneers 6 and 7 despite the thicker cover glasses tried on Pioneer 8. (See Ch. 4, Vol. II.) |
| 2130          | Type-I orientation command dispatched. Telemetry indicated a single valve pulse.  |
| 2145          | Command sent to turn off orientation power and enter cruise mode.   |

TABLE 4-5.—*Highlights of the Pioneer-9 Flight:  
Acquisition to Cruise*

| Date,<br>GMT | Event and remarks   |
|--------------|---|
| Nov. 8, 1968 |   |
| 1012         | Momentary signal picked up at DSS-51.   |
| 1024         | Initial acquisition by DSS-51. Acquisition delayed by a malfunctioning driver. Predicts were also late. First telemetry (one-way mode) indicated spacecraft systems were all performing normally. |
| 1030         | Two-way coherent mode established between DSS-51 and spacecraft.  |
| 1045         | Spacecraft commanded to switch from 64 to 512 bps.  |

TABLE 4-5.—*Highlights of the Pioneer-9 Flight:  
Acquisition to Cruise—Concluded*

| Date,<br>GMT  | Event and remarks  |
|---------------|--|
| 1046          | Type-I orientation maneuver commanded.   |
| 1047          | Three-way lock with DSS-51 and DSS-42 established.   |
| 1100          | Undervoltage Protection On command sent.   |
| 1130          | First experiment turned on. On the first pass over DSS-12, a partial Type-II orientation maneuver was performed. A total of 58 counterclockwise pulses were transmitted, rotating the spacecraft spin axis an estimated 15°.   |
| Nov. 9, 1968  |  |
| 2215          | First of the final Type-II orientation commands were transmitted from DSS-12. A total of 250 counterclockwise pulses were commanded before the signal maximum was reached. Three test clockwise pulses were initiated to insure that the return to signal maximum could be made. A total of 26 clockwise pulses brought the spin axis back to maximum after the 6.7-dB point beyond the maximum was reached. |
| Nov. 10, 1968 |  |
| 0600          | Type-II orientation complete. Pioneer 9 enters cruise mode.  |



## CHAPTER 5

# Spacecraft Performance During the Cruise Phase

THE PIONEER SPACECRAFT WERE DESIGNED for a minimum life of 6 months each, and each greatly exceeded this goal. In fact, each spacecraft functioned well for several years, confirming in their longevities the design decisions made by Ames and TRW Systems in the early 1960's. This chapter is concerned with spacecraft performance in orbit around the Sun: How did each subsystem perform in practice? What components and design features finally encountered trouble? This introspection is well worthwhile because the basic Pioneer design philosophy has proved so successful that much of it is being applied to other spacecraft destined for the outer planets, such as the Jupiter fly-by probes, Pioneers F/G, which require years rather than months of successful operation.

As a chronological framework for the following discussion of spacecraft performance, table 5-1 provides a list of major engineering and scientific events during the cruise phase. An engineering event, of course, is one involving subsystem performance; say, the failure of a key component. Because improvements in ground support equipment have been so critical to extending Pioneer operation to greater and greater distances, some of these changes are also presented in the chronology. A scientific event might be a solar flare or the passing of the spacecraft behind the Sun. Thus, table 5-1 also identifies astronomical events of significance to the next chapter which deals with scientific results.

### PIONEER-6 PERFORMANCE

The nominal Pioneer-6 mission extended from the launch date (December 16, 1965) to June 13, 1966—a total of 180 days. However, because spacecraft performance at the end of 180 days continued to be good and the 210-ft dish at DSS-14 became available for long distance tracking, the mission was extended. (All subsequent Pioneer missions were also extended, as spacecraft lifetimes greatly exceeded the 180-day design level.)

Although each Pioneer surpassed the goals set for it, each of the spacecraft provided its share of minor problems. On Pioneer 6, for example,

TABLE 5-1.—*Major Events During the Cruise Phases  
of Pioneers 6, 7, 8, and 9*

| Date, GMT        | Event  |
|------------------|--|
| <b>Pioneer 6</b> |  |
| Dec. 23, 1965    | First Goddard magnetometer flip command executed.  |
| Dec. 24, 1965    | First Duty Cycle Store mode commanded due to first lack of DSS coverage.   |
| Jan. 3, 1966     | First acquisition by a DSS station without GOE equipment; DSS-61 (Robledo, Spain).   |
| Jan. 13, 1966    | Spacecraft control shared between Ames and SFOF for the first time.  |
| Feb. 23, 1966    | Transfer of mission control to Ames completed.   |
| Mar. 2, 1966     | Inferior conjunction or syzygy, with spacecraft 1.84° below Sun as seen from Earth.  |
| Mar. 17, 1966    | Bit error rate at DSS-12 reaches $10^{-3}$ ; spacecraft bit rate reduced from 256 to 64 bps.   |
| Apr. 13, 1966    | Bit rate reduced from 64 to 16 bps. Pioneer 6 34.2 million km from Earth.  |
| Apr. 29, 1966    | Spacecraft receiver 2 switched to high-gain antenna.   |
| May 8, 1966      | Bit rate reduced from 16 to 8 bps. Pioneer 6 55.3 million km from Earth.   |
| May 20, 1966     | Perihelion; spacecraft 64 701 502 km from Earth, 121 821 430 km (0.814 AU) from Sun.   |
| June 4, 1966     | Type-I orientation maneuver; number of gas impulses indeterminate (4 to 10). Type-II orientation maneuver to confirm spacecraft altitude.      |
| June 9, 1966     | Type-II orientation maneuver for the purpose of attaining a more favorable spacecraft altitude for the extended mission. Battery switched off. |
| July 11, 1966    | Stanford radio propagation experiment turned off because spacecraft was too far away.  |
| Dec. 16, 1966    | Magnetometer flipped by command.   |
| Nov. 23, 1968    | Superior conjunction. Excellent scientific data acquired as spacecraft passes behind the Sun.  |
| Nov. 28, 1969    | First simultaneous tracking of Pioneers 6 and 7 in "radial-spiral" experiment.   |
| July 6, 1970     | Magnetometer data all zeros.   |
| Oct. 26, 1970    | First simultaneous tracking of Pioneers 6 and 8 in "radial-spiral" experiment.   |
| Oct. 30, 1970    | Bit rate of 64 bps now standard.   |
| May 19, 1971     | Pioneers 6 and 8 aligned with Earth.   |
| <b>Pioneer 7</b> |  |
| Aug. 25, 1966    | Magnetometer flipped by command for first time.  |
| Aug. 31, 1966    | TWT 2 switched in to replace erratic TWT 1.  |
| Sept. 20, 1966   | Syzygy, Pioneer 7 enters Earth's magnetic tail.  |
| Nov. 6, 1966     | Went to 64 bps because of high error rate.   |
| Jan. 19, 1967    | Lunar occultation pass from DSS-12.  |
| Mar. 16, 1967    | Type-II orientation maneuvers.   |

TABLE 5-1.—*Major Events During the Cruise Phases  
of Pioneers 6, 7, 8, and 9—Concluded*

| Date, GMT        | Event  |
|------------------|--|
| Mar. 21, 1967    | Bit-error rate of $10^{-8}$ reached with 85-ft antenna. Goldstone tracking continued using narrowed bandwidth and lowered noise temperatures.  |
| June 13, 1967    | Battery commanded off.   |
| Aug. 17, 1967    | Type-II orientation maneuvers.   |
| Jan. 23, 1968    | DSS test with linear polarization cone.  |
| Feb. 16, 1969    | Lack of Sun pulses noted in spacecraft telemetry. These returned later.  |
| May 7, 1969      | Undervoltage problems. (See text.)   |
| Nov. 10, 1969    | Aphelion.  |
| Nov. 28, 1969    | First simultaneous tracking of Pioneers 6 and 7 in "radial-spiral" experiment. Battery turned off.   |
| <hr/>            |  |
| <b>Pioneer 8</b> |  |
| Jan. 17, 1968    | Syzygy, Pioneer 8 in Earth's tail.   |
| Jan. 25, 1968    | Magnetometer flipped by command for first time.  |
| Jan. 27, 1968    | Spacecraft emerges from geomagnetic tail.  |
| Feb. 9, 1968     | Type-I and partial Type-II orientation maneuvers.  |
| Mar. 30, 1968    | Type-I and Type-II orientation maneuvers revealed that Sun-sensor D was inoperative. Battery turned off.   |
| June 27, 1968    | Another orientation maneuver attempt showed that Sun-sensors A, B, and C were also out of action.  |
| Sep. 21, 1969    | Battery commanded off.   |
| Jan. 20, 1970    | Began electromagnetic interference tests to determine whether Goddard cosmic-dust experiment was being affected by spacecraft.   |
| Oct. 26, 1970    | First simultaneous tracking of Pioneers 6 and 8 in "radial-spiral" experiment.   |
| May 19, 1971     | Pioneers 6 and 8 aligned with Earth.   |
| <hr/>            |  |
| <b>Pioneer 9</b> |  |
| Jan. 14, 1969    | Solar-array temperature on this inbound flight had begun rising, causing the primary bus voltage to decrease. Battery was disconnected.  |
| Jan. 30, 1969    | Inferior conjunction or syzygy.  |
| Feb. 5, 1969     | Special test using Type-I and Type-II orientation commands showed that the spacecraft orientation subsystem was working well, inferring that the Sun-sensor ultraviolet filters had solved the Sun-sensor degradation problem. |
| Apr. 8, 1969     | First perihelion at 0.754 AU, which was within the 0.8-AU design goal.   |
| Jan. 20, 1970    | Began electromagnetic interference tests to determine whether Goddard cosmic-dust experiment was being affected by spacecraft.   |
| Sep. 29, 1970    | Ames magnetometer turned off temporarily to eliminate 1.9-dB degradation of Stanford radio propagation experiment.   |
| Dec. 18, 1970    | Syzygy.  |

the gas leak in the orientation control subsystem caused some concern. The degradation of the Sun sensors plagued every Pioneer until Pioneer 9's ultraviolet filters finally solved the problem. Future designers of long-lived spacecraft should benefit from Pioneer experience; therefore, these summaries of engineering performance are organized on a subsystem basis.<sup>6</sup> Many of the observations concerning spacecraft design also apply to the rest of the spacecraft in the series.

### Orientation Control Subsystem

The initial Pioneer-6 orientation maneuvers have already been described in Ch. 4. The orientation control subsystem operated flawlessly during these maneuvers and also during the attitude adjustments made in June 1966 to prepare the spacecraft for the extended mission. The fact that these maneuvers were executed successfully at the end of nominal life indicated that the gas leak that had developed during the launch phase did not compromise the mission at all. The shape of the gas pressure curve drawn from telemetered data (fig. 5-1) implies that the gas leakage rate was proportional to a pressure less than the bottle pressure itself. The inference is that gas escaped through the relief valve or a poorly sealed nozzle valve. At the conclusion of the June 9, 1966, maneuver, the gas pressure was approximately 100 psi, and leakage was apparently near zero. A reconstruction of the Pioneer-6 spin rate is provided in table 5-2. Apparently the gas leak was responsible for slight changes in the spin rate.

### Thermal Control Subsystem

No problems arose with this subsystem; all temperatures were maintained well within the design limits. All temperature measurements gradually rose as the spacecraft approached perihelion 155 days after launch, falling slowly afterwards. Approximately one month after launch, predictions were made of spacecraft temperatures at 0.9 and 0.8 AU based upon known orbital conditions and the results of the thermal-vacuum tests. All except three parameters fell within 2.5 percent of the predictions (fig. 5-2). The nitrogen temperature was off 4 percent and the two Sun-sensor temperatures, 6 percent, at 0.814 AU. In addition, the upper part of the solar array ran at a higher-than-expected temperature. Minor discrepancies in spacecraft thermal-vacuum simulation and the protrusion of the Sun-sensor shields accounted for these larger-than-expected deviations.

<sup>6</sup>These performance summaries are based largely upon discussions in the TRW Systems final report: Pioneer Spacecraft Project, Final Project Report, Rept. 8830-28, Dec. 1969.

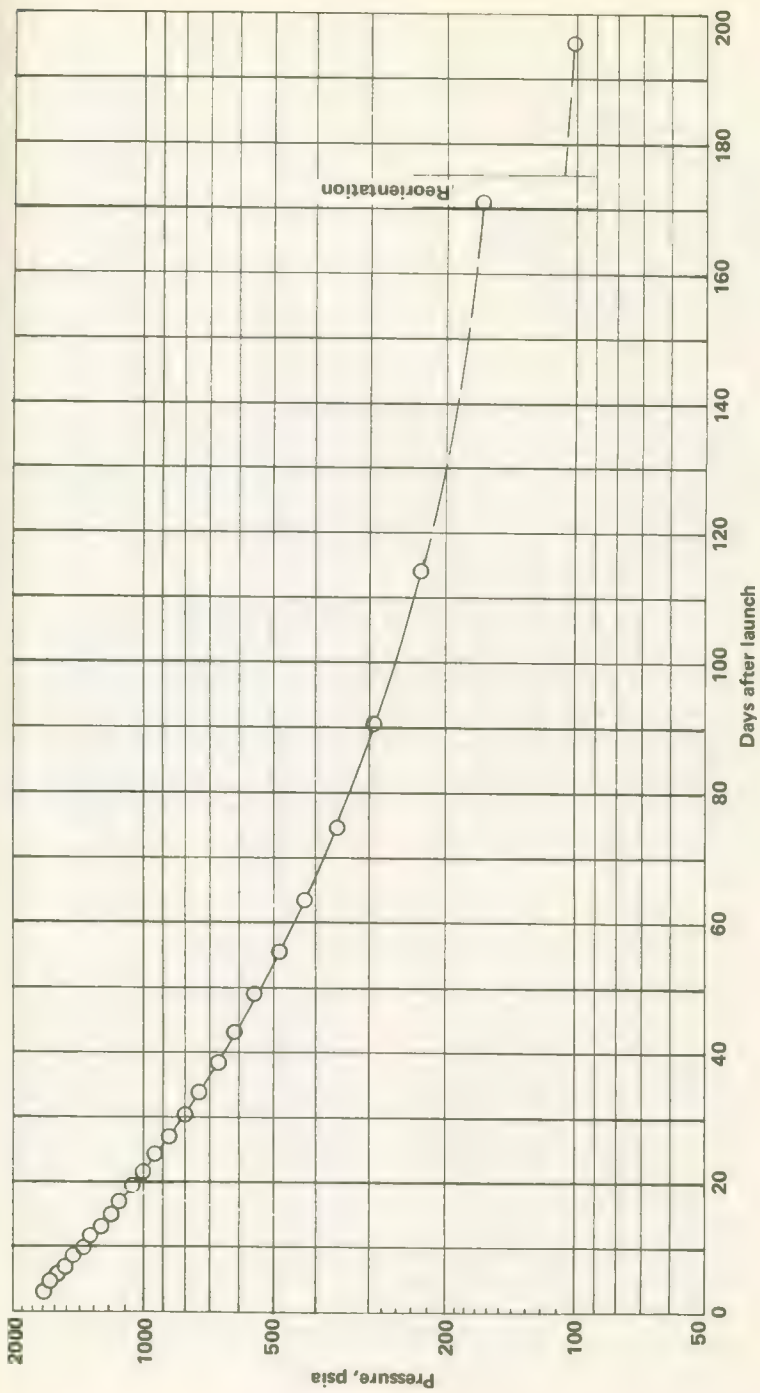


FIGURE 5-1.—Variation of Pioneer-6 nitrogen bottle temperature after initial orientation.

TABLE 5-2.—*Early Pioneer-6 Spin-Rate History*

| Stage                                  | Estimated spin rate, rpm |
|--|--------------------------|
| After boom deployment                  | 58.88                    |
| After the automatic Type-I orientation | 59.01                    |
| Before the partial Type-II orientation | 58.99                    |
| After the partial Type-II orientation  | 59.11                    |
| Before the June 1966 maneuvers         | 57.77                    |
| After the June 1966 maneuvers          | 51.79                    |

**Electric Power Subsystem**

Initial telemetry confirmed that the spacecraft power supply was operating normally (fig. 5-3). During the automatic Type-I orientation maneuver, the primary bus showed evidence of a ripple, but several groups of high-bit-rate, Format-C, telemetry data taken later in the revision did not indicate any ripple.

Right after boom deployment, the battery was recharged at an average 0.1 A. Fifteen min later, the charging current dropped to 0.024 A, and after 4 hr the battery was trickle charging or floating. On June 9, 1966, the battery was switched off the primary bus as a protective measure.

The spacecraft load history is summarized in table 5-3 and figure 5-4. Over the years the performance of the solar array has been degraded by solar particles, but this has not been considered a serious problem because of the favorable orbit.

TABLE 5-3.—*Pioneer-6 Electrical Load History*

| Day of flight | Spacecraft condition            | Volt | Primary bus Ampere | Watt <sup>a</sup> |
|---------------|---------------------------------|------|--------------------|-------------------|
| 1             | Experiments off, orientation on | 31.6 | 1.39               | 44.0              |
| 1             | Experiments on, orientation on  | 31.1 | 1.63               | 50.7              |
| 2             | Experiments on, orientation on  | 31.1 | 1.67               | 51.9              |
| 3             | Experiments on, orientation on  | 31.1 | 1.67               | 51.9              |
| 3             | Experiments on, orientation off | 31.1 | 1.63               | 50.7              |
| 39            | Experiments on, orientation off | 31.1 | 1.63               | 50.7              |
| 53            | Experiments on, orientation off | 30.4 | 1.67               | 50.8              |
| 156           | Experiments on, orientation off | 28.2 | 1.79               | 50.5              |
| 171           | Experiments on, orientation off | 28.8 | 1.79               | 51.5              |
| 171           | Experiments on, orientation on  | 28.8 | 1.83               | 52.6              |
| 208           | Experiments on, orientation off | 29.4 | 1.75               | 51.4              |

<sup>a</sup> Resolution was approximately  $\pm 2$  W.

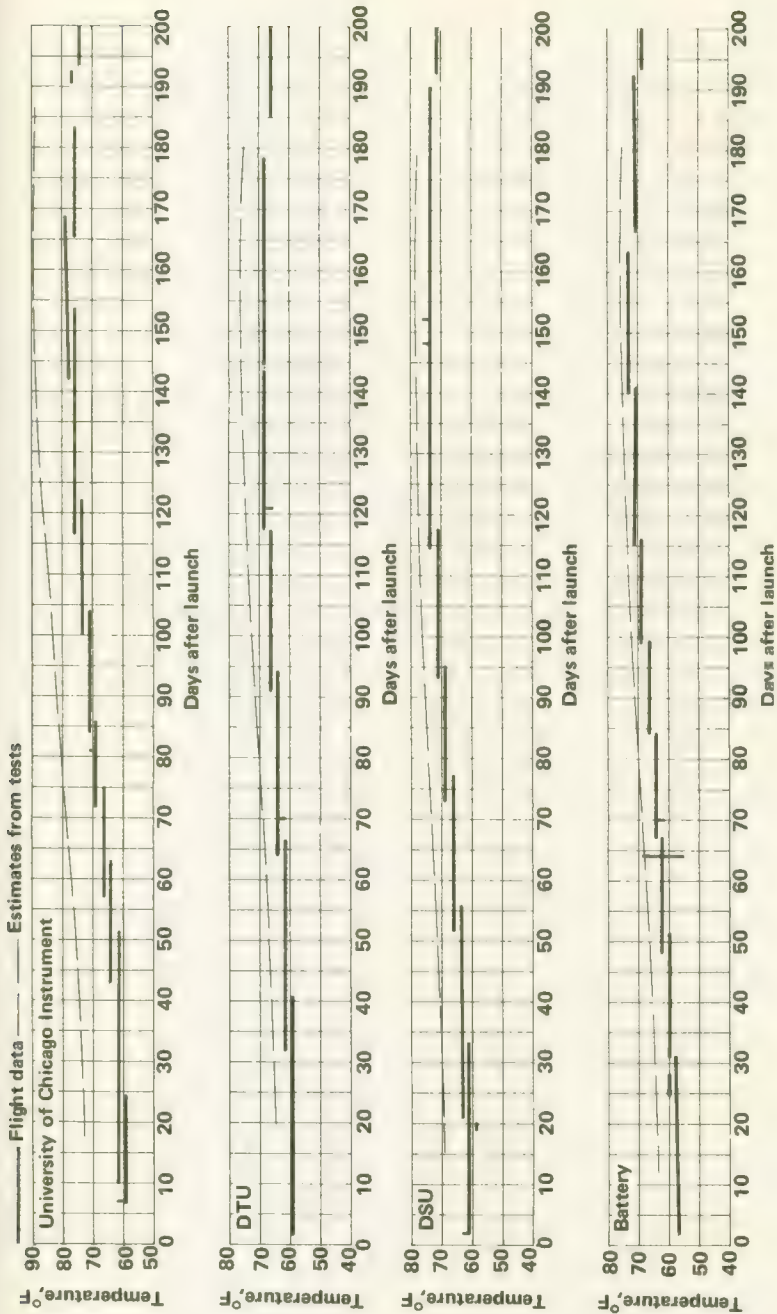


FIGURE 5-2.—Selected temperatures telemetered from Pioneer 6.

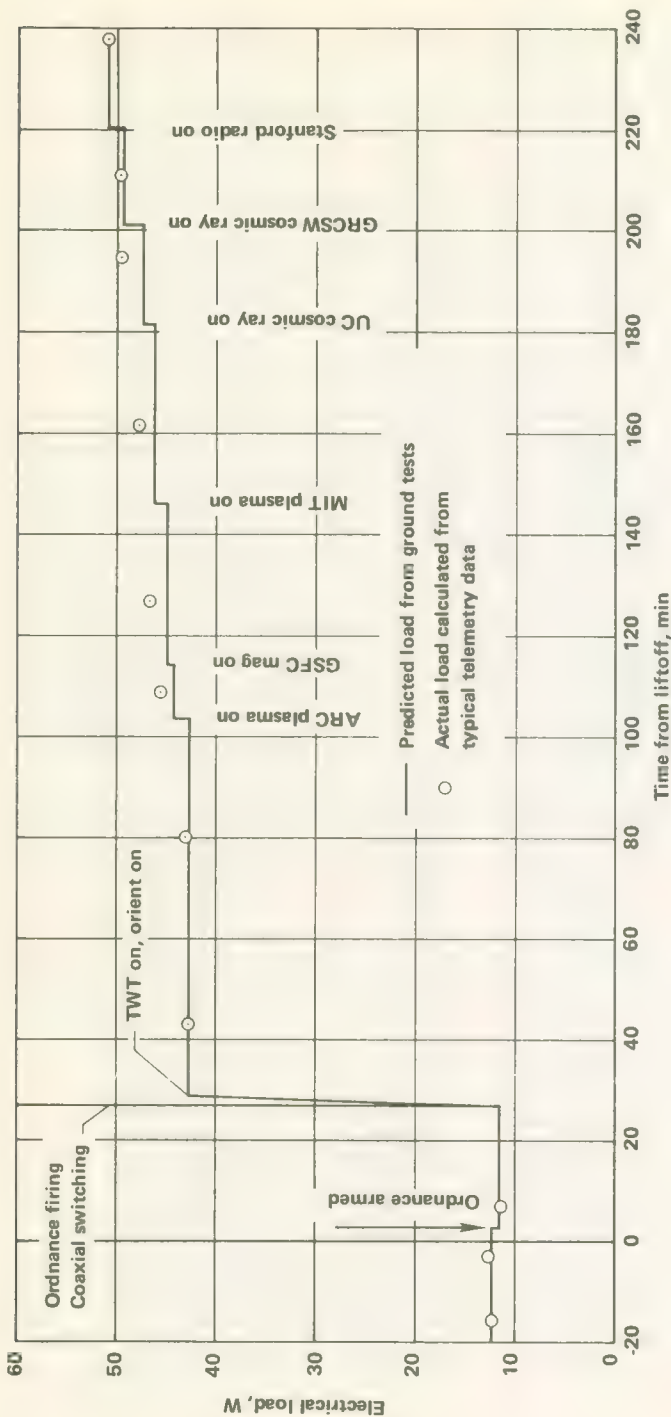


FIGURE 5-3.—Electrical loads on Pioneer 6 during the first 4 hr.

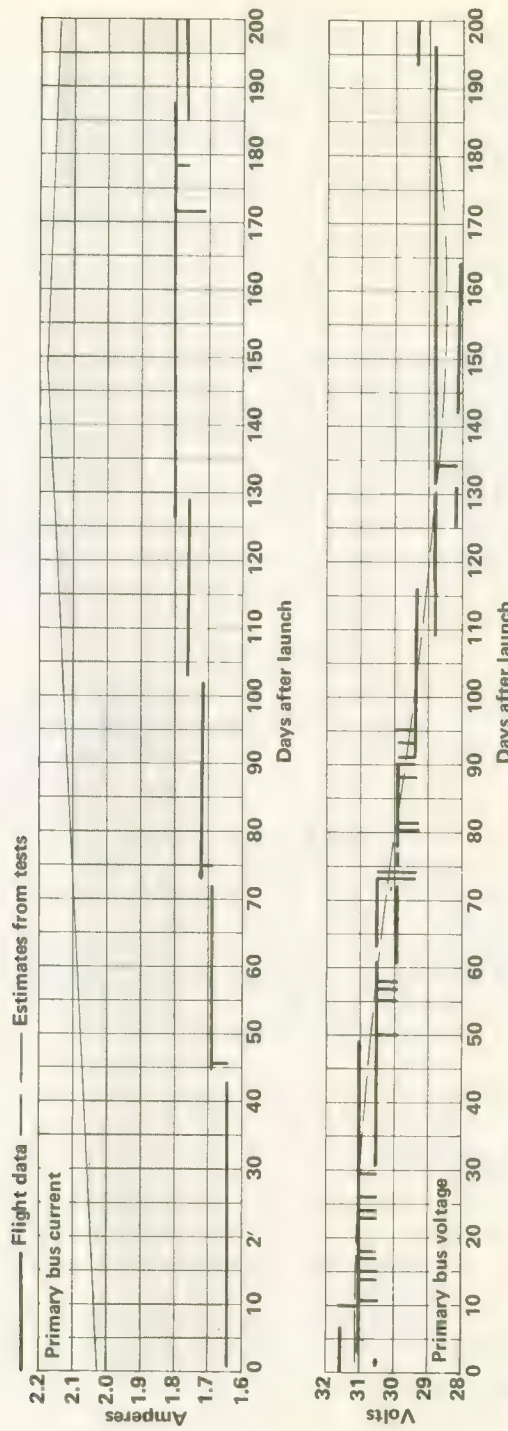


FIGURE 5-4.—Early history of the Pioneer primary bus voltage and current.

### Communications Subsystem

The performance of this subsystem was generally better than predicted during the first 6 months of flight (fig. 5-5). The data in table 5-4 substantiate this observation for the March 1966 period. Figure 5-1 shows the actual bit-error rate for the same period. During these 6

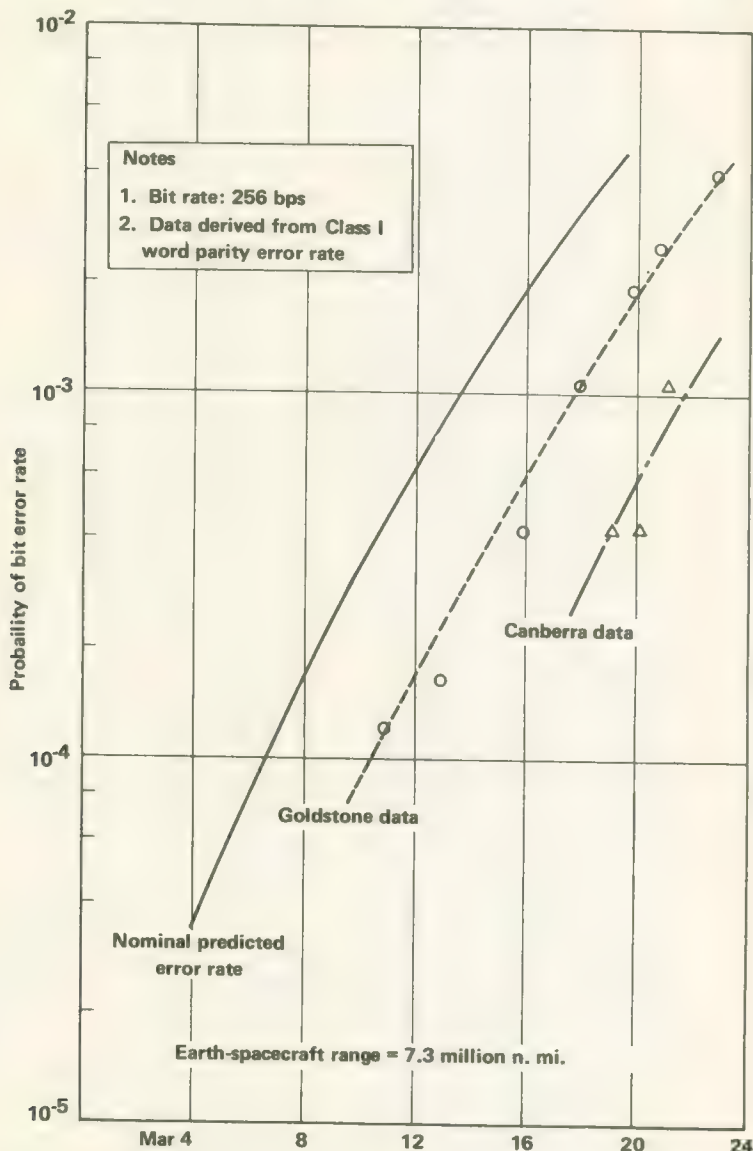


FIGURE 5-5.—Pioneer-6 telemetry bit-error rate during part of Mar. 1966.

months about 3500 commands from the Earth were executed satisfactorily by the spacecraft.

Housekeeping telemetry indicated a slight upward drift of the helix current of TWT 1 during the first 6 months. From 7 mA after initial stabilization, the current level crept up to between 7.50 and 7.75 mA during the first 175 days. In early 1971, the level had reached an 8.0-mA average. The TWT threshold lies within this range, but no further drift has been noted, and no degradation of TWT performance was apparent. The operating life of this TWT exceeded the life tests made by the manufacturer.

Inferior conjunction or syzygy occurred on March 2, 1966, at 0530 for Pioneer 6. As the spacecraft moved nearer the Sun, the bit-error rate rose as indicated in figure 5-6. The radio noise contributed by the Sun had, of course, adversely affected the signal-to-noise ratio and thus the bit-error rate. Signal deterioration was most severe within 2.5° of the Sun. By mid-1969, the high-gain antenna characteristics had degraded to a level equal to those of the low-gain antenna. A malfunction in receiver 2 prevented the use of channel 7.

### Structure Subsystem

The spacecraft structure subsystem functioned perfectly during separation and boom deployment. The stability of the signal received by the DSS stations showed further that the spacecraft was aligned and balanced with high precision.

### Data Handling Subsystem

During the first 6 months of operation, all of the various modes, formats, and bit rates were commanded for one reason or another (fig. 5-7). This subsystem responded properly to all commands. During the first 200 days of operation, the spacecraft procured nearly 3 billion bits of information for transmission to Earth (table 5-5). These bits fell in the following categories:

| Category                 | Bits, millions |
|--------------------------|----------------|
| Science data             | 2060           |
| Engineering data         | 160            |
| Parity check bits        | 370            |
| Data identification bits | 260            |
| Other                    | 20             |
| Total                    | 2870           |

About 96 percent of the scientific data were transmitted in Format A, less than 4 percent in Format B, and less than 0.03 percent in Format D.

TABLE 5-4.—*Pioneer-6 Communication Subsystem Performance*

| Date<br>(1966) | Time<br>after<br>launch<br>(days) | Representative received signal strength<br>at Deep Space Stations —dBm |        |        |        | Predicted<br>signal<br>strength,<br>—dBm |
|----------------|-----------------------------------|--|--------|--------|--------|--|
|                |                                   | DSS-11   | DSS-12 | DSS-41 | DSS-42 |  |
| March          |                                   |  |        |        |        |  |
| 8              | 82                                | 148.0  |        | 146.0  |        | 148.7                                    |
| 9              | 83                                | 149.3  |        | 149.0  |        | 148.9                                    |
| 10             | 84                                | 148.5  |        | 149.1  |        | 149.1                                    |
| 11             | 85                                |  |        |        | 150.0  | 149.3                                    |
| 12             | 86                                | 148.0  | 149.3  |        | 149.2  | 149.5                                    |
| 13             | 87                                | 149.2  | 149.5  |        | 149.5  | 149.7                                    |
| 14             | 88                                | 150.2  |        | 148.0  |        | 150.0                                    |
| 15             | 89                                |  | 149.0  |        |        | 150.2                                    |
| 16             | 90                                |  |        |        | 150.8  | 150.4                                    |
| 17             | 91                                |  |        | 150.6  | 150.5  | 150.6                                    |
| 18             | 92                                |  |        |        | 151.2  | 150.8                                    |
| 19             | 93                                |  |        | 153.3  |        | 151.0                                    |
| 20             | 94                                |  | 150.4  | 151.6  | 152.3  | 151.2                                    |
| 21             | 95                                |  | 150.7  |        | 151.1  | 151.4                                    |
| 22             | 96                                |  |        | 151.0  | 152.2  | 151.7                                    |
| 23             | 97                                |  |        | 152.0  | 153.5  | 151.9                                    |
| 24             | 98                                |  | 150.8  |        | 150.1  | 152.1                                    |
| 25             | 99                                |  | 152.7  | 152.2  |        | 152.3                                    |
| 26             | 100                               |  | 152.9  | 153.4  |        | 152.5                                    |
| 27             | 101                               |  | 152.5  |        | 153.8  | 152.7                                    |

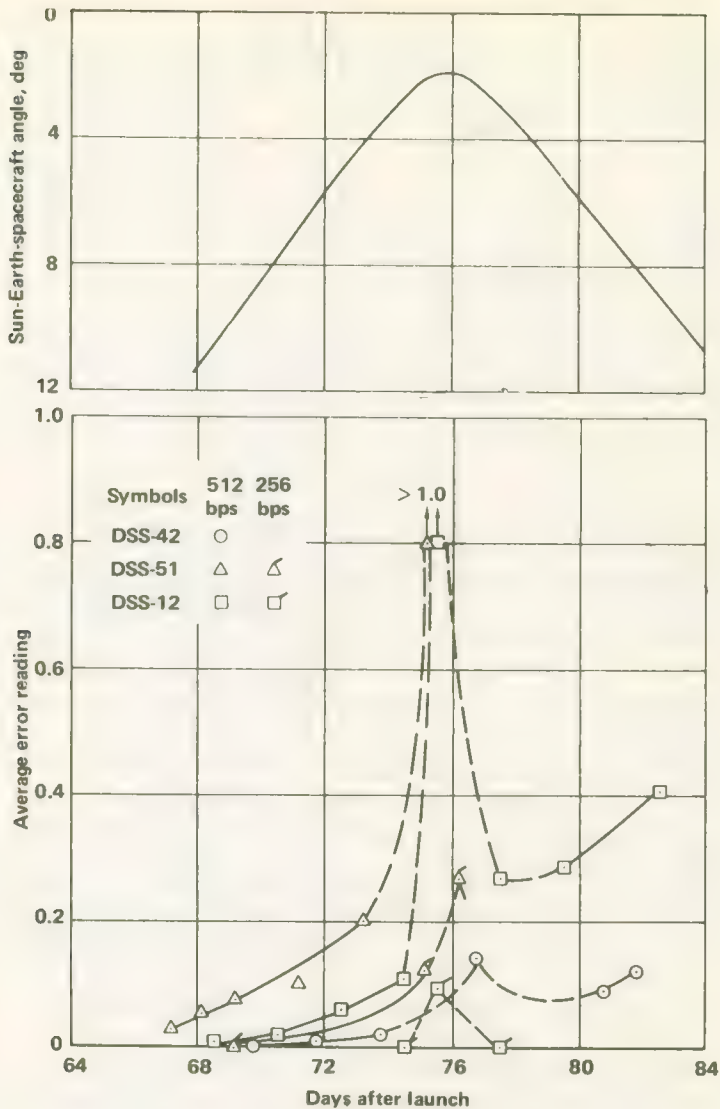


FIGURE 5-6.—The effect of proximity of Pioneer 6 to the Earth-Sun line of the telemetry data error rate.

The Real-Time Mode of data transmission was employed predominantly whenever DSS stations were available—in fact, almost all data received at Earth arrived via this mode. The Duty Cycle Store Mode provided about 18 percent of the data coverage, but because of intermittent sampling of stored data, this mode contributed less than 0.05 percent of the data received at Earth (fig. 5-8).

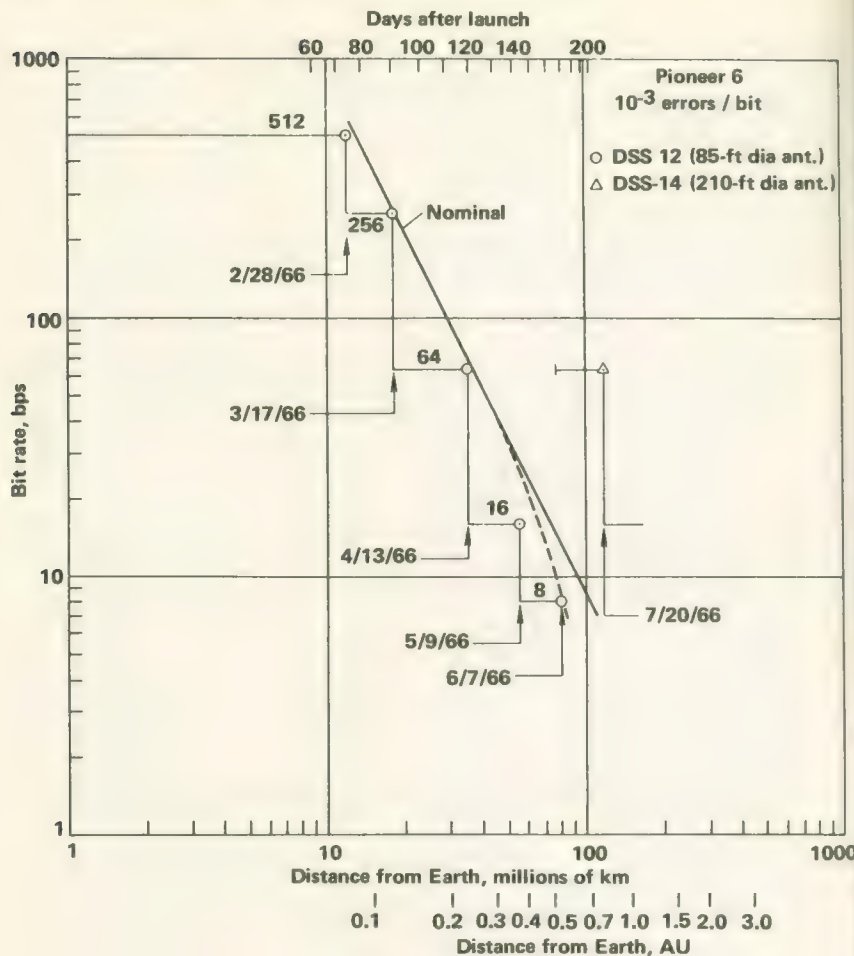


FIGURE 5-7.—Distance limitations for Pioneer-6 telemetry.

### PIONEER-7 PERFORMANCE

As the spacecraft began the long cruise phase, all spacecraft subsystems appeared to be operating normally. On August 25, 1966, however, TWT 1 began to display anomalous performance in the noncoherent mode of operation although operation was normal in the coherent mode. For example, the helix current jumped to 10.2 mA compared to the nominal 6.1 mA, and the temperature rose to 180° F against the normal 101° F. On August 31, 1966, Ames personnel decided to switch in TWT 2. This TWT behaved normally in every respect. Except for this difficulty, overcome by redundancy in the design, spacecraft performance during the basic 180-day mission was excellent. Some subsystem details follow.

TABLE 5-5.—Summary of Pioneer Data Acquisition Through 1969<sup>a</sup>

| Flight    | Time in solar orbit, months | Billions of bits acquired | DSN telemetry support, hrs | Books of printed data <sup>b</sup> |
|-----------|-----------------------------|---------------------------|----------------------------|------------------------------------|
| Pioneer 6 | 48                          | 3.030                     | 6330                       | 154                                |
| Pioneer 7 | 40                          | 2.260                     | 6271                       | 118                                |
| Pioneer 8 | 25                          | 6.032                     | 4455                       | 306                                |
| Pioneer 9 | 14                          | 6.518                     | 2275                       | 332                                |
| Total     | 127                         | 17.840 <sup>c</sup>       | 29173                      | 910                                |

<sup>a</sup> Adapted from Table 2, JPL Space Programs Summary 37-61, Vol. II, p. 13.

<sup>b</sup> Data printed in alpha-numeric form in 1000-page books.

<sup>c</sup> Of this total, 72 percent was scientific information, 6 percent engineering information, and 22 percent parity and data identification.

### Orientation Subsystem

The orientation subsystem was turned off at 1102 GMT, August 19, 1966, after completing the usual series of Type-I and Type-II orientation maneuvers. Telemetry indicated a gas leakage rate of about 9 cc/hr, which was well within the specified maximum of 15 cc/hr. Some of these telemetered data are listed below. By 1970, essentially all of the nitrogen had leaked away (table 5-6).

On February 16, 1969, telemetry from the spacecraft indicated that the spacecraft was no longer generating Sun pulses. The precise time of failure is unknown, but it was between February 9 and 16. The opinion was that Sun-sensor E had degraded during the 914 days of flight to the point where the Sun no longer activated it. This failure was, all Sun sensors except those of Pioneer 9 with ultraviolet filters. The lack of course, part of the ultraviolet degradation problem encountered with of a reference Sun pulse has negated the magnetometer experiment and precluded anisotropy measurements with the GRCSW experiment.

### Communication Subsystem

The performance of this subsystem has been excellent except for the difficulty of operating TWT 1 in the coherent mode, which was mentioned above. All five of the coaxial switches were activated once—successfully. Throughout the mission the redundant receivers were addressed occasionally; these, too, worked flawlessly. On January 4, 1967, receiver 2 was connected to the high-gain antenna. After January 10, all commands were transmitted to the spacecraft through this receiver.

It is interesting to compare the performance of the Pioneer-7 telemetry link with that of Pioneer 6. This is done in tables 5-7 and 5-8, by indicating the distance at which telemetry bit rate had to be reduced to keep the bit-error rate below  $10^{-3}$ .

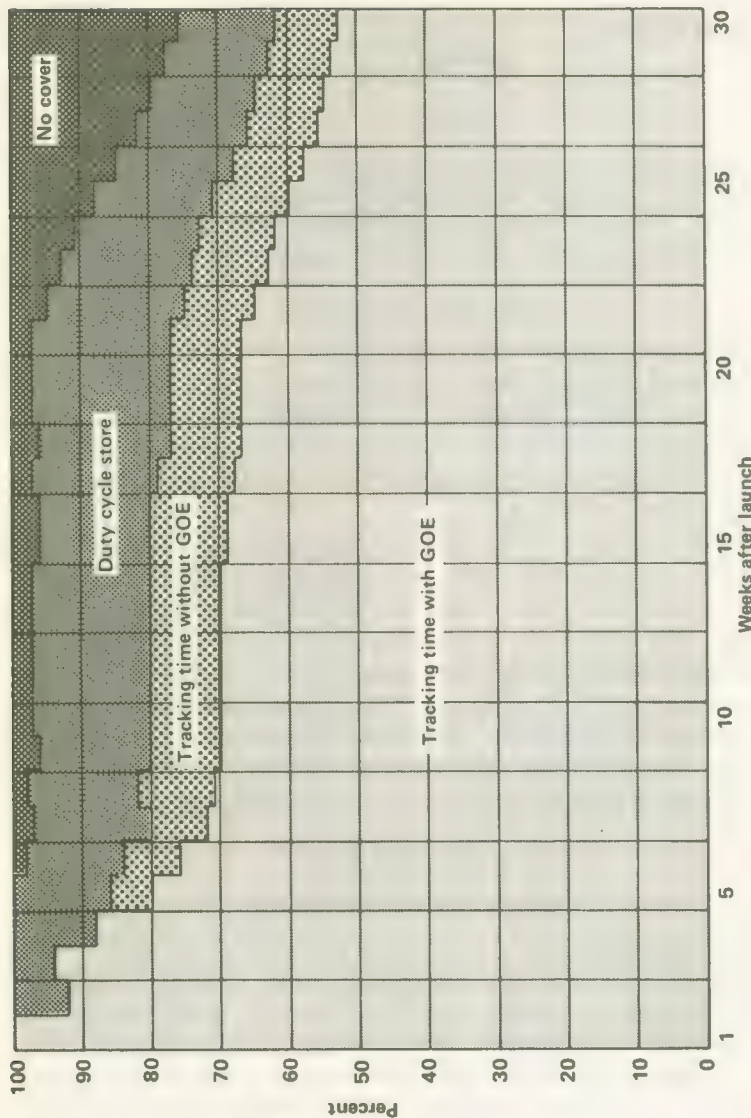


FIGURE 5-8.—Cumulative telemetry data coverage during the early part of the Pioneer-6 flight.

TABLE 5-6.—*Sun-Sensor E Degradation*

| Date          | Gas pressure,<br>psia | Bottle temperature,<br>°F |
|---------------|-----------------------|---------------------------|
| Aug. 19, 1966 | 2112                  | 26.3                      |
| Sept. 2, 1966 | 2112 to 2048          | 23.9                      |
| Oct. 5, 1966  | 2048 to 1983          | 23.9                      |
| Nov. 10, 1966 | 1983 to 1918          | 23.9                      |
| Dec. 15, 1966 | 1918                  | 21.5                      |
| Jan. 15, 1967 | 1853                  | 21.5                      |
| Feb. 15, 1967 | 1789                  | 19.1                      |

TABLE 5-7.—*Comparative Telemetry Link Performance,  
Pioneers 6 and 7*

| Threshold, bps | Pioneer-6<br>range, 10 <sup>6</sup> km | Pioneer-7<br>range, 10 <sup>6</sup> km | Predicted<br>range, 10 <sup>6</sup> km |
|----------------|--|--|--|
| 512            | 12.4                                   | 12.2                                   | 12                                     |
| 256            | 18.3                                   | 15.0                                   | 17                                     |
| 64             | 34.3                                   | 32.3                                   | 33                                     |
| 16             | 57.0                                   | 59.1                                   | 60                                     |
| 8              | 79.5                                   | 76.8                                   | 80                                     |

TABLE 5-8.—*Received Carrier Strengths at DSS Receivers*

| Range, 10 <sup>6</sup> km | Pioneer-6<br>signal<br>strength, dBm | Pioneer-7<br>signal<br>strength, dBm | Predicted<br>signal<br>strength, dBm |
|---------------------------|--------------------------------------|--------------------------------------|--------------------------------------|
| 1                         | -127.5                               | -127                                 | -125.5                               |
| 5                         | -139                                 | -139                                 | -139.4                               |
| 10                        | -145                                 | -145.5                               | -145.5                               |
| 20                        | -151.5                               | -152                                 | -151.5                               |
| 40                        | -158                                 | -158.2                               | -157.5                               |
| 60                        | -162                                 | -162                                 | -161                                 |
| 80                        | -164                                 | -                                    | -163.5                               |

### Electric Power Subsystem

During all phases of flight the spacecraft power supply operated as predicted. During the eclipse of the Sun by the Earth, which began approximately 100 min after liftoff, the battery supplied 1.76 A. By the

end of the eclipse, the solar-array temperature had dropped to  $-130^{\circ}$  F and the bus voltage to 24.3 V. Entering sunlight again, the solar array picked up the load and began recharging the battery. The cold solar array generated a bus voltage of about 35 V and a current that saturated the current sensor at 0.562 A. To avoid overcharging the battery while the solar array warmed up, the battery was commanded off for 11 min. When the battery was reconnected, the voltage had dropped to 33.6 V and the recharging current to 0.130 A. Equilibrium conditions were gradually attained, and all parameters were normal.

On May 7, 1969, near the 1.125 AU aphelion, tests indicated that the undervoltage relay was being tripped when the MIT plasma experiment was switched to its high power mode. The implication was that the 9-W extra power requirement exceeded the capabilities of the degraded solar array. To provide the required power, the Goddard magnetometer and Stanford radio propagation experiments were turned off. This was acceptable because the magnetometer data were useless without the pulses from Sun-sensor E, which was out of action, and the spacecraft was beyond the range of the Stanford experiment. The MIT instrument was left in a low-power mode which prevented it from operating in its four highest energy steps.

### Thermal Control Subsystem

Performance here has also been excellent. Temperatures of the Sun sensors did not decay as rapidly as prior analysis had indicated. This was attributed to the conservative approach used in the analysis. In this instance a conduction path to the spacecraft was not included in the analysis because it was too difficult to take into account.

During the ascent phase, the aft, uninsulated end of Pioneer 7 was illuminated by the Sun. Platform temperatures during this phase were a few degrees higher than those of Pioneer 6 which was illuminated on its insulated end. After the orientation maneuvers, Pioneer 7 continued to operate a little warmer as described below.

The equilibrium temperatures at various points on the spacecraft are listed in table 5-9 for the Pioneer-6 and Pioneer-7 flights. It is interesting to note that the Pioneer-7 platform ran a few degrees warmer than Pioneer-6 and that the solar-array temperature was a little lower. The inference is that Pioneer 7 was better insulated than Pioneer 6.

### Structure Subsystem

Performance was good throughout the mission. The absence of ripple on the primary bus and signal stability at the DSS receivers inferred precision balance and alignment.

TABLE 5-9.—*Equilibrium Temperatures at 1 AU, Pioneers 6 and 7*

| Telemetry measurement  | Pioneer 6, °F | Pioneer 7, °F |
|------------------------|---------------|---------------|
| Sun-sensor A           | 58            | 55            |
| Sun-sensor B           | 80            | 82            |
| Receivers              | 57            | 62            |
| TWT 1 (operating)      | 103           | 106           |
| TWT 2 (in reserve)     | 70            | 79            |
| TWT converter          | 76            | 81            |
| Transmitter driver     | 52            | 52            |
| Digital telemetry unit | 62            | 64            |
| Data storage unit      | 64            | 67            |
| Equipment converter    | 62            | 67            |
| Battery                | 60            | 70            |
| Upper solar panel      | 41            | 27            |
| Lower solar panel      | 41            | 27            |
| Platform 1             | 83            | 86            |
| Platform 2             | 57            | 60            |
| Platform 3             | 52            | 52            |
| Wobble-damper boom     | 54            | 63            |
| High-gain antenna      | 64            | 64            |
| Lower actuator housing | 73            | 79            |
| Nitrogen bottle        | 27            | 28            |

### Data Handling Subsystem

All formats, modes, and bit rates were used successfully during the mission.

### PIONEER-8 PERFORMANCE

The Earth-escape hyperbola for Pioneer 8 was less energetic than planned. Instead of occurring at roughly 500 Earth radii, syzygy took place at 463 Earth radii. The heliocentric orbit was less eccentric and more inclined than the planned orbit, but the differences were not significant. The spacecraft performed normally except for the deviations noted below.

Early in the mission, trouble was experienced with the Ames plasma probe, and it was subsequently turned off. However, the difficulty was ultimately traced to a corona discharge resulting from outgassing. Later, the Ames experiment was switched back on, and it operated without further trouble.

Receiver 2 drifted somewhat, with a drift of 10 kHz being measured 3 months after launch.

During an orientation maneuver in March 1968, Sun-sensor D was found to be inoperative. On another orientation attempt in June 1968,

Sun-sensors A, B, and C were also found to be out of commission. The heavier Sun-sensor covers installed on Pioneer 8 had obviously not solved the degradation problem.

### PIONEER-9 PERFORMANCE

Pioneer 9, an inbound flight, was subjected to increasing solar radiation, higher solar-array temperatures, and, consequently, falling bus voltages. To prevent the discharge of the battery, it was switched out on January 14, 1969.

To check the effects of the ultraviolet filters newly installed on the Sun sensors, a special test was conducted on February 5, 1969, the 89th day of flight. Telemetry indicated that Type-I and Type-II commands were executed properly. The ultraviolet filters had apparently solved the Sun-sensor degradation problem.

The spacecraft reached perihelion at 0.754 AU on April 8, 1969. The spacecraft was designed to penetrate to only 0.8 AU. It reached 0.754 AU without overheating although the cosmic-ray experiment reached 90° F, its upper limit.

All spacecraft systems operated normally throughout the nominal 180-day mission. During the extended mission in May 1969, the communication range reached 130 million km (78 million miles) using only the 85-ft DSS antennas, and a bit-error rate of  $10^{-3}$ . This extension of the communication range can be attributed to three factors:

- (1) Use of linear polarizers at some DSS stations
- (2) Improvement of noise temperatures at the DSS stations
- (3) Use of the Convolutional Coder Unit on Pioneer 9

Later in 1969, the communication range was extended still further to 152 million km (95 million miles) by allowing the bit-error rate to increase to  $10^{-2}$ . During part of 1970, an improved, low-temperature cone (an "ultracone") was installed at DSS-12. With this improvement, the communication range was extended to 260 million km (162 million miles).

Decoder 2 began operating improperly in 1969 and is no longer used for normal operations.

#### Convolutional Coder Unit (CCU) Performance

The CCU, which is described in Vol. II, was added to Pioneers D and E as an engineering experiment. It can be switched in or out of the telemetry stream. CCU performance has been good, contributing about 3 dB to the communication power budget. In effect, the CCU has nearly doubled Pioneer-9's communication range.

Between the November 6, 1968, launch and December 10, 1968, the

spacecraft operated in the uncoded mode at 512 bps except for CCU functional checks. Since December 10, the CCU has been in almost constant use except when the spacecraft is being worked by a DSS without Pioneer GOE.

About January 7, 1969, Pioneer 9 was far enough away for the CCU to provide a "coding gain" for DSS stations configured for receiving circularly polarized waves.<sup>7</sup> Up to March 6, 1969, GOE-equipped DSS stations tracked Pioneer 9 approximately 1000 hr with the CCU in operation; 680 of these hours were in the coding-gain region. As a result of the CCU's coding gain,  $4.43 \times 10^8$  additional bits were received during this period. The 3-dB gain at 512 bps was verified by direct comparison with uncoded data at 256 bps. The CCU experiment has been so successful on Pioneer 9 that convolutional coding is being applied to other spacecraft.

### REFERENCE

1. LUMB, D. R.: Test and Preliminary Flight Results on the Sequential Decoding of Convolutional Encoded Data from Pioneer IX. IEEE paper, International Conference on Communications, 1969.

---

<sup>7</sup>The Pioneers transmit linearly polarized signals. A loss is incurred when a DSS antenna receiving circularly polarized signals is used.



## CHAPTER 6

# PIONEER SCIENTIFIC RESULTS

THE COMPLETE SCIENTIFIC LEGACY of the Pioneer Program will not be known for many years. Scientific papers based upon the data telemetered back from deep space are still being published in abundance. Indeed, all four successfully launched spacecraft are still active and continue to add to our scientific store. The Pioneer scientific record of today, though incomplete, is impressive; some 137 contributions are listed at the end of this volume. These papers and some of their implications are summarized in the following pages.

The first Pioneer was launched in December 1965 to add to the substantial fund of information that Earth satellites and planetary probes had already discovered during the first 8 yr of the Space Age. It is impractical to review here the state of our knowledge of interplanetary space as of 1965. However, Glasstone's *Sourcebook on the Space Sciences*<sup>8</sup> was published about the same time as the launch of Pioneer 6, and the reader is referred to it for background information.

To set the stage properly, a brief description of the cosmic setting of the Pioneer drama is in order. The Sun controls most of what happens in interplanetary space. In 1965 solar activity was low and supposedly going to get even lower. Of course, the Pioneers were originally planned to support the world's ICSY program. However, solar activity, as measured by the sunspot number, began to climb in 1966; by 1969 it had reached its peak. The Pioneers, therefore, have already monitored solar activity in deep space for over half a solar cycle. As solar activity built up in the late 1960's, solar flares appeared more frequently, engulfing with their plasma and cosmic radiation some of the Pioneers and, on occasion, the Earth too. These flares were of great interest to science, and the Pioneers, located strategically around the Sun, in effect made the whole solar system a laboratory for Earth-bound scientists. The more important of these flares were noted in the chronology of the last chapter. Thus, the physical backdrop for the Pioneer program was one of increasing solar activity—more plasma-producing flares, more solar cosmic rays, and, in general, more opportunities to unravel the effects of the Sun on the interplanetary medium and the Earth.

<sup>8</sup>D. Van Nostrand, Princeton, 1965.

## THE GODDARD MAGNETIC FIELD EXPERIMENT (PIONEERS 6, 7, AND 8)

The magnetic field in interplanetary space is intimately associated with the hot, ionized plasma that streams outward from the Sun. In fact, it is customary to speak of the solar magnetic lines of force as "imbedded" in the plasma. Thus, data from the Pioneer magnetometers must be studied in conjunction with measurements made by the spacecraft's plasma instruments. The GRCSW cosmic-ray anisotropy experiment was also related to the magnetometer in the sense that cosmic-ray isotropy could be affected by changes in the structure of the magnetic field. In addition, on the Block-II Pioneers, the TRW Systems electric field experiment registers many of the same magnetohydrodynamic phenomena that are signaled by the magnetometer and plasma probes. The magnetometer therefore views only one dimension of the interplanetary plasma which, as we shall see, turns out to be a most complex medium indeed.

By December 1965 when Pioneer 6 was launched, satellites, such as IMP 1 (Explorer 18) and space probes, had already confirmed the theoretical prediction of a basically spiral solar magnetic field imbedded or "frozen" in the streaming solar plasma. The Sun's rotation about its axis imposed the so-called "water sprinkler" pattern on the outwardly rushing plasma (fig. 6-1). At the distance of the Earth, the solar plasma had a velocity of about 400 km/sec, and the water-sprinkler effect bent the solar magnetic lines of force until they were inclined about  $45^{\circ}$  to the Sun-Earth line. The IMP 1 magnetometer showed further that the direction of the solar magnetic field would be first directed outward and then inward, each condition lasting several days as the Sun's rotation carried the newly dubbed "sectors" past the Earth (fig. 6-1). It was first thought that the sectors might be associated with large plasma-emitting areas of the Sun, but some recent theories suggest that small nozzle-like regions may be responsible. The sectors also evolve with time (ref. 1); there were four separate sectors during the latter part of the 1960's, but their pattern varied. The Pioneer spacecraft were ideal platforms from which to monitor these gross structures of interplanetary space and also investigate any microstructure superimposed upon the sectors.

### First Results from Pioneer 6

At approximately 11 Earth radii, the magnetometer reported a marked increase in magnetic field fluctuations as shown in figure 6-2 (ref. 2).<sup>9</sup> With the penetration of the magnetopause at 12.8 Earth radii, the field

<sup>9</sup> The first Pioneer-6 results were communicated at a special Pioneer-6 symposium convened by the American Geophysical Union in 1966.

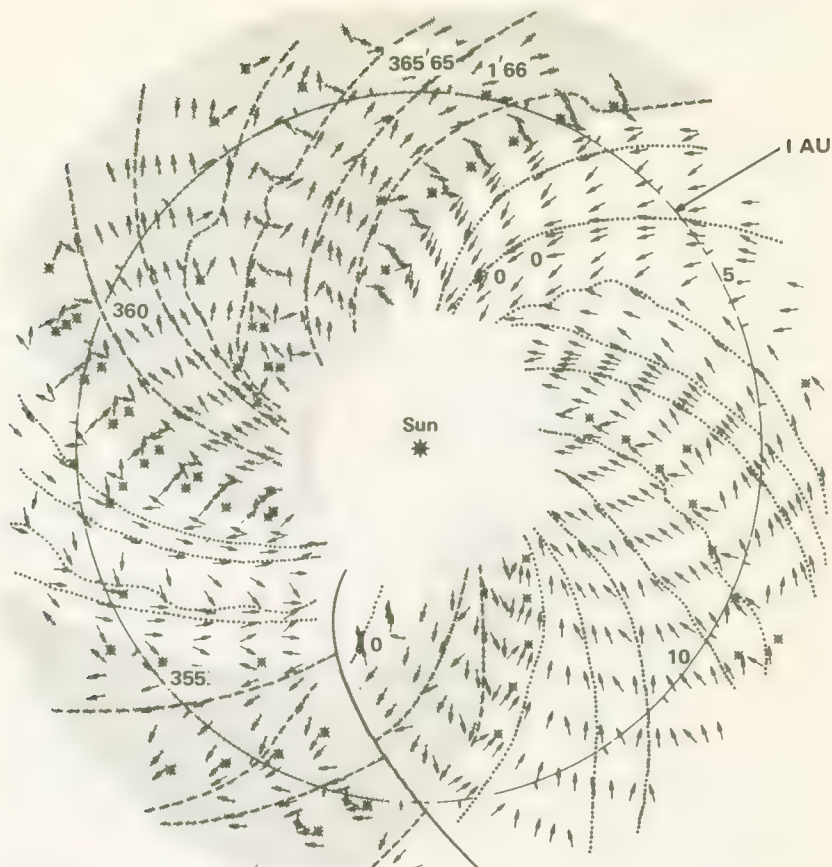


FIGURE 6-1.—Sector structure of the interplanetary magnetic field from Pioneer-6 data telemetered between Dec. 18, 1965, and Jan. 14, 1966. Each arrow represents an equivalent flux of 5 for 6 hr. Shaded regions are those where the field is directed away from the Sun; field was antisolar elsewhere. From: Schatten; et al. Solar Physics, vol. 5, 1968, p. 250.

dropped quickly to less than  $20 \gamma$ —a well-known phenomenon by 1965. The collisionless bow shock was penetrated at about 20.5 Earth radii, and the quiet-time field then fell to about  $4 \gamma$ .

Pioneer-6 data also confirmed that the interplanetary magnetic field often changes direction abruptly without changing magnitude. This phenomenon was interpreted at that time in terms of intertwined filamentary or tube-like structures in interplanetary space which mostly display the classical spiral structure but which sometimes create a twisted microstructure. The low-energy solar-proton anisotropies observed by Pioneer 6 tend to confirm this view (fig. 6-3).

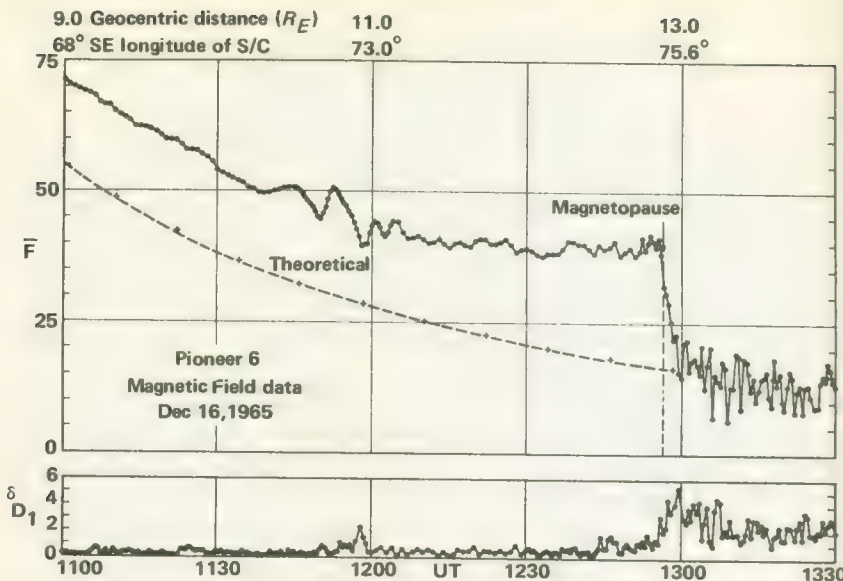


FIGURE 6-2.—Observations of geomagnetic field magnitude near the boundary of the regular field, the magnetopause, at a distance of  $12.8 R_E$  near the sunset terminator. The observed magnitude is larger than the theoretically expected because of the compression of the Earth's magnetic field by the solar wind. Note the abrupt transition from strong and regular fields to weak and rapidly fluctuating fields. The lowermost "noise" curve measures the rms deviation ( $\delta$ ) over a 30-sec interval of one component of the magnetic field. Note that the increase in noise level as the magnetopause is approached and the significantly higher noise level when within the magnetosheath. From: ref. 2.

Pioneer-6 results were compared with magnetometer readings from IMP 3 (Explorer 28) (ref. 3). This was the first time that accurate measurements of the interplanetary magnetic field had been made from two widely separated spacecraft. By considering corotation delays (due to the Sun's rotation) excellent agreement was found between the two sets of data. Using these observations, Burlaga and Ness (ref. 4) identified a tangential discontinuity.

Generally, then, early Pioneer magnetometer data tended to confirm the Earth shock structure, the magnetopause, and the spiral sector structure of the interplanetary field inferred from previous spacecraft flights. The strong experimental support for a filamentary fine structure was perhaps the most interesting result from the first few months of flight.

#### Further Observations of the Geomagnetic Tail

Outward-bound Pioneers 7 and 8 carried Goddard magnetometers through the region where the geomagnetic tail was expected to exist.

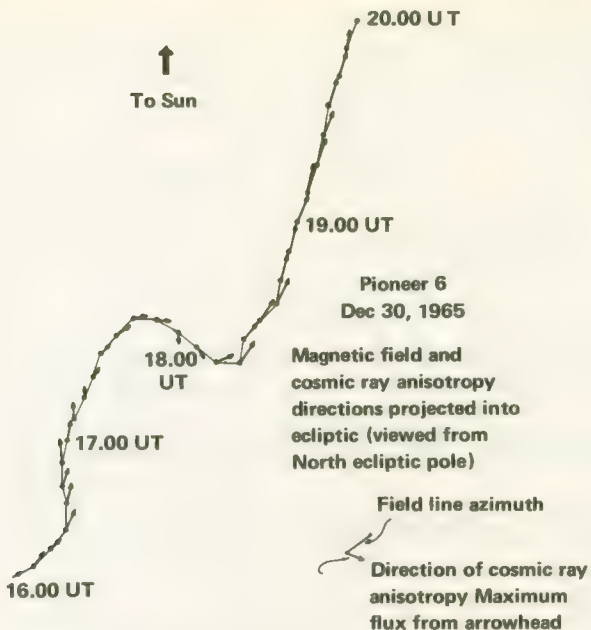


FIGURE 6-3.—Comparison of interplanetary magnetic field and solar cosmic-ray anisotropic directions projected onto the ecliptic plane. From: ref. 29.

This region was crossed by Pioneer 7 between September 23 and October 3, 1966, at distances ranging from 900 to 1050 Earth radii. Simultaneously, results from Explorer 33 demonstrated the existence of a tail out to 80 Earth radii. The Pioneer flights presented additional opportunities to explore this strange region "downwind" from the Earth.

A coherent, well-ordered geomagnetic tail with an imbedded neutral sheet was not observed by Pioneer 7 (ref. 5). However, the rapid field reversals recorded (fig. 6-4) are characteristic of the neutral sheet region observed closer to Earth. The conclusion of Ness and his colleagues at Goddard was that the geometry of the tail changes to a complex set of intermingled filamentary flux tubes at several hundred Earth radii.

In a later paper, Fairfield compared Pioneer-7 data with those obtained during the same period from Explorers 28 and 33 in the region closer to Earth (ref. 6). Comparisons revealed periods when Pioneer 7 was recording the steady, higher-magnitude solar or anti-solar fields characteristic of the tail but quite different from the fields connecting past the satellites. The presence of these isolated intervals was interpreted as due to the tail sweeping back and forth across the spacecraft in response to changing directions of plasma flow. Discontinuous features of the tail were found to connect past the three spacecraft at velocities comparable to the measured velocities of the solar wind.

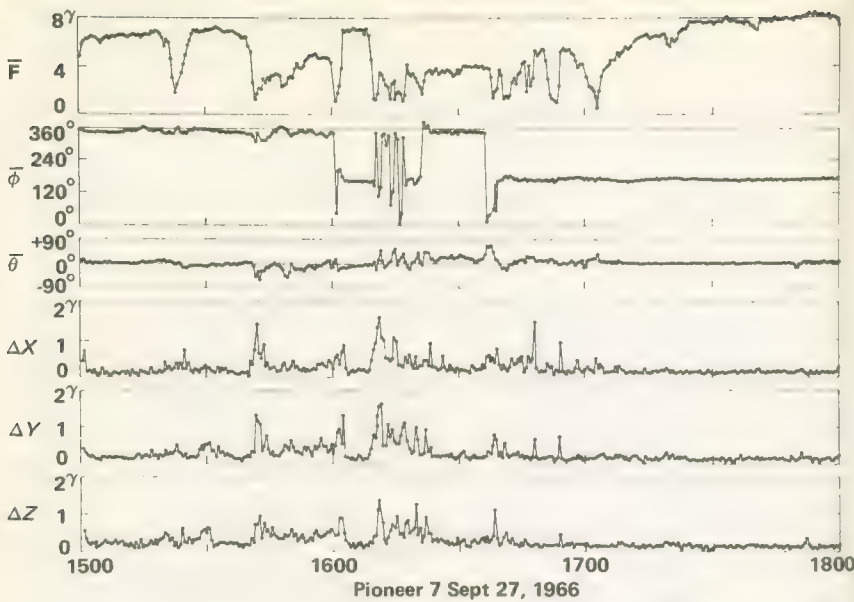


FIGURE 6-4.—Detailed 30-sec averaged magnetic field observations by Pioneer 7 on Sept. 27, 1966, when the field orientation and its rapid reversals are characteristic of the neutral sheet region of the geomagnetic tail. From: ref. 5. Throughout the 3-hr interval from 1500 to 1800 the field is observed to be directed either away from the Sun ( $\phi=180^\circ$ ) or toward the Sun ( $\phi=360^\circ$ ).

Pioneer 8 passed through the tail region at 470 to 580 Earth radii in January 1968. The results here were similar to those obtained from Pioneer 7 at 100 Earth radii (ref. 7). The geomagnetic tail may lose the clearcut structure plotted by Explorer 33 at 80 Earth radii before it reaches 500 Earth radii.

#### Mesoscale and Microscale Structures

Whereas the macroscale structures of the interplanetary field—those structures persisting 100 hr and more—generally fit theoretical expectations quite well, mesoscale structures (1 to 100 hr) and microscale structures (<1 hr) presented new experimental and theoretical problems and results. Some relevant observations and interpretations arising from Pioneer magnetometer data follow.

Directional discontinuities were correlated early with solar cosmic-ray anisotropies and explained in terms of spaghetti-like flux tubes or filaments. More thorough analysis of Pioneer data has replaced this type of model with a “discontinuous” model (ref. 8). The new model recognizes

the fact that field discontinuities on the mesoscale and microscale—in both magnitude and direction—are more prevalent than previously suspected, and that their character does not always imply the existence of filaments.

In another paper, Burlaga (ref. 9) has reported a variety of other microscale structures:

- (1) Transitional regions (called D-sheets) associated with plasma discontinuities
- (2) D-sheets possibly related to the annihilation of magnetic lines of force
- (3) Inhomogeneous, isothermal regions in which the square of the magnetic field intensity is proportional to the density and hydromagnetic tangential discontinuities in these regions
- (4) Periodic variations in magnetic field intensity associated with discontinuities in the bulk speed

Burlaga suggested that small velocity discontinuities play a fundamental role in reducing stresses in the interplanetary medium, and that large velocity discontinuities may give rise to waves and turbulence.

### Fluctuations and Power Spectra

The calculation of power spectra is useful in building theoretical models of the interplanetary milieu. For example, power spectra have been related to parameters describing the propagation of cosmic rays.

Power spectra based on early 1966 Pioneer-6 data exhibit an inverse dependence on the inverse square of the frequency as shown in figure 6-5 (ref. 10). The spectral shapes at that time were apparently dominated by microscale plasma-magnetic field discontinuities being connected outward by the solar wind. During more disturbed periods later in the flight, the discontinuities were not dominant, and the power spectra typically show an inverse 3/2 dependence on frequency.

Power spectra studies (ref. 11), using data obtained from Pioneers 7 and 8 as they passed through the magnetosheath, favor the view that fluctuations are created by the amplification of small connected irregularities occurring at the Earth's bow shock.

### Observations of Specific Interplanetary Events

Pioneer magnetometer results have helped provide insight into what happens in interplanetary space when a major solar event, usually a large flare, occurs on the Sun. One such analysis concerned the July 7, 1966, event (ref. 12). The available Pioneer-6 information was used sparingly here in combination with Explorer-33 data. Pioneer data were also applied to the event of February 25, 1969 (ref. 13). The following

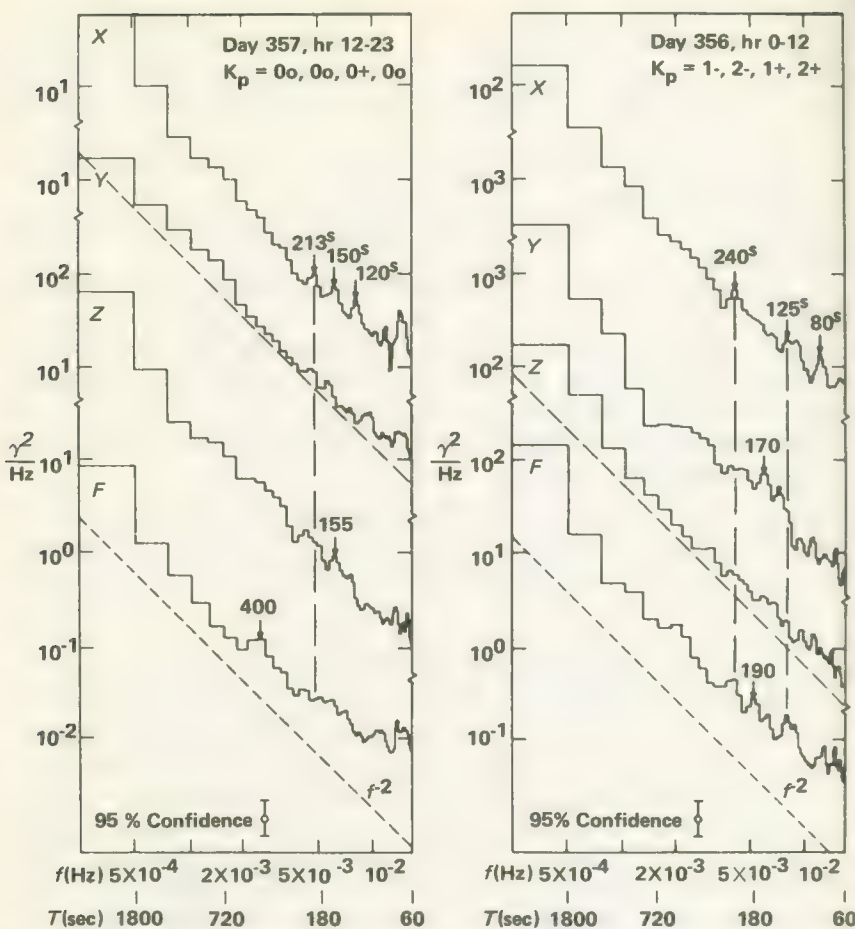


FIGURE 6-5.—Power spectra of the interplanetary magnetic field components and magnitude for two 12-hr periods in Dec. 1965. The dotted lines indicate inverse-square dependency. Data are from Pioneer 6,  $10^6$  km from Earth. From: ref. 10.

observations based on Pioneer-8 telemetry represent about what one would expect from a general model of a solar disturbance propagating through space.

(1) A rather steady field of 4 to 6  $\gamma$  was observed during the early hours of February 25.

(2) The field increased rapidly to near  $10\gamma$  between 2000 and 2022, then it rose slowly to about  $14\gamma$ .

(3) Long-period variations were observed between 0200 and 0500, February 26.

(4) A very quiet field of about  $6 \gamma$  occurred between 2000 and 0500, February 27.

(5) The next group of telemetered data at 2149, February 27, again revealed a high field (over  $10 \gamma$ ). Large variations were noticed.

(6) In the last time interval telemetered, between 0200, February 28, and 0500, February 29, the field had dropped to normal values.

### THE MIT PLASMA PROBE (PIONEERS 6 AND 7)

The preliminary MIT data presented at the American Geophysical Union Pioneer-6 Symposium indicated that, first, sharp changes in the plasma density preceded the dramatic changes in the magnetic field recorded by the Goddard magnetometer, and, second, the peaks in number density were followed by periods of increased bulk velocity (ref. 14). The early theoretical conclusions drawn from these coordinated measurements have already been covered in the preceding section.

The MIT group later published additional correlations between the plasma-probe and magnetometer data (ref. 15). In this study, the simultaneous changes in plasma and magnetic parameters were found to be consistent with what one would expect from tangential discontinuities. High-velocity shears were observed across these discontinuities, the largest being about 80 km/sec. The discontinuities observed by the MIT plasma probe were undoubtedly due to the same filament boundaries or discontinuities discussed in the papers published by the Goddard group.

The MIT plasma-probe and Goddard magnetometer data also showed that these discontinuities have preferred directions in space, with a tendency for the solar wind to be fast from the west and slow from the east. This east-west asymmetry in solar wind velocity is a natural result of the rotation of the Sun—the water-sprinkler effect again. Slow streams of plasma tend to spiral more tightly, and fast streams are straighter. The condition exists whereby slow and fast plasma streams tend to push against one another. Fast plasma streams push slow plasma away from the Sun and to the east; fast plasma, in turn, is pushed toward the Sun and to the west. The east-west asymmetry was shown strikingly when 3-hr averages of solar wind speed were correlated against flow angle in the plane of the ecliptic for a 27-day stretch of data (ref. 16). Figure 6-6 shows a conspicuous peak at zero lag, a positive correlation confirming the predicted in-phase relationship.

The correlation of plasma-probe and magnetometer data has continued to be a fruitful way to study the detailed structure of the solar plasma. For example, the general form of theoretical relation between the size of a sudden geomagnetic pulse and the associated change in solar wind stagnation pressure was confirmed in this way (ref. 17). Formisano was also shown that data from the two Pioneer instruments may be

combined to study the mechanism that controls the high energy tail of the interplanetary electron distribution (ref. 18). It seems, for example, that electron pressures are usually two to five times higher than proton pressures.

### Observation of Solar Flares

The MIT plasma probe, like the Goddard magnetometer, observed the passage of the shock front due to the solar flare of July 7, 1966 (ref. 19). The shock was first observed close to the Earth by the plasma probe and magnetometer on Explorer 33 some 45 hr after the visual observation of the solar flare. Ninety hours after the visual observation, Pioneer 6 recorded the passage of a shock. Because Pioneer 6 was closer to the Sun than Explorer 33, the anomalous time delays are difficult to explain. Even if the disturbance engulfed the Earth first, and then, through co-rotation, finally reached Pioneer 6, we have temporal inconsistencies. There may have been two separate interplanetary disturbances.

### Observations in the Magnetosheath

Pioneer 6 carried the MIT plasma probe through the magnetosheath in the dusk meridian on December 16, 1965 (ref. 20). While the data confirmed some portions of the various theories developed to describe the magnetosheath, the proton distribution measured was bi-Maxwellian (fig. 6-7) rather than the classical single-peaked curve. Roughly 10 percent of the total number density was estimated to reside in the high-energy tail. The high-energy tail was observed throughout the magnetosheath and tended to travel primarily in the direction of the bulk plasma flow (fig. 6-8). Two or three minutes before crossing the shock front, the high-energy particles began arriving from the direction of the solar plasma bulk flow; they continued to do so during the passage through the magnetosheath. After crossing into interplanetary space, the high-energy tail disappeared. Apparently, the high-energy tail was composed of solar plasma particles penetrating through the magnetosheath and eventually swerving to travel in the direction of the bulk flow within the magnetosheath. To attain the fit shown in figure 6-8, a thermal speed of 50/km sec was assumed in the direction of the bulk velocity within the magnetosheath and 70 km/sec perpendicular to this direction for the high-energy tail. Because Pioneer 6 penetrated the magnetosheath during a very quiet period, the above observations are probably characteristic of the normal interaction of the solar plasma with the Earth.

The electron flux was more complex, with three distinct regions being observed. The first region, from 9 to 11.5 Earth radii, was characterized by angularly isotropic fluxes in all four electron channels. The electron energy spectrum indicated that the electrons formed a plasma sheet in

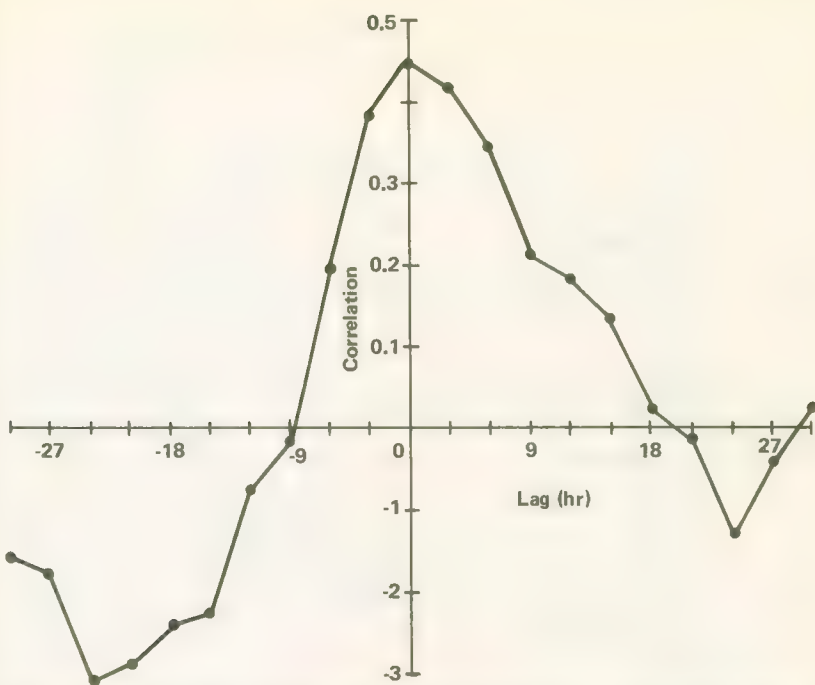


FIGURE 6-6.—Correlation between Pioneer-6 measurements of solar wind speed and angle in the ecliptic plane as a function of lag time. From: ref. 16.

this region. The second region, 1.5-Earth radii thick, was bounded at the outer edge by the magnetopause. The electron distribution in this region could be explained by two models. Using the thermodynamic model presented by Howe, the distribution matched that of a Maxwellian having a pressure of about  $300 \text{ eV/cm}^3$ , with the temperature parallel to the local magnetic field about twice that perpendicular to the field. In the third region, the magnetosheath itself, the following parameters were typical:

- (1) Thermal electron energy—40 eV
- (2) Electron speed—2700 km/sec
- (3) Electron temperature —  $100\,000^\circ \text{ K}$

Howe also compared the results of the MIT and Ames plasma probes in this region. MIT velocity measurements were consistently about 20 km/sec higher and well outside the uncertainties of the MIT experiment. There was also clear disagreement in the measurement of the out-of-the-ecliptic flow angle. The density pulse detected by the Ames instrument when the shock was crossed could not be detected by the MIT probe. It should be recalled, however, that these two instruments

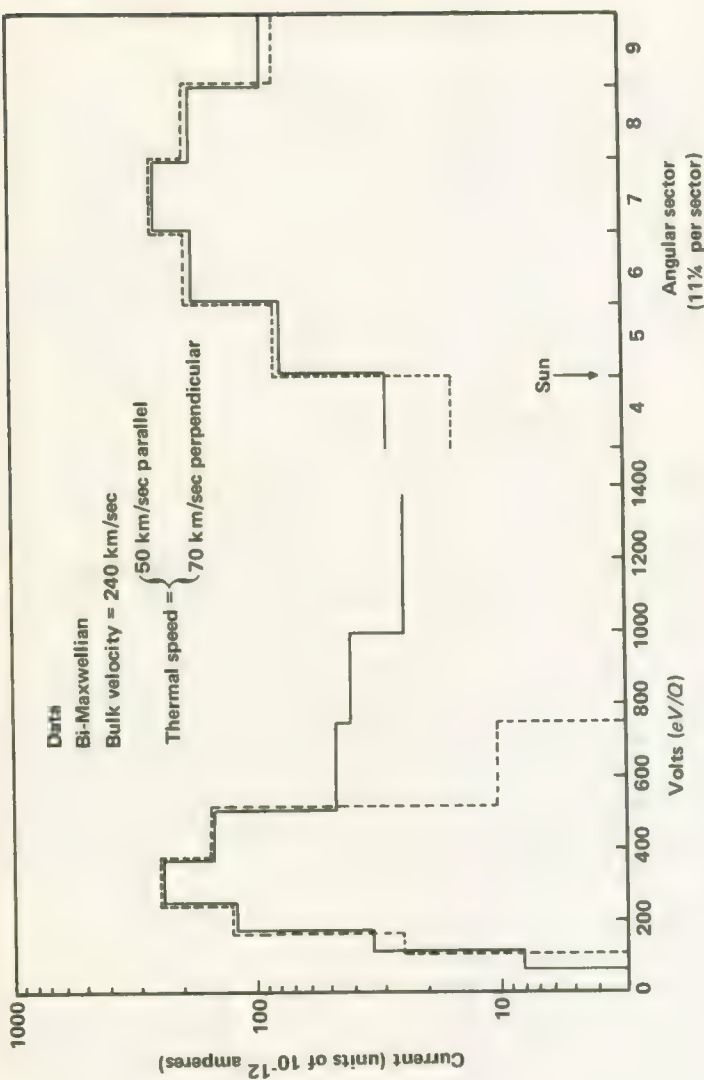


FIGURE 6-7.—Typical magnetosheath energy and angular measurements and the bi-Maxwellian fit. The two thermal speeds are parallel and perpendicular to the bulk velocity, which is within  $30^\circ$  of the magnetic field direction in the magnetosheath. From: ref. 20.

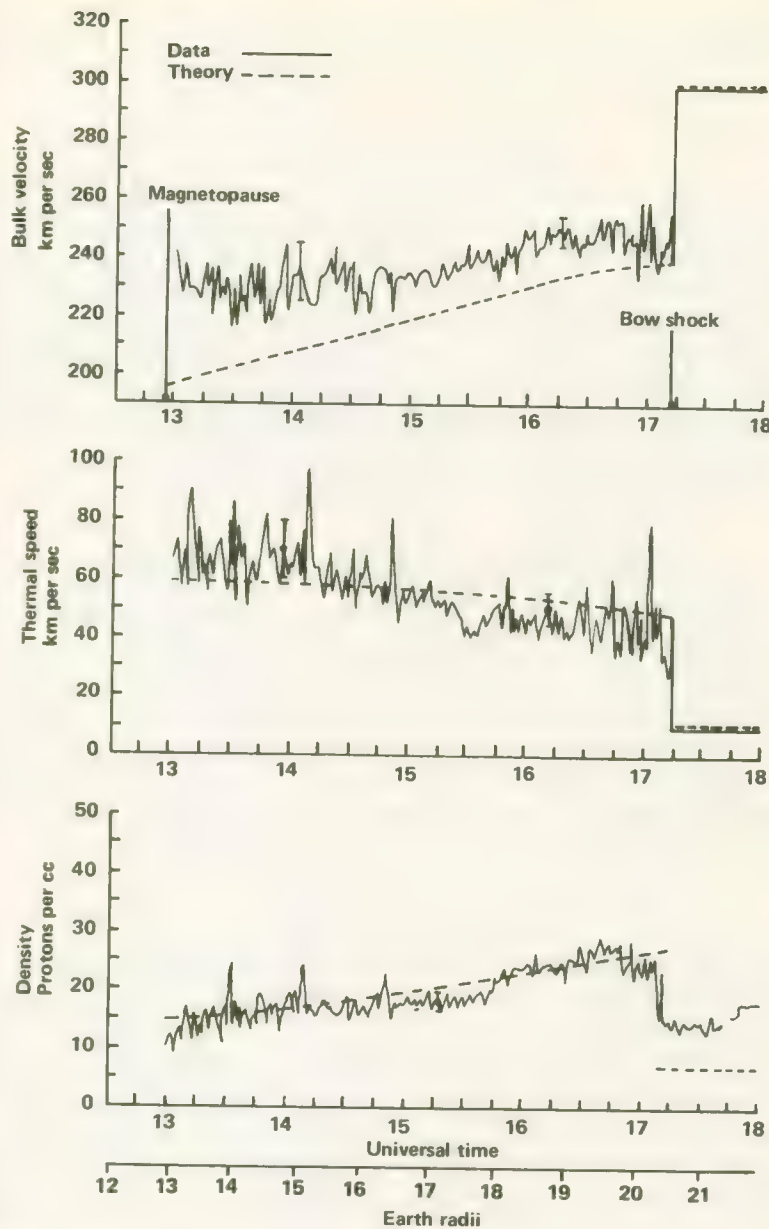


FIGURE 6-8. Pioneer-6 magnetosheath proton observations showing velocity, thermal speed, and number density. From: ref. 20.

are quite different in concept and that one would expect to have to reconcile discrepancies at this stage of their development.

### Passage Through the Earth's Tail

The passage of Pioneer 7, an outward bound spacecraft, through the Earth's magnetic tail was recounted in the preceding section. During this passage on August 17 and 18, 1966, data from the MIT probe clearly indicated the existence of a tail and the traversal of the neutral sheet (ref. 21). There was also some evidence of a second neutral sheet near the magnetopause. The data were found to be in general agreement with expectations from a quasistatic model of the geomagnetic tail, based on a balance of particle and field pressures (fig. 6-9). Also shown in figure 6-9 is the apparent correlation of a period of low particle flux with the terrestrial observation of a geomagnetic bay (insert).

### THE AMES PLASMA PROBE (ALL PIONEERS)

The Block-I and Block-II plasma probes (called quadrисpherical electrostatic analyzers) built by Ames Research Center record the energy spectra of electrons and positive ions in the solar plasma as functions of azimuth and elevation angles (see ch. 5, Vol. II). For a more complete understanding of the interplanetary medium, it is essential to relate plasma probe results to the magnetometer data and, of course, the somewhat different perspectives apparent to the MIT Faraday-cup plasma probe and the TRW Systems electric field detector.

### Some Early Results

Like the other Pioneer-6 experimenters, the Ames plasma-probe group presented preliminary results at the 1966 Pioneer-6 Symposium sponsored by the American Geophysical Union (ref. 22). Figures 6-10 and 6-11 show two basic types of data acquired by the Ames plasma probe—energy spectra and angular spectra. The energy spectrum (fig. 6-10) indicates a proton peak at 1350 V, corresponding to a proton velocity of approximately 510 km/sec. The second peak in the curve was due to alpha particles. However, analysis of subsequent data revealed the possible presence of singly ionized helium in the solar wind—the first time this had been detected. In the angular spectra (fig. 6-11), collector 5 consistently recorded higher fluxes than collector 4. The inference was that a net southward convective flow of plasma existed with respect to the plane of the ecliptic. There was also an obvious velocity dependence in ecliptic longitude. It was quite apparent from early Pioneer-6 meas-

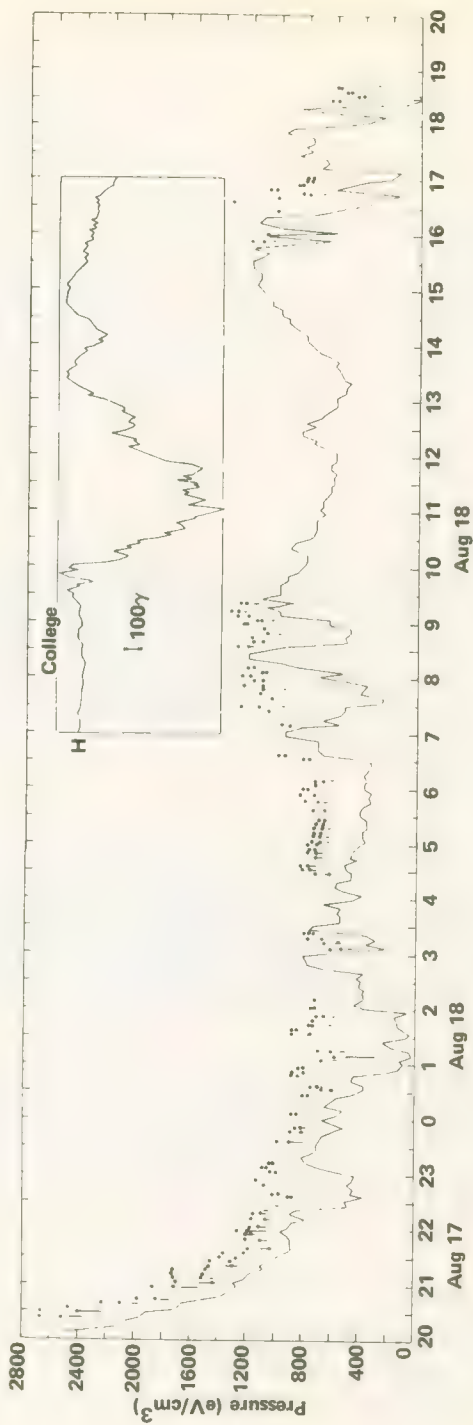


FIGURE 6-9.—Magnetic field pressure (solid line) and total pressure (data points) assuming equal proton and electron pressure. A magnetic bay at College, Alaska, is shown in the inset with the same time scale as the data record. The bay event coincides with a decrease total pressure in the tail. From: ref. 21.

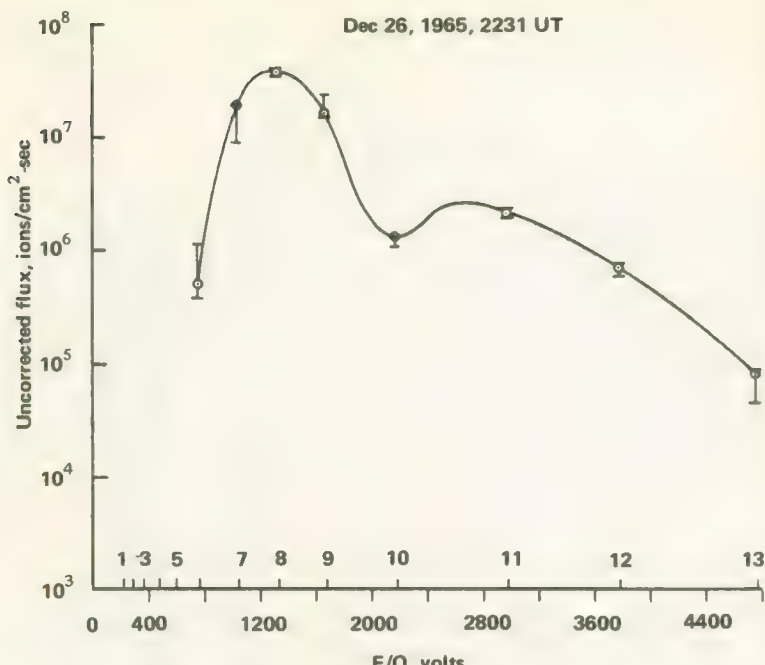


FIGURE 6-10.—Pioneer-6 Ames plasma probe E/Q spectrum, Dec. 26, 1965, 2231 UT, showing the hydrogen peak at approximately 1350 V with the helium peak estimated at 2700 V. From: ref. 22.

urements that the common assumptions of solar radial flow of plasma and thermal isotropy were not valid.

The early data also revealed an average solar wind electron temperature of about  $100\,000^\circ\text{ K}$  during quiet times when the solar wind was blowing at about 290 km/sec, with a maximum ion temperature of  $50\,000^\circ\text{ K}$ . Interplanetary electrons always seem hotter than ions during quiet periods.

As Pioneer 6 passed through the Earth's magnetopause, the Ames plasma probe measured the temperature of solar electrons in the bow shock at  $500\,000^\circ\text{ K}$ . Here, ion temperatures were about the same as electron temperatures, but, in contrast, the ions did not cool off downstream from the Earth. The ions also exhibited other non-thermal characteristics.

#### Observations of the Earth's Wake

Pioneers 7 and 8 were outward-bound missions and, as illustrated in figure 6-12, swept through the Earth's tail early in their flights. Instruments on both spacecraft detected evidence of the Earth's tail or wake

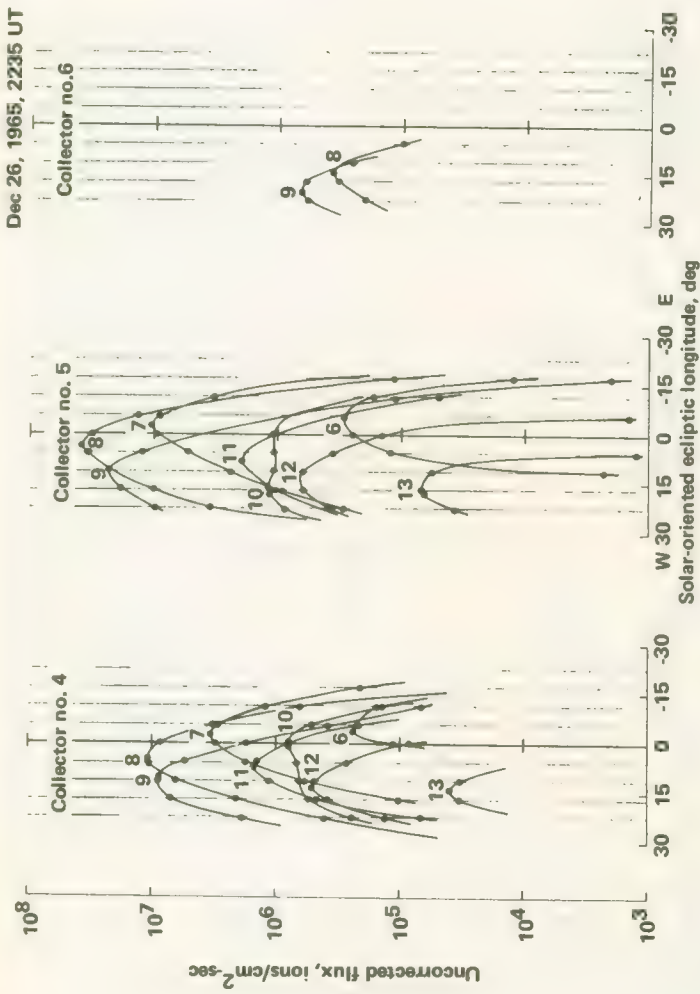


FIGURE 6-11.—Pioneer-6 Ames plasma probe angular distributions in ecliptic longitude, for energy steps 6 through 12 collectors 4, 5, and 6 obtained on Dec. 26, 1965, at approximately 2235 UT. From: ref. 22.

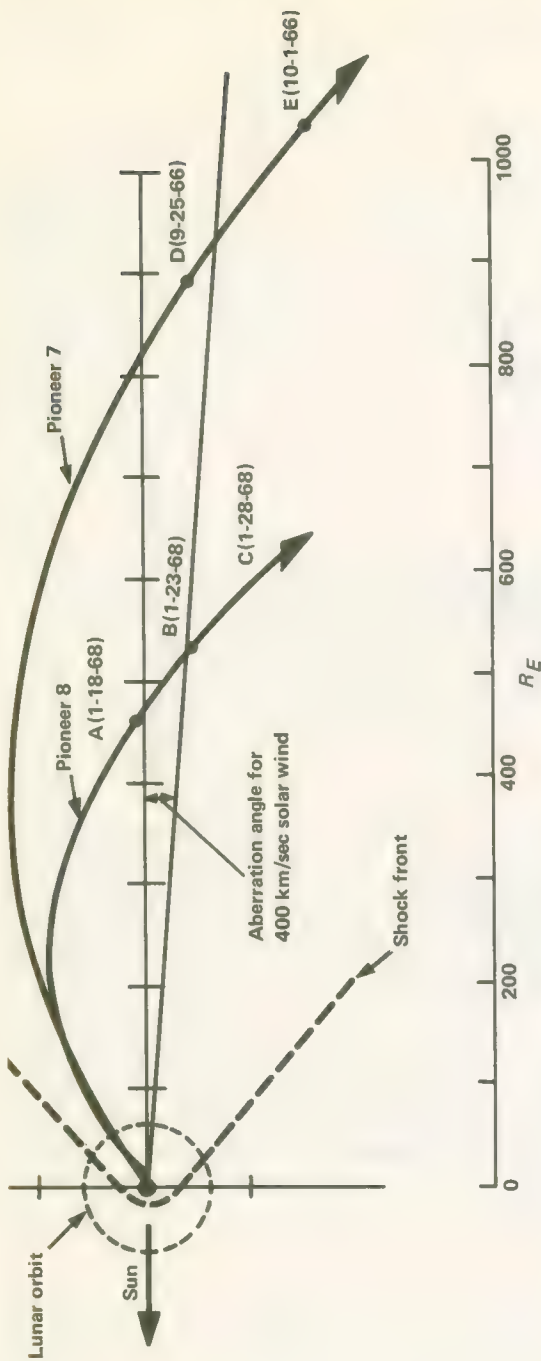


FIGURE 6-12.—Pioneers-7 and -8 trajectories; ecliptic projection. Pioneer 7, launched Aug. 17, 1966, went through the expected region of the geomagnetic tail at  $1000 R_E$  in Sept. 1966. Pioneer 8, launched Dec. 13, 1967, went through the expected region of the geomagnetic tail at  $500 R_E$  in Jan. 1968. The Pioneer-8 spacecraft coordinates at locations A, B, and C are, respectively,  $460 R_E$ ,  $525 R_E$ , and  $590 R_E$  geocentric from the Earth;  $8.5 R_E$ ,  $0.5 R_E$ , and  $12.3 R_E$  above the ecliptic at an ecliptic projection of the spacecraft-Earth-Sun angle of  $180^\circ$ ,  $185.5^\circ$  and  $190.5^\circ$ . The Pioneer-7 spacecraft locations at D and E are, respectively,  $887 R_E$  and  $1059 R_E$  geocentric from the Earth,  $25.4 R_E$  and  $28.7 R_E$  above the ecliptic at an ecliptic projection of the spacecraft-Earth-Sun angle of  $183^\circ$  and  $189^\circ$ . From: ref. 23.

with their magnetometers and plasma probes. The Ames plasma probes detected the wakes at about 1000 and 500 Earth radii for Pioneers 7 and 8, respectively (ref. 23). In each case the normally quiescent plasma ion energy spectra were interrupted by the abrupt changes in the magnitude and curve shape that one would expect near the tail boundaries.

In figure 6-13, the typical quiescent ion spectrum is compared with that measured in the Earth's wake by Pioneer 7. The peaks of the "disturbed" spectra are usually one or two orders of magnitude less than those of quiescent spectra. Further, there is often a different kind of double peak (indicated by the dashed lines) which infers that the

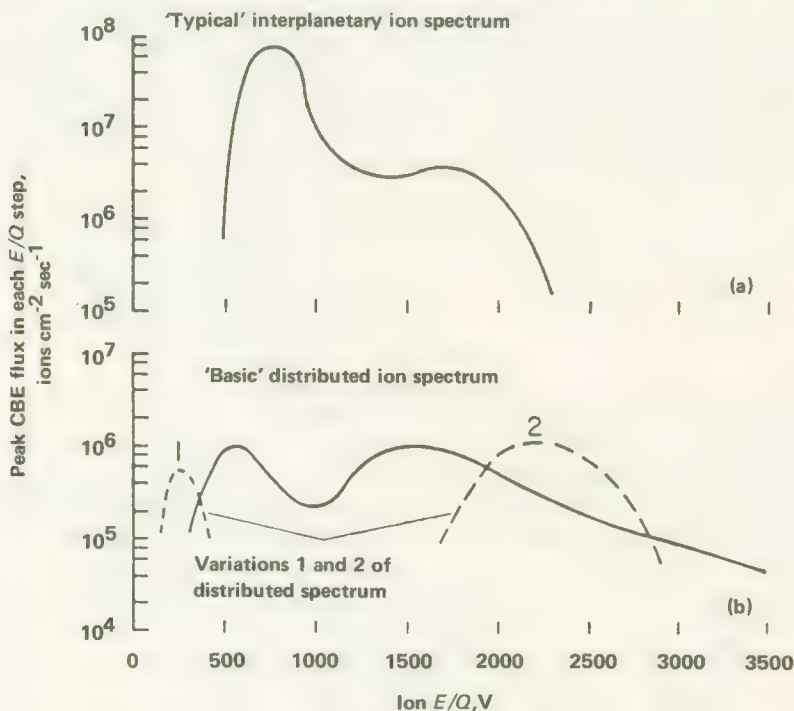


FIGURE 6-13.—Pioneer-7 ion spectrum. (a) 'Typical' interplanetary ion spectrum. The peak CBE flux of the curve (the  $H^+$  peak) is  $10^7$ - $10^8$  ions  $cm^{-2}sec^{-1}$ . The energy per unit charge is 850 V. The second peak at 1700 V ( $2 \times 850$  V) is the  $He^{++}$  peak. (b) 'Basic' disturbed ion spectrum and two variations often observed in the geomagnetospheric wake. The peak flux is  $<\sim 10^6$  ions  $cm^{-2}sec^{-1}$ . In this case the first peak of the curve (the  $H^+$  peak) occurs at  $\sim 500$  V and the second at  $\sim 1500$  V. The second peak is interpreted as a high energy tail of the proton energy distribution. Analysis of successive ion spectra show that the higher energy distribution often grows at the expense of the lower energy distribution. At times only part of the distribution is seen as indicated by the two variations. From: ref. 23.

high energy tail of the proton distribution may grow at the expense of the low energy protons in the vicinity of the Earth's wake. The disturbed nature of plasma conditions in this region is quite apparent in figure 6-14 where the energy spectra are seen to vary markedly with time. During some periods, for example, no flux could be detected at all; at other times, the spectra were either normal or disturbed, indicating a mixing that seems reasonable near the turbulent boundaries of a magnetic tail.

The Ames investigators felt, on the basis of their data, that the following interpretations were possible:

- (1) The observations could represent a turbulent downstream wake if the Earth's magnetosphere closed between 80 and 500 Earth radii.
- (2) If the solar wind diffuses into the magnetic tail, the plasma probe measurements could be due to the tail "flapping" past the spacecraft.
- (3) The tail might have a filamentary structure at these distances (500 and 1000 Earth radii), and the disturbed data could arise at filament boundaries.

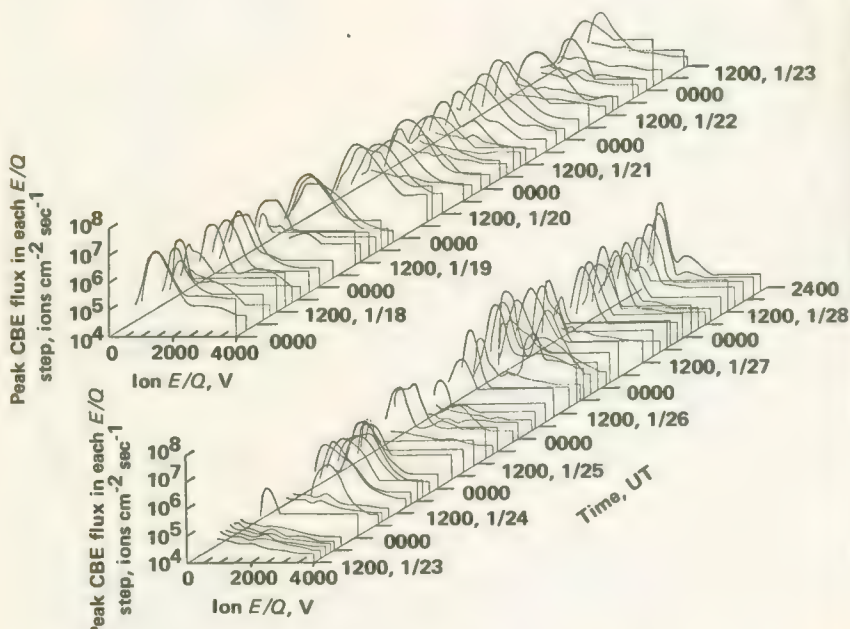


FIGURE 6-14.—Pioneer 8 ion spectra, Jan. 18-28, 1968. Eleven days of spectra (approximately 2 hr apart) are plotted. The changing nature of the measurable plasma characteristics are illustrated. Real time teletype data gaps are indicated by not plotting any spectrum (e.g., 2000-2400 UT on Jan. 23, 1968), while an absence of measurable plasma is indicated by plotting a low-lying noise spectrum (e.g., 1200-1800 UT on Jan. 23, 1968). From: ref. 23.

(4) Possibly the tail might have disintegrated into "bundles" at these distances.

(5) If magnetic merging occurred, subsequent acceleration of pinched-off gas may have caused the disturbed conditions measured.

### Plasma Instabilities

Prior to Pioneer 6, few spacecraft were capable of making detailed measurements of the solar wind. Consequently, the collisionless interplanetary plasma was treated as a single magnetofluid. However, the Ames plasma probes have revealed that the solar proton distribution is definitely anisotropic, with the temperature parallel to the local magnetic field being larger than that perpendicular to the local magnetic field (ref. 24). From these data and basic theory, it can be shown that the anisotropy can be produced by the approximate conservation of magnetic moment and thermal energy as the collisionless solar plasma flows outward and the imbedded magnetic field weakens. The positive ion distributions measured were also unstable with respect to the generation of low-frequency whistlers. The conclusion was that a generalized form of "firehose" instability must occur with the growth of whistlers near the ion cyclotron frequency.

## THE CHICAGO COSMIC RAY EXPERIMENT (PIONEERS 6 AND 7)

The Chicago cosmic-ray telescope on the Block-I Pioneers provided the opportunity for scientists to investigate the direction of arrival of cosmic-ray particles near the plane of the ecliptic. The experiment also had a short enough time resolution so that rapid fluctuations in cosmic-ray intensity could be recorded. The first test case came shortly after the launch of Pioneer 6 when solar-flare protons were detected on December 30, 1965. These early results—some of them unexpected—were reported at the Pioneer-6 Symposium by the Chicago group (ref. 25).

### Anisotropy of Solar-Flare Proton Flux

The solar flare that erupted about 2 weeks after the launch of Pioneer 6 was given an importance rating of 2. The effects were noted for almost a week, as indicated in figure 6-15. Interplanetary conditions during most of this period were remarkably free of solar-flare blast effects capable of modulating the galactic cosmic-ray flux. Solar protons in the energy range 13 to 70 MeV first arrived at the spacecraft at about 0300 UT, December 30, 1965, with lower energy particles arriving later. The anisotropy of these protons was striking (fig. 6-16), with the average direction of particle flow about halfway between the Sun line and the

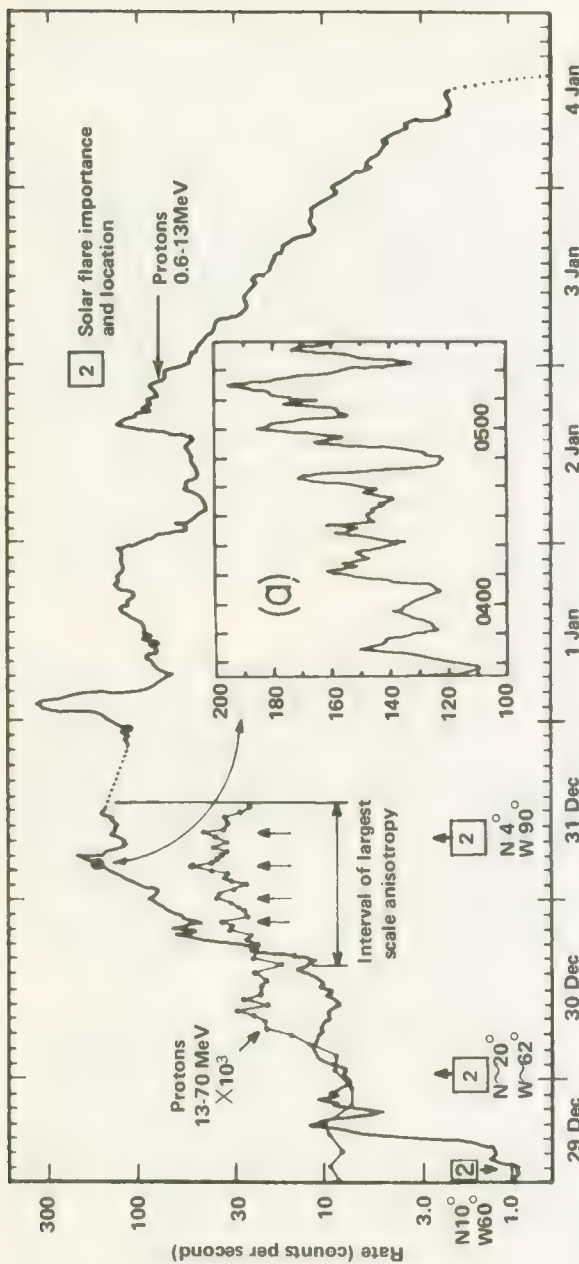


FIGURE 6-15.—The intensity-time distribution of protons of 0.6–13 MeV energy and protons 13–70 MeV energy. Anisotropies were observed for a period of approximately 2 days after the flare of Dec. 30, 1965. The arrows refer to quasi-periodic bursts of period  $\sim 4$  hr. Insert (a) is an expansion of the region shown within the circle. Data points are  $\sim 36$  sec apart. Note the quasi-periodic oscillations of  $\sim 15$  min. From: ref. 25.

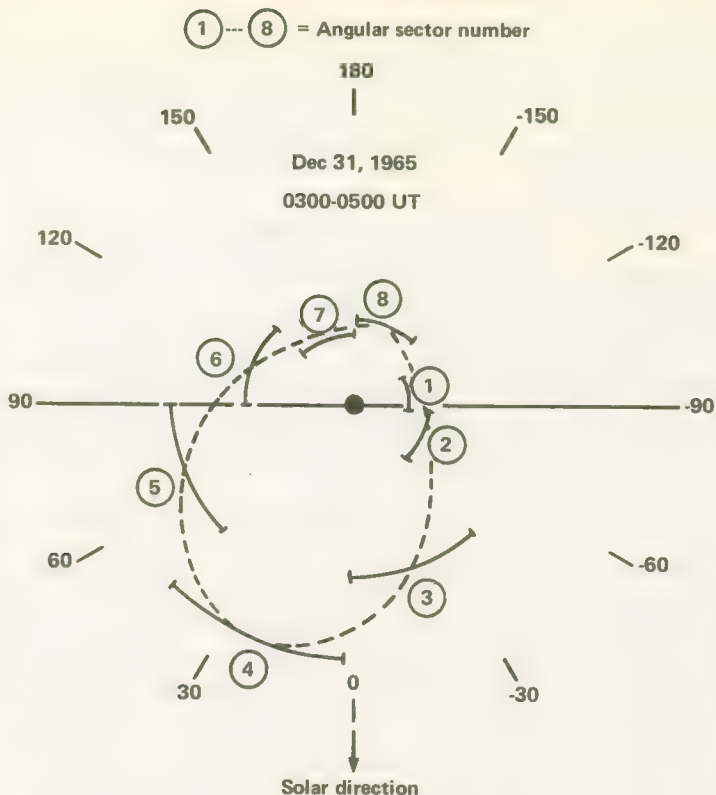


FIGURE 6-16.—Anisotropy diagram for proton flux from flare recorded Dec. 30, 1965.  
From: ref. 25.

angle one would expect if the particles travelled along the "water-sprinkler" spiral lines. However, the detailed data reveal a more complex situation:

- (1) The direction of the peak amplitude was highly variable, changing direction by as much as  $90^\circ$  within 10 min.
- (2) Relative to the intensities in other directions, the peak intensity varied rapidly.
- (3) Occasionally, the angular distribution was strongly peaked within a  $45^\circ$  sector.
- (4) Rarely, two intensity peaks  $180^\circ$  apart were noted.

The strong collimation of solar protons with energies greater than 13 MeV infers that there are few irregularities in the propagation path from the Sun that could scatter the protons. However, the rapid changes in direction of the peak flux vector supports the conclusion from Goddard magnetometer and GRCSW cosmic-ray anisotropy data that there are

many short-term, rather localized changes in the Earth's magnetic field. (See discussion of the possible filamentary character of interplanetary space under these other experiments.) The double intensity peak noted on occasion implies that some back-scattering does occur out beyond the spacecraft's orbit.

### Rapid Intensity Variations

During part of the solar-flare event (about 7 hr), the proton measurements at energies of the order of 600 keV displayed large-scale, quasi-periodic bursts with periods of about 900 sec and characteristic rise and fall times of roughly 100 to 200 sec. In addition, quasi-periodic fluctuations were noted in the 13 to 70 MeV energy range with periods of 3.5 to 4 hr. It is possible that these fluctuations indicate the existence of Alfvén waves in the inner solar system.

### Sector Structure of Interplanetary Space

Corotation effects were noted early in flight by the Chicago instrument, supporting the joint observations of several other Pioneer 6 instruments and similar instruments on spacecraft elsewhere in the solar system. For example, proton intensity structures detected at Pioneer-6 were noted some 2 hr later at the IMP-3 (Explorer 28) Earth satellite.

Proton flux increases over the period from December 1965 through September 1966 have been unambiguously associated with specific solar flares (ref. 26). Enhanced solar proton fluxes in the energy range 0.6 to 13 MeV have been recorded from specific active regions from ranges as great as  $180^\circ$  in longitude. The enhanced fluxes were characterized by definite onsets when their associated active centers reached points  $60^\circ$  to  $70^\circ$  east of the central solar meridian. Cutoffs occurred  $100^\circ$  to  $130^\circ$  west. Coupled with the detection of associated modulations of the galactic cosmic-ray flux, these observations again point to the existence of corotating magnetic regions associated with the active centers on the Sun (fig. 6-17). Observations seem to show that solar-flare protons propagate along the spiral interplanetary field from the Sun's western hemisphere. Present evidence supports the view that the solar protons arise from processes continually occurring in the solar active centers.

The protons from flares located at ranges over  $60^\circ$  in longitude seem to propagate rapidly through the corona into the interplanetary magnetic field. The short transit and rise times cannot be explained by isotropic diffusion across coronal magnetic fields. To account for these observations, a new quasi-stationary model was suggested in which some field lines rooted in or near the active center are spread out in the corona over a range of about  $100^\circ$  to  $180^\circ$  in longitude and then extended into interplanetary space by the solar wind.

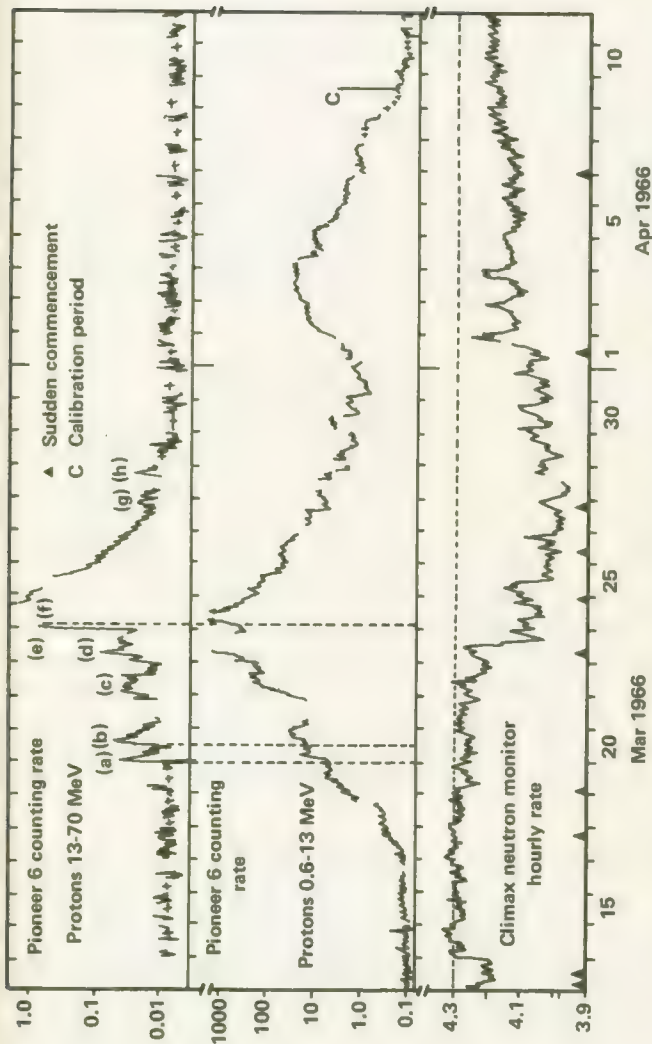


FIGURE 6-17.—Thirty-min averages of the counting rates of protons  $^{13-70}$  and  $0.6-13$  MeV. The enhanced flux of  $0.6-$  to  $13$ -MeV protons during Mar.  $15-31$  is attributed to solar region 8207. The first evidence of enhanced flux from the following region (8223) appears on Mar. 31. A magnetic sector boundary occurs on Mar. 31. Note at this time the abrupt change in the level modulation at the Climax neutron monitor. (a)-(h) denote discrete flare and shock-wave events seen at  $13-70$  MeV. From: ref. 26.

### Differential Energy Spectra

By correlating measurements from Chicago cosmic-ray telescopes aboard Pioneer 7 and OGOs 1 and 3, the Chicago group has shown that protons and helium nuclei in the 1 to 20 MeV/nucleon range are present during the so-called "quiet times" often observed in interplanetary space from 1964 to 1966 (ref. 27). Further, the observed helium nuclei flux was shown to increase from 1964 to 1965 and then decrease from 1965 to 1966—in accord with the observed variation of galactic helium nuclei by terrestrial detectors. In contrast, the proton flux detected kept increasing during these 3 yr.

These results infer that most of the particles observed by the spacecraft at the time of solar minimum are of galactic origin. As the new solar cycle began, solar particles (mostly protons) began to enhance the galactic proton flux. The H/He ratio rose from 2 in 1965 to about 10 in 1966.

### Relativistic Electrons in the Geomagnetic Tail

NASA's scientific satellites have established that a neutral sheet (where the Earth's magnetic field is essentially nil) exists within the Earth's tail between about 11 and 80 Earth radii. Satellites have also detected high energy electrons streaming along this sheet. During its passage through the geomagnetic tail in August 1966, Pioneer 7 observed relativistic electrons confined within this neutral sheet at about 19 and 38 Earth radii (ref. 28). The two high-energy-electron peaks ( $>400$  MeV), shown in figure 6-18, were coincident with Pioneer-7 passages across the neutral sheet. The relativistic electron fluxes did not extend outside the neutral sheet, and the evidence points to acceleration of the electrons by the split magnetic field within the sheet. The origin of this unique feature in nature is still controversial.

## THE GRCSW COSMIC RAY EXPERIMENT (ALL PIONEERS)

The primary mission of the GRCSW experiment was the measurement of anisotropy in the distribution of cosmic rays within the solar system but still far enough away from the Earth to avoid its perturbing magnetic field. The construction of a theoretical model describing how cosmic rays are propagated through the solar system depends upon the accurate measurement of cosmic rays with energies less than 1000 MeV. Because the weaker cosmic rays, especially those originating on the Sun, are affected by the solar magnetic field and the plasma in which it is imbedded, the GRCSW data must be examined in conjunction with the results of the Pioneer plasma and magnetometer experiments. Some

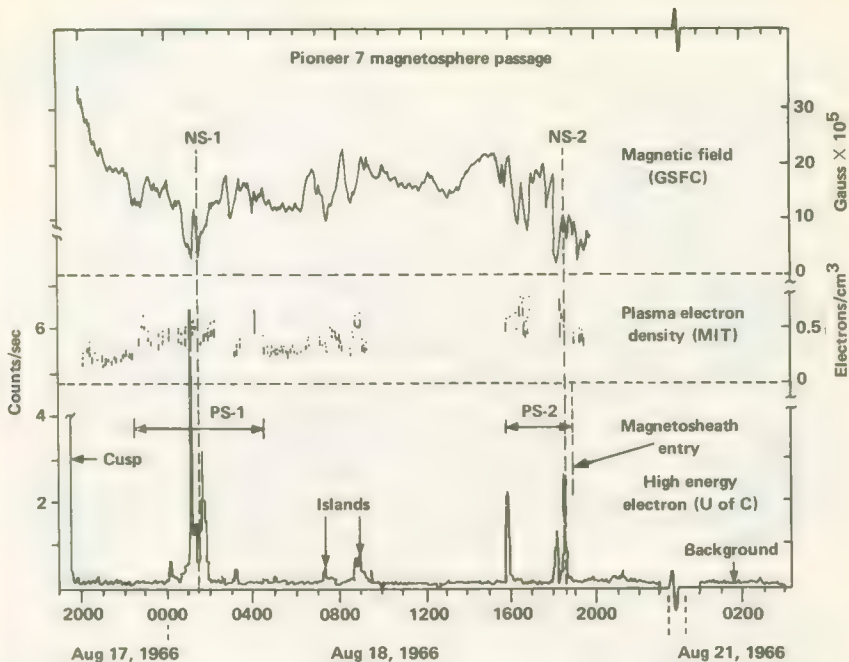


FIGURE 6-18.—The intensity of electrons  $>400$  keV as a function of time as the spacecraft emerges from the cusp region until passage into the magnetosheath (ref. 28). A typical cosmic ray background flux is shown on the right for Aug. 21. For comparison the magnetic field strength and electron concentration reported by Lazarus et al. (ref. 21) are shown on the same scale. NS-1 = neutral sheet passage no. 1.

of these interrelationships have already been discussed in the preceding sections.

### General Structure of Interplanetary Space

The early data from Pioneer 6 revealed that the low-energy cosmic-ray flux (13 MeV/nucleon) exhibited considerable anisotropy. It was this anisotropy which, when combined with Goddard magnetometer data, led to the original concept of the filamentary structure described earlier in connection with the Goddard magnetometer (ref. 29). The close correlation of these two sets of data can be seen in figure 6-3. According to this model, cosmic rays of low energy are forced to flow inside these twisting tubes, as shown in figure 6-19. The changing cosmic-ray anisotropies were ascribed to the experiment's sampling of the fluxes in the various tubes as they swept past the spacecraft. The tubes themselves were estimated to be between 0.5 and 4 million km in diameter. As the

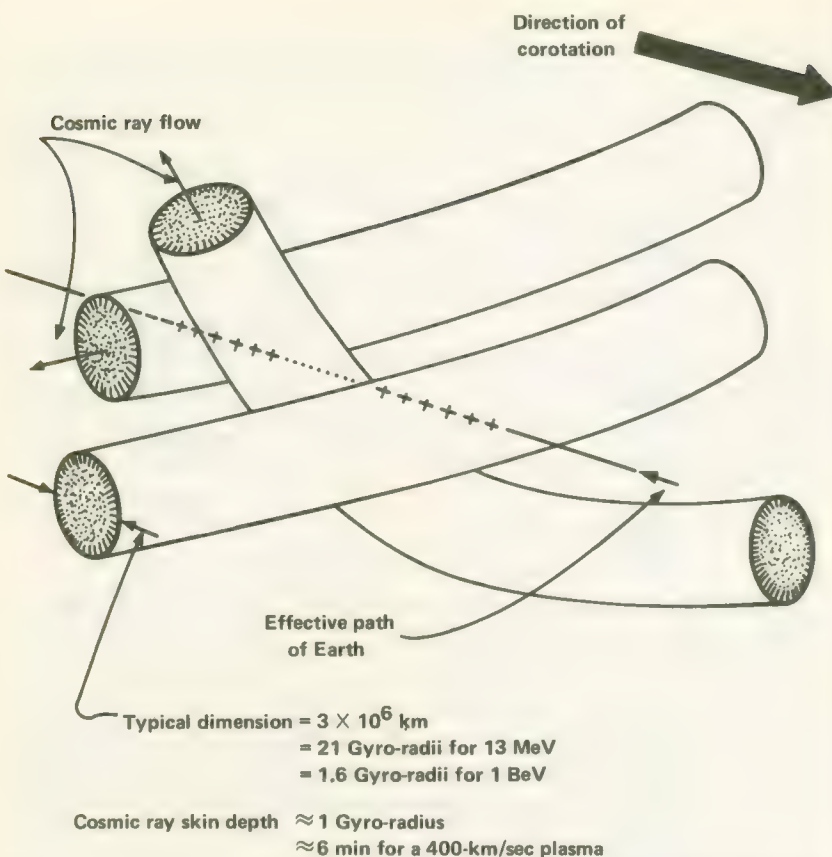


FIGURE 6-19.—A simplified model of the filamentary structure of the interplanetary magnetic field. Each filament can be thought of as a bundle of tubes of force. The cosmic rays of low energy are constrained to travel along the filament by the magnetic field. From: Bartley; et al.: J. Geophys. Res., vol. 71, Jul. 1, 1966, p. 3301.

reader will recall, later magnetometer data suggested that the filament model should be replaced by a "discontinuity" model.

The extent of the anisotropy of low-energy solar protons during early flight was striking. Since scattering normally reduces anisotropy, these results imply that little scattering transpired since the cosmic rays were injected into the interplanetary field near the Sun. In contrast, the anisotropy of relativistic cosmic rays is known to be obliterated quickly.

In 1967, Rao, McCracken, and Bartley (ref. 30) summarized these analyses of Pioneer anisotropy data collected during 1965 and 1966 for the period when solar flare effects were not seen. Considering only cosmic rays in the vicinity of 10 MeV/nucleon, their conclusions were:

(1) The 10 MeV/nucleon cosmic rays possessed a density gradient directed toward the Sun; i.e., density increases sunward, as expected.

(2) These low-energy cosmic rays are predominantly of solar origin even during the sunspot minimum.

(3) The density gradient frequently reverses in the range  $10 < E < 1000$  MeV.

(4) Cosmic radiation between 10 and  $10^5$  MeV corotates with the Sun.

Studies of the large-scale, steady-state structure of interplanetary space have also been made by comparing Pioneer data with those from other spacecraft (ref. 31). Comparison of Pioneer cosmic-ray telemetry with comparable data from the IMP 3 (Explorer 28) Geiger counter showed close agreement when the spacecraft were lined up with the sun. When separated by  $50^\circ$  in azimuth (in late 1966) the variations in cosmic-ray flux appeared to be due mainly to galactic cosmic rays. Balasubrahmanyam and his colleagues concluded that there exist numerous, long-lived regions of modulated cosmic-ray flux following the general spiral configuration of the interplanetary magnetic field as it corotates with the Sun.

#### A Closer Look at the Anisotropy-Magnetic Field Relationship

The early paper of McCracken and Ness (ref. 29), which introduced the filament concept, was modified by another joint paper in 1968 (ref. 32). The main thrust of this paper was that the observed anisotropies of low-energy cosmic rays could be divided into two groups:

(1) Equilibrium anisotropies which are most evident toward the end of a solar-flare event. The maximum cosmic-ray flux is always directed away from the Sun (fig. 6-20), and the anisotropy amplitude is low (5 to 15 percent). Perhaps of most significance is the fact that the anisotropies are not dependent upon the detailed nature of the interplanetary magnetic field.

(2) Nonequilibrium anisotropies which change direction in time and have amplitudes between 20 and 50 percent. These anisotropies are aligned—parallel or antiparallel—to the magnetic field.

These observations were interpreted as possible evidence of complex loops in the magnetic field.

#### Cosmic-Ray Propagation Processes

The GRCSW group published two general papers relating Pioneer cosmic-ray data to cosmic-ray flare effects and energetic-storm-particle events (refs. 33 and 34). The data used came from Pioneers 6 and 7 and covered 29 solar flares occurring between December 16, 1965, and October 31, 1966. Some of the more important conclusions expressed in this paper were:

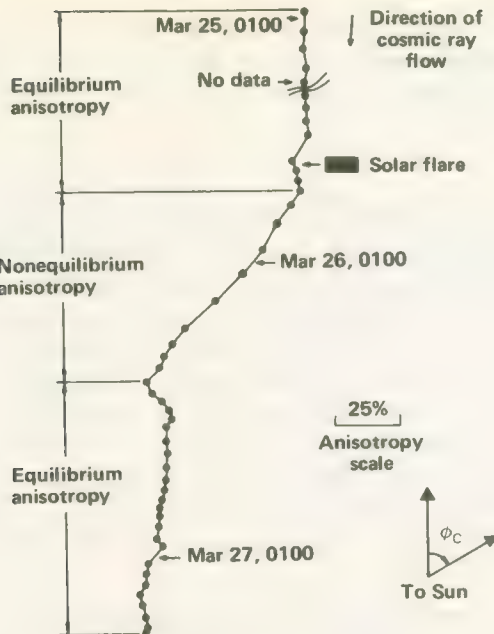


FIGURE 6-20.—The difference between the equilibrium and nonequilibrium classes of cosmic-ray anisotropy. The amplitudes and azimuths of the mean anisotropy for each hour are plotted as a vector addition diagram. Note definition of  $\phi_c$ . From: ref. 32.

- (1) Solar cosmic rays are normally extremely anisotropic with the direction of maximum flux aligned parallel to the magnetic field vector during the first part of the solar event.
  - (2) During the late portion of the flare, the cosmic rays are in diffusive equilibrium.
  - (3) Under some circumstances, the propagation of cosmic rays from the Sun to Earth is completely dominated by a "bulk motion" propagation mode. Here, the cosmic rays do not reach the spacecraft until the magnetic regime into which they were injected engulfs the Earth.
  - (4) In two cases, the anisotropy and cosmic-ray times of flight infer diffusion of the cosmic rays to a point on the western portion of the solar disk before injection into the magnetic field.
  - (5) Simultaneous observation by both Pioneers when separated by  $54^\circ$  of azimuth indicate density gradients of about two orders of magnitude per  $60^\circ$  sector during the initial stages of a solar flare.
  - (6) A study of cosmic-ray scattering within the solar system indicates a mean free path of about 1.0 AU for large-angle scattering.
- The second paper dealt with the energetic-storm-particle event which was defined as the very marked enhancement of cosmic rays in the 1 to

10 MeV range near the onset of a strong terrestrial magnetic storm. Data relating to seven such events were extracted from Pioneer-6 and Pioneer-7 telemetry. The data indicated a near one-to-one correspondence between the energetic-storm-particle events and the beginning of a Forbush decrease (fig. 6-21). It was shown further that the bulk of the energetic-storm-particles are apparently not trapped in the magnetic regime associated with the Forbush decrease. The Pioneer cosmic-ray data tend to support the Parker "blast wave" model in which the charged particles are accelerated by the magnetic field within the shock front. Further discussion can be found in reference 35.

The GRCSW group also compared the characteristics of corotating the flare-induced Forbush decreases as derived from cosmic-ray data obtained from Pioneers 6 and 7 (ref. 36). The results of this investigation are summarized in table 6-1.

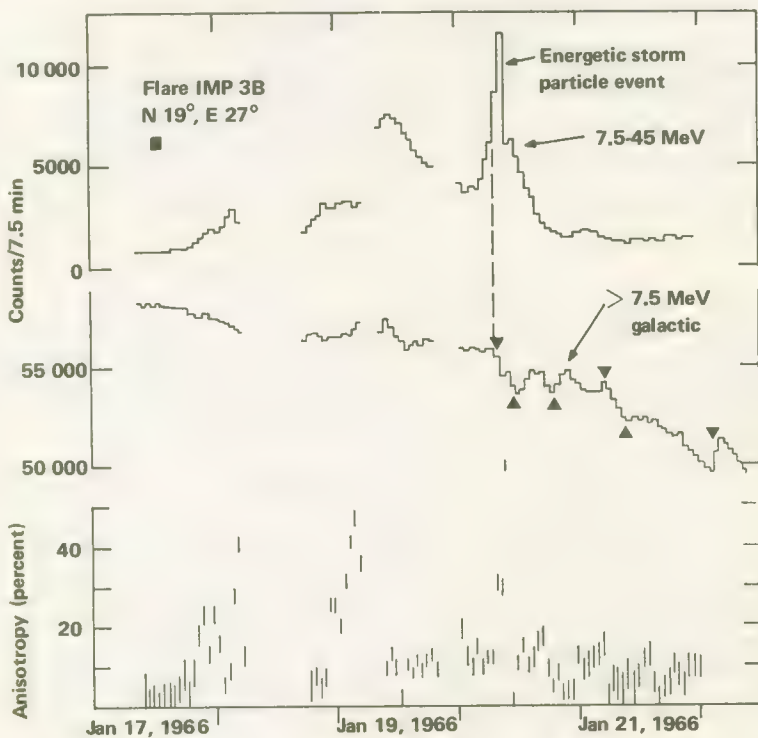


FIGURE 6-21—Temporal variations of the cosmic-ray counting rates and the cosmic-ray anisotropy amplitude during the period Jan. 17-21, 1966. Note that the major portion of the energetic storm-particle event occurred after the onset of the small Forbush decrease. The solid wedges refer to times at which major changes were observed to occur in the anisotropic nature of the cosmic radiation. From: ref. 34.

TABLE 6-1.—*Comparison of the Properties of Corotating and Flare-Initiated Forbush Decreases<sup>a,b</sup>*

| Corotating Forbush decrease                                   | Flare-initiated Forbush decrease  |
|---|---|
| Not accompanied by solar-generated cosmic rays                | Accompanied by solar cosmic rays and an energetic storm particle event                  |
| Onset time difference due to corotation                       | Probably simultaneous onset up to $\sim 100^\circ$ off the axis of the Forbush decrease |
| No amplitude dependence over $\sim 60^\circ$ of solar azimuth | Amplitude varies by a factor of $\sim 4.0$ over $\sim 60^\circ$ of solar azimuth        |

<sup>a</sup> Adapted from reference 36.

<sup>b</sup> The energy dependence of both classes of events is essentially the same.

### Galactic Alpha-Particle Flux

Some limited studies of the galactic alpha-particle flux measured by the Pioneer-6 GRCSW cosmic-ray experiment have been reported (ref. 37). An examination of the time dependence of alpha particles in the 124- to 304-MeV range shows that these particles exhibit the same recurrent Forbush decreases previously observed in the galactic proton flux.

### Studies of Specific Solar-Flare Events

Several solar-flare events have been examined in detail in the light of GRCSW cosmic-ray data and readings taken at several ground stations. By way of illustration, the results of the studies of the January 28, 1967, and March 30, 1969, events are summarized below (ref. 38). The salient features of the first event were:

- (1) The probable location of the responsible solar flare was about  $60^\circ$  beyond the west limb of the Sun.
- (2) Low-energy particles ( $< 100$  MeV) recorded by the Pioneers and the high-energy particles ( $> 500$  MeV) detected at Earth arrived after diffusion across the interplanetary magnetic field. Both groups of particles displayed remarkable isotropy.
- (3) The flux that would be observed by a detector ideally located in azimuth would be greater than 2000 particles  $\text{cm}^{-2} \text{ sec}^{-1} \text{ sr}^{-1}$  above 7.5 MeV.
- (4) Pioneer observations indicated low-energy injection commencing several hours before the high-energy main event.

Reiff has written a running account of the March 30, 1969, event (ref. 39). Solar activity was high during most of March; several active regions capable of generating solar flares were under surveillance. On March 30,

after the most active of these regions had rotated behind the west limb of the Sun, terrestrial radio telescopes recorded the largest 10-cm burst from the corona in scientific history. Within about 2 hr, the cosmic-ray instrumentation on Pioneers 6, 8, and 9 noted a sharp increase in low- and high-energy protons. About a day later, Pioneer 7 recorded the same increase in flux. Apparently a large solar flare had occurred on the other side of the Sun. The fluxes recorded by Pioneers 8 and 9 as well as those on Earth satellites subsided within a few days; by April 5, Pioneer-6 and -7 data followed suit.

By April 10, the active region of the Sun which produced these effects was only  $20^\circ$  behind the east limb. Once again a flare erupted. Within a half hour, cosmic-ray intensities at Pioneers 6 and 7 jumped more than an order of magnitude. Terrestrial instruments and those on Pioneers 8 and 9 showed little change. The relative locations of the Earth and the spacecraft are indicated on figure 6-22. Evidently the flare-generated radiation first engulfed Pioneers 6 and 7. Two days later, Pioneers 8 and 9 and terrestrial instruments were recording increases while levels at the other Pioneers dropped to near-normal levels. The motion of the active region and solar rotation had combined to turn the spray of radiation more than  $90^\circ$ .

In 1971, a key paper was published by McCracken and his colleagues describing the decay phase of typical solar flares (ref. 40). Some of the important conclusions from this paper follow:

(1) At times less than 4 days after the injection of a solar flare, the anisotropy at 10 MeV tends to be directed radially away from the Sun. After 4 days, this anisotropy is directed  $45^\circ$  east of the spacecraft-Sun line. This situation implies the dominance of convection over diffusion in the escape of solar cosmic rays late in flare life.

(2) A positive radial cosmic-ray density gradient exists at late times (more than 4 days) near the Earth's orbit. This drives a diffusive current along the interplanetary magnetic lines toward the Sun.

(3) The observed temporal variation of cosmic-ray flux can be ascribed to (a) convective removal of the cosmic radiation, and (b) the corotation of the cosmic-ray population.

(4) The observed rate of change of cosmic-ray flux is critically dependent upon the local value of the gradient in heliocentric longitude for energies less than 10 MeV.

(5) Cosmic-ray spectra indicate that the influence of the longitude gradient upon the observed temporal decay increases toward lower energies.

(6) Late in the solar flare, the spectral exponent near 10 MeV is dependent upon the longitude of the observer relative to the centroid of the cosmic-ray population injected by the flare.

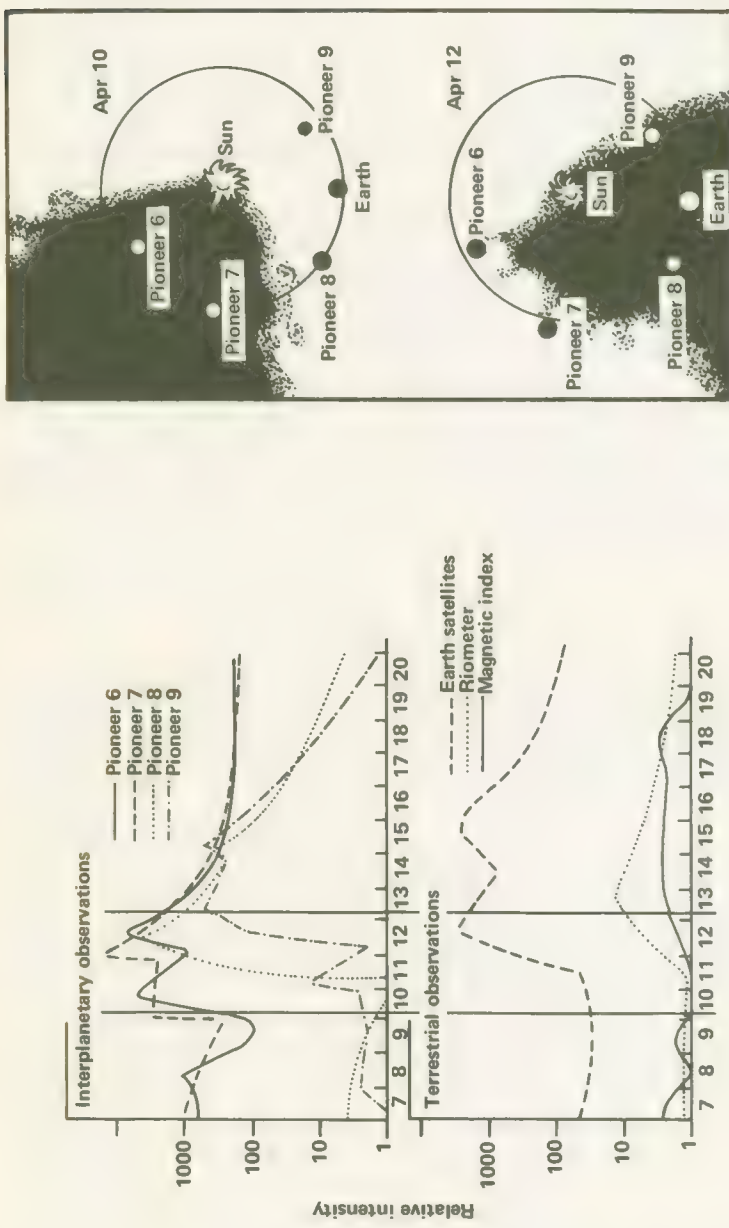


FIGURE 6-22.—Pioneer locations and data summaries for the solar proton event beginning on Apr. 10, 1969. From: ref. 39.

## THE MINNESOTA COSMIC RAY EXPERIMENT (PIONEERS 8 AND 9)

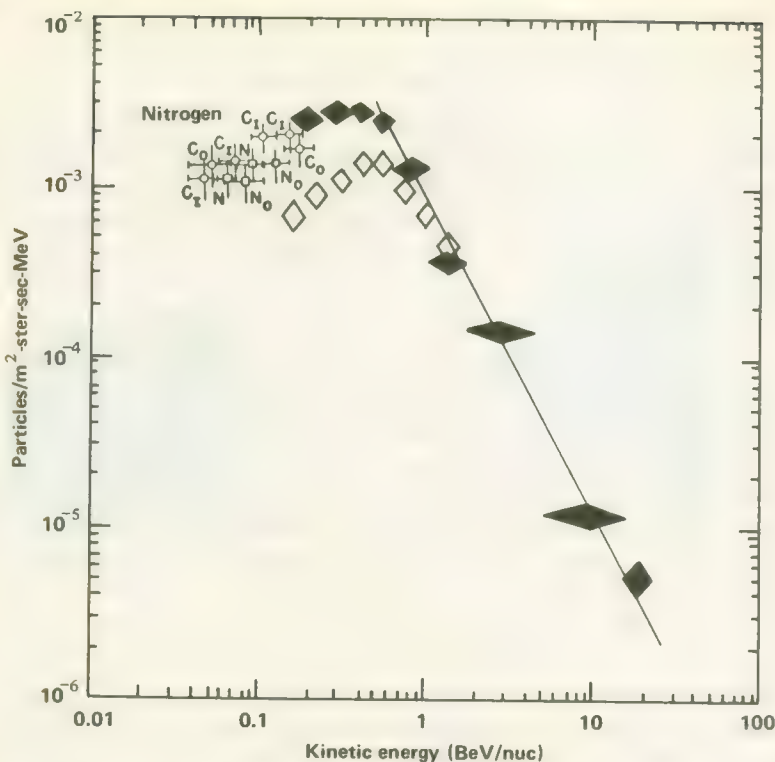
The Minnesota cosmic-ray telescopes replaced the Chicago instruments on the Block-I Pioneer flights. The energy range of the Minnesota instrument was considerably higher (4 MeV/nucleon to over 2 BeV/nucleon). The research results published to date are primarily concerned with galactic cosmic rays rather than the lower-energy particles originating on the Sun, although papers on solar cosmic rays are in preparation.

### Composition of Galactic Cosmic Rays

Although the so-called "M (medium) nuclei," carbon, nitrogen, and oxygen are the most abundant nuclei in cosmic rays except for hydrogen and helium, their relative abundances have been in question until recently. New measurements of cosmic-ray nitrogen from balloons and Pioneer 8 have provided better estimates (ref. 41). The energy spectrum of nitrogen was found to be identical with those of the other M nuclei over the range of 100 MeV to over 22 BeV/nucleon. The ratio of nitrogen nuclei to all M nuclei was found to be about 0.125, constant to within 10 percent over the above energy range (fig. 6-23). Assuming that some of the nitrogen in the cosmic-ray flux originates in fragmentation reactions with interstellar matter and knowing the proper cross sections, one can compute a "source" N/M ratio less than about 0.03. However, the solar atmospheric value for the N/M ratio is about 0.10—a disturbingly higher value. The implication is that galactic and solar cosmic rays may originate in fundamentally different processes.

The Pioneer-8 instrument also identified and measured fluorine nuclei in the galactic cosmic rays (ref. 42). The fluorine abundance was 1 to 2 percent that of oxygen for energies above 500 MeV/nucleon. These data on fluorine are consistent with the hypothesis that the fluorine is created by the fragmentation of heavier nuclei as they traverse roughly  $4 \text{ g/cm}^2$  of hydrogen in their flights through the galaxy.

In a later paper, the Pioneer-8 data were used to estimate the chemical composition and energy spectra of cosmic rays with atomic numbers from 3 to 30 (ref. 43). Briefly, the results were as follows. The ratio of light to medium elements (L/M ratio) was  $0.25 \pm 0.02$  and was constant with energy over the range of 100 MeV/nucleon to over 22 BeV/nucleon. No significant variations in the individual Li/M, Be/M, and B/M ratios were observed as a function of energy. These ratios were 0.086, 0.037, and 0.150, respectively (fig. 6-24). However, the Be/ $(\text{Li} + \text{B})$  ratio was considerably less than that predicted from known fragmentation parameters, suggesting that some  $\text{Be}^7$  had decayed in flight. The chemical composition of the heavier cosmic rays was roughly what one



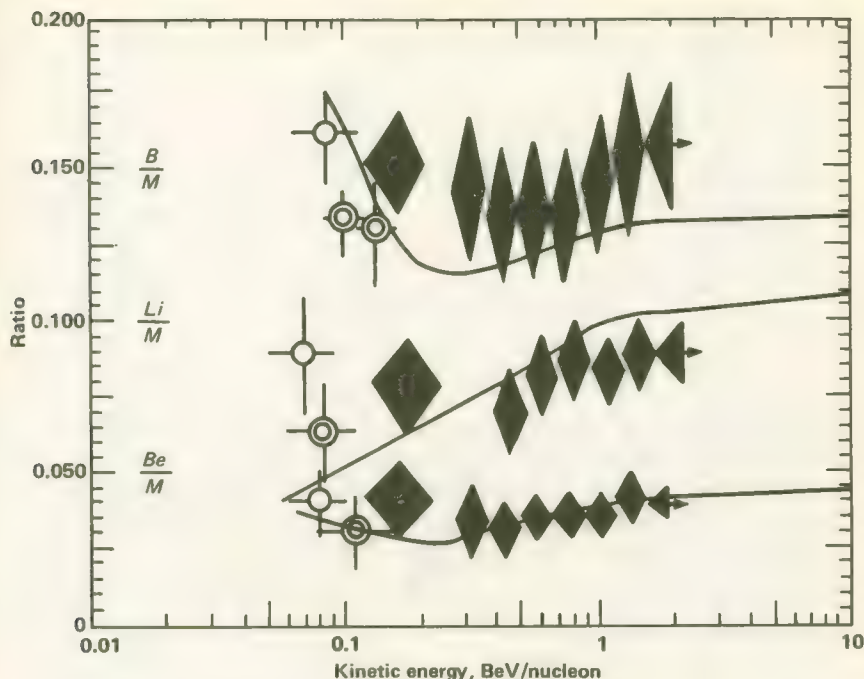


FIGURE 6-24.—The Li/M, Be/M, and B/M ratios (diamonds) as measured by Pioneer 8. The low energy measurements are from other sources. Solid lines are calculations of the energy dependences of these ratios. From: ref. 43.

TABLE 6-2.—*Chemical Abundances of Heavy Elements in the Primary Cosmic Radiation Measured by Pioneer 8<sup>a</sup>*

| Element | Abundances<br>$\text{Si} = \text{L}$ | Events<br>registered |
|---------|--------------------------------------|----------------------|
| F       | 0.13                                 | (52)                 |
| Ne      | 1.34                                 | (557)                |
| Na      | 0.26                                 | (110)                |
| Mg      | 1.39                                 | (575)                |
| Al      | 0.30                                 | (124)                |
| Si      | 1.00                                 | (415)                |
| P       | 0.13                                 | (53)                 |

<sup>a</sup> From reference 43.

ents within the solar system. First, the instrument measured differential energy spectra of protons and helium-nuclei between 40 MeV/nucleon and 2 BeV/nucleon; the analysis in this range was two-dimensional, greatly reducing the background. Second, each event was assigned to one of four quadrants, permitting a study of the anisotropies associated with the gradients. The results of these measurements are presented in

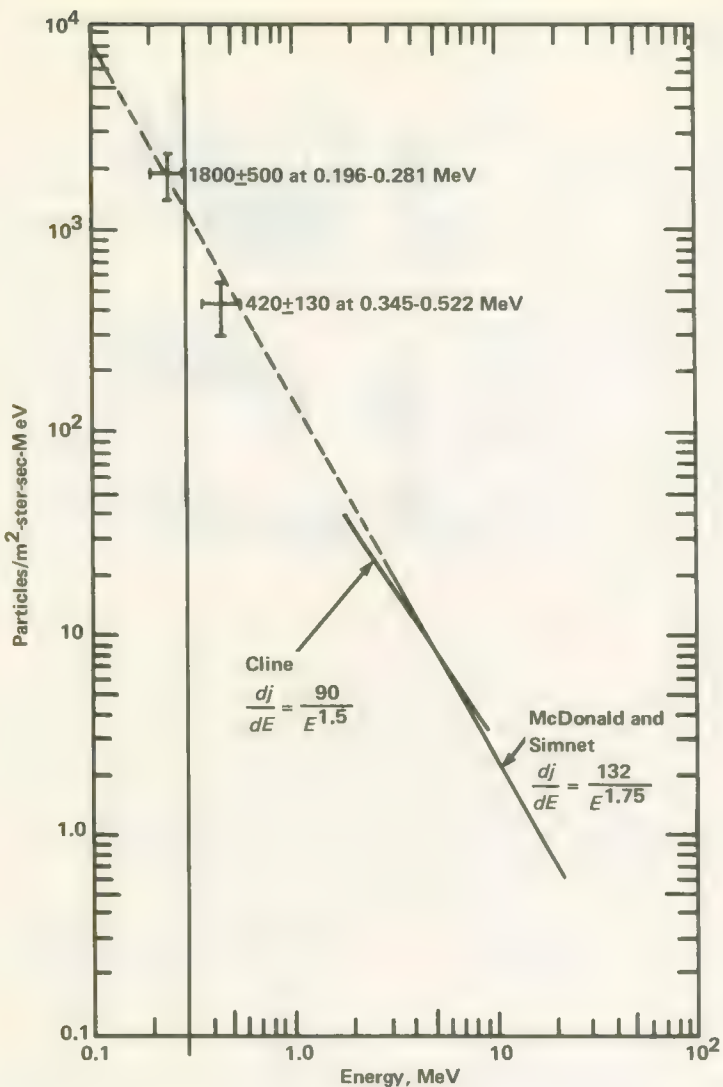


FIGURE 6-25.—Pioneer-8 measurements of low energy primary electrons. From: ref. 45.

table 6-3. In general, the cosmic ray anisotropy seems close to zero; however, it may be slightly positive in some energy ranges. The data indicate that there are no significant anisotropies above 240 MeV.

#### Effects of Solar Modulation

Pioneer 8 measurements of protons and helium nuclei were used in conjunction with data from balloons and terrestrial cosmic-ray monitors

TABLE 6-3.—*Gradient and Anisotropy Measurements on Pioneer 8*

| Energy              | Radial proton gradient | Radial proton anisotropy | Azimuthal proton anisotropy |
|---------------------|------------------------|--------------------------|-----------------------------|
| >2 BeV              | -1.5 ± 6%              | -0.31 ± 0.28%            | -0.13 ± 0.27%               |
| 1.25 BeV to 2 BeV   | 0 ± 7%                 | +0.26 ± 0.45%            | -0.38 ± 0.44%               |
| 660 MeV to 1.25 BeV | +23 ± 8%               | +0.57 ± 0.35%            | -0.55 ± 0.44%               |
| 334 MeV to 660 MeV  | +28 ± 9%               | +0.36 ± 0.38%            | -0.80 ± 0.35%               |
| 240 MeV to 334 MeV  | -7 ± 11%               | +0.7 ± 1.0%              | -0.60 ± 1.0%                |
| 63 MeV to 107 MeV   | +20 ± 15%              |                          |                             |
| >60 MeV             | 0 ± 5%                 |                          |                             |
| 12 MeV to 25 MeV    | 0 ± 25%                |                          |                             |

to observe the solar modulation of cosmic rays during the 1965 to 1968 period (ref. 45). Pioneer 8 instrumentation covered the rigidity ranges 200 MeV to 2 BeV, for protons, and 400 MeV to 2 BeV, for helium nuclei. Figures 6-26 and 6-27 show the results from Pioneer 8 compared with similar data from other sources at earlier times. The decreases noted from 1965 to 1968 are due, of course, to rising solar activity and the solar system's increasing ability to exclude galactic cosmic rays. When these changes are compared particle-by-particle, a number of new features arise that cannot be explained by the simple diffusion-convection theory of cosmic-ray modulation. The authors note, though, that models incorporating energy-loss effects are more successful in explaining these features.

### THE STANFORD RADIO PROPAGATION EXPERIMENT (ALL PIONEERS)

As described in ch. 5, Vol. II, the Stanford radio propagation experiment operates in a closed loop which employs the 150-ft paraboloidal antenna and associated transmitting equipment at Stanford University, the spacecraft receiver and transmitter, and the facilities of NASA's Deep Space Network. Basically, the experiment measures the integrated electron content between the spacecraft and the Earth. Corrections for the Earth's ionosphere are made with the help of radio-propagation measurements using Earth satellites such as the Beacon Explorers and the Applications Technology Satellites (ATSSs). The integrated electron content measurements can be very revealing scientifically when solar flares occur and when the spacecraft passes near the Sun or the Moon.

#### The Interplanetary Electron Number Density

Based upon Pioneer-6 data taken between February 20 and April 9, 1966, the average electron number density was  $8.25 \text{ cm}^{-3}$ , with an rms

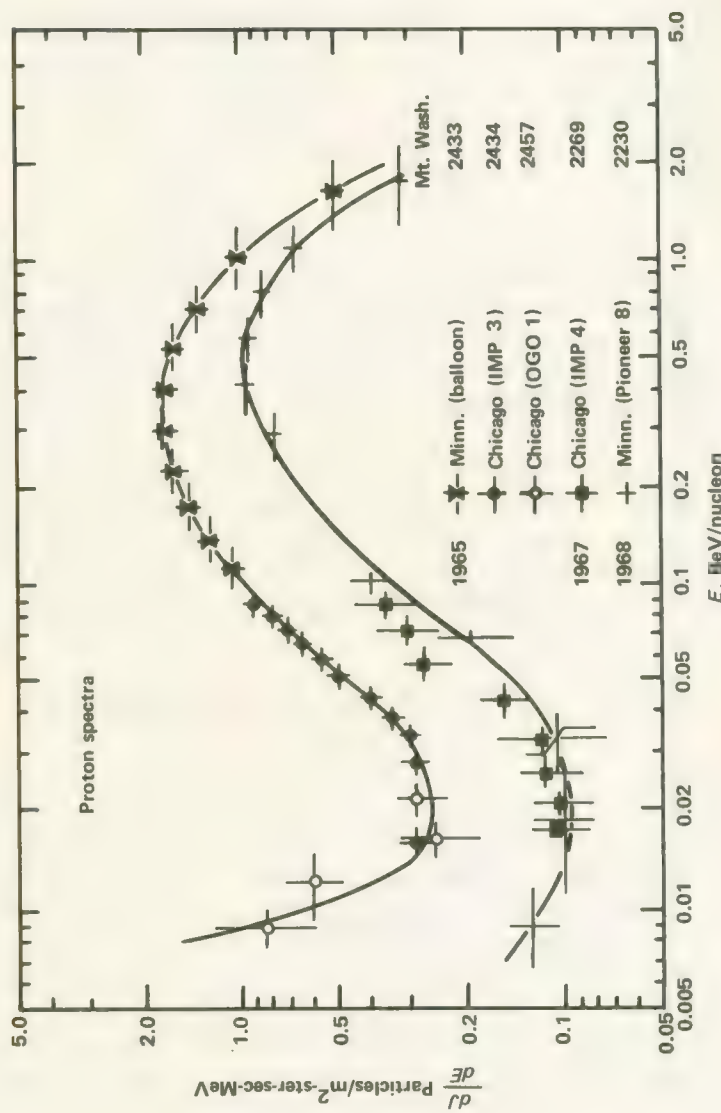


FIGURE 6-26.—Proton spectrum measured by Pioneer 8 in 1968. From: ref. 45.

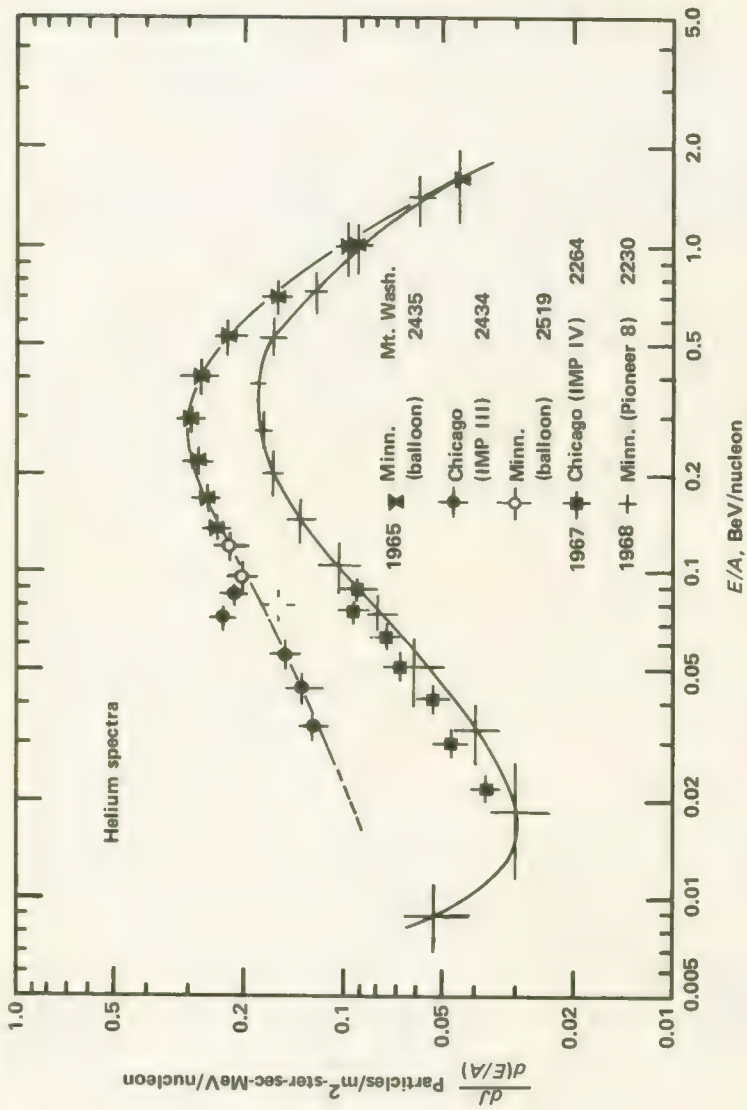


FIGURE 6-27.—Helium nuclei spectrum measured by Pioneer 8 in 1968. From: ref. 45.

of  $4.43 \text{ cm}^{-3}$  (ref. 46). As Pioneer 6 moved farther out into space, it soon became apparent that the first values reported were unusually high due to high solar activity. The spread in measured values of the total interplanetary electron content is shown for Pioneer 6 in figure 6-28. The electron number density can be computed from the slopes of the lines drawn through these scattered points. The data in the figure yield an electron number density of  $5.47 \pm 4.1 \text{ cm}^{-3}$ . A similar procedure for Pioneer-7 data leads to the value of  $8.02 \pm 3.8 \text{ cm}^{-3}$  (ref. 47).

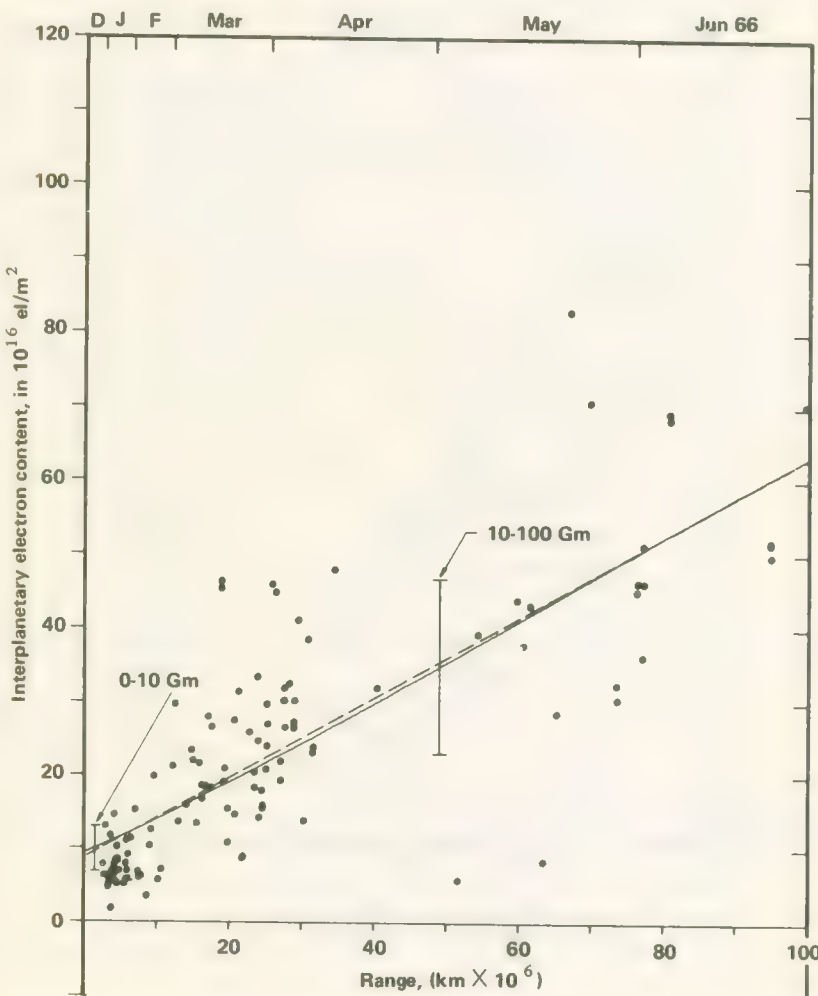


FIGURE 6-28.—Integrated electron content measured from Pioneer 6 to Earth as a function of spacecraft range. From: ref. 47.

### Plasma Pulses and Clouds

The measurements plotted in figure 6-28 owe their variation primarily to changes in solar activity and, consequently, the quantity of electrons injected into interplanetary space. Some of these injections—called plasma pulses or clouds—are fairly well-defined. Many have been “mapped” after a fashion by the Stanford radio propagation experiment. Koehler has reported on the analysis of three plasma pulses occurring on October 24, 1966, November 10, 1966, and January 25, 1967 (ref. 48).

On October 24, 1966, the integrated electron content measured between the Earth and Pioneer 6 was unusually high, as shown in figure 6-29. The difference between the electron content on October 24 and October 26, a “control” day with the usual electron content, is plotted in figure 6-30. As a first approximation, the curve is triangular in shape and can be explained as due to a rectangular pulse of increased electron density travelling radially outward from the Sun and crossing the propagation path. The peak electron content was  $40 \times 10^{16}$  electrons/m<sup>3</sup>. Dividing by the  $10.7 \times 10^6$  km propagation path, the peak increase in electron density over the background comes to 33 electrons/cm<sup>3</sup>. This particular pulse travelled the length of the propagation path in about 9 hr, leading to a calculated velocity of 330 km/sec. This figure corresponds well with the plasma velocity measured during the same period by the Ames plasma probe.

The event of November 10 was somewhat different in that the curve corresponding to that in figure 6-30 was flat-topped. The interpretation was that the pulse was shorter than the propagation path in this case. The flat-top, which represents a constant electron content, occurs before the leading edge reaches the spacecraft and after the trailing edge has passed the Earth.

The largest of the three pulses was noted on January 25. Its peak electron content was  $56 \times 10^{16}$  electrons/m<sup>3</sup> above the background. Indications were that this was approximately a spherical pulse  $5.2 \times 10^6$  km in diameter travelling at 350 km/sec.

The Stanford group made a more detailed study of the plasma cloud ejected by the July 7, 1966, solar flare (ref. 49). Although the radio propagation experiment was being operated beyond its nominal maximum range, the description of the plasma cloud derived from the measurements is compatible with the MIT plasma probe which also measured the passage of a plasma shock at the same time (ref. 19). The shape and extent of the passing plasma cloud was calculated from the integrated electron content measured from Pioneer 6. Three cloud shapes—each deduced from a different data channel—seemed to fit the data (fig. 6-31). Each cloud model has a double structure to account for the two

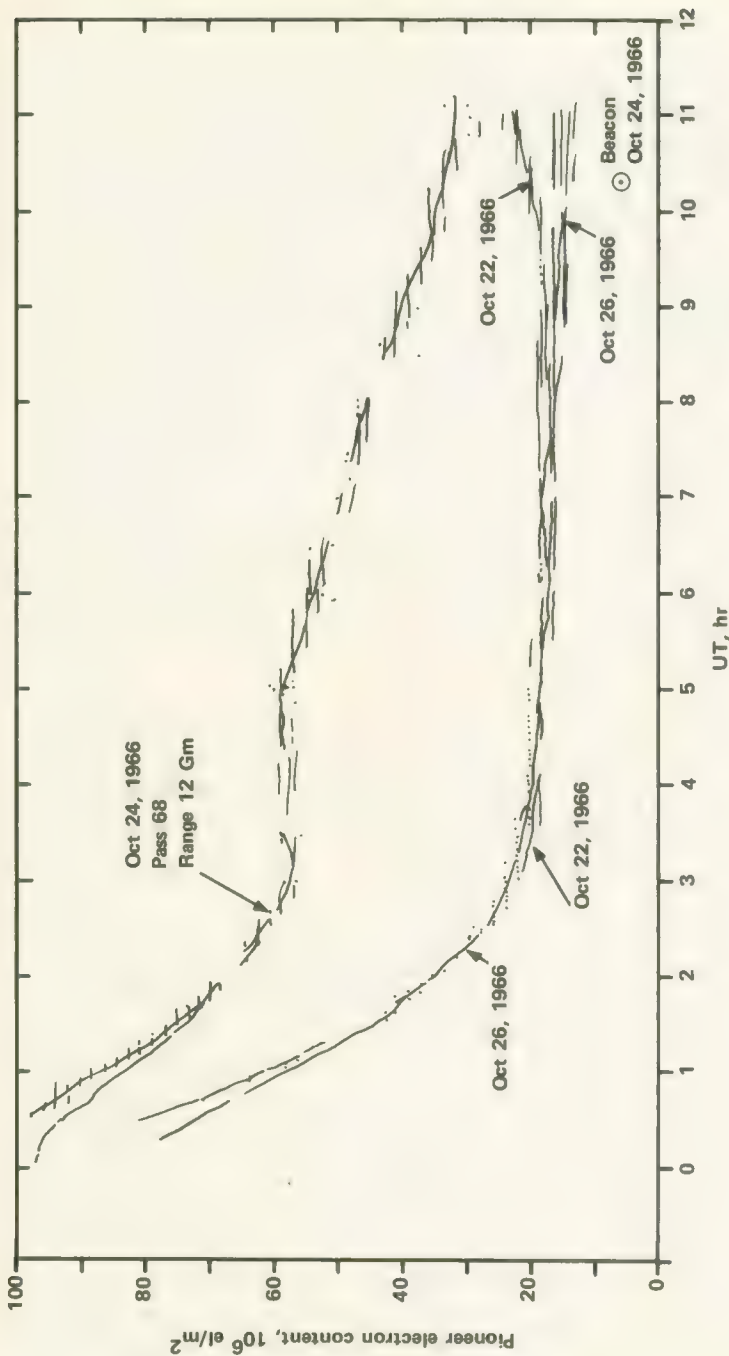


FIGURE 6-29.—The pulse of Pioneer electron content (interplanetary plus the ionospheric content) on Oct. 24, 1966. The normal content on Oct. 22 and 26 is shown for comparison.  
From: ref. 48.

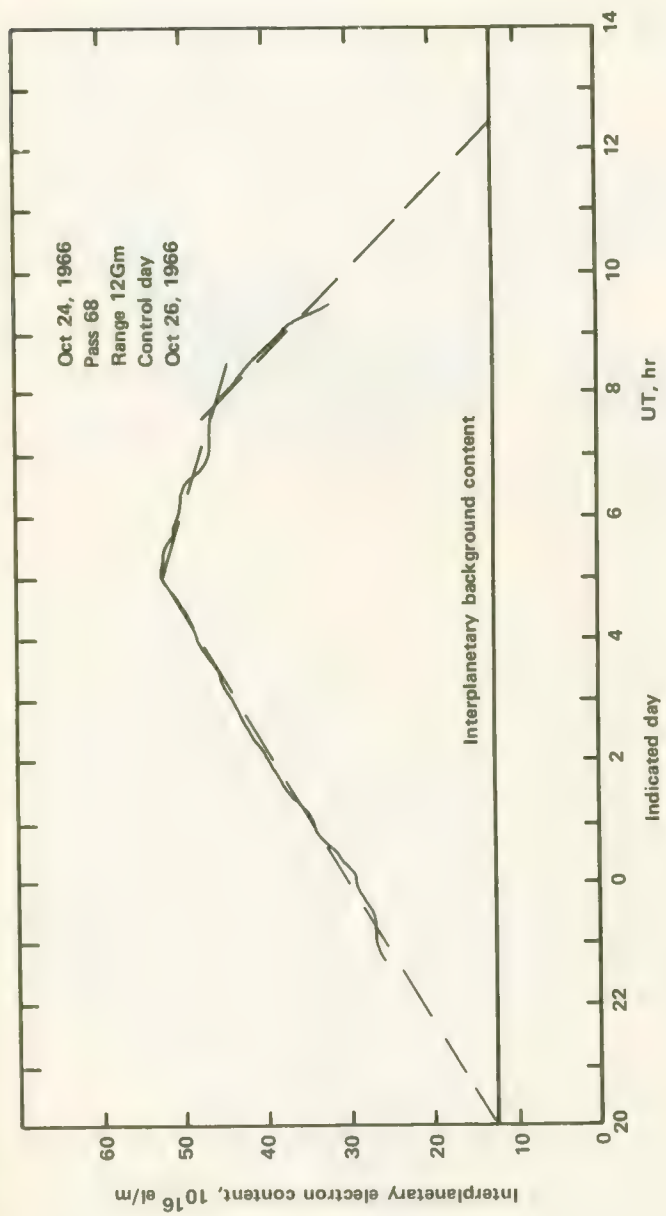


FIGURE 6-30.—The Oct. 24, 1966, pulse had a triangular shape on the electron content-time plot, inferring that it occupied the entire distance between the spacecraft and the Earth.  
From: ref. 48.

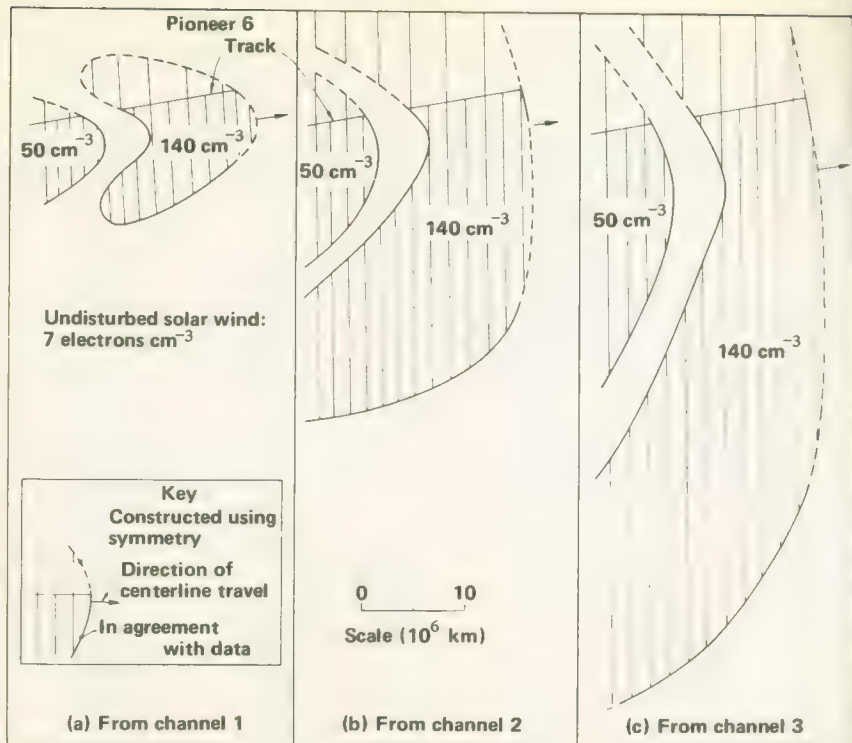


FIGURE 6-31.—Possible plasma cloud shapes. These shapes are consistent with measurements, but were restricted by simplifying assumptions and incorporate structural features based on prevailing theories about such cloud behavior. The configuration shown in (b) is considered the most likely. A gradient in density was actually measured along the Pioneer track, and a lateral gradient also probably existed; consequently, the cloud must have been broader than the outlines shown. From: ref. 49.

average density levels detected by the MIT instrument. The second cloud in figure 6-31 was thought to be the most probable configuration. Although a unique reconstruction of the cloud is impossible with the available data, the most likely models are consistent with the general conclusion that the shock fronts of the plasma clouds ejected from the Sun have radii of curvature of about 0.5 AU by the time they reach the Earth.

#### The January 20, 1967, Lunar Occultations

When the Moon occulted the Pioneer-7 spacecraft on January 20, 1967, radio signals sent from the 150-ft Stanford antenna were diffracted by the edge of the lunar disk and also refracted by the lunar ionosphere (ref. 50). The geometry of the situation is portrayed in figure 6-32. Of course, if there is no lunar ionosphere at all, only the classical Fresnel

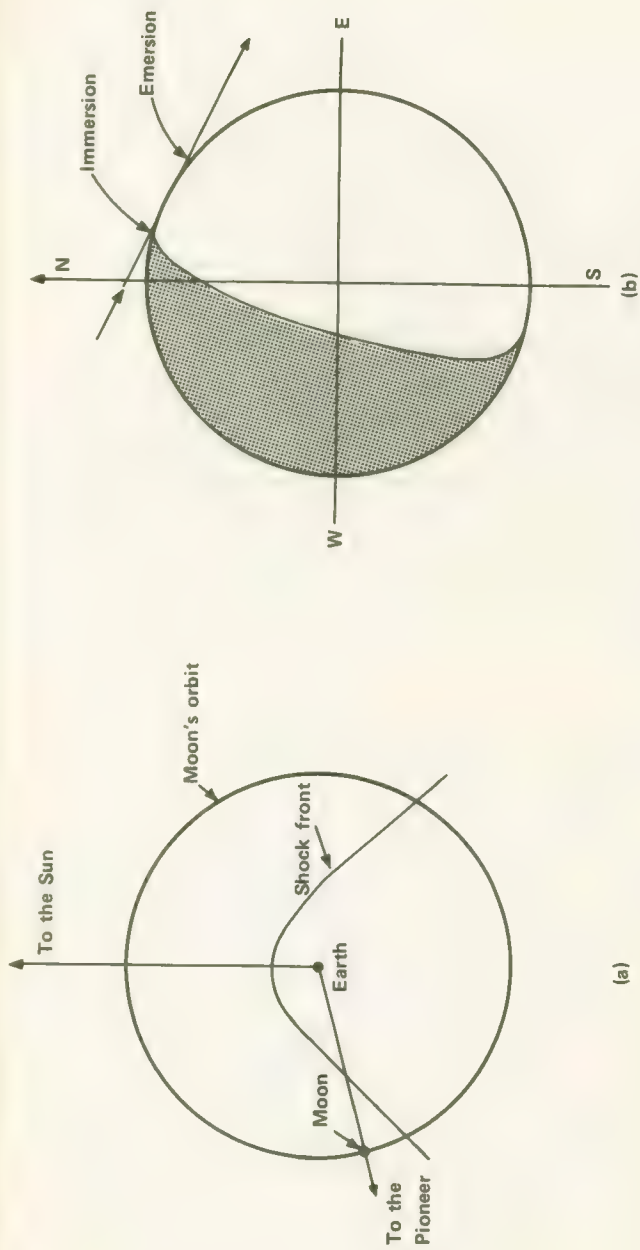


FIGURE 6-32.—(a) Relative positions of the Sun, the Moon, and Pioneer 7 in the plane of the ecliptic Jan. 20, 1967. (b) The lunar occultation of Pioneer 7 as seen from Stanford University. Immersion occurred at 05:30 UT; emersion was at 05:49 UT. From: ref. 50.

diffraction pattern will be measured (fig. 6-33). If an ionosphere is present, however, its refractive effects will displace the diffraction pattern in time. In this case, the difference in the angles of refraction for the 49.8- and 423.3-MHz signals were used to compute electron density.

The ray path from the Stanford antenna to Pioneer 7 was partially in the shadow of the Moon during immersion but was fully illuminated during emersion. The angles of refraction were  $-2.3$  microradians and  $-5.7$  microradians for immersion and emersion, respectively. The minus sign indicates that the electron density increases with height near the surface of the Moon, and that a tenuous ionosphere may be created—at least on the sunlit side—by the interaction of the solar wind with the lunar surface.

### Solar-Wind Flow Patterns

By taking measurements during two periods each day, first using a Pioneer spacecraft ahead of Earth and then another behind it, corotating solar-wind flow patterns are clearly visible (ref. 51). The density patterns observed are not consistent with the hypothesis of steady corotating flows—there are large transients which occur too rapidly. The Stanford group has observed that identifiable features recur with nearly but not exactly the same period on successive solar rotations. Croft suggests that these patterns might be due to the corotation of thin steady streams that fluctuate in direction. These data might also indicate that some corotating regions are of low density and featureless while others are dense and highly disturbed.

## RADIO PROPAGATION EXPERIMENTS USING THE SPACECRAFT CARRIER (ALL PIONEERS)

With the Stanford radio propagation experiment it is possible to measure the integrated electron density between the spacecraft and the Earth, as described in ch. 5, Vol. II. However, useful scientific information can also be obtained concerning transient space phenomena by observing changes in the Faraday rotation of the spacecraft S-band transmitter. Levy and his associates at the California Institute of Technology and the University of Southern California have used the DSN 210-ft antenna at Goldstone to measure transient Faraday rotations during solar occultation of Pioneer 6 (ref. 52). The geometry of the occultation is shown in figure 6-34. As the spacecraft line of sight approached the Sun, the S-band telemetry signal passed through increasingly dense regions of the solar corona. By November 16, however, the signal-to-noise ratio had deteriorated to the point where the experiment had to be discontinued until the signal was reacquired on November 29. At three points (marked A, B, and C on fig. 6-34) between 6 and 11 solar

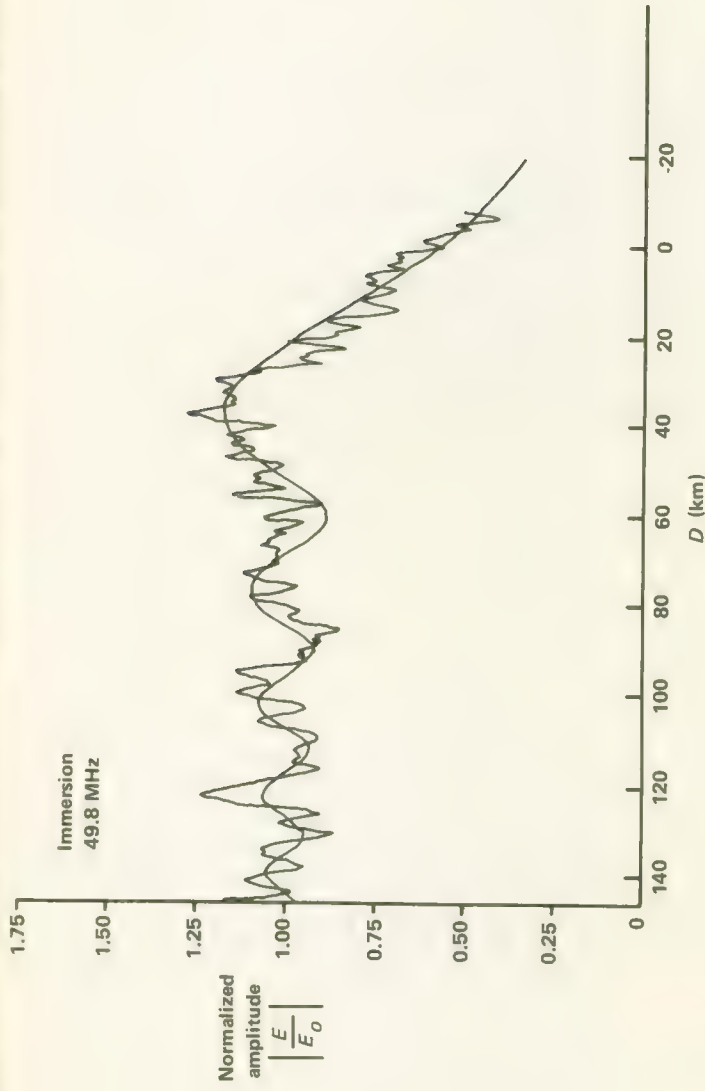


FIGURE 6-33.—Theoretical and actual diffraction pattern observed during the lunar occultation of Pioneer 7 at 49.8 MHz. From: ref. 50.

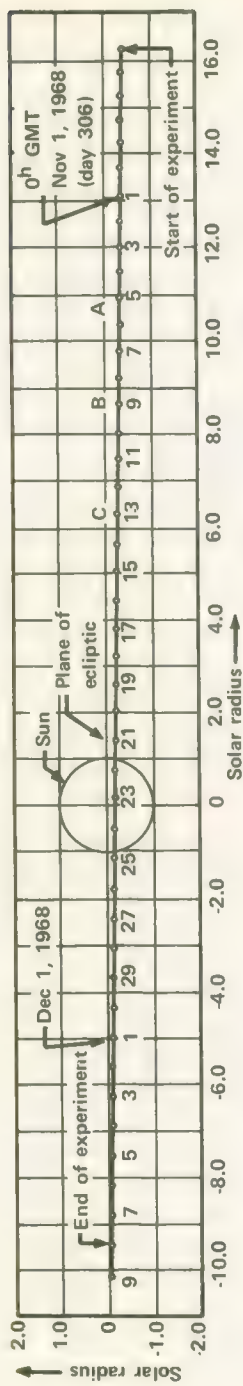


FIGURE 6-34.—Projection of Pioneer-6 orbit relative to the plane of the ecliptic. From: ref. 52.

radii, Faraday rotation transients were recorded (fig. 6-35). The duration of each event was about 2 hr. The transients were poorly correlated with solar flares, but it was noted that bursts of radio noise in the dekameter range occurred prior to the observation of the Faraday rotation phenomena.

Later studies of these transients at GSFC by Schatten led to the correlation of Levy's three events with specific Class-1 solar flares and sub-flares which preceded the events (ref. 53). Schatten interpreted Levy's evidence in terms of a magnetic bottle expanding from the corona to perhaps 10 to 30 solar radii before contracting back toward the corona. Resembling an elongated blister, the magnetic bottle and its electronic content would cause the observed Faraday rotation transients.

#### TRW SYSTEMS ELECTRIC FIELD EXPERIMENT (PIONEERS 8 AND 9)

The Pioneer Electric Field Experiment is physically associated with the Stanford Radio Propagation Experiment, utilizing its short 423-MHz antenna as a detector; but scientifically it is more closely allied with those experiments measuring characteristics of the interplanetary plasma; i.e., the Ames plasma experiment and the Ames and Goddard magnetometers. The electric field experiment was added late in the Block-II program and was thus rather limited in its allotments of weight, power, and telemetry capacity. The engineering design and physical operations of this experiment are described in ch. 5, Vol. II.

Early in the development of space physics, scientists concentrated primarily upon measuring solar plasma velocity, density, and temperature. Plasma dynamics, including the study of plasma waves and other "cooperative" phenomena, was generally not emphasized. It was recognized, of course, that waves and many other dynamic phenomena were not being detected with the usual plasma instruments. Earth satellites soon began carrying vlf (very low frequency) radio listening experiments and high-sensitivity instruments like the "LEPEDEA" analyzers. These instruments began to reveal the true complexity of the plasma environment near the Earth. It was, therefore, desirable to install a vlf or electric field experiment on the Block-II Pioneers. Fortunately, this proved possible.

Near the Earth's orbit the solar wind is very dilute, and the plasma is truly collisionless. Individual electrons and positive ions are influenced only by dc electromagnetic fields or by fields due to the organized motion of plasma particles in the form of ac plasma waves. The Pioneer Electric Field experiment was designed to detect these microscopic plasma phenomena. The overall size of the Pioneer spacecraft and its appendages is small compared to the Debye length in interplanetary

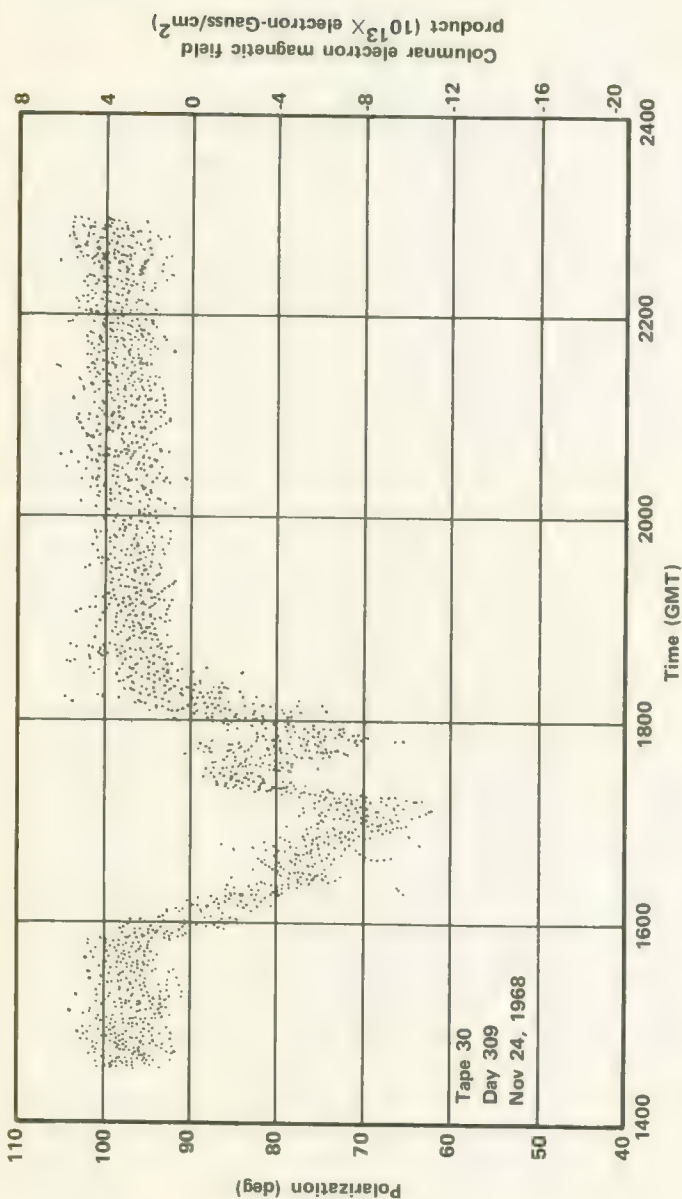


FIGURE 6-35.—One of the transient Faraday-rotation phenomena observed by Levy et al. From: ref. 52.

space and also the minimum wavelength for any undamped plasma oscillation. Thus, the spacecraft actually represents a "microscopic" measuring platform immersed in plasma phenomena of much greater fundamental size. The 423-MHz antenna is a relatively insensitive, but adequate, capacitively coupled sensor that detects plasma waves sweeping past the Pioneers in interplanetary space.

While magnetometers have helped scientists understand microscopic electromagnetic phenomena in space, the Pioneer Electric Field experiment is primarily electrostatic in nature—in fact, it was the first low-frequency (under 20 kHz) electric field experiment to be flown in deep space. The Pioneer instrument detects density fluctuations within the plasma rather than the motions of current systems indicated by magnetometers. In this sense, the electric field experiment allows us to study the plasma from an entirely different vantage point than the more conventional plasma probes and magnetometers. Electrostatic plasma phenomena can carry considerable energy in deep space and strongly affect overall plasma behavior. The following discussion of the results obtained from this experiment underscores the importance of these extremely simple, lightweight instruments in our understanding of the interplanetary medium.

### Presentation of Early Results

The initial results from the Pioneer-8 Electric Field experiment were reported by Scarf *et al.* (ref. 54). These experimental data were treated in three categories.

*Broadband measurements.*—During the spacecraft's passage across the Earth's magnetosphere, very low amplitude vlf oscillations were detected. On December 14, Pioneer 8 first encountered the streaming plasma in the distant magnetosheath, as indicated in figure 6-36. The electric field experiment detected some plasma waves before the Ames plasma probe registered its first bursts of plasma around 2140 UT. Apparently the crossing of the magnetosphere was completed about 0230 on December 15 when both the electric field experiment and the Ames plasma probe indicated enhanced activity. Almost coincident with the penetration of the magnetosheath, Earth-based magnetic field instrumentation reported a magnetic disturbance (a sudden commencement). Within minutes of the terrestrial indication, the Pioneer electric field experiment also detected the disturbance. Evidently, the phenomena stimulating terrestrial magnetic storms also intensify interplanetary plasma waves.

*The 400-Hz channel.*—When the preceding broadband data are combined with information from the narrow-bandwidth 400-Hz channel,

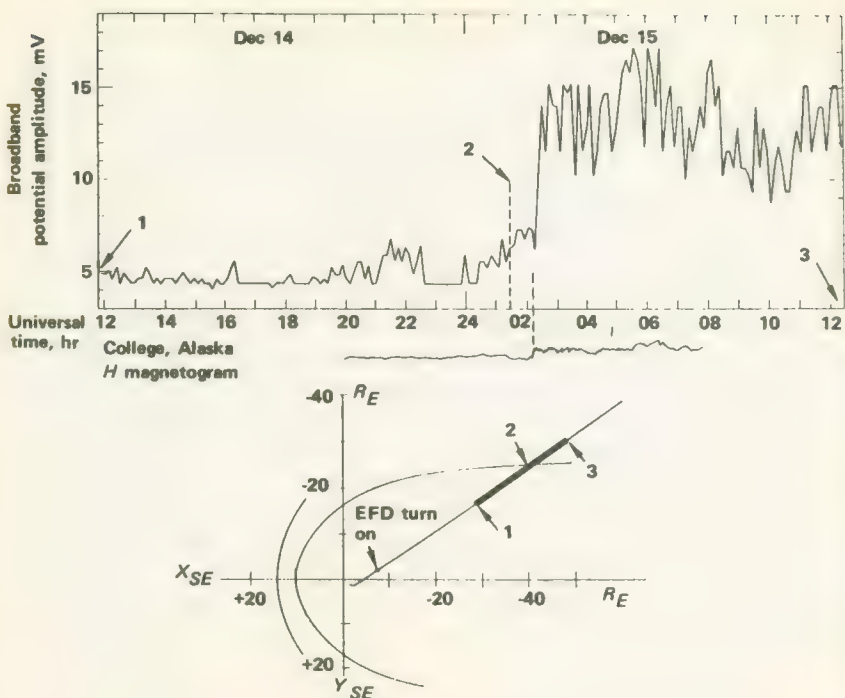


FIGURE 6-36.—Broadband wave amplitudes in the outer magnetosphere and magneto-sheath. The projection of the near-Earth trajectory in the ecliptic plane is shown, and the heavy segment represents the period from 1200 UT, Dec. 14 to 1210 UT on Dec. 15 (indicated by the numbers 1 and 3). Point 2 shows where the Ames Research Center plasma probe first started to detect continuous streaming plasma (personal communication), but bursts were encountered earlier. The H component of the College, Alaska, magnetogram shows a sudden commencement at 0215 UT, Dec. 15, followed by a storm (this ssc was categorized as a sudden impulse by some observatories), and the broadband wave amplitude rose shortly thereafter. From: ref. 54.

one obtains a measure of the spectral width of the low-frequency noise band.

Telemetry from the 400-Hz channel revealed a regular modulation that was quickly associated with the spacecraft's spin rate, more precisely with the instantaneous position in space of the Stanford antenna. The effect was greatest when this antenna was pointed toward the Sun. Apparently, the physical cause of the modulation is a Sun-aligned space-charge cloud surrounding the non-conducting spacecraft.

Despite the modulation, the 400-Hz channel is clearly sensitive to the plasma waves detected by the broadband channel. Further conclusions were not drawn at the time this initial paper was written.

*The 22-kHz channel.*—The narrow-bandwidth 22-kHz channel provides information about plasma oscillations when the electron concentration is relatively low. There is a natural noise background at this frequency, but it usually lies well below the experiment's threshold. Rarely, however, intense bursts of 22-kHz noise activate the receiver. The noise burst portrayed in figure 6-37 is typical. Although rare, these noise bursts do not appear to be random, being weakly correlated with solar and geomagnetic activity and strongly correlated with proximity to the Earth's magnetosphere.

The following tentative observations were presented by Scarf *et al.* (ref. 54) :

(1) Even when the Sun is quiet, low-frequency electric waves ( $>100\text{Hz}$ ) can be detected in the solar wind although the lowest levels are near the in-flight background.

(2) Wave amplitudes at the lowest frequencies vary markedly with changing conditions in interplanetary space. These electric field changes are correlated with local changes in the plasma environment as registered on the Ames plasma probe.

(3) As Pioneer 8 moved away from the Earth, the effects of corotation and solar-wind travel times were evident when comparing disturbances recorded at both the Earth and the spacecraft.

(4) Large-amplitude high-frequency waves, detected when the spacecraft was far from Earth, are apparently the result of bursts of interplanetary, but Earth-associated, electron oscillations.

### Shock Structures

At the 1969 Summer Advanced Study Institute at the University of California at Santa Barbara, further results were presented on the shock structures detected by the Pioneer electric field experiment (ref. 55). Data from Pioneers 8 and 9 and OGO 5 were used to demonstrate the several types of shock structures found in the high Mach-number solar plasma colliding with the Earth's magnetosphere. The most common structure reported was a large-amplitude magnetohydrodynamic pulse having a characteristic length equal to the initial gradient and a trailing wavetrain. Energy in these shock structures is apparently dissipated via electrostatic wave turbulence which arises from instabilities. Further thoughts concerning these interactions were presented in a second paper at this same meeting by Scarf and his associates (ref. 56).

### Measurements in the Distant Geomagnetic Tail

The plasma-probe and electric-field data recorded as Pioneer 8 crossed the Earth's geomagnetic tail during January 1968 were reported in 1970

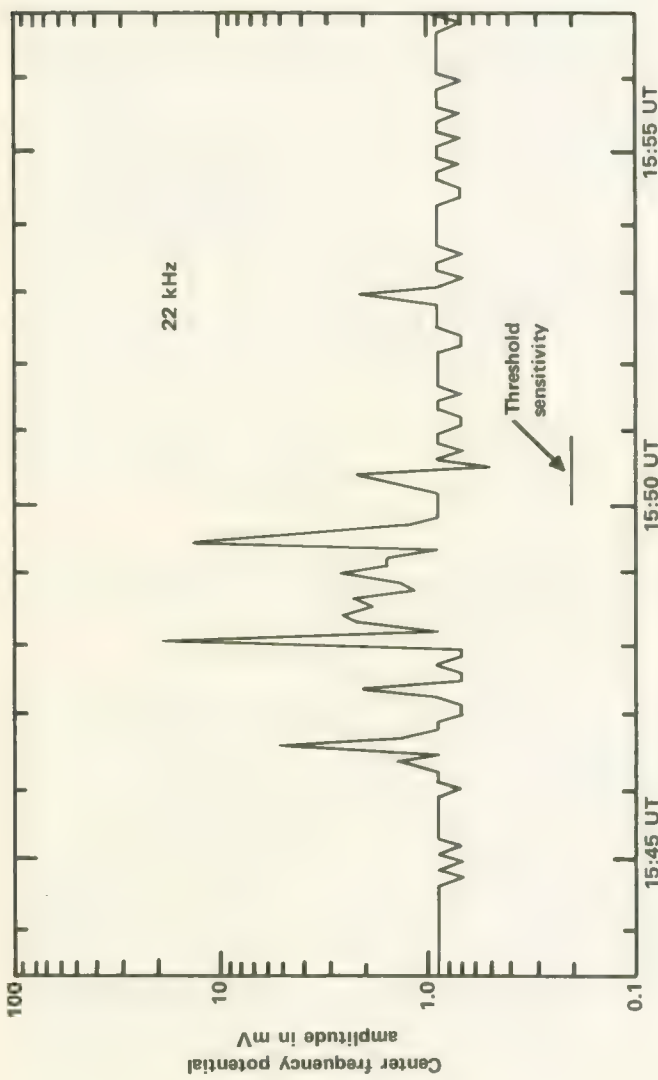


FIGURE 6-37.—Example of a 22-kHz noise burst on Dec. 21, 1967;  $r = 150 R_E$ . The in-orbit background is near 0.68-0.89 mV, and deviations below this are found only when the most intense enhancements are also detected. These large-amplitude 22-kHz bursts are observed very rarely. From: ref. 54.

by the researchers at Ames and TRW Systems (ref. 57). Both instruments recorded disturbances near the tail boundaries between 500 and 800 Earth radii downstream. The major conclusion of this paper was that tail breakup and field-line-reconnection phenomena begin within 500 Earth radii.

### Multi-Instrument Correlation of Space Disturbances

The initial results from the Pioneer-8 electric field experiment showed clearly their close correlations with terrestrially detected magnetic activity. Because the other Pioneer instruments also record space events (from a different perspective), correlations between different onboard instruments should also be obvious in many instances. Scarf, in his 1970 review paper, illustrated a three-way correlation during a Forbush decrease. Figure 6-38 indicates how the Pioneer-8 magnetometer, electric-field experiment, and the Minnesota cosmic-ray experiments all recorded the same event.

Another interesting correlation between different instruments (on different spacecraft this time) was revealed by Siscoe *et al.* (ref. 58). They illustrated the striking correlation between Pioneer-8 electric-field data and the solar-wind parameters recorded by Explorer 35 (in lunar orbit) in late February 1968 (fig. 6-39). Siscoe *et al.* noted that the electric-field noise data are of two types: (1) bursts or spikes lasting less than 10 sec, and (2) persistent signals typically lasting a day or more. The first type of data coincide with plasma and magnetic-field discontinuities, whereas the latter are available for comparison. The persistent signals, on the other hand, correlate loosely with solar-wind density, whether the density increases are due to interplanetary shocks (the so-called "snow plow" effect) or other processes.

This multi-spacecraft correlation study also proved of value in defining the spatial extent of the Earth's influence. Siscoe and his associates showed that a huge wake region surrounds the distant geomagnetic tail (ref. 59). This analysis indicated that Pioneer 8 did not encounter undisturbed solar wind for several months following launch. In a later paper, Siscoe used this fact to explain the early anomalous E-field observations (ref. 59).

In later papers, new types of correlation studies were presented (refs. 60 and 61). Nearly simultaneous wave observation from OGO 5 and Pioneer 9 were compared and used to provide an in-flight calibration for the simple Pioneer instrument. Analysis of these wave observations suggested that the wave spectrum varies with radial distance from the Sun.

In concluding the discussion of the electric-field experiment, it should be noted again that the experiment had only very limited telemetry

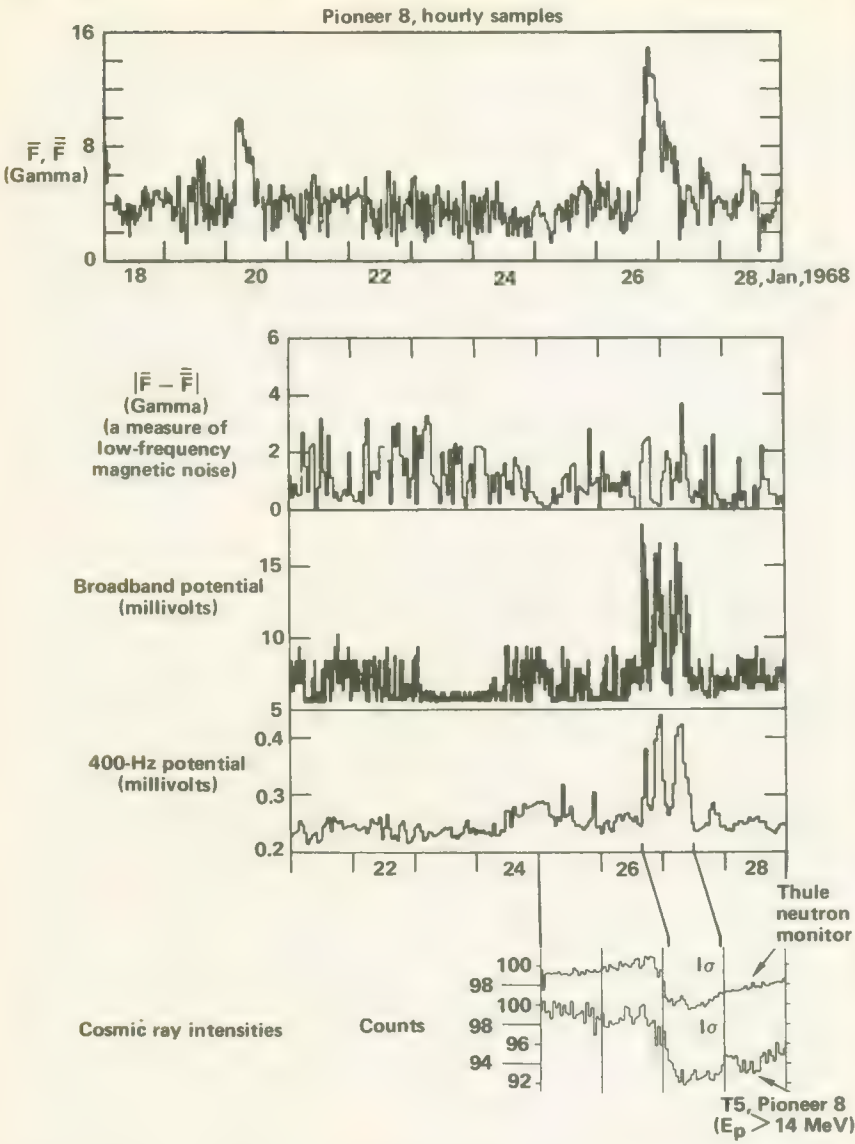


FIGURE 6-38.—Pioneer 8 magnetometer data (top) and electric-field data (middle) reveal interplanetary shock. Cosmic-ray readings (bottom) show attendant Forbush decrease.

capacity assigned, and that the interpretation of results is somewhat complicated by interactions of the interplanetary medium with the spacecraft. For example, the experiment was too limited for the unambiguous determination of plasma wave modes in interplanetary space.

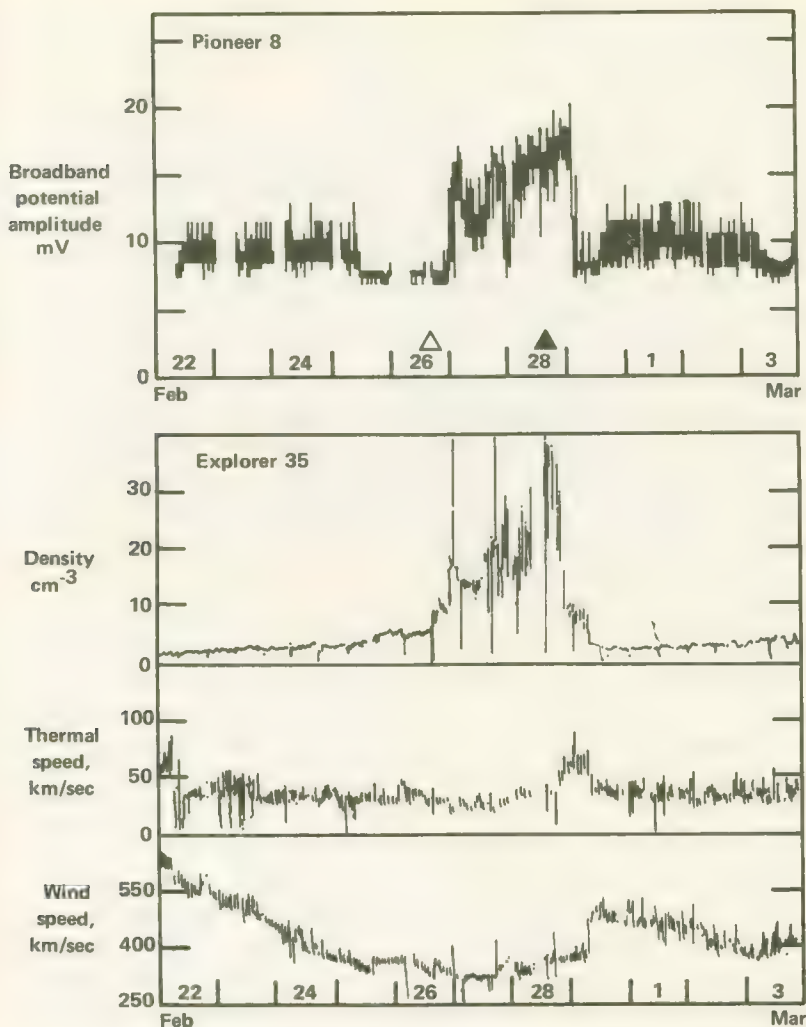


FIGURE 6-39.—Interplanetary shock registered almost simultaneously on Pioneer 8 electric field experiment and Explorer 35 plasma probe.

#### THE GODDARD COSMIC DUST MEASUREMENTS (PIONEERS 8 AND 9)

During the early days of the Space Age, cosmic dust was thought to be a serious hazard to men and machines operating outside the Earth's protective atmosphere. More accurate measurements of cosmic dust particles have since shown these fears to have been unwarranted. Sensitive external surfaces on long-lived Earth satellites may suffer some degrada-

tions, but neither manned nor unmanned spacecraft have been compromised. Nevertheless, cosmic dust particles do exist, and their presence in space demands a scientific explanation.

Are cosmic dust particles products of cometary disintegration or the debris from collisions within the asteroid belt? Most of our insight into this question at present comes from ground-based photographic and radar measurements of meteor trails. These data suggest that almost all cosmic dust trajectories are heliocentric with the orbital characteristics of comets rather than asteroids. Further, the particles seem "fluffy" and of low density. The Pioneer cosmic dust experiment, which flew on Pioneers 8 and 9, was designed to help answer this question of particle origin with *in situ* data from deep space.

The experiment itself (described in detail in Vol. II) was designed and tested by a team of scientists and engineers at Goddard Space Flight Center. Arrays of plasma and acoustical sensors can measure particle directions, energies, and, through a time-of-flight technique, velocities. The early results from Pioneer 8 described below have been reported by the Goddard group (ref. 62).

During the first 390 days of continuous exposure of the Pioneer-8 sensors, numerous events (several per day) were recorded by the front sensor array alone, the rear sensor array alone, or the microphone sensor alone. These data were not completely analyzed at the time the referenced papers were written. However, six time-of-flight events involving both front and rear sensor arrays were also registered. These are considered highly important to the question of cosmic dust origin because orbital information can be derived from the measurements.

The six time-of-flight events in a space of 390 days represent a rate  $3.8 \times 10^4$  lower than the rate recorded by a time-of-flight experiment on OGO 1. It is surmised that the high OGO-1 rate was due to coincident noise pulses in that experiment—noise was a serious problem with early scientific satellite cosmic dust experiments. Early Pioneer-8 results confirm expectations from zodiacal light measurements.

From a knowledge of the spacecraft trajectory and orientation at the instant of each event and the telemetered data indicating times of flight and the specific sensors activated in the front and back arrays, it was possible to derive the particle orbits shown in table 6-4. These data indicate a cometary origin for the six particle events, reinforcing the conclusions derived from ground-based observations.

The most interesting of the six events reported in the two papers occurred on April 13, 1968. Apparently, one front sensor segment and two rear sensors responded, inferring that the particle partially disintegrated upon first impact, showering the rear array with a conical spray

TABLE 6-4.—*Particulars for the First Six Time-of-Flight Events Detected by Pioneer 8<sup>a</sup>*

| Date    | MPS  | SCS  | MPI        | TPS   | PM   | a    | e    | q     | q'   | $\omega$ | $\Omega$ | i   | $\pi$ |
|---------|------|------|------------|-------|------|------|------|-------|------|----------|----------|-----|-------|
| 3/11/68 | 7.5  | 27.3 | $0 \pm 27$ | 19.3  | 2.1  | 0.67 | 0.58 | 0.28  | 1.07 | —        | —        | 0   | 339   |
| 3/26/68 | 18.0 | 28.8 | $0 \pm 27$ | 12.5  | 0.93 | 0.58 | 0.84 | 0.095 | 1.07 | —        | —        | 0   | 7     |
| 4/13/68 | 27.6 | 28.5 | $0 \pm 27$ | 16.05 | 2.2  | 0.62 | 0.97 | 0.019 | 1.22 | —        | —        | 0   | 24    |
| 4/14/68 | 34.0 | 28.4 | $0 \pm 27$ | 9.06  | 0.78 | 0.55 | 0.97 | 0.013 | 1.09 | —        | —        | 180 | 17    |
| 5/25/68 | 15.7 | 27.9 | $0 \pm 27$ | 13.28 | 1.2  | 0.59 | 0.81 | 0.11  | 1.07 | —        | —        | 0   | 50    |
| 1/24/69 | 5.9  | 30.4 | $33 \pm 8$ | 31.5  | 1.9  | 1.28 | 0.24 | 0.98  | 1.59 | 49.9     | 102      | 5.9 | 152   |

MPS—Measured Particle Speed (km/sec)

SCS—Spacecraft Speed (km/sec)

MPI—Measured Particle Inclination (deg)

TPS—True Particle Speed (km/sec)

PM—Particle Mass (derived) (gm  $\times 10^{-11}$ )

a—Semi-Major Axis (in AU)

e—Eccentricity

q—Perihelion Distance (in AU)

q'—Aphelion Distance (in AU)

 $\omega$ —Argument of Perihelion (deg) $\Omega$ —Longitude of the Ascending Node, deg

i—Inclination of the Orbital Plane to the Ecliptic, deg

 $\pi$ —Longitude of Perihelion (deg)<sup>a</sup> See reference 63.

of debris. No such fragmentation was observed during laboratory tests with particles fired from an electrostatic accelerator. In view of the possible friable nature of cosmic dust material, this type of event was not unexpected. The much higher rates of solitary front and back array events also tend to indicate fluffy particles with poor penetrating powers.

The April 13, 1968, event was notable in two other aspects: (1) its impact energy exceeded 80 ergs, more than any other particle recorded; and (2) it was the only particle that activated the acoustical sensor. Thus, independent measurements of the particle mass were possible from the energy and momentum equations. These were  $2.3 \times 10^{-11}$  and  $1.6 \times 10^{-11}$  grams—relatively good agreement for this kind of experiment. From this information an orbit for the particle can be computed (fig. 6-40). However, it is cautioned that the response of the acoustic sensor to the postulated spray of debris is unknown and was assumed to be the same as that of a solid particle.

Summarizing, the early Pioneer-8 cosmic dust data tend to confirm the hypotheses that cosmic dust is almost exclusively of cometary origin and rather fluffy or friable in character.

In a paper presented at the XIIIth Plenary Meeting of COSPAR in May 1970, Berg and Gerloff summarized Pioneer results to that date (ref. 63).

(1) The microphone micrometeoroid detectors employed on many early spacecraft also respond to the cosmic rays generated by solar flares. This effect was responsible for the much higher micrometeoroid fluxes "measured" by these craft in the early days of space science.

(2) The micrometeoroid flux between 0.7 and 1.1 AU is  $2 \pm 0.5 \times 10^{-4}$  particles/m<sup>2</sup>-sec- $2\pi$ sr and shows a cutoff at a mass of  $5 \times 10^{-12}$  g (fig. 6-41).

(3) Among the eight detected particles for which orbits could be computed were two that travel in the orbital planes of known comets (Encke and Grigg-Skjellerup).

### THE PIONEER CELESTIAL MECHANICS EXPERIMENT (ALL PIONEERS)

All spacecraft launched out of the Earth's gravitational "well" provide opportunities for improving solar system constants and ephemerides. Although the Pioneer spacecraft did not pass close to any other planets, their trajectories were affected by the Moon. Further, the launch of four similar spacecraft, of known mass and equipped with tracking aids, into heliocentric orbits made possible more accurate determinations of the Astronomical Unit (AU) as well as the Earth's ephemeris.

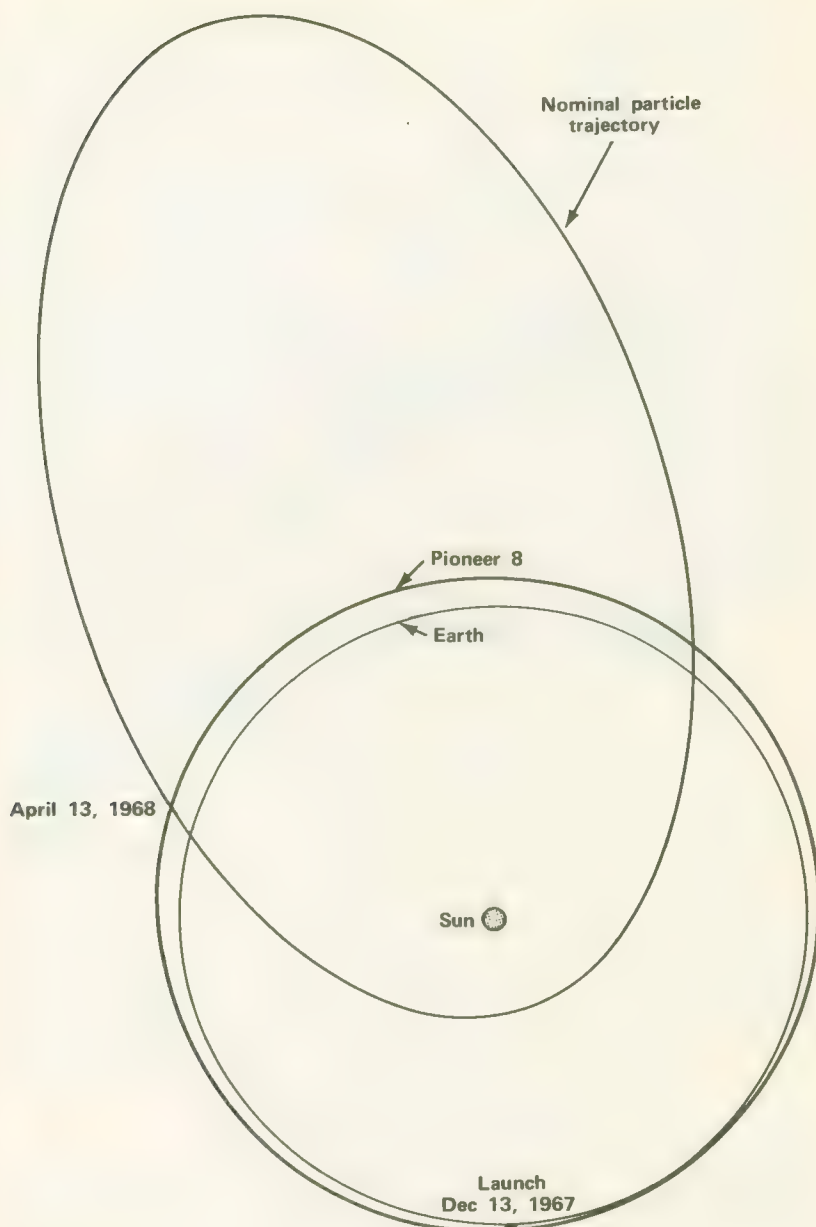


FIGURE 6-10.—Postulated orbit for the particle recorded on Apr. 13, 1968. This was a time-of-flight event. From: Berg, 1969.

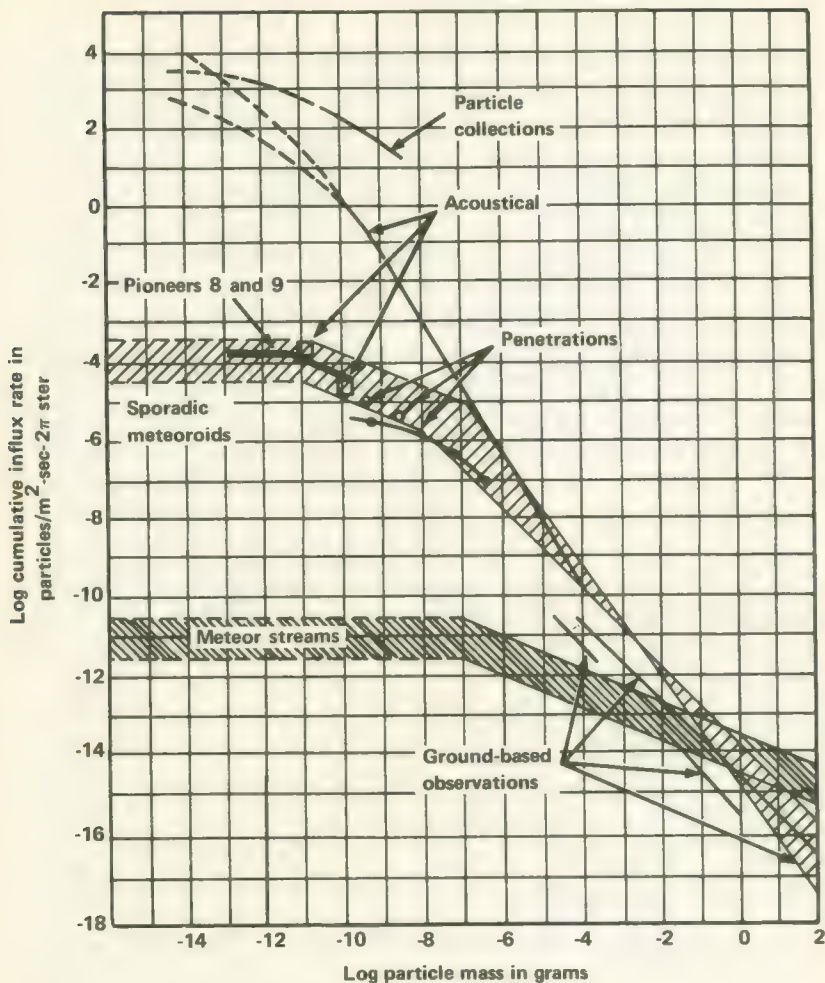


FIGURE 6-41.—Micrometeoroid fluxes as functions of mass. The heavy lines represent experimental data, while the shaded areas are theoretical. Pioneer data agree well with theory. From: ref. 63.

The three formal objectives of the experiment were:

- (1) Obtain primary determinations of the masses of the Moon and Earth and of the AU
- (2) Improve the ephemeris of the Earth
- (3) Investigate the possibility of a General Relativity test, using Pioneer orbits and data (ref. 64).

The source of all data for this experiment is the Deep Space Network. The spacecraft carried no special equipment for this experiment. DSN

two-way coherent Doppler data, judged as "good" by the tracking stations, were put on magnetic tapes. The tapes also contained mission data, such as the specific DSN station responsible for each group of data. Obvious mistakes were edited from the tapes.

Although the Pioneers, unlike the Mariners, made no midcourse maneuvers, they did carry out the two types of orientation maneuvers described in Vol. II. Tracking data indicate that some trajectory perturbations resulted from these maneuvers. Fortunately, the orientation maneuvers were usually concluded within a day or two of launch. From the tracking data on Pioneer 7, it is apparent that the Type-II orientation maneuver executed on August 19, 1966, changed the spacecraft velocity only by a few hundred millimeters per second. More serious was the gas leak on Pioneer 6, which provided an unknown source of uncompensated momentum transfer—in other words, a source of thrust that confused the analyses. The gas leak rendered the first 6 months of Pioneer-6 tracking data useless in terms of the objectives of the experiment.

In the first paper published on the Pioneer celestial mechanics experiment, Anderson and Hilt (ref. 64) reported the following preliminary Earth-Moon data:

$$\begin{aligned}\text{Geocentric gravitational constant} &= GE = \\ &398601.5 \pm 0.4 \text{ km}^3/\text{sec}^2 \\ \text{Lunar gravitational constant} &= GM = \\ &4902.75 \pm 0.12 \text{ km}^3/\text{sec}^2 \\ \text{Earth-Moon mass ratio} &= \mu^{-1} = \\ &81.3016 \pm 0.0020\end{aligned}$$

The uncertainties were believed to represent realistic standard errors. The authors reported that most of the systematic errors in the determination of  $\mu^{-1}$  probably came from the single-precision numerical computations performed on an IBM 7094. These computations were being converted to double-precision as the paper was being written.

### SOLAR WEATHER MONITORING

Solar events strongly affect all that transpires in interplanetary space from the edges of the Sun's extensive corona to well beyond the Earth's orbit. The chief carriers of solar disturbances are the solar plasma (solar wind), the Sun's magnetic field, and the bursts of cosmic rays that often accompany solar activity. The interactions of these phenomena with the Earth are not obvious as far as the ordinary citizen is concerned. Rarely, he will read or hear that intense magnetic storms triggered by solar

activity are hampering long distance communication, but in general the Earth is well insulated from any obvious effects of solar activity by its magnetosphere and atmosphere.

During intense magnetic storms, while most people go about their business unknowing and unconcerned, solar-induced electromagnetic effects wreak havoc with radio and long-landline communication. High frequency radio links depending upon forward- or back-scattering processes in the upper atmosphere are often impossible to use. There is also evidence that magnetic storms sometimes open circuit breakers and cause other disruptions in large electric power grids, particularly in the northern latitudes. Companies engaged in searching for minerals with magnetic detectors are often forced to suspend operations. Accurate forecasts of magnetic storms are useful (and worth money) in the sense that preparations can be made for use of other communication circuits and for otherwise reducing the impact of the storm.

Because of these terrestrial effects, several groups are interested in "solar weather"; i.e., the status of the interplanetary magnetic field, plasma fluxes, and cosmic radiation levels. The interest transcends pure science. NASA, for example, is concerned with solar events that might compromise manned space missions, particularly those that leave the shelter of the Earth's magnetosphere. The Environmental Science Services Administration (ESSA) desires advance information on magnetic storms and the injection of new charged particles into the Earth's belt of trapped radiation. These are the events that sometimes upset terrestrial communications and have some not-so-well-understood effects on the planet's weather. The Department of Defense (DOD) has similar interests for military reasons.

Pioneer solar weather reports began in January 1967. Usually, they are sent once a day to ESSA's Space Disturbance Forecast Center at Boulder, Colorado, to DOD's NORAD, and to other agencies. However, when manned flights are imminent, reports are sent hourly to NASA's Apollo Mission Control Center at Houston, Texas. The reports include:

- (1) The corotation delay, the expected time in days between the measurement of a disturbance at the spacecraft and its arrival at Earth
- (2) Solar-wind velocity, density, and temperature
- (3) Cosmic-ray intensities in several energy bands
- (4) The general condition of the interplanetary magnetic field.

#### REFERENCES

1. BURLAGA, L. F.; AND NESS, N. F.: Macro and Microstructure of the Interplanetary Magnetic Field. *Can. J. Phys.*, vol. 46, 1968, p. S962.
2. NESS, N. F.; SCEARCE, C. S.; AND CANTARANO, S. C.: Preliminary Results from the Pioneer 6 Magnetic Field Experiment. *J. Geophys. Res.*, vol. 71, Jul. 1, 1966.

3. NESS, N. F.: Simultaneous Measurements of the Interplanetary Magnetic Field. *J. Geophys. Res.*, vol. 71, Jul. 1, 1966, p. 3319.
4. BURLAGA, L. F.; AND NESS, N. F.: Tangential Discontinuities in the Solar Wind. *Solar Phys.*, vol. 9, Oct. 1969, p. 467.
5. NESS, N. F.; SCEARCE, C. S.; AND CANTARANO, S. C.: Probable Observations of the Geomagnetic Tail at  $10^3$  Earth Radii by Pioneer 7. *J. Geophys. Res.*, vol. 72, Aug. 1, 1967.
6. FAIRFIELD, D. H.: Simultaneous Measurements on Three Satellites and Observation of the Geomagnetic Tail at  $1000R_E$ . *J. Geophys. Res.*, vol. 73, Oct. 1, 1968, p. 6179.
7. MARIANI, F.; AND NESS, N. F.: Observations of the Geomagnetic Tail at 500 Earth Radii by Pioneer 8. *J. Geophys. Res.*, vol. 74, Nov. 1, 1969, p. 5633.
8. BURLAGA, L. F.: Directional Discontinuities in the Interplanetary Magnetic Field. *Solar Phys.*, vol. 1, Apr. 1969, p. 54.
9. BURLAGA, L. F.: Micro-scale Structures in the Interplanetary Medium. *Solar Phys.*, vol. 4, May 1968, p. 67.
10. SARI, J. W.; AND NESS, N. F.: Power Spectra of the Interplanetary Magnetic Field. NASA TM-X-63428, 1968. (Also available in *Solar Phys.*, vol. 8, Jul. 1969.)
11. MARIANI, F.; BAVASSANO, B.; AND NESS, N. F.: Magnetic Field Fluctuations on the Magnetosheath Observed by Pioneers 7 and 8. NASA TM-X-63762, 1969.
12. NESS, N. F.; AND TAYLOR, H. E.: Observations of the Interplanetary Magnetic Field, July 4-12, 1966. NASA TM-X-55842, 1967.
13. MARIANI, F.; BAVASSANO, B.; AND NESS, N. F.: Interplanetary Magnetic Field Measured by Pioneer 8 during the 25 February 1969 Event. Intercorrelated Satellite Observations Related to Solar Events. V. Manno and D. E. Page, eds., D. Reidel Publishing Co., Dordrecht, 1970, pp. 427-435.
14. LAZARUS, A. J.; BRIDGE, H. S.; AND DAVIS, J.: Preliminary Results from the Pioneer VI M.I.T. Plasma Experiment. *J. Geophys. Res.*, vol. 71, Aug. 1, 1966, p. 3787.
15. SISCOE, G. L.; TURNER, J. M.; AND LAZARUS, A. J.: Simultaneous Plasma and Magnetic-Field Measurements of Probable Tangential Discontinuities in the Solar Wind. *Solar Phys.*, vol. 6, Mar. 1969, p. 456.
16. SISCOE, G. L.; GOLDSTEIN, B.; AND LAZARUS, A. J.: An East-West Asymmetry in the Solar Wind Velocity. *J. Geophys. Res.*, vol. 74, Apr. 1, 1969.
17. SISCOE, G. L.; FORMISANO, V.; AND LAZARUS, A. J.: Relation Between Geomagnetic Sudden Impulses and Solar Wind Pressure Changes—An Experimental Investigation. *J. Geophys. Res.*, vol. 73, Aug. 1, 1968, p. 4869.
18. FORMISANO, V.: Interplanetary Plasma Electrons—A Preliminary Report of Pioneer 6 Data. *J. Geophys. Res.*, vol. 74, Jan. 1, 1969, p. 355.
19. LAZARUS, A. J.; AND BINSACK, J. H.: Observations of the Interplanetary Plasma (Associated with the July 7, 1966, Flare). Paper presented at 10th COSPAR Meeting, 1967.
20. HOWE, H. C., JR.: Pioneer 6 Plasma Measurements in the Magnetosheath. *J. Geophys. Res.*, vol. 75, May 1, 1970.
21. LAZARUS, A. J.; SISCOE, G. L.; AND NESS, N. F.: Plasma and Magnetic Field Observations during the Magnetosphere Passage of Pioneer 7. *J. Geophys. Res.*, vol. 73, Apr. 1968.
22. WOLFE, J. H.; ET AL.: Initial Observations of the Interplanetary Solar Wind by the Pioneer 6 Quadrispherical Plasma Probe. Am. Geophys. Union, 1966.
23. INTRILIGATOR, D. S.; ET AL.: Preliminary Comparison of Solar Wind Plasma Observations in the Geomagnetic Wake at 1000 and 500 Earth Radii. *Plan. and Space Sci.*, vol. 17, Mar. 1969.
24. SCARF, F. L.; WOLFE, J. H.; AND SILVA, R. W.: A Plasma Instability Associated with Thermal Anisotropies in the Solar Wind. *J. Geophys. Res.*, vol. 72, Feb. 1, 1967.

25. FAN, C. Y.; ET AL.: Anisotropy and Fluxuations of Solar Proton Fluxes of Energies 0.6-100 MeV Measured on the Pioneer VI Space Probe. *J. Geophys. Res.*, vol. 71, Jul. 1, 1966.
26. FAN, C. Y.; ET AL.: Protons Associated with Centers of Solar Activity and Their Propagation in Interplanetary Magnetic Field Regions Corotating with the Sun. *J. Geophys. Res.*, vol. 73, Mar. 1, 1968.
27. FAN, C. Y.; ET AL.: Differential Energy Spectra and Intensity Variation of 1-20 MeV/Nucleon Protons and Helium Nuclei in Interplanetary Space (1964-1966). *Can. J. Phys.*, vol. 46, May 15, 1968, p. S498.
28. RETZLER, J.; AND SIMPSON, J. A.: Relativistic Electrons Confined within the Neutral Sheet of the Geomagnetic Tail. *J. Geophys. Res.*, vol. 74, May 1, 1969, p. 2149.
29. McCracken, K. G.; AND NESS, N. F.: The Collimation of Cosmic Rays by the Interplanetary Magnetic Field. *J. Geophys. Res.*, vol. 71, Jul. 1, 1966.
30. RAO, U. R.; McCracken, K. G.; AND BARTLEY, W. C.: Cosmic-Ray Propagation Processes, 3. The Diurnal Anisotropy in the Vicinity of 10 MeV/Nucleon. *J. Geophys. Res.*, vol. 72, Sept. 1, 1967, p. 4343.
31. BALASUBRAHMANYAN, V. K.; ET AL.: Co-Rotating Modulations of Cosmic Ray Intensity Detected by Spacecraft Separated in Solar Azimuth. NASA TM-X-63654, 1969.
32. McCracken, K. G.; RAO, U. R.; AND NESS, N. F.: Interrelationship of Cosmic-Ray Anisotropies and the Interplanetary Magnetic Field. *J. Geophys. Res.*, vol. 73, Jul. 1, 1968.
33. McCracken, K. G.; RAO, U. R.; AND BUKATA, R. P.: Recurrent Forbush Decreases Associated with M-Region Magnetic Storms. *Phys. Rev. Letters*, vol. 17, Oct. 24, 1966, p. 928.
34. McCracken, K. G.; RAO, U. R.; AND BUKATA, R. P.: Cosmic-Ray Propagation Processes, 1. A Study of the Cosmic-Ray Flare Effect. *J. Geophys. Res.*, vol. 72, Sept. 1, 1967.
35. RAO, U. R.; McCracken, K. G.; AND BUKATA, R. P.: The Acceleration of Energetic Particle Fluxes in Shock Fronts in Interplanetary Space. *Can. J. Phys.*, vol. 46, 1968, p. S844.
36. BUKATA, R. P.; McCracken, K. G.; AND RAO, U. R.: A Comparison of the Characteristics of Corotating and Flare-Initiated Forbush Decreases. *Can. J. Phys.*, vol. 46, May 15, 1968, p. S994.
37. BUKATA, R. P.; ET AL.: Pioneer VI Observations of Forbush-Type Modulation Phenomena in the Galactic Alpha Particle Flux. Paper presented at 11th Intl. Conf. on Cosmic Rays (Budapest), 1970.
38. BUKATA, R. P.; ET AL.: Neutron Monitor and Pioneer 6 and 7 Studies of the January 28, 1967, Solar Flare Event. *Solar Phys.*, vol. 10, Nov. 1969, p. 198.
39. REIFF, G. A.: Radio Propagation Experiments with Interplanetary Spacecraft. *J. Spacecraft and Rockets*, vol. 6, May 1969.
40. McCracken, K. G.; ET AL.: The Decay Phase of Solar Flare Events. *Solar Phys.*, 1971.
41. LEZNIAK, J. A.; ET AL.: Observations on the Abundance of Nitrogen in the Primary Cosmic Radiation. *Astrophys. and Space Sci.*, vol. 5, Sept. 1969.
42. LEZNIAK, J.; AND WEBBER, W. R.: Observations of Fluorine Nuclei in the Primary Cosmic Radiation Made on the Pioneer 8 Spacecraft. *Astrophys. J.*, vol. 156, May 1969, p. L73.
43. LEZNIAK, J. A.; VON ROSENVINGE, T. T.; AND WEBBER, W. R.: The Chemical Composition and Energy Spectra of Cosmic Ray Nuclei with  $Z=3-30$ . *Acta Physica*, vol. 29, Supplement 1, 1970.
44. BFEDLE, R. E.; ET AL.: Measurements of the Primary Electron Spectrum in the Energy Range 0.2 MeV to 15 GeV. *Acta Physica*, vol. 29, Supplement 1, 1970.

45. LEZNIAK, J. A.; WEBBER, W. R.; AND ROCKSTROH, J.: A Comparison of Solar Modulation Effects on Protons, Electrons and Helium Nuclei. Paper presented at 11th Intl. Conf. on Cosmic Rays (Budapest), 1970.
46. STANFORD UNIVERSITY AND STANFORD RESEARCH INSTITUTE: The Interplanetary Electron Number Density from Preliminary Analysis of the Pioneer VI Radio Propagation Experiment. *J. Geophys. Res.*, vol. 71, Jul. 1, 1966, p. 3325.
47. KOEHLER, R. L.: Interplanetary Electron Content Measured Between Earth and Pioneer VI and VII Spacecraft Using Radio Propagation Effects. Stanford Electronic Laboratory SU-SEL-67-051, 1967.
48. KOEHLER, R. L.: Radio Propagation Measurements of Pulsed Plasma Streams from the Sun Using Pioneer Spacecraft. *J. Geophys. Res.*, vol. 73, Aug. 1, 1968.
49. LANDT, J. A.; AND CROFT, T. A.: A Plasma Cloud Following a Solar Wind Shock on 7 July 1966 Measured by Radio Propagation to Pioneer 6. Stanford Electronics Laboratory SU SEL-70-001, 1970.
50. POMALAZA-DIAZ, J. C.: Measurement of the Lunar Ionosphere by Occultation of the Pioneer VII Spacecraft. Stanford Electronics Laboratory SU-SEL-67-095, 1967.
51. CROFT, T. A.: Patterns of Solar Wind Flow Deduced from Interplanetary Density Measurements Taken during 21 Rotations of the Sun in 1968-70. Stanford University SU-SEL-70-063, 1970.
52. LEVY, G. S.; ET AL.: Pioneer 6—Measurement of Transient Faraday Rotation Phenomena Observed during Solar Occultation. *Science*, vol. 166, Oct 31, 1969.
53. SCHATTEN, K. H.: Evidence for a Coronal Magnetic Bottle at 10 Solar Radii. *NASA-TM-X-63811*, 1969.
54. SCARF, F. L.; ET AL.: Initial Results of the Pioneer 8 VLF Electric Field Experiment. *J. Geophys. Res.*, vol. 73, Nov. 1, 1968.
55. SCARF, F. L.; FREDRICKS, R. W.; AND KENNEL, C. F.: AC Electric and Magnetic Fields and Collisionless Shock Structures. Particles and Fields in the Magnetosphere. R. M. McCormac, ed., D. Reidel Publishing Co., Dordrecht, 1970, p. 102.
56. SCARF, F. L.; ET AL.: AC Fields and Wave-Particle Interactions. Particles and Fields in the Magnetosphere. R. M. McCormac, ed., D. Reidel Publishing Co., Dordrecht, 1970, p. 275.
57. SCARF, F. L.; ET AL.: Pioneer 8 Electric Field Measurements in the Distant Geomagnetic Tail. *J. Geophys. Res.*, vol. 75, June 1, 1970, p. 3167.
58. SISCOE, G. L.; ET AL.: VLF Electric Fields in the Interplanetary Medium: Pioneer 8. TRW Systems 10472-6016-RO-00, 1971.
59. SISCOE, G. L.; ET AL.: Evidence for a Geomagnetic Wake at 500 R<sub>E</sub>. *J. Geophys. Res.*, vol. 75, Oct. 1, 1970, p. 5319.
60. SCARF, F. L.; GREEN, I. M.; AND CROOK, G. M.: The Pioneer 9 Electric Field Experiment: Part 1, Near Earth Observations. TRW Systems 10472-6019-RO-00, 1970.
61. SCARF, F. L.; AND SISCOE, G. L.: The Pioneer 9 Electric Field Experiment: Part 2, Observations between 0.75 and 1.0 AU. TRW Systems 10472-6120-RO-00, 1970.
62. BERG, O. E.; KRISHNA SWAMY, K. S.; AND SECRETAN, L.: Cosmic Dust Radiants and Velocities from Pioneer 8. Goddard Space Flight Center X-616-69-145 and X-616-69-233, 1969.
63. BERG, O. E.; AND GERLOFF, U.: More Than Two Years of Micrometeorite Data from Two Pioneer Satellites. Paper presented at XIIIth Plenary Meeting of COSPAR (Leningrad), May 1970.
64. ANDERSON, J. D.; AND HILT, D. E.: Improvement of Astronomical Constants and Ephemerides from Pioneer Radio Tracking Data. *Am. Astronaut. Society Paper 68-130*, 1968.



# Bibliography

- ANON.: Significant Achievements in Space Science, 1966. NASA SP-155, 1967.
- ANON.: Significant Achievements in Space Science, 1968. NASA SP-167, 1968.
- BAITY, W. H.; ET AL.: Low Energy Cosmic Ray H<sup>2</sup> and He<sup>3</sup> Nuclei Intensities Measured in 1968. *Astrophys. J.*, 1970.
- BARTLEY, W. C.; ET AL.: Anisotropic Cosmic Radiation Fluxes of Solar Origin. *J. Geophys. Res.*, vol. 71, Jul. 1, 1966, p. 3299.
- ; ET AL.: Pioneer 6 Measurements of the Degree of Anisotropy of the Galactic Cosmic Radiation. COSPAR paper, 1966.
- BERG, O. E.; AND GERLOFF, U.: Orbital Elements of Micrometeorites Derived from Pioneer 8 Measurements. *J. Geophys. Res.*, vol. 75, Dec. 1, 1970, p. 6932.
- BINSACK, J. H.; AND LAZARUS, A. J.: Observations of the Interplanetary Plasma Subsequent to the 7 July Proton Flare. *Annals of ICSY*, vol. 3, 1969, p. 378.
- BUKATA, R. P.; ET AL.: Neutron Monitor and Pioneer 6 and 7 Studies of the January 28, 1967, Solar Flare Event. *Solar Phys.*, vol. 10, Nov. 1969, p. 198.
- : Pioneer 6 and 7 Observations of Solar Induced Cosmic Radiation. Paper presented at Am. Geophys. Union Meeting (Washington), 1967.
- ; McCracken, K. G.; AND RAO, U. R.: Co-rotating Modulation Phenomena. Paper presented at 10th Intl. Conf. on Cosmic Radiation (Calgary), 1967.
- ; AND PALMIRA, R. A. R.: The Effect of the Filamentary Interplanetary Magnetic Field Structure on the Solar Flare Event of May 4, 1966. *J. Geophys. Res.*, vol. 72, Nov. 1, 1967, p. 5563.
- : Anisotropic Proton Propagation Observed with Pioneers 6 and 7. Paper presented at Midwest Cosmic Ray Conf., State Univ. of Iowa, 1968.
- : Summary of Low Energy Solar Cosmic Ray Events. Paper presented at the 7th Aerospace Sci. Meeting (New York), 1969.
- BURLAGA, L. F.: Hydromagnetic Discontinuities in the Solar Wind. Significant Accomplishments in Science, 1968. NASA SP-195, 1969, pp. 127-130.
- : On the Nature and Origin of Directional Discontinuities. Goddard Space Flight Center X-692-70-462, 1970.
- : Microstructure of the Interplanetary Medium. Goddard Space Flight Center X-692-71-100, 1970.
- CANTARANO, S.; AND MARIANI, F.: Magnetic Field Measurements in Interplanetary Space. *European Space Res. Org. ESRO-SR-4*.
- ; NESS, N. F.; AND SCARFI, C. S.: Preliminary Results from Pioneer VI Magnetic Field Experiment. *J. Geophys. Res.*, vol. 71, Jul. 1, 1966, p. 3305.
- CROFT, T. A.; AND HOWARD, H. T.: The Line of Corotating Structures in the Solar Wind Deduced from Electron Content Measured Along the Line of Sight to Four Pioneers. Paper presented at Am. Geophys. Union Meeting (San Francisco), 1969.
- : Corotating Regions in the Solar Wind, Evident in Number Density Measured by Radio Propagation Technique. *Radio Sci.*, vol. 6, Jan. 1971, p. 55.
- DHANJU, M. S.; AND SARABHAI, V.: Short Period Fluctuations of Cosmic Ray Intensity at Geomagnetic Equator and Their Solar and Terrestrial Relationships. *J. Geophys. Res.*, vol. 75, Apr. 1, 1970, p. 1795.

- DRYER, M.; AND JONES, D. L.: Energy Deposition in the Solar Wind by Flare-Generated Shock Waves. *J. Geophys. Res.*, vol. 73, Aug. 1, 1968, p. 4875.
- ESHLEMAN, V. R.; ET AL.: Pioneer VIII Lunar Occultation. URSI Paper (Ottawa), 1967.
- : Bistatic Radar Astronomy. *Am. Astronaut. Society Paper* 68-182, 1968.
- FAIRFIELD, D. H.: Magnetic Field of the Magnetosphere and Tail. *The Polar Ionosphere and Magnetospheric Processes*. G. Skovli, ed., Gordon and Breach (New York), 1970, pp. 1-23.
- FISK, L. A.; AND ALEXANDER, W. I.: Radial Gradients and Anisotropies of Cosmic Rays. *NASA TM-X-63743*, 1969.
- FORMAN, M. A.: The "Equilibrium" Anisotropy in the Flux of 10 MeV Solar Flare Particles and Their Convection in the Solar Wind. *J. Geophys. Res.*, vol. 75, June 1, 1970, p. 3147.
- GERLOFF, U.; AND BERG, O. E.: A Model for Predicting the Results of "In Situ" Meteoroid Experiments, Part 1: Pioneer 8 and 9 Results and Phenomenological Evidences. Paper presented at the XIIIth Plenary Meeting of COSPAR (Leningrad), May 1970.
- GOLDSTEIN, R. M.: Pioneer 6: Measurement of Transient Faraday Rotation Phenomena Observed during Solar Occultation. *Science*, vol. 166, Oct. 31, 1969, p. 596.
- : Superior Conjunction of Pioneer 6: *Science*, vol. 166, Oct. 31, 1969, p. 598.
- GREEN, I. M.; AND SCARF, F. L.: Description of Full Data Plots for the Pioneer 8 Electric Field Experiment. *TRW Systems 10472-6005-RO-00*, 1969.
- : Pioneer 9 Solar Wind Velocity and Electric Field Data, 8 Nov. 1968 to 4 Jan. 1969. *World Data Center Report*, UAG-9, 1970, p. 40.
- GRINGAUZ, K. I.; ET AL.: Comparison of the Simultaneous Measurements of the Concentration and Velocity of Solar-Wind Ions by the Venera-3 and Pioneer 6 Space Vehicles. *Kosmicheskie Issledovaniia*, vol. 5, May 4, 1967, p. 310. (Also available as *NASA CR-84086*, 1967.)
- HOWARD, H. T.; AND KOEHLER, R. L.: Interplanetary Electron Concentration and Variability Measurements with Pioneer VI and VII. *The Zodiacal Light and the Interplanetary Medium*. J. L. Weinberg, ed., *NASA SP 150*, 1967, pp. 361-364.
- HUNDHAUSEN, A. J.: Interpretation of Positive Ion Measurements Made by the ARC Quadrisphere Electrostatic Analyzer on Pioneer 6. Preprint, no date.
- KENNEL, C. F.; AND SCARF, F. L.: Thermal Anisotropies and Electromagnetic Instabilities in the Solar Wind. *J. Geophys. Res.*, vol. 73, Oct. 1, 1968, p. 6145.
- KHOKHLOV, M. Z.: Interpretation of the Data on the Angular Distribution of Solar Wind Ions Obtained on Pioneer 6. *Geomagnetism and Aeronomy*, vol. 7, 1968, p. 874.
- LANDT, J. A.; AND ESHLEMAN, V. R.: An Estimate of the Spatial Extent of a Flare-Induced Plasma Cloud Using Columnar Electron Content. Paper presented at Am. Geophys. Union Meeting (San Francisco), 1969.
- ; AND CROFT, T. A.: Shape of a Solar-Wind Disturbance on 9 July 1966 Inferred from Radio-Signal Delay to Pioneer 6. *J. Geophys. Res.*, vol. 75, Sept. 1, 1970, p. 4623.
- LEVY, G. S.; ET AL.: Pioneer VI Faraday-Rotation Solar Occultation Experiment. Paper presented at 12th COSPAR Meeting, 1969.
- LEZNIAK, J. A.: A Measurement of Charged Particle Spectra in Interplanetary Space. Ph.D. Thesis, Univ. of Minnesota, 1969.
- ; AND WEBBER, W. R.: Measurements of Gradients and Anisotropies of Cosmic Rays in Interplanetary Space. Paper presented at 11th Intl. Conf. on Cosmic Rays (Budapest), 1970.
- : Solar Modulation of Cosmic Rays, Protons, Helium Nuclei, and Electrons. *J. Geophys. Res.*, vol. 76, Mar. 1, 1971, p. 1605.

- LOCKWOOD, J. A.; AND WEBBER, W. R.: Cosmic Ray Intensity Variations on January 26-27, 1968. *J. Geophys. Res.*, vol. 74, Nov. 1, 1969, p. 5599.
- ; ET AL.: Comparison of the Rigidity Dependence for Forbush Decreases in 1968 with that for the 11-Year Variation. *J. Geophys. Res.*, 1970.
- LOTOVA, N. A.; AND RUKHADZE, A. A.: On the Nature of the Inhomogeneous Structure of Interplanetary Plasma. *Astronomicheskiy Zhurnal*, vol. 45, 1969, p. 343.
- MARIANI, F.: Recent Observations of the Geomagnetic Tail. The Earth Explored and Served by Satellites, 1969. In Italian, *AIAA abstract A70-13851*.
- ; AND NESS, N. F.: Reinterpretation of the Pioneer 6 Bow Shock Crossing. Goddard Space Flight Center X-690-71-24, 1971.
- MCCRACKEN, K. G.; ET AL.: A Co-Rotating Solar Cosmic Ray Enhancement Observed by Pioneer 8 and Explorer 34 on July 13, 1966. Paper presented at 11th Intl. Conf. on Cosmic Radiation (Budapest), 1970.
- MCDONALD, F. B.: IQSY Observations of Low-Energy Galactic and Solar Cosmic Rays. *Annals of the IQSY*, vol. 4, 1969, p. 187.
- MERRITT, R. P.; AND BARON, M. J.: Ionospheric Integrated Electron Content for Use with Pioneer Interplanetary Spacecraft. URSI Paper (Ottawa), 1967.
- MIHALOV, J. D.; SONETT, C. P.; AND WOLFE, J. H.: Hugoniot Equations Applied to Earth's Bow Shock Wave. *J. Plasma Phys.*, vol. 3, Sept. 1969, p. 449.
- ; ET AL.: Pressure Balance Across the Distant Magnetopause. *Cosmic Electrodynamics*, vol. 1, Dec. 1970, p. 389.
- NESS, N. F.: Solar Wind and the Interplanetary Magnetic Field. *Astronaut. Aeron.*, vol. 5, Oct. 1967, p. 8.
- ; AND WILCOX, J. M.: Interplanetary Sector Structure, 1962-1966. *Solar Phys.*, vol. 2, Nov. 1967, p. 351.
- ; Direct Measurements of Interplanetary Magnetic Field and Plasma. *Annals of the IQSY*, vol. 4, 1969, p. 88.
- ; The Magnetic Structure of Interplanetary Space. NASA TM-X-63634, 1969.
- ; MARIANI, F.; AND BAVASSANO, B.: Interplanetary Magnetic Field Measured by Pioneer 8 during the 25 February 1969 Event. NASA TM-X-63790, 1969.
- ; AND SCHATTEN, K. H.: Detection of Interplanetary Magnetic Field Fluctuations Stimulated by the Lunar Wake. *J. Geophys. Res.*, vol. 74, Dec. 1, 1969, p. 6425.
- NUNAMAKER, R. R.; HALL, C. F.; AND FROSOLONE, A.: Solar Weather Monitoring—Pioneer Project. *Am. Inst. of Astronaut. and Aeron. Paper 68-36*, 1968.
- PICHLER, H.: Analysis of the Solar Wind Data from Pioneer VI. *Archiv fur Meteorologie, Geophysik und Bioklimatologie, Series A*, vol. 19, No. 2, 1970, p. 187.
- RAO, U. R.; MCCRACKEN, K. G.; AND BUKATA, R. P.: Cosmic-Ray Propagation Processes, 2. The Energetic Storm Particle Event. *J. Geophys. Res.*, vol. 72, Sept. 1, 1967, p. 4325.
- ; Pioneer 6 Observations of the Solar Flare Particle Event of 7 July 1966. *Annals of the IQSY*, vol. 3, 1967, p. 329.
- REIFF, G. A.: Summary Results from Interplanetary Spacecraft Radio Propagation Experiments. NASA, no date.
- SARI, J. W.: Power Spectral Studies of the Interplanetary Magnetic Field. *Acta Physica, vol. 29, supp. 2, 1970*, p. 373.
- SCARF, F. L.: In-Orbit Interference Problems. *JPL Electro-Magnetic Interference Workshop*, NASA CR-100697, 1968, pp. 149-162.
- ; AND FREDRICKS, R. W.: Ion Cyclotron Whistlers in the Solar Wind. *J. Geophys. Res.*, vol. 73, Mar. 1, 1968, p. 1747.
- ; Interplanetary Waves and Their Effects on the Magnetosphere. TRW Systems 10472-6009-RO-00, 1969.
- ; ET AL.: Observations of Plasma Waves in Space. Proceedings of the NATO Ad-

- vanced Study Institute's Plasma Waves in Space and in the Laboratory, 1969. J. O. Thomas and B. J. Landmark, eds., American Elsevier Publishing Co., 1969, pp. 379-404.
- : Analysis of Pioneer C and D EFD Data. Final Report. TRW Systems 10472-6013 RO-00, 1970.
- : Microstructure of the Solar Wind. TRW Systems 10472-6015 RO 00, 1970.
- ; ET AL: Magnetic and Electric Field Changes Across the Shock and in the Magnetosheath. TRW Systems 05402 6011-RO-00, 1969. (Also in: Intercorrelated Satellite Observations Related to Solar Events. V. Manno and D. E. Page, eds., D. Reidel Publishing Co. (Dordrecht), 1970, pp. 181-189.)
- SCHATTEN, K. H.: Large-Scale Configuration of the Coronal and Interplanetary Magnetic Field. Univ. of Calif. Rept., 1968.
- ; NESS, N. F.; AND WILCOX, J. M.: Influence of a Solar Active Region on the Interplanetary Magnetic Field. *Solar Phys.*, vol. 5, 1968, p. 240.
- : Large-Scale Properties of the Interplanetary Magnetic Field. Goddard Space Flight Center X-692 71-96, 1971.
- STANFORD UNIVERSITY AND STANFORD RESEARCH INSTITUTE: Interplanetary and Terrestrial Wake Electron Number Density Measurements with Pioneer 6 and 7. 1966.
- STELZRIED, C. T.: A Faraday Rotation Measurement of a 13 cm Signal in the Solar Corona. Ph.D. Thesis, Univ. of Southern California, 1969.
- WILCOX, J. M.; AND NESS, N. F.: Quasi-Stationary Corotating Structure in the Interplanetary Medium. *J. Geophys. Res.*, vol. 70, Dec. 1, 1965, p. 5793.
- : The Interplanetary Magnetic Field—Solar Origin and Terrestrial Effects. *Space Sci. Rev.*, vol. 8, Apr. 1968, p. 258.
- WOLFF, J. H.; ET AL.: The Compositional, Anisotropic, and Nonradial Flow Characteristics of the Solar Wind. *J. Geophys. Res.*, vol. 71, Jul. 1, 1966, p. 3329.
- ; ET AL.: Preliminary Observations of a Geomagnetospheric Wake at 1000 Earth Radii. *J. Geophys. Res.*, vol. 72, Sept. 1967, p. 4577.
- ; ET AL.: Preliminary Pioneer 8 Observations of the Magnetospheric Wake at 500 Earth Radii. *Trans. of the Am. Geophys. Union*, vol. 49, 1968, p. 517 (abstract only).
- ; AND MCKIBBIN, D.D.: Pioneer 6 Observations of a Steady-State Magnetosheath. *Planetary and Space Sci.*, vol. 16, 1968, p. 953.
- : Review of Ames Research Center Plasma-Probe Results from Pioneers 6 and 7. *Physics of the Magnetosphere*. R. L. Carovillano, J. F. McClay, and H. R. Rodoski, eds., D. Reidel Publishing Co. (Dordrecht), 1968, pp. 435-460.

# Index

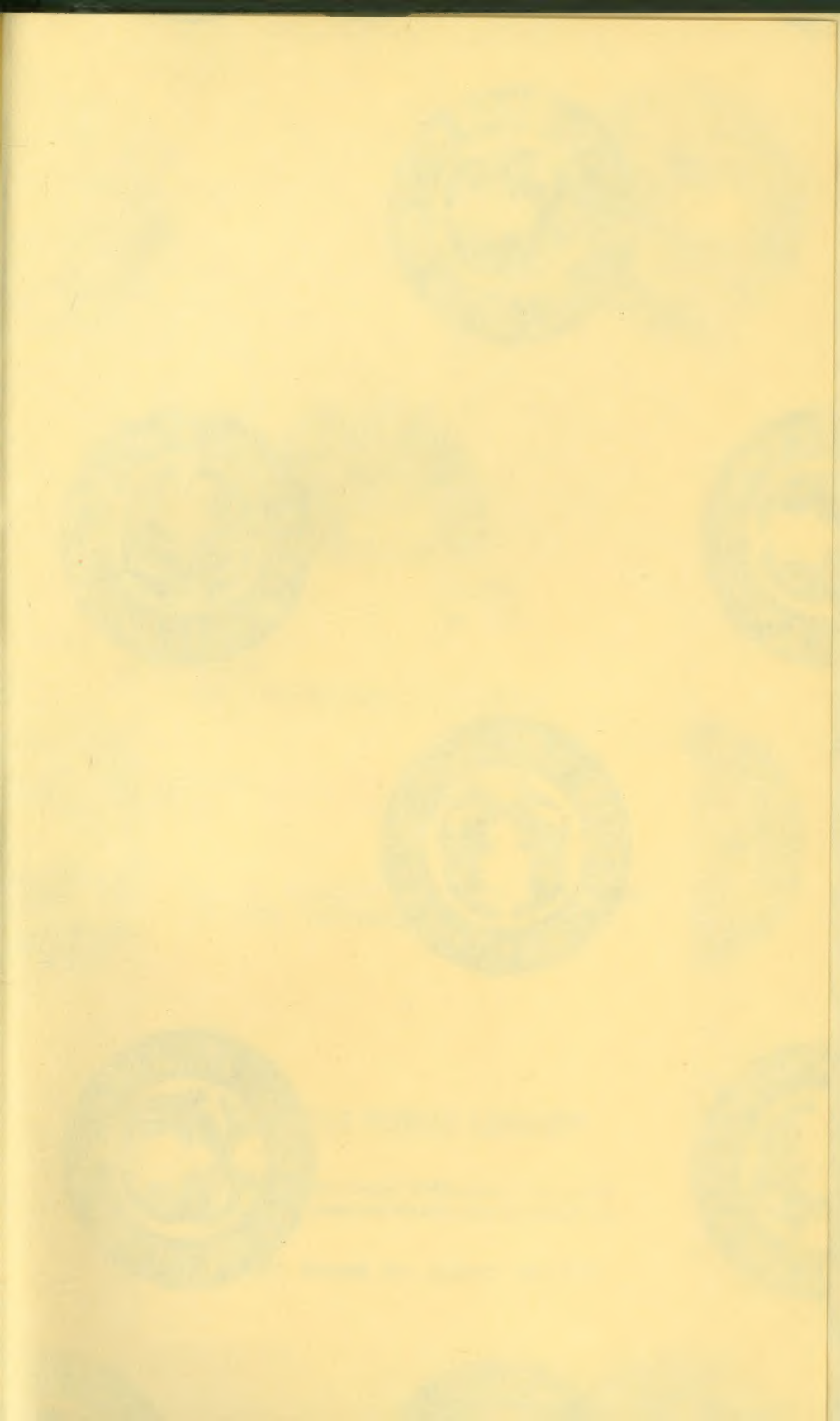
- Ames magnetometer, 23, 127  
Ames plasma probe, 127  
    scientific results, 90, 92-97, 130  
Ames Research Center, 1, 2, 6, 7, 9,  
    13, 55, 133  
    (See also Ames magnetometer, Ames  
    plasma probe)  
California Institute of Technology, 124  
Cape Canaveral (Cape Kennedy), 3, 4,  
    5, 13, 37  
Celestial mechanics experiment results,  
    138, 140-141  
Chicago cosmic-ray experiment, 20  
    scientific results, 97-102  
Communication subsystem performance,  
    64-65, 66, 69, 70, 71  
Convolutional coder, 23  
    performance, 74-75  
Cosmic dust, 135-138, 139, 140  
    (See also Goddard cosmic-dust ex-  
    periment)  
Cosmic rays, 97-115  
    (See also Chicago cosmic-ray experi-  
    ment, GRCSW cosmic-ray experi-  
    ment, Minnesota cosmic-ray experi-  
    ment)  
Data-handling subsystem performance,  
    65, 67-68, 73  
Deep Space Network (DSN), 3, 4, 6,  
    7, 9, 25, 115, 124  
    launch configuration, 37  
    (See also Tracking and data acquisi-  
    tion)  
Delta launch vehicle, 3, 4, 11, 17, 25  
    performance, 26-36  
Department of Defense, 142  
DSN. See Deep Space Network.  
Earth, magnetic field, 78-83, 86-87,  
    88-91, 92, 95-97, 102, 129-131  
Eastern Test Range (ETR), 3, 4, 8-9,  
    11, 17, 25, 36, 37, 38, 39  
Electrical Ground Support Equipment  
    (EGSE), 3, 10  
Electric-power subsystem performance,  
    60, 62, 63, 71-72  
Environmental Science Service Admin-  
    istration (ESSA), 142  
Goddard cosmic-dust experiment, sci-  
    entific results, 135-138, 139, 140  
Goddard magnetometer, 72, 103, 127  
    scientific results, 78-85, 86, 103, 133,  
    134  
Goddard Space Flight Center (GSFC),  
    2, 8, 9, 127  
GRCSW cosmic-ray experiment, 78  
    scientific results, 102-110  
Ground Operational Equipment  
    (GOE), 4, 6, 7  
International Quiet Sun Year (IQSY),  
    77  
Jet Propulsion Laboratory (JPL), 1, 2,  
    6-7, 38, 39  
    (See also Deep Space Network, JPL  
    celestial mechanics experiment)  
JPL celestial mechanics experiment, sci-  
    entific results, 138, 140-141  
Launch sequence, 27, 30  
Launch vehicle. See Delta launch ve-  
    hicle.  
Magnetometers. See Goddard magne-  
    tometer.  
Manned Space Flight Network  
    (MSFN), 25, 37, 38  
McDonnell-Douglas Astronautics Co., 2,  
    8  
Micrometeoroids. See Cosmic dust.  
MIT Faraday-cup plasma probe, 72  
    scientific results, 85-90, 119  
NASA Communications Network  
    (NASCOM), 11  
NASA Headquarters, 8, 142

- Orientation, Type I maneuver, 25, 41, 44, 45, 46-49  
(*See also* specific spacecraft, flight operations)  
Type II maneuver, 7, 11, 12, 46-49  
(*See also* specific spacecraft, flight operations)
- Orientation subsystem performance, 58, 59, 60, 69  
(*See also* Sun-sensor degradation)
- Pioneer A. *See* Pioneer 6.
- Pioneer B. *See* Pioneer 7.
- Pioneer C. *See* Pioneer 8.
- Pioneer D. *See* Pioneer 9.
- Pioneer E, 12, 22, 26  
flight operations, 43-44  
launch-vehicle performance, 30, 36  
prelaunch narrative, 23
- Pioneer 6, 21  
flight operations, 38, 40, 41, 49-51  
gas leak, 58, 59  
launch-vehicle performance, 26-28, 29, 30  
prelaunch narrative, 20  
spacecraft performance, 55-56, 58-68, 70  
trajectory, 32
- Pioneer 7, flight operations, 41, 43, 51  
launch-vehicle performance, 28, 30  
prelaunch narrative, 20-21  
spacecraft performance, 56-57, 68-69, 71-73  
trajectory, 33
- Pioneer 8, 14  
flight operations, 41-52  
launch-vehicle performance, 28, 30  
prelaunch activities, 18-19  
prelaunch narrative, 21-22  
spacecraft performance, 57, 73-74  
trajectory, 34
- Pioneer 9, countdown schedule, 16-17  
detailed task sequence, 13, 15-16
- flight operations, 41, 43, 52-53  
launch-vehicle performance, 30, 36  
prelaunch narrative, 23  
spacecraft performance, 57, 74-75  
trajectory, 35
- Plasma probes. *See* Ames plasma probe, MIT Faraday-cup plasma probe.
- Radio propagation experiments, scientific results, 124  
(*See also* Stanford radio propagation experiment)
- SFOF. *See* Space Flight Operations Facility.
- Solar weather monitoring, 141-142
- Space Flight Operations Facility (SFOF), 1, 3, 4, 6, 7, 11, 13, 38, 45
- Stanford radio propagation experiment, scientific results, 115, 118-124, 125
- Structure subsystem performance, 65, 72
- Sun, magnetic field, 78-85, 92, 95-97, 100, 103-105  
plasma, 78, 81, 83, 85-90, 92-97, 100, 119-124, 129-135  
solar weather, 141-142
- Sun-sensor degradation, 58, 69, 71, 73-74
- Test and Training Satellite (TETR), 9, 21, 44
- Thermal control subsystem performance, 58-61, 72, 73
- Tracking and data acquisition, launch to DSS acquisition, 36-44  
launch trajectories, 32-35  
Pioneer-6 ground track, 29  
(*See also* Deep Space Network)
- TRW Systems, 2, 7, 9, 55, 133
- TRW Systems electric field detector, 78  
scientific results, 90, 127-135
- University of Southern California, 124
- U.S. Air Force, 2  
(*See also* Eastern Test Range)

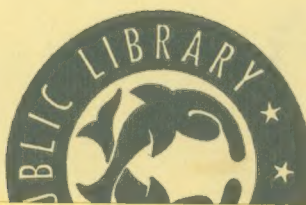


1

1







R629.435  
C813i

2768227  
v. 1-3

Corliss  
The interplanetary pioneers

R629.435 IDOTONIC TECHNOLOGY 2768227  
C813i v.1-3

TO BE SIGNED FOR AND RETURNED  
TO THE TECHNOLOGY LIBRARIAN.

## SEATTLE PUBLIC LIBRARY

Please keep date-due card in this pocket. A borrower's  
card must be presented whenever library materials are  
borrowed.

REPORT CHANGE OF ADDRESS PROMPTLY

